Gravity-Driven Water Flow in Networks

Gerard F. Jones

WILEY

This page intentionally left blank

GRAVITY-DRIVEN WATER FLOW IN NETWORKS

This page intentionally left blank

GRAVITY-DRIVEN WATER FLOW IN NETWORKS

Gerard F. Jones
Villanova University

WILEY
A JOHN WILEY & SONS, INC., PUBLICATION

Published by John Wiley & Sons, Inc., Hoboken, New Jersey
Published simultaneously in Canada

Library of Congress Cataloging-in-Publication Data:

Jones, Gerard F.
Gravity-driven water flow in networks : theory and design / Gerard. F. Jones.
p. cm.
Includes bibliographical references and index.
ISBN 978-0-470-28940-2 (hardback)
1. Hydrodynamics. 2. Water—Distribution. 3. Drainage. I. Title.
TC171.J66 2010
628.1'44—dc22 2010031088

Printed in the United States of America.

oBook ISBN: 978-0-470-93965-9
ePDF ISBN: 978-0-470-93964-2
ePub ISBN: 978-1-118-00208-7

10 9 8 7 6 5 4 3 2 1

To Nicki, Lauren, and
Chris, and in loving
memory of Eric

This page intentionally left blank

Contents in Brief

This page intentionally left blank

List of Symbols

English Symbols

A	area, m^2
a	cost-per-length coefficient, US$/m
a_w	wave speed in liquid, m/s
B	bulk modulus for liquid, Pa
b	exponent
C	coefficient
C'	cost per unit length, US$/m
C_T	total cost, US$
$\hat{C}$	constant in inequality constraint
c_v	specific heat at constant volume, J/kg·K
D	inside, or nominal, diameter of pipe, m
E	elastic modulus of pipe, Pa
e	internal energy per unit mass, J/kg
F	dimensionless static pressure at delivery location, $p_2/\rho g z_1$
$\hat{F}$	dimensionless static pressure at a pipe end, $p/\rho g(z_1 - z_2)$

English Symbols (Cont'd)

Fr	Froude number
f	Darcy friction factor (friction factor)
f^*	factor in Eqn (2.16)
g	gravitational acceleration, 9.807 m/s^2
$\hat{g}$	inequality constraint function
H	head, (m/s)^2
h	head, m
$\hat{h}$	height, m
i	growth rate, %/100
K	minor loss coefficient
L	pipe length, m
ℓ	pipe length from inlet to outlet measured in horizontal plane, m
$\hat{l}$	equality constraint function
M	number of minor-loss elements accounted for using L_e/D values
m	integer
$\dot{m}$	mass flow rate, kg/s
N	number of minor-loss elements accounted for using K values
n	integer
p	static pressure, Pa
P	population
PF	peak factor
Q	volume flow rate, L/s
$\dot{q}$	heat transfer rate to system, W
Re	Reynolds number
r	radius, m
s	mean slope between source and delivery points
S	hydraulic gradient
$\hat{s}$	slack variable
T	temperature, °C
t	time
$\hat{t}$	dummy variable
u	local velocity in the direction of fluid flow, m/s
$\overline{u}$	cross-sectional average flow speed, m/s
V	volume, L
$\dot{w}$	rate of work done by system, W
x, y	horizontal coordinates (x is alternately a pipeline coordinate), m
$\hat{x}$	independent parameters in optimization
$\hat{Y}$	objective function
z	vertical coordinate, m

Greek Symbols

α	kinetic energy correction factor
β	factor in Eqn (11.55)
γ	r/z_1 for syphon geometry
Δ	change
ϵ	roughness of pipe wall, m
η	efficiency
λ	tortuosity; ratio of actual length of pipe to pipe length if run straight
$\hat{\lambda}$	Lagrange multiplier
ν	kinematic viscosity, m^2/s
ρ	density, kg/m^3
ξ	dummy variable of integration

Subscripts

a	actual
$a, b, c, \ldots$	pipe labels for multiple-pipe networks
b	pertaining to branch
app	approximate
atm	atmospheric
$1, 2$	inlet and outlet states
$1, 2, 3, \ldots$	node numbers for multiple-pipe networks
d	demand
D	discharge
del	delivery
e	equivalent
$entry$	at entry of pipe
f	final
F	future
fr	friction
g	generator
$high$	high point
i, j	indices
j	at a junction
in	in
L	loss
low	low point
ℓ	local
m	pertaining to main
mod	modified

Subscripts (Cont'd)

out	out
p	peak
P	present
R	souRce
ref	reference
S	storage tank
s	start
sys	system
sc	scale
$shaft$	shaft
T	total
t	turbine
th	theoretical
u	unit
∞	refers to surroundings or terminal conditions
99%	99% of total

Superscripts

n	natural
new	most-recent result from an iterative procedure
old	result before most-recent from an iterative procedure
opt	optimal
$'$	measured from a peak
$*$	refers to a liquid-filled pipe segment

Preface

Several of the key elements of the mission statement for the Nicaraguan-aid organization, Agua Para la Vida (www.aplv.org), follow:

- Help small, rural communities of Nicaragua develop and maintain access to safe drinking water.
- Provide training and education to local people in all aspects of designing, building, and maintaining drinking water systems so that they can achieve autonomy in rural drinking water development.
- Develop design tools and teaching methods for use by other groups involved in village water system construction.

Even with the considerable aid of the many organizations like Agua Para la Vida and Youth Action For Rural Development (YARD) in Kenya (www.wsp.org), much of the population of these countries and others like them lack access to clean water. In Nicaragua it is most ironic that this deficit occurs in mountainous regions where the wet-season lasts 8 months of the year or more and rain water is plentiful! The need for the careful design of gravity-driven clean water networks in these, and many other similar parts of the world community is well established. This book is a small attempt to help in this worthy endeavor by presenting information to support technologists, engineers and engineering students, and practitioners who carry out these designs.

When the topic of analysis and design for water flow in pipes is raised, the saying "...there is nothing new under the sun" likely comes to mind. Certainly, many references on this are readily available. I began to teach this subject as a part of service learning projects at Villanova University in early 2004. The focus of the projects was to provide clean water for the people of central Nicaragua who had no easy access to this and often drank nearby, but contaminated water with dire consequences. With the guidance of faculty, the mostly mechanical engineering students assessed, analyzed, and designed the networks, and in some cases followed up by helping to install the network they or others had designed. I found teaching the analysis of gravity-driven water networks to the students to be a challenge. Most had already taken a course in fluid mechanics and had learned some things about pipe flow. However, gravity-driven flow in a closed pipe is very different than the flow problems to which they had been exposed. In my lectures that stressed fundamentals related to the importance of mean slope in a single-pipe network, local static pressure distributions near low and high points, and cost–minimization to determine unique solutions to the energy equation, it was as if I were teaching an entirely new subject. After some reflection, I would recall from my own teaching of fluid mechanics that the elevation change in nearly all problems was neglected (certainly for gases) or assumed negligible compared with a specified pressure difference between the pipe ends. The important elements of gravity-driven pipe flow are, in fact, never taught! I recognized a clear need for a good learning and teaching tool on this topic.

The literature was of little help. The treatment of gravity-driven flow in the existing text, trade, and hand books, if presented at all, is technology based so there were few, if any, fundamentals to which the students could relate and use as a sound basis for understanding and insight. In short, in the literature where gravity-driven flow appeared there was little educational value, and in sources like textbooks where the educational value is high, there was little or no treatment of gravity-driven flow networks. Simple and fundamentally sound design tools and algorithms using modern-day software were also missing.

Thus, this book is written in an attempt to place the analysis and design of gravity-driven water networks on a sound fundamentals footing and to provide easy-to-use algorithms and charts for analysis and design computations. In this way, I have attempted to bridge the gap between fundamental fluid mechanics and the applied and useful technology-based material in the various existing references on gravity-driven water networks. In particular, the topics have been chosen to add clarity, a sound technical basis, and support to many of those contained in the currently popular handbook by Thomas Jordan, Jr. (2004), which is cited in many places in this text. A benefit of the fundamentals approach is the production of original design graphs, formulas, and computational algorithms for the correct, sustainable designs of single- and multiple-pipe gravity-driven water networks.

Both theory and design are covered in this work, along with the analysis that must join the two. It is a considerable challenge to span this range effectively. For the theory I have, of course, relied on past work from classical fluid mechanics in which the focus may be thought of as the *discipline of engineering*. The design and practical content, that is, the *practice of engineering*, comes from reflection on past written

works and our team's experience in the field with actual gravity-driven water networks and with industry applications.

In addition to practitioners, this book is written for engineers, technologists, and scientists and for students preparing for these fields. To help the readers relate to the technical material, the presentation style has been chosen to be consistent with what students normally encounter in an undergraduate college-level course in the United States. In some cases, an advanced-level high school physics course that covers the energy equation for a moving fluid and the topic of flow in a pipe may suffice as adequate background to understand much of the material presented in this text.

Most of this book can be covered in about half of a 14-week term. This is the time that could perhaps be allotted for a college or high school level design course. The main Chapters 1–13, and 15 should be coverable in ~7 weeks, along with most of the relevant problems in Chapter 16. Chapters 10 and 14, on optimization and air blocks, may be added at the discretion of the instructor.

Double-outlined textboxes, like this one, will be employed to provide periodic breaks for the reader where there is an extended amount of technical material and will include examples, clarifying and reinforcing comments, supplemental information, and questions for exploration.

Fundamental equations and final forms of the most useful ones will be boxed.

This should not be confused with the double-outlined textboxes.

In addition to textboxes, annotations in the form of footnotes appear very frequently throughout the text. This is a personal preference of the author[1].

Other than the chapter on optimization and local static pressure, the mathematics required to understand the material in this book is algebra including the solution of single and simultaneous nonlinear algebraic equations using numerical methods. Many chapters require this. For readers who have forgotten or are not familiar with nonlinear algebraic equations, a section in Chapter 4 is included to refresh memories or introduce the basics of this topic. References to integrals and to ordinary differential equations are made in several chapters including those on local static pressure and minor losses, so it is worthwhile for the reader to recall some of the basics surrounding the calculus when covering this material. Some understanding of the calculus is needed for optimization, which always requires the derivative to determine so-called "stationary" points for a function. Of course, it is assumed that the reader has, at least, a familiarity with fluid mechanics.

Most pipe-flow problems of the types considered in this book require numerical solutions carried out on a computer. The traditional way of solving the systems of nonlinear algebraic equations that arise in pipe flows is iteration and linearized scaling (often referred to as "Regula Falsi" in texts on numerical methods), covered in Chapter 11, which for simple problems, could be executed by hand. A similar

[1]It is hoped that the readers will find the history, clarifications, and extensions presented by these aids useful without distracting from the principal thrust of the material.

method that "compartmentalizes" the terms from the energy equation and then uses trial-and-error to determine pipe diameter is the normal method of solution where just a single pipe is involved (Chapter 4). However, computer programs to quickly and efficiently solve the equations of pipe flow are well developed and have been for very many years. These fall into two classes. Nearly all are "opaque" in that the user is not made aware, or chooses not to be aware, of the program's basis. This means that an executable file is run on a computer, which is the result of a compilation of a source program written in perhaps Fortran or C++ (see comments below).

The other class is composed of "transparent" computer programs that present the solution in an easy-to-read manner, and appear as if written on paper. The solution for a given design is obtained by modifying an already-developed program for a closely related one. The commercial package Mathcad[2] is chosen for use in this book. In particular, the root and Given...Find constructs in Mathcad are very valuable for the solution of nonlinear algebraic equations. There are frequent references to these. Mathcad is also the only commercial package that explicitly includes units in equations. The conversion from one unit to another, say inches to mm, as required by the problem is accomplished automatically and is transparent. For various reasons, the use of units and the associated need to include them when solving engineering problems are a challenge for students today. Mathcad worksheets that solve the equations for many types of gravity-driven water networks are supplied with this text (downloaded from http://www.wiley.com/WileyCDA/WileyTitle/productCd-0470289406,descCd-DOWNLOAD.html). If familiarization with Mathcad is needed, a brief tutorial is presented in Appendix C.

As is the case with all technological tools, the lifetime of Mathcad may be finite. That is, at some time in the future it may be replaced with a "new and improved" version or it may even disappear. This is not a concern because the fundamental equations for analysis and design appearing in this text remain unchanged and can be solved with any programming language or tool, such as C++, Matlab[3], Microsoft's Excel, or a new and improved Mathcad. Even a programmable hand-held calculator is sufficient for some problems. More-senior engineers may recall a similar discussion in the 1970s concerning Fortran, then the dominant programming language in engineering, as to what the computational tool of the future will be. The answer that was often given was that no one knew for certain, but it would probably be called Fortran. Presently, after numerous revisions over the years, Fortran continues to be used by scientists and engineers worldwide.

G. F. JONES

Villanova, Pennsylvania
September, 2006

[2]Mathcad, Parametric Technology Corporation, 140 Kendrick Street, Needham, Massachusetts
[3]Matlab, The MathWorks, Inc. 3 Apple Hill Drive, Natick, Massachusetts 01760, USA.

Acknowledgments

I want to acknowledge the support from and stimulating discussions with James O'Brien and Jordan Ermilio of Villanova University. The three of us began a service-learning project at Villanova in 2003 and the book is an outgrowth of this initiative that continues today. Also due thanks are the mechanical engineering students at Villanova, whose interest and dedication in helping those less-fortunate than themselves over the past 7 years in their travels to central Nicaragua were the principal motivation for writing this book. The author also appreciates the thoughtful comments of Gary Gabriele, Ron Parise, Louis Velez, and Kevin Woods who, along with Jim and Jordan, reviewed the text and added their insight. Jordan also co-authored Chapters 13 and 15 and supplied many of the photographs for which I am very grateful.

I also wish to thank Villanova University for giving the time for me to finish a large part of this book during a sabbatical in the fall of 2007.

I am grateful to the staff at Wiley including my editor Bob Esposito, production manager Christine Punzo and her production staff, and LaTeX guru Amy Hendrickson, for their persistence and patience in seeing this project through to completion.

Lastly, I thank my wife, Nicki, for her patience, love, and support during the brief, but intense, period of time spent writing this book and during my travels to Central America.

G. F. J.

This page intentionally left blank

CONTENTS

CHAPTER 1

INTRODUCTION

"Give a Man a Fish, and Feed Him for a Day. Teach Him to Fish, and Feed Him for Life."
– Traditional

1.1 WATER DISTRIBUTION NETWORKS AND THEIR DESIGN

It is generally recognized that water distribution networks date to thousands of years BC. Those in Greece, Syria, Jordan, Turkey (Mays, 2000), Palestine, Persia (Salzman, 2006), and Crete (Trifunovic, 2006), as well as Rome (Chanson, 2002; Salzman, 2006; Trifunovic, 2006), Machu Picchu (Wright et al., 1997) and, later, New York City (Koeppel, 2000) have been extensively documented in print and the visual media. The networks consisted of "aqueducts," open channels and lead and wooden pipes, that used gravity to move water over large distances with reasonable losses. Despite these very early successful efforts at the design and construction of water distribution networks, it is estimated that today nearly 1 billion people live without access to clean drinking water throughout the world (Trifunovic, 2006); more than 15% of the total population. In particular, the probability of access to clean water in rural populations in South and Central America and Africa ranges from a scant 40–60%.

Gravity-Driven Water Flow in Networks. By Gerard F. Jones

The design of water networks has undoubtedly had a much shorter history, at least in terms of what we now know as engineering design. Consider evidence of the different elements used in the aqueducts in Rome in the first century, AD (Chanson, 2002). Culverts,[1] flow regulation with overflow and underflow gates,[2] and dropshafts to dissipate energy in steep regions using vortical motion appeared frequently. The relatively high levels of technical and construction expertise for this time period are remarkable. However, design was carried out by rules-of-thumb, based on simple observations and experiences, passed down through generations and across vast regions by word of mouth or perhaps script, not through the understanding of mass, momentum, and energy conservation that we use today. Certainly, there were no fast computational tools in ancient times to carry out the sophisticated calculations for the design and performance of these networks.[3]

In contrast to the likely design of the Roman aqueducts, imagine the following exchange that may occur on a day this week in the District Engineer's Office in a remote town in a developing country.

Community Member: Good morning Sr. Engineer. Last year, our community of San Pedro identified clean water as a priority development concern. In addition to this, we understand that your office has also been promoting small hydroelectric facilities for rural areas such as ours. There are currently 23 families living in the main section of San Pedro, which also has a school, a church, and a community center. There are an additional 80 families who live in more isolated areas of San Pedro and we believe that these families will start to build their homes closer to the village center once we have completed a water supply system and have reliable access to electricity.

District Engineer: Well, the local government is very interested in assisting areas, such as San Pedro, and we hope to be able to work with your community in the near future. Perhaps you can help us by providing some more information. For example; how many sources of water are there in San Pedro? Where will you get the water?

Community Member: There are several sources for water that we have already been using, but the water sometimes is dirty, especially during the rainy season. Also, every household does not have equal access to this water, so only a few families are benefiting from these sources. Most of these sources are from natural springs and are usually very clean because they are in a forested area in the mountains. There are some people who use this forested area for collecting wood for cooking or building houses but, we believe that the land owners will offer these sites for our needs if we have funding from the municipal government.

District Engineer: Okay, this is very useful information. Before we can even consider developing a water system, we will have to have an agreement with the local land owner and designate a protected area above the source so that no one can enter or

[1] A culvert is a passageway for flow constructed under a larger structure, such as a roadway or bridge.

[2] A gate, or sluicegate, is a plate of material that is used to partially or fully block flow, usually in an open channel. An overflow type allows the flow pass over the upper edge of the sluice; an underflow forces the flow below its lower edge.

[3] The abacus dates from about the 5th century BC and would have been used where appropriate by the Romans at later times. It was primarily a tool for the merchant rather than the hydraulic engineer.

disturb the watershed that is supplying these springs. This will ensure that the sources will continue to produce clean water. We will also have to design a protected spring intake so that runoff does not contaminate the source. Finally, if other conditions look favorable, I will have my assistant and one of our student interns visit your community to survey the site. Bear with me as I make a few quick calculations. Taking out his calculator, the engineer enters numbers, speaking the entries as he pushes buttons. "23 families $\times$ 6 persons per family $\times$ 100 liters per day per person $\times$ 1.1 raised to the tenth power is about 35,800 liters of water per day." Punching a few more numbers into his calculator the engineer notes, "any single water source that produces more than 0.42 liters per second will be able to satisfy your water needs."

Community Member: Is there any funding that we can use to build the system? How much do you estimate the water network will cost?

District Engineer: Assuming the community provides the labor for installation, there are several costs including the pipe, fittings, and valves, concrete, and reinforcement for a storage tank and the reservoir at the source, and we will need to build several tapstands[4] to distribute water at several locations including the school. Once my team surveys the site and determines the flow rate from an acceptable water source, I will have enough data to locate and size the reservoir and storage tank. I will also know where the pipes need to be run from the source to the tank, and from the tank to the delivery locations and tapstands. Once I have this information, I will calculate the volume of cement and amount of reinforcing steel mesh. I can then calculate the cost for these materials . . . .

Community Member: . . . (Impatiently interrupting) but, the distances to the water sources I have in mind are great, more than two kilometers each. And, the houses are spread over large distances. Surely, this much pipe will be very expensive. Do we need to have any counterpart funding from the community?

District Engineer: Well, first we will need to calculate the sizes of all pipes. I have a computer program that solves dozens of equations and models the flow of water in the network before it is actually built. This way, I can investigate many different designs and how they will perform before we actually build them. This saves money because if we do not design the system properly, your community will not have a reliable distribution of clean water even after we finish construction. I will pick from among the many designs the one that works the best from an engineering viewpoint and that has a reasonable cost.

Community Member: Interesting... (being curious, the community member continues), how can you trust that your equations will really work? We have tried many times to improve the water supply system in our community and have never really succeeded in making a difference because the water flow is always small and does not have good pressure.

Taking the opportunity to teach the community member about engineering, the District Engineer explains:

[4]See Section 1.3.5.

District Engineer: In engineering school we study fluid systems and hydraulics for an entire year and we learn about the equations and their history. We even verify the results from these equations in carefully designed experiments in a laboratory; we learn to have confidence in them. These equations are over 150 years old and have been used to design water systems all over the world. We almost always see that the designs work according to what the computer model predicts. Once the computer model is "validated" in this manner, we can trust that the equations will accurately predict how the system will work and we can make designs based on these results.

The reason why I am explaining this to you is because, after the water system is built, we will ask you to monitor the water flow rate from the source and the demand in your community. This is done for two reasons. First, if the network is not performing as we designed, there may be a need for correction to our design equations and methods, or construction techniques. This, we would certainly want to do for future designs. Second, we can perhaps correct your network so that it will perform as designed.

Community Member: Wow! This sounds like magic to me but, (being tentative) I am sure that it will work. Thank you for considering this request.

District Engineer: You are welcome Sr. Member. Engineers call this "analysis and design" and it is something that engineers are trained to do. I am very comfortable with this.

I will ask my assistant and his team to meet you later this week to begin to collect these data for your network. Now, regarding your request for hydroelectric power, we will need to discuss this after we determine the cost of the water network. You may wish to reconsider your request once you see this figure.

Community Member: Thank you again, Sr. Engineer, I look forward to working with you on this project.

We see from this exchange that the engineering design of gravity-water networks is really *analysis and design*, based first and foremost, on the mathematical solution of the equations for fluid flow in networks; equations that have been validated in the laboratory and field for more than a century. Essentially, we are confident of the ability of these equations to predict the future (that is, how networks will perform based on the solutions to these equations). There is a strong focus on analysis in this book. We will also see the importance of network cost. Cost is of interest not only because of its fundamental importance, but also since it is used to supply a needed constraint on the flow problem. The design is based loosely on fundamentals but, in addition, has a large contribution from engineering wisdom accumulated over many years of successful practice. We also see from the above dialog that measurements taken in the field before and after the analysis and design (collecting measurements before is sometimes referred to as "assessment") are crucial to assure a high-quality design that meets all requirements and provides feedback to the analysis and design process for continuous improvement where needed.

B.1.1 The Different Types of Water Sources

There are three different types of water sources that we commonly encounter. The first is surface water like a flowing stream or river, or a nonflowing pond. Second, a groundwater source is a quantity of subsurface water similar to a river or pond, except that it resides below the surface and is recharged by rain and run-off from rain. These subsurface reservoirs are known as *aquifers*. A spring is where groundwater rises to the surface of the ground due to an impermeable layer near the surface. Springs are typically located in mountainous areas and form because of the large rate of change of elevation of the terrain.

1.2 FEASIBILITY FOR GRAVITY-DRIVEN WATER NETWORKS

Communities that are candidates for a successful gravity-driven water network will have the following physical and social characteristics (Mihelcic et al., 2009):

- A source(s) of clean water, free from pathogens and large amounts of suspended solids, within relatively short distance from the community, elevated above the highest point of water delivery to the community, and with a flow rate sufficient to meet the present and future demands of the community,
- If the source(s) is a spring, it should be properly protected by its native vegetation (to preserve ground-water movement) and, for all types of sources, from possible surface contamination, such as pasture runoff,
- Level surface areas located between the source(s) and the highest point of water delivery to the community on which to site a storage tank and, if needed, a break-pressure tank,
- Binding commitments from the land owner(s) of the source(s), and that where the tank(s) will be located and pipelines run,
- Commitment from members of the community to provide labor for construction, maintenance, and continued successful operation of the network.

1.3 THE ELEMENTS

The elements of a gravity-driven water network are shown in the schematic of Fig. 1.1. As discussed in further detail below, the network is composed of a reservoir at the source, pipe, valves and fittings (fittings, such as elbows and tees, which are not shown in this figure), storage and perhaps break-pressure tanks, and points where the water is available for distribution to the communities, referred to as tapstands. Elements, such as vacuum breakers and air vents, may be necessary in the network under certain

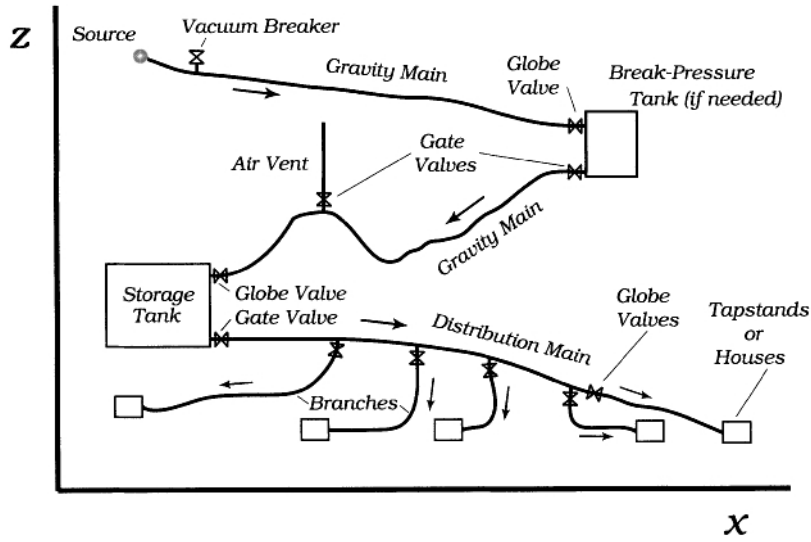

Figure 1.1 The elements of a gravity-driven water network.

conditions that are described below. The pipe segments that transport water between two points without a change in the flow rate between them are sometimes referred to as "gravity mains." Those that deliver water to branches are called "distribution mains." Valve types, such as globe and gate, will always be used to isolate parts of the network for maintenance and repair, and for flow control.

1.3.1 Reservoir at the Source

Reservoirs and several of their features are shown in Fig. 1.2. For example, a spring or freshwater stream may be dammed using reinforced concrete, as in Fig. 1.2. Besides providing for the water outlet through a gate-valved (see Section 1.3.4) pipe, a clean-out drain of at least 4-in. diameter, and an overflow pipe need to be provided for in the dam. A filter screen is normally installed at the point of water intake inside of the reservoir. A clean-out pipe accommodates periodic cleaning of the reservoir, if needed. The overflow pipe allows the water to drain away from the tank in a sanitary manner. A concrete cap, also shown in this figure, ensures cleanliness of the reservoir over time and reduces the frequency of screen cleaning. A door in the cap provides access to the filter.

1.3.2 Pipe and Fittings

Pressure pipe is used to transport water in these networks. As discussed in detail in Chapter 3, plastic pipe [polyvinyl chloride (PVC), high-density polyethylene (HDPE), acrylonitrile–butadiene–styrene (ABS)] is normally chosen because of economy, per-

Figure 1.2 Photos of reservoirs. All are constructed of poured concrete. Clockwise from upper left: a covered reservoir separated from uncovered section by a screen filter (PVC pipe in foreground awaits installation), a totally covered reservoir with a concrete valve box in front, a totally covered reservoir with cover partially removed for access to clean filter inside, a dam to hold back water before construction of the reservoir (the vertical PVC pipe downstream from the dam is a vacuum breaker; see the discussion in Section 1.3.6), inside view of a totally covered reservoir.

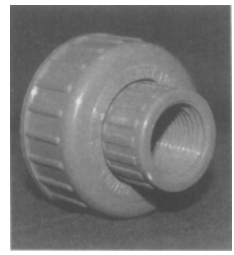

Figure 1.3 A nut union of PVC. Photo courtesy of Nicki Jones.

formance, and availability. In cases where large pressures are expected, galvanized steel (galvanized iron or GI) pipe is used, however this is heavy and more expensive than plastic so its use is chosen carefully. Rigid-wall pipe is manufactured in various lengths up to about 6 m. Flexible-wall pipe is supplied in long rolls.

The scale of the networks addressed in this work is such that pipe diameters of the order of 6 in. are about the largest encountered.[5] Dimensional and pressure data for pipe up to nominal 12-in.-size are presented in Chapter 3.

Typical fittings that join segments of pipe are elbows (90°, 45°, and 22.5°), which turn the flow at the angle specified, tees for flow branching, reducers (or expanders) for decreasing (or increasing) the pipe diameter, and couplings. Unions (or "nut" unions, Fig. 1.3) are sometimes used in situations where there is a need to separate assemblies of pipe for maintenance or repair. Unions allow pipe segments to be removed without cutting and reassembly.

A photo of workers preparing to glue a PVC pipe joint with a coupling is shown in Fig. 1.4. The transition between PVC (at the top) and galvanized iron pipe (at the bottom) is visible in Fig. 1.5. A 22.5° elbow joins the two.

1.3.3 Tanks

In all water-supply networks, there is nearly always a mismatch between water demand and supply flow rates. *Storage tanks*, such as shown in Fig. 1.6, accumulate water from the source over time for use as required by the time-dependent demand. The topic of sizing a storage tank is addressed in Chapter 13. Where it is available, large tanks (say, > 30 m^3) are almost always constructed on site of cement block or reinforced concrete. Plastic tanks are becoming more common and can be cost-competitive with concrete tanks, but for large volumes may be difficult to transport to the site. The reinforced concrete tank in Fig. 1.6 is typical of those built in central Nicaragua and in the Pacific rim. A close inspection of this photo will reveal an access ladder built into the side of the tank on its left and a water overflow pipe on the right. As with

[5]The exception to this is for microhydroelectric power systems (Chapter 12) where pipe sizes can be 12 in. and larger.

Figure 1.4 Workers preparing to glue a PVC pipe joint.

Figure 1.5 A 22.5° elbow joining PVC (top) and galvanized iron pipe (bottom).

Figure 1.6 A concrete storage tank. The capacity is ~14 m^3.

those installed in dams, the overflow pipe allows the water to drain away from the tank in a sanitary manner.

A *break-pressure tank*, such as that shown in Fig. 1.7, is not used for water storage but to reduce the static pressure in the flow to atmospheric pressure. Break pressure tanks are used in high-head gravity-driven water networks where the build-up of static pressure at lower elevations would require thick-wall plastic or GI pipe; both are expensive alternatives. The capacity of these tanks is not a major design consideration since there should be no accumulation within the tank; inflow and outflow rates should match.

The design of a beak-pressure tank is discussed briefly in Chapter 13.

If there are considerable suspended solids in the water, a *sedimentation tank* will be needed. This type is different than the previous two in that its role is to *filter* and to reduce the flow speed of water while passing through the tank. The filtration

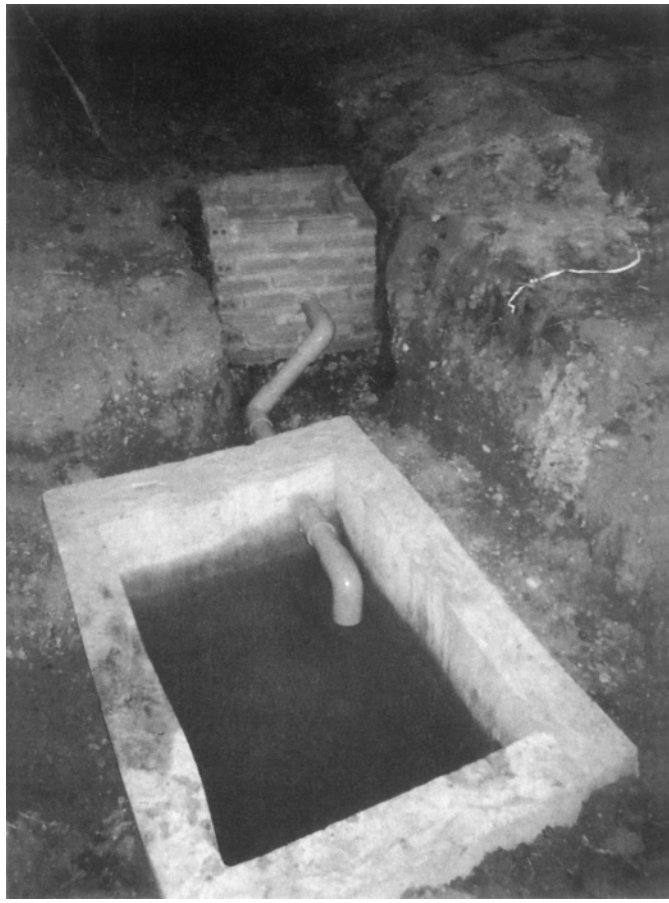

Figure 1.7 A break-pressure tank.

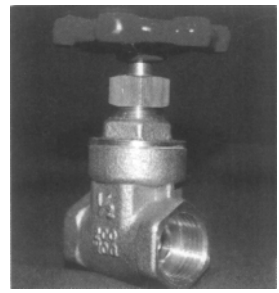

Figure 1.8 Outer view of bronze-body $\frac{1}{2}$-in. gate valve. Valve height is ~3 in. Valve photos courtesy of Nicki Jones.

directly removes some of the larger suspended solids, while the long residence time in the tank allows most of the remaining solids to settle under the effect of gravity. From this description, a sedimentation tank will look very different than a storage tank. Contrasted with the storage tanks in Fig. 1.6, a sedimentation tank has a filter bed, provides a long flow path for water between its inlet and outlet, and has a large cross-sectional flow area to slow down the flow.

1.3.4 Valves

Both gate and globe valves are heavily used in gravity-driven water networks. A gate valve belongs to a class that may be generally thought of as "block" valves. The purpose of these is to either allow the full flow to pass or be totally turned off. No throttling or pressure reducing should be performed with a gate valve because they are not designed for this purpose and will prematurely fail if operated in this way[6]. The gate in this valve is moved up or down by rotating the handle. When the gate is down, the flow is blocked, and when up fully open. The slot in which the gate travels creates a characteristic rectangular shape for the mid-section of the body of the gate valve as seen from the outside (see Fig. 1.8).[7]

Another type of block valve is a ball valve. A ball valve of PVC construction is shown in Fig. 1.9. In this valve, a spherical ball with a hole drilled through its middle is rotated to either allow the flow to pass (the hole aligned with the valve inlet and outlet) or be blocked (no part of the hole is aligned with the valve inlet and outlet). Because of difficulties with fine flow control, throttling is not recommended for a ball valve.

[6]The "gate" in a gate valve is just that, a metal plate the slides up or down in a slot to open or close the valve. There is considerable play in this slot, such that the gate can move back and forth with the passing flow. When partially closed, it will do so and prematurely wear. The first piece of knowledge I learned as a project engineer at an oil refinery in the early 1970s was never to use a gate valve to attempt to throttle the flow in a pipe.

[7]The photographs in this chapter are intended to simply familiarize the reader. Where possible, actual hardware, such as small gate and globe valves, and a union should be inspected to get a better sense for the components actually used in water networks.

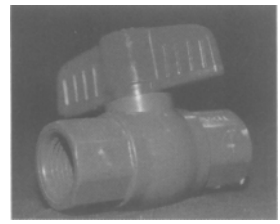

Figure 1.9 Outer view of $\frac{1}{2}$-in. plastic ball valve. Valve height is ~2.5 in.

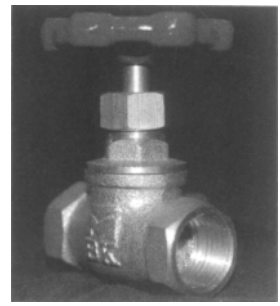

Figure 1.10 Outer view of bronze-body $\frac{1}{2}$-in. globe valve. Valve height is ~3 in.

Although a globe valve (Figs. 1.10 and 1.11 (Wikipedia, 2009)) can be used as an "on–off" valve, its primary function is to throttle or reduce the static pressure in the flow. The flow passageway between the metallic disk and valve seat, as seen in Fig. 1.11, is adjustable. When the passageway is adjusted to be small, a large pressure drop occurs in the flow between the valve inlet and outlet. Because of the importance of energy management in gravity-driven water networks (see Section 1.5.1), the globe valve is used in many locations, especially where appropriate for control and flow balancing, in addition to intentional energy dissipation.

1.3.5 The Tapstand

A tapstand (Fig. 1.12) is often the final delivery location for water. The tapstand consists of a suitably supported delivery pipe normally of PVC and ~$\frac{1}{2}$-in. nominal size, a water tap valve[8] or a ball valve, and a base of concrete that maintains cleanliness of the tapstand area and allows unused water to drain away from the site.

Tapstands, as well as other elements discussed in this introduction, are covered more completely in the design sections of this text (chapters 13 and 15).

[8]This valve is recommended to be bronze and will have a flow pattern that resembles that for a globe valve. The seat that is opposite the disk (see Fig. 1.11) is normally made of a rubber-type material for a water tap valve.

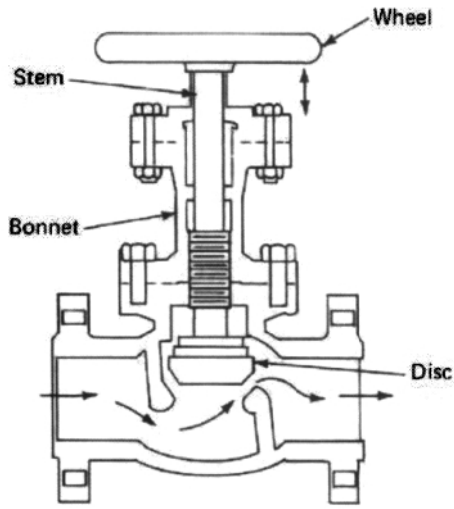

Figure 1.11 cross-sectional view of large globe valve.

1.3.6 Miscellaneous Elements

There is a need for air vents at local high points to vent trapped air in any water distribution network. This is discussed more fully in Chapter 14, where models for the potentially penalizing effect of trapped air in the network are also developed. A bucket-type air vent, shown in Fig. 1.13, automatically opens to vent air when there is an air–water interface in the body of the unit. This level indicates the presence of air in the network. Alternately, a gate valve on the branch of a tee fitting installed at the local high point can be used to manually vent trapped air. A long vertical pipe attached to the local high point may also be used to vent air automatically. In this case, the top end of the pipe is open to the atmosphere and its elevation must be approximately above the surface level of the reservoir or nearest tank upstream from it.

A vacuum breaker prevents the formation of negative gage pressure in a flowing pipe. Negative pressures in the flow are undesirable for several reasons that will be described in detail later in this book. A vacuum breaker can be a purchased unit that is installed in-line in the pipe. In this case, a spring in the body of the vacuum breaker allows air from the outside to enter the flow should the pressure fall below a preset value. In a more-simple form, a vacuum breaker can be a vertical piece of pipe with an open end at the top. This would automatically bring air into the network when the pressure of the flow falls below atmospheric.

Pipe anchors (Fig. 1.14) are used to support pipe where there may be large forces due to water flow, such as where the flow turns in a 90° elbow. Buried concrete and steel rods are normally used for this purpose.

Figure 1.12 A completed tapstand.

Figure 1.13 An air vent.

Figure 1.14 A pipe anchor.

1.4 ENGINEERING DESIGN

Engineering design is distinguished from graphical or conceptual design by its *quantitative* nature. The latter two types of design use drawings or sketches to convey information about the object intended to be produced. For example, an artist would produce a conceptual design for the shape and perhaps features of a new car. In engineering design, not only are the conceptual elements addressed, all of the equations for the appropriate physical laws of nature are included and solved to produce results that successfully demonstrate feasibility of the design. The equations referred to here are normally the conservation laws of mass, energy, momentum, and electrical charge, where appropriate, the particular laws that relate fundamental properties to measurable or observed quantities,[9] and perhaps others including economics, environmental impact, and safety. Clearly, engineering design is broader and more comprehensive and challenging than conceptual or graphical design alone.

1.4.1 Hydraulic and Nonhydraulic Design

Hydraulic design forms the largest piece of the overall design for gravity-driven water networks. Hydraulic design is engineering design that consists of mathematical models and calculations, drawings, and reports that characterize all of the hydraulic components of the network, including the reservoir, pipe, fittings and valves, tanks, and associated components that are discussed in detail in Section 1.3. Only the fluid-flow aspects of these components are included in the hydraulic design. Nonhydraulic design consists of the engineering design of all of the remaining components and elements of components.

For example, the hydraulic design of the pipe network will determine the pipe materials and diameters, wall thicknesses, lengths, and the internal pressure distribution under various operating and nonoperating conditions. The support of the pipe, say across a stream or river, the structural means to connect the pipe to a reservoir or tank, and the location of possible clean-out connections are part of the nonhydraulic design phase of the project. Another example is the storage tank. The volume of the tank will be calculated from the results of a water demand model for the community in need and the volume flow rate of water that can be supplied to the tank from the source or sources. In addition to locating the tank in the network, these are parts of the hydraulic design. The nonhydraulic design of the tank addressed its structural attributes, including the wall thickness and reinforcement if needed, and perhaps even methods to build the tank, as well as a cover for water cleanliness. The location and size of an overflow pipe and possible clean-out connections, even though related to water flow, may also likely fall under the nonhydraulic design umbrella.

[9]Examples of this are laws that relate heat to temperature, stress to strain in a solid, shear stress to velocity gradients in a fluid, and flow of electrical current to charge potential. As we will see in Chapter 2, there are also quantities, like Reynolds number (Re) , that are not laws, but simply definitions to support an analytical framework.

In this text, hydraulic design will include conservation of mass (referred to as the continuity equation) and mechanical energy (referred to as the energy equation). For multiple-pipe networks there is the need for an additional equation to produce unique solutions where pipe diameters are sought. In this case, engineering economy comes into play and we will consider minimizing network cost where appropriate. In equation form this is $dC_T = 0$, where C_T is the total cost of the network. Loosely, this simple expression may be though of as an equation of "cash conservation" in addition to mass and energy conservation.

Hydraulic analysis and design forms the bulk of this book. This includes Chapters 2–12, most of which are based on analysis. Chapter 3 considers pipe materials, dimensions, and pressure ratings. Chapter 4, which discusses the classes of pipe-flow problems, is included as a supplement. Readers who are already familiar with solving these problems may need to spend little time on this chapter. Design results for a single-pipe network, described below, appear in Chapter 5. The important role played by local pressure in the pipe is emphasized in Chapter 6, and energy losses from pipe fittings and valves in Chapter 7. The treatment of single-pipe networks culminates with Chapter 8 in which several examples of these are presented and solutions for them obtained. Simplified design formulas are useful to obtain quick, approximate design results for single-pipe networks and as a supporting role in the understanding of multiple-pipe networks. These are explored in Chapter 9. Optimization, where the network cost is minimized, will be highlighted (Chapter 10) because of its usefulness in allowing us to calculate unique pipe sizes for our designs. The basics covered in this chapter are applied in Chapter 11 to multiple-pipe networks, which forms the technical core and largest fraction of this book. This topic covers all of the types of multiple-pipe designs encountered in gravity-driven water networks including serial networks, multiple branches, loops, and large-scale, complex networks.

The complimentary topic of microhydroelectric power is briefly presented in Chapter 12. Design, including hydraulic and nonhydraulic design, is the focus in Chapters 13–15, which includes the design process and some hydraulic-design issues, as well as those concerned with air pockets in the network. The treatment of gravity-driven water networks is completed with Chapter 15 where a case study is thoroughly presented.

Exercises, with solutions, appear in Chapter 16.

1.5 GRAVITY-DRIVEN WATER NETWORK DISTINGUISHING CHARACTERISTICS

1.5.1 Energy Management

In water networks, where the flow is driven by a pump, the designer normally has some degree of control over how much and where the energy is put into the network. This is done by either adding a pump or increasing or decreasing the pump size or power to meet the design specifications. Analysts and designers of gravity-driven water networks are not afforded the same luxury. In these networks, for all points

beyond the atmospheric-pressure source of water, the energy that drives the flow comes from only static pressure in the water when converted from potential energy. This statement will become clearer after we have digested material related to the energy equation in Section 2.2. The concept that underlays this statement will be explored in more detail and in various contexts at several locations in this book. Thus, the overarching problem, and our challenge as analysts and designers, is to *effectively manage the conversion of pressure energy* because no energy from an outside source can be supplied. Energy management and cost of the network are also related. Pipe sizes that are too small cost less than large ones, but dissipate too much of the pressure energy in friction that gives the designer little flexibility at distances far from the source. More freedom in a design would come about if pipe sizes are larger than needed, but this increases the cost of the network and could present flow control problems including possible premature failure of throttling valves. Static pressure in the flow network is our friend because it allows us flexibility in our designs and potential for expansion of the network in the future should the need arise.

The dissipation, or removal, of pressure energy from the network is the same for both pumped and gravity-driven types. Dissipation must come from friction in the pipe either at discrete locations ("minor" losses; see Section 2.2.1) or distributed over the pipe length (referred to as a "major" loss; see Section 2.2.2). As will be discussed frequently, one of the more useful minor-loss devices is the throttling, or globe, valve.

Of course, it is clear that once the source and delivery locations are fixed for a gravity-driven water network, the contour of the ground in which the network is installed plays no role in the network overall performance. For example, changing the run of a pipeline to pass through regions of locally large slope has no effect on the overall potential available to drive the flow. A locally large slope simply means that in other parts of the network the slope must be locally small or even of the opposite sign. There may, however, be adverse effects on the performance of the network should the local elevations be too large or too small, as discussed in the next paragraph.

While recognizing that the energy from static pressure is our friend, we also need to be aware that we may have an enemy in the same pressure. Should the pressure rise above that which can be withstood by the pipe or fittings that join pipe, the pipe or joint will rupture with obvious dire consequences. At the other extreme, low-pressure conditions are also a concern. If the static pressure in a pipe falls below that outside the pipe, possible contamination of the clean water flow with dirty surroundings outside of the pipe will occur if there is any leakage path in the pipe wall. Vacuum conditions,[10] which can easily occur in an improperly design gravity-driven water network, are worse yet. Not only is the contamination potential present but, as discussed in Chapter 8, the collapse of pipe walls could occur under an extreme vacuum.

[10]Pressures below atmospheric.

1.5.2 Single- and Multiple-Pipe Networks

It is convenient to categorize gravity-driven water networks *or parts of them* as single- or multiple-pipe types. In networks or parts of networks that consist of branches or loops of multiple numbers of pipes, it is clear to the analyst/designer that the design methodologies associated with multiple-pipe networks (presented in Chapter 11) will apply. The distribution main appearing in Fig. 1.1 is an example of a segment of a gravity-driven network that is a multiple-pipe type because of the branches. The definition of a single-pipe network, which may be part of a larger network, is one where a pipe of a single diameter is used, the pressures at each end of the pipe are known or prescribed, and the flow rate of water remains unchanged between the pipe inlet and outlet (that is, there are no branches). See, for example, the gravity mains in Fig. 1.1.[11] The most elementary case for a single-pipe network is flow in a pipe of a single diameter that is run *directly* from an atmospheric-pressure source to a delivery location like a reservoir or break-pressure tank. The flow for this case remains at atmospheric pressure at each and every point[12] along the flow path. This simple result makes for a simple design procedure to determine, for example, the pipe diameter required to pass a prescribed water flow rate. We can take advantage of this simplicity once we recognize the single-pipe character of the network. The easy-to-use design charts in Chapter 5 and the elementary algebraic formulas for pipe diameter in Chapter 9 are evidence of this simplicity.

If we now imagine the pipe to have locally very high and/or very low points along the flow path, the problem takes on a different character. Along with the local high and low points comes the *need* for us to investigate the flow at, and near, these extreme points to determine static pressures. This is done for two reasons. First, we want to be certain that the pressures are not too large or small such that the undesirable consequences noted in the above section will occur. Second, the designer will want to consider possible pipe diameter changes at the extreme points and to investigate the effects of these changes on the network performance and cost. If the diameters change in an otherwise single-pipe network the pipe is called a "serial" network, which is a multiple-pipe type.

Thus, we see that a single-pipe network must satisfy not only the condition of being just one pipe of a single diameter with no branches and known pressures at each end, but it must also be absent of large local high or low points that would necessitate a local investigation of the flow and static pressures. If large local high or low points are present in a single pipe, the network is then treated as if it were a multiple-pipe type and the analysis and design methodologies of Section 11.5.1 would apply.

Once we consider the energy equation for pipe flow in Chapter 2, the meaning of "locally very high and/or very low points" in the above paragraphs will be quantified to some extent.

[11]The gravity main leading from the source to the reservoir (or storage) tank is sometimes referred to as the "intake pipe."

[12]This statement will be interpreted in light of the energy equation for pipe flow in the Chapter2.

1.6 THE FUNDAMENTAL PROBLEM

We begin this book by considering the basic problem of steady liquid flow in a single full pipe due to an elevation change between its inlet and outlet. The ideas for flow in a single pipe are extended to multiple pipes in Chapter 11; a more general and challenging problem. The intended application is the analysis and design of a clean-water distribution network that is fed by a reservoir (the "source," see the textbox B.1.1) and delivered, possibly through a storage and/or break-pressure tanks, to a "delivery" location for distribution to multiple houses in a community. Other applications come to mind, including water flow from an elevated reservoir to a turbine for producing mechanical or electrical power to end users. We touch briefly on this topic in Chapter 12.

Although the scale of the networks targeted by this text is that for small communities in developing countries, the fundamental principles and analysis and design methodologies are exactly those for much larger networks, including large urban areas and towns. As will be discussed in Chapter 11, the technology (that is, the computer programs) is the primary change when traversing from the small to large scale.

The fundamental problem of hydraulic design for a gravity-driven water distribution network of the type considered in this book is normally as stated in textbox B.1.2.

B.1.2 Fundamental Problem of Hydraulic Design for a Gravity-Driven Water Network

For a required volume flow rate of water to be delivered to an end use, and known dimensions of the site (positions and elevations of source, storage tank, and tap-stands, total length of pipe, contour of the land, etc.), calculate the pipe diameters and wall thicknesses for the network that satisfy these conditions, produce an acceptable static pressure distribution throughout the network, and if needed or desired, minimize network cost.

Included in the overall design will be sizing and locating storage and break-pressure (if required) tanks, the locations and types of valves and fittings, and the consideration of issues like the elimination of undesirable low-pressure conditions along the flow path that may lead to infiltration of contaminated water into the pipe flow.

The statement on the fundamental problem in textbox B.1.2 is an example of a "demand-driven" design for a fluid-flow network. This is one where the fluid flow rates are specified and the pipe diameters calculated such that they provide these flows. Alternatively, one could specify the pipe diameters in the network and calculate the flow rates at all relevant points with the intent of finding one or more combinations of pipe diameters that meet the desired delivered flow rates. This "supply-driven" approach requires tedious and time-consuming trial-and-error calculations where guesses are made for the pipe size for each segment of the network. Analyses for designs carried

out in this way are especially taxing for large multiple-pipe networks where there may be hundreds or more possible pipe-size combinations. For example, a relatively small multiple-pipe network consisting of 10 pipe segments where one might guess the possibility of any one of three pipe diameters for each segment requires considering more than 59,000 total possible diameter combinations.

1.7 A BRIEF BACKGROUND

Among the references for the design of gravity-driven water networks,[13] none present a strong foundation for fluid flow that can be connected with design-related material. For example, see Jordan Jr. (2004); Corcos (2004). A recently published and very thorough text on water-network design by (Trifunovic, 2006) contains < 4 pages on gravity-driven flow networks. The work of Swamee and Sharma (2000) addresses design based on cost minimization (discussed in Chapter 11) and presents a criterion for choosing between gravity-driven and pumped networks. One of the better references to date is the recent one by Swamee and Sharma (2008) that has broad coverage and is generally well written, but lacks a consistent and strong connection with pipe-flow fundamentals that are crucial for pedagogical soundness when teaching inexperienced students. Most of the qualitative and sparse quantitative data for gravity-driven water networks are published by various Non-Governmental Organizations (WaterAid, 2008), and the `NeatWork` code (Agua Para La Vida, 2002–2008), usually available on the internet, and government agencies (U.S. Peace Corps., 2008; National Park Service, 2008). There are also several sources from master's thesis work at various universities (Niskanen, 2003). Surprisingly, even the latest (7th) edition of the Piping Handbook (Nayyar, 2002) contains no obvious reference to gravity-driven fluid flow in pipes, nor does the Plastic Piping Handbook (Willoughby et al., 2002).

Because the aforementioned references focus heavily on design, the present work is not intended to be a comprehensive treatment of the *design* subject matter. It is, however, an attempt to bridge the gap between the classical fluid mechanics that may have been learned in an undergraduate engineering or perhaps physics curriculum, with which the reader may already be familiar, and the applied, technology-oriented coverage of this topic in a book, such as Jordan Jr. (2004), and a tool such as the `NeatWork` code from Agua Para La Vida (Agua Para La Vida, 2002–2008). Although the book of (Jordan Jr., 2004) contains a wealth of information on many of the important aspects of a gravity-water system, all of the technical topics like flow in single and parallel pipes, and air blocks are explained in ways that target a nonengineer, and in some cases a nontechnical, audience. This, apparently, is author intended. For engineers or engineering students, the solutions to many of these problems may greatly benefit from a sound, more-fundamental approach that their education and

[13]The scale of the water flow rates for the networks addressed here is of the order of liters per second. Gravity-driven water networks for major population centers that require tens of liters per second and larger, for example, can be designed with the methods presented in this book, but will require larger-size pipe and associated hardware than is discussed here. As noted in Chapter 11, the scale of the computational tool used to carry out the analysis and design will need to be larger as well.

training can provide. Indeed, after completing this book, the reader may consider it an engineering analysis and design companion to the handbook of Jordan Jr. (2004).

Another purpose for this book is to provide original design graphs, formulas, and computational algorithms for the fundamental problem of determining pipe sizes for a single- and multiple-pipe gravity-driven water systems that produce acceptable static pressure distributions, and to provide information concerning other critical technical and design topics pertinent to a gravity-driven water distribution network. Among these is included optimization of the network to achieve minimum cost.

1.8 APPROACH

In this text, we will focus on two levels of analysis and design. The first level will key on the performance of a water flow network based on *overall characteristics*, (that is, the mean slope, and inlet and outlet states). The second level addresses the *distribution of properties*, say static pressure, in the flow. The former is valuable in predicting the pipe size needed for a required volume flow rate and a given set of design conditions, and the latter is critical to assure the integrity of a design at each and every point along the flow path in a network having local peaks and valleys. The concept of "Natural flow" in a pipe (explored in Chapter 2) and a new concept of the "Natural diameter" for a pipe (in Chapter 6) are outgrowths of these two levels of analysis and design.

Following the review of the fundamentals of fluid flow in a pipe (in Chapter 2), including the all-important mass conservation and energy equations, we will first focus on several cases of interest and, in Chapters 5 and 9, provide a series of design formulas and graphs to calculate the diameter, D, for a single-pipe network to satisfy a prescribed water flow rate, Q. A design worksheet in `Mathcad`, a copy of which appears in the text and supplied herewith, extends this analysis by including the effects of minor losses and eventually flow in the more-complex multiple-pipe networks that are most common for this application. Note that all of the theory and results presented in this book can be applied to the flow of any common fluid having constant density and viscosity, but all design graphs and numerical calculations will be for water, which is obviously the principal focus in this work. Of course, although the term "fluid" is being used here, only dense fluids (that is, liquids) can flow in a gravity-driven network.

1.9 KEY FEATURES OF THIS BOOK

The following lists several of the principal features of this text. As a group, these will provide an effective, distinctive, and innovative framework for the analysis and design of gravity-driven water networks.

1. The fundamental theory of flow in pipes, including mass and mechanical energy conservation, the Darcy–Weisbach equation, Darcy friction factor, laminar and turbulent flow, and major and minor losses is thoroughly covered in its own chapter.

2. Every topic begins with, or references, fundamentals of pipe flow and other relevant theory. This enables readers with technical backgrounds to quickly relate to new ideas, methodologies, and solutions. Also, because all developments have a solid, well-defined background, the assumptions on which the topics are based will be clear as will the range of problems appropriate to the topics.

3. Single- and multiple-pipe networks are precisely defined. These classifications provide the analyst and designer with the ability to use simple analysis and design methodologies where appropriate. The generally weak role played by minor losses is discussed and quantified, the outcome that allows the neglect of minor loss as a first approximation to a design. Thus, simple design charts and formulas are presented for the case of minor-lossless flow in single-pipe networks, not computer programs with their inherent complexity.

4. Where computer programs are necessary for solutions to multiple-pipe and some single-pipe network problems, the Mathcad worksheets supplied with the text (see the list of these in Appendix A) are described in full detail including input and output information, solution methodologies, and if needed hints on how to run the programs effectively. Many textboxed examples in this book that address the worksheets take the reader through a step-by-step process of the changes to an existing worksheet, perhaps already understood by the reader, to solve a related, but different, problem. The intent is to supply worksheets that perform all of the fundamental calculations covered in this book. Clearly, not all problems, nor variations of them, can or should be included. In addition, there may be user-preference mismatches, like the preferred use of metric pipe data in the worksheets on multiple-pipe networks (which are supplied with pipe data in in.). One of the reasons for choosing Mathcad is that adjustments of preferences and modifications to solve different problems are easily made in Mathcad's transparent graphical interface.[14] To assist in this, a brief Mathcad tutorial is included in Appendix C.

5. The inclusion and relevance of cost minimization to produce a unique solution to the problem of determining pipe sizes in multiple-pipe networks subject to designer-prescribed volume flow rates is explained in detail. The underlying theory behind this is developed and equations derived and then applied to several example problems and exercises. The Given . . . Minimize construct is liberally used for cost minimization, which is fully explained and demonstrated in the Mathcad worksheets supplied with this text and in the Mathcad tutorial in Appendix C.

[14]The graphical interface referred to makes Mathcad simpler to use compared with line-by-line-type programming languages such as C++ and Fortran, as well as Matlab. For example, an equation written in Mathcad appears as it would on paper. There is no need for the user to "translate" the equation and, in fact, the logical flow of the entire solution, all of which would be necessary if using line-by-line-type programming languages.

6. Where appropriate in many places throughout the text where nontraditional approaches are used to analyze problems, new methods are compared with the traditional ones to emphasize the benefits of the new methodologies and place them in proper perspective.

7. More than 100 exercise and example problems and their solutions appear in the final chapter or elsewhere throughout this book.

References

Agua Para La Vida. Neatwork: A user guide — a decision support program for the design of gravity water distribution networks. Technical report, Agua Para La Vida, Berkeley, CA, 2002–2008.

H. Chanson. Some aspects of the hydraulic design of Roman aqueducts. *La Houille Blanche*, 2002(6/7):43–57, 2002.

G. Corcos. Air in water pipes, a manual for designers of spring-supplied gravity-driven drinking water rural delivery systems. Technical report, Agua Para La Vida, Berkeley, CA, 2004.

T. D. Jordan Jr. *Handbook of Gravity-Flow Water Systems*. ITDG Publication, London, UK, 2004.

G. T. Koeppel. *Water for Gotham: A History*. Princeton University Press, Princeton, NJ, 2000.

L. W. Mays. *Water Distribution Systems Handbook*. McGraw-Hill, New York, NY, 2000.

J. R. Mihelcic, L. M. Fry, E. A. Myre, L. D. Phillips, and B. D. Barkdoll. *Field Guide to Environmental Engineering for Development Workers*. ASCE Press, Reston, VA, 2009.

U.S Department of the Interior National Park Service. Guiding Principles of Sustainable Design. `http://www.nps.gov/dsc/dsgncnstr/gpsd/ch8.html`, 2008.

M. L. Nayyar. *Piping Handbook*. McGraw-Hill, New York, NY, 7th edition, 2002.

A. Niskanen. The design, construction, and maintenance of a gravity-fed water system in the dominican republic. Master's thesis, Michigan Technological University, Houghton, MI, 2003.

J. Salzman. Thirst: A short history of drinking water. *Yale J. Law and the Humanities*, 17(3), 2006.

P. K. Swamee and A. K. Sharma. Gravity flow water distribution network design. *J. Water Supply: Res. and Technol.-AQUA*, 49(4):169–179, 2000.

P. K. Swamee and A. K. Sharma. *Design of Water Supply Pipe Networks*. John Wiley & Sons, Inc., Hoboken, NJ, 2008.

N. Trifunovic. *Introduction to Urban Water Distribution*. Taylor & Francis, New York, NY, 2006.

U.S. Peace Corps., 2008. `http://www.peacecorps.gov`.

WaterAid. Technology Notes. `http://www.wateraid.org`, 2008.

Wikipedia. Globe valve — wikipedia, the free encyclopedia, 2009. URL `\url{http://en.wikipedia.org/w/index.php?title=Globe\_valve\&oldid=300120956}`. [Online; accessed 25-August-2009].

D. A. Willoughby, R. D. Woodson, and R. Sutherland. *Plastic Piping Handbook*. McGraw-Hill, New York, NY, 2002.

K. R. Wright, J. M. Kelly, and A. V. Zegarra. Machu Picchu: Ancient Hydraulic Engineering. *J. Hydraulic Eng.*, 123(10):838–843, 1997.

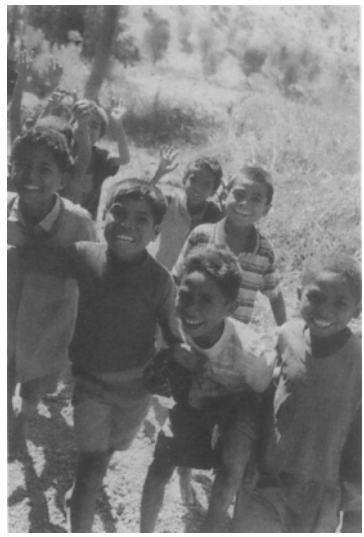

Children in a village in East Timor react
to a new water system in their community.

CHAPTER 2

THE FUNDAMENTAL PRINCIPLES

"If you don't know where you're going, you will probably end up somewhere else."
– The Peter Principle, 1969

2.1 THE PROBLEM UNDER CONSIDERATION

Generally, there are four properties of interest to engineers and designers when solving a problem of fluid flow in a pipe. The first is the elevation since, for the present context, this property provides the driving force for the flow. The second is the velocity. As we will see below, velocity is proportional to the fluid flow rate, the value of which is often one of the specified conditions in a design. The third property is static pressure,[1] defined in more detail below. We all have a sense of pressure from our experiences, say, from a deep dive into a swimming pool where we sense water pressure on our ears. Lastly, because of the fluid property of viscosity, a moving fluid experiences

[1] Static pressure is often simply referred to as pressure in some texts on fluid flow in pipes. For clarity purposes, the choice is made in this text to distinguish between static pressure in a moving fluid and hydrostatic pressure in a standing column of fluid.

Gravity-Driven Water Flow in Networks. By Gerard F. Jones

shear where it meets the walls of pipe, valves, and fittings that gives rise to frictional energy losses.

It is very interesting that the modifier "gravity-driven" that appears in this book title produces quite a different problem than engineers normally encounter when solving pipe-flow problems where the difference in pressure between the pipe inlet and outlet is often specified as the driving force. Instead, when the weight of the water (referred to as its body force) drives the flow, the pressure takes on a different role in the problem. Where both ends of a single pipe are open to the atmosphere, pressure does not appear at all in the design formulas. In other cases, the pressure at the delivery point of the water may be prescribed by the designer so that this value appears as a constant in the design. In still other cases, for example, in multiple-pipe networks, the pressure can be prescribed or it may be a *dependent variable* whose value must be within a range of acceptability as defined by the designer. All of these instances will be explored fully in the chapters that follow.

In this chapter, first we consider the problem of developed fluid flow in a single round pipe due to an elevation change between the pipe inlet and outlet. The flow is assumed to be steady, the pipe flows full, and we ignore the presence of dissolved gases and any suspended foreign matter in the fluid, both in its physical properties and in the equations for flow. The reader will note that this problem differs from the transient flow of a fluid and that in a partially filled pipe. These types of flows, which may include that resulting from the flushing of a toilet or the short-term running of water from a wash basin or sink in a house, are characterized by constant (atmospheric) pressure and are very different than those treated in this text. Another category, called "open-channel" flow, also differs in that not only is the pressure constant at the atmospheric value, but the pipe itself does not bound the fluid on all sides. Open-channel flows are covered in nearly every undergraduate fluid mechanics textbook, many of which are referenced herein (White, 1999; Fox and McDonald, 1992; Gerhart et al., 1992; Munson et al., 1994; Potter and Wiggert, 2002).

2.2 THE ENERGY EQUATION FOR STEADY PIPE FLOW: FLUID DYNAMICS

The movement of fluids in pipes is well understood and is described in various levels of detail in many texts and handbooks. For our purposes, the analysis of the problem of pipe flow comes down to solving the equations for mass and energy conservation for the fluid between any two locations along the water-flow path. For a single-pipe network that was discussed in Chapter 1, the two locations referred to above are the beginning and end of the pipe that connect the source and delivery locations. For a multiple-pipe network, the upstream and/or downstream locations are normally at naturally occurring branch points, such as a tee fitting. In still other cases, where there is an interest in the local distribution of fluid properties in the pipe flow, the two locations are separated by a differential distance measured along the flow path. This approach, for example, is used in Chapter 6.

First, we define some of the variables needed for this work. Throughout this book, the pipe inside diameter is D, the cross-sectional average flow speed[2] in the pipe is $\overline{u}$, and the water has constant density ρ. The static pressure at any location in the pipe is p, and the elevation measured from an arbitrary location in the pipe is the vertical coordinate z.

Static pressure is the pressure that would be measured in a *flowing*, incompressible fluid where there is no direct effect from the flow speed. In a conceptual sense, the static pressure would be measured by a pressure gage that flows along with the fluid. In a practical sense, it would be measured by a small tap or hole installed in the pipe wall so that the opening of the tap is parallel to the motion of the fluid and thus sees no direct impact from the fluid velocity. A pressure gage would be connected by a small hose or pipe to this hole. By understanding the conceptual idea of how to measure static pressure, we can begin to appreciate the true meaning of the modifier "static," namely, *static pressure is really a dynamic quantity*. It is static only in the sense that the value of p has no direct effect from the local velocity of the moving fluid and the measurement of p does not affect the local velocity.

We begin with the energy equation for steady, *hydrodynamically developed* flow of an incompressible fluid, like water, in a long, round pipe. In a hydrodynamically developed flow that exists in all long pipelines, the shape of the velocity distribution[3] is the same at all locations along the flow path. Another consequence of hydrodynamically developed flow *for a horizontal pipe of constant diameter* is that the static pressure gradient is constant in the direction of fluid flow. Thus, *the static pressure decreases linearly along the flow path.* For an incompressible fluid, the flow is independent of the size of the static pressure; it depends only on the gradient of this. The above comments apply to laminar, as well as turbulent flow.[4] The energy equation for pipe flow is covered in a variety of formal courses including thermodynamics, fluid mechanics, and physics. The highlights of this coverage will be presented in this chapter.[5]

[2]Velocity is a vector. Flow speed is the component of the velocity vector in the direction of fluid flow. If there is no need to calculate reaction forces and thus no use for a vector, the term flow speed is more appropriate to use for $\overline{u}$.

[3]This is the distribution of the local flow speed of the fluid as a function of the local radial position through the pipe cross section.

[4]The character of laminar and turbulent flows is discussed in detail below with the presentation of the friction factor. As a preview, a laminar flow is orderly with no mixing of the fluid in the directions normal to the principal movement of the flow. In turbulent flow, cross-mixing dominates over nearly all of the flow cross section. Turbulent flow is most common in pipes of diameters typical of most gravity-driven water networks. Laminar flow can occur in small gravity-driven water networks where the water flow rates are small.

[5]A word of caution is appropriate here. As noted above, the literature on water distribution networks abounds. Some of these works, even those of reputable governing bodies (American Water Works Association, 2006), may use different definitions and sometimes inappropriate formulas for gravity-driven water networks of the scale considered in this book. For example, at least one book has been uncovered that defines static pressure in the hydrostatic sense, meaning no motion of the fluid. This is unfortunate because of confusion caused by an alternate definition of an important concept at such a fundamental level. The reader should be aware that such writings exist, and that the basics presented in this book are classical

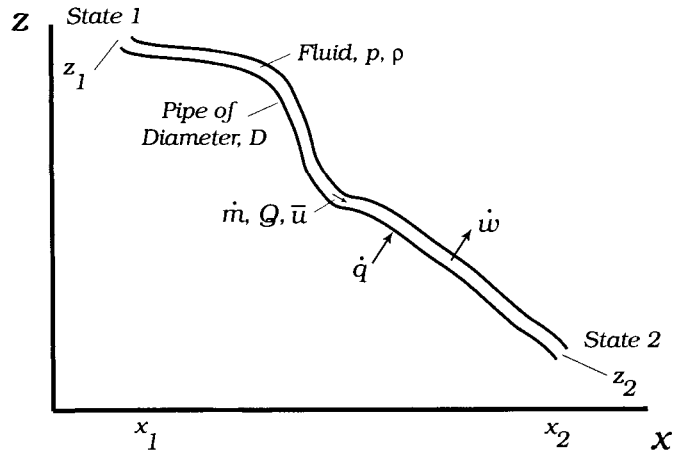

Figure 2.1 Geometry and nomenclature for flow in a single pipe. Gravity acts in the negative-z direction.

Referring to Fig. 2.1, the energy equation for an open system, that is, a system with mass flow through its boundaries, consisting of a pipe of variable diameter having a single inlet and outlet is[6] (see any text on thermodynamics or fluid mechanics)

$$\dot{m}[(\frac{p_1}{\rho} + e_1 + \alpha_1 \frac{\overline{u}_1^2}{2} + gz_1) - (\frac{p_2}{\rho} + e_2 + \alpha_2 \frac{\overline{u}_2^2}{2} + gz_2)] = \dot{w} - \dot{q} \qquad (2.1)$$

where $\dot{m}$ is the mass flow rate, e is the internal energy per unit mass, g is the acceleration of gravity, and $\dot{q}$ and $\dot{w}$ are the rates of heat transfer to and work done by the system, respectively. States 1 and 2 are at any two arbitrary locations along the pipe-flow path where the normal convention is that state 1 is upstream and state 2 is downstream. The terms in each parentheses on the left side of Eqn (2.1) account for pressure energy,[7] kinetic energy, and potential energy, all per unit mass of fluid. The term α is the ratio of the kinetic energy in the flow to the kinetic energy based on the mean flow speed, $\overline{u}$. It accounts for the non-uniform velocity distribution through the cross section of the flow and is connected with the acceleration of the flow between two different flow speeds in the pipe. For example, if the velocity distribution were uniform through the cross section of the pipe, α would equal 1. For fully developed turbulent flow, normal for most gravity-driven water flows, $\alpha \approx 1.05$, which reflects a nearly uniform velocity distribution. A sketch depicting the velocity distributions

in that the concepts, definitions, and terms are consistent within the narrow framework of gravity-driven water flows *and* over the broader framework of the body of fluid mechanics.

[6]Equation (2.1) is alternately referred to as the first law of thermodynamics.

[7]In the fundamentals treatment of fluid mechanics, $(p_1 - p_2)/\rho$ is often referred to as "flow work" that is the work required to move the fluid between states 1 and 2. However, p/ρ is the pressure energy per unit mass of fluid associated with a given state.

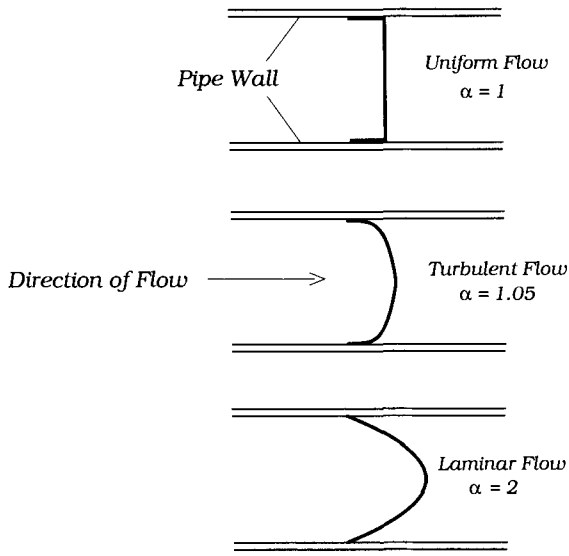

Figure 2.2 Velocity distributions for flow in a round pipe and accompanying values of α. The velocity where the fluid meets the pipe wall is zero. The main focus is on laminar and turbulent flow. Uniform flow, which would occur if the flow were inviscid, is shown for comparison purposes only.

for laminar and turbulent flows and the accompanying values of α for each is shown in Fig. 2.2.

For readers already familiar with the above developments, Eqn (2.1) is sometimes referred to as the "steady-flow energy equation" (White, 1999).

The field of thermodynamics provides us with the definition of work. Work is a quantity that passes through the boundary of the system and has the effect of raising or lowering a weight. Clearly, since there is no turbine installed in the pipe, the rotation from which could be used to lift or lower a weight (this case will be considered in Chapter 12), there is no work for incompressible flow in a pipe. Upon rearranging Eqn (2.1), we obtain

$$\left(\frac{p_1}{\rho} + \alpha_1 \frac{\overline{u}_1^2}{2} + g z_1\right) - \left(\frac{p_2}{\rho} + \alpha_2 \frac{\overline{u}_2^2}{2} + g z_2\right) = -\frac{\dot{q}}{\dot{m}} + e_2 - e_1 \equiv H_L \qquad (2.2)$$

This is the energy equation for pipe flow (the flow must be steady, but we will not include this modifier in the interest of brevity) and this equation and its solutions will be the principal focus of the analysis content of this book. Readers who may not be familiar with the energy equation and the terms that comprise it will find the example in textbox B.2.1 useful.

Equation (2.2) is sometimes referred to as a "modified Bernoulli equation" because it resembles the Bernoulli equation.[8] Jordan Jr. (2004) refers to it as the "Bernoulli equation for a real system". In contrast to the Bernoulli equation,

$$(\frac{p_1}{\rho} + \frac{u_1^2}{2} + gz_1) - (\frac{p_2}{\rho} + \frac{u_2^2}{2} + gz_2) = 0 \tag{2.3}$$

which is only valid for steady, inviscid (that is, frictionless) flow of an incompressible fluid along a streamline (see the discussion in textbox B.2.3), included in the energy equation for pipe flow is a positive-valued term that accounts for energy loss due to friction, H_L, which is referred to as "head[9] loss." Head can be expressed as a height, a dimensional length given the symbol h, or as the product of height and the acceleration of gravity, g, given the symbol H. Then,

$$H \equiv gh \tag{2.4}$$

By comparing Eqs (2.2) and (2.4), we obtain an equivalence between static pressure and head as

$$\boxed{h \equiv \frac{p}{\rho g}} \tag{2.5}$$

where h is referred to as "static pressure head." This is a term we will use frequently, especially where we deal with multiple-pipe networks. If subscript L appears with h or H, as indicated above, it would be referred to as "head loss."

We see that the energy equation for pipe flow equates the change in total mechanical energy (the sum of pressure, kinetic, and potential energy) between the pipe inlet and outlet to the energy "loss" in the pipe due to friction. Any gravity-driven water network will flow provided the change in total mechanical energy between the pipe inlet and outlet is positive valued. Our inspection of Eqn (2.2) shows that this energy loss is really a transformation from mechanical energy to internal energy and heat transfer from the pipe wall. If heat transfer, $\dot{q}$ is nonzero and negative valued (heat transfer from the pipe to the surroundings). If internal energy, the temperature of the water increases slightly as it flows along its path. To see this, we focus on the internal energy equation of state for a liquid, which is

$$e_2 - e_1 = c_v(T_2 - T_1) \tag{2.6}$$

where c_v is the specific heat at constant volume. Thus, the change in internal energy from frictional effects from the flow inlet to outlet causes a temperature increase

[8]The Bernoulli equation has a very interesting history. Its origin as it appears in Eqn (2.3) is traced loosely to Daniel Bernoulli (in his book of 1738, *Hydrodynamica*) but apparently his father Johann (1667–1748) in his book *Hydraulica* first recognized the static pressure as a dynamic quantity. Leonhard Euler (1707–1783) was the first to characterize pressure as a pointwise quantity. He developed a differential form of an equation that relates the forces acting on a moving inviscid fluid and integrated it to obtain what we now call the Bernoulli equation. As discussed by Anderson (1990), because of these contributions, the Bernoulli equation could legitimately be called the Bernoulli–Euler equation.

[9]The word head comes from early developments in hydraulics in the 19th century and described an elevation of water above an arbitrary location. Though it is not certain, head probably referred to the elevation at eye level or the level of the human head.

between these two points. It turns out that for most cases this change is so slight it is ignorable (see Exercise 3). From this outcome, we conclude that all thermal contributions to the energy equation are negligible and, for design purposes, the fluid behaves as if it is isothermal. An exception to this will be made in Chapter 10, where we may consider temperature changes in the fluid when optimizing the design.

B.2.1 Example: The Energy Equation Applied to Human Movement

You and your partner are planning a hike through the hilly woods in a Pennsylvania state park. Though you are both not fluids, interpret as well as possible the three terms in the energy equation, pressure, kinetic, and potential energy, in light of your characteristics while on this trek. Assume that your speed is uniform once you begin the walk and that potential energy is relative to that at the lowest point on the hike.

The interpretation: The three terms of interest on the right side of Eqn (2.2) are, in order, the change between any two states for pressure, kinetic, and potential energy; all written per unit of mass. Once you are moving at uniform walking speed $\overline{u}$, the kinetic energy of the system (you and your partner) remains constant. If you would write Eqn (2.2) between any two states along your walking path, the kinetic energy change is zero and thus does not contribute to the mechanical energy of your system. However, if the starting state is you at rest, the kinetic energy at this state is zero and $\overline{u}^2/2$ at any other state. The kinetic energy would contribute in this case.

By contrast, the change in potential energy per unit mass, $g(z_1 - z_2)$, will not be zero because you are told that the route is hilly. For example, an upward climb will require an energy input to the system (supplied by the chemicals in your body) that power the muscles needed to make the climb. One could imagine this coming from a chemical form of the pressure energy, or a new energy "source" term that could be included in Eqn (2.2). The character of the pressure energy will be explored more fully below. A downward descent results in the reduction of potential energy of the system. This change in potential energy per mass, $g(z_1 - z_2)$, where $z_1 > z_2$, must be balanced by a dissipation of energy that occurs in the loss term, H_L [see Eqn (2.2)]. This is why the muscles in our legs ache or "burn" during a long downhill hike or run as they must work internally to dissipate the potential energy change. Of course, in both our bodies and in fluids there is always an energy loss due to friction (shear in fluids and muscular contractions in us) whenever there is motion in either.

Pressure is unique to a fluid, which you are not, so it is a challenge to apply the concept of pressure energy to the movement of your body. Nonetheless, we can get a good sense for static pressure and pressure energy if we use our imagination.

Example: The Energy Equation (Cont'd)

One property of the process that results in the change of pressure in a flow is that of *reversibility*. This means that pressure energy may increase or decrease in response to a change in another form of energy and the conversion between the two forms of energy is reversible. Another way of saying this is that the energy transformation process is 100% efficient or "loss-free." A good example of this is within a static fluid (see Section 2.3), where we see a balance between pressure energy and potential energy; a decrease in one causes an increase in the other. The pressure felt on your eardrums upon a deep dive into a swimming pool provides evidence of this.

How can this translate to our hike? Imagine that you have a spring attached to you in such a way that it can reversibly (that is, without friction) wind up using the potential energy as we descend a hill. Thus, potential energy on the descent is stored in the form of energy in the spring in what is really another form of potential energy. The sense that our bodies would get during this downward trek is equivalent to a walk on level ground. In the ascent that may follow, we allow the spring to reversibly unwind, adding energy to the system to aid in the climb. Again, because of the energy added to the system from the unwinding spring, this upward walk would feel as though it is on level ground.

The simple analog in the above paragraph implies that in a conceptual sense, *pressure energy is like stored spring energy in a fluid*; indeed, modeling the "spring of air" is a topic several hundred years old (Brockman, 2009; Boyle, 1660). Anyone who has cracked open a valve on a pressurized water pipe, or worse yet, mistakenly drilled through the side of a pressurized pipe, can bear witness to this fact. It is worthwhile remembering this concept for several reasons. One of these is that it will become clear after digesting Chapter 6 that pressure energy is the *sole energy source* for the motion of fluid from the lower to higher parts of a gravity-driven water network. While the spring (potential) energy analog is valuable from a conceptual standpoint, from fundamental ideas, pressure energy is really a form of internal energy or *flow work* that will be described in Section 2.3.

There are two classifications for the energy loss in the pipe. The first is the energy loss due to shear stress between the moving fluid and the stationary pipe wall (major loss). The second is the energy loss due to the same process in pipe fittings and valves installed in the flow path and is referred to as a "minor loss."[10] Various investigators have determined through laboratory experiments that the head loss, H_L, is proportional to the kinetic energy per unit mass of the flow. With this, the energy

[10]The terms major and minor are standard in fluid dynamics. Of course, the loss in a very short length of pipe may be of the same order of magnitude as that in a number of fittings. The terminology of major and minor is based on assumed large pipe lengths.

equation for flow in a pipe of diameter D and length L becomes

$$\boxed{(\frac{p_1}{\rho} + \alpha_1 \frac{\overline{u}_1^2}{2} + gz_1) - (\frac{p_2}{\rho} + \alpha_2 \frac{\overline{u}_2^2}{2} + gz_2) = H_L} \tag{2.7}$$

where H_L is from

$$\boxed{H_L = [f(\frac{L}{D} + \sum_{i=1}^{M} \frac{L_e}{D}\Big|_i) + \sum_{i=1}^{N} K_i]\frac{\overline{u}^2}{2}} \tag{2.8}$$

The term on the right side of Eqn (2.7) is the energy change due to friction, H_L. It is an extended form of the classical, empirical-based, Darcy–Weisbach equation (White, 1999),

$$\boxed{H_L = f\frac{L}{D}\frac{\overline{u}^2}{2}} \tag{2.9}$$

where terms for the minor loss (see Section 2.2.1) have been included. Combining Eqn (2.4) with Eqn (2.9) produces an alternate form for the Darcy–Weisbach equation. Obtain,

$$\boxed{\frac{h_L}{L} = f\frac{\overline{u}^2}{2gD}} \tag{2.10}$$

where h_L/L is the dimensionless group head loss per unit length of pipe that appears frequently in the pipe-flow literature. The Darcy–Weisbach equation has, through observation, been validated extensively for major and minor energy losses in pipe flow.

The first term on the right side of Eqn (2.7) is the major loss and the second and third terms account for the minor loss. The parameter f in the major loss will be discussed in detail in Section 2.2.2 and the minor losses in Section 2.2.1.

2.2.1 The Minor Loss

The minor loss can be characterized by a dimensionless loss coefficient K which, when summed over all minor-loss elements (N), accounts for the total minor loss along the pipe-flow path [see Eqn (2.7)]. For example, the minor loss coefficient for flow entering a pipe protruding through and beyond the wall of a reservoir (this condition is termed a "re-entrant") ranges from 0.8 to 1.0 depending on wall thickness, pipe diameter, and length of the protrusion (Streeter et al., 1998).

There is an alternate, less-common, way of expressing minor losses. In Eqn (2.7), L_e is called the "equivalent length" and the procedure for accounting for the minor losses is called the "equivalent-length" method. In the equivalent-length method, we calculate the energy loss for a pipe fitting or similar minor-loss element as if it occurs in a number of pipe-diameters of straight-pipe length that is referred to as the equivalent length. This method is commonly used for certain types of fittings. For example, the minor loss for an elbow is sometimes accounted for using the equivalent-length

method. For a standard 90° elbow, the reported equivalent length[11] is $L_e/D = 30$ (Fox and McDonald, 1992). In Eqn (2.7), the total minor loss for those elements using the equivalent length method is from the sum of M total elements. Please note that only the loss-coefficient approach *or* the equivalent length method is used, never use both methods for the same minor loss elements or else the effect of the minor losses will be erroneously doubled. Also, note that the energy equation for pipe flow developed here [Eqn (2.7)] applies to a length of pipe of a fixed diameter. Therefore, the summations in the minor loss terms in these equations must likewise be taken over a pipe of a single diameter.

B.2.2 Why The Bernoulli Equation Does Not Apply to Pipe Flows

The Bernoulli equation is simple and thus very appealing to use, including pipe flow and other cases where it should not be, so we need to give serious consideration to the problem at hand before possibly applying it. The assumptions on which it is based are sometimes not well understood or ignored by its potential users. Fundamentally, Eqn (2.3) applies only if the flow is steady, incompressible, inviscid, and states 1 and 2 lie on a single streamline. In steady flow, a streamline is the locus of points traversed by a small "particle" of fluid as it travels in the flow. Steady says that the flow cannot depend on time (that is, the flow cannot be accelerating or decelerating with time.) Incompressible means that the density can be approximated as constant in value. Flows of liquids are normally incompressible, as well as gases, if the flow speed is sufficiently small. Inviscid implies that there is no effect of shear acting on the flow along the streamline on which Eqn (2.3) is written. For nearly all real flows, the viscosity of the fluid will never be zero, so inviscid does not mean the absence of viscosity. Rather, inviscid is a statement of the lack of a velocity gradient in the direction normal to the fluid flow (perhaps, recall Newton's law of viscosity from fluid mechanics). Even with the restrictions, there are many examples of where the Bernoulli equation accurately applies. Namely, in the free-stream of external flows over wings and other streamlined surfaces, and in laminar, internal flow in a pipe or other internal flow along only the centerline. It can be approximately applied in some turbulent flows, although with less certainty of the results since many of these are highly viscous, and there is little hope of following a streamline.

To be fair, many authors of undergraduate texts on fluid mechanics are at least partly to blame for some misunderstanding concerning the Bernoulli equation. For example, illustrative problems like internal flow in a tube that are clearly viscous but, without explanation, the students are instructed to treat as inviscid are a possible source of confusion.

[11]The equivalent length under discussion here is a number for a particular fitting. This number is the value of the ratio L_e/D.

Minor loss coefficients and/or equivalent lengths for the most common fittings and valves are presented in Table 2.1. Included are the elbow, tee, union, coupling; gate, globe and ball valve; expander and contractor; and loss coefficients for entry and exit losses. More comprehensive lists and charts and, for readers unfamiliar with them, descriptions of these fittings and valves can be found in nearly all undergraduate fluid mechanics textbooks. Munson et al. (1994), for example, has numerous sketches of valves and fittings among their minor-loss charts. The globe valve, which is commonly used to dissipate the potential energy in a gravity-driven water network, is discussed in many locations in the this text. A few comments on the data in Table 2.1 are in order. Much of these data are extracted from industry publications, such as The Crane Company (1970) and data from the Hydraulic Institute (Hydraulic Institute, 1990). As pointed out by White (1999) these data are relatively old and many are questionable. After comparing a few published results with data obtained from tests of more-recently manufactured fittings, one concludes that most data from the above sources are likely very conservative. For example, the value of K for a standard 90° elbow in Table 2.1 calculated from the recent correlation appearing in White (1999) is ~0.31 for Re of 5×10^5. This is clearly much less than the other two reported values of 0.9 and 1.5. Also, note the variability of the reported values for the same fitting or valve in Table 2.1. This is not surprising since the loss coefficients will reflect variations in *specific manufacturing methods and dimensional details* of the fitting or valve. This is expected because standards at this level of manufacturing detail generally do not exist. Fortunately, the sensitivity of our designs to these variabilities is expected to be weak because the minor loss is not large for most gravity-driven water networks, except where needed for flow control. The latter concerns the intentional dissipation of energy in a partially closed globe or faucet valve, an important function that is to produce a minor loss.

An exception to the conservative estimates for K values in Table 2.1 is that for a fully-open globe valve. Gray (1999) suggests that the effect of diameter dependence on K may be written as

$$K = 85 \log_{10}^{-2}\left(\frac{0.0135 \text{ mm}}{D}\right) \qquad \text{globe or faucet valve} \tag{2.11}$$

which, for the pipe sizes of interest in this work, gives K in the range of 6–10, or about twice that from Table 2.1. It would appear that a conservative estimate of K for a fully-open globe or faucet valve ranges from 8–10. Swamee and Sharma (2008) report a value of 10. Of course, K values increase unbounded with continued closing of the valve. As demonstrated in Exercise 7, K values can approach 500,000 before nearly fully restricting the flow in this valve.

Table 2.1 Coefficients and Equivalent Lengths for Calculation of Minor Loss

Fitting Type	Equivalent Length (L_e/D)	K
Standard 90° Elbow[a]	30[b]	$1.49\,\mathrm{Re}^{-0.145} \pm 10\%$[c], 0.9[d], 1.5[e]
Standard 45° Elbow[a]	16[b]	≈ 0.3[f,c], 0.4[e]
Standard Tee - Flow Through Run[a]	20[b]	0.9[c], 0.9[e]
Standard Tee - Flow Through Branch[a]	60[b]	≈ 1.7[f,c], 2.0[e]
Union		Negligible[e]
Coupling		Negligible
Gate Valve (Fully Open)		Negligible[e]
Globe or Faucet Valve (Fully Open)	340[b]	4[c], 10[d,e]
Globe or Faucet Valve (75% Open)		4[c]
Globe or Faucet Valve (50% Open)		6[c]
Globe or Faucet Valve (25% Open)[g]		20[c]
Ball Valve (Fully Open)	3[b]	0.05[e]
Ball Valve (2/3 Open)		5.5[e]
Ball Valve (1/3 Open)		210[e]
Sudden Expansion into Large Area ("Exit" Loss)		1 (based on theory)
Sudden Contraction ("Entrance" Loss)		0.78:re-entrant[b], $0.8 \sim 1.0$:re-entrant[d]
		0.5:square-edge[b]
Gradual In-line Reducer		$0.05 \sim 0.43$[b], estimate as 0.4
Gradual In-line Expander		$0.4 \sim 1.2$[c], estimate as 1.0

[a] "Standard" means that this type of fitting is most commonly used. For example, long radius and short radius elbows used for special purposes in industry are not standard. Re is Reynolds number.
[b] Fox and McDonald (1992)
[c] White (1999)
[d] Streeter et al. (1998)
[e] Munson et al. (1994)
[f] The approximation symbol ($\approx$) refers to an average over several pipe sizes.
[g] Globe or faucet valves less than 25% open will have minor loss K values in the range of 100 or more (theoretical K value for such valves approaching the fully closed position tends toward infinity).

2.2.2 The Friction Factor

The term f in Eqs (2.8)–(2.10) is the Darcy friction factor[12] that accounts for energy loss due to friction for flow in a straight, horizontal pipe. We write it as $f(\overline{u}, D)$ to keep in mind that the friction factor depends on the mean flow speed in the pipe and the pipe diameter through the Reynolds number, Re, defined below. For laminar flow, an exact formula for $f(\overline{u}, D)$ may be developed from the solution of the momentum equations (referred to as the Navier–Stokes equations) and the equation for mass conservation for fluid flow and is explored in textbox B.2.3. Recourse to data from experiments is needed to write $f(\overline{u}, D)$ for turbulent flow, wherein the friction factor is also known to depend on the relative roughness of the pipe wall, ϵ/D, discussed further below. In design, ϵ is always a prescribed value (that is, a parameter) from laboratory measurements and we normally do not include this parameter in the argument list along with $\overline{u}$ and D. For smooth pipe, typical values for $f(\overline{u}, D)$ range from ~0.05 to ~0.01 for turbulent flow from the near-transition regime to highly turbulent, respectively. That is, an order-of-magnitude estimate is $f \approx 0.03 \pm 0.02 = 0.03(1 \pm 0.67)$ for turbulent flow.

The value of $f(\overline{u}, D)$ is determined from different formulas for laminar and turbulent flow. These are (White, 1999)

$$f(\overline{u}, D) = \begin{cases} 64/\mathrm{Re}, & \text{laminar, Re} < 2300 \\ \{-2\log_{10}[\frac{2.51}{\mathrm{Re}\sqrt{f(\overline{u},D)}} + \frac{\epsilon/D}{3.7}]\}^{-2} & \text{turbulent} \end{cases} \tag{2.12}$$

where Re is the Reynolds number

$$\mathrm{Re} = \frac{\overline{u}D}{\nu} \tag{2.13}$$

that clearly depends on $\overline{u}$ and D, but is never written as $\mathrm{Re}(\overline{u}, D)$, and ν is the kinematic viscosity of water at its ambient temperature. The value for ν can be found in most textbooks on fluid mechanics or heat transfer. The kinematic viscosity for water at, or near, atmospheric pressure as a function of temperature can also be estimated to accuracies within $< 1\%$ over the temperature range $1 \sim 99°\mathrm{C}$ from the

[12]The Darcy friction factor can be obtained from Moody's publication (Moody, 1944) of the now-famous friction factor chart. This chart appears in many sources including textbooks on fluid mechanics and in Fig. 2.4. An interesting and very readable history of the friction factor for pipe flow and the Darcy–Weisbach equation is available (Brown et al., 2000). To produce his diagram for friction factor, Moody, in a relatively simple manner, restructured the existing friction-factor diagram of Rouse (1943) "in a more conventional form". According to Ettema (2006), in addition to f and Re, plotted on secondary axes, Rouse included on the primary axes two different quantities. One of these was $f^{-1/2}$, and the other $\mathrm{Re}f^{1/2}$. This was done to identify the turbulent-smooth curve $f^{-1/2} = -0.8 + 2\log(\mathrm{Re}f^{1/2})$ from the then-recent work of Colebrook and White (1937) and Colebrook (1938, 1939). Since very few, if any, of us use the "Rouse" diagram today, this is one among several instances in engineering of an individual whose archival contributions came from very basic observations and actions. From Rouse and Ince (1963) and the inclusion of an exclamation point in Rouse (1975), Rouse thought Moody received undue credit for the work of himself and his colleagues. Further brief discussion on the history of f for turbulent flow is presented in Chapter 9.

formula (Streeter et al., 1998),

$$\nu = \frac{15.72 \times 10^{-6} \mathrm{m}^2/\mathrm{s}}{(T/T_{ref} + 4.25)^{1.5}} \tag{2.14}$$

where T/T_{ref} is dimensionless and $T_{ref} = 283.16$ K (K$=$ 273.16 + °C). A plot of the kinematic viscosity of water and Eqn (2.14) is presented in Fig. 2.3. For reference and convenience, the kinematic viscosity of water at 10°C is $\nu = 1.307 \times 10^{-6}$ m^2/s.

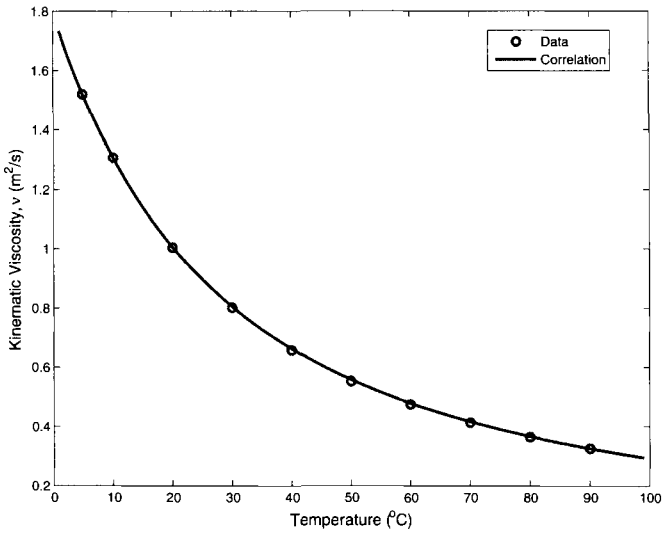

Figure 2.3 Kinematic viscosity of water. Data are from Streeter et al. (1998) and correlation is from Eqn (2.14).

From fundamental fluid mechanics, we know that Re "characterizes"[13] the flow regime. In particular, flow is very likely to be laminar for Re < 2300 (and *will* be laminar for Re slightly less than 2300) and turbulent flow occurs for Re $\gtrsim$3000–4000. In a laminar flow, there is no mixing of the fluid in the directions normal to the principal movement of the flow. This is contrasted with turbulent flow where mixing in all directions dominates over most of the flow cross section[14]. The transition regime,

[13]Another word for characterize is "describe" or "distinguish," like the term "mile-high city" is used in United States-based jargon to describe the elevation of Denver, Colorado. While true that Denver is approximately 1 mile above sea level, there are probably relatively few locations that are exactly 5280 feet above sea level within the limits of the city.

[14]We do not yet have a complete understanding of turbulence due, in part, to the complexity of turbulent flows and the multiplicity of length and time scales that it possesses. Sir Horace Lamb, the notable British hydrodynamicist and applied mathematician is reported to have said "I am an old man now, and when I die and go to Heaven there are two matters on which I hope for enlightenment. One is quantum electrodynamics and the other is the turbulent motion of fluids. And about the former I am rather more optimistic" (Anderson et al., 1984).

which lies between the laminar and turbulent limits, is a region of some uncertainty for the friction factor, even though the recommended Eqs (2.16) and (2.17) for $f(\overline{u}, D)$, presented below, model this regime. In general, it is best to stay clear of the transition regime when designing a water network. In the results presented below, we will see that for small values of z_1 and volume flow rate Q, the flow in the pipe may indeed be laminar or transitional though turbulent flow is most common.

The formula for $f(\overline{u}, D)$ from Eqn (2.12) for laminar flow is from the solution of the Navier–Stokes equations for incompressible, constant–viscosity flow (see textbox B.2.3). The formula for $f(\overline{u}, D)$ from Eqn (2.12) for turbulent flow is referred to as the Colebrook equation (Colebrook and White, 1937; Colebrook, 1938, 1939) and is the industry-accepted design formula for the friction factor for turbulent flow in pipes. Note that it is implicit in $f(\overline{u}, D)$ and requires iteration or a numerical root-finder to solve. An explicit approximation that produces results to within $\pm 3\%$ of the Colebrook equation is

$$f(\overline{u}, D) = \begin{cases} 64/\mathrm{Re} & \text{laminar, Re} < 2300 \\ \{-1.8 \log_{10}[\frac{6.9}{\mathrm{Re}} + (\frac{\epsilon/D}{3.7})^{1.11}]\}^{-2} & \text{turbulent} \end{cases} \tag{2.15}$$

which is from Haaland (White, 1999), and is easier to implement. A similar expression is from Swamee and Jain (1976) although many explicit and implicit forms for $f(\overline{u}, D)$ have been proposed (see Romeo et al. (2002) for a brief review up to 2001).

As noted, the term ϵ in Eqs (2.12) and (2.15) is the absolute roughness of the pipe inside wall that is relevant for only turbulent flow. The roughness is an average height, in a root-mean-square sense, of the roughness elements on the wall surface. For plastic pipe (Polyvinyl Chloride, etc., see Chapter 3), $\epsilon \approx 5 \times 10^{-6}$ ft $\pm 60\%$ (White, 1999) or $\approx 1.5 \times 10^{-3}$ mm $\pm 60\%$; generally considered to be smooth[15]. For galvanized steel or iron pipe, ϵ is ~100 times larger than this value. It is well known that ϵ itself does not affect $f(\overline{u}, D)$, but rather the ratio ϵ/D, which is referred to as the relative roughness of the pipe. This is not surprising since, as demonstrated by dimensional analysis, often a part of a course in fluid mechanics, only dimensionless groups ultimately appear in homogeneous mathematical formulas. Both ϵ and D have dimensions of length.

In this book, use is made of $f(\overline{u}, D)$ from a correlation of friction factor data [for a representative set of friction factor data, see Schlichting (1979)], which spans the laminar, transition, and turbulent regimes from Churchill (1977)[16] and Churchill et al. (2002). Thus, no conditional statement (e.g., an `if` statement) in a computer algorithm, is needed to evaluate $f(\overline{u}, D)$ as would be needed for Eqs (2.12) and (2.15).

[15]The term smooth means that the scale of pipe-wall roughness is much less than the thickness of the viscous sublayer in a turbulent flow. The sublayer is a thin layer of moving fluid immediately next to the pipe wall that has a laminar character.

[16]From Churchill (2006), the correlation of Eqs (2.16) and (2.17) has appeared in the literature in the past with several typographical errors. The expression presented here is error free.

The friction factor correlation is written as

$$\boxed{\begin{aligned} 0 = \frac{f^*}{2} - \{&(\frac{4}{\mathrm{Re}\sqrt{f^*/8}})^{24} + [(\frac{18765}{\mathrm{Re}\sqrt{f^*/8}})^{8} \\ &+(3.29 - \frac{227}{\mathrm{Re}\sqrt{f^*/8}} + (\frac{50}{\mathrm{Re}\sqrt{f^*/8}})^{2} \\ &+\frac{1}{0.436}\ln(\frac{\mathrm{Re}\sqrt{f^*/8}}{1+0.602\frac{\epsilon}{D}\mathrm{Re}\sqrt{f^*/8}}))^{16}]^{-\frac{3}{2}}\}^{\frac{1}{12}} \end{aligned}} \tag{2.16}$$

where

$$\boxed{f(\overline{u}, D) = 4f^*} \tag{2.17}$$

Swamee (1993) presents a slightly simpler variation of this formula that spans all regimes.

Though it is surprising to most, research continues on the understanding and models for turbulent flow in pipes and over surfaces (Marusic et al., 2010). The recent data for flow in rough and smooth pipes for $57 \times 10^3 < \mathrm{Re} < 21 \times 10^6$ reported by Allen et al. (2007) and others (McKeon et al., 2004, 2005; Shockling et al., 2006; Langelandsvik et al., 2008) have not yet been incorporated into Eqs (2.16) and (2.17).

The rather cumbersome-looking equation, Eqn (2.16), is just an implicit formula for $f(\overline{u}, D)$ as a function of Re and relative roughness of the pipe. Just like Eqn (2.12), its solution requires iteration or a numerical root-finder. A plot of Eqn (2.16) for a broad range of Re appears in Fig. 2.4 which is commonly referred to as the Moody chart or Moody diagram (see footnote 12). Shown in Fig. 2.5 is the friction factor for PVC and galvanized iron pipe, two materials normally used in gravity-driven water networks, over a Re range normally encountered in them. Also in Fig. 2.5 is the friction factor for the "smooth" limit ($\epsilon/D \to 0$). The implicit formula for the friction factor for this limiting case is from the work of Colebrook (1938, 1939) and Colebrook and White (1937),

$$f(\overline{u}, D)^{-1/2} = -0.8 + 2\log[\mathrm{Re} f(\overline{u}, D)^{1/2}] \tag{2.18}$$

Note from our inspection of Fig. 2.5 that the friction factor for PVC and smooth pipe are practically indistinguishable. This outcome will be very useful when we explore the development of simplified design formulas in Chapter 9.

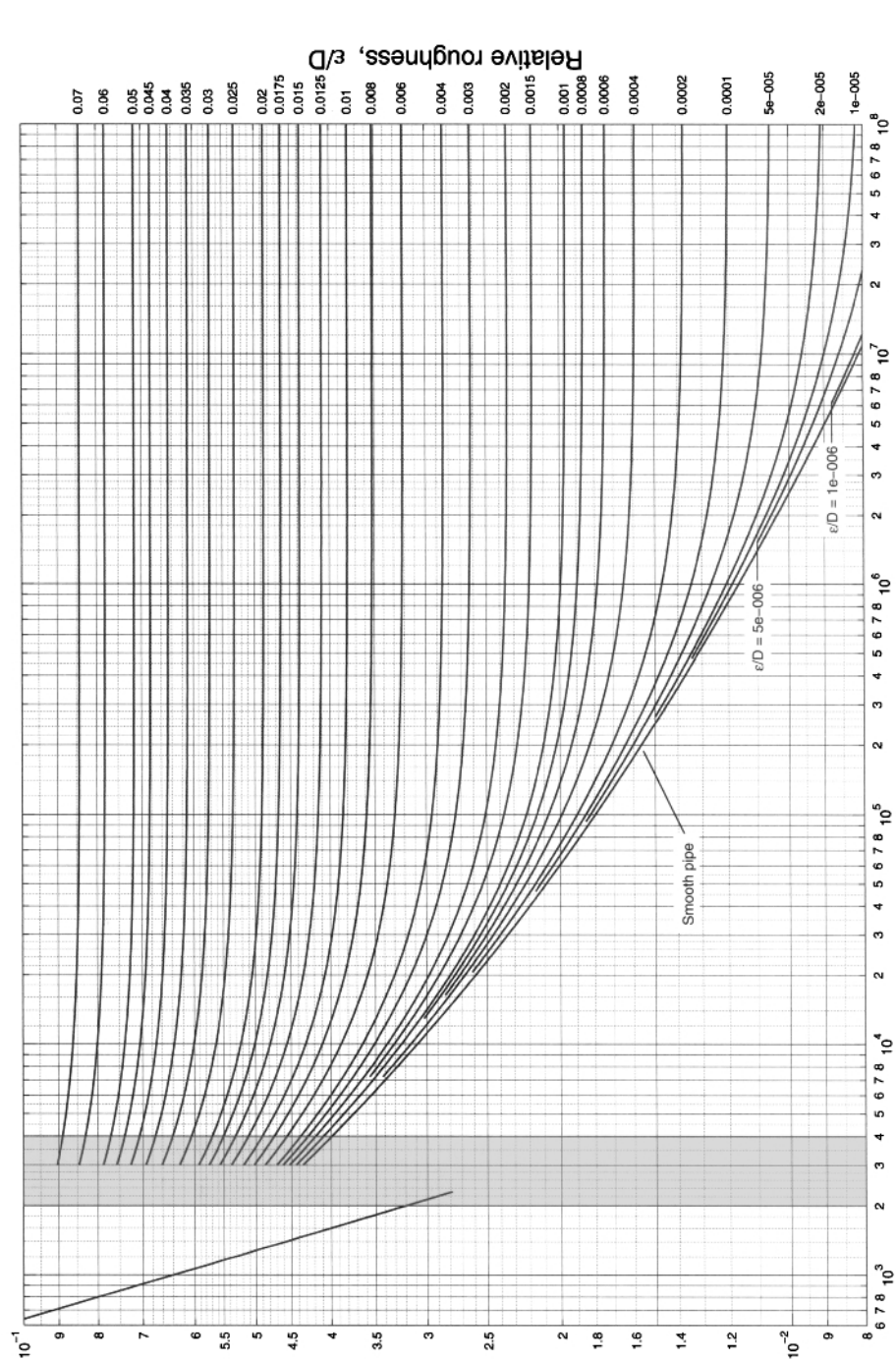

Figure 2.4 The friction factor. Relative roughness appears on the right side of this figure. The laminar ($\mathrm{Re} \lesssim 2300$) and turbulent ($\mathrm{Re} \gtrsim 3000$) regimes are clearly identifiable. The transition regime is sandwiched between these two. Produced in MatLab from Metzger & Willard Inc., Okeechobee, FL.

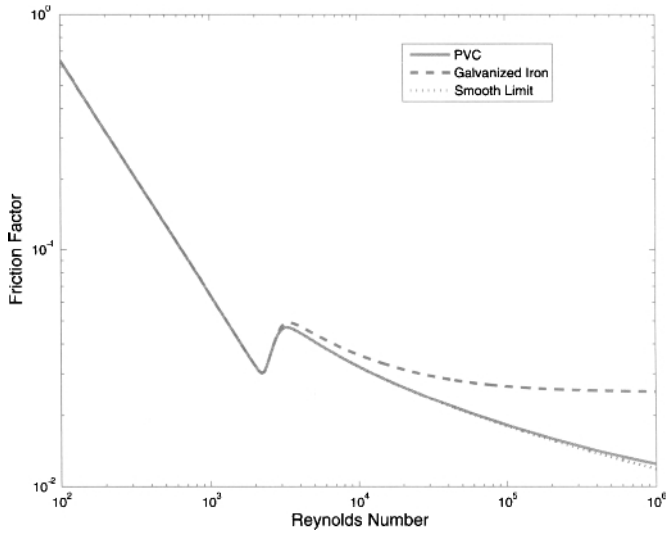

Figure 2.5 Friction factor for PVC and galvanized iron pipe, and the "smooth" limit ($\epsilon/D \rightarrow 0$) from Eqn (2.16). Laminar flow occurs for Re $\tilde{<}$ 2300 and turbulent flow for Re $\tilde{>}$ 3000. Transition flow is sandwiched between the two. Assumed is $D = 2.067$ in. to provide a value for ϵ/D. The friction factor for PVC and smooth pipe are practically indistinguishable.

B.2.3 The Navier–Stokes Equations

The Navier–Stokes equations are the momentum equations, Newton's second law of motion, for a Newtonian fluid. Together with the equation of mass conservation, the solution of the Navier–Stokes equations gives the velocity and static pressure distributions for any flow of a Newtonian fluid, like water and many other fluids encountered every day. Thus, the Navier–Stokes equations are the universal equations for fluid flow, including turbulent flow. Because they are a set of second-order, nonlinear, partial differential equations, they are very difficult to solve for most practical problems. Numerical methods (referred to as Computational Fluid Dynamics, or CFD) must normally be used. For pipe flow there is one very common case where the length of the pipe is very large compared with the diameter. Here, the velocity distribution in a laminar, incompressible, constant-viscosity pipe flow is termed "fully developed," and a closed-form solution for the velocity can be obtained from the Navier–Stokes equations. From this, an expression for the friction factor, $f(\overline{u}, D) = 64/\mathrm{Re}$, can then be developed that appears in Eqs (2.12) and (2.15). An approximate solution for the friction factor may be obtained in the same manner for turbulent flow, but modifications guided by experimental data are needed for accuracy. Please see the chapter on Differential Analysis of Fluid Flow in any fluid mechanics textbook for more details.

The solution for $f(\overline{u}, D)$ using Mathcad, which includes the use of the root function to solve Eqs (2.16) and (2.17), is illustrated in Fig. 2.6. Fortunately, this solution is included in all of the Mathcad worksheets presented in this text so there is no need for the designer to type Eqs (2.16) and (2.17) into Mathcad.

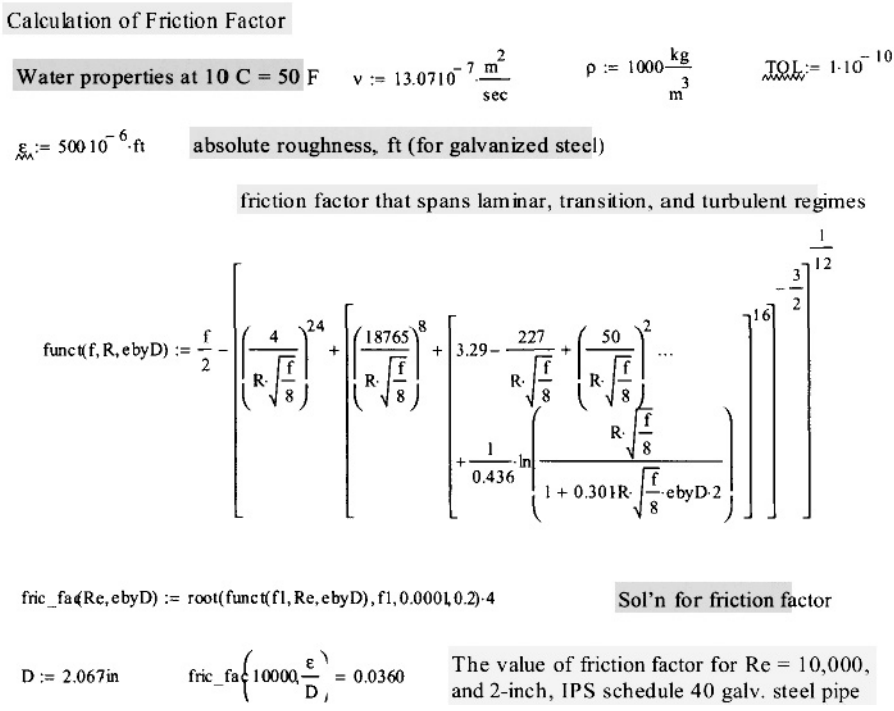

Figure 2.6 Mathcad solution for $f(\overline{u}, D)$ for 2.067-in. inside-diameter galvanized iron (or steel) pipe and Re of 10,000. $f(\overline{u}, D)$ is from the function `fric_fac` evaluated by the `root` solver. The term `ebyD` is relative roughness ϵ/D. The final two arguments in the function `root(funct(f1,Re,ebyD),f1,0.0001,f1)` of 0.0001 and 0.2 are the assumed lower and upper bounds, respectively, for the value of the friction factor, `frict_fac(Re,ebyD)`. Compare the result from this example with that from Fig. 2.5. Mathcad worksheet `friction factor.xmcd`.

An approximation to the friction factor is the Blasius formula [from Blasius in 1913 appearing in Munson et al. (1994)],

$$f(\overline{u}, D) = 0.316\,\mathrm{Re}^{-1/4} \tag{2.19}$$

normally reported as being valid for turbulent flow, where $10^4 < \mathrm{Re} < 10^5$ and for smooth pipe. As noted in the above paragraph, the smooth-pipe approximation applies to PVC and other plastic pipe but less accurately to steel or cast iron, the galvanized form of which is sometimes referred to as galvanized iron or GI. On the Moody chart,

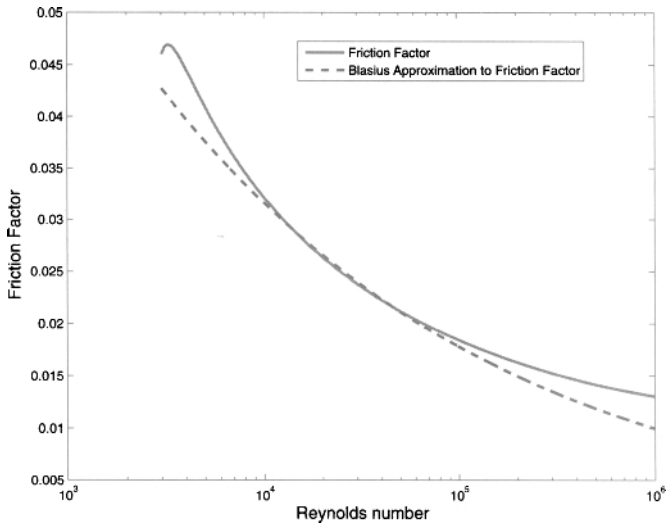

Figure 2.7 Friction factor in turbulent regime for smooth pipe and the Blasius approximation to it.

the limiting-case of smooth pipe appears as the lowest (that is, smallest ϵ/D) curve in the turbulent regime. A form of the energy equation where this approximation is evoked for $f(\overline{u}, D)$ is developed in Chapter 9 [Eqs (9.2)–(9.10)]. A plot of the friction factor for smooth pipe and the Blasius approximation to it appears in Fig. 2.7 and the extent of agreement between the two appears in Fig. 2.8. The relative error between the two at Re of ~4000 is 12% and about twice this value at Re of 1×10^6. For Re between 4,000 and 325,000, the relative error is 12% or less; except for a small band near the middle of this range the Blasius approximation underestimates the friction factor over this span of Re.

B.2.4 A Brief Assignment

Take a few minutes to compare the plot appearing in Figs. 2.4 or 2.5 with a few points calculated from Eqn (2.16) using the `Mathcad` worksheet `friction factor.xmcd`. Convince yourself that Eqn (2.16) is indeed an accurate representation of the friction factor. In particular, focus on how the friction factor changes from the laminar regime, through transition, and into the turbulent regime. Can you attribute a cause to the trends that you observe? How does the friction factor behave as a function of Re for pipe that is very rough, say, in the upper-right corner of Fig. 2.4? What do you think causes this? Why does the friction factor for smooth pipe show the greatest dependence on Re?

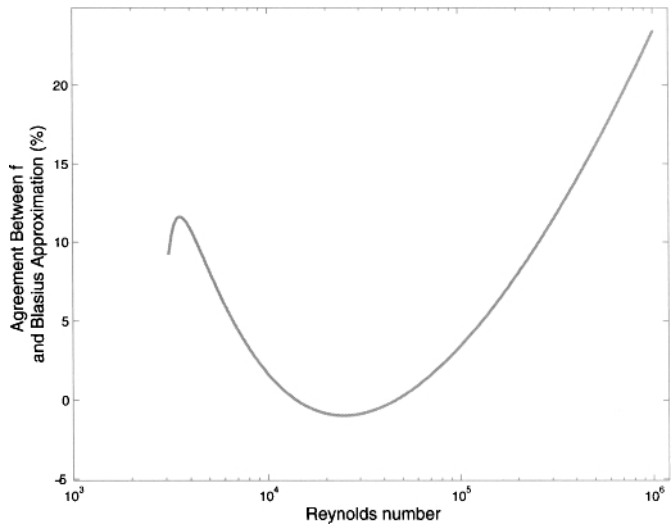

Figure 2.8 Percentage difference between the friction factor for smooth pipe and the Blasius approximation to it.

2.3 A STATIC FLUID

A condition that is sometimes of interest in a fluid-flow network is that where the fluid motion ceases. In this case, the fluid is referred to as "static". A subfield of fluid mechanics called *fluid statics* was developed to study fluids under this condition where applications include manometer theory and forces that are exerted on flat and curved surfaces (e.g., some dams and submarine hulls). Since there is no motion in a static fluid, all terms in the energy equation [Eqn (2.7)] that relate to fluid motion including head loss and velocity are zero. The energy equation for a static fluid becomes[17],

$$\frac{p_1 - p_2}{\rho} + g(z_1 - z_2) = 0 \tag{2.20}$$

This equation shows that in the absence of fluid motion, there is simply a balance between the pressure and potential energy; an increase in one results in the decrease in the other. If the fluid motion is zero, the pressure is referred to as "hydrostatic" pressure to distinguish the stationary state of the fluid from that in motion. However, the concept of pressure as stored energy in a fluid spring (as discussed in textbox B.2.1) still loosely applies. One of the reasons why the static state of a gravity-driven water network is of interest to analysts and designers is that the maximum pressures

[17]For readers knowledgeable about fluid statics, Eqn (2.20) is easily rewritten in the more-familiar form of the energy equation for a static fluid, $dp/dz + \rho g = 0$, by assuming the difference $z_1 - z_2$ to be differential in size. This equation is immediately obtained once we recognize $z_1 - z_2 = dz$ and thus $p_1 - p_2 = dp$.

in the network are most severe under this condition. This is because the frictional head loss, the right side of the energy equation [Eqn (2.7)], always serves to reduce static pressure along the fluid flow path. If the flow ceases, the pressures, which are then termed hydrostatic, become larger than when fluid is in motion.

2.4 LENGTH SCALES FOR GRAVITY-DRIVEN WATER NETWORKS

It is interesting to note that the ratio L/z_1 in the energy equation [Eqn (2.25)] contains, as a single term, two of the three lengths associated with a gravity-driven water system. These are the elevation of the source, z_1, and the length of the pipe, L. To further explore this term, and to set the stage for the solutions of the energy equation for the pipe diameter needed to supply a prescribed volume flow rate of water, we will consider two cases below. The first is an ideal case (Section 2.6.1), where the pipe is straight (that is, no bends or curves in the pipe) between the source and delivery location, and the second is for a case where the pipe may have curves and bends and, thus, is of arbitrary length. The latter case appears in Section 2.6.5.

The third length in the problem is D. D contributes to the characterization the regime of flow in the pipe through the Re. Actually, the ratio of D to $\nu/\overline{u}$ characterizes the regime of the flow. As noted above, for values of Re less than about 2300, the flow is orderly, has no mixing in the direction normal to fluid flow, and is termed laminar. For values of this ratio much greater than 2300, the length scale D is large enough such that disturbances normally present in the flow become amplified. After some distance downstream from the disturbance, the flow becomes chaotic and possesses large rates of mixing in the direction normal to fluid flow in what we know as turbulent.

Through the ratio with z_1, D also characterizes the strength of the minor loss in the problem, as we will see from the discussion in Section 2.6.2. It is appropriate to note how all three lengths characterize the problem. First, recalling that $z_2 = 0$ by definition, it is clear that z_1 establishes the potential energy that drives the flow. Second, it is also clear that the pipe length, L, contributes to characterizing the frictional head loss; larger pipe lengths have larger frictional head loss than do shorter lengths. However, the dependence of L on the details of where the pipe is run unnecessarily complicates this characterization. Instead, the appropriate length scale that characterizes the pipe length is indeed the straight-pipe length which, as is explored in Section 2.6.1, is completely defined by z_1 and the location of the delivery point of the water relative to the source. The use of the straight-pipe length, in combination with z_1, produces a very simple dependence of the problem on the "mean," or average, slope of the pipe and eliminates the dependence on both of these lengths.

2.5 MASS CONSERVATION

Conservation of energy is the first of two fundamental equations that are our focus in the analysis and design of water-flow networks. The second is mass conservation which states that mass can neither be created nor destroyed during any process of

interest in this text. For the one-dimensional (1D), steady flow in a round pipe that occurs in the networks considered, mass conservation is written as (refer to Fig. 2.1),

$$\boxed{Q = \overline{u}A = \overline{u}\pi D^2/4} \tag{2.21}$$

where Q is the volume flow rate[18] and A is the cross-sectional flow area. Equation (2.21) is often referred to as the "continuity equation" for it must be satisfied for the flow to be continuous. Application of Eqn (2.21) to quasi-1D flow between two pipes of the same or different diameters clearly leads to,

$$Q^+ = Q^- \tag{2.22}$$

where the $+$ and $-$ superscripts refer to just downstream and upstream of the pipe junction, respectively. For the more general case of flow through a junction of multiple pipes, we have

$$\boxed{\sum Q_{in} - \sum Q_{out} = 0} \tag{2.23}$$

where Q_{in} and Q_{out} are inflows and outflows from a junction, respectively. Unless otherwise stated, all values for Q are positive values.

Where it may be needed, the mass flow rate, $\dot{m}$, is related to the volume flow rate through the density of the fluid. Thus,

$$\boxed{\dot{m} = \rho Q} \tag{2.24}$$

B.2.5 A Problem for Exploration

A waterfall (Fig. 2.9) is an example where water flows at constant atmospheric pressure from high–to–low elevations. Suppose a particular site has a clean water source that feeds an existing waterfall. The flow rate in the waterfall is large enough to supply a community downstream. You are to consider the alternative of piping water from the source for delivery to the community. Discuss the energy changes in the waterfall and pipe flow for these two cases and identify each with the relevant terms in the energy equation. How does the continuity equation enter the problem? Suggestions to focus your discussion include the nature of the energy loss in the waterfall versus that for the pipe flow, water cleanliness in both cases, and the possibility of delivering electrical power to the community in addition to water.

[18]Normally reported in liters per second, L/s, or m^3/s. There are 1000 L in 1 m^3. A liter is about 0.264 gallons, or slightly more than a quart.

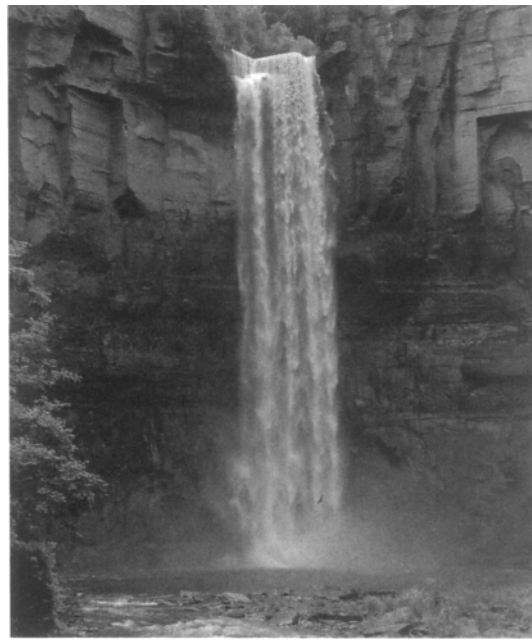

Figure 2.9 The waterfall at Taughannock Falls, New York. Photo courtesy of Nicki Jones.

Exploration (Cont'd)

A start of the exploration. We first consider piping the flow. The static pressure and vertical velocity of the flow are both zero at the top of the falls. Application of the energy equation [Eqn (2.7)] between this location and any lower point in the pipe flow shows that the reduction in potential energy is balanced by the increase in static pressure less the energy loss from accumulated friction. The kinetic energy change of $\overline{u}^2/2$, where $\overline{u}$ is the flow speed in the pipe, is generally negligible. For instance, if $\overline{u} = 3$ m/s, the change in kinetic energy is 4.5 m^2/s^2, whereas the change in potential energy is more than 100 times this for the falls of Fig. 2.9 (65 m high). Application of the continuity equation between the top of the pipe and any location downstream shows that $\overline{u}$ is constant throughout the flow.

Next, consider the waterfall where the static pressure is atmospheric everywhere despite the reduction in potential energy from the fall. The local kinetic energy for the waterfall can be estimated by considering that the flow accelerates during its downward movement under the influence of gravity. Since the volume flow rate, Q, is constant, the continuity equation [Eqn (2.21)] requires a reduction in cross-sectional flow area as the water proceeds downward. This is seen by noting that the waterfall appears wispier at the lower elevations compared with the middle. If we apply Eqn (2.7) to the flow between the top of the falls and the

Exploration (Cont'd)

point just before it reaches the pool of water below, there is a near-perfect balance in energy between potential and kinetic as the loss in potential energy fuels the increase in kinetic energy during the fall; any difference is attributable to energy supplied to evaporate water, an effect that tends to cool the water along its flow path. However, because the velocity in the vertical direction is zero at both the origin of the waterfall and in the pool, there is a zero net change in kinetic energy between these two points. By applying the energy equation between these points we see that, overall, the energy loss (H_L) balances the potential energy, $g(z_1 - z_2)$, where $z_1 - z_2$ is the elevation change of the waterfall. The energy loss in this case comes from mixing and splashing in the pool and, more importantly, evaporation at the pool surface. The mist rising from the pool surface and wetted walls of the canyon in Fig. 2.9 are evidence of this dissipation. This case is an example where the energy loss is not a true "head loss" (that is, a reduction in static pressure) but turbulent mixing and a partial evaporation of the flow. The thermal energy change in the flow must be considered to complete the understanding of this problem.

We see from this brief analysis that piping the flow is desirable if static pressure is needed to transport the flow to a community beyond the reach of the stream. It also allows for the installation of a microhydroelectric power plant if desired (see Chapter 12). Piping also facilitates greater control over maintaining water cleanliness in the supply.

B.2.6 The Friction Factor and Head Loss

As an illustration of the calculation of $f(\overline{u}, D)$ and the head loss due to pipe friction, consider the following simple problem. Calculate the friction factor and the head loss per 100 m of nominal 1-in. PVC pipe (D=1.049 in.) for a flow rate, Q, of 0.45 L/s. Is the flow laminar or turbulent?

With the flow rate specified, the Re can be written from the continuity equation (see Eqn (2.21)) as

$$\mathrm{Re} = \frac{4Q}{\pi \nu D}$$

For water at 10°C, refer to Fig. 2.3 or Eqn (2.14) to find $\nu = 1.307 \times 10^{-6}$ m^2/s.

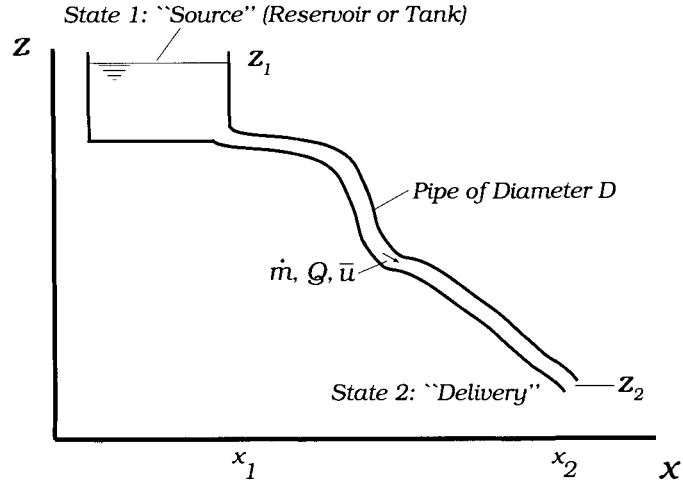

Figure 2.10 Single-pipe geometry with source at atmospheric pressure. The source is located at (x_1, z_1) and the delivery location is at (x_2, z_2), where $x_1 = z_2 = 0$.

The Friction Factor and Head Loss (Cont'd)

Then

$$\mathrm{Re} = \frac{4 \cdot 0.45 \times 10^{-3}\ \mathrm{m^3/s}}{\pi \cdot 1.307 \times 10^{-6}\ \mathrm{m^2/s} \cdot (1.049/39.372)\ \mathrm{m}} = 16,450$$

clearly a turbulent flow. For 1.049-in. inside diameter PVC pipe with $\epsilon = 5 \times 10^{-6}$ ft, $\epsilon/D = 5.720 \times 10^{-5}$ and Eqs (2.16) and (2.17) gives $f(\overline{u}, D) = 0.0278$. This result can be calculated using the `Mathcad` worksheet as seen in Fig. 2.6. Please take this opportunity to compare this result with what you would obtain graphically from the Moody chart in Figs. 2.4 or 2.5. The values for f should be identical from both sources. The head loss per unit length of pipe is from Eqn (2.10),

$$\frac{h_L}{L} = f(\overline{u}, D)\frac{\overline{u}^2}{2gD} = 8f(\overline{u}, D)\frac{Q^2}{g\pi^2 D^5}$$

$$\frac{h_L}{L} = 8 \cdot 0.0278 \cdot \frac{(0.45 \times 10^{-3}\ \mathrm{m^3/s})^2}{9.807\ \mathrm{m/s^2} \cdot \pi^2 \cdot ((1.049/39.372)\ \mathrm{m})^5} = 0.0346 = 3.46\%$$

Thus, head loss of 3.46 m/100 m of straight, horizontal 1-in. nominal PVC pipe occurs due to friction. Head loss per length of pipe is referred to as the "hydraulic gradient" in the hydraulics community. Normally given the symbol S, if using S do not confuse it with the lower-case s used in this book for mean slope.

2.6 SPECIAL CASE OF RESERVOIR AT STATE 1

In this section we begin our discussion of a single-pipe network by first referring to Fig. 2.10, which is Fig. 2.1 applied to the case of flow from a large reservoir or reservoir tank (the "source") at atmospheric pressure to a pipe of uniform diameter, D. State 1 is labeled the source and state 2 is the delivery point. *All remaining material in this section is based on this geometry and the assumptions that follow.* We will assume that the static pressure is to be measured from the local atmospheric value, so that at the reservoir surface (state 1) $p_1 = 0$ by definition. Also at the surface of the reservoir $\overline{u}_1$ may be approximated as zero because the reservoir is assumed to contain a very large volume. The large volume translates into a large cross-sectional area for water flow. The continuity equation, Eqn (2.21), predicts a vanishingly small value for $\overline{u}$ in the limit of infinitely large cross-sectional flow area. In addition, since we define the coordinate z to be measured from the lowest point in the pipe, $z_2 = 0$ (see footnote 19 for the definition of the mean and local slope of the pipe.). With these developments, Eqn (2.7) simplifies to,

$$1 - \frac{p_2}{\rho g z_1} = [f(\overline{u}, D)(\frac{L}{z_1} + \frac{D}{z_1}\sum_{i=1}^{M}\frac{L_e}{D}\Big|_i) + \frac{D}{z_1}(\alpha_2 + \sum_{i=1}^{N} K_i)]\frac{\overline{u}^2}{2gD} \qquad (2.25)$$

As noted, for turbulent flow, $\alpha_2 \approx 1.05$ and for laminar flow, $\alpha_2 = 2$. A schematic diagram of Fig. 2.10 is presented in Fig. 2.11, where the pipe is shown as a single line and other details that will be needed below appear. The use of a single line to represent a pipe is consistent throughout the remainder of this book, except where it is necessary to show liquid levels in, or size of, a pipe, such as in Chapter 14.

2.6.1 The Straight-Pipe Limit

We now consider the first of the two cases referred to in Section 2.4. As illustrated in Fig. 2.11, if the pipe is straight, the pipe length L is related through the Pythagorean theorem to the elevation, z_1, and the horizontal run of the pipe, ℓ, which is equal to $x_2 - x_1$, the distance between the inlet and outlet of the pipe measured in the horizontal plane. Thus,

$$L = \sqrt{z_1^2 + \ell^2} = z_1\sqrt{1 + (\ell/z_1)^2} = z_1\sqrt{1 + s^{-2}}, \qquad (2.26)$$

where s (lower case) is the mean slope[19] of the pipe (rise/run) or $s = z_1/\ell$. z_1 and ℓ may be determined by an instrument such as a GPS, an altimeter (for z_1), perhaps a

[19]The following convention is used throughout this book. The mean slope s is the ratio of the elevation of the source above the delivery location measured in the *downward* direction to the run (i.e., the distance between the source and the delivery location measured in the horizontal plane). Thus, s is positive valued for water flow downward. In later chapters, the *local* slope, given the symbol s_l, will be needed that depends on local position along the flow path. This too is taken to be a positive number if the orientation of the pipe assists the flow of water downward. The upward direction of the coordinate z in Fig. 2.11 and similar figures is conventional. The issue of whether the slope is positive or negative valued is mitigated

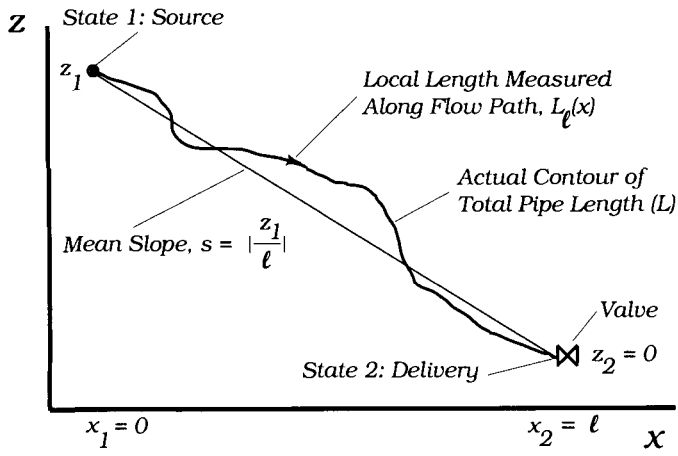

Figure 2.11 Schematic diagram for a single-pipe geometry of Fig. 2.10. The mean slope is average rise/run of pipe, where run is the distance measured between the pipe ends in the horizontal plane and the rise is the height of the source above the delivery location. See footnote 19.

tape measurement of the site (for ℓ), or from commercial satellite data (e.g., Google Maps®, maps.google.com). See Appendix B for a sample calculation of s.

With Eqn (2.26), Eqn (2.25) becomes,

$$1 - \frac{p_2}{\rho g z_1} - [f(\overline{u}, D)(\sqrt{1+s^{-2}} + \frac{D}{z_1}\sum_{i=1}^{M}\frac{L_e}{D}\Big|_i) + \frac{D}{z_1}(\alpha_2 + \sum_{i=1}^{N} K_i)]\frac{\overline{u}^2}{2gD} = 0 \tag{2.27}$$

Equation (2.27) is the energy equation for gravity-driven flow in a single pipe of uniform D. We see from Eqn (2.27) that the mean slope of the pipe, s, and the dimensionless static pressure at the delivery location, $p_2/\rho g z_1$, are the controlling parameters in the design. All other terms in Eqn (2.27) are related to the minor losses that, as discussed below, generally play a weak role in the design except where needed for flow balancing. In later chapters, the static pressure at the delivery location will be written as the static pressure head at the delivery location, or

$$\boxed{h_{del} = \frac{p_2}{\rho g}} \tag{2.28}$$

by the fact that s relates to the overall or local path length for flow along the pipe that, by definition, is always positive. Mathematically, s almost always appears as s^2 in all of the relevant equations so that the sign of s is immaterial. In cases where tbe slope is written as simply s, normally by taking the square root of $1/(1 + 1/s^{-2})$, where $s \ll 1$, the absolute value sign that formally appears after the square root is taken will be suppressed for the sake of convenience.

from which $p_2/\rho g z_1 = h_{del}/z_1$. The term h_{del} will appear frequently throughout this book. To emphasize and reinforce the fundamentals in this chapter and the few that follow, we will treat the pressure at delivery as a pressure for now.

It is intuitive to expect the mean slope to be important in the problem that we are considering. For any system that is gravity driven, whether solid (say, a pendulum) or, as in the present case of a fluid, the inclination of the system in the direction of the gravity vector affects the net driving force. For example, if a pipe containing water is oriented horizontally (perpendicular with respect to the gravity vector), we expect no gravity-driven flow to occur. At the other extreme, with the pipe oriented in the direction of the gravity vector, we would expect the largest possible fluid flow, since there can be no larger value for the inclination. The latter case is referred to as "terminal" and will be explored in further detail in Section 5.3.

Before the final form of the energy equation for flow in a straight pipe is presented, a discussion of two facets of this problem is needed. These are the importance of the minor loss term and the significance of the term $p_2/\rho g z_1$ in the energy equation.

B.2.7 Appearances can be Deceiving; Eqn (2.27) is Really the Energy Equation!

Though its appearance is probably unfamiliar, it is easy to demonstrate that Eqn (2.27) is the energy equation. Ignoring for the moment all minor losses (terms that contain D/z_1), and multiplying Eqn (2.27) by gz_1, we obtain

$$gz_1 - \frac{p_2}{\rho} - \underbrace{f(\overline{u}, D)\, z_1 \sqrt{1+s^{-2}}\, \frac{\overline{u}^2}{2D}}_{\Delta p_{fr}/\rho} = 0 \tag{2.29}$$

where Δp_{fr} is the positive-valued pressure drop due to major-loss friction. In Eqn (2.29), we see the balance between the potential energy at the source (state 1), pressure energy at the delivery point (state 2), and frictional energy due to the major loss, all per unit of mass flow. Recalling that $s = z_1/\ell$ and $L^2 = z_1^2 + \ell^2$, the major-loss term in Eqn (2.29) may be rewritten using the following steps,

$$\begin{aligned} H_L \equiv \frac{\Delta p_{fr}}{\rho} &= f(\overline{u}, D)\, z_1 \sqrt{1+s^{-2}}\, \frac{\overline{u}^2}{2D} \\ &= f(\overline{u}, D)\, z_1 \sqrt{1+(\frac{\ell}{z_1})^2}\, \frac{\overline{u}^2}{2D} \\ &= f(\overline{u}, D)\, \frac{z_1}{z_1} \sqrt{z_1^2+\ell^2}\, \frac{\overline{u}^2}{2D} = f(\overline{u}, D)\, \frac{L}{D}\, \frac{\overline{u}^2}{2} \end{aligned}$$

which is the Darcy–Weisbach equation, Eqn (2.9).

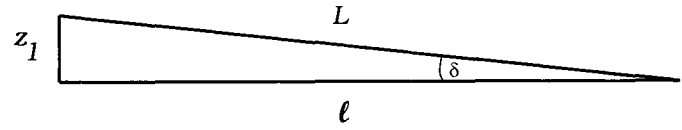

Figure 2.12 Graphical illustration of $s = \tan(\delta) = z_1/\ell \approx z_1/L$ in the limit of small slope, s.

Appearances (Cont'd)

For a straight pipe, it is worthwhile to rewrite Eqn (2.26) for emphasis,

$$L = \sqrt{z_1^2 + \ell^2}$$

or

$$\frac{L}{z_1} = \sqrt{1 + s^{-2}} = |s|^{-1}(1 + s^2)^{1/2} \tag{2.30}$$

For the normal case of $s \ll 1$, expanding the square-root term in a binomial series, which states $(1 + \epsilon)^n = 1 + n\epsilon$ to dominant order where ϵ is a dimensionless number, $\epsilon \ll 1$, and n is an exponent, gives

$$\frac{L}{z_1} = \sqrt{1 + s^{-2}} = |s|^{-1} + \frac{|s|}{2} \approx |s|^{-1} \quad \text{for} \quad |s| \ll 1 \tag{2.31}$$

For convenience, we will suppress writing the absolute value of s in this book. For example, if $s = 0.10$ or 10%, $L/z_1 = \sqrt{1 + s^{-2}} = 10.05$ or 10.05 m of pipe length for every 1 m of rise. From Eqn (2.31), the approximation $L/z_1 = s^{-1} = 10$ differs from the exact answer by just 0.5%. We see that the approximation of Eqn (2.31) to Eqn (2.30) is clearly acceptable for small values of the mean slope. From our inspection of Fig. 5.30, which we will focus on in Chapter 5, the practical meaning of $s \ll 1$ is $s \lesssim 0.5$ (an angle between a line drawn from the source to delivery location and level ground of $< 27°$). This condition is satisfied by most gravity-driven water networks.

A graphical illustration of this approximation appears in Fig. 2.12, where it is clear that $s = \tan(\delta) = z_1/\ell \to z_1/L$ in the limit as $s \to 0$.

2.6.2 Justification for Neglect of Minor Losses

For all gravity-driven water networks, the ratio $D/z_1 \ll 1$. For example, if a pipe of diameter of $1\frac{1}{2}$ in. has an elevation head of 100 m, $D/z_1 = 4.09 \times 10^{-4}$, clearly a very small number. Thus, the minor losses and α_2 in Eqn (2.27) can be neglected as a first approximation. We will assess the effect of these terms on the flow speed

in Chapter 7, but because the minor losses are generally not large (except where needed for flow balancing; more on this in Chapter 11), in future treatments we will sometimes neglect the effect of the minor loss and α_2 terms in the energy equation, even though there may be minor-loss elements installed in the network.

2.6.3 The Meaning of $p_2/\rho g z_1$: "Natural Flow" in a Pipe

The term $p_2/\rho g z_1$ in Eqn (2.27) is the ratio of the static pressure at the delivery location (i.e., at the low end of the pipe to the hydrostatic pressure caused by the reservoir). Alternately, it is the ratio of the static head at the delivery location, $p_2/\rho g$, to the elevation head, z_1. Before discussing the concept of Natural flow, which is the main thrust of this section, several observations are worth noting. First, this ratio is dimensionless, which means that the numerical values for it are independent of the system of units used in the analysis and design of the network. At this point it is also worthwhile to recall that the hydrostatic pressure, $\rho g z_1$, is that caused by a stationary head of fluid, z_1. This should not be confused with the static pressure, which is the pressure measured in a fluid when it is in motion; as discussed in Section 2.2, static pressure is a dynamic quantity. Finally, the term $p_2/\rho g z_1$ is a design parameter that we, as designers, are either free to adjust to our needs or the value of it is constrained by other parts of the design. For the case of a single pipe with only a single delivery location, $p_2/\rho g z_1$ is a parameter whose value we prescribe. In contrast with multiple-pipe networks, considered in Chapter 11, the value of $p_2/\rho g z_1$ may depend on other parts of the design including the flow in every other pipe segment in the network.

Referring to Fig. 2.11, we will consider two bounding values for p_2. For the first one, imagine that the valve at the delivery point in Fig. 2.11 is fully opened and presents no restriction to the water flow that leaves the end of the pipe at this location. When water leaves the delivery point it is surrounded by an environment at atmospheric pressure. The result is that the pressure within each point in the water flow at state 2 is at atmospheric pressure. Thus, p_2 or $p_2/\rho g z_1$ has a lower-bound value of 0; the case for which water flows from the end of the pipe due only to its kinetic energy and has no assistance from static pressure at this point. This condition is the "Natural flow" of the system [Jordan Jr. (2004) and others]; the flow rate that will be moved by gravity for a given pipe and system geometry (including elevations, diameters, and lengths). In other words, the flow speed for Natural flow in a pipe is that which exactly balances the frictional energy loss with the potential energy at the source, $\rho g z_1$. The concept of Natural flow in a pipe, though introduced in the present context of flow in a straight pipe, applies to any pipe, straight or otherwise.

At the other extreme, imagine that the valve at the delivery point in Fig. 2.11 is fully closed so that there is no flow. Recalling the developments from Section 2.3, for this bounding case $p_2/\rho g z_1 = 1$ and the static pressure at the delivery point is termed *hydrostatic*. The pressures within the network achieve their largest possible values for the hydrostatic case. Because of this, the designer will always check to ensure that the pipe and fittings in the network can withstand the pressures that will exist in this limiting case. Also note that the pipe diameters have no effect on the

pressures in the network since pressure comes from from only the local elevation in the pipe (see Section 2.3).

To summarize the above discussion, we can write

$$\boxed{\text{(Natural flow)} \quad 0 \leq \frac{p_2}{\rho g z_1} \leq 1 \quad \text{(Hydrostatic limit)}} \tag{2.32}$$

It is worthwhile noting that for Natural flow, where the static pressure at delivery is zero, no pressure term will appear in the energy equation. This is because both the reservoir and the delivery locations are at atmospheric pressure. In addition, *the case for Natural flow will provide a lower bound on the pipe diameter(s) in the network.* This is because without any other flow restrictions, the pipe itself must dissipate the total potential energy of the source. The smallest of acceptable pipe sizes are needed to accomplish this. Another consequence of Natural flow is that minor-lossless flow in a straight, constant-diameter pipe between the source and delivery location will be at atmospheric pressure at all points along the flow path. The explanation for this comes from the following. The static pressures at the source and delivery locations are atmospheric and at each and every location along the pipe-flow path there is an exact balance between the potential energy and the energy dissipated by friction both per unit length of pipe. Thus, there is no "excess" energy at any point in the flow available to raise the static pressure of the flow above atmospheric conditions.

It is recommended that the reader keep the simple limiting-case values for $p_2/\rho g z_1$ from Eqn (2.32) in mind as an aid in understanding and interpreting the material in several of the following chapters and, certainly, in the execution of a design.

The normal case for p_2 would be between the extremes of $p_2/\rho g z_1 = 0$ and $p_2/\rho g z_1 = 1$, where there is a need to control the flow rate of water from the end of the pipe at the delivery location or to distribute water from the delivery point to houses in a village far from this point. This requires $0 < p_2/\rho g z_1 < 1$ so that flow is possible. To accommodate a realistic range of possible static pressures at the delivery location for use in the design charts presented in Chapter 5, we will give the designer-specified term $p_2/\rho g z_1$ the symbol F, that is, $\boxed{F \equiv p_2/\rho g z_1.}$ For the design charts presented in this chapter, we will allow F to take on the specific fixed values of 0, 0.1, 0.25, and 0.50; a reasonable range of interest for gravity-driven water networks.

2.6.4 Final Form of Energy Equation for Flow in a Straight Pipe

With the substitution for F in Eqn (2.27), the final form of the energy equation for the case of a straight pipe of diameter D becomes

$$1 - F - [f(\overline{u}, D)(\sqrt{1+s^{-2}} + \frac{D}{z_1}\sum_{i=1}^{M}\frac{L_e}{D}\Big|_i) + \frac{D}{z_1}(\alpha_2 + \sum_{i=1}^{N} K_i)]\frac{\overline{u}^2}{2gD} = 0 \tag{2.33}$$

where, if we neglect the minor loss (the terms involving D/z_1) as discussed in Section 2.6.2, we obtain

$$1 - F - f(\overline{u}, D)\sqrt{1+s^{-2}}\frac{\overline{u}^2}{2gD} = 0 \tag{2.34}$$

where the approximation of $\sqrt{1+s^{-2}} = |s|^{-1}$ from textbox B.2.7 is valid for $|s| \ll 1$. For convenience, we will suppress the absolute value sign in the foregoing expressions throughout this book (see footnote 19).

From our inspection of Eqs (2.33) or (2.34), we see that $\overline{u}$ is indeed a maximum for $F = 0$ (i.e., Natural flow). Also, the only solution possible from either of these equations is $\overline{u} = 0$ for $F = 1$, the hydrostatic case. Both of these observations provide support and validation for the discussion in Section 2.6.3.

Of course, few gravity-driven water networks have only a single pipe and even fewer have a single straight pipe. In Section 2.6.5, we will turn our attention to the extension of Eqs (2.33) and (2.34) applied to single-pipe networks that have an arbitrary length. The topic of multiple-pipe networks is covered in Chapter 11 which, along with the treatment of air pockets in the network and optimization, is the culmination of the analytical content of this book.

B.2.8 An Interim Recap

Thus far in this chapter we have applied the principle of conservation of energy, one of the fundamental conservation laws in engineering and science, to the steady flow of an incompressible, constant-viscosity fluid in a pipe. The outcome is a balance between the change in total mechanical energy (consisting of pressure, kinetic, and potential energy) and energy loss between known inlet and outlet states. From many past observations in the laboratory and in practice, the energy loss is known to be proportional to the kinetic energy per unit mass, $\overline{u}^2/2$, through a friction factor to account for the loss in a run of straight pipe (the "major loss") and empirical minor loss coefficients accounting for the loss in fittings and valves (the "minor loss"). For laminar flow, the friction factor is from the solution of the Navier–Stokes equations and for turbulent flow from a correlation of data collected in experiments. With the generally small minor losses neglected for gravity-driven water flow in a straight pipe we see that the mean flow speed, or volume flow rate, of water depends on just D, the slope of the pipe, and the dimensionless static pressure at the delivery location, F. Here F is bounded from above by 1, where there is no flow in the pipe (hydrostatic limit) and below by zero, where there is maximum flow in the pipe (Natural flow limit) for the given conditions. Since pressures are maxima for the hydrostatic limit, the required wall thicknesses of the pipe in the network are determined based on this case. In addition to conserving energy, we saw that mass also needs to be conserved. The equation for mass conservation, referred to as the continuity equation [Eqn (2.21)], is simple in form for 1D pipe flows that are of interest in the present context.

The reader should keep in mind that the energy equation that is the basis for all of the analysis and design in this book is the same one that the reader may have encountered in courses in thermodynamics, fluid mechanics, heat transfer, and other subjects. The only differences that you might observe are the appearance

Recap (Cont'd)

or disappearance of terms that model processes that may not be relevant to the topic being considered. An example of this is the "disappearance" of the work term for the case of pipe flow where there clearly is none of this.

2.6.5 A Circuitously Run Pipe of Arbitrary Length

In this case, the pipe length, L, is not unique to the elevation of the reservoir and the run, but is arbitrary. The length may consist of straight pipe and fittings including elbows, and so on, or it may be bent in a curved manner to conform to the contour of the earth in which it is buried. For the case of a pipe of arbitrary length, L is written as

$$L > \sqrt{z_1^2 + \ell^2} = z_1\sqrt{1 + s^{-2}} \tag{2.35}$$

or

$$L = \lambda\sqrt{z_1^2 + \ell^2} = \lambda z_1\sqrt{1 + s^{-2}} \tag{2.36}$$

where λ is a dimensionless number normally greater than one[20], defined as

$$\lambda = \frac{L}{\sqrt{z_1^2 + \ell^2}} = \frac{L}{z_1\sqrt{1 + s^{-2}}} \tag{2.37}$$

Thus,

$$\frac{L}{z_1} = \lambda\sqrt{1 + s^{-2}}, \quad \text{or} \quad \frac{z_1}{L} = \frac{1}{\lambda\sqrt{1 + s^{-2}}} \tag{2.38}$$

λ is the ratio of the actual length of the pipe to the pipe length if it were straight between the source and delivery points (see Fig. 2.11). In the field of hydrogeology (or hydrology) where engineers and scientists explore the movement of groundwater in the earth, λ is referred to as the tortuosity (Domenico and Schwartz, 1998), one of terms we will use in this text. Here λ also appears as a characterizing parameter in the treatment of fluid flow and heat transfer in porous media (Nield and Bejan, 1992). A porous medium is a permeable solid generally having nonregular shaped passages through which a fluid can flow. In terms of the length scales discussed in Section 2.4, λ may be thought of as a "dimensionless length" of the pipe in a flow network. For a pipe of arbitrary length, it is worthwhile to note from Eqn (2.38) and the normal case of $s \ll 1$, we can write

$$\boxed{\frac{s}{\lambda} \approx \frac{z_1}{L}} \tag{2.39}$$

Please see textbox B.2.7 for the development of Eqn (2.39) for $\lambda = 1$.

[20]See textbox B.2.10 and the discussion in Section 5.4 on the effective size-limitations of the parameter λ.

Substitution of Eqn (2.36) into Eqn (2.25) produces the final form of the energy equation for the case of flow in a pipe of diameter D and arbitrary length,

$$\boxed{1 - F - [f(\overline{u}, D)(\lambda\sqrt{1+s^{-2}} + \frac{D}{z_1}\sum_{i=1}^{M}\left.\frac{L_e}{D}\right|_i) + \frac{D}{z_1}(\alpha_2 + \sum_{i=1}^{N} K_i)]\frac{\overline{u}^2}{2gD} = 0,} \tag{2.40}$$

where, if we neglect the minor loss (the terms involving D/z_1), we obtain

$$1 - F - f(\overline{u}, D)\,\lambda\sqrt{1+s^{-2}}\,\frac{\overline{u}^2}{2gD} = 0 \tag{2.41}$$

or

$$\frac{1-F}{\lambda\sqrt{1+s^{-2}}} - f(\overline{u}, D)\frac{\overline{u}^2}{2gD} = 0 \tag{2.42}$$

The approximation of $\sqrt{1+s^{-2}} \approx s^{-1}$ from textbox B.2.7 is valid for $s \ll 1$, the practical meaning of which is $s \tilde{<} 0.5$ (an angle between the source and level ground of $< 27°$), a condition satisfied by most gravity-driven water networks. Substituting this into Eqn (2.42), we obtain a simpler form of Eqn (2.42),

$$\frac{s(1-F)}{\lambda} - f(\overline{u}, D)\,\frac{\overline{u}^2}{2gD} = 0 \qquad \text{for } s \tilde{<} 0.5 \tag{2.43}$$

We recognize the second term in each of Eqs (2.42) and (2.43) as the dimensionless frictional head loss per length of pipe, h_L/L, in the network [see Eqn (2.10)]. This is referred to as the "hydraulic gradient" in the hydraulics community and often given the symbol S (not to be confused with the lower-case s used for mean slope). Thus, the first terms in Eqs (2.42) and (2.43), $(1-F)/(\lambda\sqrt{1+s^{-2}})$ or $s(1-F)/\lambda$ are, by equivalence, the dimensionless frictional head loss per length of pipe and both can be given the symbol S. For Natural flow, where $F = 0$, the hydraulic gradient becomes $\boxed{S = s/\lambda}$. An example of the calculation of the hydraulic gradient is presented in textbox B.2.6.

For the demand-driven designs that are the focus in this book, it is always of interest to solve any one of Eqs (2.40)–(2.43) for D in terms of Q instead of $\overline{u}$. One equation is easily obtained from the other by using the continuity equation, Eqn (2.21), to eliminate $\overline{u}$ in favor of Q. The resulting form of energy equation from Eqn (2.42) for example, is one the more useful forms for minor-lossless flow (see next paragraph) in a single-pipe network,

$$\boxed{\frac{1-F}{\lambda\sqrt{1+s^{-2}}} - \frac{8Q^2}{\pi^2 g}\,\frac{f(Q,D)}{D^5} = 0} \tag{2.44}$$

For the case of small s, this is written as

$$\boxed{\frac{s(1-F)}{\lambda} - \frac{8Q^2}{\pi^2 g}\frac{f(Q,D)}{D^5} = 0} \tag{2.45}$$

Equation (2.40) is the energy equation for steady, gravity-driven, incompressible, developed flow in a full round pipe of diameter D, tortuosity λ, and where the source is a reservoir at atmospheric pressure. The existence of laminar, transition, or turbulent flow in the pipe is accommodated by the friction factor, $f(\overline{u}, D)$, through Eqs (2.16) and (2.17). The variants of the energy equation for pipe flow are Eqs (2.42)–(2.45) where minor losses are neglected (i.e., they apply to "minor-lossless" flow). Equations (2.40)–(2.45) are nonlinear algebraic equations in D and $\overline{u}$ or Q [recall that the friction factor depends on $\overline{u}$ (or Q) and D]. The solutions for any of these equations requires a numerical root-finder or, as is the tradition, iteration. Both of these methods are explored in Chapter 4. Several chapters in this book will be devoted to the solutions of Eqn (2.40) and its variants including Chapter 5, where design charts for minor-lossless flow in a single-pipe network from the solution of Eqn (2.44) are presented, Chapter 9 where an approximation to the friction factor is considered, and Chapter 11 where Eqn (2.40) is extended to include flows in multiple-pipe networks as defined in Chapter 1. In the case of multiple-pipe networks, where the static pressure at the inlet to a pipe segment may not be zero, there will be the need to modify Eqn (2.40) slightly to account for the addition of this pressure. See Section 2.9 for this adjustment.

It is enlightening to inspect the roles played by the terms s, λ, and $1 - F$ in the analysis and design of a single-pipe network where the source is a reservoir at atmospheric pressure. Our inspection of Eqn (2.45) shows that s and $1 - F$ enter the problem as multiplicative factors. That is, a change in s has the same effect on D and Q as the same change in $1 - F$. The term λ enters the problem as an inverse multiplicative factor. For example, this means that an increase in λ of, say, 10% is equivalent to decreasing s by ~10%. It is convenient to think about the roles of s, λ, and $1 - F$ in this manner as you move forward with the tools for further analysis and design. In fact, at this point the astute reader will question why the role of a single parameter, $s(1 - F)/\lambda$, which is the hydraulic gradient, is not being discussed. This is a legitimate question, but because the parameters s, λ, and $1 - F$ are prescribed independently and have very different meanings, a deliberate choice is made to treat each one separately for now, including this chapter, and in Chapter 5, where design charts are presented for diameter as a function of the delivered volume flow rate of water for independently fixed values of s, λ, and F. In Chapter 9, it will be convenient, however, to treat the group $s(1 - F)/\lambda$ as a single parameter.

B.2.9 Example: A Circuitously Run, Single-Pipe Network

Consider a single-pipe network that is required to pass 4.8 L/s of water flow from the source at atmospheric pressure to an open reservoir tank. The mean slope, s, is 6.3% as determined by a few simple measurements made with an Abney level (see Section 8.2), and the tortuosity, λ, is estimated as 1.35. Calculate the theoretical pipe diameter required to meet these design conditions. Neglect all minor loss and assume the pipe to be galvanized iron (GI). To investigate the possibility of using plastic pipe, calculate the diameter if the pipe were PVC.

The slope is small enough ($s < 0.5$) that the energy equation of Eqn (2.45) applies to this problem. $F = 0$ because the reservoir is at atmospheric pressure. Upon substitution of numbers and units into Eqn (2.45), we get

$$\frac{0.063}{1.35} - \frac{8(4.8 \times 10^{-3}\ \mathrm{m^3/s})^2}{\pi^2 \cdot 9.807\ \mathrm{m/s^2}} \frac{f(Q,D)}{D^5} = 0$$

or

$$\frac{f(Q,D)}{D^5} = \frac{2.591 \times 10^{-4}}{\mathrm{in.}^5}$$

The friction factor from Eqs (2.16) and (2.17) depends on Re, which is written as it was in textbox B.2.6. Obtain

$$\mathrm{Re} = \frac{4Q}{\pi \nu D} = \frac{1.841 \times 10^5}{D}$$

where D is in inches. For GI pipe $\epsilon \approx 1.5 \times 10^{-1}$ mm. Using the `Mathcad` worksheet `friction factor.xmcd` for the friction factor, we obtain the solution $D = 2.52$ in. For these conditions, the flow speed in the pipe is 1.50 m/s, the friction factor is 0.0260, and Re is 73,200, which corresponds to turbulent flow.

For PVC pipe $\epsilon \approx 1.5 \times 10^{-3}$ mm and the results become $D = 2.48$ in. The diameters for GI and PVC pipe are nearly identical. The larger roughness of the GI pipe, by a factor of 100 compared with PVC, plays a minor role in this problem. For larger flow rate and slope, differences will be greater.

B.2.10 The Scales of λ, s, and F

As it turns out, and as discussed in more detail in Chapter 5, the dimensionless length of the pipe, λ, does not have a strong influence on the outcomes of most designs for two reasons. First, the common-sense practice is to connect the source, tank, and tapstands at the delivery locations by as short a pipe length as possible to minimize pipe cost. Thus, L will approach the value it would have if run along a straight path between the source and delivery locations. Second, the mean slope of a typical design is small. Thus, the run of a water-delivery pipe is very much larger than the elevation of the source so that peaks and valleys in the pipeline and also a normal amount of circuitousness in the horizontal plane does not add much overall length to the pipe. For both of these reasons, values for λ larger than one plus a small fraction are unusual for most actual designs. To support this observation, consider Table 2.2, where we present dimensional data for several gravity-driven networks in central Nicaragua and other countries that were assessed and designed by students and faculty at Villanova University. From our inspection of these data, we see that values for λ for real networks are clearly of the order of 1. In fact, an estimate of $\lambda \approx 1.2 \pm 0.15$ is representative of this data set. Based on the dependencies established in Chapter 9 for a restricted range of Re and smooth pipe wall, the effect of λ on D may be written as $D \approx \lambda^{0.211}$, or $D \approx (1.2 \pm 0.15)^{0.211}$. Thus, the variation in λ for the range of real networks appearing in Table 2.2 has only a $\pm 2.5\%$ effect on pipe diameter, D. Obviously, the scales of s and F are expected to vary greatly among the networks. Table 2.2 shows a sampling of these for s. In the case of F, for a shallow network with small s, F of 0.5 may be required to provide the static pressure needed for water distribution beyond the point where the distribution main meets the branches. For a larger network where the mean slope is greater, F of 0.1 may be more than adequate.

2.7 SINGLE- AND MULTIPLE-PIPE NETWORKS REVISITED

Single- and multiple-pipe networks were introduced in Chapter 1. A single-pipe network, or gravity main, must satisfy not only the condition of being just one pipe of a single diameter with no branches and known pressures at each end, but it must also meet one additional condition as described in this section. The existence of local peaks or valleys in a pipe will require that we investigate the network at a greater level of detail than for cases where these do not appear. A local peak or valley is defined by the vertical distance between the actual local elevation of the pipe and the elevation at this point if the pipe were run straight between the source and delivery locations (Fig. 2.13). For convenience, we refer to this distance as Δz_p and take as positive

Table 2.2 Dimensional Data and s and λ for Several Gravity-Driven Water Networks

Project Name	z_1 (m)	ℓ (m)	$\sqrt{z_1^2 + \ell^2}$ (m)	L (m)	s	λ
Baan Bo Kau Village - Thailand (Leg 1)	62.50	1456.6	1457.9	1889.9	0.0429	1.296
Baan Bo Kau Village - Thailand (Leg 2)	50.30	505.7	508.2	533.5	0.0995	1.050
Baan Bo Kau Village - Thailand (Leg 3)	30.20	631.6	632.3	729.6	0.0478	1.154
San Benito, Central Nicaragua	24.70	1414.0	1414.2	1695.6	0.0145	1.199
Kiangan, Ifugao - Philippines (Leg 1)	80.90	197.4	213.3	216.4	0.410	1.014
Kiangan, Ifugao - Philippines (Leg 2)	14.90	297.4	297.8	297.8	0.0502	1.000
Kiangan, Ifugao - Philippines (Leg 3)	41.40	299.7	302.5	302.6	0.138	1.000

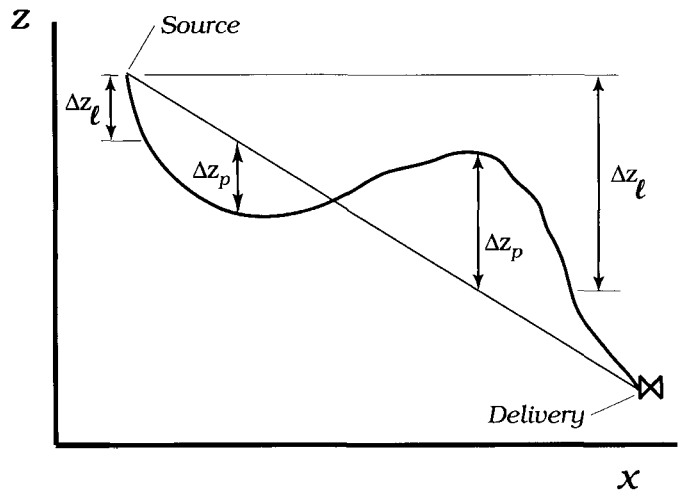

Figure 2.13 Geometry to support definition of local peak and valley.

for both a peak and valley. If Δz_p is nonexistent or small,[21] and the peak occurs far enough downstream of the source, we are generally not concerned with the *local* static pressure distribution in the network. The term local refers to *each position along the water flow path.* Alternately, for networks where local peaks or valleys are not small, there will be a need to prescribe or bound the static pressures at each peak and valley to ensure the proper performance of the network. A possible outcome of prescribing or bounding static pressures at these locations might be a change in the pipe diameter. For these cases, the *need* to address the local static pressures at, or near, each peak or valley, along with the possible consequence of a change in the pipe diameter, will classify the design as a multiple-pipe network. Analysis of networks where there is a single flow path in a pipe of varying diameter is covered in Section 11.5.1.

In summary, a single-pipe network where there are local peaks or valleys with large changes in elevation, or with a local peak near the source, should be analyzed as if it is a multiple-pipe type. The procedures described in Chapter 11 apply. Otherwise, the network may be analyzed as single-pipe using the energy equation for pipe flow, Eqn (2.40) and its variants, and the graphical solutions of these equations that are presented in Chapters 5, 8, and 9.

Aside from the practical need for the treatment of a single-pipe network, note that there is another benefit of discussing them in detail. It is easier to understand and appreciate the energy equation and its application in the simpler context of a single-pipe network than for one that has multiple branches that add to complexity

[21]The meaning of small is arbitrary. Δz_p of less than about 20% of Δz_ℓ as seen in Fig. 2.13 may be considered small for a peak. The size of Δz_p for a local valley has a smaller effect than that for a local peak provided the valley is not lower than the delivery location.

and where the same fundamental principles apply. Therefore, for both practical and pedagogical reasons we will spend time on this type of network and its solutions.

B.2.11 Understanding of Concepts and Use of Precise Terminology in Engineering

There have been numerous terms defined and described in precise ways in this chapter. Precision is crucial for success in engineering and science. In the present context, precision refers to the understanding, appreciation, and accurate use of the *terminology* and *technical concepts*. Terms that appear above like *steady state*, *incompressible*, and *constant viscosity* have precise, well-defined meanings that collectively fully characterize the nature of the flow that we are analyzing. This precision also serves to improve our own level of understanding. Analysis and design are always performed in a team environment. This demands precise and accurate communication among team members. Loose, or imprecise, terminology and hazy, or inaccurate, concepts are not desirable for effective communication. If a designer says to her teams members, "... our design will provide for the steady water flow of 0.25 L/s in a straight, round pipe, assuming to flow full, with a mean slope of 3% and a static pressure at the delivery location equivalent to a 3 m head," others in the team will know precisely about the conditions at hand and can proceed with the next steps to execute a successful design. This may be considered "over-stating" the problem from certain cultural points of view, but the idea behind it is clear and the intent is sound.

An illustration of the above comes from the popular Web site Wikipedia (`http://en.wikipedia.org`), used by many including students, concerning the definition of the power term Btu per hour. "When used as a unit of power, BTU per hour (BTU/h) is the correct unit, though this is often abbreviated to just 'BTU'." When confronted with a mislabeled unit such as this, the designer needs to decide either to let the context guide the correct units or, alternately, question the author. Both the uncertainty or extra time required are undesirable outcomes of this imprecision.

The engineer, as an individual in the design team, cannot expect a design to succeed if they, themselves, do not have a thorough understanding of the terminology and technical concepts associated with the design work. This is one reason why much attention has been paid to precise wording in the above writings. See, for example, the discussion in textbox B.2.2, and the common error of referring to the energy equation for pipe flow as the Bernoulli equation. However, we must be aware that most engineers, as well as some engineering professors, often fall short in the use of precise and accurate words, terminology, and concepts. As with most skills, improvements in these areas are realized with practice, maturity, and broadened experiences, and given sufficient time and thought about a technical problem.

2.8 THE ROLE OF THE MOMENTUM EQUATION

It is well understood that the analysis and design of components and systems requires the fundamental laws of engineering science be satisfied. These are conservation of mass, momentum, energy, and electrical charge. It is clear that mass and energy conservation have been thoroughly addressed through Eqs (2.7) and (2.21) and that conservation of electrical charge is irrelevant in the present context.

At this point, the curious student may wonder where momentum conservation, or Newton's second law of motion, $\vec{F} = m\vec{a}$, fits into the picture. The momentum equation for developed (that is, nonaccelerating) flow in a straight pipe reduces to a force balance on a flowing fluid and accounts for pressure and shear forces, and ultimately the reaction force, or the force that is required to be applied on the pipe to keep it from moving. If we focus on the fluid flow, Newton's second law enables us to calculate the force arising from pressure and shear on the pipe wall, both of which result from the major and minor losses discussed above (Gerhart et al., 1992). In turn, if we focus on the interaction between the fluid and pipe wall, the pressure and shear force may then be used to calculate the reaction forces in the pipe wall.[22] The reaction forces in the pipe wall may be internal, if the pipe wall itself resists them, or external if the pipe wall needs support from an outside force. Internal reaction forces are normally balanced by the strength of the pipe itself and joints between the pipe and fittings. External reaction forces always require an outside "restraining" force. A good example of this is water flow from a hose when the nozzle at the end of the hose is opened. If the hose is released (or unrestrained), it undulates wildly as the momentum from the discharging water flow seeks a balance by a restraining force. Since this force can come only from the inherent stiffness of the hose, which is flexible, the undulations are the result of the movement of the variable stiffness hose.

Thus, we see that the momentum equation is especially valuable when used to calculate forces required to hold the pipe in place when, in particular, the pipe is not straight. For example, the design of an anchor to tie down the pipe in the region of a 90° elbow needs to begin with the solution of the momentum equation considering the momentum changes in two directions, one leading into the elbow where there is a loss of momentum in one coordinate direction, and the other away from it where there is a gain of momentum in a coordinate direction orthogonal to the first. These types of problems are covered in all textbooks on fluid mechanics in the chapters on the control-volume or open-system formulations of Newton's second law for a flowing fluid.

Another application for the momentum equation relevant to water networks is water hammer. Water hammer is a condition that occurs when the momentum from a flowing liquid is suddenly stopped, such as by the sudden closing of a valve. It is a

[22]The details of this are as follows. The reaction force may be obtained by first solving the problem where the focus is only on the fluid. This means that the control volume surrounds only the fluid. To satisfy equilibrium, we recognize that at the fluid-pipe wall interface, the shear and pressure force acting on the fluid must be balanced by that supplied by the pipe wall. A control volume that focuses on the pipe and the attachment to its surroundings enables the calculation of the reaction force for the pipe.

rapid-transient process and the resulting "shock," similar to that of a sonic-boom or shock wave in the air when disturbed by an explosion or a vehicle moving at a speed from below to above the local speed of sound, produces a pressure wave that travels at high speeds through the fluid, causes noise, and normally results in movement of the pipe. The perturbation could be severe enough to break joints between pipe and fittings, or loosen pipe anchors. This topic is treated in Section 13.17.

Although not of primary interest in the present work, calculations of forces from momentum changes and shear in pipe flows are very important in pipe systems where the successful anchoring of pipe and stresses in the pipe wall and fittings are always critical, such as in power and chemical processing plants, and oil refineries.

2.9 FORCED FLOWS

For comparison purposes, and to broaden the range[23] of use for the analysis and design tools developed in this book, it is of interest to consider the energy equation for pipe flow where the flow is driven by a static pressure at the source, p_1, where $p_1 > 0$. This type of flow is referred to as "forced" and is contrasted with a gravity-driven flow for which $p_1 = 0$. Forced flow, where the flow is driven by a pump (for a liquid) is the primary type of pipe flow considered in an most courses on fluid mechanics. Retaining p_1 in the energy equation, Eqn (2.40) becomes,

$$1 - \frac{p_2 - p_1}{\rho g z_1} - \left[f(\overline{u}, D)\left(\frac{L}{z_1} + \frac{D}{z_1} \sum_{i=1}^{M} \left. \frac{L_e}{D} \right|_i \right) + \frac{D}{z_1}(\alpha_2 + \sum_{i=1}^{N} K_i) \right] \frac{\overline{u}^2}{2gD} = 0 \tag{2.46}$$

If minor losses are negligible, we get

$$1 - \frac{p_2 - p_1}{\rho g z_1} - f(\overline{u}, D)\, \frac{L}{z_1}\, \frac{\overline{u}^2}{2gD} = 0 \tag{2.47}$$

where the L/z_1 appears instead of λ/s [Eqn (2.39)] because it is more convenient to write the pipe length directly in terms of L for the present situation.

If we compare Eqs (2.40) and (2.41) with Eqs (2.46) and (2.47), respectively, we see that their forms are identical provided F takes on the meaning $(p_2 - p_1)/\rho g z_1$ instead of simply $p_2/\rho g z_1$. Thus, we define a modified term, F_{mod}, where

$$F_{mod} = \frac{p_2 - p_1}{\rho g z_1} \tag{2.48}$$

[23] Parts of some networks that are candidates for gravity-driven flow may also be candidates for pump-driven flow. Thus, the fit of the treatment of forced-flow in this text along with gravity-flow is a natural one.

Substituting Eqn (2.48) into Eqn (2.47) the energy equation for the case of minor-lossless forced pipe flow is

$$\frac{z_1(1 - F_{mod})}{L} - f(\overline{u}, D)\frac{\overline{u}^2}{2gD} = 0 \tag{2.49}$$

By comparing Eqs (2.49) with Eqs (2.42) or (2.43), we see that any analysis and design result in this book where F, s, and λ appear in the context of a gravity-driven flow may be applied to a forced-flow problem by simply replacing

- F with F_{mod}
- $\lambda\sqrt{1 + s^{-2}}$ or λ/s (for $s \ll 1$) with the ratio L/z_1.

It is worth noting that in contrast to gravity-driven flow where F is always a positive value, in most cases where the flow is pump or blower-driven[24] $p_1 > p_2$ such that F_{mod} is negative valued. In fact, in many industrial pipe flows, especially where the fluid is a gas, F_{mod} is so large in an absolute-value sense that the contribution from gravity [the 1 in Eqn (2.49)] becomes numerically negligible.

The solution of Eqn (2.49) for D, where through the continuity equation $\overline{u}$ is eliminated in favor of a prescribed volume flow rate Q, is included in several chapters including Chapters 4 and 5.

As a closing comment to this section, a small amount of reasoning can be applied to convince oneself of the validity of the form of the energy equation for a pipe flow like Eqn (2.49). It is most easy to explain for the case of Natural flow, where the pressure at the delivery location is atmospheric, or zero gage pressure. For this case, $F_{mod} = 0$ and Eqn (2.49) is written as

$$\frac{z_1}{L} - f(\overline{u}, D)\frac{\overline{u}^2}{2gD} = 0 \tag{2.50}$$

As noted in Section 2.6.5, the second term in this equation is the head loss per length of pipe, h_L/L. Substituting this into Eqn (2.50), we get the simple result

$$z_1 = h_L,$$

which is simply the obvious statement that the head loss must be equivalent to the elevation for a Natural flow. *Voilà!*

Once the fundamentals of any subject are understood, small exercises like the one just performed here are great for reinforcing our understanding of the material, and to convince ourselves that "we are on the right track." They can also serve the uncertain student by being a point of illumination; much like the proverbial light bulb that suddenly glows over the student's head.

[24]The fluids of interest in this text are liquids, but the energy equation for pipe flow applies to any fluid including gases where, for forced flow, a blower or fan is used.

2.10 SUMMARY

There is a wealth of information in this chapter, so it is worthwhile for the reader to take some time to digest it, reflect, and pursue some of the exercises in Chapter 16. Moving forward from textbox B.2.8, we have discovered that the analysis and design of a gravity-driven (or forced flow, for that matter, as we saw in Section 2.9) network consists of requiring that energy and mass be conserved. Practically, this means that we must be sure that the energy and continuity [Eqn (2.21)] equations are satisfied. The above treatment for a straight pipe reduced the energy equation to a relatively simple form [Eqn (2.33)], especially for minor-lossless flow [Eqn (2.34)]. For the more common case, where the pipe is of arbitrary length, we saw that the energy equation remained nearly unchanged from these forms; the only difference being the inclusion of the tortuosity, λ, for which data show is of the order of 1.2 for small gravity-driven water networks. The most-useful form of the energy equation for our purposes will be Eqn (2.42) or its minor-lossless variant, Eqn (2.45). Considerable attention will be given to the application of these forms of the energy equation in the few chapters that follow.

As discussed in Chapter 1, the classification of single-pipe and multiple-pipe networks allows us to establish a framework that leads to insight and understanding about how gravity-driven water networks perform, in addition to the development of easy-to-use design formulas and charts for the simpler single-pipe networks. Thus, it is important to recognize the characteristics that distinguish the two. In short, a single-pipe network acts as if it is multiple-pipe if it possesses significant local low and high points, and if there is a need to examine the properties of the flow at these points. This was addressed in more detail in Section 2.7.

References

J. J. Allen, M. A. Shockling, G. J. Kunkel, and A. J. Smits. Turbulent flow in rough and smooth pipes. *Trans. Roy. Soc., (London)*, 365:699–714, 2007.

The American Water Works Association. PE Pipe-Design and Installation, Manual of Water Supply Practices, M-55. `http://www.awwa.org`, 2006.

D. A. Anderson. *Modern Compressible Flow*. McGraw Hill, New York, NY, 1990.

D. A. Anderson, J. C. Tannehill, and R. H. Pletcher. *Computational Fluid Mechanics and Heat Transfer*. Hemisphere, New York, NY, 1984.

R. Boyle. *New Experiments in Physico-Mechanicall, Touching the Spring of Air, and its Effects*. H. Hall, Oxford, UK, 1660.

J. B. Brockman. *Introduction to Engineering*. John Wiley & Sons, Inc., Hoboken, NJ, 2009.

G. Brown, J. Rogers, and J. Garbrecht. Task Committee Planning: Darcy Memorial Symposium on the History of Hydraulics. *J. Hydraulic Eng.*, 126(11):799–801, 2000.

S. W. Churchill. Friction factor equation spans all regimes. *Chem. Eng. J.*, 84:91–92, 1977.

S. W. Churchill. Personal communication. 2006.

S. W. Churchill, M. Shinoda, and N. Arai. An appraisal of experimental, predictive and correlative contributions to fully developed turbulent flow in a round tube. *Thermal Sci. Eng.*, 10(2):1–11, 2002.

C. F. Colebrook. Turbulent flow in pipes. *Proc. Inst. Civil Eng.*, 11:133–156, 1938.

C. F. Colebrook. Turbulent flow in pipes with particular reference to the transition region between the smooth and rough pipe laws. *Proc. Inst. Civil Eng.*, 12:393–422, 1939.

C. F. Colebrook and C. M. White. Experiments with fluid-friction in roughened pipes. *Proc. Roy. Soc. (London)*, 161:367–381, 1937.

P. A. Domenico and W. Schwartz. *Physical and Chemical Hydrogeology*. John Wiley & Sons, Inc., New York, NY, 2nd edition, 1998.

R. Ettema. Hunter Rouse - His Work in Retrospect. *J. Hydraulic Eng.*, 132:1248–1258, 2006.

R. W. Fox and A. T. McDonald. *Introduction to Fluid Mechanics*. John Wiley & Sons, Inc., New York, NY, 4th edition, 1992.

P. M. Gerhart, R. J. Gross, and J. I. Hochstein. *Fundamentals of Fluid Mechanics*. Addison Wesley, New York, NY, 1992.

D. D. Gray. *A First Course in Fluid Mechanics for Civil Engineers*. Water Resources Publications, LLC, 1999.

Hydraulic Institute. *The Engineering Data Book, 2nd Edition*. Cleveland, OH, 1990.

T. D. Jordan Jr. *Handbook of Gravity-Flow Water Systems*. ITDG Publication, London, UK, 2004.

L. I. Langelandsvik, G. J. Kunkle, and A. J. Smits. Flow in a commercial steel pipe. *J. Fluid Mech.*, 595:323–339, 2008.

I. Marusic, R. Mathis, and N. Hutchins. Predictive model for wall-bounded turbulent flow. *Science*, 329:193–196, 2010.

B. J. McKeon, C. J. Swanson, M. V. Zagarola, R. J. Donnelly, and A. J. Smits. Friction factors for smooth pipe flow. *J. Fluid Mech.*, 511:41–44, 2004.

B. J. McKeon, M. V. Zagarola, and A. J. Smits. A new friction factor relationship for fuly developed pipe flow. *J. Fluid Mech.*, 538:429–443, 2005.

L. F. Moody. Friction factors for pipe flow. *Trans. ASME*, 66:671, 1944.

B. R. Munson, D. F. Young, and T. H. Okiishi. *Fundamentals of Fluid Mechanics*. John Wiley & Sons, Inc., New York, NY, 2nd edition, 1994.

D. A. Nield and A. Bejan. *Convection in Porous Media*. Springer-Verlag, New York, NY, 1992.

M. C. Potter and D. C. Wiggert. *Mechanics of Fluids*. Brooks/Cole (Thomson), Tampa, FL, 2002.

E. Romeo, C. Royo, and A. Monzón. Improved explicit equations for estimation of the friction factor in rough and smooth pipes. *Chem. Eng. J.*, 86:369–374, 2002.

H. Rouse. Evaluation of boundary roughness. Technical report, Iowa Institute of Hydraulics Research, University of Iowa, Iowa City, IA, 1943.

H. Rouse. Hydraulics in the United States, 1776-1976. Technical report, Iowa Institute of Hydraulics Research, University of Iowa, Iowa City, IA, 1975.

H. Rouse and S. Ince. *History of Hydraulics*. Dover, New York, NY, 1963.

H. Schlichting. *Boundary Layer Theory*. McGraw-Hill, New York, NY, 1979.

M. A. Shockling, J. J. Allen, and A. J. Smits. Roughness effects in turbulent pipe flow. *J. Fluid Mech.*, 564:267–285, 2006.

V. L. Streeter, E. B. Wylie, and K. W. Bedford. *Fluid Mechanics*. McGraw-Hill, New York, NY, 1998.

P. K. Swamee. Design of a submarine oil pipeline. *J. Trans. Eng.*, 119(1):159–170, 1993.

P. K. Swamee and A. K. Jain. Explicit equations for pipe-flow problems. *J. Hydraulic Div., ASCE*, 102(5):657–664, 1976.

P. K. Swamee and A. K. Sharma. *Design of Water Supply Pipe Networks*. John Wiley & Sons, Inc., Hoboken, NJ, 2008.

The Crane Company. *Flow of Fluids Through Valves, Fittings, and Pipe*. New York, NY, 1970.

F. M. White. *Fluid Mechanics*. McGraw-Hill, New York, NY, 4th edition, 1999.

Villanova University engineering and nursing students and faculty in Managua enroute to Waslala, Nicaragua.

CHAPTER 3

PIPE MATERIALS AND DIMENSIONS

"... Give us the tools and we will finish the job."
– W. Churchill, 1941

3.1 INTRODUCTION

In this chapter, we present pipe sizes, dimensions, and pressure ratings for several different kinds of materials and for the dimensioning systems normally used in gravity-driven water networks (iron pipe size, standard diameter ratio, and metric). There is a considerable body of data in this chapter that has been culled and distilled from the many sources referenced herein. Only a few text and handbook sources were found worthwhile in this regard. As seen below, most data come from the technical literature of trade groups like the Plastic Pipe and Fitting Association, and piping manufacturers and marketers. The wide range of materials including metals and plastics, together with vastly different standards that govern pipe sizes and dimensions in different parts of the world, contribute to the lack of ability for the designer to find these data in even a few sources; the search is often challenging and time consuming. For example, the Plastic Piping Handbook (Willoughby et al., 2002) surprisingly presents no dimensional data whatever for plastic pipe. The latest (7th) edition of the Piping

Gravity-Driven Water Flow in Networks. By Gerard F. Jones

Handbook (Nayyar, 2002) contains dimensional data for some pipe (both steel and plastic from the IPS and SDR systems) though not a complete set. Even worse is the near-total absence of data for metric pipe in the available US-based literature.

It is the hope that engineers, engineering students, technologists, and designers will find the pipe data in this chapter useful as a stand-alone final source for at least polyvinyl chloride (PVC), chlorinated polyvinyl chloride (CPVC), and polyethylene (PE), or as a productive first step toward this end.

3.2 PIPE MATERIALS

The industry manufactures pressure pipe from many different types of materials. As the name indicates, pressure pipe is designed to transport fluids under pressure. There are also types of pipe used for liquid service, including water, that are not suitable for internal pressure. Plastic drainage or sewer pipe, where the pressure at any point in the pipe is nearly atmospheric, are examples of this. From everyday observations, most of us are aware that common materials for pressure pipe are steel (pipes supplying natural gas to a heater in many houses in the United States), copper (hot and cold water supply pipes in many houses in the United States), cast iron (sewer pipe in older houses in the United States), and aluminum. The latter two are generally not of interest for gravity-driven water systems because of their cost, weight, and lack of availability in developing regions, among other reasons. In addition to these there are several varieties of plastic pipe including PE (produced in a range of densities); the high-density polyethylene given the abbreviation HDPE, PVC, sometimes abbreviated as PVC-U or uPVC, where U or u stands for unplasticized[1]), CPVC, and acrylonitrile–butadiene–styrene (ABS). Plastic pipe was introduced in the United States around 1940, it is comparably inexpensive, lightweight, rugged and strong, UV-resistant or easily treated to be so, will not corrode like ferrous metals, is immune to attack from most organics and other chemicals in soil, resistant to abrasives at normal flow speeds, and available in many countries around the world. For these reasons, it is normally the candidate of choice for pipe in many applications including many gravity-driven water networks.

Plastic pipe is produced from polymers that belong to a class called *thermoplastics*. Thermoplastics soften with increased temperature and harden upon cooling. A *thermosetting* plastic is a different class that does not have this characteristic. Thermoplastics are ideal for the formation (at elevated temperatures) of extruded tube and other shapes like fittings including elbows, tees, reducers, nut unions, and so on, and valve bodies.

Among all thermoplastic materials, PVC has the largest strength and the least cost per unit volume making it the most commonly used type of plastic pressure pipe. Polyvinyl chloride pipe is rigid and strong. It is sold in lengths ranging from $\approx$10 ft to >6 m ($\approx$20 ft). The preferable method of joining is by solvent cementing, where

[1]Plasticizers may be added to PVC to soften it for use in plastic covers, luggage, and so on. The type of PVC used in the manufacture of pressure pipe is unplasticized making it rigid and stiff.

the inside of the fitting and outside of the pipe are coated with a volatile solvent and quickly joined together. Over a few minutes time, the solvent melts the PVC material in the region of the joint and effectively welds the two pieces together. Heat fusion, where the pipe and fitting are simultaneously heated to their melting point, is not generally used since the melt viscosity of PVC is too large for the two pieces to blend and form a joint with integrity (Nayyar, 2002). Threaded PVC is not common because of the increased installation time and additional equipment and labor to carry this out. If the pipe is to be joined by threading, sch. 80 pipe should be used because the penetration depth of the threads would weaken the joints of a thinner pipe wall.

The impact strength of PVC is very low. As such, the pipe should be buried underground where possible in a stabilized or backfilled trench with a depth of ≈ 1 m. The use of sharp rock or stone near the pipe should be avoided in favor of fine gravel or sand. Depths >6 m should be avoided to reduce the possibility of too large an earth loading. Burying also protects the pipe from the UV part of solar radiation that, over time, can make the pipe brittle. Most types of PVC pipe have additives to resist UV which will often be indicated on the pipe outside diameter (OD) (Plastic Pipe & Fittings Association , PPFA). For exposed pipe that is not treated with these additives, painting the outside of it with a light-colored latex or water-based acrylic paint will protect the pipe. Exposure of the pipe to UV during installation is normally not a problem.

Both PVC and PE pipe have smooth inside surfaces. The absolute roughness, as noted in Chapter 2, is $\approx 5 \times 10^{-6}$ ft $\pm 60\%$ (White, 1999) and is about 100 times less rough than steel or galvanized iron. Thus, PVC pipe has very good abrasion resistance from particulates that may find their way into the water flow.

Expansion of PVC and PE pipe need not be accommodated (say, with expansion joints) in situations where the pipe is buried because the temperature of the water and its surroundings are approximately equal. Long runs of straight pipe of large diameter, say 4 in. or more, should have expansion accounted for if the pipe is run above ground. Often, several 90° elbows are adequate for this purpose.

The PE pipe is available in a range of densities. Low-density PE is relatively flexible and, for the smaller diameters, is often found in spooled form. Medium-density PE pipe is less flexible, and high-density PE pipe is the most rigid. Coiled PE pipe has the advantage of much longer native lengths than PVC, say in the hundreds of feet. This feature requires fewer joints in the system and a subsequent saving on labor and installation time. The reliability of the system also increases relative to that of PVC because of the fewer number of joints.

The joining process for PE pipe is not as simple as that for PVC. The PE pipe cannot be joined by solvent cementing. For small pipe sizes, PE pipe may be joined by insert fittings or compression fittings. Insert fittings fit tightly inside the pipe and compression fittings fit over the outside of the pipe. For large PE pipe sizes, a butt-fusion process is required where a tool heats the two pieces to be joined to their melting temperature to establish a weld. This machine requires electrical power and movement into remote locations. Thus, large-size PE pipe would not be suitable for use in cases where electrical power is not available.

3.3 THE DIFFERENT CONTEXTS FOR PIPE DIAMETER

There are two contexts in which we deal with pipe diameter. The first is a calculation from an equation that produces the inside diameter, D, for a pipe. This is the *theoretical* value for the pipe inside diameter needed to satisfy a prescribed set of conditions for a design. In this context, D will almost always be an irrational number that we write to two-to-four significant digits of accuracy. It is not, however, the pipe diameter that will be installed for a given design. This is the second context. The manufacturers of pipe of all kinds, including plastic, steel, copper, and so on, produce pipe in "nominal" sizes, such as $\frac{3}{4}$ in., 1 in., and so forth. The nominal diameter is not the inside or outside diameter, but a label that loosely characterizes the size of the pipe. Because the nominal pipe size is a label and not an actual number for the inside diameter, in this book we will generally write the nominal pipe sizes as, say, $1\frac{1}{2}$ in. instead of the decimal representation, 1.5 in.

The worldwide standard of specifying pipe by its nominal size, rather than an actual dimension, and the fact that a pipe has at least two dimensions (wall thickness, inside diameter, or outside diameter) that may, in principle, be independently specified, necessitate a mapping of sorts between nominal size and actual pipe dimensions. These will be explored for different pipe materials in the sections that follow.

3.4 SYSTEMS FOR SPECIFYING PIPE DIMENSIONS

In this section, we will discuss the most common systems that define the dimensions of pipe normally used for gravity-driven water networks. There are two categories within this framework. The first are the English-based systems including the Iron Pipe Size (IPS) and the Copper Tube Size (CTS). The pipe in these systems appears in the United States as well as in many other developed and developing countries outside the United States. The second is the metric-based system. Metric pipe enjoys mostly international use and is not widely available or installed in the United States. The Standard Diameter Ratio (SDR) series, described below, spans both the English- and metric-based classifications and is perhaps the widest used system for the specification of pipe dimensions.

3.4.1 English-Based Pipe Sizes

The most commonly used system for pipe dimensions in this category is IPS. Cast iron, ductile iron, steel (plain or galvanized inside and outside the pipe to help prevent corrosion), and nearly all plastic pipe is manufactured to meet the dimensional specifications, including diameters and wall thicknesses, of the IPS system. Copper tube, which is not generally used for the present application because of its cost and subsequent lack of good availability, follows the CTS system, which is different than IPS. In the CTS system, the outside diameter of the tube is $\frac{1}{8}$-in. larger than the nominal tube size. For a fixed pipe size, the inside diameter decreases in value with increased pressure rating and thus increased wall thickness. There are three wall thicknesses

available when choosing a copper tube: type "K" tube pertains to thick wall, type "L" tube standard wall thickness, and type "M" tube thin wall. Domestic hot water systems of copper tube typically use a wall thickness corresponding to type L.

For a given pipe diameter, the wall thickness determines the maximum allowable working pressure. If the wall thickness for an IPS pipe is of a standard value, we refer to this pipe as "schedule 40" or a sch. 40 wall thickness. For higher-pressure resistance pipe, the terminology for an IPS pipe is "schedule 80" or a sch. 80 wall thickness. Pipe dimensions for the IPS series of pipe sizes are designed so that the outside diameter is independent of the wall thickness. Thus, sch. 40 and 80 pipes of the same nominal pipe size have the same outside diameter so that they can both use the same fittings (like elbows and tees), which require that the pipe be fit into them; for this reason the IPS system is sometimes referred to as an "outside diameter controlled" system. Pipe walls thicker than sch. 80 (schedules 120, 160, etc.) are manufactured, but these are generally not needed or used for gravity-driven water systems.

The correspondence between nominal pipe sizes and actual dimensions for schedule, 40 and 80 IPS pipe is given in Tables 3.1 and 3.2 (Fox and McDonald, 1992; Gagliardi and Liberatore, 2002) for the range of pipe sizes normally used in gravity-driven water systems. Note that there are relatively few nominal sizes from among which to choose; a result of manufacturing companies producing just a few nominal sizes of a pipe of a particular material, and local suppliers of the pipe who choose to stock only a few nominal sizes. This is one small example of the interplay between economics and engineering in real-world terms.

The dimensions of plastic pipe can alternately be characterized by another outside-diameter-controlled series referred to as the "Standard Diameter Ratio" (SDR) system[2] or series. The objective of this system is to maintain equal pressure ratings for all pipe diameters of a fixed type of pipe material. In the SDR system, this is accomplished by increasing the wall thickness in direct proportion to the OD of the pipe[3]. Thus, *SDR is defined as the ratio of the outside diameter to the minimum wall thickness*. Rated pressures are larger for pipes that have smaller SDR values (that is, larger wall thicknesses for a given pipe OD) and vice versa. With the SDR series, there may be many more wall thickness (that is, pressure rating) choices available compared with IPS pipe. For example, a particular type of 2-in. nominal plastic pipe that has an outside diameter of 2.375 in. (consistent with the OD of sch. 40 and sch. 80 IPS pipe) is manufactured with SDR values of 7.3, 9.0, 11.0, 13.5, and 17.0[4]. Recall from the discussion above that only two commonly used wall thickness for the IPS system, schedules 40 and 80. Since the SDR system is OD controlled, any

[2]This is sometimes referred to as the SDR–PR system or series where PR refers to pressure rating. Also, there exists a less-popular, inside-diameter-controlled series called *SIDR*. Information on this series, which is not covered in this book, can be found mostly in the trade literature.

[3]The formula for the circumferential or "hoop" stress in a pipe (referred to as a "thin-wall" pipe because the wall thickness is much smaller than the pipe radius) shows that for a given material the ability of the pipe to resist internal pressure is proportional to the ratio of wall thickness and pipe diameter.

[4]Note that each number differs from the previous one by ~25%. This has the effect of producing pressure ratings in approximately the same steps; 25% smaller than that for the previous SDR value.

Table 3.1 Correspondence Between Nominal Pipe Sizes and Actual Dimensions for sch. 40 IPS Pipe

Nominal Size (in.)	Outside Diameter (in.)	Max. Inside Diameter (in.)	Min. Wall Thickness (in.)	Equivalent SDR
$\frac{1}{2}$	0.840	0.622	0.109	7.71
$\frac{3}{4}$	1.050	0.824	0.113	9.29
1	1.315	1.049	0.133	9.88
$1\frac{1}{2}$	1.900	1.610	0.145	13.1
2[a]	2.375	2.067	0.154	15.4
$2\frac{1}{2}$	2.875	2.469	0.203	14.2
3	3.500	3.068	0.216	16.2
$3\frac{1}{2}$	4.000	3.548	0.226	17.7
4[b]	4.500	4.026	0.237	19.0
5	5.563	5.047	0.258	21.6
6	6.625	6.065	0.280	23.7
8	8.625	7.981	0.322	26.8
10	10.75	10.02	0.365	29.5
12	12.75	12.00	0.375	34.0

[a]Note the local increase in SDR for 2-in. pipe indicating a reduction in the relative wall thickness for this size compared with the neighboring sizes.
[b]The inside diameter is within 1% of the nominal size for nominal size of 4 in. and larger.

Table 3.2 Correspondence Between Nominal Pipe Sizes and Actual Dimensions for sch. 80 IPS pipe

Nominal Size (in.)	Outside Diameter (in.)	Max. Inside Diameter (in.)	Min. Wall Thickness (in.)	Equivalent SDR
$\frac{1}{2}$	0.840	0.546	0.147	5.71
$\frac{3}{4}$	1.050	0.742	0.154	6.82
1	1.315	0.957	0.179	7.35
$1\frac{1}{2}$	1.900	1.500	0.200	9.50
2	2.375	1.939	0.218	10.9
$2\frac{1}{2}$	2.875	2.323	0.276	10.4
3	3.500	2.900	0.300	11.7
$3\frac{1}{2}$	4.000	3.364	0.318	12.6
4	4.500	3.826	0.337	13.4
5	5.563	4.813	0.375	14.8
6	6.625	5.761	0.432	15.3
8	8.625	7.625	0.500	17.3
10	10.75	9.594	0.593	18.1
12	12.75	11.376	0.687	18.6

given nominal pipe size will be able to use the same fittings whether it is SDR or IPS based; only the wall thickness, and thus pressure rating, will differ depending on the schedule (if IPS based) or SDR (if SDR based).

We present pressure ratings for PVC (and CPVC), PE, and ABS IPS series pipe in Tables 3.3 and 3.4 for the most commonly available SDR-series PVC pipe. Our inspection of the latter table reveals that SDR 26 is probably the most recommended wall thickness, with a pressure rating of 160 psig, for SDR-series, PVC pipe. From Table 3.3 for IPS pipe, sch. 40 should be used in most cases for all plastic pipe. In networks of PVC pipe where the pipe is joined by threading instead of the normal solvent cementing, sch. 80 is recommended to improve reliability in the joint regions by having a thicker-wall pipe. For PE pipe, the pressure ratings are considerably smaller than PVC for the same schedule and pipe size. This may necessitate using sch. 80 PE pipe for the larger pipe sizes in certain instances where pressure ratings >90 psig are needed. Dimensions and pressure ratings for a broad range of SDR-series, PVC pipe appear in Table 3.5.

Note that the local reduction in pressure ratings for the 2-in. nominal IPS pipe size, as seen in Table 3.3 for ABS, PVC (and CPVC), and PE materials, is the result of the dimensions for this pipe size. This is explained by noting that the equivalent SDR (see Tables 3.1 and 3.2 for these) for 2-in. pipe is locally high compared with the neighboring pipe sizes indicating a relatively thinner wall thickness for 2-in. nominal IPS pipe. For conversion purposes, note that 100 psig is equivalent to 70.31 m of water head.

Dimensions and pressure ratings for a range of SDR-series, English-based PE pipe is presented in Table 3.6 where, as with the recommended pressure rating for PVC from above, SDR 11 is the recommended wall thickness for PE pipe with a pressure rating of 160 psig.

3.4.2 Metric Pipe Sizes

Though not used very often, if at all, in the United States, metric-dimensioned PVC and PE pressure pipe is used throughout the rest of the world. In central America, as well as many other locations, both English- and metric-based pipe enjoy wide use. Manufacturing facilities in Asia, Europe, England, Australia, and New Zealand produce metric pipe to various standards. Unfortunately, the differences in the standards can create considerable uncertainty in availability and the correspondence between actual dimensions and nominal metric sizes. Dimensional and pressure-ratings data for metric-based, SDR series PVC pipe are presented in Tables 3.7 and 3.8 and in Tables 3.9 and 3.10 for metric-based, SDR-series PE pipe. For metric pipe, the pressure rating is defined through a "PN" (*pressure nominel*) value. In Table 3.11, the mapping between the PN value and pressure in various units is displayed.

One thing to note by inspecting Tables 3.7–3.10 is that the OD and nominal pipe size (sometimes referred to as the "DN" or *diametre nominel*) are equal for the metric-based plastic pipe manufactured to the standards on which these tables are based. As briefly noted above, there are several different standards, normally associated with distinct geographic regions of the world, that when followed produces pipe with

Table 3.3 Pressure Rating (in psig) at 73.4°F for Selected Types of IPS series, English-Based Plastic Pipe

Nominal	ABS Pipe[a]		PVC & CPVC Pipe[a]		PE Pipe[a]	
Size (in.)	Sch. 40	Sch. 80	Sch. 40	Sch. 80	Sch. 40	Sch. 80
$\frac{1}{2}$	480	680	600	850	240	340
$\frac{3}{4}$	390	550	480	690	195	275
1	360	500	450	630	180	250
$1\frac{1}{2}$	260	380	330	470	130	190
2	220	320	280	400	110	160
$2\frac{1}{2}$	240	340	300	420	120	170
3	210	300	260	370	105	150
$3\frac{1}{2}$	190	280	240	350	95	140
4	180	260	220	320	90	130
5	160	230	190	290	80	115
6	140	220	180	280	70	110
8	120	200	160	250	60	100
10	110	190	140	230	55	95
12	110	180	130	230	55	90

[a]From Plastic Pipe & Fittings Association (PPFA) and Harvel Plastics, Inc. (2005–2006).

Table 3.4 Dimensions and Pressure Ratings for Common SDR-Series, English-Based PVC Pipe

Nominal Size (in.)	Outside Diameter (in.)	Inside Diameter (in.)	Min. Wall Thickness (in.)	SDR	Pressure Rating[a] (psig)
$\frac{1}{2}$	0.840	0.696	0.062	13.5	315
$\frac{3}{4}$	1.050	0.910	0.060	21.0	200
1	1.315	1.175	0.060	26.0	160
$1\frac{1}{2}$	1.900	1.734	0.064	26.0	160
2	2.375	2.173	0.073	26.0	160
$2\frac{1}{2}$	2.875	2.635	0.091	26.0	160
3	3.500	3.210	0.110	26.0	160
$3\frac{1}{2}$	4.000	3.672	0.135	26.0	160
4	4.500	4.134	0.173	26.0	160
5	5.563	5.108	0.214	26.0	160
6	6.625	6.084	0.255	26.0	160
8	8.625	7.921	0.332	26.0	160
10	10.75	9.874	0.413	26.0	160
12	12.75	11.711	0.490	26.0	160

[a]Temperature is based on 73.4°F. Note that the pressure rating corresponds only to the SDR value, which is the objective of this series, and that the OD corresponds to the IPS series for the given nominal size (see Tables 3.1 or 3.2). The ratio of OD to the min. wall thickness is not exactly equal to SDR because of dimensional tolerances. The same reason applies to any inequality between OD-2·Wall Thickness and ID (Gagliardi and Liberatore, 2002; Harvel Plastics, Inc., 2005–2006).

Table 3.5 Dimensions and Pressure Ratings for SDR series, English-Based PVC Pipe[a]

Nominal Size (in.)	SDR 13.5 315 psig		SDR 21 200 psig		SDR 26 160 psig		SDR 32.5 125 psig		SDR 41 100 psig	
	ID	Wall	ID	Wall	ID	Wall	ID	Wall	ID	Wall
$\frac{1}{2}$	0.696	0.062								
$\frac{3}{4}$			0.910	0.060						
1			1.169	0.063	1.175	0.060				
$1\frac{1}{2}$			1.700	0.090	1.734	0.073	1.780	0.060		
2	2.023	0.176	2.129	0.113	2.173	0.091	2.229	0.073		
$2\frac{1}{2}$	2.449	0.213	2.581	0.137	2.635	0.110	2.699	0.088		
3	2.982	0.259	3.146	0.167	3.210	0.135	3.284	0.108	3.330	0.085
$3\frac{1}{2}$			3.597	0.190	3.672	0.154				
4	3.834	0.333	4.046	0.214	4.134	0.173	4.224	0.138	4.280	0.110
5			5.001	0.265	5.108	0.214	5.221	0.171	5.291	0.136
6			5.955	0.316	6.084	0.255	6.217	0.204	6.301	0.162
8			7.805	0.410	7.961	0.332	8.095	0.265	8.205	0.210
10			9.728	0.511	9.924	0.413	10.088	0.331	10.226	0.262
12			11.538	0.606	11.770	0.490	11.966	0.392	12.128	0.311

[a]Temperature is based on 73.4°F. ID is inside diameter (in.) and Wall is minimum wall thickness (in.). The OD corresponds to the IPS series for the given nominal size (see Tables 3.1 or 3.2). The ratio of OD to the min. wall thickness is not exactly equal to SDR because of dimensional tolerances. The same reason applies to any inequality between OD-2·Wall Thickness and ID. From Crestline-West Inc.; Harvel Plastics, Inc. (2005–2006); CertainTeed Corp. (2005).

Table 3.6 Dimensions and Pressure Ratings for SDR Series, English-Based PE Pipe[a]

Nom. Size (in.)	SDR 7.3 254 psig		SDR 9 200 psig		SDR 11 160 psig		SDR 13.5 128 psig		SDR 17 100 psig	
	ID	Wall	ID	Wall	ID	Wall	ID	Wall	ID	Wall
$\frac{1}{2}$	0.600	0.115	0.650	0.093	0.680	0.076				
$\frac{3}{4}$	0.750	0.144	0.816	0.117	0.850	0.095				
1	0.940	0.180	1.023	0.146	1.070	0.120				
$1\frac{1}{2}$	1.349	0.260	1.453	0.211	1.533	0.173	1.601	0.141		
2	1.686	0.325	1.815	0.264	1.917	0.216	2.002	0.176	2.078	0.140
3	2.485	0.479	2.675	0.389	2.826	0.318	2.915	0.259	3.063	0.206
4	3.194	0.616	3.440	0.500	3.633	0.409	3.794	0.333	3.938	0.265
5	3.948	0.762	4.253	0.618	4.490	0.506	3.469	0.412	4.870	0.327
$5\frac{3}{8}$	3.815	0.736	4.109	0.597	4.338	0.489	4.531	0.398	4.705	0.316
6	4.700	0.908	5.065	0.736	5.349	0.602	5.584	0.491	5.798	0.390
8	6.261	1.182	6.709	0.958	7.057	0.784	7.347	0.639	7.611	0.507
10	7.804	1.473	8.362	1.194	8.796	0.977	9.158	0.796	9.486	0.632
12	9.256	1.747	9.916	1.417	10.432	1.159	10.862	0.944	11.25	0.750

[a]Temperature is based on 73.4°F. ID is inside diameter (in.) and Wall is minimum wall thickness (in.). The OD corresponds to the IPS series for the given nominal size (see Tables 3.1 or 3.2). The ratio of OD to the min. wall thickness is not exactly equal to SDR because of dimensional tolerances. The same reason applies to any inequality between OD-2·Wall Thickness and ID. From American Water Works Association (2006); The Plastic Pipe & Fittings Association (2002); PolyPipe, Inc. (2005).

considerably different specifications for the same nominal sizes. For example, the Islex dimensional data (Islex, 2005) for PVC pipe differs greatly from that in the above referenced tables. The Australian/New Zealand standard is AS/NZS 1477:1999 for PVC pipe, whereas the PVC pipe data in Tables 3.7 and 3.8 are based on standard ISO4422-2 (International Organization for Standardization, 1996). Dimensional data for PVC pipe from British and Chinese manufacturers appear to follow the latter standard. There is evidently little or no difference between the PE pipe manufactured in Australia and New Zealand and that made elsewhere in the world, however.

The main message for the designer to be derived from this discussion is the need to obtain reliable information on local pipe materials and dimensions certainly before finalizing a design, but perhaps even before beginning it. Engineering tradeoffs on the pipe sizes for a system and their availability from near (say, local hardware stores) and remote sources (like plumbing supply houses in larger but more-distant cities) will need to be considered. For example, larger and more costly pipe from a local supplier may be more economical than smaller sizes once the transportation and delivery costs are factored into the design.

As a final note on this topic, the United States and other countries sometimes report metric-based sizes for IPS series pipe. Table 3.12 shows this conversion that is sometimes referred to as a "soft metric conversion". Note that the pipe having these metric dimensions is not metric pipe but IPS series pipe with its English units converted to the metric system.

3.5 CHOOSING AN APPROPRIATE NOMINAL PIPE SIZE

When the designer calculates the theoretical value for the inside diameter, D, from the energy equation he/she must choose an appropriate corresponding nominal pipe size[5]. Normally, the choice is made for the nominal size that produces an inside diameter slightly larger than the theoretical value.[6] The logic here is that a pipe of diameter slightly greater than that required by theory will, for a fixed pressure drop, accommodate more flow than that required for the design. For the end user, having more flow is usually better than less, at least in the situations where it can indeed be supplied; the larger-than-theoretical pipe size can be viewed as a safety factor of sorts. Alternately, for a fixed water flow rate, a larger pipe diameter will produce larger static pressures along the flow path (for a fixed flow rate the flow in a larger pipe diameter will have less friction since the flow speed is reduced). Higher pressures give the designer more flexibility since the flow will have more energy. This point is subtle. Pressure energy can always be *dissipated* in a pipe flow by using an energy dissipation device like a throttling valve but, once potential energy is converted into

[5]Note that the designations ID, OD, and Wall are labels for dimensions of pipe. D and ID have the same reference but D is a mathematical symbol whereas ID is a label.

[6]One exception to this is when the theoretical size is just slightly larger than that for a nominal size. In this case the choice is made for the nominal size that produces an inside diameter slightly smaller than the theoretical value. Also note that the need for an increase in water flow rate due to population growth in the future is *systematically* accounted for in the design. This topic is treated in Chapter 13.

Table 3.7 Dimensions and Pressure Ratings for SDR Series, Metric-Based PVC Pipe[a]

Nom. Size and OD (mm)	SDR 9 PN 25		SDR 13.6 PN 16		SDR 17 PN 12.5		SDR 21 PN 10	
	Min. Wall Thickness (mm)	ID (mm)	Min. Wall Thickness (mm)	ID (mm)	Min. Wall Thickness (mm)	ID (mm)	Min. Wall Thickness (mm)	ID (mm)
16	1.8	12.4	1.5 [1.2]	13.0 [13.6]				
20	2.3	15.4	1.5 (2.0) [1.5]	17.0 (16.0) [17.0]				
25	2.8	19.4	1.9 (2.0) [1.9]	21.2 (21.0) [21.2]	1.5	22.0		
32	3.6	24.8	2.4 (2.4) [2.4]	27.2 (27.2) [27.2]	1.9 (2.0)	28.2 (28.0)	1.6	28.8
40	4.5	31.0	3.0 (3.0) [3.0]	34.0 (34.0) [34.0]	2.4 (2.4)	35.2 (35.2)	1.9 (2.0)	36.2 (36.0)
50	5.6	38.8	3.7 (3.7) [3.7]	42.6 (42.6) [42.6]	3.0 (3.0)	44.0 (44.0)	2.4 (2.4)	45.2 (45.2)
63	7.1	48.8	4.7 (4.7) [4.7]	53.6 (53.6) [53.6]	3.8 (3.8)	55.4 (55.4)	3.0 (3.0)	57.0 (57.0)
75	8.4	58.2	5.6 (5.6) [5.6]	63.8 (63.8) [63.8]	4.5 (4.5)	66.0 (66.0)	3.6 (3.6)	67.8 (67.8)
90	10.1	69.8	6.7 (6.7) [6.7]	76.6 (76.6) [76.6]	5.4 (5.4)	79.2 (79.2)	4.3 (4.3)	81.4 (81.4)
110			8.1 (7.2) [8.1]	93.8 (95.6) [93.8]	6.6 (5.7)	96.8 (98.6)	5.3 (4.8)	99.4 (100.4)
125			9.2	106.6	7.4 (7.4)	110.2 (110.2)	6.0 (6.0)	113.0 (113.0)
140			10.3	119.4	8.3 (8.3)	123.8 (123.8)	6.7 (6.7)	126.6 (126.6)
160			11.8	136.4	9.5 (9.5)	141.0 (141.0)	7.7 (7.7)	144.6 (144.6)
180			13.3	153.4	10.7	158.6	8.6	162.8
200			14.7	170.6	11.9	176.2	9.6	180.8
225			16.6	191.8	13.4	198.2	10.8	203.4
250			18.4	213.2	14.8	220.4	11.9	226.2
280			20.6	238.8	16.6	246.8	13.4	253.2
315			23.2	233.6	18.7	242.6	15.0	250.0

[a]Temperature is based on 20°C. ID is inside diameter. OD is outside diameter. The mapping between PN and pressure is given in Table 3.11. See continuation of this table in Table 3.8. From ISO4422-2, International Organization for Standardization (1996). Parenthetical values from Fujian Zhenyun Plastic Industry Co., Ltd.. Square bracketed quantities from ISO15493, International Organization for Standardization (2003).

Table 3.8 Dimensions and Pressure Ratings for SDR Series, Metric-Based PVC Pipe[a]

Nom. Size and OD (mm)	SDR 26 PN 8		SDR 33 PN 6.3		SDR 34.4 PN 6		SDR 41 PN 5	
	Min. Wall Thickness (mm)	ID (mm)	Min. Wall Thickness (mm)	ID (mm)	Min. Wall Thickness (mm)	ID (mm)	Min. Wall Thickness (mm)	ID (mm)
16								
20								
25								
32								
40	1.6	36.8	1.5	37.0				
50	2.0 (2.0)	46.0	1.6	46.8				
63	2.5 (2.5)	58.0	2.0	59.0	1.9 (2.0)	59.2 (59.0)	1.6	59.8
75	2.9 (2.9)	69.2	2.3	70.4	2.2 (2.2)	70.6 (70.6)	1.9	71.2
90	3.5 (3.5)	83.0	2.8	84.4	2.7 (2.7)	84.6 (84.6)	2.2	85.6
110	4.2 (3.9)	101.6 (102.2)	3.4	103.2	(3.2)	(103.6)	2.7	104.6
125	4.8 (4.4)	115.4 (116.2)	3.9	117.2	(3.7)	(117.6)	3.1	118.8
140	5.4 (4.9)	129.2 (130.2)	4.3	131.4	(4.1)	(131.8)	3.5	133.0
160	6.2 (5.6)	147.6 (148.8)	4.9	150.2	(4.7)	(150.6)	4.0	142.0
180	6.9	166.2	5.5	169.0			4.4	171.2
200	7.7	184.6	6.2	187.6			4.9	190.2
225	8.6	207.8	6.9	211.2			5.5	214.0
250	9.6	230.8	7.7	234.6			6.2	237.6
280	10.7	258.6	8.6	262.8			6.9	266.2
315	12.1	290.8	9.7	295.6			7.7	299.6

[a]Temperature is based on 20°C. ID is inside diameter. OD is outside diameter. The mapping between PN and pressure is given in Table 3.11. See continuation of this table in Table 3.7. From ISO4422-2, International Organization for Standardization (1996). Parenthetical values from Fujian Zhenyun Plastic Industry Co., Ltd..

Table 3.9 Dimensions and Pressure Ratings for SDR Series, Metric-Based PE Pipe[a]

	SDR 9		SDR 11		SDR 13.6		SDR 17	
PE 80 PE 100	PN 16 PN 20		PN 12.5 PN 16		PN 10 PN 12.5		PN 8 PN 10	
Nom. Size (mm)	Min. Wall Thickness (mm)	ID (mm)	Min. Wall Thickness (mm)	ID (mm)	Min. Wall Thickness (mm)	ID (mm)	Min. Wall Thickness (mm)	ID (mm)
16	1.8	12	1.6	13	1.6	13	1.6	13
20	2.2	16 (15.4)	1.6	17	1.6	17	1.6	17
25	2.8	19	2.3	20	1.9	21	1.6	22
32	3.6	26 (24.6)	2.9	26	2.4	27 (27.4)	1.9	28
40	4.4	31	3.6	33	2.9	34	2.4	35
50	5.6	39 (38.8)	4.5	41	3.7	43 (42.8)	2.9	44
63	7.0	49 (48.8)	5.7	52	4.6	54 (54)	3.7	56
75	8.3	58	6.8	61	5.5	64	4.4	66
90	10.0	70 (69.8)	8.2	74	6.6	77 (77.2)	5.3	79
110	12.2	86	10	90	8.1	94	6.5	97
125	13.9	96	11.4	102	9.2	107	7.4	110
140	15.6	109	12.7	115	10.3	119	8.2	124
160	17.8	124	14.5	131	11.8	138	9.4	141

[a]Temperature is based on 20°C. ID is inside diameter. The minimum value for the outside diameter is equal to the nominal size. The mapping between PN and pressure is given in Table 3.11. The PE number corresponds to the strength of the polyethylene used in the pipe; PE 100 is stronger than PE 80. Parenthetical numbers correspond to the dimensions from Jordan Jr. (2004) for Class III (normal-wall; SDR 9) and Class IV (thick-wall; SDR 13.6) HDPE pipe. See continuation of this table in Table 3.10. From Islex (2005); The Engineering Toolbox (2010). The dimensions generally agree with those reported by Durapipe (2005).

Table 3.10 Dimensions and Pressure Ratings for SDR Series, Metric-Based PE Pipe[a]

	SDR 21		SDR 26		SDR 33		SDR 41	
PE 80 PE 100	PN 6.3 PN 8		PN 6.3		PN 4		PN 3.2 PN 4	
Nom. Size (mm)	Min. Wall Thickness (mm)	ID (mm)	Min. Wall Thickness (mm)	ID (mm)	Min. Wall Thickness (mm)	ID (mm)	Min. Wall Thickness (mm)	ID (mm)
16	1.6	13	1.6	13	1.6	13	1.6	13
20	1.6	17	1.6	17	1.6	17	1.6	17
25	1.6	22	1.6	22	1.6	22	1.6	22
32	1.6	29	1.6	29	1.6	29	1.6	29
40	1.9	36	1.6	37	1.6	37	1.6	37
50	2.4	45	2.3	46	1.6	47	1.6	47
63	3.0	57	2.4	58	2	59	1.6	60
75	3.6	68	2.9	69	2.3	70	1.9	71
90	4.3	81	3.5	83	2.7	84	2.2	86
110	5.2	100	4.2	102	3.3	103	2.7	105
125	6.0	113	4.8	115	3.8	117	3.1	119
140	6.7	127	5.4	129	4.2	131	3.5	133
160	7.6	145	6.2	148	4.8	150	4.0	152

[a]Temperature is based on 20°C. ID is inside diameter. The minimum value for the outside diameter is equal to the nominal size. The mapping between PN and pressure is given in Table 3.11. The PE number corresponds to the strength of the polyethylene used in the pipe; PE 100 is stronger than PE 80. See continuation of this table in Table 3.9. From Islex (2005); The Engineering Toolbox (2010). The dimensions generally agree with those reported by Durapipe (2005).

Table 3.11 Mapping Between PN and Pressure for Metric-Based Pipe

PN	Head of water (m)	kPa	Head of water (ft)	psig	bar[a]	Class
3.2	32	320	105	47	3.2	
4	40	400	131	58	4	
6.3	63	630	207	92	6.3	~B (6 bar)
8	80	800	262	117	8	~C (9 bar)
10	100	1000	328	147	10	~C (9 bar)
12.5	125	1250	410	183	12.5	~D (12 bar)
16	160	1600	524	235	16	
20	200	2000	655	294	20	

[a]One bar is 100 kPa which is approximately 1 atm (101.325 kPa or 14.7 psia). From Islex (2005); Plastics Industry Pipe Association of Australia, Ltd. (2010).

Table 3.12 The Metric Equivalent of IPS series sch. 40 and 80 Nominal Pipe Sizes

Nominal Size[a]		Outside Diameter	Sch.	Min. Wall Thickness	Inside Diameter
(IPS - in.)	(Metric - mm)	(mm)		(mm)	(mm)
$\frac{1}{2}$	15	21.336	40	2.769	15.798
			80	3.734	13.868
$\frac{3}{4}$	20	26.670	40	2.870	20.930
			80	3.912	18.846
1	25	33.401	40	3.378	26.645
			80	4.547	24.307
$1\frac{1}{2}$	40	48.260	40	3.683	40.894
			80	5.080	38.100
2	50	60.325	40	3.912	52.501
			80	5.537	49.251
$2\frac{1}{2}$	65	73.025	40	5.156	62.713
			80	7.010	59.005
3	80	88.900	40	5.486	77.928
			80	7.620	73.660
$3\frac{1}{2}$	90	101.60	40	3.048	95.504
			80	5.740	90.120
4	100	114.30	40	6.020	102.26
			80	8.560	97.180
6	150	168.28	40	7.112	167.77
			80	10.97	146.33

[a]See Tables 3.1 and 3.2 for the equivalences in English units. Note that the actual inside diameters and wall thicknesses of metric dimensioned pipe can vary especially in developing regions where dimensional standards for pipe may be different than other regions or not followed. From The Engineering Toolbox (2010).

pressure energy in a gravity-driven water network, energy from the outside is never *added* to the flow. A companion consideration is that the local slope of the pipe is determined by the contour of the ground; it cannot be simply adjusted as needed by the designer to add potential energy. This scenario is in contrast to a pumped-water network where a larger or additional pump may perhaps be added where needed to meet the design specifications.

In summary, the choice of a larger pipe diameter than required by the solution of the energy equation adds *flexibility* to the values of the flow parameters including flow rate and static pressure at the delivery location by use of a throttling valve. Throttling valves are discussed in greater detail in Sections 4.7, 11.6.5, and 13.14.

In addition to footnote 6, there may be cases encountered where it is desirable to choose a nominal pipe size corresponding to a slightly smaller diameter. Examples of this are in designs where costs need to be tightly controlled, since larger pipe sizes are more costly, or where the choice of the larger pipe produces a flow speed well below that recommended to prevent the internal build-up of debris. A composite pipe, two series-connected pipes of different diameters as discussed in Section 13.16, may be used in place of a single pipe to more-precisely match the design constraints for a pipe network.

Some details on these topics and the broader problem of designing a pipe having too large a diameter for a prescribed flow rate are considered in Chapter 13.

References

The American Water Works Association. PE Pipe-Design and Installation, Manual of Water Supply Practices, M-55. `http://www.awwa.org`, 2006.

CertainTeed Corp. Certainteed Pressure Pipe. `http://www.certainteed.com`, 2005.

Crestline-West Inc. `http://www.crestline.com`.

Durapipe. `http://www.durapipe.co.uk`, 2005.

R. W. Fox and A. T. McDonald. *Introduction to Fluid Mechanics*. John Wiley & Sons, Inc., New York, NY, 4th edition, 1992.

Fujian Zhenyun Plastic Industry Co., Ltd. `http://www.Zhenyunplastic.com`.

M. G. Gagliardi and L. J. Liberatore. *Piping Handbook*, chapter on Water Systems Piping. McGraw-Hill, New York, NY, 7th edition, 2002.

Harvel Plastics, Inc. `http://www.harvel.com`, 2005–2006.

International Organization for Standardization. Pipe and Fittings Made of Unplasticized PVC for Water Supply - Specifications. `http://www.iso.org`, 1996.

International Organization for Standardization. Plastic Piping Systems for Industrial Applications. `http://www.iso.org`, 2003.

Islex. http://www.islex.com.au, 2005.

T. D. Jordan Jr. *Handbook of Gravity-Flow Water Systems.* ITDG Publication, London, UK, 2004.

M. L. Nayyar. *Piping Handbook.* McGraw-Hill, New York, NY, 7th edition, 2002.

The Plastic Pipe & Fittings Association (PPFA). Plumbing Apprentice Training Manual for Plastic Piping Systems. http://www.ppfahome.org, 2002.

Plastics Industry Pipe Association of Australia, Ltd. http://www.pipa.com.au, 2010.

PolyPipe, Inc. *Polypipe: Design and Engineering Guide for Polyethylene Piping.* Gainesville, TX, 2005.

The Engineering Toolbox. http://www.engineeringtoolbox.com, 2010.

The Plastic Pipe & Fittings Association. *Polyethylene Water Service: Pipe and Tube Installation Guide.* Glen Ellyn, IL, 2002.

F. M. White. *Fluid Mechanics.* McGraw-Hill, New York, NY, 4th edition, 1999.

D. A. Willoughby, R. D. Woodson, and R. Sutherland. *Plastic Piping Handbook.* McGraw-Hill, New York, NY, 2002.

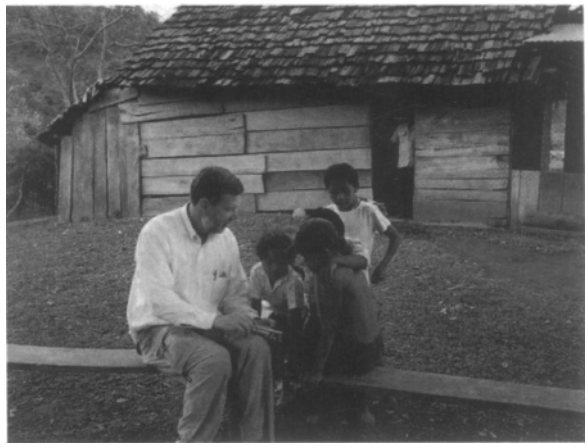

The author explaining a GPS to
children of Arena Blanca in Nicaragua.

CHAPTER 4

CLASSES OF PIPE FLOW PROBLEMS AND SOLUTIONS

"When you drink the water, remember the spring."
– Chinese Proverb

4.1 THE CLASSES

To place the present developments in perspective, it is worthwhile to compare the problem of gravity-driven flow in a pipe with the other pipe-flow problems normally encountered in the fields of fluid mechanics or hydraulics. The energy equation, Eqn (2.7), is obviously the same for all pipe-flow problems but, traditionally, the manner of how the solutions have been executed depended on the type of problem, or class, being solved. Four classes of problems for flow in a single pipe are considered.

1. L, Q, and D are known, $p_2 - p_1$ is unknown.
2. $p_2 - p_1, Q$, and D are known, L is unknown.
3. $p_2 - p_1, L$, and D are known, Q is unknown.
4. $p_2 - p_1, L$, and Q are known, D is unknown.

Gravity-Driven Water Flow in Networks. By Gerard F. Jones

The first two classes are particularly simple because with both Q and D known, the flow speed, $\overline{u}$, is easily calculated from the continuity equation (that is, the equation of mass conservation), Eqn (2.21). From this, the Reynolds number (Re) and friction factor ($f(\overline{u}, D)$) are calculated and the remaining unknown, either L or $p_2 - p_1$, is easily found from application of the energy equation, Eqn (2.7).

The last two classes are slightly more challenging since, with Q or D unknown, Re is not known so that $f(\overline{u}, D)$ is also not known. That is, the unknown of either Q or D appears in a nonlinear way in the energy equation. Either a pencil-and-paper iterative method is needed or a root-finder in a program like `Mathcad` or `Excel` may be used to solve Eqn (2.7) for $\overline{u}$. An example of this is presented in Section 4.2. The present work is a special case of class 4, where the inlet static pressure, p_1, is zero and the effect of gravity on the flow is critically important. Thus, the reader may have already solved a problem similar to that being considered in this work in a course like fluid mechanics. However, examples in a typical fluid mechanics course focus mostly on systems where the flow is driven by a pump (that is, $p_1 \neq 0$) and particular attention is paid to the calculation of the major and minor losses.[1] In fact, the elevation change in many problems is most often neglected, certainly when the fluid is a gas. Of course, this effect is the only driving force for flow in the present case.

4.2 AN ILLUSTRATIVE PIPE FLOW PROBLEM OF CLASS 4

Consider the following example of a pipe flow problem of class 4. The object of this exercise is to compare and contrast the different approaches to the solution of a pipe-flow problem where D is unknown. With the value for D, and thus Re and $f(\overline{u}, D)$, unknown as discussed above, the approaches used below may also be employed to solve flow problems of Class 3, where Q is unknown.

4.3 THE PROBLEM STATEMENT

A processing plant requires a flow rate of 1.100 m^3/min (18.33 L/s) from a water main located 275 ft from the plant and 10 m below the plant delivery location. It is known that the run of the pipe is relatively straight so that only a few 45° elbows will be required. Determine the minimum sch. 40, galvanized-iron (GI) pipe size required if the supply (that is, the source) and delivery static pressures are known to be 950 and 120 kPa, respectively. Assume the water temperature to be 10°C.

[1] As noted at numerous places in this text, except where needed for flow balancing, minor losses are not very important for many gravity-driven water distribution systems.

4.4 SETTING UP THE PROBLEM

We begin by writing the energy equation, Eqn (2.7), and simplify it by noting that $z_2 = 0$ as above. Also, because the pipe is uniform diameter, $\overline{u}_1 = \overline{u}_2$ is obtained from the continuity equation [Eqn (2.21)]. We may also assume that the total minor loss will be small compared with the major loss since the pipe is relatively long and there will be but a few elbows. For instance, a 45° elbow has an equivalent length of 16 (Table 2.1). Three elbows would then increase the pipe length by about 50 ft, about a 20% increase in the true length. We can often accommodate this by choosing the nominal pipe size having the next largest value for D, once it is calculated; the normal procedure as discussed in Section 3.5. In all cases, we can check for the accuracy of neglecting the minor loss after the solution for D is obtained.

Using Eqn (2.4), Eqn (2.7) becomes

$$\frac{p_1 - p_2}{\rho g L} + \frac{z_1}{L} = \frac{h_L}{L} = f(\overline{u}, D)\frac{\overline{u}^2}{2gD} \tag{4.1}$$

Also note that this equation appears in a slightly different form as Eqn (2.49) [F_{mod} includes the pressure difference in Eqn (2.49)].

The flow rate is prescribed for this problem, not $\overline{u}$. Thus, it is convenient to write $\overline{u}$ in terms of Q using Eqn (2.21),

$$\overline{u} = \frac{4Q}{\pi D^2} \tag{4.2}$$

whereupon Eqn (4.1) becomes

$$\frac{p_1 - p_2}{\rho g L} + \frac{z_1}{L} = \frac{h_L}{L} = \frac{8Q^2}{\pi^2 g}\frac{f(Q, D)}{D^5} \tag{4.3}$$

where $z_1 = -10$ m (see Fig. 2.11).

The left side of Eqn (4.3) contains only constants and for the far right side, constants and the dependent variable, D. Because D appears in a nonlinear way through both D^5 and $f(Q, D)$, Eqn (4.3) is a nonlinear algebraic equation and will be solved by a numerical method. Inserting the values for all parameters along with their units into Eqn (4.3), we get

$$0.8904 = \frac{h_L}{L} = 2.628 \times 10^3 \frac{f(Q, D)}{D^5} \tag{4.4}$$

where the unit of D is inches. It is interesting to note that the potential energy term in Eqn (4.3), z_1/L, is 0.0364 in absolute value or only ~4.1% of the total energy of 0.8904 dimensionless units. This is clearly a problem that is dominantly pressure driven, very different than those that are gravity driven.

To solve this equation, Re will be needed to calculate the friction factor. Written in terms of Q (as in textbox B.2.6), this becomes

$$\mathrm{Re} = \frac{6.463 \times 10^5}{D} \tag{4.5}$$

Equations (4.4), (4.5), and that for friction factor, Eqs (2.16) and (2.17), are a system of three nonlinear algebraic equations in three unknowns, D, Re, and $f(Q, D)$. Three methods for the solution of this problem will be considered below.

4.4.1 The Nonlinear Algebraic Equation[3]

In informal terms, a nonlinear algebraic equation is one where the unknown variable, while appearing in just a single location, is not able to be positioned alone on one side of the equal sign in the equation. The more-formal definition is that it is an equation where the unknown appears in a nonlinear way. Examples of a nonlinear algebraic equations are

$$\begin{aligned} g(x) &= x^4 + x - 10 = 0 \\ g(x) &= \sin(x) + 5 = 0 \\ g(x) &= \cosh(2x) + 2x + 3 = 0 \\ g(x) &= \ln(x) + 2xe^{6x} = 0 \\ g(x) &= x + \frac{2}{x} + 5\sqrt{x} = 0 \end{aligned} \tag{4.6}$$

where $g(x)$ denotes a function of the unknown variable, x (the symbols in this section, g, x, a, b, and c, as well as superscripts new and old below, are used only in their contexts in this section; as such, they do not appear in the Nomenclature and where possibly used in other parts of this book will have different meanings). For each of these examples, we are unable to isolate the unknown variable x, alone, on one side of the equal sign in the respective equation and not have it appear elsewhere in the equation. That is, the terms x^4, $\sin(x)$, $\cosh(2x)$, $\ln(x)$, e^{6x}, $2/x$, and $\sqrt{x}$ are all nonlinear functions of x. In the same way, Eqn (4.4), rewritten here in a slightly different form,

$$r(Q, D) = D - 4.943 f(Q, D)^{1/5} = 0$$

is also a nonlinear algebraic equation because, in the function $r(Q, D)$, the unknown D appears in a nonlinear way through term $f(Q, D)^{1/5}$. We have seen by our inspection of Eqs (2.16) and (2.17) or Fig. 2.6 that $f(Q, D)$ is also a nonlinear function of D through Re which appears in a nonlinear way in the $f(Q, D)$ function.

Some nonlinear algebraic equations can be solved by analytical methods; that is, we can obtain an exact solution in terms of elementary functions. A quadratic equation is an example of this,

$$ax^2 + bx + c = 0 \tag{4.7}$$

where a, b, and c are real numbers. From algebra, we will recall that Eqn (4.7) has the solution

$$x = \frac{-b \pm \sqrt{b^2 - 4ac}}{2a} \tag{4.8}$$

[3]This section may be skipped if appropriate without loss of continuity.

We refer to the values for x that satisfy the algebraic equation as the "roots" of that equation. In a graphical sense, a real root (one that is not imaginary) of a single nonlinear algebraic equation is the value of x that results in $g(x) = 0$, or the value of x where the function $g(x)$ crosses the x axis.

In general, the roots of nonlinear algebraic equations may be real, imaginary, or a combination of the two. The latter is referred to as a "complex" number. For example, in the illustrative case presented below the function possesses two real and two imaginary roots. Since the volume flow rate and pipe diameter, normally determined from the solution of the energy equation for pipe flow, are real quantities we are concerned only with real roots from the solution of this equation. In addition, since the pipe diameter is always positive-valued, the requirement $D > 0$ must always be satisfied.

Except for quadratic and cubic polynomials that are known to have solutions written as a function, such as Eqn (4.8) was for a quadratic polynomial (we refer to these as "analytical" solutions), no general solution of nonlinear algebraic equations exists. Thus, the lack of analytical solutions requires that nearly all nonlinear algebraic equations be solved by *numerical methods*. Normally, these solutions are carried out on a computer although, in principle, iteration using paper and pencil may be used.

As an example of a solution carried out on paper, consider the first of Eqs (4.6). Begin the solution by rewriting this equation in the following form,

$$x = (10 - x)^{1/4} \tag{4.9}$$

We will solve this equation by iteration, a method referred to *Gauss–Seidel iteration* (Gerald and Wheatley, 1999). The procedure is simple. We guess a value for x and substitute this value into the right side of Eqn (4.9). Upon evaluation of the right side, which is equal to x, we are presented with an updated estimate of x. Again, upon substituting into the right side and evaluating, we obtain another, hopefully more accurate, estimate for the value of x. This procedure continues until, with further iterations, the value of x no longer changes to our desired level of accuracy. The solution is then said to have "converged." The results of this procedure are best presented in a table (Table 4.1), where the iteration number and the values for x at that iteration number are written. From our inspection of Table 4.1, we see that one root of Eqn (4.9) is $x = 1.697$. Other roots may exist, but what we have found is the root closest to the guessed value for x of 1. A plot of the function of Eqn (4.9) may perhaps reveal other real roots and we can find their values by following the procedure of Table 4.1 after making a guess for x near this root.[4]

Clearly, one could implement this iterative solution on a computer, and provided with a meaningful initial guess, obtain a single root of a nonlinear algebraic equation, such as that from the energy equation for pipe flow, Eqn (4.4). However, Gauss–Seidel iteration is not very efficient and the success at converging to a solution in the

[4]For this example, there are two real roots, 1.697 and -1.856, and two complex conjugate roots, $0.0791 \pm 1.780i$, referred to as a "complex conjugate" pair. If, for example, x were the pipe diameter, the value for the diameter would be 1.697 units. That is, since the diameter is a quantity that is both positive and real (not imaginary), the only physically allowable root is 1.697.

Table 4.1 Solution of a Nonlinear Algebraic Equation by Gauss–Seidel Iteration

Iteration[a]	x^{old}	x^{new}
1	1	1.732
2	1.732	1.696
3	1.696	1.698
4	1.698	1.697

[a]The value for the initial guess is 1. The designation "new" means the updated value of x after the "old" value of x is substituted into the right side of Eqn (4.9).

region of the initial guess depends on the way in which the nonlinear equation [say, Eqn (4.9)] is written. In other words, convergence to a solution is not guaranteed with the Gauss–Seidel method. Fortunately, more robust numerical methods, such as the Newton–Raphson method (Gerald and Wheatley, 1999), have been developed and are very widely used by engineers and scientists in everyday practice. In particular, in `Mathcad` the function `root` is used to find a single root of a nonlinear algebraic equation is known to be quite robust.

In Chapter 11, we will need to solve not just a single nonlinear algebraic equation, but many such algebraic equations simultaneously. These are referred to as systems of nonlinear algebraic equations. The idea behind the numerical solution for these systems is similar to that from the discussion above. Numerical methods of solution, such as Newton–Raphson, are very good at solving systems of nonlinear algebraic equations. In `Mathcad`, the `Given...Find` construct is used for this purpose so there is no need to write a computer program when carrying out the solution. The designer needs to be aware that the `root` function and `Given...Find` construct in `Mathcad` are numerical-based, like the example explored in this section. Thus, a good initial guess[5] for each of the unknowns in the single or system of nonlinear algebraic equations needs to be provided as a start for the solution.

4.5 DIFFERENT APPROACHES TO THE SOLUTION

4.5.1 Method 1: Trial and Error

The first method, presented in most textbooks on fluid mechanics, is trial and error. The values for D corresponding to a series of guessed values of nominal sizes for GI pipe are substituted into the above system of equations. The value of D that satisfies the equality required by Eqn (4.4) is the solution. The results from this procedure

[5]The meaning of good is that guesses should not be too far from the eventual solution. For a single equation, it is easy to find the approximate solution (i.e., the guess) by plotting the equation for the variable whose value you wish to obtain, thus finding its approximate root. For a system of nonlinear algebraic equations coming up with a good set of values for the initial guesses may be more challenging. Often, good guesses for the system are had by using the solutions for a similar case that has already been solved. Other than this, trial and error is usually needed, along with a sense for approximately what the solutions will be.

are presented in Table 4.2, where we see that Eqn (4.4) is satisfied for a nominal pipe size between 2 and 3 in., that is, right-side values for Eqn (4.4) of 1.779 and 0.2277 bound the left-side value of 0.8904. As discussed in Section 3.5, we choose a nominal 3-in. pipe, the larger of the two[6]. An inspection of Fig. 5.31 will reveal that, under the prescribed conditions, a 3-in. nominal GI pipe will pass ~40 L/s of water flow, much larger than required for this design. The problem with this "oversized" pipe is discussed in Section 4.7.

4.5.2 Method 2: Use of Head-Loss Data

In this method, which has found the broadest usage when the graphical hydraulic-gradient-line method is employed for the design of gravity-driven water networks (Section 6.6.2), we focus on the middle term in Eqn (4.4), the hydraulic gradient, which is sometimes referred to as the "head loss per unit length of pipe" or "head-loss factor." This was the subject of a calculation in textbox B.2.6. Tables and plots of hydraulic gradient, h_L/L, for different types of pipe and a range of wall thicknesses are published in the literature including tables in handbooks (Jordan Jr., 2004) and technical trade publications, such as The Plastic Pipe & Fittings Association (2002) both for PE pipe. Two such plots, one for sch. 40 GI pipe and the other for sch. 80, were generated and appear in Figs. 4.1 and 4.2.[7] These were produced by the two right-most terms in Eqn (4.3),

$$\boxed{\frac{h_L}{L} = \frac{8Q^2}{\pi^2 g}\frac{f(Q,D)}{D^5}}$$

where $f(Q, D)$ is the friction factor from Eqs (2.16) and (2.17). From our inspection of Fig. 4.1, we find that nominal 3-in.pipe is required for Q of 18.3 L/s and h_L/L of ~0.9. Obviously, this is a relatively quick and simple method compared with the trial-and-error approach of Method 1. However, this method can be used only if the designer has the head loss table or curves for the particular pipe of interest.[8] That is, the head-loss data are specific to pipe material (because of roughness) and schedule or SDR because the inside diameter (ID) changes with wall thickness for all outside diameter (OD)-controlled pipe. Since it is not always practical or possible to obtain

[6]Note that if $2\frac{1}{2}$-in. nominal pipe (which has D of 2.469 in.) is available, this would be the best choice. Though they exist, local suppliers of plastic pipe may not stock the larger pipe sizes, say >2 in., in half-inch increments.

[7]Note there is very little quantitative difference in these two graphs, especially for the larger pipe sizes. The differences between the inside diameters for sch. 40 and sch. 80 pipe are not large. For this detail, see Section 3.4.1.

[8]Many such tables have been found to have values for the head-loss that differ by as much as 35% from those calculated from the friction factor recommended for use in this book. Before relying on the accuracy of data from these tables, the designer should verify several of these tabular entries over the range where they will be used. This can be easily done with the `Mathcad` worksheet `HydraulicGradient.xmcd`. Please see Exercise 13. One source reporting reliable head-loss data from the Darcy–Weisbach equation is Appendix 4 of Trifunovic (2006), for specified wall roughness ϵ, and D in integer metric sizes (not actual ID for nominal pipe sizes).

Table 4.2 Trial and Error Method of Solution where D is Unknown[a]

Nominal Size (in.)	Inside Diameter, D (in.)	Reynolds Number, Re	Friction Factor, $f(Q, D)$	Right Side of Eqn (4.4)	Comment
1	1.049	6.703×10^5	0.03028	62.64	Excessive friction
$1\frac{1}{2}$	1.610	4.367×10^5	0.02709	6.582	Excessive friction
2	2.067	3.402×10^5	0.02554	1.779	Excessive friction
3	3.068	2.292×10^5	0.02356	0.2277	Insufficient friction

[a]The left side of Eqn (4.4) is 0.8904. The value for D that satisfies Eqn (4.4) is between 2.067 in. (2-in nominal) and 3.068 in. (3-in nominal). We choose the larger of the two.

these sources of head-loss data, Method 2 will not always be the choice of the designer. In the next method, we will use a commercial software package to solve the problem; the preferential method is used in this book.

An additional difficulty with Method 2 is including minor losses. *Because of the limitless combinations of fittings and valves that could be installed in a pipe network, head-loss data are only for a straight pipe and, thus, do not include minor loss.* Iteration must be used to include minor losses as illustrated in Exercise 12; specifically, h_L/L for straight pipe is multiplied by $(1 + \frac{L}{D}\sum_{i=1}^{M} \frac{L_e}{D}|_i)$, where $\frac{L_e}{D}|_i$ is the equivalent length of the minor loss contributors, to obtain h_L/L for the network that includes minor loss. At most, about one or two iterations will be required to accurately determine D using Method 2 because, as discussed above, minor losses are not large for gravity-driven water networks. However, for networks where the minor loss is $> 10 \sim 20\%$ of the major loss, several iterations may be required.

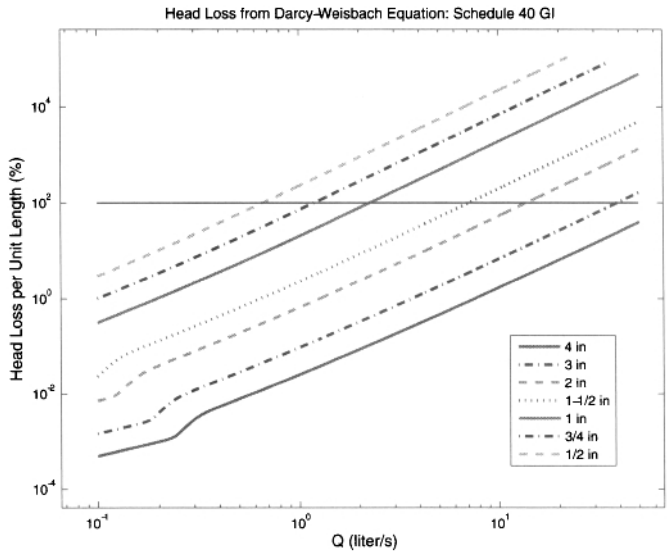

Figure 4.1 Head-loss factors, h_L/L, for sch. 40 galvanized iron (that is, galvanized steel) pipe. Horizontal line at $h_L/L = 1$ corresponds to Natural flow in a vertical pipe (please see Fig. 5.3). Gravity-driven water flow in the pipe corresponds to the region below this line. Pump-driven water flow, where $p_1 > 0$, can occur above this line.

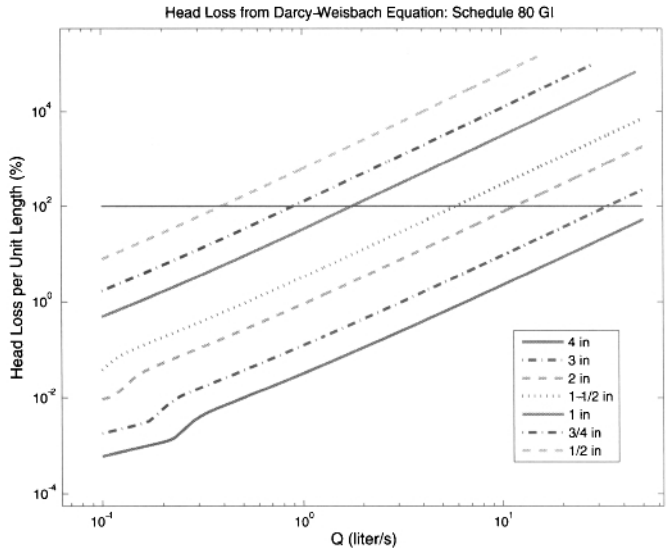

Figure 4.2 Head-loss factors, h_L/L, for sch. 80 galvanized iron (that is, galvanized steel) pipe. Horizontal line at $h_L/L = 1$ corresponds to Natural flow in a vertical pipe. Gravity-driven water flow in the pipe corresponds to the region below this line. Pump-driven water flow, where $p_1 > 0$, can occur above this line.

B.4.1 Care When Using Head-Loss Charts

Care should be taken when using head-loss data from the available charts and tables. There are several assumptions concerning the friction-factor model (for example, Darcy–Weisbach or Hazen–Williams, please see Chapter 9), actual pipe inside diameters versus nominal pipe sizes versus inside diameter values not connected with actual dimensions or nominal sizes, the pipe roughness, and the kinematic viscosity of the water (that is, the temperature upon which this property is based) that vary among the sources. The kinematic viscosity of water should be based on 10°C. See Exercises 13, 14, and 28.

4.5.3 Method 3: Use of a Computer Program

In the previous two methods two independent calculations are made based on terms in the energy equation. The first is the net mechanical energy, the left side of Eqn (4.3). This part may be thought of as the net mechanical energy "compartment". The frictional losses in the pipe are calculated next from the right side of Eqn (4.3), the result from which may be thought of as the frictional energy or dissipation "compartment". The results of these two independent calculations are compared through the energy

equation [Eqn (4.4)] and a choice made for the pipe diameter that best matches the values from the two compartments. This is how the pipe flow problems of class 4 have traditionally been solved.

A different approach is taken in Method 3. The flow in the pipe in this example must satisfy energy conservation. Thus, by writing the energy equation for pipe flow, Eqn (4.4), between the inlet and outlet states, we can solve (using a root solver in the package `Mathcad`) this equation for the unknown pipe diameter. The solution for Re and friction factor are also solved along with the energy equation in a procedure referred to as the "simultaneous" solution of the subject three algebraic equations. This is the approach used throughout this book. The main benefit of the use of a software package to solve pipe-flow problems of the current type is that it *eliminates compartmentalization of the solution* by simultaneously solving the three nonlinear algebraic equations that determine the solution for D; energy, and the equations for friction factor and Re. Thus, the numerical value for D is determined directly from the solution after which the designer can easily choose the nominal pipe size having an ID equal to or slightly larger than this value. A copy of the `Mathcad` worksheet that shows this calculation is presented in Fig. 4.3 where use is made of the `root` function.[9] The result (D of 2.360 in., the nominal pipe size having the next largest value for D is 3 in.) is, of course, identical to that from the first two methods.

The clear advantages of Method 3 are that, given the `Mathcad` worksheet and, of course, a working copy of `Mathcad` on a computer, this approach is just as quick as Method 2 and, most importantly, *it requires no source of head-loss data.* That is, these data are produced by the friction factor function already in the worksheet. Method 3, which automatically accommodates any minor losses, is clearly much quicker and less tedious and prone to error than the approach of Method 1. Should the designer not have `Mathcad`, other programs, such as `Excel` or a hand-held calculator, may be programmed with the same equations that appear in the `Mathcad` worksheet. This has been done by the author and other practitioners in piping system design. An additional benefit of Method 3 compared with Method 2 is that uncertainty in the accuracy of head-loss data is eliminated. The friction factor that is used [Eqs (2.16) and (2.17)] is accurate and includes not only the turbulent flow regime over the range of Re encountered in gravity-driven and forced-flow water networks, but the laminar and transition regions should they arise.

4.6 A NOTE OF CAUTION

After completing this chapter, it may be tempting for readers with a background in pipe flow calculations to be cavalier about the material that remains ahead, including local pressure distribution and analysis and design of multiple-pipe networks. If among this group, do not let this premature sense of understanding interfere the learning process. Unless you have had considerable experience analyzing and designing gravity-flow

[9]The `root` function in `Mathcad` is equivalent to the `Given. . .Find` construct except that it solves for the root of a single nonlinear algebraic equation instead of multiple ones.

Method 3

Water properties at 10 C = 50 F $\nu := 13.0710^{-7}\cdot\frac{m^2}{sec}$ $\rho := 1000\frac{kg}{m^3}$ $TOL := 1\cdot10^{-10}$

$\varepsilon := 50010^{-6}\cdot ft$ absolute roughness, ft (for galvanized steel) $kPa := 1000Pa$

$p_1 := 950kPa$ $p_2 := 120kPa$ $L := 275ft$ $z_1 := -10m$ $Q := 1.1\cdot\frac{m^3}{min}$ $\frac{8\cdot Q^2}{\pi^2\cdot g} = 2.628\times 10^3\, in^5$

$\frac{p_1 - p_2}{\rho\cdot g\cdot L} + \frac{z_1}{L} = 0.8904$ $Re(D) := \frac{4\cdot Q}{\pi\cdot\nu\cdot D}$ $Q = 18.333\frac{liter}{s}$

friction factor that spans the laminar/turbulent range. ebyD is relative roughness.

$$funct(f,R,ebyD) := \frac{f}{2} - \left[\left(\frac{4}{R\cdot\sqrt{\frac{f}{8}}}\right)^{24} + \left[\left(\frac{18765}{R\cdot\sqrt{\frac{f}{8}}}\right)^{8} + \left[3.29 - \frac{227}{R\cdot\sqrt{\frac{f}{8}}} + \left(\frac{50}{R\cdot\sqrt{\frac{f}{8}}}\right)^{2} \cdots + \frac{1}{0.436}\cdot\ln\left(\frac{R\cdot\sqrt{\frac{f}{8}}}{1 + 0.301R\cdot\sqrt{\frac{f}{8}}\cdot ebyD\cdot 2}\right)\right]^{16}\right]^{-\frac{3}{2}}\right]^{\frac{1}{12}}$$

$f1 := 0.2$ $fric\_fac(Re,ebyD) := root(funct(f1,Re,ebyD),f1,0.0001,f1)\cdot 4$

$$D := root\left[\left(\frac{p_1 - p_2}{\rho\cdot g\cdot L} + \frac{z_1}{L} - \frac{8\cdot Q^2}{\pi^2\cdot g}\cdot\frac{fric\_fac\left(Re(D),\frac{\varepsilon}{D}\right)}{D^5}\right), D, 0.0001in, 8\cdot in\right] \qquad D = 2.360in$$

Figure 4.3 Mathcad worksheet solution for solving a pipe-flow problem where D is unknown. The function `fric_fac` is the friction factor evaluated by the `root` solver. The final two arguments in the function `root(funct(f1,Re,ebyD,f1),0.0001,f1)` of 0.0001 and `f1` are the assumed lower and upper bounds for the value of the friction factor, `frict_fac(Re,ebyD)`. Here, D is determined using the same `root` solver where the lower bound is assumed to be 0.0001 in. and the upper bound 8 in. $\mathrm{Re}(D) = 4Q/(\pi\nu D)$ is Re written as function of D. Mathcad worksheet `single pipe example-method 3.xmcd`.

networks, the content awaiting you is not trivial nor obvious. To entice participation in service projects that use the theory and applications in this book, I have heard one student say to another that the material is "easy." Indeed, in the overall scale of college-level learning in engineering, for example, all evidence points to the fact that the material is not. In particular, the solution of systems of nonlinear algebraic equations (using Mathcad or any other technology) is never simple. Minimization of network cost to provide static pressure heads at junctions of multiple pipes (a uniqueness problem), the modeling of flow in a loop network where flow rates and pipe sizes are unknown, and the effect of trapped air in network pipelines, among many others, are not simple topics.

Whether you are an experienced engineer/designer or a novice engineering or technology student, you are encouraged to move forward with an open mind while exploring the remainder of this book.

4.7 SUMMARY

To summarize the solution of a pipe-flow problem of class 4, where either D or Q is the unknown, three basic methods are described to carry out the solution. Trial and error is a "brute force" method that will normally work, but is tedious and time consuming, especially, as we will see in Chapter 11, for multipipe flow networks. Method 2 requires that the designer have access to the head-loss curves or tables for the specific pipe material and wall thickness under consideration, and to include minor losses using potentially tedious iteration. Since this is not always practical, Method 3, which uses the computer package Mathcad and the friction factor presented in Chapter 2 instead of head-loss charts, is the method of preference.

A closing comment is needed concerning the lack of ability to choose a nominal pipe size that has the exact value for D calculated from the energy equation. The ID of a sch. 40 nominal 3-in. pipe is 3.068 in. whereas the pipe diameter required to satisfy the conditions stated in the above example problem is 2.360 in. One or more of the parameters must therefore be adjusted in value to accommodate this change. Often, industry restricts adjustability of the prescribed flow rate and static pressures p_1 and p_2 because they are constrained by other parts of the flow network. This also applies to gravity-driven water networks. A quick calculation with the Mathcad worksheet shown in Fig. 4.3, where we fix D at 3.068 in. and allow p_2 to vary, shows that a 3-in. nominal pipe will supply the required flow rate (subject to the given inlet pressure and elevation change) for p_2 equal to 665 kPa. Thus, a throttling valve is needed at the point of delivery of the water to reduce the static pressure from 665 kPa to the required 120 kPa. As discussed in Section 13.14, this type of adjustable valve, a globe valve, is used at various locations in nearly every pipe network to allow flexibility in the flow and pressure conditions (i.e., for flow control). From this, we see that a globe valve in the pipe has the effect of a reducing the pipe diameter from one corresponding to a nominal size. The globe valve allows the designer to more-closely match the diameter corresponding to the chosen nominal pipe size with the required theoretical

inside diameter. The reader may find it convenient to remember that *a globe valve is, in effect, a device that can reduce the diameter of the pipe in which it is installed.*

References

C. F. Gerald and P. O. Wheatley. *Applied Numerical Analysis.* Addison Wesley, New York, NY, 5th edition, 1999.

T. D. Jordan Jr. *Handbook of Gravity-Flow Water Systems.* ITDG Publication, London, UK, 2004.

The Plastic Pipe & Fittings Association. *Polyethylene Water Service: Pipe and Tube Installation Guide.* Glen Ellyn, IL, 2002.

N. Trifunovic. *Introduction to Urban Water Distribution.* Taylor & Francis, New York, NY, 2006.

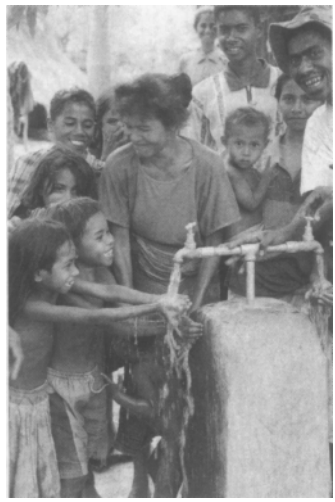

A community in East Timor enjoys the fruits of a successful design.

CHAPTER 5

MINOR-LOSSLESS FLOW IN A SINGLE-PIPE NETWORK

"Do Something for Somebody Everyday for which you do not get Paid."
– A. Schweitzer

5.1 INTRODUCTION

This chapter presents results pertaining to the analysis and design of a single-pipe network. This refers to a pipe of uniform diameter, and possible fittings and valves, that connect a source of water to a delivery location. If, for any reason, the pipe has multiple diameters, then the network is of the multiple-pipe type. The theory and part of the design for multiple-pipe networks is presented in Chapter 11. Applications for the material in this chapter include any water source, such as groundwater or a spring (see Chapter 1 for these definitions), that is open to atmospheric pressure, or a storage or break-pressure tank under the same condition. The static pressure at the delivery location can be atmospheric (that is, zero-gage pressure) or any positive value such that $p_2/\rho g z_1 < 1$, as discussed in Chapter 2. The positive static pressure at the delivery location is physically produced by a minor-loss element, such as a faucet or globe valve. Only in this sense is minor loss considered in this chapter; that is, no minor losses are considered at any other location along the pipe-flow path.

Gravity-Driven Water Flow in Networks. By Gerard F. Jones

As indicated in Chapter 2, although the minor loss elements may certainly be present in the network, their effects on the selection of pipe sizes is normally small except where intentionally included for flow control. The reader is referred to Chapter 8 for the appropriate Mathcad worksheet where minor losses are to be considered. Because single-pipe networks are so common, the design charts presented in this chapter are expected to be useful, especially in the field, for rapid estimation of pipe sizes for these simple networks.

Also included in this chapter are design charts for the more-general case of *forced flow* in a single-pipe, uniform-diameter, minor-lossless flow network. In this case, *the pressure at the source can take on any nonzero value.* These formulas and design charts are useful as a complement to the present work on gravity-driven water networks in cases where a pump is used to deliver the flow.

From our inspection of the general form of the energy equation for gravity-driven pipe flow, Eqs (2.33) and (2.40), we see that Eqn (2.33) is a special case of the more-general Eqn (2.40) with tortuosity λ set equal to 1. Thus, Eqn (2.40) and its restrictive cases, Eqs (2.41) and (2.43), are the energy equations of interest. In any of these, mean slope s, tortuosity λ, and the dimensionless static pressure at delivery, F, can be given any values specified by the designer. The neglect of minor losses means ignoring all terms in Eqn (2.40) that include D/z_1. This gives Eqs (2.41) or (2.42). After being written in terms of Q instead of $\overline{u}$ as in Section 5.2, the solution of Eqn (2.42), a nonlinear algebraic equation, is carried out in Mathcad using the root function.[1] The friction factor is from Eqn (2.16).

5.2 SOLUTION AND BASIC RESULTS

The focus of this chapter is on the solution of the energy equation for minor-lossless pipe flow, Eqn (2.44), rewritten here for convenience

$$\frac{1-F}{\lambda\sqrt{1+s^{-2}}} - \frac{8Q^2}{\pi^2 g}\frac{f(Q,D)}{D^5} = 0$$

A comment on the dependencies appearing in Eqn (2.44) is in order. Equation (2.44) includes $Q, D, F, s, f(Q,D)$, and λ, along with constants. From among this list, $f(Q,D)$ will always be a function of the solution though Eqn (2.16). That is, the value for $f(Q,D)$ will never be prescribed by the designer. Each of the terms F, s, and λ are almost always treated as either a parameter or an independent variable;[2] in many of the design graphs appearing in this book for a single-pipe network, s is normally the independent variable. Q and D are either the dependent variable or a parameter. For example, in the next paragraph, we will plot $Q = Q(s)$, where D, F, and λ are parameters. In the design plots that form the bulk of this chapter, $D = D(s,Q)$,

[1] The root function in Mathcad is equivalent to the Given. . .Find construct except that it solves for the root of a single nonlinear algebraic equation instead of multiple ones.

[2] An independent variable is one that is varied according to our wishes to investigate the response of a dependent variable. A parameter is typically a variable held constant during this investigation.

which produces a contour plot, where there are two independent variables, s and Q, and F and λ are parameters. Throughout all of this discussion and for all cases, the solution for the problem of pipe design is from the same energy equation, the only thing that changes is for what variable we are solving.

B.5.1 Example: The Solution of Eqn (2.44)

The solution of Eqn (2.44) will ultimately be carried out using a root-finder in Mathcad. However, here we will use Gauss–Seidel Iteration, discussed in Chapter 4, to illustrate the solution. For this example, $Q = 1.43$ L/s, $s = 3.3\%$, $\lambda = 1.32$, and $F = 0.20$ and the pipe is SDR-26 metric polyvinyl chloride (PVC, where $\epsilon = 1.52 \times 10^{-3}$ mm). Following the procedure of Chapter 4, Eqn (2.44) is rewritten as

$$D = [\frac{8Q^2}{\pi^2 g} \frac{\lambda\sqrt{1+s^{-2}}}{1-F} \cdot f(Q,D)]^{1/5}$$

Note that the friction factor $f(Q, D)$ depends on the Reynolds number (Re) and relative roughness as discussed previously. Thus,

$$f(Q,D) = f(\mathrm{Re}, \epsilon/D)$$

where, as we saw in Section 2.5, Re is

$$\mathrm{Re} = 4Q/\pi\nu D$$

After substituting the values for Q, s, λ, ϵ, and F and rewriting the above expression for D to accommodate the Gauss–Seidel algorithm, we get

$$D^{new} = [\frac{8 \cdot (1.43 \times 10^{-3}\ \mathrm{m^3/s})^2 \cdot 1.32}{\pi^2 \cdot 9.807\ \mathrm{m/s^2} \cdot 0.033 \cdot 0.8} \cdot f(\mathrm{Re}^{old}, \epsilon/D^{old})]^{1/5}$$

or

$$D^{new} = 96.70\ \mathrm{mm} \cdot f(\mathrm{Re}^{old}, \epsilon/D^{old})^{1/5} \tag{5.1}$$

where

$$\mathrm{Re}^{old} = \mathrm{Re}(Q, D^{old})$$

We begin by supplying a guess for $D = D^{old}$ of 25 mm. Substituting this into the right side of Eqn (5.1) gives $D^{new} = 44.53$ mm. This procedure is repeated until, after just three iterations, we obtain a converged solution for $D = 45.72$ mm (Table 5.1). From Table 3.8, a nominal 50-mm size [inside diameter (ID) of 46.0 mm] is chosen based on this value of D.

The fundamental results from the solution of Eqn (2.44) are now explored. We present a graph of Q versus s for two pipe diameters and two values for λ and $F = 0.5$ (see Fig. 5.1). We see that the water flow rate increases with slope and with pipe diameter. This can be explained from an intuitive argument. Imagine a

Table 5.1 Solution of Eqn (2.44) by Gauss–Seidel Iteration

Iteration	D^{old} (mm)	$D^{\text{new}a}$ (mm)
1	25	44.53
2	44.53	45.61
3	45.61	45.72

[a]The term D^{new} is the updated value of D after the "old" value of D (D^{old}) is substituted into the right side of Eqn (5.1).

single, straight, open-ended pipe of length L held in your hands where the pipe has a constant source of water at the top opening. If the slope of the pipe is zero, (i.e., horizontal), there is no effect from gravity pulling the water downward because of the zero slope and the flow rate is zero. Note how all of the curves in Fig. 5.1 tend to zero flow rate as the slope approaches zero. As the slope of the pipe increases, the flow rate increases because of the increase in z_1; recall Eqn (2.39) where $s \approx z_1/L$ for small slope. For example, for a pipe with a slope of one, a pipe inclination of 45°, the flow rate increases to the largest value seen in Fig. 5.1. It is easy to explain how energy is conserved as s increases. An increase in flow rate in a pipe of fixed diameter caused by an increase in s means an increase in flow speed. The greater flow speed, in turn, means greater energy dissipation over the pipe length and this comes from the increase in potential energy caused by increasing z_1 and s.

Water flow rate also increases with pipe diameter, as seen in Fig. 5.1. For a given length of pipe, the frictional energy loss (which comes from shear between the pipe wall and water) is proportional to the circumference of the pipe (πD) and for a given flow speed, the flow rate is dependent on the pipe cross-sectional area ($\pi D^2/4$). The ratio of the area to the circumference is proportional to D so that, as D increases, more water can pass through the cross section of the pipe per unit of shear stress at the pipe wall. We also see in Fig. 5.1 that, as expected, the water flow rate decreases as the pipe gets longer because of the additional friction. This is the effect of λ.

5.3 RESULTS FOR LIMITING CASE OF A VERTICAL PIPE: FROUDE NUMBER

As the slope of the pipe approaches infinity (that is, a vertical pipe), the pipe length becomes equal to the elevation at the top of the pipe and the flow rate reaches a maximum value. This is seen in Fig. 5.2, which is identical to Fig. 5.1 except that the slope axis now ranges from 0.2 to 10. The maximum flow rate in this case can be compared with the classical "terminal velocity" of a body falling in a fluid under its own weight. In this situation, the speed of the fall is such that the drag acting on the body is exactly balanced by the body's weight. The acceleration is zero and the speed that the body achieves under this condition is referred to as "terminal." Thus, with a large slope (10 is large enough to be considered infinite), water is simply free-falling vertically in the pipe and will reach a speed where the weight of the water is exactly

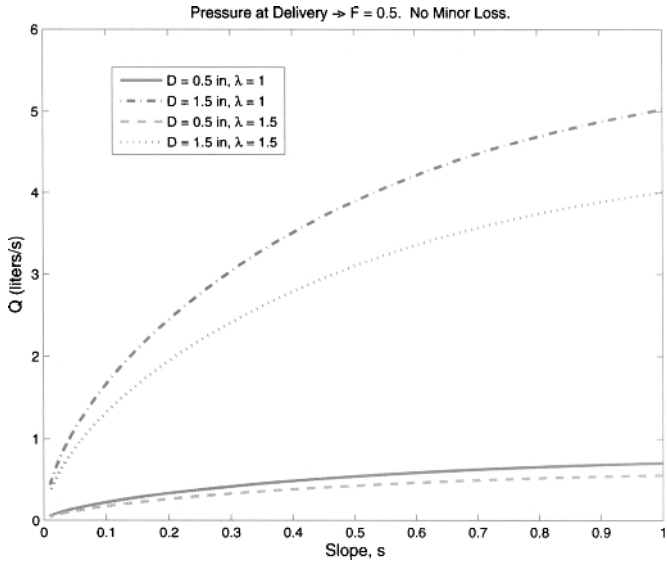

Figure 5.1 Volume flow rate of water versus mean slope of pipe for two different diameters of PVC IPS pipe and two values for pipe length. $\lambda = 1$ corresponds to the straight pipe case. Here, $\lambda = 1.5$ is for a pipe length 50% greater than the straight pipe case. Dimensionless static pressure at delivery corresponds to $F \equiv p_2/\rho g z_1 = 0.5$. No minor loss.

balanced by the friction force at the pipe wall. Under these conditions the energy equation to be solved for the terminal velocity of the water is from Eqn (2.40) with $s \to \infty$. With minor losses neglected, $\lambda = 1$, and the delivery pressure of zero for Natural flow [Eqn (2.43)], we get

$$1 - f(\overline{u}_\infty, D)\frac{\overline{u}_\infty^2}{2gD} = 0 \tag{5.2}$$

The solution of Eqn (5.2), with $\overline{u}_\infty$ converted to volume flow rate, Q_∞, appears in Fig. 5.3 for a broad range of pipe diameter (see related Exercise 15).

While this limiting case is of interest from a theoretical perspective and as an upper bound on the volume flow rate of water in a gravity-driven flow, it has little relevance in an actual design since few, if any, reservoirs are located vertically or near vertically above the delivery spot.

It is worth mentioning at this point that since 1 and $f(\overline{u}, D)$ in Eqn (5.2) (dropping subscript ∞) are clearly dimensionless numbers, then the group $\overline{u}^2/2gD$ must be a dimensionless group. In fluid dynamics, $\overline{u}^2/2gD$ is related to the Froude number, Fr, defined as

$$\text{Fr} \equiv \frac{\overline{u}}{\sqrt{gD}} \tag{5.3}$$

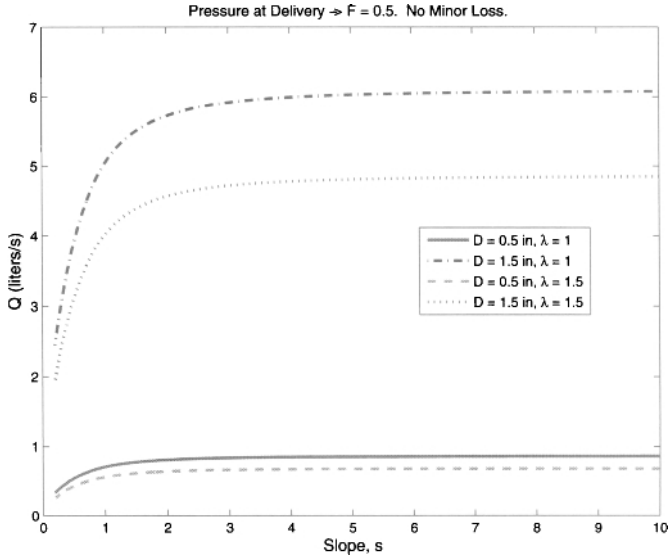

Figure 5.2 Same as Fig. 5.1 except slope axis ranges from 0.2 to 10. Terminal values for Q are seen in this figure as slope$\rightarrow \infty$.

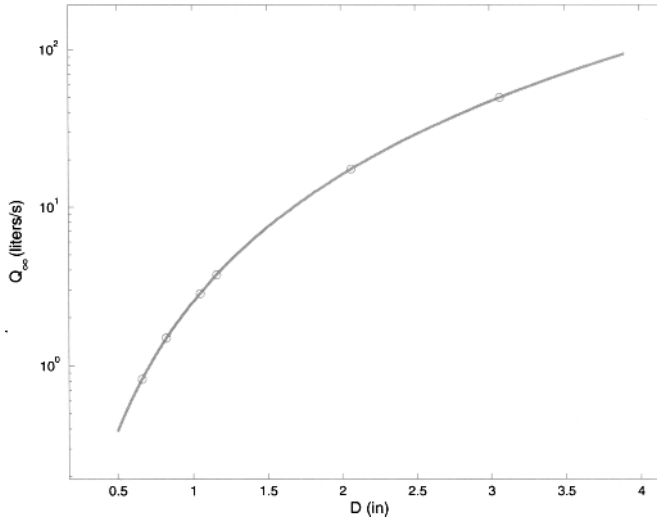

Figure 5.3 Limiting case for the terminal volume flow rate of water in a vertical pipe. The circles correspond to PVC IPS nominal pipe sizes of $\frac{1}{2}$, $\frac{3}{4}$, 1, $1\frac{1}{2}$, 2, and 3 in.

which may be interpreted as proportional to the ratio of the inertia force to the body, or gravity, force on the flow.

Thus, we see that Eqn (5.2) can be rewritten as

$$f(\overline{u}, D)\mathrm{Fr}^2 = 2 \tag{5.4}$$

where Fr depends on the flow speed $\overline{u}$, as in Eqn (5.3).

If the reader has covered Dimensional Analysis, normally part of a fluid mechanics course, Fr may be readily recalled. Fr always arises in fluid dynamics when there is gravity or a similar force field, such centrifugal force in the problem. Since the friction factor is of the order of 0.02, Fr is seen through Eqn (5.4) to be of the order of 10, a result that reflects the small length scale (that is, the pipe diameter) for gravity-driven flow in a pipe. As the length scale increases, say, for example, for large waves acting on the bow of a ship, the value of Fr decreases indicating a greater effect from the gravitational influences in the problem. No further discussion of Fr is necessary here. It is more convenient to deal with the group $\overline{u}^2/2gD$ rather than Fr since in the present work we will be solving for $\overline{u}$, or Q derived from $\overline{u}$, directly.

5.4 DESIGN GRAPHS FOR A SINGLE PIPE FOR MINOR-LOSSLESS FLOW

The design graphs for a single-pipe network for minor-lossless gravity-driven flow are presented in Figs. 5.4–5.11 below for English-based, sch. 40 PVC pipe (Section 5.4.2), Figs. 5.13–5.20 for sch. 40 galvanized-steel pipe, often referred to as galvanized iron (GI) pipe (Section 5.4.3), and in Figs. 5.22–5.29 for metric-based, SDR 21 PVC pipe (Section 5.4.5). The plots are of Q as a function of the mean slope, s, for a range of nominal pipe diameters (the actual inside diameters differ from the nominal size as discussed in Chapter 3 and were used as D in the calculations)[3] and for different values for F and λ as parameters. The F values are 0 (atmospheric pressure at the delivery location or Natural flow), 0.1, 0.25, and 0.5, and the λ values are 1 (straight pipe) and 1.5 (50% longer than straight pipe). This relatively large value for λ is chosen as a realistic upper bound of its affect on Q and D. The plots noted above are similar to that of Fig. 5.1 except that the design plots are presented with log–log axes and grid lines to be able to better read the numbers for s and Q over a large range of values.

Generally, all figures show that the volume flow rate increases in proportion to nearly the square root of s for a given D. Increasing D also increases Q, as discussed above, with the largest changes from size to size in the smallest diameter range. Increasing the pipe length by 50% over the straight-pipe case of $\lambda = 1$ (Figs. 5.4–5.7) decreases Q by ~25% (see Figs. 5.8–5.11 for $\lambda = 1.5$), which is not a very

[3]The pressure ratings for the sch. 40 pipe range from 600 to 180 psig for the smallest to the largest pipe size appearing in these figures (see Table 3.3). The pressure rating for metric-based, SDR 21 PVC pipe is PN 10 or 147 psig (please see Table 3.7). These results from these charts are expected to approximately apply to the lower pressure rated, SDR 26 PVC pipe because the ID values for SDR 21 and SDR 26 are nearly identical.

large impact on the design. As discussed in textbox B.2.10, the tortuosity λ is not a strong influence for two reasons. First, the common-sense practice is to connect the source, tank, and tapstands by as short a pipe length as possible to minimize pipe cost. Second, the mean slope of a typical design is very small. Thus, the run of a water-delivery pipe is very much larger than the elevation of the source so that peaks and valleys in the pipeline and a normal degree of circuitousness in the horizontal plane does not add much overall length to the pipe. For both of these reasons values for λ larger than one plus a very small fraction are unusual for most actual designs.

In Fig. 5.13, for galvanized straight steel pipe and delivery static pressure of zero, we see that the water flow rate is considerably smaller than that for the smoother PVC pipe (cf. Fig. 5.4) of the same diameter. A quick consult with the Moody chart from Fig. 2.5 or any fluid mechanics textbook shows that, for Re approximately $< 10^5$, the difference between the friction factors for relative roughness of 1×10^{-6} and 100×10^{-6} is as much as a factor of two. The difference becomes larger with larger Re, but these are not common for gravity-driven water flows. It is also noteworthy in Fig. 5.12 that laminar flow is obvious for the smallest values of s and the smallest pipe sizes. Note the marked difference in slopes of the curves for this range compared with the rest of the figure that are in the turbulent regime.

A `Mathcad` worksheet has been produced that solves for the nominal pipe diameter for prescribed values of Q, s, λ, and F and includes the effects of minor losses. This code, a copy of which appears in Fig. 8.1, is supplied with this book. Compared with the above design graphs, the program has the advantages of including the minor losses where they may be needed. The `Mathcad` worksheets for multiple-pipe networks where the inlet and outlet static pressures may not be zero for one or more of the pipes are also supplied with this text. Copies of these appear throughout the text.

The design charts are presented below as a tool that can be used in the field for rapid estimation of pipe sizes. For more-thorough design calculations, the `Mathcad` worksheet is a more-appropriate tool, but may not be convenient in the field.

5.4.1 Use of the Design Graphs

First, we address the choice of the appropriate figure to use. It is assumed that values for Q and s are known from assessment of the potential site. In many cases, the designer will not know accurate values for F and λ for the proposed network at an early point in the design process. Even if they were known, the graphs corresponding to these exact values are not likely to appear in Figs. 5.4–5.29. The suggested procedure for using these figures in this situation is as follows. This discussion will use English-based, sch. 40 PVC pipe as an example (Figs. 5.4–5.11). If the designer is interested in GI pipe, Figs. 5.13–5.20 should be used, and for metric sizes, Figs. 5.22–5.29.

- Use Fig. 5.4 to estimate the pipe diameter based on the known volume flow rate and mean slope between the source and delivery. This is for assumed values of $F = 0$ (Natural flow) and $\lambda = 1$ which, as discussed in Section 2.32, will produce a lower-bound estimate of the pipe size. The pipe size will always be the smallest possible for the given site geometry because friction is the only

effect balancing the potential energy for Natural flow. That is, a small pipe size is required to produce the large flow speeds needed to generate the necessary friction.

- Repeat this step using Fig. 5.8, which is for $F = 0$ and $\lambda = 1.5$. If there is a difference in pipe sizes between these two steps, either choose the largest pipe size between the two or a more-detailed analysis needs to be carried out to calculate the diameter. This step addresses the effect of pipe length on the pipe diameter. Note, however, that D determined from this step is likely to be "worst case" or larger than required by the design because values for λ are normally < 1.5 for most networks.

- To determine the sensitivity of D to static pressure at the delivery location, repeat the first step using Fig. 5.5, for $F = 0.1$ and $\lambda = 1$, then Fig. 5.6, for $F = 0.25$ and $\lambda = 1$, and so on. If necessary, repeat with Fig. 5.9, for $F = 0.1$ and $\lambda = 1.5$, then Fig. 5.10, for $F = 0.25$ and $\lambda = 1.5$, etc. For most systems, where the elevation head of the source is $\tilde{>}20$ m, a pipe having $F > 0.5$ is not likely. An inspection of the results by sequential use of the above figures will give the designer a sense for the appropriate pipe diameter to use.

Recall that in all of the figures presented in this section, minor losses have been neglected. We will consider the impact of minor losses on the design in Chapter 7. For all design graphs, water temperature is assumed to be 10°C.

In Section 5.5 and in Chapter 9, we demonstrate that all of the design graphs for a given pipe material and wall thickness or schedule can be condensed to a *single* plot. Essentially, this is done by simply rearranging the solution for the dimensionless form of the energy equation, say in terms of Q or D. See Eqn (9.7) or Fig. 9.4. Note that the two dimensionless groups that appear in these plots are what would be obtained if dimensional analysis, say the use of the Buckingham Pi theorem, is performed on the problem of gravity-driven flow in a single pipe. See the topic of Dimensional Analysis in most fluid mechanics textbooks for information on the Buckingham Pi theorem.

5.4.2 Design Graphs for IPS, Sch. 40 PVC Pipe

The design graphs for English-based (IPS), sch. 40 PVC pipe are presented in this section in Figs. 5.4–5.11. A plot of Re for this type of pipe appears in Fig. 5.12.

5.4.3 Design Graphs for IPS, Sch. 40 GI Pipe

The design graphs for English-based (IPS), sch. 40 GI pipe are presented in this section in Figs. 5.13–5.20. A plot of Re for this pipe appears in Fig. 5.21.

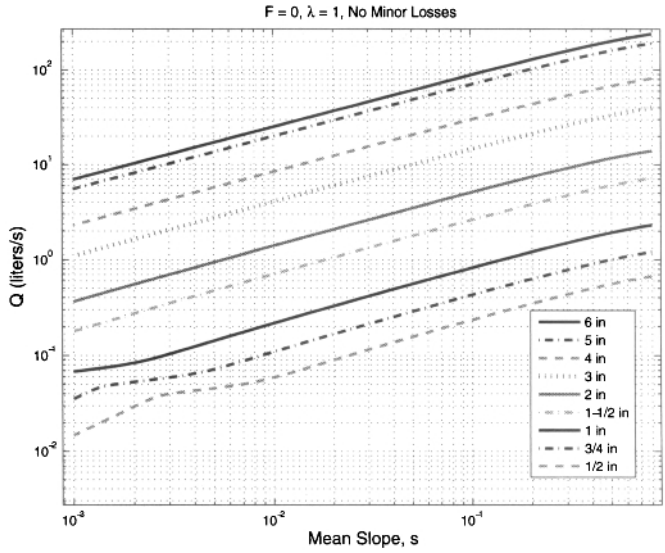

Figure 5.4 Volume flow rate of water versus mean slope of pipe for nine nominal sch. 40 PVC pipe diameters. Delivery pressure corresponds to $F \equiv p_2/\rho g z_1 = 0$ (Natural flow) and $\lambda = 1$ (straight pipe case). Laminar flow is evident for the smallest pipe sizes and the lowest values for the slope. This is followed by the transition regime, and then fully turbulent flow. These characteristics appear in the remaining design plots in this chapter.

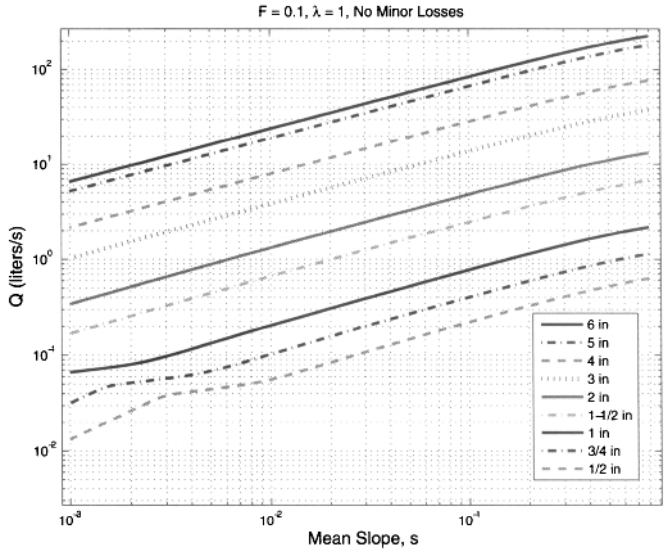

Figure 5.5 Volume flow rate of water versus mean slope of pipe for nine sch. 40 nominal PVC pipe diameters. Delivery pressure corresponds to $F \equiv p_2/\rho g z_1 = 0.1$ and $\lambda = 1$.

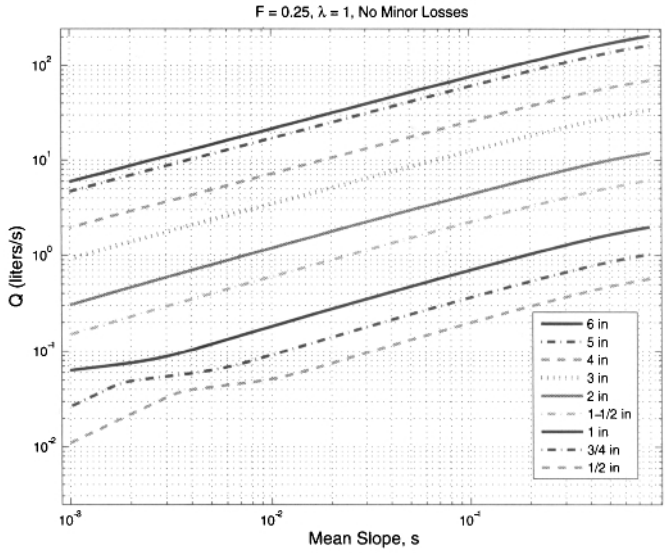

Figure 5.6 Volume flow rate of water versus mean slope of pipe for nine sch. 40 nominal PVC pipe diameters. Delivery pressure corresponds to $F \equiv p_2/\rho g z_1 = 0.25$ and $\lambda = 1$.

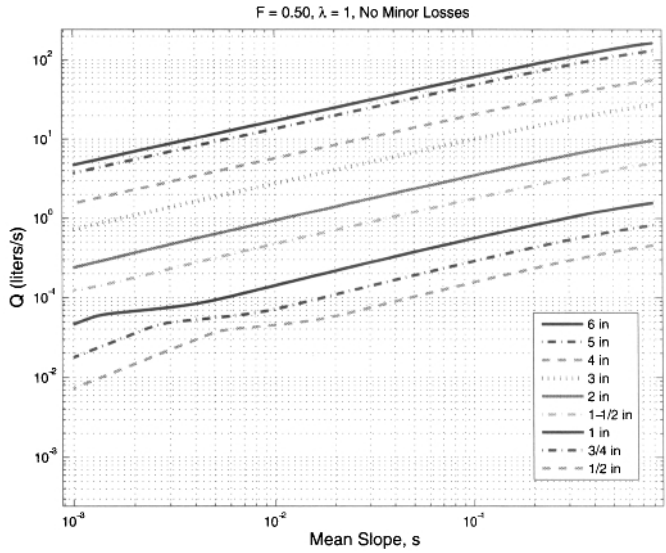

Figure 5.7 Volume flow rate of water versus mean slope of pipe for nine sch. 40 nominal PVC pipe diameters. Delivery pressure corresponds to $F \equiv p_2/\rho g z_1 = 0.5$ and $\lambda = 1$.

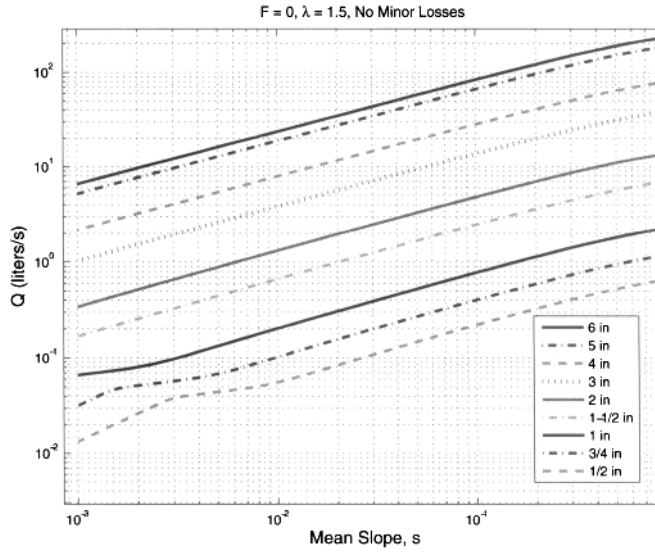

Figure 5.8 Volume flow rate of water versus mean slope of pipe for nine sch. 40 nominal PVC pipe diameters. Delivery pressure corresponds to $F \equiv p_2/\rho g z_1 = 0$ (Natural flow) and $\lambda = 1.5$ (50% longer than straight-pipe case).

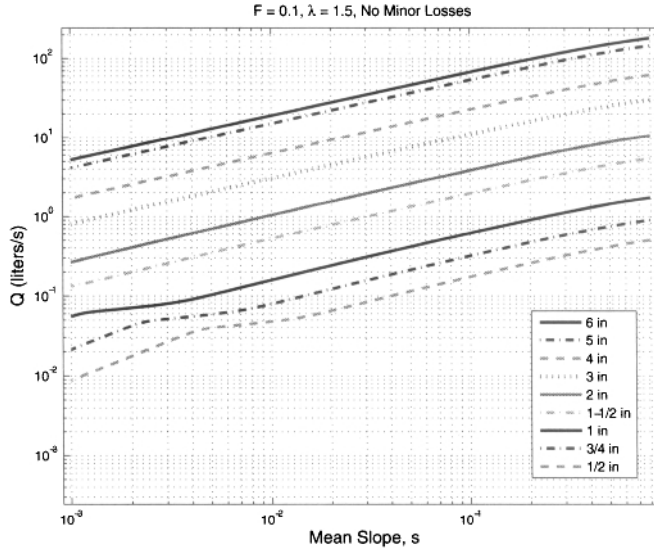

Figure 5.9 Volume flow rate of water versus mean slope of pipe for nine sch. 40 nominal PVC pipe diameters. Delivery pressure corresponds to $F \equiv p_2/\rho g z_1 = 0.1$ and $\lambda = 1.5$.

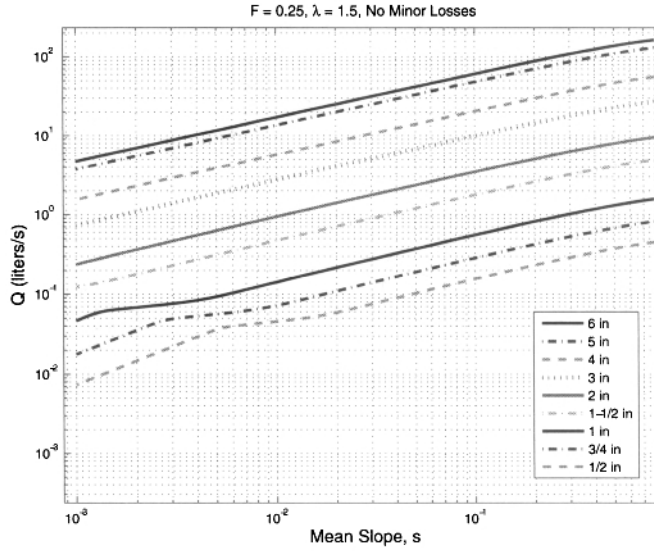

Figure 5.10 Volume flow rate of water versus mean slope of pipe for nine sch. 40 nominal PVC pipe diameters. Delivery pressure corresponds to $F \equiv p_2/\rho g z_1 = 0.25$ and $\lambda = 1.5$.

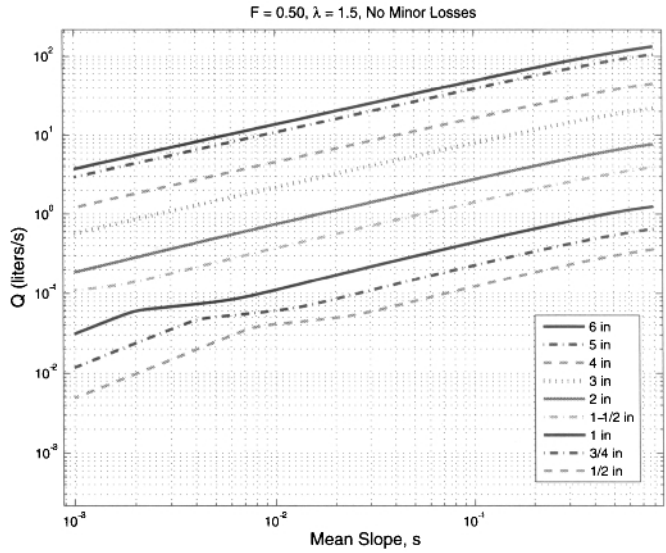

Figure 5.11 Volume flow rate of water versus mean slope of pipe for nine sch. 40 nominal PVC pipe diameters. Delivery pressure corresponds to $F \equiv p_2/\rho g z_1 = 0.5$ and $\lambda = 1.5$.

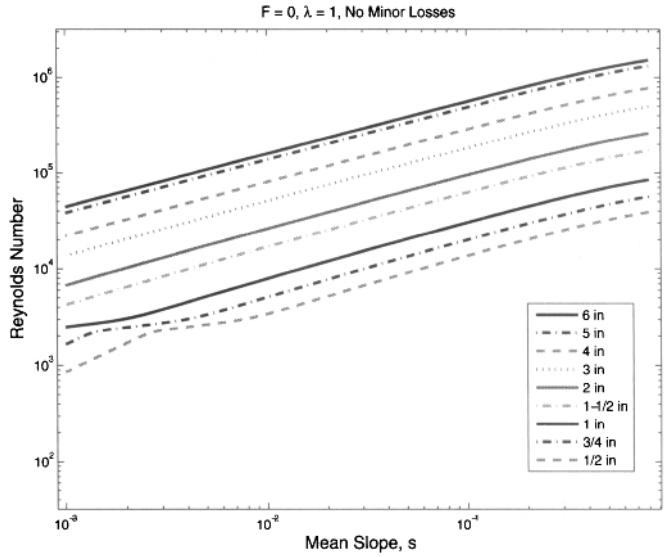

Figure 5.12 Reynolds number versus mean slope of pipe for nine sch. 40 nominal PVC pipe diameters. Delivery pressure corresponds to $F \equiv p_2/\rho g z_1 = 0$ (Natural flow) and $\lambda = 1$ (straight-pipe case). Recall that the flow is laminar for Re $\lesssim$ 2300 and that turbulent flow is assured for Re $\gtrsim$3000.

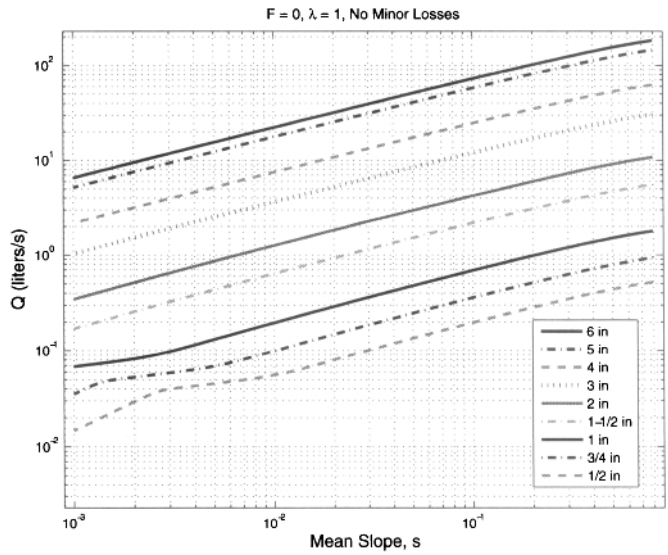

Figure 5.13 Volume flow rate of water versus mean slope of pipe for nine nominal sch. 40 galvanized-steel (GI) pipe diameters. Delivery pressure corresponds to $F \equiv p_2/\rho g z_1 = 0$ (Natural flow) and $\lambda = 1$ (straight pipe case). Compare with Fig. 5.4 for PVC pipe.

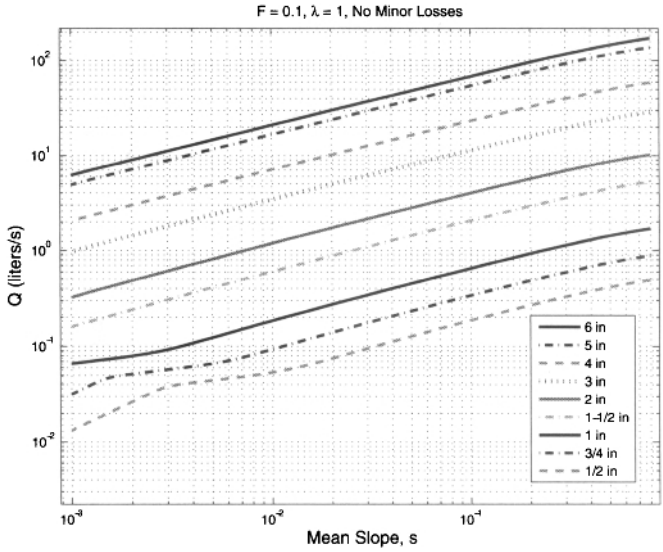

Figure 5.14 Volume flow rate of water versus mean slope of pipe for nine nominal sch. 40 galvanized steel (GI) pipe diameters. Delivery pressure corresponds to $F \equiv p_2/\rho g z_1 = 0.1$ and $\lambda = 1$.

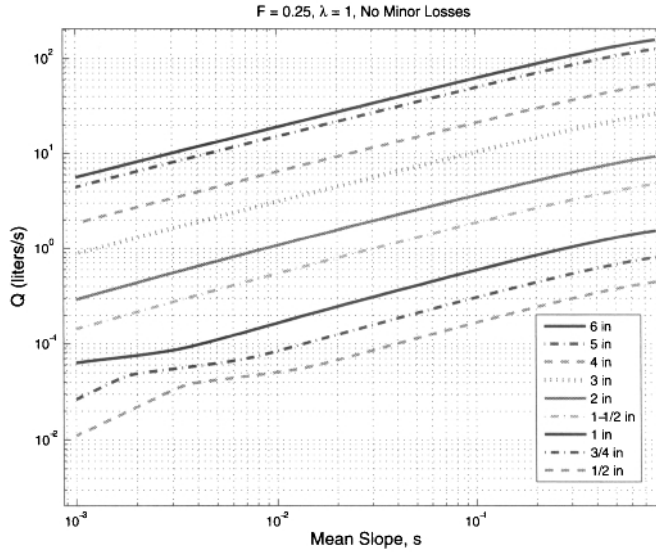

Figure 5.15 Volume flow rate of water versus mean slope of pipe for nine nominal sch. 40 galvanized steel (GI) pipe diameters. Delivery pressure corresponds to $F \equiv p_2/\rho g z_1 = 0.25$ and $\lambda = 1$.

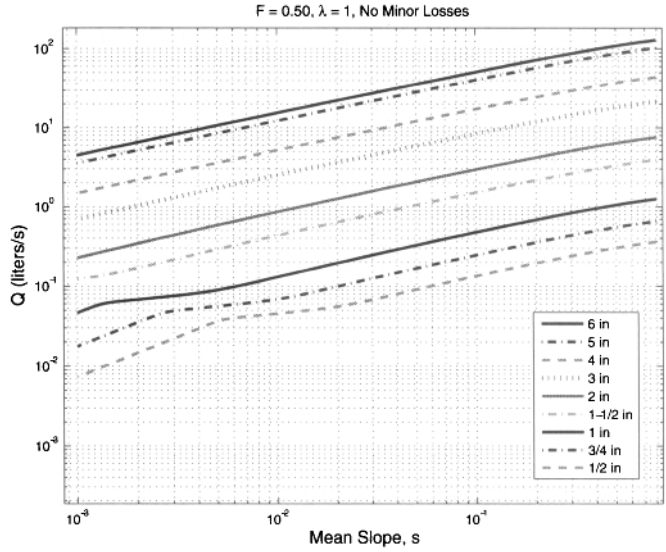

Figure 5.16 Volume flow rate of water versus mean slope of pipe for nine nominal sch. 40 galvanized steel (GI) pipe diameters. Delivery pressure corresponds to $F \equiv p_2/\rho g z_1 = 0.5$ and $\lambda = 1$.

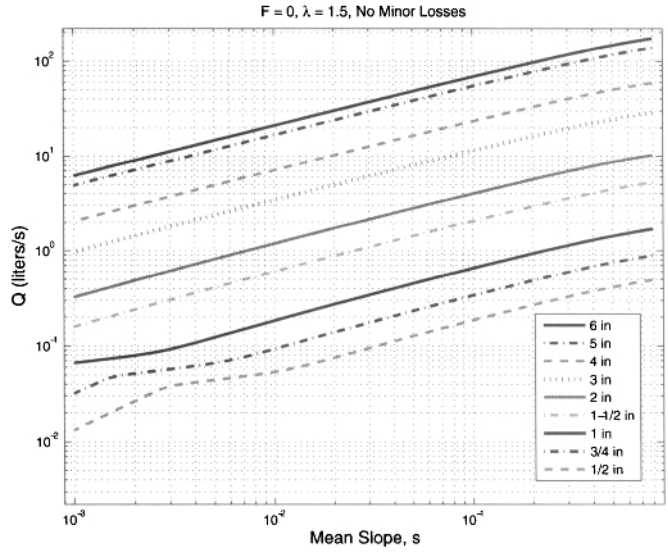

Figure 5.17 Volume flow rate of water versus mean slope of pipe for nine nominal sch. 40 galvanized steel (GI) pipe diameters. Delivery pressure corresponds to $F \equiv p_2/\rho g z_1 = 0$ (Natural flow) and $\lambda = 1.5$ (50% longer than straight-pipe case).

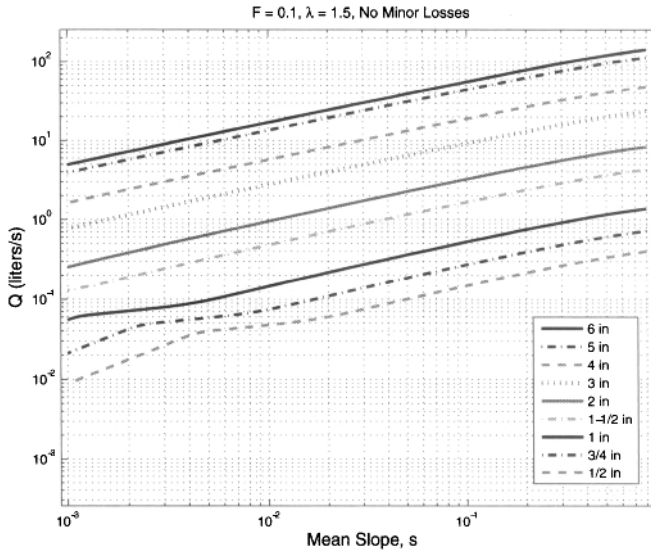

Figure 5.18 Volume flow rate of water versus mean slope of pipe for nine nominal sch. 40 galvanized steel (GI) pipe diameters. Delivery pressure corresponds to $F \equiv p_2/\rho g z_1 = 0.1$ and $\lambda = 1.5$.

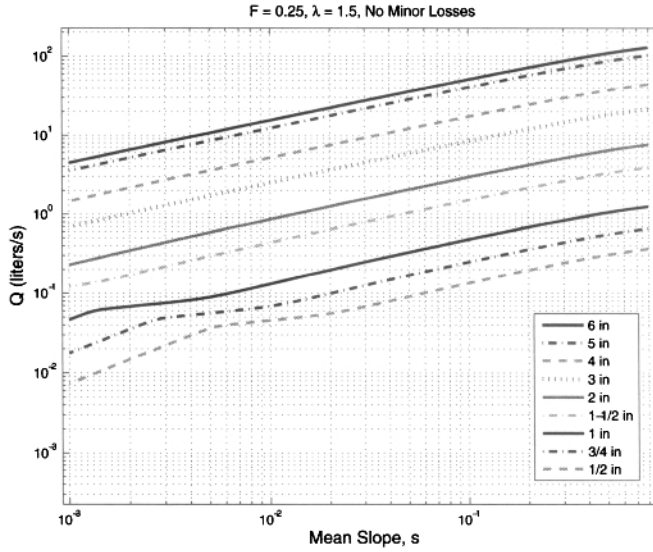

Figure 5.19 Volume flow rate of water versus mean slope of pipe for nine nominal sch. 40 galvanized steel (GI) pipe diameters. Delivery pressure corresponds to $F \equiv p_2/\rho g z_1 = 0.25$ and $\lambda = 1.5$.

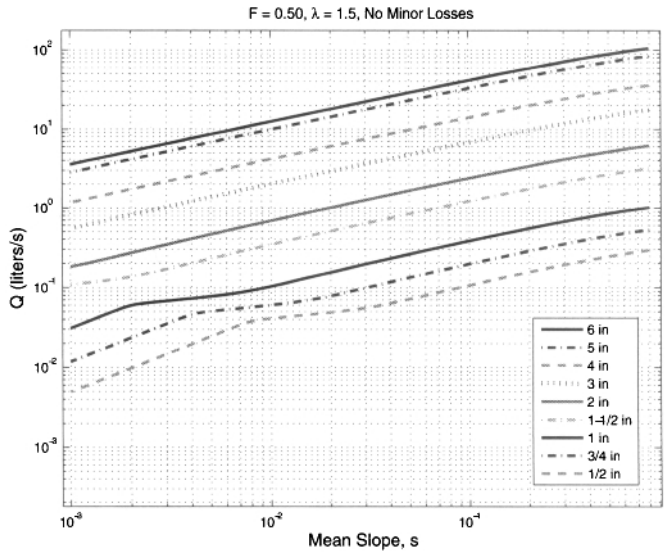

Figure 5.20 Volume flow rate of water versus mean slope of pipe for nine nominal sch. 40 galvanized steel (GI) pipe diameters. Delivery pressure corresponds to $F \equiv p_2/\rho g z_1 = 0.5$ and $\lambda = 1.5$.

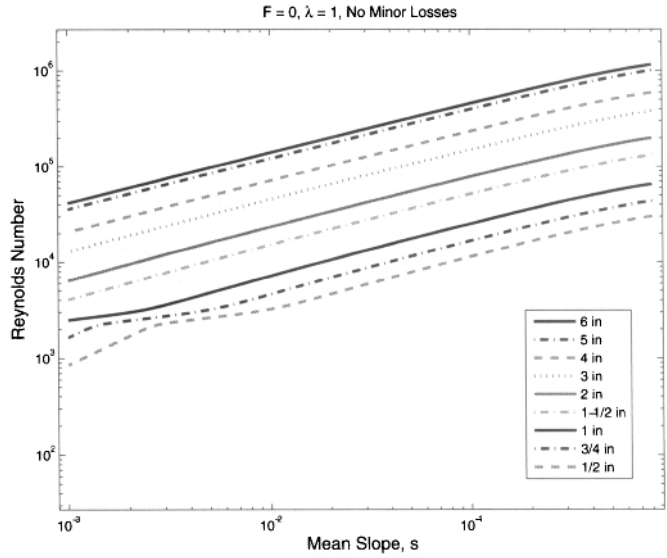

Figure 5.21 Reynolds number versus mean slope of pipe for nine nominal sch. 40 galvanized steel (GI) pipe diameters. Delivery pressure corresponds to $F \equiv p_2/\rho g z_1 = 0$ (Natural flow) and $\lambda = 1$ (straight-pipe case). Recall that the flow is laminar for Re $\tilde{<}$ 2300 and that turbulent flow is assured for Re $\tilde{>}$3000.

5.4.4 Approximate Formulas for D: A Preview

In Chapter 9, we will explore the use of an approximation for the friction factor for smooth pipe and a restricted range of Re. One consequence of this approximation is a simple formula for theoretical pipe diameter D as a function of Q, s, and λ. The result [Eqn (9.3)] is previewed here for convenience,

$$D \approx 0.741 \left[\frac{s\,(1-F)}{\lambda}\right]^{-4/19} \left(\frac{\nu^{1/7} Q}{g^{4/7}}\right)^{7/19} \tag{5.5}$$

where $g = 9.807$ m/s^2 and, for water at 10°C, $\nu = 1.307 \times 10^{-6}$ m^2/s. Recall that based on previous discussions, λ may be approximated to leading order as $\lambda \approx 1.2$. Equation (5.5), which assumes a restricted range of Re and smooth pipe[4], is easily programmed on a handheld calculator and may be used to make a quick estimate of D or a verification of D obtained by the design charts in this chapter or `Mathcad` worksheets.

Swamee and Sharma (2008) report an extension of this approximate formula to include laminar flow and, for turbulent flow, the effect of pipe roughness, ϵ, for nonsmooth pipe. They present,

$$\begin{aligned} D \;\approx\; & 0.66\left\{\left[214.75\frac{\nu Q}{g(h_L/L)}\right]^{6.25}\right. \\ & + \left.\epsilon^{1.25}\left[\frac{Q^2}{g(h_L/L)}\right]^{4.75} + \nu Q^{9.4}(g h_L/L)^{-5.2}\right\}^{0.04} \end{aligned} \tag{5.6}$$

where the hydraulic gradient, h_L/L, is $s\,(1-F)/\lambda$, as discussed in textbox B.2.6.

B.5.2 Example: Use of the Design Charts for Gravity-Driven Flow

Calculate the minimum IPS PVC nominal pipe size for a single-pipe, minor-lossless flow network having a maximum volume flow rate of $Q = 0.40$ L/s and a mean slope of $s = 6\%$. Investigate the sensitivity of the pipe size to delivery pressure and pipe length. Calculate Re for the recommended pipe size. Compare your result with that from Eqn (5.5).

We begin with Fig. 5.4 to estimate D. This is for assumed values of $F = 0$ and $\lambda = 1$ which will produce a lower-bound estimate of the pipe size. For the prescribed values of Q and s, we obtain a pipe diameter between $\frac{3}{4}$ and 1 in. We choose the larger of the two, $D = 1$ in. From Fig. 5.8, which is for $F = 0$ and $\lambda = 1.5$, find the same result. We move on to examine the effect of delivery pressure to determine if a larger pipe size will be required with higher pressures at delivery. Using Fig. 5.9 (for $F = 0.1$ and $\lambda = 1.5$), we find the same result as above for D. From Fig. 5.11 (for $F = 0.5$ and $\lambda = 1.5$), we find that D of 1 in. is slightly too small.

[4]Refer to Section 9.3 for the details.

Use of the Design Charts for Gravity-Driven Flow (Cont'd)

Thus, we conclude if the delivery pressure is to be at least 50% of the elevation head, a $1\frac{1}{2}$-in. PVC pipe is recommended. For static pressure at the delivery location less than this value and tortuosity < 1.5, D =1 in. is adequate. Keep in mind that the flow rate was stated to be a maximum. We must be aware of the need for increasing Q, if appropriate, to accommodate growth of the population over time. From Fig. 5.12, Re for $1\frac{1}{2}$-in. PVC pipe is ~50,000, clearly a turbulent flow. For the given conditions, Eqn (5.5) becomes

$$D = 0.930(1 - F)^{-4/19} \text{ in.}$$

For $F = 0, 0.1$, and 0.25, we obtain $D = 0.930, 0.951$, and 0.988 in., respectively. From Table 3.1, we see that this simple design formula predicts the need for a 1-in. PVC pipe. This is a slight under-prediction for the largest λ compared with the above charts. Note that Eqn (5.5) is valid for only smooth pipe, such as PVC and PE. This excludes its use for GI pipe. However, Eqn (5.6) may be used in this case.

5.4.5 Design Graphs for Metric, SDR 21 PVC Pipe

The design graphs for metric-based, SDR 21 PVC pipe are presented in this section in Figs. 5.22–5.29.

5.5 COMPREHENSIVE DESIGN PLOTS FOR GRAVITY-DRIVEN OR FORCED FLOW

Gravity-driven water flows are the principal topic in the book. However, the curious reader will wonder if the formulas and design charts in this and Chapters 2 and 9 can be applied when flow in a pipe network is driven by a pump or, for a gas, a blower (both referred to as "forced" flow). The answer to this question is yes, and was addressed in Section 2.9, where we saw that upon rearranging the energy equation for pipe flow, Eqn (2.42) (for gravity-driven flow), and comparing with Eqn (2.49) (for forced-flow), the term

$$S = \frac{(1 - F)}{\lambda\sqrt{1 + s^{-2}}} \tag{5.7}$$

and

$$S = \frac{z_1(1 - F_{mod})}{L} = \frac{z_1}{L} - \frac{p_2 - p_1}{\rho g L} \tag{5.8}$$

play the exact same roles for flow in a pipe of diameter D. The first of these two equations applies to a minor-lossless gravity-driven flow, and the second, under the

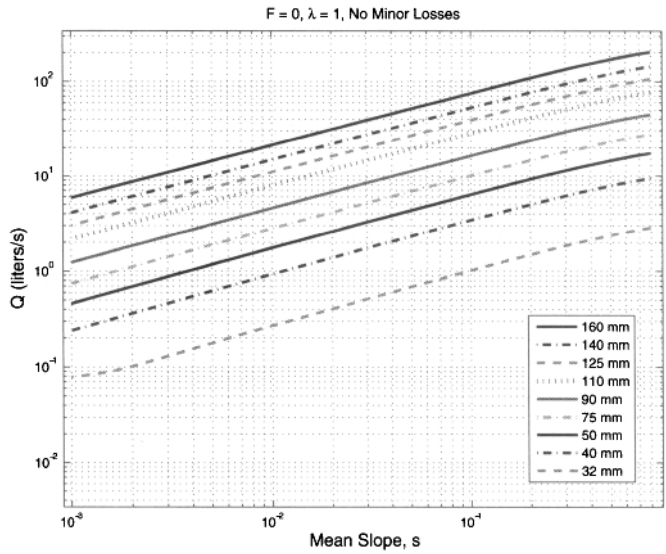

Figure 5.22 Volume flow rate of water versus mean slope of pipe for nine PVC pipe diameters. Delivery pressure corresponds to $F \equiv p_2/\rho g z_1 = 0$ (Natural flow) and $\lambda = 1$ (straight pipe case). Laminar flow is evident for the smallest pipe sizes and the lowest values for the slope. This is followed by the transition regime, and then fully turbulent flow.

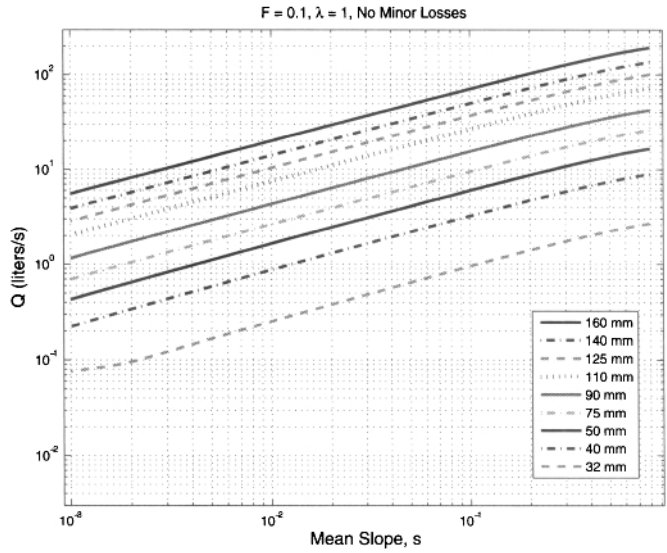

Figure 5.23 Volume flow rate of water versus mean slope of pipe for nine PVC pipe diameters. Delivery pressure corresponds to $F \equiv p_2/\rho g z_1 = 0.1$ and $\lambda = 1$.

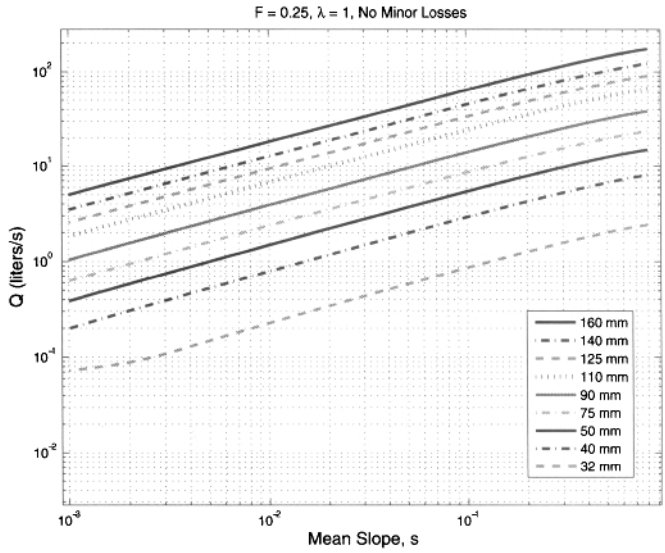

Figure 5.24 Volume flow rate of water versus mean slope of pipe for nine PVC pipe diameters. Delivery pressure corresponds to $F \equiv p_2/\rho g z_1 = 0.25$ and $\lambda = 1$.

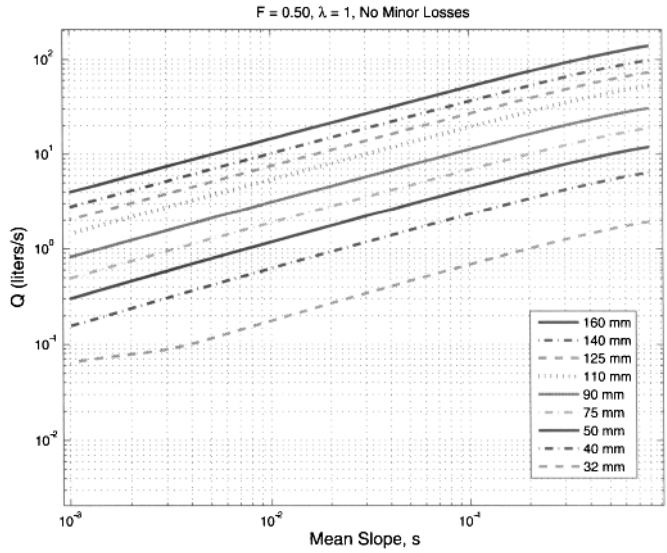

Figure 5.25 Volume flow rate of water versus mean slope of pipe for nine PVC pipe diameters. Delivery pressure corresponds to $F \equiv p_2/\rho g z_1 = 0.5$ and $\lambda = 1$.

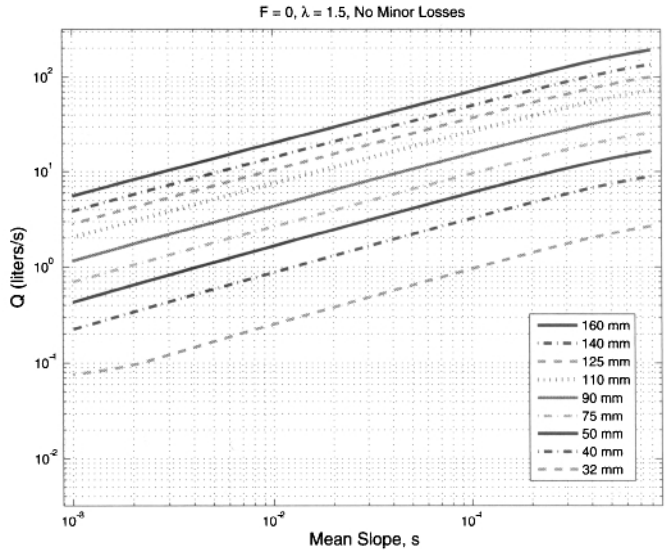

Figure 5.26 Volume flow rate of water versus mean slope of pipe for nine PVC pipe diameters. Delivery pressure corresponds to $F \equiv p_2/\rho g z_1 = 0$ (Natural flow) and $\lambda = 1.5$ (50% longer than straight-pipe case).

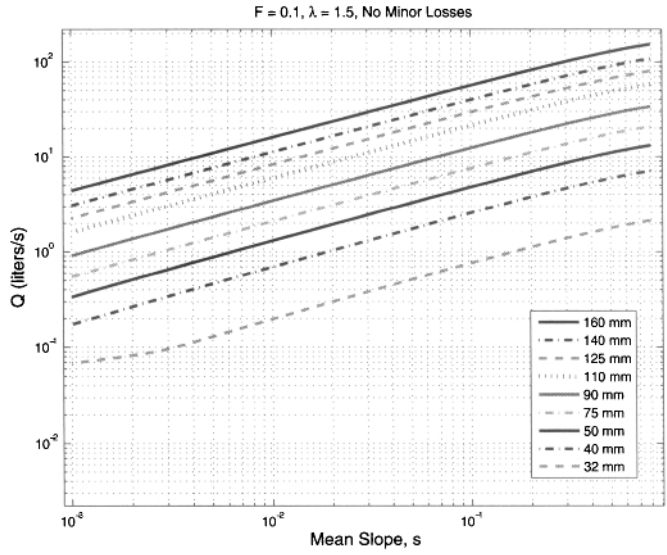

Figure 5.27 Volume flow rate of water versus mean slope of pipe for nine PVC pipe diameters. Delivery pressure corresponds to $F \equiv p_2/\rho g z_1 = 0.1$ and $\lambda = 1.5$.

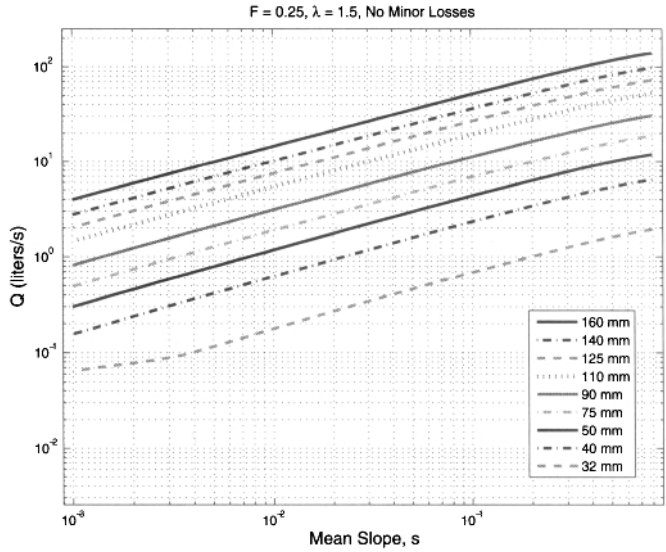

Figure 5.28 Volume flow rate of water versus mean slope of pipe for nine PVC pipe diameters. Delivery pressure corresponds to $F \equiv p_2/\rho g z_1 = 0.25$ and $\lambda = 1.5$.

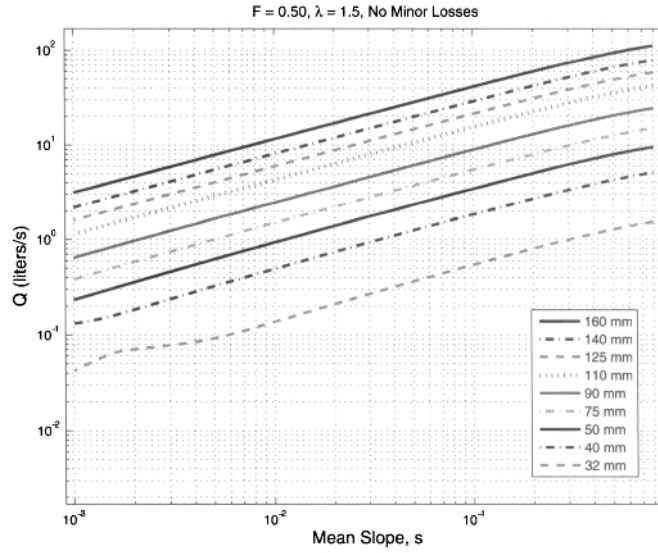

Figure 5.29 Volume flow rate of water versus mean slope of pipe for nine PVC pipe diameters. Delivery pressure corresponds to $F \equiv p_2/\rho g z_1 = 0.5$ and $\lambda = 1.5$.

same conditions for flow driven by a pump or blower[5] Thus, both Eqs (2.41) and (2.49) may be written as the same comprehensive equation in terms of Q,

$$S - \frac{8Q^2}{\pi^2 g}\frac{f(Q,D)}{D^5} = 0 \tag{5.9}$$

Plots of Q versus S for forced or gravity-driven flow are presented in Figs. 5.30 and 5.31 for nine nominal IPS, sch. 40 PVC and GI pipe sizes, and in Fig. 5.32 for nine metric, SDR 13.6 PVC pipe sizes, respectively. Our inspection of either reveals the same trends evident in any one of the design graphs above, as well as the terminal effect for gravity-driven flow. This occurs for $S > 1$ as terminal flow speed, and thus volume flow rate, is encountered. Note that Fig. 5.30 is the same as Fig. 5.4 and Fig. 5.31 the same as Fig. 5.13 except that the group S, as defined above, appears on the abscissa, and the upper range on the abscissa is larger to accommodate the larger values for S that typically occur for forced-flow problems. The reason for comparing the gravity-driven results with those for forced flow in Figs. 5.30–5.32 is to show that the physics of the flow problem is identical; only the mechanism that drives the flow is different. In fact, the designer will use Figs. 5.30–5.32 only for forced-flow networks, since Figs. 5.4–5.29, as they appear, apply only to gravity-driven water flow networks.

In Eqs (5.5) and (5.6), we have approximate formulas for D for gravity-driven flow in single-pipe networks based on an approximation for the friction factor.[6] The equivalent forms for these for the case of gravity-driven *or* forced flow is,

$$D \approx 0.741\, S^{-4/19}\left(\frac{\nu^{1/7} Q}{g^{4/7}}\right)^{7/19} \tag{5.10}$$

and

$$D \approx 0.66\left\{(214.75\frac{\nu Q}{gS})^{6.25} + \epsilon^{1.25}\left(\frac{Q^2}{gS}\right)^{4.75} + \nu Q^{9.4}(gS)^{-5.2}\right\}^{0.04} \tag{5.11}$$

where $g = 9.807$ m/s^2 and, for water at 10°C, $\nu = 1.307 \times 10^{-6}$ m^2/s. As noted above, these may be easily programmed on a handheld calculator to facilitate making a quick estimate of D, or a verification of D obtained by the design charts in this chapter or `Mathcad` worksheets.

5.6 THE FORGIVING NATURE OF SIZING PIPE

Because of the limited number of pipe sizes from which one has to choose, the process of selecting a pipe size for a given set of design conditions can be, by its very nature, a forgiving process. To illustrate this, consider any one of Figs. 5.4–5.11, say Fig. 5.5.

[5]The fluids of interest in this text are liquids, but as noted in Chapter 2, the energy equation for pipe flow applies to any fluid including gases.

[6]Please refer to Chapter 9 for the details and restrictions on the accuracy of these formulas.

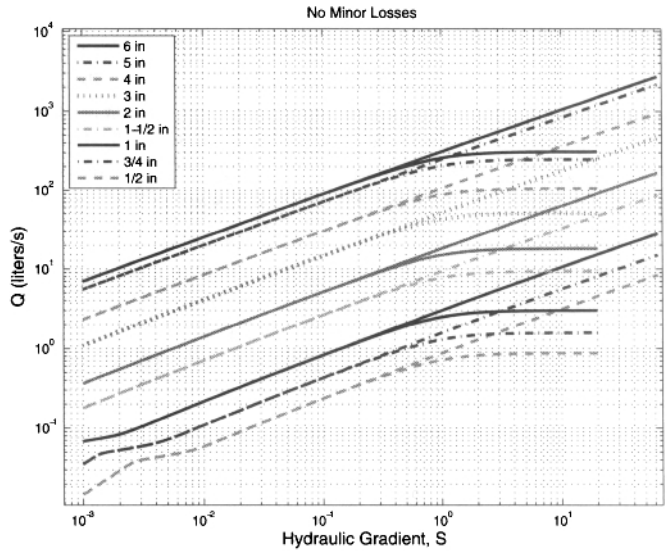

Figure 5.30 Volume flow rate of water versus $S = (1 - (p_2 - p_1)/\rho g z_1)/(L/z_1)$ (for forced flow) and $S = (1 - F)/(\lambda\sqrt{1 + s^{-2}})$ for gravity-driven flow for nine nominal sch. 40 PVC pipe diameters. The curves for gravity-driven flow are for Natural flow and $\lambda = 1$ and become horizontal at an abscissa value of ~2, indicating terminal flow. For $s \ll 1$, $S = (1 - F)/(\lambda\sqrt{1 + s^{-2}}) = s$ for Natural flow and $\lambda = 1$. Our inspection of this figure shows the practical meaning of $s \ll 1$ is $s \tilde{<} 0.5$.

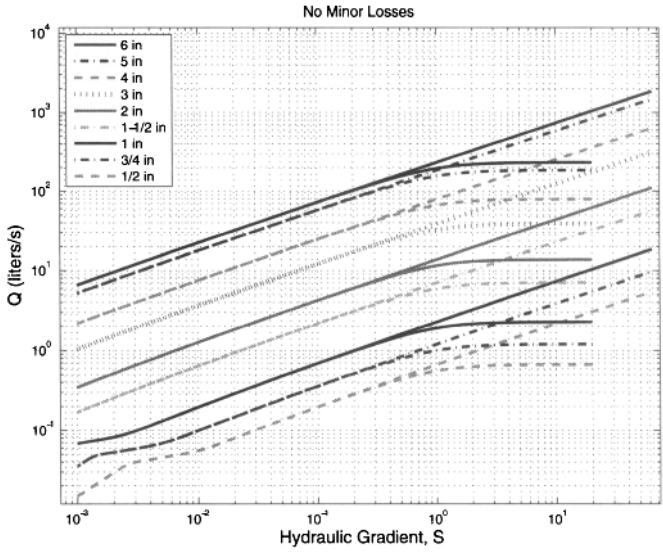

Figure 5.31 Volume flow rate of water versus $S = (1 - (p_2 - p_1)/\rho g z_1)/(L/z_1)$ (for forced flow) and $S = (1 - F)/(\lambda\sqrt{1 + s^{-2}})$ for gravity-driven flow for nine nominal sch. 40 GI pipe diameters. The curves for gravity-driven flow are for Natural flow and $\lambda = 1$.

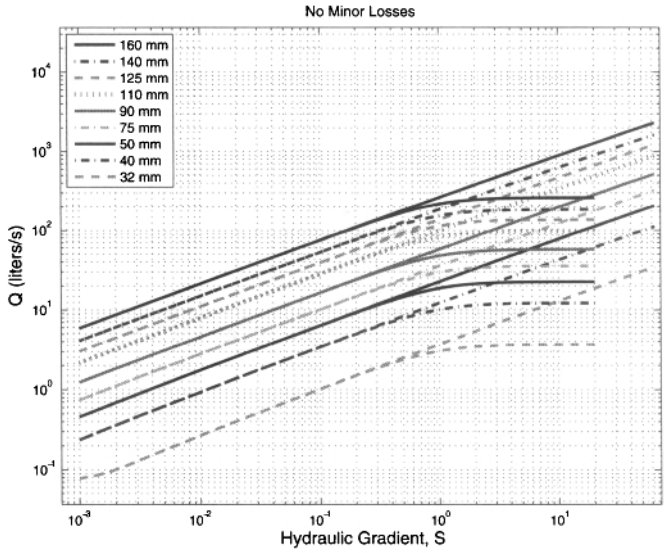

Figure 5.32 Volume flow rate of water versus $S = (1 - (p_2 - p_1)/\rho g z_1)/(L/z_1)$ (for forced flow) and $S = (1 - F)/(\lambda\sqrt{1 + s^{-2}})$ for gravity-driven flow for nine metric, SDR 21 PVC pipe diameters. The curves for gravity-driven flow are for Natural flow and $\lambda = 1$.

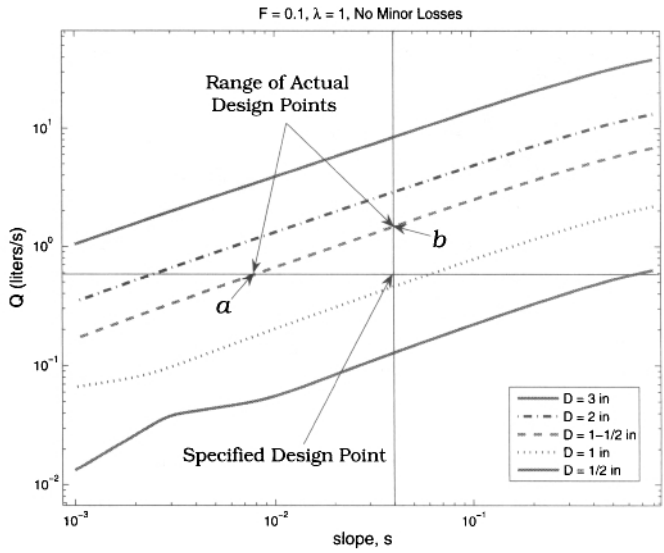

Figure 5.33 A replot of Fig. 5.5 demonstrating the forgiving nature of sizing pipe.

We have modified this figure to emphasize certain points for discussion as follows and present it as Fig. 5.33.

Consider the following example. The design slope and flow rate are given as 0.04 and 0.6 L/s, respectively, for a minor-lossless flow where $F = 0.1$ and $\lambda = 1$. The specified design point can be easily located in the appropriate design plot for these conditions (Fig. 5.5) and is labeled in Fig. 5.33. Since the design point requires a tube size slightly >1-in. nominal PVC, we choose a $1\frac{1}{2}$-in. pipe to satisfy the flow requirements. By our inspection of Fig. 5.33, we see that by choosing this pipe size, we have changed the design point from that specified to an infinite number of *actual design points* that lie along a line (the operating line) connecting points a and b as seen in Fig. 5.33. In particular, the system can pass the required flow of 0.6 L/s for a slope of ~0.008 (much less than the specified 0.04; see point a), and will pass a much larger-than-specified flow of nearly 1.2 L/s for the specified slope of 0.04 (point b). As long as $F = 0.1$, $\lambda = 1$, and the minor losses are negligible, the system will operate at some point on the operating line. Of course, this assumes that the source can supply the peak flow rate of water (of ~1.2 L/s) that sits on this line. In general, this may not be possible and to accommodate the lack of the source's ability to provide this flow, the designer needs to plan for a fitting in the pipeline to reduce the static pressure[7] in the pipe under consideration (see Section 13.15 for issues on oversized pipe). Normally this is installed at the lowest end of the pipe.

[7]For example, a globe valve. With the pressure drop that it causes, a globe valve essentially acts like a reduction in the pipe size. In this way, the effective pipe size for this example is somewhere between 1 in. and $1\frac{1}{2}$-in. See Section 13.14 for a discussion on energy dissipation and globe valves.

We see from this brief discussion that selecting the next largest pipe size above the theoretical value for D adds a degree of forgiveness to the design process. Of course, the extent of forgiveness depends on the location of the design point relative to the operating line for the selected nominal pipe size. If the design point is very close to this line there will not be much forgiveness. Because of this, small errors in slope, flow rate, F, and λ may not adversely impact the success of the operation of the network. However, the conscientious designer will never rely solely on this forgiveness when it comes to planning for an expansion of the network to accommodate additional water flow rate for more houses, schools, community centers, and churches. This should be built into the design in the normal, systematic way.

B.5.3 Example: Comprehensive Design Chart for Forced Flow

Investigate the sensitivity of the volume flow rate Q to the range of nominal-GI pipe sizes from $\frac{3}{4}$ in. to $1\frac{1}{2}$ in. The elevation of the pump is 14 m *below* the delivery location, the pipe length is 730 m, the discharge pressure of the pump is $p_1 = 281$ kPa, and the delivery pressure is atmospheric.

The problem is clearly one of forced flow. Therefore we plan to use Fig. 5.31 which applies to GI pipe. First calculate the value for parameter S from Eqn (5.8),

$$\begin{aligned} S &= \frac{z_1}{L} - \frac{p_2 - p_1}{\rho g L} = \frac{-14\text{ m}}{730\text{ m}} - \frac{0 - 281{,}000\text{ N/m}^2 \cdot 1\text{ kg} \cdot \text{m}/(\text{s}^2 \cdot \text{N})}{1000\text{ kg/m}^3 \cdot 9.807\text{ m/s}^2 \cdot 730\text{ m}} \\ &= -0.0192 + 0.0393 = 0.0201. \end{aligned}$$

Note that the elevation, z_1, is -14 m since the discharge of the pump (the source) is below the delivery location.

The volume flow rates for $S = 0.02$ from Fig. 5.31 for GI nominal pipe sizes of $\frac{3}{4}$ in., 1 in., and $1\frac{1}{2}$ in. are 0.15, 0.29, and 0.90 L/s, respectively.

References

P. K. Swamee and A. K. Sharma. *Design of Water Supply Pipe Networks*. John Wiley & Sons, Inc., Hoboken, NJ, 2008.

Students and faculty from Villanova University work with technicians in Waslala, Nicaragua preparing to construct a reservoir.

CHAPTER 6

"NATURAL DIAMETER" FOR A PIPE: LOCAL STATIC PRESSURE

"How do you get the water to flow uphill?"
– Anita D. Jones (age 84)

6.1 MOTIVATION

In Section 2.6.1, we saw the concept of Natural flow in a pipe as the constant value of flow that produces a balance between the potential energy of the source and energy dissipated by pipe friction. In this brief chapter, we explore a related concept. For a prescribed volume flow rate in a minor-lossless flow and a given geometry of the network (elevations and pipe lengths), there exists a theoretical pipe diameter distribution that produces a desired constant value of static pressure at each and every location in the pipe. We refer to this theoretical diameter as the "Natural diameter" or "Natural diameter distribution" for a pipe.[1] For example, the desired local static

[1] Although the concept of a Natural diameter distribution of a pipe is valid for all flow networks in principle, in practice it can be obtained only for those networks where the pipe possesses a downward slope at all points. This slope is referred to as a "favorable slope" for a gravity-driven water network; one that at each and every point assists the flow with the addition of potential energy that is in turn dissipated as friction.

Gravity-Driven Water Flow in Networks. By Gerard F. Jones

pressure may be a (positive-valued) gage pressure needed to produce flow at a distance or eliminate possible flow of contaminants from the surroundings into a buried pipe. Jordan Jr. (2004) has recommended a static head of water ($p/\rho g$) of a minimum of 10 m, or ~1 atm of pressure.

As a prelude to this idea, we will need to develop the energy equation for local flow conditions along the pipe flow path. If desired, the solution from this equation is the local static pressure. This is the first instance in the text where attention is being given to the local static pressure, otherwise referred to as the static pressure distribution, $p(z)$. In the developments in the previous chapters, our focus was on only the inlet and outlet states for the flow; no attention was paid to those states in between. The static pressure varies continuously in a pipe flow and must generally be positive—valued throughout the network for the reasons described above. In addition, and to answer the quotation above, it is a positive (i.e., greater than gage in value) static pressure that forces water to flow, locally, uphill. These needs may be a challenge from a design standpoint especially in networks where there are local peaks that have an elevation near that of the source. A sound design approach must consider the local static pressure distribution to ensure that the performance of the network meets the design specifications.

For simplicity, in the first few sections below we restrict our interest to a pipe that runs in just a vertical plane, that is, a two-dimensional (2D) network (see Fig. 2.11). The local static pressure distribution in a fully three-dimensional (3D) network will be covered in Section 6.5.

6.2 THE ENERGY EQUATION WRITTEN FOR LOCAL STATIC PRESSURE

We begin by writing the energy equation for pipe flow, Eqn (2.7), in differential form. We have

$$d(\frac{p(z)}{\rho}) + \frac{1}{2}d(\alpha(z)\overline{u}^2(z)) + gdz = dH_L(z) = -d(\frac{p_{fr}(z)}{\rho}) \qquad (6.1)$$

where the negative sign in right-side friction term ($-dp_{fr}$ is a differential pressure drop) accounts for the dissipative nature of friction (i.e., a reduction of static pressure with distance in the direction of water flow). Note that this negative sign would also appear as a multiplier of the friction term of Eqn (2.7) if its left side were written in reverse order, state 2 energy values minus those at state 1. The argument z is included in the appropriate terms in Eqn (6.1) to remind us that the terms may depend on local elevation. Ultimately, z, in turn depends on the local horizontal coordinate, x, through the geometry of the pipe network. This gives $z = z(x)$, where x is assumed to be measured from the location of the source.

Upon integrating Eqn (6.1) from $z(x = 0)$ to any arbitrary $z(x)$ location, we obtain

$$\begin{aligned} \frac{p(z) - p_1}{\rho} &+ \frac{1}{2}[\alpha(z)\overline{u}^2(z) - \alpha_1\overline{u}_1^2] + g(z - z_1) \\ &= -\int_0^{L_\ell(z)} f(\overline{u}(z), D(z))\frac{\overline{u}(z)^2}{2D(z)}\, dL\,(z) \end{aligned} \tag{6.2}$$

where L_ℓ is the length of the flow path to any arbitrary location, and $z = z(x)$. In Eqn (6.2) the differential form of the Darcy–Weisbach equation, Eqn (2.9), was used,

$$d(\frac{p_{fr}}{\rho}) = f(\overline{u}, D)\frac{\overline{u}^2}{2D}dL \tag{6.3}$$

where dL is a differential pathlength for the flow.

As usual, p_1 and $\overline{u}_1$ are both zero (at the source). Dividing Eqn (6.2) by gz_1, where z_1 is the elevation of the source, and rearranging, Eqn (6.2) becomes

$$\frac{p(z)}{\rho g z_1} = 1 - \frac{z}{z_1} - \frac{\alpha(z)\overline{u}^2(z)}{2gz_1} - \frac{1}{2gz_1}\int_0^{L_\ell(z)} f(\overline{u}(z), D(z))\frac{\overline{u}(z)^2}{D(z)}\, dL(z) \tag{6.4}$$

In Eqs (6.2) and (6.4), the static pressure p, elevation z, and flow speed $\overline{u}$ are states and, as such, the differentials of them are *exact* differentials.[2] For an exact differential da, $\int_1^2 da = a_2 - a_1$. In particular, note that the static pressure at any location depends only on the local value for $\overline{u}$, not an integrated value to that point; an effect that is referred to as the "static pressure regain", which you may have discussed in fluid mechanics. The exact-differential nature of p, z, and $\overline{u}$ is the reason why these terms do not appear under an integral sign in Eqs (6.2) and (6.4). Friction, however, is not a state but a path-dependent quantity. Friction arises from work done by shear forces on the pipe wall from motion of the fluid; it is well understood work (and heat transfer, for that matter) are path-dependent quantities; longer path lengths cause larger total frictional forces on the fluid. In the frictional term in Eqs (6.2) and (6.4), the length from the origin to any arbitrary location along the flow path affects the local static pressure, not simply the friction at that location. This is why the frictional term appears under an integral sign in Eqs (6.2) and (6.4).

The differential flow-path length, dL, may be written in terms of differential elevation change, dz, and differential coordinate, dx, as

$$dL = \sqrt{dx^2 + dz^2} = \sqrt{1 + (\frac{dz}{dx})^2}\, dx = \sqrt{1 + s_\ell^2}\, dx \tag{6.5}$$

where s_ℓ is the local slope of the pipe. For a discussion on the sign of s_ℓ, see footnote 18 in Section 2.6.1.

[2]The distinction between a "state" variable like energy, static pressure p, elevation z, and flow speed $\overline{u}$ and "nonstate", or path-dependent, variables like work due to friction is made in classical thermodynamics. Please see any thermodynamics textbook for this.

With Eqn (6.5), Eqn (6.4) becomes

$$\begin{aligned}\frac{p(x)}{\rho g z_1} &= 1 - \frac{z(x)}{z_1} - \frac{\alpha(x)\overline{u}^2(x)}{2gz_1} \\ &- \frac{1}{2gz_1}\int_0^x f(\overline{u}(\xi), D(\xi))\frac{\overline{u}(\xi)^2}{D(\xi)}\sqrt{1+s_\ell(\xi)^2}\,d\xi \end{aligned} \tag{6.6}$$

where ξ is a dummy variable of integration.

As a final step we employ the continuity equation, Eqn (2.21), to write $\overline{u}$ in terms of Q as done above. Equation (6.6) is written as

$$\boxed{\begin{aligned}\frac{p(x)}{\rho g z_1} = 1 - \frac{z(x)}{z_1} - \frac{8Q^2}{\pi^2 g z_1}\{\frac{\alpha(x)}{D(x)^4} \\ + \int_0^x \frac{f(Q, D(\xi))}{D(\xi)^5}\sqrt{1+s_\ell(\xi)^2}\,d\xi\}\end{aligned}} \tag{6.7}$$

Equations (6.6) and (6.7) are the energy equations (the first in terms of $\overline{u}$ and the second in terms of Q) for gravity-driven, minor-lossless[3] flow in any straight or curved pipe, of constant or variable diameter, which govern the local static pressure distribution in the flow, $p(x)$. The first two terms on the right side of Eqs (6.6) and (6.7) account for a static pressure increase with reduction in elevation and the last term on the right side represents the major frictional loss and the energy to accelerate the flow locally. It is a relatively straightforward task to show that Eqn (6.6), when written at $x = \ell$, reduces to Eqn (2.34) for a straight pipe of constant cross section (where s_ℓ and D are both constant)[4], and to Eqn (2.41) for any general curved pipe of constant cross section.[5] In both cases, recall that F in Eqs (2.34) and (2.41) are defined as $p(z=0)/\rho g z_1$ or $p(x=\ell)/\rho g z_1$. A variation of Eqn (6.6) will appear in Chapter 7 to describe the static pressure distribution in a pipe where minor losses are included.

In the present context, the static pressure, $p(x)$, is taken to be a prescribed constant and we solve the energy equation for the diameter. For this case, we designate this theoretical diameter from the solution of Eqn (6.7) as $D(x) = D^n(x)$ to show that it is special (i.e., the Natural diameter distribution that produces the required uniform static pressure in the pipe).

[3]Note that the term α, which accounts for the local acceleration of the flow over a small length of the pipe, has been included; this is not a minor loss.

[4]Please see Exercise 18.

[5]Note that for constant D and constant volume flow rate, f is also constant and the integral in Eqn (6.7) reduces to $\int_0^x \sqrt{1+s_\ell(\xi)^2}d\xi = \int_0^x dL_\ell = L_\ell(x)$, where $L_\ell(x)$ is the pipe length from the source to any arbitrary x (that is, horizontal) location measured along the flow path. Please take a few minutes to prove this to yourself.

6.3 AN ILLUSTRATION: THE "NATURAL DIAMETER"

Once the geometry of the pipe is specified, $z(x)$ and slope $s_\ell(x)$ are known and with a prescribed uniform value for $p(x)/\rho g$, Eqn (6.7) can be solved for $D^n(x)$. The numerical solution of Eqn (6.7) was carried out (in the package `Matlab`) for two cases of straight pipe ($\lambda = 1$) in a minor-lossless flow having a uniform slope of 1% (small slope) and 100% (large slope of 45°), respectively, with Q of 1.0 L/s and z_1 of 100 m. The value for $p(x)/\rho g$ was set to 0 (atmospheric pressure throughout the pipe)[6]. The friction factor, $f(Q, D)$ from Eqs (2.16) and (2.17), is used in obtaining this solution. The kinetic energy correction factor, α, is 2 for laminar flow and 1.05 for turbulent flow.

The results for this case are shown in Fig. 6.1, where $D^n(x)$ is plotted against the x coordinate. Our inspection of this figure reveals a considerable variation in pipe diameter that occurs over the first meter, or so, of x. Over this distance[7] the pathlength for the flow is small enough that friction may be neglected in favor of acceleration in Eqn (6.7). With the neglect of the integral term, and for $p(x)/\rho g z_1$ of zero, we may rewrite Eqn (6.7) as

$$D^n_{app}(x) = \left(\frac{8\alpha Q^2}{\pi^2\, g\, x\, s}\right)^{1/4} \tag{6.8}$$

where the subscript app indicates an approximate value for $D^n(x)$ and s is the mean slope. A plot of this function appears in Fig. 6.1, where we note near-perfect agreement between Eqn (6.8) and the numerical solution of Eqn (6.7) for the entrance region of the pipe. From our inspection of Fig. 6.1, we see that $D^n(x)$ approaches a large value (in theory, approaching infinity) as $x \to 0$, a reflection of the need for the water to remain quiescent to satisfy the imposed zero static pressure. For x values larger than ~10 meters, friction dominates the flow and $D^n(x)$ becomes constant. This is a consequence of the constant slope for this example. For a fixed value of $p(x)/\rho g z_1$ and constant slope, the only solution admitted by Eqn (6.7) is constant D. To explain this, first note that for constant slope the incremental decrease in potential energy per unit change in x is constant over the entire flow path of the pipe. Since this energy change must be consumed by friction, the frictional energy change per unit change in x must be constant. This can only occur with a uniform value for D over the entire flow path.[8]

Finally, by our inspecting Fig. 6.1, we see that the value of D from this figure in the friction-dominated region is in perfect agreement with that from Fig. 5.4, the

[6]This value is chosen because the required static pressure is arbitrary and a zero value is the simplest case. The results presented below will be identical in character for any value of $p(x)/\rho g$, say $p(x)/\rho g$ equal to 10 m, except that the designer will not be able to satisfy this condition for at least the first 10 m of pipe measured vertically from the source.

[7]The distance referred to in this sentence is established by comparing the friction and inertia terms on the right side of Eqn (6.7). A balance between them shows that the water will need to travel about 10-30 pipe-diameter lengths before friction becomes of the same order of magnitude as inertia.

[8]From a mathematical viewpoint, note that Eqn (6.7), when written for constant D and slope, contains two terms that are linear in x. The first is $1 - z(x)/z_1$, and the second is the friction term $f(Q, D)/D^4 \cdot L_\ell(x)/D$. Thus, the value for D is established by a balance between these two terms.

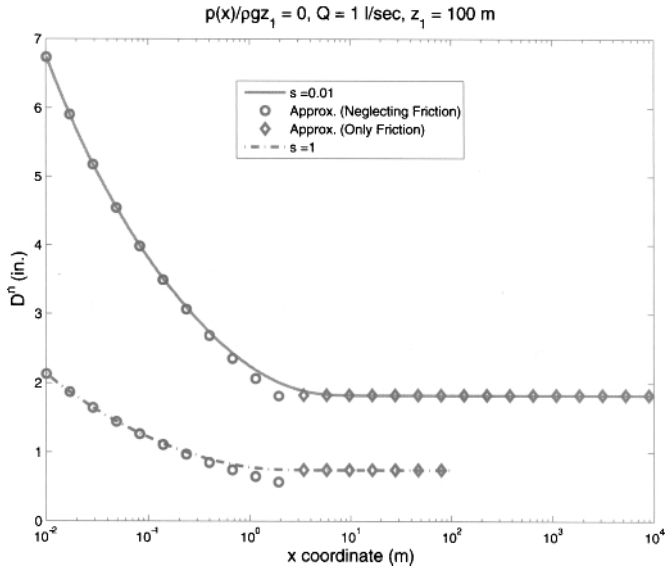

Figure 6.1 The Natural diameter distribution, $D^n(x)$, for $p(x)/\rho g z_1 = 0$ and large and small constant-slope pipes. The approximate values for $D(x) = D^n_{app}(x)$ are from Eqn (6.8) for the first few meters of the pipe where friction is negligible and, after this location, from Fig. 5.4, where friction dominates. The values for D for the two slopes are 1.83 and 0.748 in., respectively, in the friction-dominated region.

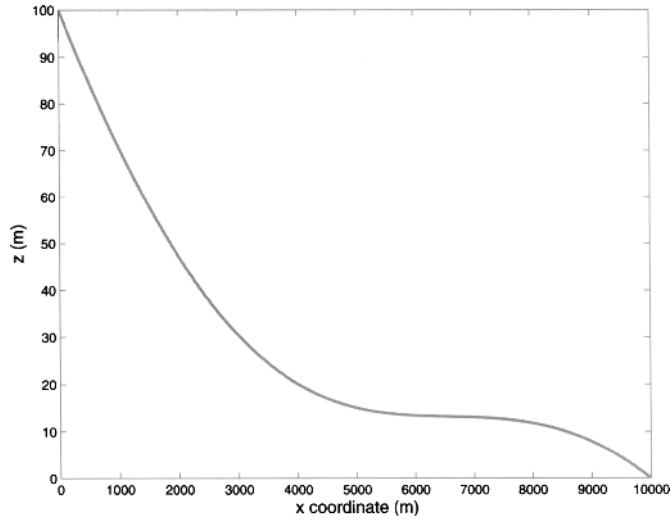

Figure 6.2 A realistic contour for a gravity-driven water pipe.

appropriate design curve for the set of conditions in this example. It is worthwhile checking for this consistency in problems that present us with this opportunity.

Let us consider a more realistic example where the slope of the pipe varies with x (see Fig. 6.2). The results for this example are presented in Figs. 6.3 and 6.4, where the focus is on $D^n(x)$ for the inertia-dominated region near the pipe entrance, and the bulk of the pipe flow, respectively. Two points concerning Fig. 6.4 are noteworthy. First, there is a variation in pipe diameter of about a factor of 3 as the result of the variation in local slope, $s_\ell(x)$, and the need for the constancy of the local static pressure. Second, it is clear that the pipe diameter varies inversely with local slope. Note that the largest change in $D^n(x)$ occurs where the contour of the pipe has a near-zero value for a local slope that occurs between x of 6000 and 7000 meters. This observation is explained as follows. As the local slope decreases, the local driving force (or potential energy) per unit of pipe length decreases. To satisfy the energy equation, the energy dissipated by friction must also decrease. This is accomplished by reducing the flow speed or, since Q is constant for these examples, increasing the pipe diameter, $D^n(x)$.

6.4 COMMENTARY

From the above examples, it is clear that the pipe diameter and local static pressure are intimately connected by the contour of the pipe (along with Q and z_1 whose effects were not investigated in the examples presented here). In particular,

- The pipe diameter and local slope are inversely proportional to each other, where there is a uniform local static pressure in the pipe flow,

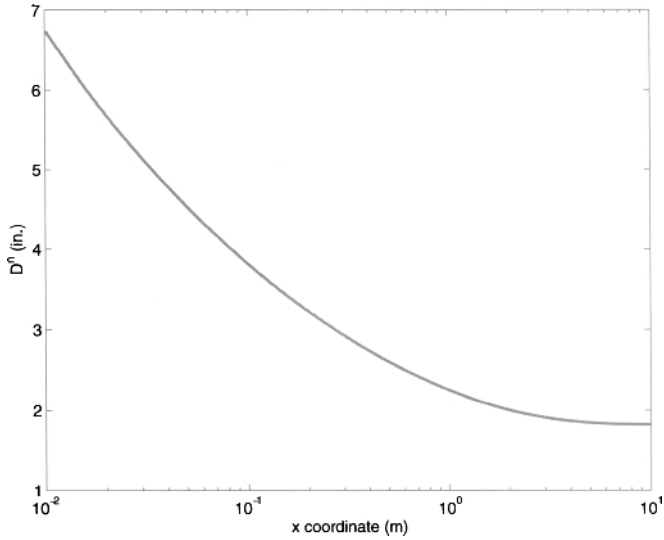

Figure 6.3 Natural diameter distribution, $D^n(x)$, for $p(x)/\rho g z_1 = 0$, $Q = 1.0$ L/s, $s = 0.01$, $z_1 = 100$ m, and the pipe contour of Fig. 6.2. Only the near-source region is shown.

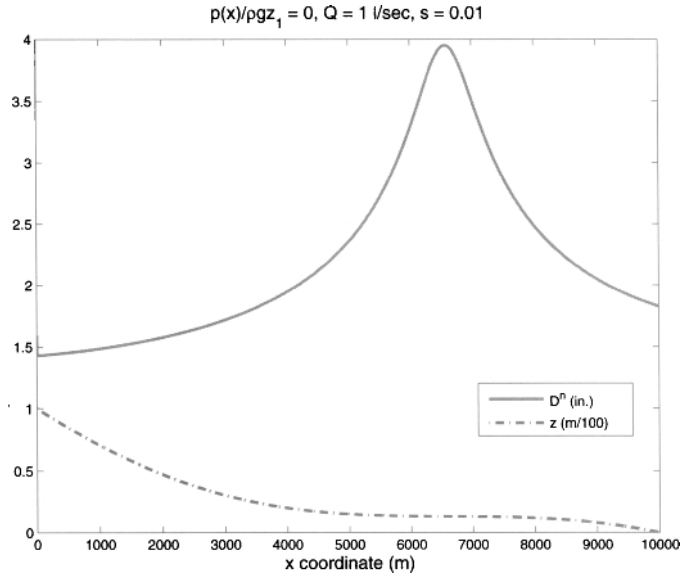

Figure 6.4 Natural diameter distribution, $D^n(x)$, for $p(x)/\rho g z_1 = 0$, $Q = 1.0$ L/s, $s = 0.01$, $z_1 = 100$ m, and the pipe contour of Fig. 6.2. The bulk of the pipe flow is shown. The pipe contour appears for reference.

- For the region away from the pipe inlet, where the flow is dominated by friction not inertia, D is constant and finite for the case of constant nonzero slope (cf. Fig. 6.1) and approaches infinity as the local slope approaches zero (cf. Fig. 6.4).

Of course, no one designs a gravity-driven water network with a variable-diameter pipe as depicted in Figs. 6.1, 6.3, and 6.4; pipes of infinitely variable diameters do not exist and if they did their cost would likely make them prohibitive to install. Instead, we use pipes of constant diameter over large flow paths and the designer needs to choose nominal pipe sizes that produce a static pressure distribution that is *acceptable*. This designation means a static pressure large enough to prevent contaminants from entering the water flow from the outside but not too large such that the pipe costs will become prohibitive. This is clearly where engineering tradeoffs need to be considered.

In summary, the combination of the need to provide acceptable pressures and the lack of ability for the designer to control these pressures by locally varying the pipe diameter as he/she chooses, necessitates that close attention be paid to the effect of pipe size distribution in networks that have local peaks and valleys. A good example for this is presented in Section 8.6.

The ideas from the this section will now be extended to a 3D pipe flow network.

6.5 LOCAL STATIC PRESSURE FOR A THREE DIMENSIONAL NETWORK

For a 3D flow network, where the flow path can be described as $z(x, y)$, we begin with Eqn (6.5) and extend this to include a second coordinate in the horizontal plane, y. The differential of the flow path length becomes

$$dL = \sqrt{dx^2 + dy^2 + dz^2} \tag{6.9}$$

where dy is the differential length of the pipe in the y direction. If we restrict our interest to those cases where the pipe diameter, D, is uniform over the flow path, Eqn (6.7) is written as

$$\frac{p(x, y(x))}{\rho g z_1} = 1 - \frac{z(x, y(x))}{z_1} - \frac{8Q^2}{\pi^2 g z_1}\left[\frac{\alpha}{D^4} + \frac{f(Q, D)}{D^5}\int_0^{L_\ell(x, y(x))} d\xi\right]. \tag{6.10}$$

The symbol ξ is a dummy variable of integration as before. $L_\ell(x, y(x))$ is the length from the source to any arbitrary location along the pipe flow path as a function of the position of the pipe in the y direction ($y(x)$) and the assumed independent variable, x. That is, the coordinates of the pipe at any location are $(x, y(x), z(x))$. We see from our inspection of Eqn (6.10) that there is little need to refer to local slope as we did for the simpler case of a 2D network. In the present 3D case, there are two slopes that affect the local flow path length along the pipe, $dz(x)/dx$ and $dz/dy = (dz(x)/dx)/(dy(x)/dx)$. These are cumbersome to use. Instead, the

designer normally solves the energy equation in the coordinate of the pipe itself, the local pipe length L_ℓ, or "pipeline coordinate.[9]" Thus, the final form of the energy equation for minor-lossless pipe flow and constant D for a 3D flow network is

$$\frac{p(L_\ell(x))}{\rho g z_1} = 1 - \frac{z(L_\ell(x))}{z_1} - \frac{8Q^2}{\pi^2 g z_1 D^4}[\alpha + \frac{f(Q,D)}{D}\int_0^{L_\ell(x)} d\xi] \tag{6.11}$$

or, after carrying out the integration,

$$\boxed{\frac{p(x)}{\rho g z_1} = 1 - \frac{z(x)}{z_1} - \frac{8Q^2}{\pi^2 g z_1 D^4}[\alpha + f(Q,D)\frac{L_\ell(x)}{D}]} \tag{6.12}$$

An inspection of Eqn (6.12) for a 3D flow network shows that it is identical to that for the 2D analysis above for constant D. That is, Eqn (6.7) when written for constant D and combined with Eqn (6.5) is identical to Eqn (6.12) if the independent variable x is replaced by $L_\ell(x)$. Since the quantities of interest are energies (which are scaler, not vector in character), any 3D flow network described by the coordinates (x, y, z) may be effectively "flattened" in the y direction so that the component of the network in this direction is eliminated. This is valid provided that the overall length of the pipe is unchanged and the elevation, z, as a function of the independent variable x or $L_\ell(x)$ is maintained. Thus, we see that the independent variable x takes on a new meaning in light of this discussion. x can be the horizontal coordinate in the usual Cartesian coordinate sense, or the coordinate measured along the line of the pipe. We will refer to the x coordinate in the latter case as a "pipeline coordinate."

A consequence of the above discussion is that there is no need to distinguish between 2D and 3D flow networks provided the horizontal coordinate is measured in the vertical plane of the pipe for which the energy equation is written. The energy equation, written for local conditions in a minor-lossless pipe flow [Eqn (6.12)], will be referred to as needed in the chapters that follow.

6.6 GRAPHICAL INTERPRETATIONS: ENERGY LINE AND HYDRAULIC GRADE LINE

6.6.1 Energy Line

Engineers working in the field of hydraulics, who perform calculations for pipe and open-channel fluid flows, sometimes rewrite Eqn (2.2) by dividing both sides by g. With the use of Eqn (2.4), we obtain

$$\frac{p(z)}{\rho g} + \alpha_2 \frac{\overline{u}(z)^2}{2g} + z = h_T - h_L(z) \tag{6.13}$$

[9]The reader may remember from fluid mechanics that this is the usual way that the Bernoulli equation is developed; by integrating the inviscid momentum equation along a streamline thereby putting it in a "streamline coordinate system."

where h_T is the total head at $z = z_1$, and $h_L(z)$ is the z-dependent head loss due to frictional energy losses, both major and minor. In writing Eqn (6.13), we have taken state 2 to be at any arbitrary location z along the flow path. At $z = z_1$, $\overline{u}_1 = p_1 = h_L = 0$ and Eqn (6.13) gives $h_T = z_1$. Thus, Eqn (6.13) may be written as

$$\frac{p(z)}{\rho g} + \alpha_2 \frac{\overline{u}(z)^2}{2g} + z = z_1 - h_L(z) \tag{6.14}$$

Since Eqn (6.14) must be dimensionally homogeneous, each term on the left side is a height, or "head," above $z = 0$. Specifically, $p(z)/\rho g$ is the "pressure head" due to the static pressure $p(z)$, $\alpha_2 \overline{u}(z)^2/2g$ is the "velocity head," (also referred to as inertia or acceleration in this text) and z is the "elevation head." We see from Eqn (6.14) that the three heads must add up to the total head less that due to energy losses. A plot of $z_1 - h_L(z)$, or alternately, $p(z)/\rho g + \alpha_2 \overline{u}(z)^2/2g + z$, versus horizontal distance over which the pipe runs produces on the vertical axis an "Energy Line" or EL (Munson et al., 1994). For a lossless flow (inviscid, for which the energy equation becomes the Bernoulli equation), $h_L = 0$ and the EL is a constant height, z_1. Otherwise, the EL has a negative slope for real flows, the value of which depends on the major frictional loss and the distribution and magnitude of the minor loss coefficients. For example, a minor loss will result in a sudden (i.e., vertical) reduction in the EL height, whereas the major loss affects only the slope of the EL over a finite distance. This slope of the EL is h_L/L, which is the hydraulic gradient or head-loss factor, is seen in many places in this text [e.g., Eqs (2.42) and (2.43)].

6.6.2 Hydraulic Grade Line

As pointed out by Jordan Jr. (2004), the maximum recommended flow speed for pipe flow is ~3 m/s. The velocity head calculated from this flow speed is ~0.5 m (< 1 psig). This is normally small compared with the other head terms in the energy equation so that it is sometimes able to be neglected. This conclusion is consistent with the above justification for the neglect of minor loss and inertia for cases where D/z_1 is small.

The "Hydraulic Grade Line" or HGL is defined as (Munson et al., 1994),

$$\frac{p(z)}{\rho g} + z \approx z_1 - h_L(z) \tag{6.15}$$

or

$$z_1 \approx z + h(z) + h_L(z) \tag{6.16}$$

and thus includes only the pressure and elevation heads; the change in kinetic energy per unit mass is neglected. However, the kinetic energy due to acceleration from zero speed to $\overline{u}$ near the source can be included among the minor losses in h_L.

Equation (6.16) states that the potential energy at the source is conserved and is composed of the sum of the potential (z) and pressure energy [or static pressure head, $h(z)$], and the frictional energy loss [$h_L(z)$] at any elevation, z. For a horizontal pipe, the HGL height is a measure of the static pressure distribution in the pipe and for any flow of a viscous fluid, will have a negative slope due to frictional loss. The

difference between the EL and the HGL is a measure of the velocity in the pipe. For a pipe of uniform diameter, the velocity is constant and the difference between the EL and HGL lines will be constant (i.e., the slopes of each line will be the same, and the differences between the two will be small). Minor loss will affect the HGL in the same manner as they do the EL; a minor loss results in a sudden drop in the HGL due to a localized loss of static pressure.

An example where the results are presented in terms of the HGL and compared with a plot of local static pressure distribution is presented in Section 8.6. For further details on the EL and HGL, and examples of pipe flow with the EL and HGL illustrated, please consult any undergraduate fluid mechanics textbook.

6.6.3 The Relevance of the HGL and EL

In engineering, we often need to calculate and plot the distribution of a property in space. For example, in solid mechanics this may be the stress in, or deformation of, a material due to a prescribed set of loading conditions, say a beam loaded uniformly over its span. In a similar manner, in fluid mechanics, we often need to calculate the pressure or velocity distribution in a flow. For example, a graph of the HGL is nothing more than a distribution of *pressure and potential energy per unit mass* in the flow. That is, the same information would come from a plot of just static pressure and elevation versus local horizontal distance or local distance measured along the pipe flow path, $L_\ell(x)$. Mechanical engineers, by virtue of their training, tend to do the latter, whereas hydraulic engineers for the same reason tend toward the former.

Since the local static pressure is of key importance when designing networks with peaks and valleys, a plot of $p(x)$ and $z(x)$ are adequate to highlight and understand the performance of a gravity-driven water network design; no plot of HGL or EL is needed. The personal preference of the author is to plot the dimensionless static pressure, $p(x)/\rho g z_1$, and dimensionless elevation, $z(x)/z_1$. The reasons are that both of these are dimensionless quantities (values are independent of the system of units) have maximum values of 1 *in any system of units* and zero for their lower limit. Also, the value of $p(x)/\rho g z_1$ between 1 and 0 at the delivery location is a measure of the frictional losses in the design; as discussed in Section 2.6.3 the friction losses increase as $p(x_2)/\rho g z_1$ approaches 0.

An example for flow in three dimensional gravity-driven flow network and the use of the HGL and EL is presented in Section 8.6.

6.7 SUMMARY

In this chapter, we began our focus on the *local* states between the source and delivery for a gravity-driven water network. This is motivated by the need to assure that acceptable pressure conditions will exist at all points along the flow path, including possible low points, where pressures will be locally high, and possible high points, where the pressure will be locally low. As a companion to the Natural flow defined in Chapter 2, and to emphasize and quantify the distinct connection between the pipe

diameter and local static pressure, we defined a concept called the "Natural diameter" for a pipe. The Natural diameter distribution is that needed to produce a desired static pressure distribution in the pipe flow. The results from a simple integration along the flow path of the energy equation for pipe flow showed that for a specified uniform local static pressure:

- Large pipe sizes are needed in the region of the reservoir due to the acceleration of the flow from the quiescent source to the flow conditions in the pipe,
- In the regions away from the source, very large pipe sizes are needed where the local slope approaches zero,
- From the examples given in this chapter, we conclude that the pipe diameter and local slope are inversely proportional to each other to maintain a uniform static pressure.

Of course, pipe sizes that are infinitely variable do not exist. Therefore, the designer needs to choose pipe sizes that produce an *acceptable* pressure distribution in the flow where this designation means a static pressure large enough to prevent contaminants from entering the water flow from the outside. This means a pipe size large enough to maintain a sufficiently large static pressure, but small enough to keep network costs within budget. The combination of the need to provide acceptable pressures and the lack of ability for the designer to control these pressures by locally varying the pipe diameter as (s)he chooses, necessitates that close attention be paid to the effect of pipe size distribution in networks that have local peaks and valleys.

Because the energy equation is a scaler, not vector, any three dimensional gravity-driven water network may be modeled as if it is 2D by measuring the x coordinate along a line that is the projection of the vertical center plane of the pipe onto the horizontal plane. This is referred to as the "pipeline coordinate".

The traditional HGL plot for a gravity-driven water network is appropriate for us to assess network performance. This is most convenient as a tool to quickly highlight potential problems with a proposed design, such as unacceptably low static pressure heads at junctions, and so on. The HGL has enjoyed broad use in the hydraulics community because graphical data are easy to understand and interpret. However, the energy equation (or systems of energy equations), which the HGL graphically represents, still need to be solved to determine pipe diameters in designs where these are unknown. Otherwise, as pointed out in Section 1.6, tedious and time-consuming trial-and-error methods are required. In addition, as we will see in Chapter 11, there will be a need for us to work with the energy equations, not their graphical representations, to uniquely determine the static pressure heads at junctions in multiple-pipe networks. The HGL approach will fail in this regard. The bottom line is that just a plot of $p(x)$ and $z(x)$ are adequate to highlight and understand how the network will function; no plot of HGL is needed. It is most convenient, and hence strongly recommended, for the designer to plot the dimensionless elevation and static pressure distribution; both of these quantities have maximum values of 1 *in any system of units* and 0 for their lower limits.

References

T. D. Jordan Jr. *Handbook of Gravity-Flow Water Systems.* ITDG Publication, London, UK, 2004.

B. R. Munson, D. F. Young, and T. H. Okiishi. *Fundamentals of Fluid Mechanics.* John Wiley & Sons, Inc., New York, NY, 2nd edition, 1994.

A motivation for continued efforts in water network development.

CHAPTER 7

THE EFFECTS OF MINOR LOSSES

"Rivers and Streams Forming Springs, These Belong to Every Man."
– The Talmud

7.1 NATURE OF THE MINOR LOSS

Minor losses, embodied by the terms K and L_e/D in Eqn (2.40), enter into the design as an energy loss added to that due to friction in the straight pipe. There is a subtle difference between the major and minor losses. The major loss is one that is uniformly distributed along the pipe length. In contrast, the minor losses occur at discrete locations along the flow path. By acting at discrete locations, minor losses impose a localized effect on the static pressure in the flow. For example, the minor loss associated with a partial blockage in a pipe flow will cause a reduction in static pressure at the blockage location and immediately downstream. Should the pressure fall to vacuum conditions, contaminated ground water may enter the pipe flow, which is obviously undesirable.

From a modeling perspective, one must consider a localized model of the pipe flow to investigate the effect of the minor loss. This is contrasted with a "lumped" type of model when one considers just an entering and an exiting state, say Eqn (2.40).

Gravity-Driven Water Flow in Networks. By Gerard F. Jones

The latter model will yield only "overall" performance, never local conditions at any arbitrary point along the flow path.

The energy equation for local conditions is Eqn (6.7), which was developed in Chapter 6. We now rewrite this equation here and include minor losses,

$$\frac{p(z(x))}{\rho g z_1} = 1 - \frac{z(x)}{z_1} - \frac{8Q^2}{\pi^2 g z_1}\left\{\frac{1}{D(x)^4}\left[\alpha + \int_0^x dK(\xi)\right] + \int_0^x \frac{f(Q, D(\xi))}{D(\xi)^5}\sqrt{1 + s_\ell(\xi)^2}\, d\xi\right\} \tag{7.1}$$

where, for this general form, we have allowed D and the local slope, s_ℓ, to vary along the pipe flow path. The form of the energy equation for the case of constant D is presented in Eqn (7.2).

All terms on the right side of Eqn (7.1) contribute to the dimensionless static pressure, $p(z(x))/\rho g z_1$, on the left side. The term $1 - z/z_1$ in Eqn (7.1) is the increase in dimensionless static pressure as the result of reducing z from z_1 at the source to $z = 0$ at the delivery location. This is the hydrostatic pressure contribution to the static pressure. The integral term that includes $f(Q, D(\xi))$ is the change in the dimensionless static pressure due to major-loss friction. The rest of Eqn (7.1) represents the pressure change due to the acceleration from zero flow speed at the source to $\overline{u}$ in the pipe (embodied by the term α and referred to a acceleration or inertia in this text) and the minor losses. The integral in Eqn (7.1) that involves $K(\xi)$ can be thought of as a running sum of the minor loss coefficient values between the top of the network (at $z = z_1$ or $x = x_1$) and the location at any elevation $z(x)$ along the pipe. These need to be specified by the system designer. Also note in Eqn (7.1) that we have chosen to include the effects of the minor loss using the more-common K coefficients alone (i.e., any equivalent-length-type coefficients, if they exist, have been converted to K-type).

We see from our inspection of Eqn (7.1) that the value of the local static pressure results from a competition between the tendency for it to increase with a reduction in elevation z (the hydrostatic effect) and the loss of static pressure due to major and minor losses along the flow path (note the negative sign before the major and minor loss terms in Eqn (7.1)). The major loss causes a uniformly distributed static pressure loss along the flow path, but the minor loss causes sudden losses in static pressure at specific locations where the minor loss elements, such as fittings and valves, are installed.

Equation (7.1) shows that the dimensionless static pressure distribution in the pipe, $p(z(x))/\rho g z_1$, depends on the dimensionless elevation of the pipe, $z(x)/z_1$, the local slope, s, pipe diameter, D, and reservoir elevation, z_1, as well as the distribution and size of the loss coefficients, K.

7.2 A NUMERICAL EXAMPLE

Because of the near-limitless combinations of types and locations of minor loss elements there is no simple way to represent the solution of Eqn (7.1) in the form of a few graphs, as done in Chapter 5, where we neglected minor losses. Instead, we will consider a few cases of interest and attempt to draw some general conclusions from these.

We consider a gravity-driven water network consisting of a single straight pipe of uniform slope and pipe diameter with a re-entrant loss or larger at the inlet (the end of the pipe protrudes into the reservoir) at $z = z_1$, where $K = K_1 = K_{entry}$ and two other minor losses. One is at $z = 0.5z_1$, where $K = K_2 = 50$ and the other is at $z = 0$, where $K = K_3 = 100$. Normally, there is a filter installed at the pipe inlet to prevent the entry of dirt and debris that could, over time, plug the system. To model this effect, we consider 20 and 200 times the re-entry $K = K_{entry}$ value of 0.78 (see Table 2.1); the factor 20 corresponds to a small filter blockage, and 200, a larger one. We consider two nominal polyvinyl chloride (PVC) pipe sizes of 2 in. and $\frac{3}{4}$ in., and assume a slope, s, of 1 and 10%. The case that will produce the lowest static pressures in the pipe (i.e., worst case) is one where the static pressure at the delivery location, p_2, is zero. We assume this value here to produce the most conservative results relative to this parameter. We also take $z_1 = 50$ m. The results will show not much sensitivity to z_1, but large sensitivity to s and D, as well as the K distribution.

The local static pressure distribution is shown in Figs. 7.1 and 7.2 for the small and large filter blockage, respectively. Both figures show a sharp reduction in static pressure immediately after the flow leaves the reservoir at $z/z_1 = 1$. As the flow moves down the pipe toward smaller z the static pressure increases due to the fact that the pressure gain due to the decrease in potential energy is more than the frictional energy loss per unit of pipe flow path. At $z/z_1 = 0.5$, the static pressure falls suddenly due to the minor loss at this location. Between $z/z_1 = 0.5$ and the bottom of the pipe, the static pressure rises again and then falls suddenly due to the minor loss at $z = 0$. Clearly, the main region of concern in the pipe is immediately downstream from the reservoir where the pressure may be very low; further downstream the hydrostatic pressure has contributed to the increase in static pressure. For the small blockage, there is slight concern for the designer due to ~ -3 psig (gage) pressure or 3 psi less than atmospheric pressure. For the large blockage, the results are clearly catastrophic. If the values for static pressure appearing in Figs. 7.2 are realized, all PVC pipe would fail under the extreme vacuum conditions. However, the volume flow rate will surely decrease in response to the vacuum, lessening the extent of the vacuum seen in this figure. One way to correct the problem of unacceptably low pressures in the pipe is to install vacuum breakers (valves that automatically allow air into the system should the pressure become too small) at the low-pressure locations. This will be discussed in more detail in Chapter 13.

An additional concern with the formation of negative gage pressures in a pipe is that small leaks in the pipe wall or fitting joints may cause contaminated ground water to pass into clean water in the pipe. This problem is particularly egregious

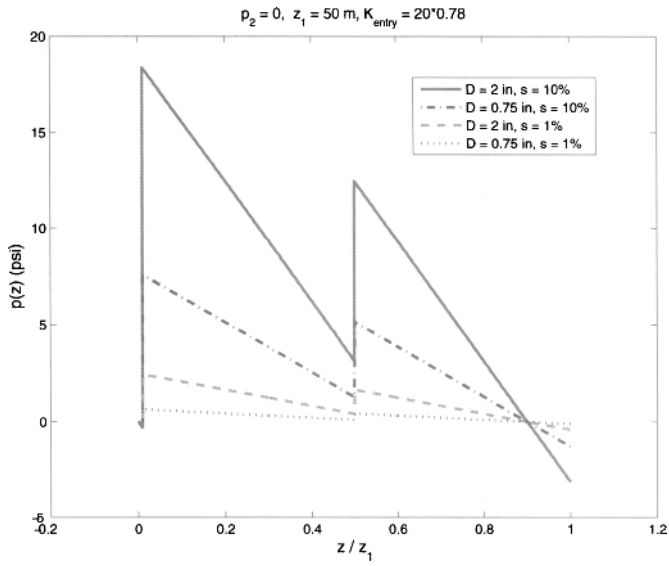

Figure 7.1 Minor loss effects on static pressure in a single straight pipe. Small blockage at entrance to pipe in reservoir. $z/z_1 = 1$ is located at the reservoir. $z/z_1 = 0$ is at the delivery location.

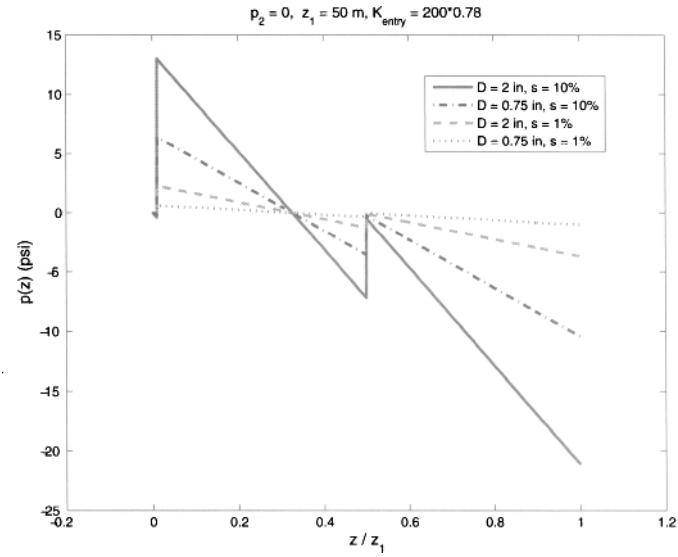

Figure 7.2 Minor loss effects on static pressure in a single straight pipe. Large blockage at entrance to pipe in reservoir. $z/z_1 = 1$ is located at the reservoir. $z/z_1 = 0$ is at the delivery location.

since such leaks are virtually impossible to find and, if found, very expensive and time consuming to repair.

From this example, we conclude that minor losses may be an issue especially as they affect the design of the filter system in the reservoir. We may generalize the results of this study by noting that static pressure will become more negative with increases in s, D, and z_1. For all other parameters fixed, increasing the delivery static pressure, p_2, reduces the velocity in the pipe and thus, reduces the effect of the minor loss.

7.3 THE CASE FOR UNIFORM D

For a pipeline of uniform diameter starting at the source, the equation to be solved for the static pressure distribution is Eqn (6.12) where the minor loss coefficient distribution K is included,

$$\boxed{\frac{p(z(x))}{\rho g z_1} = 1 - \frac{z(x)}{z_1} - \frac{8Q^2}{\pi^2 g z_1 D^4}[\alpha + \int_0^x dK(\xi) + f(Q,D)\frac{L_\ell(x)}{D}]} \quad (7.2)$$

As in Eqn (6.12), $L_\ell(x)$ is the distance from the reservoir (at $x = x_1$) measured along the run of the pipe. This function needs to be specified by the designer.

7.4 IMPORTANCE THRESHOLD FOR MINOR LOSSES

When determining the pipe diameter, it may be of interest to the designer to identify the threshold value of the sum of the minor loss coefficients below which minor losses may be neglected. With minor losses justifiably neglected, the design graphs from above or a simple closed-form design formula [Eqs (9.2)–(9.6)] may be confidently applied to determine D. Consider Eqn (2.40) and focus on the competition between the major and minor loss terms, $\lambda\sqrt{1+s^{-2}}$ and $\frac{D}{z_1}\sum_{i=1}^{M}\frac{L_e}{D}\big|_i$, respectively. If the minor loss term is significant with respect to the major loss, say, $\geq 10\%$ of it, then the minor loss may be considered to affect the calculation of the pipe diameter. If the ratio of the minor loss term to the major loss term is $< 10\%$, then we may be able to ignore the minor loss when calculating the diameter.[1] For this condition, take the ratio of the minor loss to the major loss to get

$$\boxed{\sum_{i=1}^{M}\frac{L_e}{D}\Big|_i \tilde{>} 0.1\frac{\lambda\ell}{D}} \quad (7.3)$$

[1]By integrating Eqn (7.2) over the entire length of pipe in the network, the energy equation relates Q to L, z_1, ν, g, and the total minor loss in the network. Based on the dependencies established in Chapter 9 for a restricted range of Reynolds numbers (Re) and smooth pipe wall, we use this equation to calculate that the 10%-threshold affects D by, at most, 4%.

where the "run," ℓ, is the pipe length from inlet to outlet measured in the horizontal plane.

Equation (7.3) addresses the relative strength of the minor loss if it is in the form of L_e/D terms. If the minor loss is in terms of K values, the same procedure as above gives,

$$\boxed{\sum_{i=1}^{N} K_i \gtrsim 0.003\frac{\lambda\ell}{D}} \tag{7.4}$$

That is, the minor losses are important only if Eqs (7.3) or (7.4) are satisfied.[2] Otherwise, we may ignore minor losses inasmuch as they affect the determination of the pipe diameter. Because the ratio $\lambda\ell/D$ is generally very large, normally of the order of 1000 or more for most gravity-driven water distribution networks, *minor losses may often be ignored when calculating the pipe diameter.*[3] The exception is where a partially open globe valve is used for flow control. For a partially closed globe valve, the value of K may be very large. The conclusion drawn from these developments was the motivating factor for the neglect of minor loss in the design graphs presented in Chapter 5. However, particular attention needs to be paid to the minor loss for systems where the run, ℓ, is small.

Examples of pipe flow that include the effect of minor losses are presented in the Chapter 8.

7.5 FIXED AND VARIABLE MINOR LOSSES

Before completing this brief chapter, we discuss the distinguishing features of fixed and variable minor loss elements. A fixed minor loss is one that is geometrically constant over time. The elbow, tee, coupling, union, and a fully open valve (e.g., gate valve)[4] are fixed minor loss elements since, except for a small amount of fouling from elements in the flowing fluids, their shapes do not change over time. By contrast, a globe valve, which is a variable minor-loss element, is designed for the user to partially restrict the flow by opening it a fraction of its full-open position; the changing geometry is the degree of openness.[5] The reason for the need to distinguish between these two classes of minor loss elements is that when a variable minor loss is included in the design, the loss coefficient that is included in the analysis is always based on

[2]With little loss of accuracy, D in these equations may be first estimated by neglecting minor losses.

[3]This observation is made in Jordan Jr. (2004), but with different quantification. He notes "frictional losses caused by fittings ... are considered negligible if the distance between the individual fittings is at least 1000 pipe diameters."

[4]The design of a gate valve is such that its purpose is to allow all or no flow to pass. Thus, a gate valve is operated as fully open or fully closed and should never be used to partially restrict the flow. Please see a further discussion on this topic in Section 13.14.

[5]Note that a ball valve may also be used to partially restrict flow, but these are used for this purpose less frequently than a globe valve. For one reason, a ball valve has a much greater nonlinear loss characteristic than does a globe valve. This means that a very fine adjustment may need to be made near its fully closed position to achieve the desired flow rate. Slight shifts in this position due to a small disturbance will adversely affect this setting.

a *minimum* or, in the case of a globe or faucet valve, a *fully open* condition. From Section 3.5, recall that, when sizing pipe for a network, the designer normally chooses the nominal pipe size having an inside diameter slightly larger than that calculated from the solution of the energy equation. The resulting oversized pipe will not perform as designed because the frictional loss is less than that for the specified water flow rate. The globe valve enters the design by adding friction loss to the flow while simultaneously reducing the volume flow rate to meet the design value. In this way, the *variable-minor loss globe value is an integral part of a gravity-driven water network because of its ability to control the flow and, ultimately, to shut off the flow completely to facilitate inspection and repair to parts of the network.*

Note that the minor-lossless flow approximation, on which the charts in Chapter 5 are based, includes the neglect of *all* minor losses, including those from any globe valves in the network. From Table 2.1, we saw that the loss coefficient for a fully open globe is valve is of the order of 10 and thus not a large contributor to the total frictional loss.

References

T. D. Jordan Jr. *Handbook of Gravity-Flow Water Systems.* ITDG Publication, London, UK, 2004.

Villanova University engineering students and faculty work on a pipeline of a water network in Waslala, Nicaragua

This page intentionally left blank

CHAPTER 8

EXAMPLES FOR A SINGLE-PIPE NETWORK

"When the well is dry, we know the worth of water."
– Poor Richard's Almanac, 1746

8.1 INTRODUCTION

It is worthwhile to summarize the models for pipe flow that have been developed thus far. After identifying the energy equation as the fundamental governing equation for this text (Chapter 2), first we focused on the performance of a single-pipe network driven only by the end states (i.e., the pressure at the inlet, at atmospheric conditions, and at the outlet). It was quantitatively demonstrated that minor losses are small in many gravity-driven networks. Because of this, a single chapter (5) was devoted to the solution of the energy equation for minor-lossless flow in a single pipe of a fixed diameter. Several simple design charts were the outgrowth of these solutions. The energy equation for pipe flow where minor losses are important (say, for flow control purposes), and its solution, is a hint at the importance of the *local* flow conditions in the pipe; this because of the local nature of a minor loss (see Chapter 7). The local character of the flow also bears on the integrity of a design, as we found that the local static pressure at each and every point along the flow path needs to be maintained at a

Gravity-Driven Water Flow in Networks. By Gerard F. Jones

positive gage pressure, first explored in Chapter 6. Also introduced in this chapter was the concept of the Natural diameter distribution for a pipe, developed to emphasize the strong connection between pipe size and static pressure distribution. From these ideas, we are led to understand the importance of assessing local states in networks, especially for those where there are local peaks.

Several examples for single-pipe systems are presented in this chapter to consolidate the material appearing in the above chapters and to reinforce the concepts presented therein. One example is for a straight pipe for which we can use the design graphs from above (minor losses are negligible) or the `Mathcad` worksheet. The second example is one where the pipe run is circuitous and has numerous fittings and valves that contribute to the minor loss. A variation of this example is included for a pipe delivering water from a reservoir tank to a tapstand, where there is a prescribed static pressure just upstream from the tapstand. Finally, in the last few examples we explore the importance of accessing the static pressure distribution in a network where there is a local peak. The classical problems of the time to drain a tank (the only time-dependent problem in this book) and flow in a syphon are two of these examples. We also explore the design of a simple gravity-driven water network where site is mapped by survey data.

The object of each of the examples presented below is to determine the pipe size to meet the specified design requirements. Unless otherwise specified, IPS sch. 40 polyvinyl chloride (PVC) pipe is to be used. Where minor loss coefficients are used they reference Table 2.1 unless otherwise noted.

8.2 A STRAIGHT PIPE

Consider the example for the following system where the contour of the ground provides a uniform slope from the source to a storage tank. Because of this, we will consider the pipe between the source and the tank region to be straight (i.e., it will have no bends from elbows). A flow rate measurement at the source has determined $Q = 0.40$ L/s and an Abney level[1] is used to find the slope of the system of $s = 0.0080$. Both an altimeter and a GPS give the elevation difference between the source and the tank (z_1) of 64 m. Two instruments are used to find elevation since this may be one of the most uncertain of all of the measurements characterizing the network. Four or more satellites are required to obtain a reliable altitude measurement from a GPS. This is difficult to achieve if there is a tree canopy that covers the source. Even with a multitude of satellites, the altitude reading from a GPS is still subject to a minimum

[1] An Abney level is an optical device, like a small telescope, which is used to determine the position of an object in space. By sighting a point at a distance to the position of the Abney level, the angle between this point and the Abney level can be read directly from a scale on the body of the level. When complemented with readings from a measuring tape, an approximate topographical survey of land may be produced by repeated measurements of angles and distances between successive locations along a potential pipe flow path. This may be compared with the survey obtained from GPS latitude, longitude, and elevation measurements as discussed below. See Chapter 13 or (Jordan Jr., 2004) for further details.

of ± 10 m uncertainty.[2] The uncertainty dictates that the designer consider the lowest value of z_1 rather than the reading. Thus, we take $z_1 = 64 - 10$ m = 54 m.

A filter at the inlet of the source is known to give a K value of 200 [extrapolation from Potter and Wiggert (2002)], there are 2–90° elbows ($L_e/D = 2 \cdot 30$) entering the tank, a full-open globe valve ($K = 4$, but if a conservative estimate is used, this should be increased to $K = 10$) at the inlet to the tank, and a sudden enlargement from the supply pipe where it enters the tank (K=1).

The surface of the storage tank is at atmospheric pressure ($p_2 = 0$) and, thus, $F = 0$ for this example. If we neglect minor losses for the moment, the solution for the pipe diameter is from Fig. 5.4 for a straight pipe ($\lambda = 1$) with zero delivery static pressure. For the prescribed values for Q and s, obtain D to be $< 1\frac{1}{2}$ in.. The designer would specify a $1\frac{1}{2}$ in. pipe to satisfy the prescribed conditions.

Consider the effect of the minor losses. The solution from the `Mathcad` worksheet (Fig. 8.1) with the prescribed values for L_e/D and K as above gives $D = 1.381$ in.. This corresponds to a $1\frac{1}{2}$-in. pipe (D=1.61 in. for a nominal $1\frac{1}{2}$ in. pipe). Thus, we see that the minor losses have no effect on the pipe size for this example. The values for K and/or L_e/D would need to increase $>$ 1000-fold to necessitate a 2-in. pipe size. However, should the elevation head, z_1, be reduced to a small value of 4 m, and the slope maintained as above, ℓ is reduced by a factor of 13.5 and the solution shows that a 2-in. pipe size will be required. Thus, we see further evidence that minor losses are important when sizing pipe for networks where there is a small run.

8.3 FORMAT OF MATHCAD WORKSHEETS FOR SINGLE-PIPE NETWORKS

Before continuing with examples, the format of the `Mathcad` worksheets for a single-pipe network, such as that for Fig. 8.1, is presented. With slight variations, the entries appearing in the worksheets are as follows:

1. Definition of water properties of density, ρ, and viscosity, ν.
2. A convergence tolerance, `TOL`, used in `Mathcad` to determine when a root-finding algorithm has found the root to sufficient accuracy.
3. Definition of Reynolds number (Re) as a function of Q and D.
4. Definition of the absolute roughness of the pipe wall.
5. The friction factor function as defined by Eqs (2.16) and (2.17).
6. The correspondence between nominal pipe size and D for the pipe material and type (schedule or SDR) of pipe under consideration.

[2]Errors come from several sources including ionospheric effects, shifts in the satellite orbits, errors of the satellites" clocks, multipath effects, tropospheric effects, and calculation and rounding errors (Anon., 2009). Recent reports of a GPS and coupled barometric altimeter with auto-calibration may provide elevation accuracies of better than ± 10 m. See Appendix B.

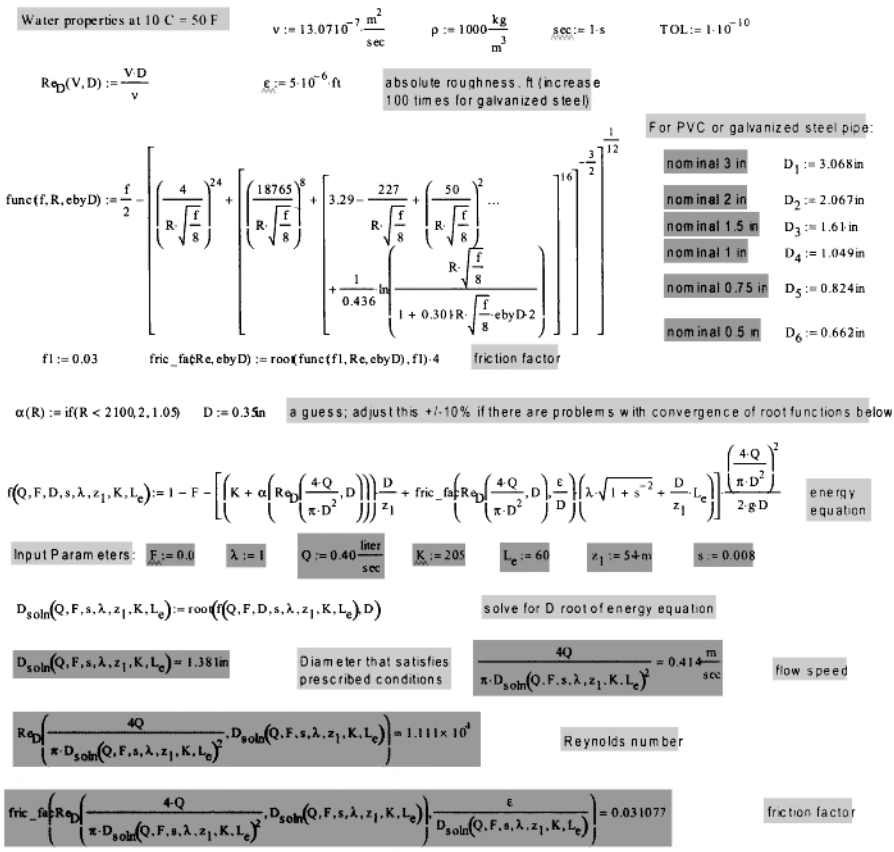

Figure 8.1 Mathcad worksheet `SinglePipeNetworkDesign_Appendix.xmcd` for example problem of Section 8.2.

7. Definition of α as a function of Re.
8. Initial guesses for the values of D (diameters ranging from 0.2 to 4 in. are good guesses for nearly all problems considered in this book).
9. The energy equation with the needed functional dependence.
10. Values for the input parameters including F, λ, and Q, the appropriate minor loss coefficients, K and L_e/D (referred to as L_e), elevation z_1, and the mean slope, s.
11. The solution of the energy equation using the `root` function.
12. The results that include the theoretical value for D, flow speed based on this value, Re, and the value for the friction factor.

The worksheets for a single-pipe network appearing in various places in this text are intended for general cases instead of those specific to the examples in this chapter. These have results that are slightly more extensive which may include the following:

- Definition of nominal diameter and actual inside diameter based on the nominal size.
- In addition to the value for friction factor, the recommended nominal pipe size based on the theoretical value for D, and the value for Q that is based on nominal pipe size are reported.
- A message called "warning." If warning says "Pipe size out of range", dimensional data for the pipe need to be extended to include either smaller or larger pipe sizes.

Though not visible in the figures of `Mathcad` worksheets in this book, input parameters in the worksheets are colored green, output parameters are red, and comments are generally yellow. A tutorial in `Mathcad` is presented in Appendix C.

8.4 A CIRCUITOUSLY RUN PIPE WITH ATMOSPHERIC DELIVERY PRESSURE

Consider the same example as in Section 8.2, but allow the pipe to follow a contour different than the straight path from the source to the tank. This would be required when there is a structure between the source and the tank, such as a mountain or a house and, in this case, the ratio of the actual pipe length to the one if the pipe were straight, λ, is > 1. In Section 2.6.5, we saw that for a range of actual water-driven networks, the values for λ are not much more than 1 plus a small fraction. However, in the present example, let us assume an extreme case where there is a hill separating the source reservoir from the delivery location whose peak elevation is larger than that of the source. Even with the neglect of friction in the flow, water cannot flow to an elevation $> z_1$. Thus, the designer must route the pipeline around the hill instead

of over it. In this case, because of the size of the hill, the pipe length is extreme such that $\lambda = 2.5$ and, because of the circuitousness, there are 20–90° elbows in the flow path ($L_e/D = 20 \cdot 30 = 600$). Assuming a total K value of 205 as above, we obtain $D = 1.67$ in. from the Mathcad worksheet (Fig. 8.2). This corresponds to a 2-in. pipe (D=2.067 in. for a nominal 2-in. pipe and D=1.61 in. for a nominal $1\frac{1}{2}$ in. pipe). Because the diameter required to satisfy the given conditions is only slightly larger than $1\frac{1}{2}$ in. and we choose a 2-in. pipe, the volume flow rate that the 2-in. pipe can pass is $Q = 0.716$ L/s, a value nearly twice that currently produced by the source. Under most conditions, this pipe size would accommodate plenty of additional flow rate for the possible planned flow rate increase in the future, assuming the source can produce it. Calculating water demands in the future is presented in Chapter13.

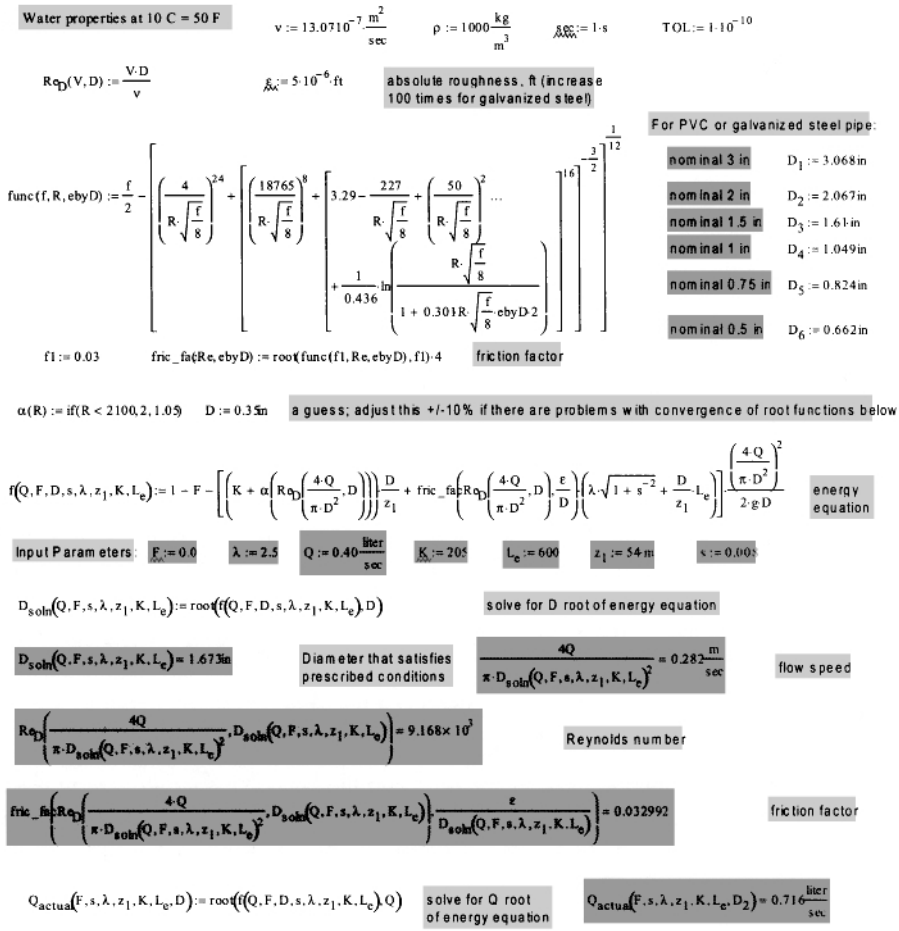

Figure 8.2 Mathcad worksheet `SinglePipeNetworkDesign_Appendix.xmcd` for example problem of Section 8.4.

8.5 A CIRCUITOUSLY RUN PIPE WITH SPECIFIED NONZERO DELIVERY PRESSURE: "SENSITIVITY" STUDIES

We reconsider the example of Section 8.4 where, instead of the pipe running from the source to a reservoir tank, it goes from the tank to a tapstand. At the tapstand there is required a static pressure equivalent to $h_{del} = 5.4$ m of water. The tank surface is open to the atmosphere so $p_1 = 0$. As above, the ratio of the actual pipe length to the one if the pipe were straight is λ. Let us consider the situation where $\lambda = 1.5$ instead of the value of 2.5 as above. There are 20–90° elbows in the flow path ($L_e/D = 20 \cdot 30 = 600$) and a total K value of 205. With an elevation for the source of $z_1 = 54$ m as above, we obtain $F = p_2/\rho g z_1 = h_{del}/z_1 = 5.4/54 = 0.10$. Ignoring minor losses for the moment, we use Fig. 5.9 to predict a pipe size of nominal $1\frac{1}{2}$ in. PVC. From the same figure, the actual volume flow rate of water for this pipe size is about 0.46 L/s, not too much larger than that specified for this problem. With minor losses include (the design charts Figs. 5.4–5.13 can no longer be used because they neglect minor losses) the `Mathcad` worksheet (Fig. 8.3) produces the need for a $1\frac{1}{2}$ in. nominal pipe. Thus, there is no measurable effect from the minor loss for this example. The maximum flow rate for this condition of 0.454 L/s is even less than when minor losses were neglected. This provides very little excess if water demand in the future increases even slightly. If the cost differential between the $1\frac{1}{2}$ in. and 2-in. nominal pipes could be absorbed, the careful designer would require a 2-in. PVC pipe for this problem.

It is interesting to note that if the value for λ of 2.5 is used as in the example of Section 8.4, a 2-in. PVC pipe is necessary and, with a maximum flow rate of 0.673 L/s, there is plenty of additional capacity for expansion in the future. The maximum flow rate of 0.673 L/s is less than that for the example of Section 8.4 of 0.716 L/s because the static pressure at the delivery location in the current example is larger than zero (the value from the previous example). The smaller driving force for flow in the current example, which is proportional to $p_1 - p_2$, reduces the flow rate. The reader is encouraged to make this change to verify the above outcome. In fact, with the `Mathcad` worksheets in hand, it is very easy to investigate the sensitivity of the designs to changes in the values for all of the design parameters. In analysis and design, these small investigations are referred to as "sensitivity studies" ("parametric studies" or "case studies" are often used as substitute terms) and are universally considered part of a sound analysis and design procedure. The results from the sensitivity studies will be very educational in that the designer will get a better "feel" for their designs. This is also a first step toward making engineering "tradeoffs," where parameter values are changed to produce a design that, in a overall sense, satisfies the needs of multiple constituencies. When making an engineering tradeoff, the designer will need to, in some sense, relinquish an aspect of the design to produce a gain in a different aspect.

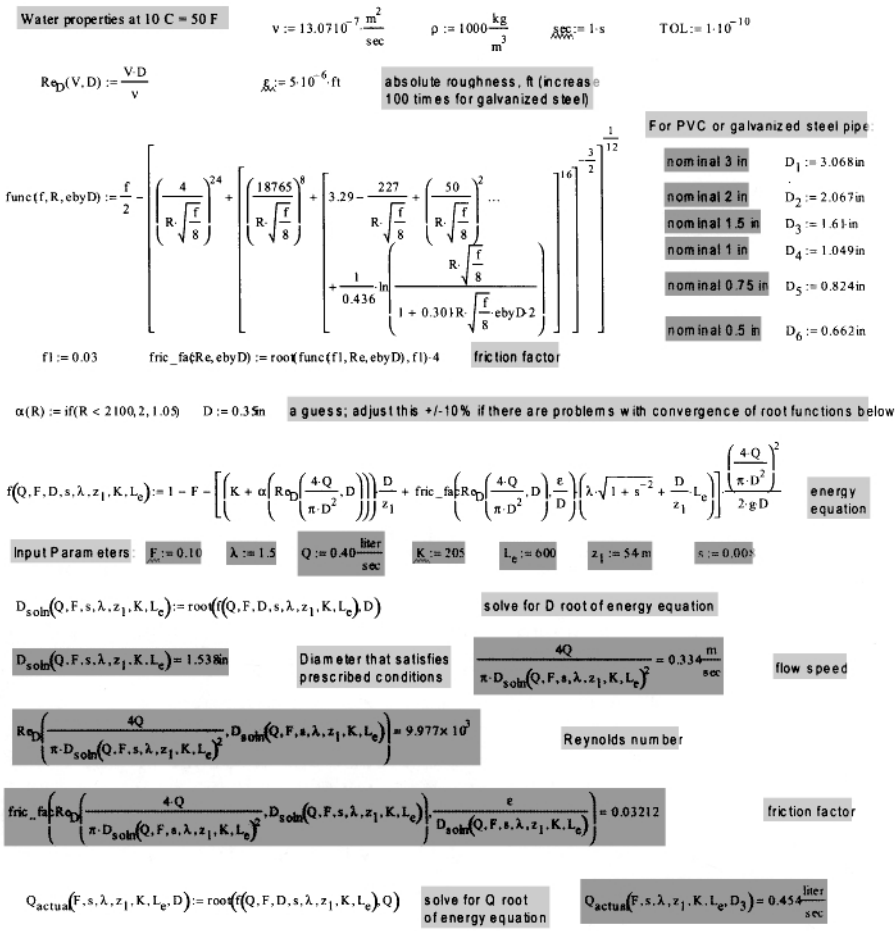

Figure 8.3 Mathcad worksheet `SinglePipeNetworkDesign_Appendix.xmcd` for example problem of Section 8.5.

8.6 THE EFFECT OF LOCAL PEAKS IN THE PIPE

The above examples have ignored the possibility of local peaks in the pipe. In networks where these exist, as discussed in Section 2.7, the local static pressure should be calculated along the flow path to insure that a minimum *positive* static pressure, as specified by the designer, is satisfied at all locations. This was discussed in some detail in Chapter 6. As noted elsewhere in this text, a positive elevation of about 10 m, or ~1 atm of pressure, is considered adequate although a lower pressure than this may be quite acceptable. A negative gage pressure (i.e., the pressure relative to atmospheric pressure) may allow the passage of contaminants from the ground

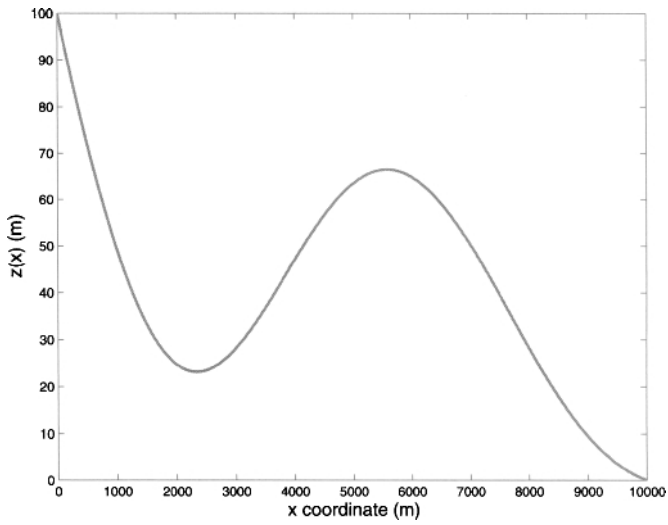

Figure 8.4 Contour of pipe to illustrate the effect of peaks on local static pressure. $s = 0.01$ and $z_1 = 100$ m. Note the large difference between the vertical and horizontal scales in this figure. If both axes were drawn in the horizontal scale, the contour of the pipe would appear nearly straight between the source and delivery locations.

into the pipe flow and in extreme cases, could result in pipe-wall collapse because of the negative pressure difference between water in the pipe and the surroundings. This is obviously undesirable. If there are no local peaks in the pipe, with downward flow, the static pressure generally increases as the loss of potential energy converts to pressure energy less that removed by major and minor losses (see Figs. 7.1 and 7.2. If there are local peaks in a uniform-diameter pipe, this situation is reversed. That is, the local static pressure decreases as the flow proceeds upward toward the peak, reaching a local minimum at a location slightly downstream from the peak, and increases in the direction of flow further downstream. This behavior resembles that for a syphon where vacuum conditions at the network peak can lift a liquid upward from a much lower point. See Section 8.9 for this example.

To illustrate this problem, consider the example, as shown in Fig. 8.4, for minor-lossless flow in a pipe having a high peak. The volume flow rate, mean slope, and elevation of the source are $Q = 0.5$ L/s, $s = 0.01$, and $z_1 = 100$ m, respectively.[3]

After determining the local slope distribution, by taking the derivative $[s_\ell(x) = dz(x)/dx]$ for this geometry, the local static pressure distribution is calculated using Eqn (6.7) by assuming three values for D: 1-in., $1\frac{1}{2}$-in., and 2-in. nominal sch. 40

[3]In several example and exercise problems in this book, elevations that appear in them may be greater than recommended in the design chapters (13 and 15) when pressure limitations of valves are considered. The large values of elevation are simply illustrative for that problem and not to be interpreted as recommended. Elevation head limitations on pipe, valves, and fittings must be taken seriously by the designer.

$$P_{rat}(D,Q,x) := 1 - \frac{z(x,a,b)}{z(0,a,b)} - \frac{8\cdot Q^2}{\pi^2\cdot g\cdot z(0,a,b)\cdot m}\left(\frac{alpha\left(Re_D\left(\frac{4\cdot Q}{\pi\cdot D^2},D\right)\right)}{D^4} + \int_{0.0\,m}^{x\cdot m} \frac{fric\_fa\left(Re_D\left(\frac{4\cdot Q}{\pi\cdot D^2},D\right),\frac{\varepsilon}{D}\right)\sqrt{1+sl\left(\frac{y}{m},a,b,s\right)^2}}{D^5}\,dy\right)$$

Energy equation

$x := 0, 10..x_{max}$

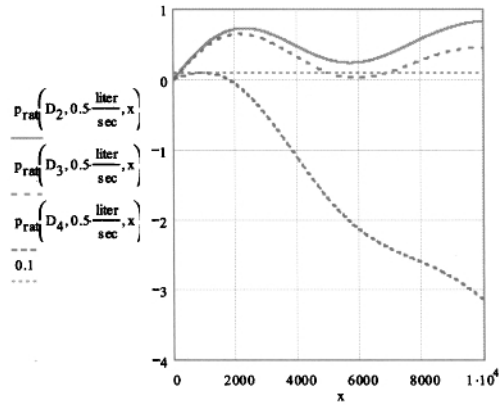

Figure 8.5 `Mathcad` worksheet `example problem on peaks.xmcd` for example problem of Section 8.6. The functions $z(x, a, b)$ (the local height) and $sl(y, a, b)$ (the local slope), as well as the preliminaries (items 1-7 in Section 8.3), are defined elsewhere in this worksheet and do not appear.

PVC pipe. The evaluation of this equation is straightforward and was done in `Mathcad` (Fig. 8.5). The resulting local static pressure distribution, $p(x)/\rho g z_1$, is presented in Fig. 8.6 as a function of local coordinate, x.

In Fig. 8.6, we see that the static pressure distribution for the 1-in. pipe falls below atmospheric pressure after about $x = 1000$ m. Obviously, this pipe size is unacceptable for the specified volume flow rate. On the other hand, the nominal 2-in. pipe has a local static pressure that is positive throughout its length and greater than an assumed minimally acceptable static pressure corresponding to $p(x)/\rho g z_1 = 0.1$ [i.e., $p(x)/\rho g$ equal to 10 m]. This pipe size is an acceptable candidate. In between these two pipe sizes, the local static pressure for the $1\frac{1}{2}$-in. nominal pipe is positive everywhere. However, the static pressure becomes very close to zero (atmospheric pressure) near $x = 6000$ m. Depending on the economics of the design (the cost of the 2-in. pipe versus that for the $1\frac{1}{2}$-in. one), the designer may choose this marginal candidate. If the cost differential is not a significant factor, the 2-in. pipe would be recommended for this problem.

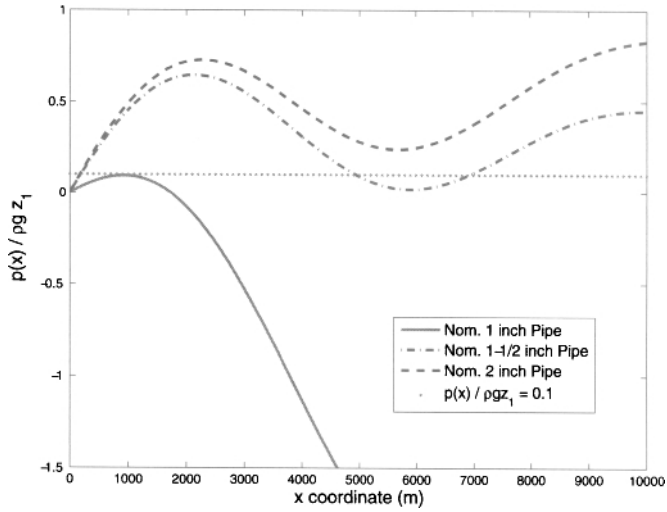

Figure 8.6 Dimensionless local static pressure distribution, $p(x)/\rho g z_1$, for geometry of Fig. 8.4. $Q = 0.5$ L/s, $s = 0.01$, and $z_1 = 100$ m.

As a final note on this example, the pipe size as determined from Figs. 5.4 (for $\lambda = 1$) for this minor-lossless flow[4] and $F = 0$ is $1\frac{1}{2}$-in. nominal PVC. That is, the use of the design charts in Chapter 5, or the associated design formulas, both of which are based on only the inlet and outlet states do not reveal the local static pressure approaching atmospheric at some point along the flow path. Equation (6.12) needs to be evaluated to shed light on this important aspect of a design.

Upon further inspection of Fig. 8.6, we see that the dimensionless static pressure, $p(x)/\rho g z_1$, at the pipe outlet at $x = 10,000$ m is ~0.80 for the 2-in. and ~0.45 for the $1\frac{1}{2}$-in. pipe. Recalling that the largest value for $p(x)/\rho g z_1$ is 1 under hydrostatic conditions, we see that the dimensionless frictional pressure drop for the two pipes (neglecting the inertia or acceleration of the flow which, as discussed above, is small for small D/z_1) is 0.20 and 0.55, respectively. The static pressure available at the outlet of the pipe speaks to the network's ability to distribute the flow, say, to houses in the surrounding community, though a distribution pipe network. It also points to the need for a globe valve at the bottom of the pipe to control the volume flow rate by dissipating some or all of the energy represented by the static pressure at this location.

The HGL for this example is presented in Figs. 8.7–8.9 for each of the three pipe diameters under consideration in this problem. Please see Section 6.6.2 for a discussion of the HGL. Several things are noteworthy from our inspection of these three figures. First, if the major friction loss is not dominant, the pressure and elevation heads are complementary; when elevation head falls, the pressure head rises. Second,

[4]The value for λ for this example is 1.0021, corresponding to a nearly straight pipe between the source and delivery locations.

the HGL is nearly a linear function of x as seen in all three figures[5] This outcome, which is a result of the small value for mean slope, is not valid for all gravity-driven networks in general, but is certainly true for this example where $s = 100/10,000 = 0.01$. In addition, the uniform diameter of the pipe results in a constant flow speed[6] and therefore a constant friction loss per unit of pipe length. The slope of the HGL is thus a measure of the frictional energy loss in the pipe. Finally, and most importantly, the proximity of the HGL to the elevation head at any x location is a measure of value of static pressure above atmospheric pressure at this location. That is, if the elevation head is equal to the HGL, the pressure head must be zero or the static pressure is equal to atmospheric pressure [see Eqn (6.12)].

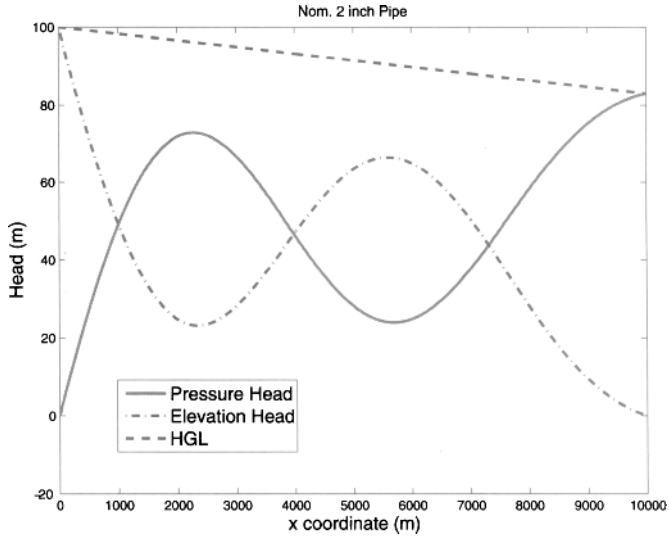

Figure 8.7 The HGL for geometry of Fig. 8.4 and 2-in. nominal PVC pipe, where $Q = 0.5$ L/s, $s = 0.01$, and $z_1 = 100$ m.

In Fig. 8.7, we see that the elevation head approaches the HGL to within ~25 m at $x \approx 6000$ m. The static pressure is much greater than the recommended value of the product of 10 m and ρg, or ~1 atm of pressure. This condition produces a satisfactory design. In Fig. 8.8, the elevation head and HGL are nearly equal at this x location. That is, the static pressure at this location is only slightly above atmospheric in value; the design is marginal in this case. Finally, in Fig. 8.9, for 1-in. nominal pipe, the friction loss per unit length of pipe is so large that the elevation head crosses over the HGL at $x \approx 1700$ m resulting in a negative pressure head from this point onward along

[5]The HGL is, in fact, a linear function of distance traveled along the pipe flow path if the pipe is of constant diameter. However, if plotting HGL against x instead of against $L_\ell(x)$ possible changes in the local values for the slope of the pipe may make the HGL nonlinear with x. That is, the HGL will be nonlinear with x if $L_\ell(x)$ is a nonlinear function of x. For an example of this, see the syphon problem in Section 8.9 below.
[6]Recall that mass conservation requires that the volume flow rate be constant in the pipe.

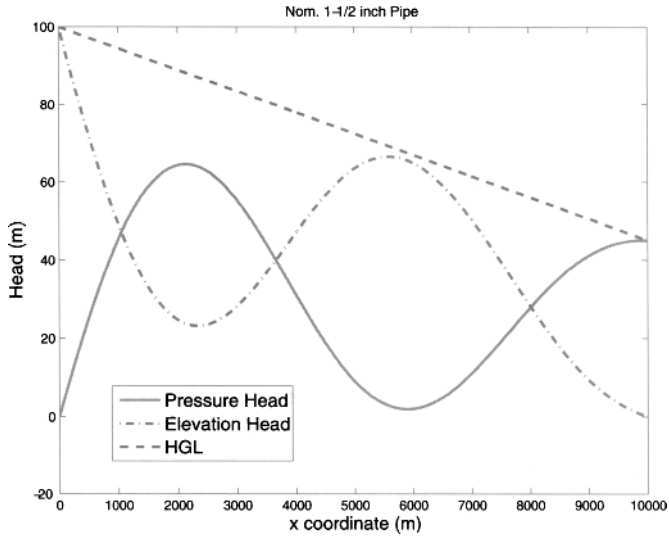

Figure 8.8 The HGL for geometry of Fig. 8.4 and $1\frac{1}{2}$-in. nominal PVC pipe, where $Q = 0.5$ L/s, $s = 0.01$, and $z_1 = 100$ m.

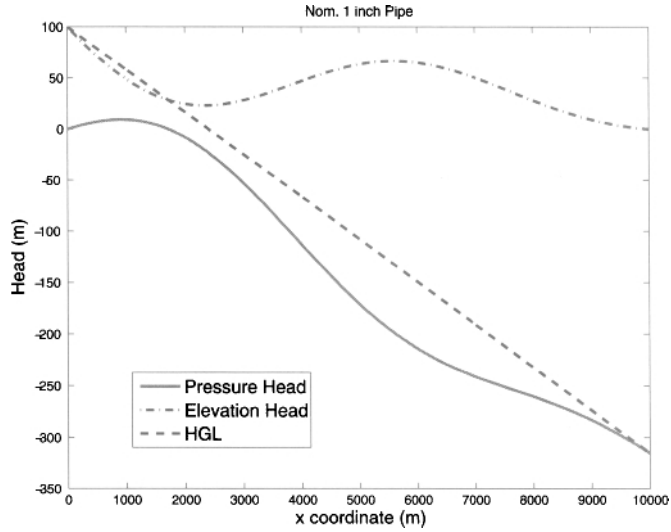

Figure 8.9 The HGL for geometry of Fig. 8.4 and 1-in. nominal PVC pipe, where $Q = 0.5$ L/s, $s = 0.01$, and $z_1 = 100$ m.

the flow path. The large negative pressures, even below that for a perfect vacuum that cannot exist, imply that the flow rate of 0.5 L/s is not possible for a 1-in. nominal pipe and the other conditions of this problem.

The effects of local peaks are treated more-fully in Chapter 14, which covers the potential problem of air pockets in the pipe.

8.7 A NETWORK DESIGNED FROM SITE SURVEY DATA

The first step in the design of gravity-driven water network is most often an assessment of the site. This is normally an identification of the proposed coordinate location of the pipe, $z(x, y)$. These data are obtained by using a transit or an Abney level and a measuring tape. A brief note on the Abney level is given in Section 8.2.

We consider a data set obtained from a site survey for a network in San Benito, Nicaragua, where the measured flow rate of water from the source is 0.5 L/s. The survey data is presented in Table 8.1. A contour plot of z as a function of (x, y) is shown in Fig. 8.10 and z versus y is the focus of a plot shown in Fig. 8.11. For information purposes, a plot of the local pathlength distribution from these data is shown in Fig. 8.12.

Table 8.1 Survey Data for the San Benito Site

Station	x (m)	$y(x)$ (m)	$z(x)$ (m)	$L_\ell(x)$ (m)
0	0.0	0.0	24.7	0.0
5	−37.2	-52.1	11.1	65.5
8	−77.4	9.6	9.93	139.0
C3	−241.0	75.7	14.8	315.6
C4	−277.8	95.8	16.8	357.6
C5	−312.5	148.4	12.6	420.7
C6	−336.2	184.7	8.8	464.2
C7	−374.7	208.4	11.2	509.6
C8	−420.8	216.0	10.9	556.2
C9	−439.1	228.7	10.0	578.6
C11	−412.6	335.1	11.2	688.2
C12	−428.9	373.1	6.7	729.8
C13	−481.8	463.7	8.3	834.8
C15	−471.9	552.1	7.5	923.7
C17	−533.9	659.1	12.4	1047
C19	−544.5	720.5	21.5	1110
C21	−536.1	864.9	19.5	1255
C23	−688.4	974.3	2.6	1443
C24	−712.3	988.9	2.0	1471
C28	−920.1	1073	0.0	1695

A quick inspection of the data in Table 8.1 (or Fig. 8.10 or 8.11) reveals that one of the challenges in this problem is to design the pipe to produce a positive static pressure at station C19 where the $z = 21.52$ m, just 3.12 m less than that at the source. This problem is made more difficult because the pathlength between the source and this station, over which pipe friction occurs, is 1110 m.

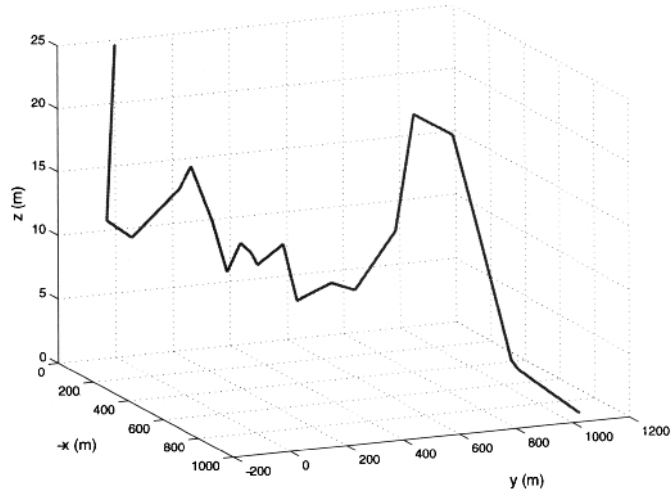

Figure 8.10 Three dimensional plot for proposed pipe contour of the San Benito site.

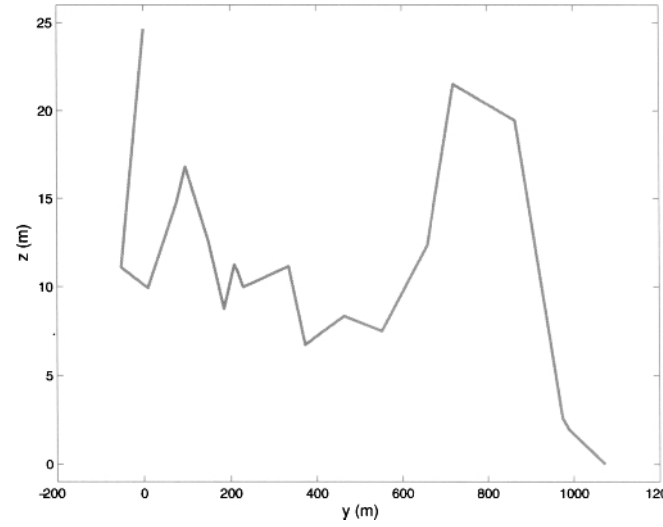

Figure 8.11 Elevation plot for the San Benito site.

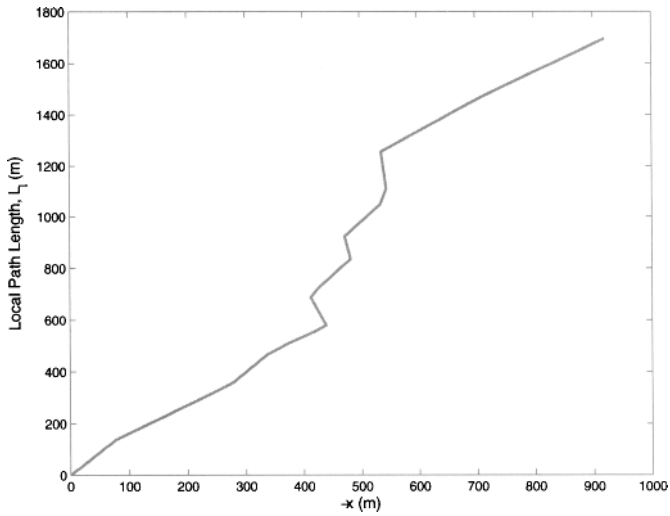

Figure 8.12 Local pathlength distribution for the San Benito site.

The Mathcad worksheet used to solve this problem is shown in Fig. 8.13. A plot of pressure head for station C19 from the solution of Eqn (6.12) as a function of pipe diameter for $z = 21.52$ m, $z_1 = 24.65$ m, and $L_\ell = 1110$ m is presented in Fig. 8.14. This figure also appears in the above-referenced Mathcad worksheet. From our inspection of this figure, we see that a vacuum occurs at this station if $1\frac{1}{2}$-in. PVC pipe is used. For 2-in. pipe and larger, the gage pressure is positive at about 1.3 m of head and larger. Further, for pipe sizes > 3 in., there is little increase in the static pressure at this station. Therefore, nominal $2\frac{1}{2}$-in. PVC pipe, if available, will result in an acceptable, but relatively low, static pressure corresponding to ~2 m of head.

For the remaining length of this network, where the elevation change is 21.52 m and the pipe length is 1695 m−1110 m = 585 m, we can use the design charts in Chapter 5 if we approximate the pressure at station C19 as atmospheric. However, it is not simple to calculate s and λ from station C19 to the delivery location using the data of Table 8.1. Instead of the design charts, we again solve Eqn (6.12) for D required to produce a zero delivery pressure assuming zero pressure at station C19, $z_1 = 21.52$ m and $L_\ell = 585$ m. Obtain $D = 1.077$ in. or a nominal 1-in. PVC pipe. Note that we have neglected all minor losses including that for a coupling to join the nominal 2-in. or $2\frac{1}{2}$-in. PVC pipe to the 1-in. pipe at station C19. This minor loss is indeed negligible (see Table 2.1).

It is interesting to note that if we ignored the local peak at station C19, and considered just the mean slope, s of 0.01743, between the source and delivery locations and overall flow pathlength embodied by λ (of 1.199), the design charts in Chapter 5 would give D of 1.310 in., or a nominal $1\frac{1}{2}$-in. pipe. As noted above, this would lead to a negative gage pressure at station C19. This is yet another example of the need

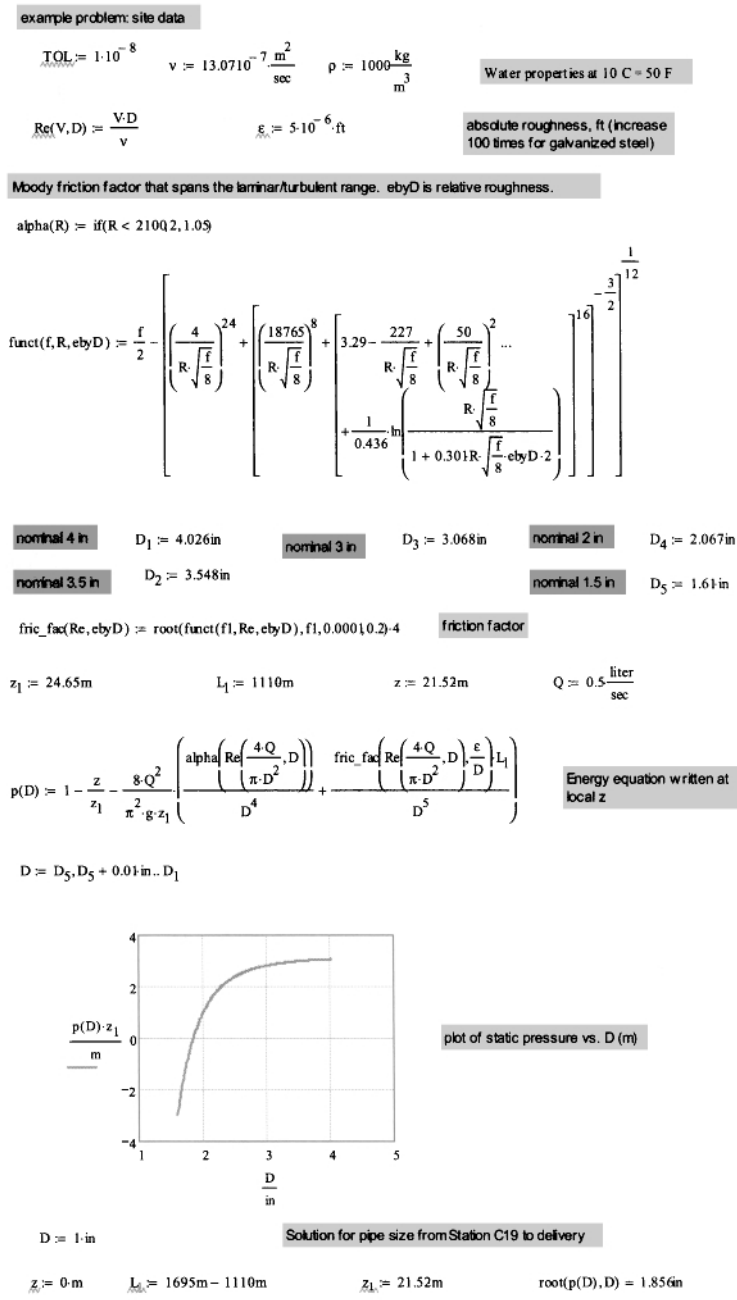

Figure 8.13 `Mathcad` worksheet for example using site survey data. `Mathcad` worksheet `site_survey_data.xmcd`.

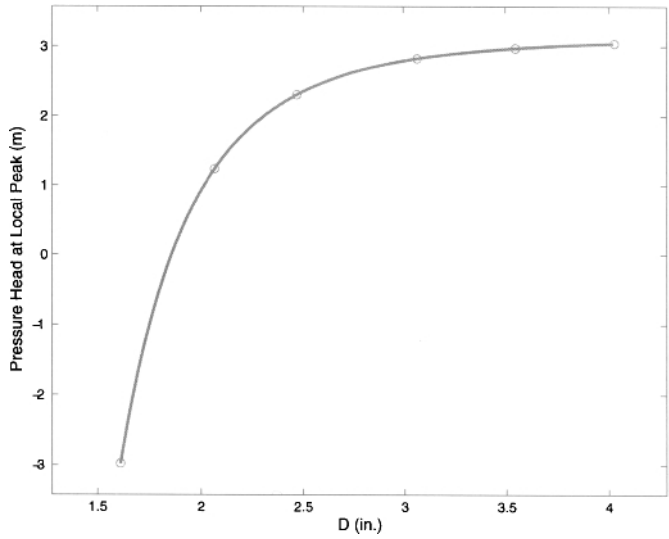

Figure 8.14 Pressure head versus pipe size for highest local peak for the San Benito site. Circles correspond to $1\frac{1}{2}$, 2, $2\frac{1}{2}$, 3, $3\frac{1}{2}$, and 4-in. nominal sch. 40 PVC pipe.

to solve Eqn (6.12), for at least at the local high points in the network, to verify that positive gage pressures are established throughout.

8.8 DRAINING A TANK: A TRANSIENT PROBLEM[8]

So far, we have focused only on steady flow problems that are of general interest in our analysis and design of gravity-driven water networks. However, there are several relevant cases where transient, or unsteady, flows are of prime interest. One of these is the time required to drain a tank through a long pipe.

A related, but simpler, problem is to predict the time that it takes to drain a tank through an opening at its bottom with no attached pipe. The Bernoulli equation, Eqn (2.3), is easily applied in a quasi-steady manner to solve for the instantaneous discharge flow speed, $\overline{u}_2(t)$, at the base of a tank of instantaneous height of liquid, $\Delta z_t(t)$. The result is referred to as Torricelli's formula,

$$\overline{u}_2(t) = \sqrt{2g\Delta z_t(t)} \tag{8.1}$$

Since it is known that the discharge flow speed is not cross-sectionally uniform nor one dimensional (the converging nature of the flow at the opening causes a radially

[8]Though most relevant to the topic at hand, this problem came to light while the author was watering a Christmas tree with a watering can. The process took more time than expected and prompted the developments in this section to determine why this was so.

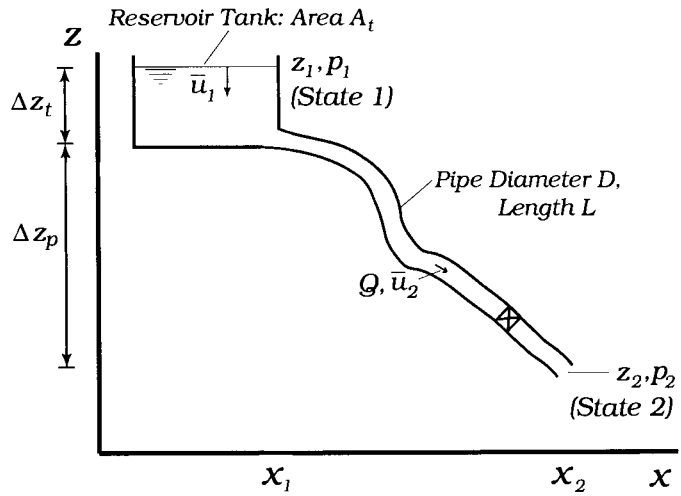

Figure 8.15 Geometry for draining a tank through a long pipe.

inward fluid motion), we apply a discharge coefficient, C_D, and express the volume flow rate through the use of the continuity equation, Eqn (2.21),

$$Q(t) = C_D A_D \overline{u}_2(t) \tag{8.2}$$

where A_D is the cross-sectional area at the tank discharge. Empirically determined values for C_D range from ~0.6 to 1.0 depending on the shape of the discharge opening and flow regime.

The above results were obtained by assuming the flow to be inviscid. This is accurate because the flow speeds are small where they occur in the presence of a walled structure (the tank) and, where the flow speeds are large at the discharge, the surface area for friction is small. Thus, frictional effects are negligible in all regions. However, when the discharge is through a long pipe, it is clear that the flow cannot be assumed inviscid. This requires use of the energy equation, not the Bernoulli equation, to model draining of a tank with a connected pipe.

Consider the geometry in Fig. 8.15. The tank of cross-sectional area A_t having an *initial* height of water Δz_t is to drain through a long pipe of length L. The pipe may have valves and fittings that we can characterize with a combined loss coefficient K, and the elevation change between the two ends of the pipe is fixed at Δz_p. Over time, Δz_t decreases as the tank is drained. The problem is to find the time at which Δz_t is zero, which is the time required to drain the tank.

The energy equation is from Eqn (2.2),

$$\left(\frac{p_1}{\rho} + \alpha_1 \frac{\overline{u}_1^2}{2} + g z_1\right) - \left(\frac{p_2}{\rho} + \alpha_2 \frac{\overline{u}_2^2}{2} + g z_2\right) = H_L + \int_1^2 \frac{dV}{dt}\, dx \tag{8.3}$$

where an integral term has been included.[9] $\int_1^2 \frac{dV}{dt}\,dx$ is the energy per unit mass required to accelerate the fluid at speed V between points 1 and 2 in Fig. 8.15 at any instant in time.[10] When the flow reaches steady state, $\frac{dV}{dt} = 0$, and the integral's contribution to the energy equation disappears as it should.

The friction term in Eqn (8.3) is from the Darcy–Weisbach equation, Eqn (2.9),

$$H_L = [f(V, D)\,\frac{L}{D} + K]\frac{V^2}{2} \tag{8.4}$$

The flow speed V varies over distance between the tank and pipe and is $\overline{u}_1$ in the tank and $\overline{u}_2$ in the pipe.

In Eqn (8.3) $p_1 = p_2 = 0$ since the static pressure at both ends of the pipe is zero and the elevation change is $z_1 - z_2 = \Delta z_t + \Delta z_p$. With these substitutions, $\alpha_1 = 1$, and Eqs (8.3) and (8.4) become,

$$\frac{\overline{u}_1^2}{2} + g(\Delta z_t + \Delta z_p) - \alpha_2\frac{\overline{u}_2^2}{2} = [f(V, D)\,\frac{L}{D} + K]\frac{V^2}{2} + \int_1^2 \frac{dV}{dt}\,dx \tag{8.5}$$

At time zero and earlier, the fluid in the tank and pipe is at rest, $V(0) = 0$. For $t > 0$, two time scales appear for this problem. The first is the time required to accelerate the flow from zero speed to that corresponding to the elevation head $\Delta z_t + \Delta z_p$; over the span of this time scale the elevation in the tank has changed very little. We will refer to this as the "short" time solution. The energy equation for this case is Eqn (8.5) that becomes,

$$L\frac{d\overline{u}_2}{dt} = g(\Delta z_t + \Delta z_p) - [f(\overline{u}_2, D)\,\frac{L}{D} + 1 + K]\frac{\overline{u}_2^2}{2} \tag{8.6}$$

where $\overline{u}_1 = 0$ reflects the fact that the elevation change in the tank is negligible over the short time scale. In addition, the acceleration of the fluid, $\frac{dV}{dt} = \frac{d\overline{u}_2}{dt}$, is spatially uniform and takes place only over the pipe-length L.

Equation (8.6) has been solved for constant friction factor and the use of equivalent length, L_e, instead of the additive K (Streeter et al., 1998). The result is

$$t_{99\%} = 2.646\frac{\overline{u}_{2,\infty 1}}{g(\Delta z_t + \Delta z_p)/L} \tag{8.7}$$

where $\overline{u}_{2,\infty 1}$ is the flow speed in the pipe subject to the hydraulic gradient $(\Delta z_t + \Delta z_p)/L$, and $t_{99\%}$ is the time that it takes to reach 99% of this flow speed; a reasonable approximation for the short time scale. Thus, $\overline{u}_{2,\infty 1}$ is the solution of

$$g(\Delta z_t + \Delta z_p) - f(\overline{u}_{2,\infty 1}, D)\,\frac{L_e}{D}\,\frac{\overline{u}_{2,\infty 1}^2}{2} = 0 \tag{8.8}$$

[9]The symbol V means velocity, not volume, in this section.

[10]From Newton's second law of motion, we note that $\frac{dV}{dt}$ is force per mass. Integrating this force over distance x between points 1 and 2 produces the energy per mass resulting from this force.

B.8.1 Draining a Tank: Short Time Solution

A tank of 30,000 L capacity and 3.5 m high is to be drained. The tank is connected to a $1\frac{1}{2}$-in. nominal sch. 40 PVC pipe, 240 m long, open to the atmosphere at its end. There are 6–90° elbows and an open globe valve in this pipeline. The elevation change from the bottom of the tank to the end of the pipe is 4 m. Calculate the steady state flow speed (subject to the initial height in the tank), $\overline{u}_{2,\infty 1}$, and the time that it takes to reach 99% of this flow speed.

The hydraulic gradient is $(\Delta z_t + \Delta z_p)/L = 0.0313$. Neglecting minor losses for the moment, use the `Mathcad` worksheet `HydraulicGradient.xmcd` to calculate $\overline{u}_{2,\infty 1} = 0.900$ m/s for the pipe of inside diameter $D = 1.61$ in. (see Table 3.1). The friction factor is $f(\overline{u}_{2,\infty 1}, D) = 0.0309$. From Eqn (8.7), we obtain

$$t_{99\%} = 2.646 \frac{0.900 \text{ m/s}}{9.807 \text{ m/s}^2 \cdot 0.0313} = 7.77 \text{ s}$$

We see that the short time scale is of the order of seconds for tank dimensions of the scale given in this example.

The assumption of constant f is approximate because f is undefined for zero flow. Here, f increases immediately as flow becomes nonzero, decreases through the laminar regime, and increases as flow perhaps passes from laminar to turbulent, where it decreases thereafter. Thus, the solution from Eqn (8.7) is approximate but is an excellent indicator of the scale of the short-time solution.

The length equivalent of an open globe valve [$K = 10$; see Eqn (2.11)] and 6–90° elbows is ~$504 \cdot D \approx 20.5$ m. This reduces the hydraulic gradient by only ~8%. If minor losses were included, the value for $t_{99\%}$ will be nearly that as above.

The solution for longer times (i.e., the actual draining of the tank) is now considered. The integral in Eqn (8.3) for the long time solution may be written in two parts,

$$\int_1^2 \frac{dV}{dt}\, dx = \Delta z_t \frac{d\overline{u}_1}{dt} + L\frac{d\overline{u}_2}{dt} \tag{8.9}$$

Since $L \gg \Delta z_t$, the first term on the right side of Eqn (8.9) is neglected in favor of the second term. In addition to this, $\overline{u}_1^2 \ll \overline{u}_2^2$ because of the of the large surface area of the tank relative to the cross-sectional area of the pipe.

We see from this that Eqn (8.6) is also the governing equation for the long time solution except that Δz_t is not constant. It depends on time so that $\Delta z_t = \Delta z_t(t)$. This effect may be included by taking the time derivative of Eqn (8.6) and recognizing that

$$g\frac{d(\Delta z_t)}{dt} = -g\overline{u}_1 = -\frac{\pi g D^2}{4A_t}\overline{u}_2 \tag{8.10}$$

where the second term on the right side is from the continuity equation. With Eqn (8.10), Eqn (8.6) becomes upon taking the time derivative of each term,

$$L\frac{d^2\overline{u}_2}{dt^2} + \frac{\pi g D^2}{4A_t}\overline{u}_2 + \frac{d}{dt}\{[f(\overline{u}_2, D)\,\frac{L}{D} + 1 + K]\frac{\overline{u}_2^2}{2}\} = 0 \qquad (8.11)$$

Equation (8.11) is the governing equation for the pipe flow speed, $\overline{u}_2$, corresponding to the long time solution for draining a tank. The initial conditions are

$$\overline{u}_2(0) = \overline{u}_{2,\infty 1}, \quad \frac{d\overline{u}_2(0)}{dt} = 0 \qquad (8.12)$$

where $\overline{u}_{2,\infty 1}$ is from the solution of Eqn (8.8).

We may define a time scale for tank draining as the ratio of the initial tank volume to the volume flow rate at based on the initial flow speed in the pipe, $\overline{u}_{2,\infty 1}$,

$$\Delta t_{sc} = \frac{4A_t \Delta z_t(0)}{\pi D^2 \overline{u}_{2,\infty 1}} \qquad (8.13)$$

which is of the order of thousands of seconds or more for realistic tank sizes. This is the "scale" or order of magnitude of the tank-draining time. By scaling Eqn (8.11) with this time scale, we see that the acceleration term, $Ld^2\overline{u}_2/dt^2$, is negligible compared with the remaining two terms. With this term eliminated, Eqn (8.11) becomes

$$[f(\overline{u}_2, D)\,\frac{L}{D} + 1 + K]\frac{d\overline{u}_2}{dt} + \frac{\overline{u}_2}{2}\,\frac{L}{D}\,\frac{df(\overline{u}_2, D)}{dt} + \frac{\pi g D^2}{4A_t} = 0 \qquad (8.14)$$

The single initial condition is the first of Eqs (8.12). The time to drain a tank is from the solution of Eqn (8.14).

Because of the time dependence of Δz_t it is not possible to obtain a closed-form solution of Eqn (8.14) of the type above for the short time case. Equation (8.14) is solved numerically in `Mathcad` (see textbox B.8.2 example). The derivative in the second term of Eqn (8.14) is evaluated symbolically in `Mathcad`. The time to drain the tank is found when the solution of Eqn (8.14) is equal to the flow speed in the pipe, $\overline{u}_{2,\infty 2}$, resulting from the hydraulic gradient $\Delta z_p/L$. The solution for $\overline{u}_{2,\infty 2}$ comes from Eqn (8.8) with $g(\Delta z_t + \Delta z_p)$ replaced by $g\Delta z_p$ alone (i.e., $\Delta z_t = 0$).

The flow speeds in the drain pipe, $\overline{u}_2(t)$, are plotted in Fig. 8.16 for three cases and for an initial tank volume of 30,000 L, initial Δz_t of 4.5 m, $L = 100$ m, $D = \frac{1}{2}$ in. nominal GI pipe, and $\Delta z_p = 0.1, 1.0$, and 10 m. Each curve terminates when the tank is empty. We see that $\overline{u}_2(t)$ decreases linearly over time for the largest value of Δz_p, but nonlinear $\overline{u}_2(t)$ occurs for the two smaller elevation heads. Evidence of transition and laminar flow is visible beginning at the knee of the curve for $\Delta z_p = 0.1$ m. It is clear that drain times ranging from more than a day to many days are possible for large tanks and under the conditions of Fig. 8.16.

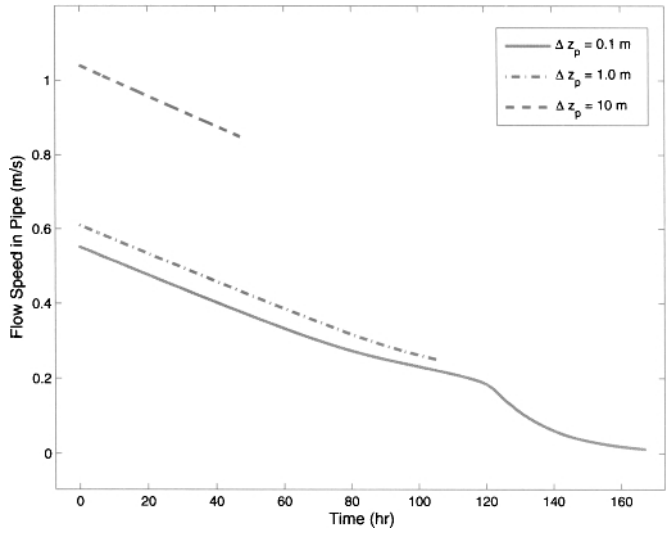

Figure 8.16 Tank-draining results.

B.8.2 Draining a Tank: Long Time Solution

Calculate the time to drain the tank for the example in textbox B.8.1.

Use the `Mathcad` worksheet `Tank_Draining.xmcd` to calculate $\overline{u}_{2,\infty 2} = 0.643$ m/s for the data given in textbox B.8.1. The friction factor is $f(\overline{u}_{2,\infty 2}, D) = 0.03924$. Equations (8.11) and (8.12) are solved numerically to obtain a drain time of ~8.7 h. The few seconds to accelerate the flow from zero speed in the short time solution are clearly negligible here.

The minor losses were included in this solution.

A quick check on the validity of this result can be made by averaging the flow speeds $\overline{u}_{2,\infty 1}$ and $\overline{u}_{2,\infty 2}$. The ratio of the tank volume to the mean volume flow rate obtained by averaging the flow speeds gives a drain time of 8.2 h, within 30 minutes of the exact solution. For cases where there are small D and Δz_p, and large values of L, the use of the average value of the volume flow rate to estimate the drain time can under-predict the exact value by 40% or more (see Fig. 8.16). For these cases there is considerable curvature in the flow speed $\overline{u}_2(t)$ versus t.

For comparison, Torricelli's formula [Eqn (8.1)], predicts a drain time of 1.26 h. This is much less than the actual solution because of the neglect of friction.

8.9 THE SYPHON

A syphon is a pipe arranged such that it is capable of lifting a liquid from a reservoir upward against gravity. This happens when the weight of water in a pipe below the reservoir level is greater than the weight of water in the pipe above the reservoir.

To model the performance of a syphon we consider a pipe of inside diameter D having a circular arc of radius r. The open end of this pipe is immersed in the water at the source at elevation z_1. At the other end, the pipe is joined by a vertical pipe of length z_1, (i.e., this leg of pipe extends to elevation $z_2 = 0$). The contours of three different syphons are shown in Fig. 8.17. All syphons have $z_1 = 20$ m, constant diameter, assumed minor-lossless flow, and a static pressure of zero (atmospheric pressure) at the delivery location at $z_2 = 0$. They each have a different value for r. The larger the value for r the further the water will need to be raised above z_1 and delivered to the outlet of the syphon.

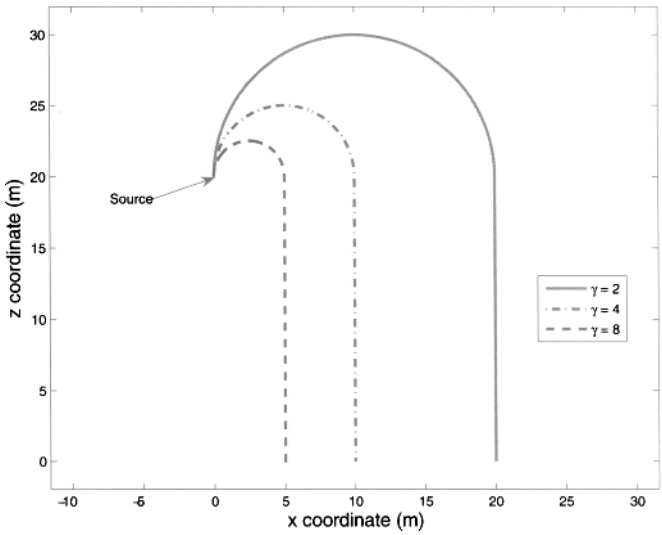

Figure 8.17 Contours for three syphon geometries.

If we let $\gamma = z_1/r$, the expressions for mean slope, s, tortuosity, λ, and the energy equation are able to be written in simplified forms. For s and λ, we have

$$s = \frac{\gamma}{2} \tag{8.15}$$

and

$$\lambda = \frac{\pi + \gamma}{\sqrt{4 + \gamma^2}} \tag{8.16}$$

The theoretical values for the volume flow rate, Q, can be estimated using figures in Section 5.4 or calculated from the Mathcad worksheet.[11] Note that this result could also be obtained by solving Eqn (6.12) at $x = x_2$, with $L_\ell(x) = L_\ell(x_2) = L$, where L is the total length of the pipe, and with the delivery pressure $p(x) = p(x_2) = 0$ and $z(x) = z(x_2) = 0$. Thus, Q is determined from the solution of the energy equation where the static pressure is zero at both ends of the syphon,

$$0 = 1 - \frac{8Q^2}{\pi^2 g z_1 D^4}\left(\alpha + f(Q,D)\frac{z_1(\pi+\gamma)}{\gamma D}\right) \tag{8.17}$$

In this equation, the term $z_1(1 + \pi/\gamma)$ is the total length of the pipe, L.

The values for s and λ for the three syphon geometries in Fig. 8.17 having γ of 2, 4, and 8 are 1 and 1.818, 2 and 1.597, and 4 and 1.351, respectively. A plot of Q versus D (Fig. 8.18) shows Q ranging from < 1 L/s for nominal $\frac{1}{2}$-in. PVC pipe to nearly 40 L/s for $3\frac{1}{2}$-in. PVC pipe. However, the question that remains unanswered at this point is what is the local static pressure distribution in the syphon. In particular, *is the static pressure distribution in the pipe even possible?*

To answer this question, we need to solve Eqn (6.12) for $p(x)$ using the local path length distributions for the three syphons appearing in Fig. 8.19. These are obtained by breaking up the syphon into small pieces having components Δx wide and Δz high. Then, a running sum of $\sqrt{\Delta x^2 + \Delta z^2}$ is calculated, which is the pathlength distribution $L_\ell(x)$. The dimensionless static pressure distribution, $p(x)/\rho g z_1$, is presented in Fig. 8.20 for a nominal $1\frac{1}{2}$-in. PVC pipe. The static pressure for all syphons behaves in the same manner. We see a reduction of pressure with distance in the direction of flow as the liquid climbs upward (potential energy is increasing at the expense of pressure energy). The pressure continues to fall even as the liquid begins to move downward. This is the result of pipe friction. At some distance beyond the highest point of the syphon, the static pressure starts to increase and, once in the vertical leg of the pipe, increases sharply to atmospheric pressure at the outlet as required by this problem. Note that the pressure in the entire syphon is negative relative to the atmospheric pressure conditions that surround it.[12] The question posed above is answered by considering the smallest static pressure possible of -14.7 psig at which we have a perfect vacuum.[13] The value of the dimensionless static pressure, $p/\rho g z_1$, for this condition is -0.517. From our inspection of Fig. 8.20, the static pressures at some locations for the syphons having $\gamma = 2$ and $\gamma = 4$ fall below the

[11] Recall that Q is obtained from the solution of Eqn (2.41) for minor-lossless flow in a pipe that is not straight. This equation can first be solved for $\overline{u}$ and then Q calculated using the continuity equation, Eqn (2.21).

[12] If the surroundings were at a sufficiently large positive gage pressure, the static pressure in the syphon would still operate below this pressure but the gage pressure in the syphon will be positive everywhere. This condition is required where there may be syphoning in a gravity-driven water flow.

[13] This condition is used as a convenient benchmark. Really, the pressure can fall no lower than that which causes the water to vaporize. When the pressure of a constant-temperature fluid is reduced, a value of the pressure is eventually reached where the water begins to form vapor. This is referred to as the saturation pressure for the given temperature, or more simply, the "vapor pressure." For water at 10°C, the vapor pressure is ~0.178 psia (absolute), very close to absolute zero pressure (see Exercise 26).

case of a perfect vacuum. Because no pressure can be less than that of a perfect vacuum, no flow will occur in the syphon for the cases of $\gamma = 2$ and $\gamma = 4$. This is easily verified in your own kitchen with a length of tubing, a sink filled with water, and a bucket into which the water can run. With the syphon running (after you have "primed" it) gradually move the tube upward creating a greater height for the water to rise. At some point, the flow will reduce to a trickle and eventually stop. The above is the correct result despite the calculations of volume flow rate based on overall states of the syphons appearing in Fig. 8.18. The flow rates appearing in this figure will occur only if the pressure is greater than a perfect vacuum at each and every point in the flow.

This is yet another example of the need to consider performance of the network based on both overall and *local* conditions. Of course, syphoning in gravity-driven networks does occur in many designs. The acceptability of these cases relies on the static pressure being large enough so that if syphoning does occur, the reduction in pressure is not severe enough to cause negative gage pressures in the network. Please see the nearby footnote for additional comments on this.

To solve the interesting problem of the maximum height of a syphon of diameter D and elevation z_1 for a fluid at a prescribed temperature, we first need to determine the x or z coordinate location where the pressure is a minimum. Then, knowing that the pressure at this location can be no smaller than the vapor pressure at the prescribed temperature, the problem can then be solved for the value of γ that produces this pressure. The height of the syphon, r is easily found from $r = z_1/\gamma$. The x coordinate where pressure is a minimum is found by taking the derivative, d/dx, of the dimensionless static pressure, $p(x)/\rho g z_1$, setting it equal to zero, and solving for the x value (see Exercise 26).

References

Anon. The GPS System. `http://www.kowoma.de/en/gps/errors.htm`, 2009. [Online; accessed 26-November-2009].

T. D. Jordan Jr. *Handbook of Gravity-Flow Water Systems*. ITDG Publication, London, UK, 2004.

M. C. Potter and D. C. Wiggert. *Mechanics of Fluids*. Brooks/Cole (Thomson), Tampa, FL, 2002.

V. L. Streeter, E. B. Wylie, and K. W. Bedford. *Fluid Mechanics*. McGraw-Hill, New York, NY, 1998.

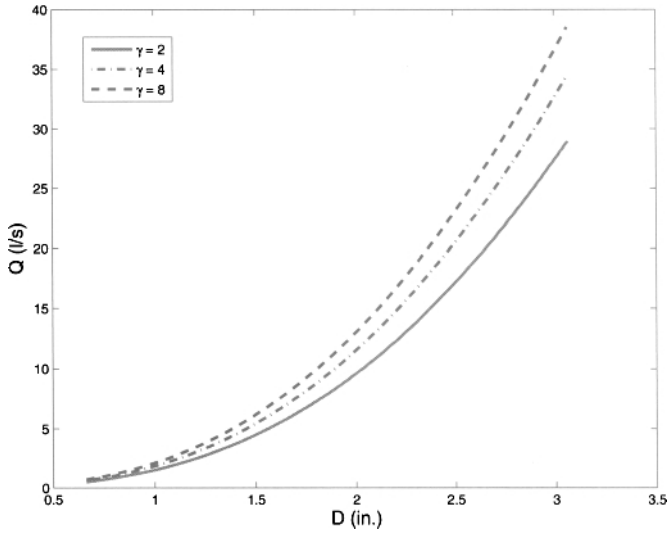

Figure 8.18 Theoretical volume flow rates, Q, for the syphon geometries of Fig. 8.17 for range of pipe diameters.

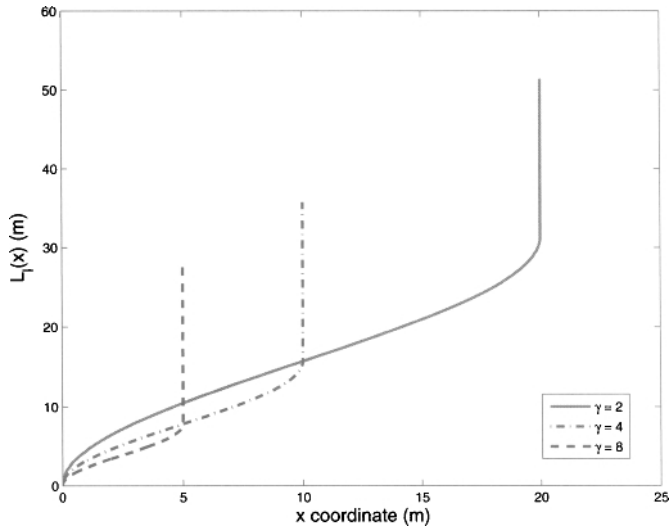

Figure 8.19 Local pathlength distribution, $L_\ell(x)$, for the syphon geometries of Fig. 8.17.

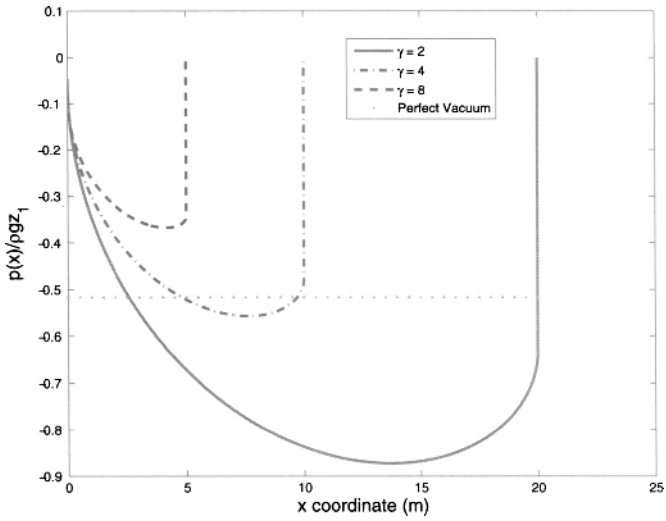

Figure 8.20 Dimensionless local static pressure distribution, $p(x)/\rho g z_1$, for the syphon geometries of Fig. 8.17 and nominal $1\frac{1}{2}$-in. PVC pipe.

CHAPTER 9

THE ENERGY EQUATION BASED ON APPROXIMATE FRICTION FACTOR

"Things should be made as simple as possible, but not any simpler."
– A. Einstein

9.1 THE PROBLEM

There are many types of design tools employed in engineering practice. For flow in pipes, these range from commercially available and in-house-written computer codes to formulas and nomographs for restrictive applications (The Crane Company, 1970; Copper Development Association, 2006). One such group of formulas is from Hazen–Williams (Williams and Hazen, 1933), first developed ~1906. In various forms, they are curve fits of pipe-flow data that relate the head loss to flow speed or volume flow rate through a "hydraulic resistance." Hazen and Williams developed their formulas in the years before Rouse and his colleagues were formalizing the use of design charts for pipe flow from the data and correlations of Blasius (in 1913), von Karman (1930); Nikuradse (1950); Colebrook and White (1937); Colebrook (1938, 1939), among others. These correlations were based on knowledge of fundamentals of fluid flow in pipes, where the friction factor is known to depend only on the Reynolds number (Re) and, for turbulent flow, relative roughness. Obviously, there were no widely

Gravity-Driven Water Flow in Networks. By Gerard F. Jones

used high-speed electronic calculators or computers at the time, so comprehensive, easy-to-use design charts were the order of the day. As pointed out in footnote 12 in Chapter 2, the Rouse chart (Rouse, 1943, 1975) ultimately spawned the Moody chart that is familiar to many.

One of the problems with the Hazen–Williams formula is that, until very recently, its accuracy and range of applicability have not been widely understood and quantified (Liou, 1998). Consequently, it has probably been used in many instances where it should not have been. This is unfortunate because the generally broad acceptance of this formula by designers of fluid flow networks has evolved, especially in the United States, and extensive data bases on coefficients for the curve fits for a variety of pipe sizes and inside surface treatments have been produced and compiled. Even today, there continues an active debate on the suitability of these formulas for analysis and design driven partially by their past widespread acceptance in the hydraulics community and the recently understood lack of accuracy for a wide range of pipe flows[1]; see Christensen (2000); Locher (2000); Swamee (2000); Travis and Mays (2007); Bombardelli and Garcia (2003).

One such Hazen–Williams formula reported by Liou (1998) is

$$Q = 0.278\, C\, D^{2.163} \left(\frac{h_L}{L}\right)^{0.54} \tag{9.1}$$

where C is a coefficient that depends on the friction factor, D, the flow speed, and the kinematic viscosity of the fluid which, we recall, depends on the fluid temperature. In addition, the coefficient 0.278 is a *dimensional* quantity whose value needs to be increased by ~55% if working in the English system of units, rather than S.I. Only the numerical values for C are reported Potter and Wiggert (2002), which for smooth pipe is ~140. The lack of units for 0.278, C, and D makes Eqn (9.1) *dimensionally nonhomogeneous.*[2] From a fundamentals standpoint, the nonhomogeneous character of the Hazen–Williams formulas forms the basis of a difficulty that is explored further in the next paragraph. For this reason, and the accuracy limitations noted above, the use of these formulas is strongly discouraged in favor of the Darcy–Weisbach equation. The possible exception to this would be for cases where the pipe-wall

[1] In particular, Christensen (2000) concludes that the minimum value for D, wherein the Hazen–Williams formula may be accurately applied is 1.44 m (56.7 in.). The pipe sizes typical of gravity-driven water networks considered in the present context are considerably smaller than this size. Cristensen concludes "...that usage of the Hazen–Williams formula should be strongly discouraged." An additional dimension to this issue was noted by Rouse (1975), "In the long run, however, it is debatable whether it [the Hazen–Williams formula] did more good or harm, for it not only concealed the principles behind the resistance phenomenon but made acceptance of later, more rigorous analyses like those of Blasius a very slow process." The reference to "...concealing the principles..." in this quote pertains to the Hazen–Williams approach of ignoring that simple dimensional analysis shows that the hydraulic gradient depends on just two quantities, the relative roughness of the pipe wall and Re.

[2] In a dimensionally homogeneous equation, like $\vec{F} = m\vec{a}$, all terms, $\vec{F}$ and $m\vec{a}$, have the same dimensions. For a dimensionally nonhomogeneous equation, the dimensions of two or more terms are not the same. In the case of Eqn (9.1) this comes about because $0.278C$ and D are dimensional quantities written without units. For example, a dimensionally nonhomogeneous form of Newton's second law of motion would be $F = 9.807\, m$.

conditions are special, such that the friction factor is unknown and the value for C is available.

Our inspection of the nonhomogeneous formula of Eqn (9.1) shows it to be like a "pencil-and-paper" computer program where numbers alone are input and a numerical answer is the output; the units for both input and output are ignored in the calculations. The potential problems with this type of model are twofold. First, one must be certain of the units for input and output, as would be the case with any computer program. Second, there is considerable variability in the Hazen–Williams coefficient that depends on the fluid type and temperature as well as D and flow speed (Trifunovic, 2006)[3]. The restriction of the Hazen–Williams formulas to turbulent flow is particularly egregious. Since the calculation of Re is not part of the design process when Hazen–Williams formulas are used, the user is left to either calculate this for themselves or, as is often the case, the possibility of laminar flow is just simply ignored. Note that this flow regime will occur for the lower left side of Figs. 5.4–5.13 for gravity-driven water networks; perhaps not likely with many large industrial liquid flows.

The combined effect of the above limitations means that the Hazen–Williams formula may provide only a coarse approximation to the solution for flow in a gravity-driven pipe-flow problem. Potter and Wiggert (2002) show a plot of the friction factor, f, from several sources including the Colebrook equation [Eqn (2.12], the industry-accepted formula for friction factor [or Eqn (2.16)] and the equivalent one from Hazen–Williams. The lack of agreement between these two is clear with differences varying to about $\pm 35\%$.[4] The results from the Hazen–Williams formula bear considerable uncertainty when compared with those from the Darcy–Weisbach equation.

9.2 A RECOMMENDATION

The bottom line of this story is, where possible, adhere to the fundamentals in the work that you do including pipe-flow calculations. For the equations and formulas you use, know and understand the assumptions on which they are based[5]. In general, the use of *nonhomogeneous* formulas in engineering should be cautiously approached. This includes formulas as well as computer programs which, with the exception of at least `Mathcad` and EES[6], are always nonhomogeneous. Remember that nonhomogeneous implies that there are one or more simplifications that have been incorporated, such as the substitution of a fixed number for an algebraic symbol of a quantity that is dimensional. These simplifications are sometimes ignored or not completely understood, which could easily result in the inappropriate use of the formula.

[3] Similar variability does not exist in the use of the Darcy–Weisbach equation where the only free parameter is the absolute wall roughness which is normally well characterized, at least for new pipe. There is no explicit dependence on D and flow speed other than through the dimensionless Reynolds number.

[4] Perform Exercise 13 to verify this result.

[5] See textbox B.2.2.

[6] F-Chart Software, Madison WI, available at info@fchart.com.

In particular, for the pipe flow calculations that are made in the normal course of formal or informal (that is, self-taught) learning, where interest is in understanding and acquiring insight as opposed to mere practice and application, there is no good reason to use nonhomogeneous formulas like the Hazen–Williams type. However, be aware that for a number of reasons mostly related to economy, tradition, and consistency with supporting methodologies, restrictive formulas are used every day in industry, including the Hazen–Williams variety in the hydraulics and related communities. The reader will also find Hazen–Williams formulas in use in Corcos (2004); Trifunovic (2006) and in many other common references that you will perhaps use in further study of gravity-driven water networks.

9.3 ENERGY EQUATION: FRICTION FACTOR FROM THE BLASIUS FORMULA

If we wish to use a simple, approximate formula to get a sense for or make a quick estimate of pipe diameter, the following development should be considered. We restrict our interest to *minor-lossless flow* [the assumption of $D/z_1 = 0$ in Eqn (2.40)], and further assume that the flow is turbulent (and $4,000 < \mathrm{Re} < 325,000$, the region where agreement between the approximate and exact friction factors is 12% or better; see Section 2.2.2) and that the pipe is smooth. The Blasius formula from Eqn (2.19), $f(\overline{u}, D) = 0.316\,\mathrm{Re}^{-1/4}$, applies (Munson et al., 1994). Upon substituting this formula for $f(\overline{u}, D)$ into Eqn (2.41) we obtain after several steps of algebra[7]

$$D = 0.741\left[\frac{\lambda\,(1+s^{-2})^{1/2}}{1-F}\right]^{4/19}\left(\frac{\nu Q^7}{g^4}\right)^{1/19} \tag{9.2}$$

which, for the normal condition of $s \ll 1$, may be simplified to

$$D = 0.741\left[\frac{\lambda}{s\,(1-F)}\right]^{4/19}\left(\frac{\nu Q^7}{g^4}\right)^{1/19} \tag{9.3}$$

The group $\nu Q^7/g^4$ has the dimension of length raised to the power of 19 and all of the remaining terms on the right-hand sides in Eqs (9.2) and (9.3) are dimensionless. We can clearly see that this group raised to the one-nineteenth power gives a dimension of length. For cases that obey the assumptions on which they are based, the dimensionally homogeneous Eqs (9.2) and (9.3) can be used to predict the pipe diameter quite accurately.[8]

[7] It is very easy to develop this formula yourself and you are encouraged to do so. See Exercise 29. Be aware that you first need to substitute the continuity equation into Eqn (2.41) to eliminate $\overline{u}$ in favor of Q.

[8] A simple, first-order estimate of the accuracy can be made by assuming that the friction factor is 0.03 ± 0.02 as cited in Section 2.2.2. After a few steps of algebra and for minor-lossless flow, Eqn (2.41) becomes $D = 0.455(1 \pm 0.158)\{\lambda Q^2/[(1-F)gs]\}^{1/5}$. The accuracy of this formula is thus $\pm 15.8\%$. A more detailed assessment is shown in Fig. 9.3.

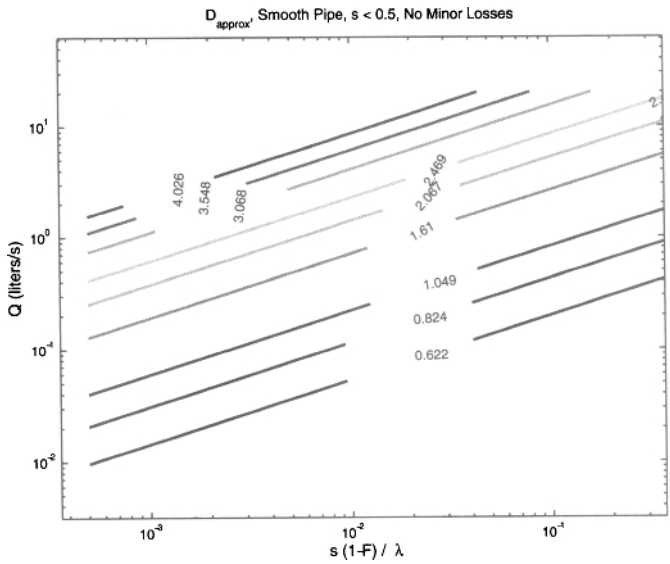

Figure 9.1 The parameter D from Eqn (9.4). The contour lines from bottom-to-top correspond to $\frac{1}{2}$, $\frac{3}{4}$, 1, $1\frac{1}{2}$, 2, $2\frac{1}{2}$, 3, $3\frac{1}{2}$, and 4 in. nominal sch. 40 PVC pipe. Compare with the design graphs in Chapter 5.

For ease of use in graphical form, Eqn (9.3) can be recast as,

$$\boxed{D = 0.741\,[\frac{s\,(1-F)}{\lambda}]^{-4/19}\,(\frac{\nu^{1/7}\,Q}{g^{4/7}})^{7/19}} \tag{9.4}$$

A plot of Eqn (9.4), D as a function of Q and the hydraulic gradient, $s(1-F)/\lambda$ (one can visualize this as a modified slope), is presented in Fig. 9.1, where the contour lines correspond to $\frac{1}{2}$, $\frac{3}{4}$, 1, $1\frac{1}{2}$, 2, $2\frac{1}{2}$, 3, $3\frac{1}{2}$, and 4 in. nominal PVC pipe. The reader may wish to compare this figure with Fig. 5.30. Note that the parameters s, F, and λ appear as a group in Fig. 9.1,[9] whereas the effect of the parameters F and λ is presented on individual design graphs in Chapter 5. When making this comparison, recall the restrictions concerning the results shown in Fig. 9.1. Namely, minor-lossless, turbulent flow with $4,000 < \mathrm{Re} < 325,000$, $s < 0.5$, and smooth pipe. Because of the restriction to turbulent flow, an inspection of Fig. 9.1 reveals no laminar or transition regions that appear in the lower-left corners of each of the pipe design plots in Chapter 5.

[9]That is, increasing λ and $F(= p_2/\rho g z_1)$ have the same effect as reducing the mean slope, s. In all of these cases, the hydraulic gradient would decrease.

Swamee and Jain (1976) report an extension of Eqn (9.4) to include the effect of pipe roughness, ϵ, for nonsmooth pipe,

$$D \approx 0.66\{\epsilon^{1.25}[\frac{Q^2}{g(h_L/L)}]^{4.75} + \nu Q^{9.4}[gh_L/L]^{-5.2}\}^{0.04} \tag{9.5}$$

where the hydraulic gradient is h_L/L, as noted in Chapter 2. A comparison between Eqs (9.4) and (9.5) for smooth pipe shows agreement to within $\pm 2\%$ over 0.1 L/s $\leq Q \leq$ 3 L/s and $0.001 \leq h_L/L \leq 1$. The inclusion of roughness in the correlation of Eqn (9.5) necessarily excludes its application to laminar flow. The stated ranges for Q and h_L/L generally produce $4,000 <$ Re $< 325,000$. Swamee and Sharma (2008) present a correlation for D that spans from laminar to turbulent flow

$$\begin{aligned} D \approx\ & 0.66\{([214.75\frac{\nu Q}{g(h_L/L)}]^{6.25} \\ +\ & \epsilon^{1.25}[\frac{Q^2}{g(h_L/L)}]^{4.75} + \nu Q^{9.4}[gh_L/L]^{-5.2}\}^{0.04} \end{aligned} \tag{9.6}$$

For minor-lossless flow in a GI pipe, differences between D evaluated by Eqn (9.6) and the Mathcad worksheets of Chapter 5 are $< 12\%$ (see Exercise 31). For smooth pipe, the agreement is 5% or better. Recall that the worksheets include minor losses if important, such as a partially closed throttling valve needed for flow control.

As an aid, a plot of Re, $4Q/\pi\nu D$, versus Q and $s(1-F)/\lambda$ is presented in Fig. 9.2 from which we note that Re $< 4,000$ are likely for small values of the hydraulic gradient, $s(1-F)/\lambda$. In Chapter 2, a comparison of the friction factor and the Blasius approximation revealed agreement to within 12% for $4,000 <$ Re $< 325,000$. Thus, we expect the accuracy of the results from Fig. 9.1 and Eqn (9.4) to be questionable in the left-most region of Fig. 9.2, where Re < 4000, a region that spans a broad range of practical values for the flow rate and hydraulic gradient.[10] We wish to further explore the extent of agreement between the solutions from the approximate and exact forms of the energy equation. Figure 9.3 shows the ratio of the pipe diameter from two independent calculations, one from the solution of the complete energy equation (D_{exact}) and one from Eqn (9.4) (D_{approx}). This ratio varies from 1 to ~1.05 for large values of the hydraulic gradient, and ~0.65-0.70 for small slope.[11] For the case of $s = 0.001$ and $Q = 0.1$ L/s, for example, $D_{approx}/D_{exact} \approx 0.9$. Obviously, under-sizing of pipe by using the approximate solution from Eqn (9.4) is not generally desirable, but because the object of this section is to get a sense for or make a quick estimate of D from the simpler, approximate form of the energy equation, the results from Eqn (9.4) may very well be accurate enough depending on the problem at hand and the demands of the designer. Of course, a final analysis and the complete design should be carried out using the appropriate Mathcad worksheet where the effects of minor losses and sensitivity studies may be easily investigated.

[10] Values for the hydraulic gradient of 0.01 and smaller are not unusual.

[11] For small values of hydraulic gradient the flow is laminar or transitional so one would expect D from Eqn (9.4) to be approximate.

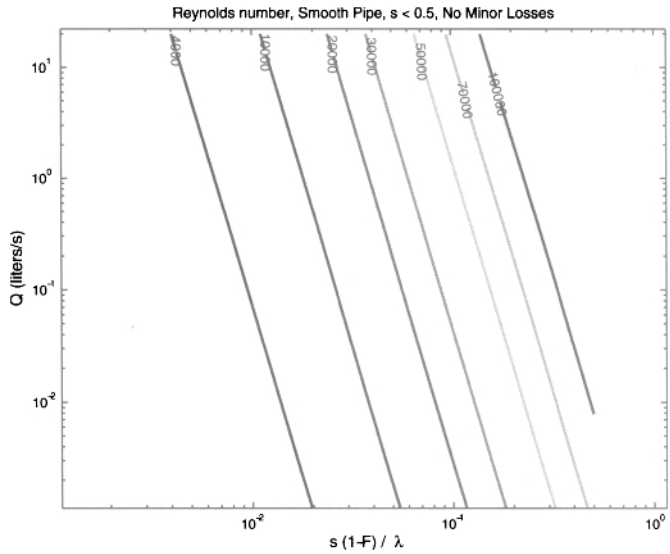

Figure 9.2 Reynolds number versus hydraulic gradient, $s(1-F)/\lambda$, and Q. Region of inaccuracy is to the left of the line corresponding to Re of 4000.

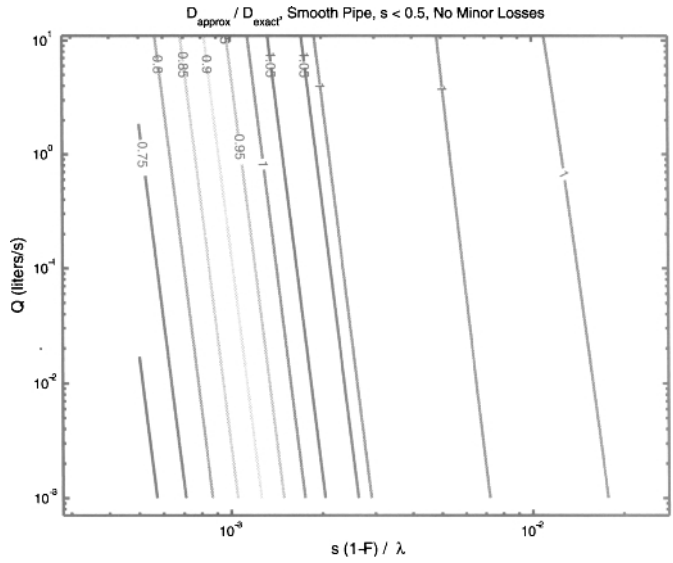

Figure 9.3 D_{approx}/D_{exact} versus hydraulic gradient, $s(1-F)/\lambda$, and Q.

As a final comment on Fig. 9.2, note that it reveals that Re$> 10^5$ are not to be expected; the upper limit on Re of 325,000 for the accuracy of the Blasius approximation is not an issue.

A particularly simple result is obtained if Eqn (9.4) is put into dimensionless form,

$$\boxed{\frac{Q\,\nu^{1/7}}{g^{4/7}\,D^{19/7}} = 2.25\,[\frac{s\,(1-F)}{\lambda}]^{4/7}} \tag{9.7}$$

where the group on the left side of Eqn (9.7) can be interpreted as the dimensionless volume flow rate and the one on the right side is the hydraulic gradient. In this form, we see that the solution of the energy equation for minor-lossless, turbulent flow (where $4000 < \text{Re} < 3.25 \times 10^5$) in smooth pipes gives a power-law relation between the dimensionless volume flow rate and the hydraulic gradient according to Eqn (9.7). A plot of this equation appears in Fig. 9.4. Also made clear by our inspection of either Eqs (9.4) or (9.7) is that for any given set of conditions, Q is proportional to $D^{19/7}$. This result is discussed in the paragraph that follows.

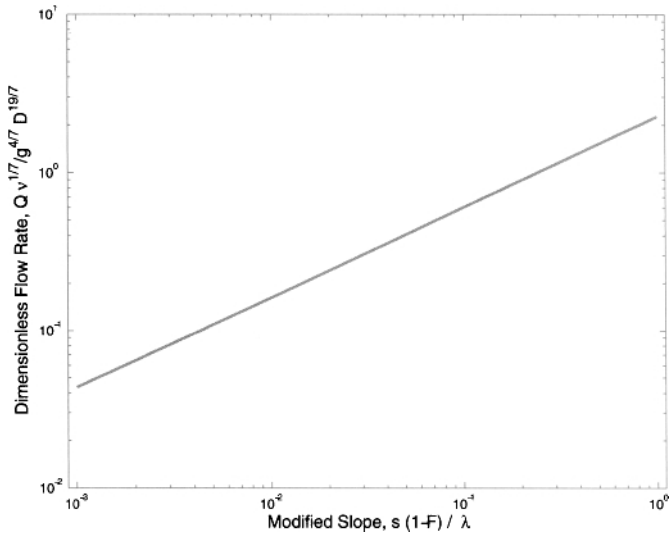

Figure 9.4 A plot of Eqn (9.7).

As we will see in Chapter 11, it is worthwhile at this point to rewrite Eqs (9.4) and (9.7) in general form. That is, both of these equations are based on $z_2 = p_1 = 0$. If we allow nonzero values for these two parameters, we obtain

$$\boxed{D = 0.741\,(\frac{\Delta z + \Delta h}{L})^{-4/19}\,(\frac{\nu^{1/7}\,Q}{g^{4/7}})^{7/19}} \tag{9.8}$$

and

$$\boxed{\frac{Q\,\nu^{1/7}}{g^{4/7}\,D^{19/7}} = 2.25\,(\frac{\Delta z + \Delta h}{L})^{4/7}} \tag{9.9}$$

where Δz is the elevation change between the two ends of a single-diameter pipe, and $\Delta h = \Delta p/\rho g$ is the change in static pressure head between these two locations. Both Eqs (9.8) and (9.9) will be convenient for use in the analysis and design of multiple-pipe networks where the values for the static pressures and elevations at the ends of each pipe are nonzero. The term $(\Delta z + \Delta h)/L = h_L/L$ is the hydraulic gradient.

Besides the obvious utility of these simple formulas, the origins of which are clear because they were derived by the readers themselves, we can see that D depends only on $Q^{7/19} = Q^{0.368}$, $\lambda^{4/19} = \lambda^{0.211}$, $(1-F)^{-4/19}$ and, for the normal situation where $s \ll 1$, $s^{-4/19}$. The sensitivity of D to the key parameters that determine it is thus established. It is interesting to note that the lack of sensitivity of D to s, λ, and F for a prescribed value for Q makes the task of sizing a system for D particularly forgiving, especially when one considers the narrow choice of nominal pipe sizes from among which to choose (see Section 5.6). The more challenging task is to determine pipe sizes for a multiple-pipe network as discussed in Chapter 11 because the static pressures at both ends of a given pipe are nonzero and unknown.

If the designer requires a delivery static pressure of head h_{del}, say, at a tapstand, where $p_{del} = \rho g h_{del}$, knowing that $F = 1 - p_{del}/\rho g z_1 = 1 - h_{del}/z_1$, Eqn (9.3) becomes

$$D = 0.741[\frac{s\,(1 - h_{del}/z_1)}{\lambda}]^{-4/19}[\frac{Q\,\nu^{1/7}}{g^{4/7}}]^{7/19} \tag{9.10}$$

From the above results, we see that for values of the hydraulic gradient > 0.001, where D from the approximate form of the energy equation for pipe flow is to within reasonable agreement with the exact value, the dimensionally homogeneous Eqs (9.2)–(9.10), subject to their restrictive assumptions may be considered acceptable alternatives to the Hazen–Williams formulas discussed above. Also, one of the key observations from the material presented in this section is the importance of calculating Re for all parts of the network. Combining Eqs (9.4) or (9.10) with the definition of Re, we obtain

$$\mathrm{Re} = 1.718\,[\frac{Q^3\,g\,s\,(1-F)}{\lambda\,\nu^5}]^{4/19} = 1.718\,[\frac{Q^3\,g\,s\,(1 - h_{del}/z_1)}{\lambda\,\nu^5}]^{4/19} \tag{9.11}$$

valid for $4000 < \mathrm{Re} < 3.25 \times 10^5$.

For reference and convenience, the kinematic viscosity of water at 10°C is $\nu = 1.307 \times 10^{-6}$ m^2/s.

9.4 FORCED FLOWS

As discussed in Section 2.9 if the flow is driven by a pump the energy equation applies where

$$\frac{1-F}{\lambda\sqrt{1+s^{-2}}}$$

or

$$\frac{s(1-F)}{\lambda} \quad \text{for} \quad s \ll 1$$

is replaced by

$$\frac{z_1(1-F_{mod})}{L} = \frac{z_1}{L} - \frac{p_2 - p_1}{\rho g L}$$

Thus, the appropriate equations and graphs in Section 9.3 will apply to pump- or blower-driven flows by simply making this replacement. To ensure accuracy, the restriction of $4000 < \text{Re} < 3.25 \times 10^5$ still applies.

B.9.1 Example: Blasius Formula Approximation to Friction Factor for Gravity-Driven Flow

Consider a gravity-driven single-pipe network that is required to flow 1.7 L/s. The mean slope between the source and delivery locations is 6.3% based on measurements taken by an Abney level (see Chapter 13 for a discussion of this instrument). The pipe length is unknown, but is estimated to be between straight from the source to delivery locations and 25% longer than this length. Using the results based on the Blasius formula approximation to the friction factor, calculate the minimum polyethylene (PE) English-based pipe size required for this flow. The rated pressure for the recommended pipe should be no less than 160 psig. Assume the delivery pressure is such that $F = h_{del}/z_1 = 0.15$ and that minor losses are small. Verify that your answer is accurate.

PE pipe is smooth, so that we can use Eqn (9.10) to calculate the actual diameter. Then, the appropriate table in Chapter 3 can be inspected to recommend a PE nominal pipe size. Equation (9.10) becomes with $\lambda = 1.25$ and $\nu = 13.07 \times 10^{-7}$ m^2/s,

$$\begin{aligned} D &= 0.741\left[\frac{0.063 \cdot (1-0.15)}{1.25}\right]^{-4/19} \\ &\cdot \left[\frac{(13.07 \times 10^{-7}\ \text{m}^2/\text{s})^{1/7} \cdot 1.7 \times 10^{-3}\ \text{m}^3/\text{s}}{(9.807\ \text{m/s}^2)^{4/7}}\right]^{7/19} \\ D &= 0.741 \cdot 1.941 \cdot 0.0289\ \text{m} \\ D &= 0.0416\ \text{m} = 1.638\ \text{in.} \end{aligned}$$

For $\lambda = 1$, this result becomes $D = 1.563$ in.

Example: Blasius Formula Approximation (Cont'd)

From Table 3.6 for PE pipe, for a rated pressure of 160 psig and D between 1.64 and 1.56 in., we recommend 2-in. nominal pipe with a standard diameter ratio (SDR) of 11 (ID of 1.917 in.). If a pipe in the IPS system is chosen, a consult with Tables 3.2 and 3.3 shows that a sch. 80, 2-in. pipe is needed (ID of 1.939 in.).

From Eqn (9.11), Re for this flow is

$$\begin{aligned} \mathrm{Re} &= 1.718\left[\frac{(1.7\times10^{-3}\ \mathrm{m^3/s})^3\cdot 9.807\ \mathrm{m/s^2}\cdot 0.063\ (1-0.15)}{1.25\cdot(13.07\times10^{-7}\ \mathrm{m^2/s})^5}\right]^{4/19} \\ \mathrm{Re} &= 39{,}805 \end{aligned}$$

This is a turbulent flow and Re> 4000. Therefore the equations in this section are valid and the results are judged to be accurate. Additional confidence in the solution is obtained by a quick comparison with Fig. 5.9 for IPS polyvinyl chloride pipe (PVC) for $\lambda = 1.5$ and $F = 0.1$ which gives D between $1\frac{1}{2}$ and 2 in. nominal. This finding is in agreement with the above solution.

9.5 SUMMARY

As analysts and designers, the use of *nonhomogeneous* formulas should be approached with some caution. This includes formulas, as well as computer programs, that are always nonhomogeneous.[12] Nonhomogeneous implies that there are one or more simplifications incorporated, such as the substitution of a fixed number for an algebraic symbol of a quantity that is dimensional. This may result in the formula's inappropriate use. For pipe-flow calculations, there is no good reason to use nonhomogeneous formulas like the Hazen–Williams type because the Darcy–Weisbach equation and the friction factor are well established and documented, and have virtually no restrictions on their use.[13]

In this chapter, a set of formulas to estimate D for prescribed values of s, F, λ, and Q to within possible acceptable levels of accuracy were produced. The summary forms of this result appear in Eqs (9.7)–(9.10) and Figs. 9.3–9.4. Two dimensionless groups appear in these formulas. The first is a combination of s, F, and λ is the hydraulic gradient or "modified slope" $(s(1-F)/\lambda)$. The other group is a dimensionless volume flow rate made up of the dimensional terms Q, g, ν, and D. For example, for a

[12] Mathcad and EES are exceptions to this.

[13] The Darcy–Weisbach equation and the friction factor apply not only to the steady-state pipe flows of incompressible fluids considered in this text but, almost without exception, in all cases including transient and compressible flows (high-speed gas flows), and flows having variable viscosity. The only restrictive assumptions on the use of the friction factor is that the flow must be a continuum (no rarified gas flows) and the fluid must be Newtonian. A Newtonian fluid is discussed in Chapter 1. Clearly, these two conditions place no restrictions at all in the context of water flow in pipes.

hydraulic gradient > 0.001, D from the approximate form of the energy equation for pipe flow is to within ~10% of the exact value. The assumptions that must be satisfied for the successful use of these formulas are minor-lossless, turbulent flow ($4000 < \text{Re} < 3.25 \times 10^5$), $s < 0.5$, and smooth pipe. The recent correlations from Swamee and Sharma (2008) appear to be adequate substitutions for the Mathcad worksheets from Chapter 5 for minor-lossless flow in a single-pipe network. However, it is important we note that the worksheets can include minor losses where they are critical such as a partially closed globe valve needed for flow control.

Finally, one of the substantive learning outcomes from this chapter is the importance of calculating Re for all designs. Recall that Re characterizes the flow, so that the value of Re tells the designer about the nature of the flow occurring in the design.

Consistent with the developments in Section 2.9, the energy equation for pipe flow based on the approximate friction factor that was solved to produce the simplified set of formulas to estimate D, could also be applied to cases where there is forced, instead of gravity-driven, flow. The only difference is the representation of the hydraulic gradient term as discussed in Section 9.4.

B.9.2 Example: Blasius Formula Approximation to Friction Factor for Forced Flow

Consider a pressure-driven single-pipe network where water at 10°C is to be pumped upward a distance of 67 m through a 3-in. nominal sch. 40 PVC pipe. The discharge pressure is 225 psig, and pressure at the delivery location is 7 m of head. Calculate the volume flow rate, Q, delivered by this single-pipe network if the length of the pipeline is 1280 m. Neglect minor losses.

PVC pipe is smooth, so that Eqn (9.7) can be used to calculate Q. As directed in Section 9.4, the term

$$\frac{s(1-F)}{\lambda}$$

in this equation is replaced by

$$\frac{z_1(1-F_{mod})}{L} = \frac{z_1}{L} - \frac{p_2 - p_1}{\rho g L} \equiv S$$

to accommodate forced flow. Rearranging Eqn (9.7) as if solving for Q, we get

$$Q = 2.25 \frac{g^{4/7} D^{19/7}}{\nu^{1/7}} \left(\frac{z_1}{L} - \frac{p_2 - p_1}{\rho g L}\right)^{4/7}$$

Blasius Formula Approximation for Forced Flow (Cont'd)

With $\nu = 13.07 \times 10^{-7}$ m^2/s, $p_2 = \rho g h_{del} = 1000$ kg/m$^3 \cdot 9.807$ m/s$^2 \cdot 7$ m $= 6.865 \times 10^4$ Pa (recognize that 1 kg·m/s^2 = 1 N and 1 Pa = 1 N/m^2), $p_1 = 225$ psig $= 1.551 \times 10^6$ Pa, $z_1 = -67$ m, and D= 3.068 in = 0.0779 m, Eqn (9.7) becomes

$$Q = 2.25 \frac{(9.807 \text{ m/s}^2)^{4/7} \cdot (0.0779 \text{ m})^{19/7}}{(13.07 \times 10^{-7} \text{ m}^2/\text{s})^{1/7}} \cdot \left(\frac{-67 \text{ m}}{1280 \text{ m}} - \frac{6.865 \times 10^4 \text{ Pa} - 1.551 \times 10^6 \text{ Pa}}{1000 \text{ kg/m}^3 \cdot 9.807 \text{ m/s}^2 \cdot 1280 \text{ m}}\right)^{4/7}$$

$$Q = 2.25 \cdot 0.02505 \text{ m}^3/\text{s} \cdot (0.06577)^{4/7} = 2.25 \cdot 0.02505 \text{ m}^3/\text{s} \cdot 0.2112$$

$$Q = 11.92 \text{ L/s}$$

This result can be checked by using Fig. 5.30. In this problem, $S = 0.06577 \approx 0.066$ and for nominal 3-in. PVC pipe, we obtain $Q \approx 12$ L/s, in agreement with the above result. A quick calculation of Re [Eqn (9.11)] will show that this flow is turbulent. Therefore, the formulas from the above section are valid. It is also worthwhile to verify that the pressure rating of the PVC pipe is acceptable for the conditions stated in the problem. From Table 3.3, the rated pressure for sch. 40 3-in. PVC pipe is 260 psig. Thus, the pipe will withstand the 225-psig pump discharge pressure with a factor of safety of $(260 - 225)/260 = 0.135 = 13.5\%$.

References

F. A. Bombardelli and M. H. Garcia. Hydraulic design of large-diameter pipes. *J. Hydraulic Eng.*, 129(11):839–846, 2003.

B. A. Christensen. Discussion on 'Limitations and proper use of the Hazen-Williams equation'. *J. Hydraulic Eng.*, 126(2):167–168, 2000.

C. F. Colebrook. Turbulent flow in pipes. *Proc. Inst. Civil Eng.*, 11:133–156, 1938.

C. F. Colebrook. Turbulent flow in pipes with particular reference to the transition region between the smooth and rough pipe laws. *Proc. Inst. Civil Eng.*, 12:393–422, 1939.

C. F. Colebrook and C. M. White. Experiments with fluid-friction in roughened pipes. *Proc. Roy. Soc. (London)*, 161:367–381, 1937.

The Copper Development Association. The Copper Handbook. `http://www.copper.org`, 2006.

G. Corcos. Air in water pipes, a manual for designers of spring-supplied gravity-driven drinking water rural delivery systems. Technical report, Agua Para La Vida, Berkeley, CA, 2004.

C. P. L. Liou. Limitations and proper use of the Hazen–Williams equation. *J. Hydraulic Eng.*, 124(9):951–954, 1998.

F. A. Locher. Discussion on 'Limitations and proper use of the Hazen–Williams equation'. *J. Hydraulic Eng.*, 126(2):168–169, 2000.

B. R. Munson, D. F. Young, and T. H. Okiishi. *Fundamentals of Fluid Mechanics*. John Wiley & Sons, Inc., New York, NY, 2nd edition, 1994.

J. Nikuradse. Laws of flow in rough pipes. Technical Report NACA Tech. Mem. 62, NACA, Washington, DC, 1950. From German, 1933.

M. C. Potter and D. C. Wiggert. *Mechanics of Fluids*. Brooks/Cole (Thomson), Tampa, FL, 2002.

H. Rouse. Evaluation of boundary roughness. Technical report, Iowa Institute of Hydraulics Research, University of Iowa, Iowa City, IA, 1943.

H. Rouse. Hydraulics in the United States, 1776-1976. Technical report, Iowa Institute of Hydraulics Research, University of Iowa, Iowa City, IA, 1975.

P. K. Swamee. Discussion of 'Limitations and proper use of the Hazen-Williams equation'. *J. Hydraulic Eng.*, 125(2):169–170, 2000.

P. K. Swamee and A. K. Jain. Explicit equations for pipe-flow problems. *J. Hydraulic Div., ASCE*, 102(5):657–664, 1976.

P. K. Swamee and A. K. Sharma. *Design of Water Supply Pipe Networks*. John Wiley & Sons, Inc., Hoboken, NJ, 2008.

The Crane Company. *Flow of Fluids Through Valves, Fittings, and Pipe*. New York, NY, 1970.

Q. B. Travis and L. W. Mays. Relationship between the Hazen-Williams and Colebrook-White roughness values. *J. Hydraulic Eng.*, 133(11):1270–1273, 2007.

N. Trifunovic. *Introduction to Urban Water Distribution*. Taylor & Francis, New York, NY, 2006.

T. von Karman. Mechanical similitude and turbulence. Proc. Third Inter. Cong. Appl. Mech. Part 1 (NACA Tech. Mem. 611), 1930.

G. S. Williams and A. Hazen. *Hydraulic Tables*. John Wiley & Sons, Inc., New York, NY, 1933.

CHAPTER 10

OPTIMIZATION

"You're an Engineer, Everything You Say is Abnormal."
– The Boss in the Comic Strip **Dilbert**, *by S. Adams, 2008*

10.1 FUNDAMENTALS

Optimization is an important part of any design process. Generally, the goal of a designer is to produce a design that has the best performance at the lowest possible total cost. Thus, with an optimized design, the design characteristics (geometry, heat and fluid flows, temperatures, materials, weight, volume, etc.) are not just acceptable, but are the best possible subject to constraints that are imposed on the design.

A word like "best" used in the above description implies an optimal ("maximal" or "minimal") value if we are able to cast all aspects of the design in quantitative terms. Not all aspects that affect a design are quantitative. We sometimes refer to nonquantitative aspects as "intangibles." Some soft-engineering topics such as those involved with safety, the law, environment, society, manufacturability, and sustainability among others, are sometimes intangible. In this regard, the relatively new field of *sustainability*, or sustainable engineering, has attempted to quantify aspects of production, manufacturing, design, and retirement of materials and products that

Gravity-Driven Water Flow in Networks. By Gerard F. Jones

were formerly difficult to do so. Even though intangibles are not able to be explicitly modeled, we nonetheless consider them in our selection of the final design. In this way, experience, engineering judgment, and good sense contribute to the selection of an optimal design.

In the optimization process, the designer considers not only the mathematical optimal cases, but also the sensitivity of the total cost to less-than-optimal ("off-optimal") designs and the relation of the design to the intangibles. In some cases, off-optimal designs may be given serious consideration if they produce a better design once the intangibles are considered.

The existence of an optimum for a design requires that there be a *competition between at least two different effects in the problem, both of which influence a common element, such as cost.* To illustrate this, consider as a simple example the optimization of a cylindrical water storage tank of fixed volume, V, the cost for which we are told is proportional to tank surface area, A. Thus, to minimize cost, we wish to minimize the surface area of the tank. The problem is to solve for the optimal tank radius and height that produce the smallest, or optimal, tank area, and thus cost.

Let the radius and height of the tank be r and $\hat{h}$, respectively. The volume of the tank is then written as

$$V = \pi r^2 \hat{h}$$

and the surface area of the tank is

$$A = 2\pi r^2 + 2\pi r \hat{h}$$

where the first term accounts for the surface area of the tank top and bottom, and the second term the tank side.

We wish to minimize A. To do this, we first write $\hat{h}$ in terms of V as

$$\hat{h} = \frac{V}{\pi r^2} \tag{10.1}$$

and, upon substitution into the expression for A, obtain

$$A = 2\pi r^2 + \frac{2V}{r} \tag{10.2}$$

where only one independent parameter, r, now appears.

Our inspection of Eqn (10.2) reveals that r affects the surface area of the tank in opposite ways for the tank top and bottom, and the tank sides. The first term on the right side of Eqn (10.2) indicates that the top and bottom surface area increases in proportion to r^2. The second term on the right side of Eqn (10.2) shows that the sidewall surface area is proportional to $1/r$ (recall that this is for a fixed tank volume where, from Eqn (10.1), $\hat{h}$ is proportional to $1/r^2$). Thus, we can see the competing effects on A from r; decreasing r produces a smaller value of A based on the first term in Eqn (10.2), but a larger value of A based on the second term in Eqn (10.2). The question to be answered is what is the value of r the produces the smallest valuc for A.

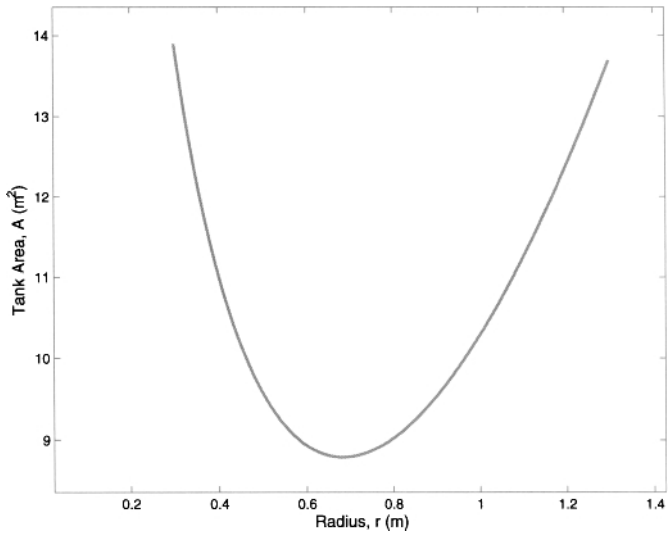

Figure 10.1 Optimal tank area as a function of tank radius. The radius that minimizes tank area is obtained by inspection. The value of r at this location is called r_{opt}. For $r < r_{opt}$, the area is dominated by the sidewall, for $r > r_{opt}$ the area is dominated by top and bottom.

One way to provide this answer is to make a plot of A versus r to locate the optimal point for A, A_{opt}, in a graphical manner (see Fig. 10.1). While acceptable for this simple example, this graphical method is time consuming and lacks generality that will be needed for more complex, realistic problems. We will explore two alternate methods for optimization in the sections below and obtain the solution for this example problem.

10.2 THE OPTIMAL FLUID NETWORK

There are at least two contexts in which we discuss optimization of fluid flow networks. The first refers to optimization of a *network of a specific type*, say a gravity-driven water system, where we size the components and carry out the design based on minimum cost, or another related outcome. The second context refers to the choice of the *most-desirable among several systems of different types*, such as a water supply from a gravity-driven system, an electrical pump system, and a dug-well system. Each of these systems may first be optimized within its own structure using the first context and then an appropriate choice made from among these optimized units. Both are important but, because the first is more fundamental than the second, we will focus on only the first context in this chapter. That is, once each system in a group is optimized subject to an over-arching set of constraints, it is a straightforward task to pick the most appropriate solution from among this group.

There are several instances that come to mind where there optimal conditions exist for a gravity-driven water network. By far, the most important from among these is the optimal static pressure head at a branching junction (where three or more pipes meet through which water is distributed). As will be discussed in Chapter 11, this arises from competition between upward and downward changes in pipe diameters at opposite sides of the branch with increasing head. Cost is proportional to pipe diameter, so this competition results in the existence of minimal cost, which yields optimal pipe diameters. Other instances may be considered from the following list.

1. In a network, where there is a water storage tank and a prescribed water flow rate, increasing the elevation of the tank to supply a larger elevation head of water will enable a reduction in the pipe diameter. In this case, there is added cost to elevate the tank and reduced cost due to the smaller pipe size. The competition here is evident. This problem is solved in Section 10.6.

2. In any network having multiple delivery points, increasing the number of delivery points, say, from one every 10 houses to one every 2 houses, will result in the need for smaller delivery pipe sizes, since each pipe will carry a smaller flow rate. The competition is between the larger number of pipes, on the one hand, and smaller diameter pipes on the other.

3. In systems where there are multiple sources, there is a choice between independent piping of small diameter from each source to a common water storage tank, and a much larger, single pipe that is manifolded near the sources. Note here that there is an embedded complication of a potential flow from one source to another, instead of to the tank (see Exercise 50).

4. In a single-pipe network with or without local peaks, should the pipe diameter change, and at what locations, to cause a gradual reduction in excess static pressure due to the elevation change? In addition to the cost of throttling valves, certain nontangibles will need to be considered in this problem including maximum acceptable pressure drop across a valve, vibration and noise in the network, and possible premature valve wear and leakage (see Exercise 35).

5. In a hybrid gravity-driven water and microhydroelectric power network, what is the optimal fraction of electrical power and what are the pipe sizes that satisfy this fraction? See Section 12.4.1 for more on this topic.

6. In a hybrid gravity-driven water and photovoltaic-powered pumped network, what is the optimal pumped fraction and what are the pipe sizes that satisfy this fraction?

Other examples can be given based on the reader's experience and creativity (see Exercise 33).

10.3 THE OBJECTIVE FUNCTION

Optimization is performed by first defining an objective function. The objective function is one that we choose to maximize or minimize[1] that contains all of the relevant information about the design. Designating the objective function as $\hat{F}$, we may write[2]

$$\hat{F}(\hat{x}_1, \hat{x}_2, \hat{x}_3, \ldots, \hat{x}_n) \rightarrow \text{Minimum or Maximum} \tag{10.3}$$

where $\hat{x}_1, \hat{x}_2, \hat{x}_3, \ldots, \hat{x}_n$ are the independent parameters in our design. For instance, $\hat{F}$ may be the total cost of the design that we wish to minimize, the surface area of a tank that we wish to minimize, or the heat transfer from the heating system that we wish to maximize. Since the objective function $\hat{F}$ is so often the total cost of a system, we often refer to the objective function as the "cost" function.

In nearly every real case, optimization is not without restrictions. We refer to the restrictions placed on the optimization of a design as "constraints." These arise from perhaps conservation principles (mass, momentum, energy, and charge conservation) or physical limitations in the problem, such as pressure, temperature, length, volume, or weight. Constraints are categorized as equality or inequality types. These are, respectively,

$$\hat{l}_i(\hat{x}_1, \hat{x}_2, \hat{x}_3, \ldots, \hat{x}_n) = 0 \tag{10.4}$$

and

$$\hat{g}_j(\hat{x}_1, \hat{x}_2, \hat{x}_3, \ldots, \hat{x}_n) \leq \hat{C}_j \tag{10.5}$$

where $\hat{C}_j$ is the largest allowable value for the inequality constraint $\hat{g}_j$. For example, an equality constraint placed on the above tank example is that the volume is fixed. There are no inequality constraints for the tank problem.

For the simple case of a design having an objective function, $\hat{F}$, that depends on a single parameter $\hat{x}$, an optimization is carried out by taking the first derivative of $\hat{F}$ with respect to $\hat{x}$. The optimal $\hat{x}$ (referred to as $\hat{x}_{opt}$) is obtained by equating this derivative to zero, and solving for the $\hat{x}_{opt}$ value. Thus

$$\frac{d\hat{F}}{d\hat{x}} = 0 \rightarrow \text{solve for } \hat{x} = \hat{x}_{opt} \tag{10.6}$$

This method falls into a class of methods referred to as Indirect and is illustrated in textbox B.10.2.

[1]Note that maximizing a function is equivalent to minimizing the negative of the function and vice versa.
[2]The appropriate symbols in this and the following sections in this chapter have been given hats to distinguish them from those used for different meanings elsewhere in this book.

B.10.1 Calculus I Refresher

It is worthwhile to recall from calculus that the point where a function is a maximum or minimum is an extreme point and has a zero slope (i.e., a zero first derivative). This is the reason for setting the first derivative to zero to obtain the location of this extreme point or "extremum." The reader may also recollect that if the second derivative of the function at the extremum is negative valued (a tendency for the value of the function to decrease with an increase in the value of $\hat{x}$ measured from the point of the extremum), then the extremum is a maximum. Otherwise, the extremum is a minimum.

B.10.2 Tank Example Completed

Consider the numerical solution for the above example of the water storage tank for which $V = 2\ \text{m}^3$. In Eqn (10.2), we differentiate A with respect to r and set the derivative equal to zero and solve to determine the optimum. Obtain

$$\frac{dA}{dr} = 4\pi r - \frac{2V}{r^2} = 0$$

Solving for $r = r^{opt}$ and then $\hat{h}^{opt}$ gives

$$r^{opt} = (\frac{V}{2\pi})^{1/3}, \qquad \hat{h}^{opt} = \frac{V}{\pi(r^{opt})^2} = (\frac{4V}{\pi})^{1/3}$$

and from Eqn (10.2),

$$A^{opt} = 3(2\pi)^{1/3}V^{2/3}$$

With $V = 2\ \text{m}^3$, get $r^{opt} = 0.683$ m, $\hat{h}^{opt} = 1.37$ m, and $A^{opt} = 8.79\ \text{m}^2$ in agreement with the results of Fig. 10.1. This area is the smallest possible value for a cylindrical tank of the given volume and, since we were told that cost is proportional to A, we have then found the smallest, and thus optimal, tank cost.

To assure that the minimum area has been found, we take the second derivative of A with respect to r to get

$$\frac{d^2A}{dr^2} = 4\pi + \frac{4V}{r^3}$$

The Tank Example (Cont'd)

which is always positive. Therefore, because the second derivative of A with respect to r is positive, the extremum found above is indeed a minimum. If the second derivative of A with respect to r is negative, the extremum found above is a maximum.

10.4 A GENERAL OPTIMIZATION METHOD

Several methods have been developed to obtain possible optimal solutions to mathematical functions. Among these are Lagrange Multipliers, Gradient Methods (including the Conjugate Gradient method), Search Methods, and Linear Programming. The commercial package `Matlab` has a variety of very powerful built-in functions for optimization that are contained in the basic package and in the Optimization Toolbox. This package is recommended for optimization of large, complex problems. The commercial package `Mathcad` also contains a small number of functions available for use in optimization problems one of which is the `Given ...Minimize` construct, as discussed below.

The method of Lagrange multipliers will be covered here. While the Indirect method, as described above, can be used for only the simplest of problems (e.g., the above tank example) where the design problem contains only a single independent parameter, the method of Lagrange Multipliers is among the most fundamental of methods for more than one independent parameter where the objective function and constraints may be nonlinear. The curious reader is encouraged to pursue the above methods presented in many references (Burmeister, 1998; Bejan et al., 1996; Jaluria, 1998) including several directed specifically at water-distribution networks (Swamee and Sharma, 2000, 2008).

10.4.1 Lagrange Multipliers

As discussed above, we wish to optimize the objective function

$$\hat{F}(\hat{x}_1, \hat{x}_2, \ldots, \hat{x}_n) \rightarrow \text{Optimum} \tag{10.7}$$

subject to the equality constraints

$$\begin{aligned} \hat{l}_1(\hat{x}_1, \hat{x}_2, \ldots, \hat{x}_n) &= 0 \\ \hat{l}_2(\hat{x}_1, \hat{x}_2, \ldots, \hat{x}_n) &= 0 \\ &\vdots \\ \hat{l}_m(\hat{x}_1, \hat{x}_2, \ldots, \hat{x}_n) &= 0 \end{aligned} \tag{10.8}$$

If there are inequality constraints, they may be converted to the equality type by using one or more "slack" variables. For example, the inequality constraint of Eqn (10.5)

may be written as an equality constraint by defining $\hat{s}_j^2$ as the difference between zero and $\hat{C}_j$. Thus Eqn (10.5) may be written as an equality constraint as

$$\hat{g}_j(\hat{x}_1, \hat{x}_2, \hat{x}_3, \ldots, \hat{x}_n) - \hat{C}_j + \hat{s}_j^2 = 0 \tag{10.9}$$

The term $\hat{s}_j$ is the unknown slack variable for the jth inequality constraint. The terms $\hat{s}_j$ for all of the inequality constraints are determined in the solution procedure as described below.

In the Lagrangian Multiplier method, we convert the discrete equations appearing in Eqs (10.7) and (10.8) into a single equation by adding the zeros of Eqn (10.8) to the objective function of Eqn (10.7). Obtain

$$\begin{aligned} \hat{Y}(\hat{x}_1, \hat{x}_2, \ldots, \hat{x}_n, \hat{\lambda}_1, \hat{\lambda}_2, \ldots, \hat{\lambda}_m) &= \hat{F}(\hat{x}_1, \hat{x}_2, \ldots, \hat{x}_n) \\ &+ \hat{\lambda}_1 \hat{l}_1(\hat{x}_1, \hat{x}_2, \ldots, \hat{x}_n) \\ &+ \hat{\lambda}_2 \hat{l}_2(\hat{x}_1, \hat{x}_2, \ldots, \hat{x}_n) \\ &+ \ldots + \hat{\lambda}_m \hat{l}_m(\hat{x}_1, \hat{x}_2, \cdots, \hat{x}_n) \end{aligned} \tag{10.10}$$

where the as-yet unknown terms $\hat{\lambda}_1, \hat{\lambda}_2, \ldots, \hat{\lambda}_m$ are referred to as Lagrange multipliers.

Following the above procedure, the optimal is obtained when the first derivative of $\hat{Y}$ with respect to all of the independent parameters is equal to zero. Thus,

$$\begin{aligned} &\frac{\partial \hat{Y}}{\partial \hat{x}_1} = 0, \quad \frac{\partial \hat{Y}}{\partial \hat{x}_2} = 0, \quad \ldots, \quad \frac{\partial \hat{Y}}{\partial \hat{x}_n} = 0 \\ &\frac{\partial \hat{Y}}{\partial \hat{\lambda}_1} = 0, \quad \frac{\partial \hat{Y}}{\partial \hat{\lambda}_2} = 0, \quad \ldots, \quad \frac{\partial \hat{Y}}{\partial \hat{\lambda}_m} = 0 \end{aligned} \tag{10.11}$$

or

$$\begin{aligned} &\frac{\partial \hat{F}}{\partial \hat{x}_1} + \hat{\lambda}_1 \frac{\partial \hat{l}_1}{\partial \hat{x}_1} + \hat{\lambda}_2 \frac{\partial \hat{l}_2}{\partial \hat{x}_1} + \cdots + \hat{\lambda}_m \frac{\partial \hat{l}_m}{\partial \hat{x}_1} = 0 \\ &\frac{\partial \hat{F}}{\partial \hat{x}_2} + \hat{\lambda}_1 \frac{\partial \hat{l}_1}{\partial \hat{x}_2} + \hat{\lambda}_2 \frac{\partial \hat{l}_2}{\partial \hat{x}_2} + \cdots + \hat{\lambda}_m \frac{\partial \hat{l}_m}{\partial \hat{x}_2} = 0 \\ &\qquad\qquad \vdots \\ &\frac{\partial \hat{F}}{\partial \hat{x}_n} + \hat{\lambda}_1 \frac{\partial \hat{l}_1}{\partial \hat{x}_n} + \hat{\lambda}_2 \frac{\partial \hat{l}_2}{\partial \hat{x}_n} + \cdots + \hat{\lambda}_m \frac{\partial \hat{l}_m}{\partial \hat{x}_n} = 0 \\ &\hat{l}_1(\hat{x}_1, \hat{x}_2, \ldots, \hat{x}_n) = 0 \\ &\hat{l}_2(\hat{x}_1, \hat{x}_2, \ldots, \hat{x}_n) = 0 \\ &\qquad\qquad \vdots \\ &\hat{l}_m(\hat{x}_1, \hat{x}_2, \ldots, \hat{x}_n) = 0 \end{aligned} \tag{10.12}$$

If $\hat{F}$ is continuous and differentiable, all derivatives in Eqn (10.12) are obtainable. Thus, Eqn (10.12) represents a system of $n + m$ algebraic equations that may be solved for the n values of the independent parameters $\hat{x}$ and the m values for the Lagrange multipliers $\hat{\lambda}$.

If the system of equations from Eqn (10.12) is linear, matrix inversion may be used in a straightforward manner to obtain the solutions for the optimal values for $\hat{x}_1, \hat{x}_2, \ldots, \hat{x}_n$ and the Lagrange multipliers $\hat{\lambda}_1, \hat{\lambda}_2, \ldots, \hat{\lambda}_m$. Otherwise, when the system of equations is nonlinear, successive substitution of one equation into another or a formal numerical method, such as Newton–Raphson (Gerald and Wheatley, 1999) or the `Given...Find` construct in `Mathcad` is used to obtain the solution.

B.10.3 A Nonfluid Example

Consider a shell-and-tube type of heat exchanger that perhaps you have seen in a large industrial plant. The purpose of this device is to transfer heat between a hot fluid stream and a cooler one, but this is the extent of involvement with fluids for this example. The exchanger length, L, and diameter, d, are to be selected such that the total cost for the exchanger is minimized. The cost function is

$$\hat{F}(L, d) = \$4450 + \$37.70/\mathrm{m}^{3.5} L d^{2.5} + \$28.60/\mathrm{m}^2 L d \qquad (10.13)$$

where $\hat{F}$ is in dollars, and d and L are in meters. The terms in Eqn (10.13) account for tube cost, shell cost, and floor space cost, respectively. The overall volume of the exchanger is fixed at $V = 15\ \mathrm{m}^3$.

The single equality constraint is the fixed volume,

$$\hat{l}(L, d) = \frac{\pi}{4} d^2 L - V = 0$$

We will use Lagrange multipliers to solve this problem. Equation (10.10) becomes,

$$\hat{Y}(L, d) = \hat{F}(L, d) + \hat{\lambda}\hat{l}(L, d)$$

where $\hat{\lambda}$ is the single Lagrange multiplier. Equation (10.12) becomes for this example,

$$\frac{\partial \hat{Y}}{\partial L} = 0 + \$37.70/\mathrm{m}^{3.5} d^{2.5} + \$28.60/\mathrm{m}^2 d + \hat{\lambda}\frac{\pi}{4} d^2 = 0 \qquad (10.14)$$

and,

$$\frac{\partial \hat{Y}}{\partial d} = 0 + \$94.25/\mathrm{m}^{3.5} L d^{1.5} + \$28.60/\mathrm{m}^2 L + \hat{\lambda}\frac{\pi}{2} L d = 0 \qquad (10.15)$$

A Nonfluid Example (Cont'd)

To solve these two equations simultaneously, eliminate $\hat{\lambda}$ between Eqs (10.14) and (10.15) to get

$$\$18.85/\mathrm{m}^{3.5} L d^{2.5} - \$28.60/\mathrm{m}^2 L d = 0$$

or $d^{1.5} = (\$28.6/\mathrm{m}^2)/(\$18.85/\mathrm{m}^{3.5})$. From this, we obtain $d = d^{opt} = 1.32$ m and from Eqn (10.4.1), $L = L^{opt} = 10.96$ m. The optimal total cost is then $\hat{F}^{opt} = \hat{F}(L^{opt}, d^{opt}) = \$5691$.

Next, the second derivatives of $\hat{F}$ with respect to d and L individually, and the mixed second partial derivative of $\hat{F}$ with respect to d and L need to be evaluated to verify that a minimum for $\hat{F}$ has been found. This is left as an exercise for the student.

As a final note, there are many problems for which no optimal solutions exist. For example, consider a heat-conducting metal fin, like those seen on the engine of a motorcycle, that transfers heat to a fluid moving next to it. For a motorcycle, the fluid is air passing across the hot engine. The heat transfer rate at the base of the fin increases monotonically with the fin length such that there is no optimal fin length in an unconstrained situation. Constraints on the other dimensions of the fin, flow rate of fluid, or the weight or volume of fin may produce an optimal fin length. Therefore, when the above algorithms or optimizing functions in `Matlab` or `Mathcad` produce suspicious, obviously incorrect optimal values, then perhaps no optima exist. In any event, a thorough inspection of the equations for the system will reveal this behavior without any numerical computations.

10.5 OPTIMIZATION USING MATHCAD

Let us reconsider textbox B.10.3 example and propose to solve it in `Mathcad`. We will use the `Given...Minimize` block. This is similar to the `Given...Find` block that we have already seen, except that it seeks to minimize a function of one or more variables and returns the (optimal) values of the variables once the minimal value for the function has been found. With this construct we need to define the function that we wish to minimizc and provide initial guesses for the unknowns. The constraints, if any, are placed inside of the `Given...Minimize` block. For this example, there is a single constraint of fixed volume, V. `Mathcad` does the rest.

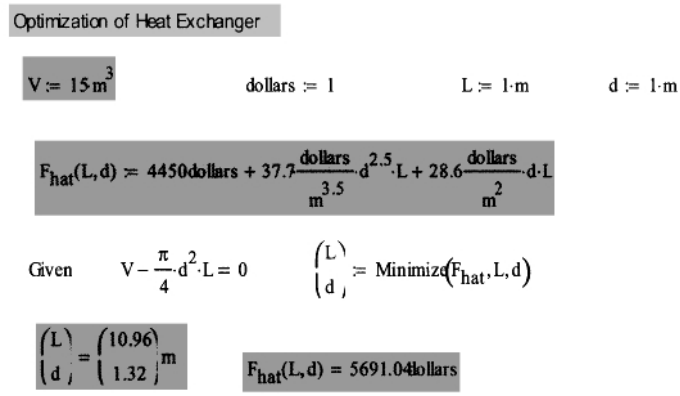

Figure 10.2 Mathcad worksheet for optimization of a heat exchanger.

The worksheet for this solution is shown in Fig. 10.2. The solution is reported in a column vector[3] and the values for d and L are identical to that in textbox B.10.3. Note that solution is compact, units are used, and it appears as it would if on paper. This construct will be used extensively for larger optimization problems in Chapter 11.

10.6 OPTIMIZING A GRAVITY-DRIVEN WATER NETWORK

10.6.1 The Problem and Cost Optimization

For some locations where there is a supply and demand for a relatively large flow rate of water, but not much elevation to drive the flow, and where the length of this single-pipe network is large, it may be cost effective to build an elevated water storage tank to produce additional elevation head. The schematic of Fig. 10.3 focuses on this situation. The flow rate is Q and the length of pipe and elevation head between the base of the tank and the delivery location are L and Δz_0, respectively. The elevation of the tank measured from its base is Δz_t.

The competition in this problem is as follows. The cost of the network includes pipe cost, typically proportional to the pipe diameter D, and the cost of the tank and structure to support it. The latter cost is composed of two terms. The first is the fixed cost of the tank (we assume the volume of the tank is fixed based on water demand) and a cost for the structure that is proportional to its height. With no tank (low elevation head) the pipe diameter will need to be large to reduce the effect of friction. In this limit, pipe cost dominates the problem. At the other extreme, where there is the tank and structure, the resulting higher elevation head will reduce the required pipe diameter and thus cost, but at the added expense of tank and structure. The question

[3]The unit of both d and L is identical, so this is not a problem. If the units of two or more dependent variables are not the same, the `Given...Minimize` block must solve as if the results are dimensionless. To do this, just divide by the unit of each term in the `Minimize` statement.

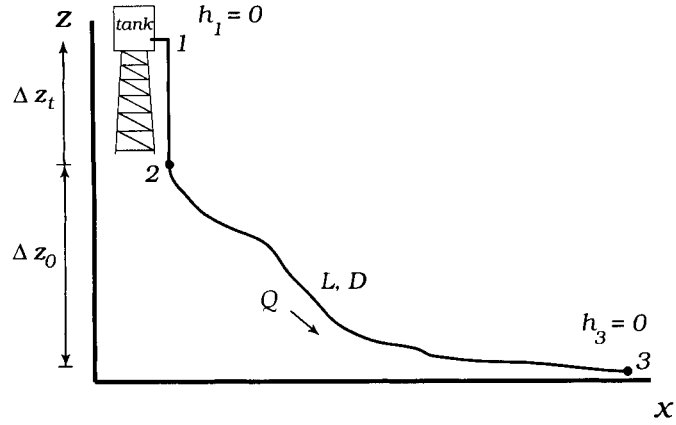

Figure 10.3 Geometry for optimization of low-head network with constructed tank.

posed is "what is the optimal height of the tank, Δz_t^{opt}, that minimizes total pipe and tank/structure cost?" After this answer is obtained, we can then calculate the optimal pipe diameter, D^{opt}, and optimal network cost, C_T^{opt}.

For the case where there is an elevated tank, water is supplied to it from the source by a small pump (not shown in Fig. 10.3), perhaps powered by photovoltaic cells. The pump is large enough to raise the water from the source to the tank, but not large enough to supply the water to the communities. It would be too large and costly to do this. It would also need to run nearly continuously to provide static pressure to the network, which would perhaps increase operating costs for electrical power.

We begin by recognizing that the pipe diameter is obtained from the solution of the energy equation, as we have seen in many problems is the past. Equation (2.23) is combined with Eqn (2.7) to eliminate $\overline{u}$ in favor of flow rate Q, to get

$$\Delta z_0 + \Delta z_t + \Delta h = \{K + \alpha + f(Q, D)[\frac{L + \Delta z_t}{D} + \frac{L_e}{D}]\}\frac{8Q^2}{\pi^2 g D^4} \qquad (10.16)$$

where $\Delta h = h_1 - h_3 = (p_1 - p_3)/\rho g = 0$, since both the tank and delivery location are at atmospheric pressure. The two minor losses embodied by K and L_e/D are included in the energy equation, as well as α to account for flow acceleration from the quiescent water in the tank to flow speed $\overline{u}$ in the pipe. The total length of the pipe is $L + \Delta z_t$ and the total elevation head is $\Delta z_0 + \Delta z_t$. Note that the continuity equation is identically satisfied for this problem.

The data that apply here are $Q = 2.5$ L/s, $L = 2000$ m, $\Delta z_0 = 4$ m, $K = 20$, and $L_e/D = 60$. The flow rate and pipe length are both relatively large, and the elevation head, Δz_0, is small.

The total cost for the network is written as

$$C_T = \$1.067(\frac{D}{D_u})^{1.4}(L + \Delta z_t) + \$1200 + \$120/\text{m}^{1.2}\Delta z_t^{1.2} \qquad (10.17)$$

where the first term on right side accounts for pipe cost, the second term for the tank and base cost of pump and structure, and the third for the height dependence of structure and pump. The coefficients and exponents are approximate and based on 2007 data from central Nicaragua.

The competition that was described above is made clear by our inspection of Eqn (10.17). The energy equation gives the solution that D is inversely proportional to Δz_t. Knowing that $L \gg \Delta z_t$, in the limit of small Δz_t, Eqn (10.17) shows that the pipe cost dominates the total cost, and for large Δz_t the tank and structure costs dominate.

10.6.2 Mathcad Worksheet

The solution is carried out in `Mathcad` and the worksheet appears in Fig. 10.4. A description of this worksheet is supplied here.

- The basics:
  - Definition of water properties of density, ρ, and viscosity, ν.
  - A convergence tolerance, `TOL`, used in `Mathcad` to determine when a root-finding algorithm has found the root to sufficient accuracy.
  - Definition of Reynolds number (Re) as a function of Q and D, and α as a function of Re.
  - Definition of the absolute roughness of the pipe wall.
  - The friction factor function as defined by Eqs (2.16) and (2.17).
  - Cost data for the pipe as a function of nominal pipe size, and for pump, tank, and structure.
- The solution:
  - Initial guesses for the values of D (diameters ranging from 0.2 in. to 4 in. are good guesses for nearly all problems considered in this book).
  - Values for the input parameters for each leg in the network, including L, Q, the appropriate minor loss coefficients, and elevation changes.
  - Definition of the energy equation for the network. This is given a symbol r and the needed functional dependence.
  - A formula for the total pipe material cost, T_{cost}.
  - The solution of the energy equation to get D as a function of Δz_t using the `Given...Find` construct and definition of the cost function, T_c, which depends on just Δz_t.
  - Plots of the results to investigate the existence of an optimum.
  - Optimization using the `Given...Minimize` construct and the solution for Δz_t^{opt}, D^{opt}, and optimal cost. A constraint on the maximum height of the tank of $\Delta z_t < 25$ m was used to prevent the structure from being unrealistically too high (a different, more nonlinear, cost model would need to be included for very tall structures).

Optimization - tank height vs. pipe diameter ORIGIN := 1

Water properties $\rho := 1000\frac{kg}{m^3}$ $v := 13.07\cdot10^{-7}\frac{m^2}{sec}$ sec := 1·s TOL := $1\cdot10^{-3}$

$\alpha(R) := if(R < 2100, 2, 1.05)$ dollars := 1

$Re(Q,D) := \frac{4\cdot Q}{\pi\cdot D\cdot v}$ $\varepsilon := 5\cdot10^{-6}\cdot ft$ absolute roughness, ft (increase 100 times for galvanized steel)

friction factor that spans the laminar/turbulent range. ebyD is relative roughness.

$$funct(f,R,ebyD) := \frac{f}{2} - \left[\left(\frac{4}{R\cdot\sqrt{\frac{f}{8}}}\right)^{24} + \left[\left(\frac{18765}{R\cdot\sqrt{\frac{f}{8}}}\right)^{8} + \left[3.29 - \frac{227}{R\cdot\sqrt{\frac{f}{8}}} + \left(\frac{50}{R\cdot\sqrt{\frac{f}{8}}}\right)^{2} \ldots + \frac{1}{0.436}\cdot\ln\left(\frac{R\cdot\sqrt{\frac{f}{8}}}{1 + 0.301\cdot R\cdot\sqrt{\frac{f}{8}}\cdot ebyD\cdot 2}\right)\right]^{16}\right]^{-\frac{3}{2}}\right]^{\frac{1}{12}}$$

fric_fac(Re, ebyD) := root(funct(f1, Re, ebyD), f1, 0.0001, 0.2)·4 friction factor

D := 3·in guess

Input Parameters: L := 2000m Q := 2.5$\frac{liter}{sec}$ K := 20 L_{ebyD} := 2·30 Δz_0 := 4·m

Define energy equation function:

$$r(\Delta z_t, Q, D, K) := (\Delta z_0 + \Delta z_t) - \left[K + \alpha(Re(Q,D)) + fric\_fac\left(Re(Q,D), \frac{\varepsilon}{D_j}\right)\left(\frac{L + \Delta z_t}{D} + L_{ebyD}\right)\right]\frac{8\cdot Q^2}{\pi^2\cdot g\cdot D^4}$$

Costs: b := 1.4

a := 1.067$\frac{dollars}{m}$ D_u := 1·in $C(D,L) := a\cdot\left(\frac{D}{D_u}\right)^b\cdot L$ c := 1200dollars d := 120$\frac{dollars}{m^{1.2}}$

$Tcost(D,\Delta z_t) := C(D, L + \Delta z_t) + c + d\cdot\Delta z_t^{1.2}$: total cost Tcost(2·in, 20·m) = 11257.32dollars : check

Solve for D vs. Δz.t in Given...Find block

Given $0 = r(\Delta z_t, Q, D, K)$ $D_p(\Delta z_t) := Find(D)$ $T_c(\Delta z_t) := Tcost(D_p(\Delta z_t), \Delta z_t)$

$\Delta z_t := 0\cdot m, 0.15m .. 25\cdot m$

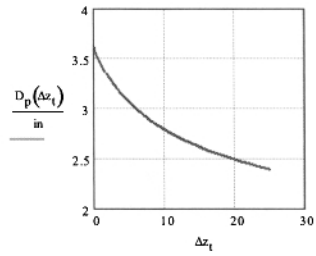

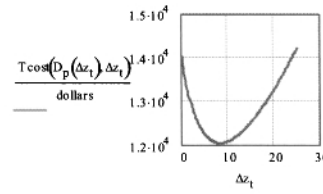

Δz_t := 5·m guess Given $\Delta z_t < 25\cdot m$ Δz_t := Minimize(T_c, Δz_t)

Δz_t = 8.23m $T_c(\Delta z_t)$ = 12041.06dollars $D_p(\Delta z_t)$ = 2.86in

Figure 10.4 Mathcad worksheet for optimization of low-head network with constructed tank.

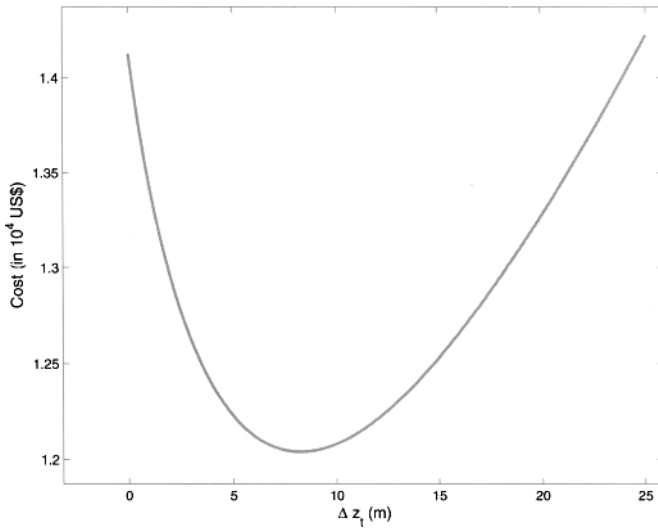

Figure 10.5 Cost versus tank height for optimization of low-head network with constructed tank.

10.6.3 Results

A plot of the total network cost as a function of Δz_t is shown in Fig. 10.5. The optimal point of $\Delta z_t^{opt} = 8.23$ m is clearly identifiable on this graph. The solution from the Mathcad worksheet gives $D^{opt} = 2.86$ in, and optimal network cost of \$12,041. From data in Chapter 3, we would select a nominal 3-in., sch. 40 IPS PVC pipe for this design. The inside diameter of this pipe is 3.068 in. Because this is larger than the theoretical diameter of 2.86 in., we would include in the design a throttling, or globe, valve to effectively reduce the pipe diameter and satisfy the design flow rate of 2.5 L/s. Otherwise, the flow rate will exceed that specified in the design. To allow for the possibility of more flow in the future, the valve opening is simply increased. This part of the design would be carried in what we refer to as the "reverse solution", which will be described in Chapter 11.

Finally, a further inspection of Fig. 10.5 reveals that halving or doubling the optimal value for Δz_t will add ~\$500 to the total network cost. This result gives the designer a "feel" for the degree of sensitivity of the design to off-optimal conditions.

10.7 MINIMIZING ENTROPY GENERATION

Minimizing network cost is one way, and given the importance of economy in engineering designs perhaps the most meaningful way, of optimizing the water-flow network. It is not the only one, however. The thermodynamic property entropy provides us with an alternate approach for this optimization. Entropy, in some contexts discussed as a measure of disorder in a system or component, is used in the classical

second law of thermodynamics to model the behavior of a system or component. In particular, the entropy increase in a real process[4] is always positive when the *total effects* of the process (that is, within the process itself and the influence of the process on its surroundings) are considered. Thus, we often seek to minimize the rate of entropy generation, $\dot{S}^{gen}$, in a process and, by doing so, guarantee the smallest possible extent of irreversibilities, or inefficiencies, associated with the process (Poulikakos and Bejan, 1982; Bejan, 1996). Many publications on entropy and the associated topics of second law, availability, and exergy analyses have appeared in the past couple of decades. In recent years, the popular concept of sustainability[5] has been formalized and frameworks for the life-cycle or sustainable analysis have been proposed and exercised. Entropy is a potentially very useful tool in sustainability analysis

The rate of entropy generation for adiabatic[6] flow in a pipe is,

$$\dot{S}^{gen} = \frac{\rho g Q(\Delta z + \Delta h)}{T_{in} + g(\Delta z + \Delta h)/2c_v} \tag{10.18}$$

where c_v is the specific heat for water (~4190 J/kg·K). $\Delta z + \Delta h$ is the head loss due to friction in the flow. The denominator in Eqn (10.18) is the absolute mean temperature of the water along the pipe flow path, where T_{in} is the water temperature at the pipe inlet.

Equation (10.18) may be used to solve for unknowns in the pipe-flow problem. For example, if the entropy generation for the tank and support structure, S^{gen}_{tank}, for the above example were known, this information could be combined with Eqn (10.18) to get an expression for the total entropy change as,

$$S^{gen}_T = S^{gen}_{tank} + \int_0^t \dot{S}^{gen}\, dt = S^{gen}_{tank} + \frac{\rho g V(\Delta z + \Delta h)}{T_{in} + g(\Delta z + \Delta h)/2c_v} \tag{10.19}$$

where V is the volume of water in the pipe. The static pressure head at the base of the tank, h_2, is unknown and can be solved for by taking the derivative of Eqn (10.19) with respect to Δh, setting this result equal to zero as done in the above examples, and solving for Δh to get h_2.

In Chapter11, we will have the need to also solve for the unknown static pressure heads at the junctions of a multiple-pipe network. Taking the derivative of Eqn (10.18) with respect to Δh and setting it equal to zero will give us an equation for this unknown. Obtain

$$0 = \frac{c_v^2 T_{in} g \rho Q}{[2c_v T_{in} + g(\Delta z + \Delta h)]^2} \tag{10.20}$$

Entropy minimization is included here mostly in the interest of completeness. Cost minimization will almost certainly be considered more important than issues of sustainability in developing regions so it is very unlikely that the equations from

[4]As opposed to one that has been idealized to obtain a limiting- or bounding-case result.

[5]Sustainability has been defined as that which "meets the needs of the present without compromising the ability of future generations to meet their own needs" (Anon., 1987).

[6]No heat transfer between the flow and its surroundings.

this section will be used in a design in this context. However, the readers should be aware of the existence of a physical law like mass and momentum conservation (i.e., the second law of thermodynamics, not economics, that can be used to determine unknown quantities like static pressure heads at junctions in multiple-pipe networks).

10.8 SUMMARY

Briefly, in this chapter we saw the importance and relevance of optimization in the analysis and design of gravity-driven water networks. The concept is very basic and we now recognize that an optimal solution may exist for problems where there is a competition of effects, as described above. A corollary to this competition is that we should be able to identify at least two limiting-cases for each optimization problem. For example, for the last problem these are zero height of the tank, where all cost is associated with only the pipe, and an infinite height of the tank, where only the tank/support cost enters the problem. It is useful to look for these limiting cases when trying to determine if a problem has an optimal solution. The Lagrange multiplier method is important and powerful for this application and we will use it again in Chapter 11. We also saw the relative simplicity of obtaining optimal solutions using the `Given...Find` and `Given...Minimize` constructs in `Mathcad`. These will also appear frequently when we consider multiple-pipe networks, where numerical solutions are nearly always required.

References

Anon. Report of the World Commission on Environment and Development: Our Common Future. `http://www.un-documents.net/wced-ocf.htm`, 1987.

A. Bejan. *Entropy Generation Minimization.* CRC, Boca Raton, FL, 1996.

A. Bejan, G. Tsatsaronis, and M. Moran. *Thermal Design and Optimization.* John Wiley & Sons, Inc., New York, NY, 1996.

L. Burmeister. *Elements of Thermal-Fluid System Design.* Prentice Hall, New York, NY, 1998.

C. F. Gerald and P. O. Wheatley. *Applied Numerical Analysis.* Addison Wesley, New York, NY, 5th edition, 1999.

Y. Jaluria. *Design and Optimization of Thermal Systems.* McGraw-Hill, New York, NY, 1998.

D. Poulikakos and A. Bejan. Fin geometry for minimum entropy generation in forced convection. *ASME J. Heat Transfer*, 104:616–623, 1982.

P. K. Swamee and A. K. Sharma. Gravity flow water distribution network design. *J. Water Supply: Res. and Technol.-AQUA*, 49(4):169–179, 2000.

P. K. Swamee and A. K. Sharma. *Design of Water Supply Pipe Networks.* John Wiley & Sons, Inc., Hoboken, NJ, 2008.

The author with Al Ortega (holding the rod) and
Jordan Ermilio (at right) and an assistant surveying in Nicaragua.

CHAPTER 11

MULTIPLE-PIPE NETWORKS

"... Learn as if you will Live Forever."
– M. Gandhi

11.1 INTRODUCTION

Thus far, we have focused on two levels of analysis and design for a single-pipe network. The first level considered the performance of a network based on *overall characteristics* (i.e., the mean slope, site geometry, and inlet and outlet states). This gave rise to a relatively simple form of the energy equation for pipe flow, Eqn (2.40) or (2.41), that linked the fluid flow rate, pipe diameter, site geometry, and static pressure at the delivery location. The second level addressed the *distribution of properties*, namely the static pressure distribution, in the flow and produced a different form of the energy equation, Eqn (6.12). The former equation is very convenient for calculating the pipe size needed for a required volume flow rate and given site geometry and delivery pressure. In Chapter 6, we saw that assessing the solution of the latter equation is crucial to assure the integrity of a design; a requirement to achieve a minimum static pressure at each and every point along the flow path in a network having local peaks. The concept of "Natural flow" in a pipe explored in Section 2.6.3

Gravity-Driven Water Flow in Networks. By Gerard F. Jones

and a new companion concept of the "Natural diameter" for a pipe in Chapter 6 were outgrowths of these two levels of analysis.

As we saw with the examples in Chapter 8, single-pipe networks are important in a gravity-driven water supply. For instance, a single pipe (a "gravity main") is used to supply water from a single source to a storage or break-pressure tank and another single pipe may be used to deliver water from the tank to a single tapstand in a community. However, a multiple-pipe network is always needed for water distribution to more than a tank or a single tapstand. Other needs would be branching flows from a "main" or "trunk" pipeline (a "distribution main") to branches of smaller-diameter distribution pipes, and networks where there are multiple water sources. Because the need for branching and single pipes of multiple diameters is so common, this substantial chapter is devoted to their study.

The developments in the above chapters may be extended to a network having more than a single pipe by making just a few changes and generalizations. We will solve energy equation for pipe flow, Eqn (2.44) (or its equivalent where minor losses are included), in a slightly modified form. The modification is very simple. In a single-pipe network, the static pressures at the end points of the network are $p_1 = 0$ (atmospheric pressure) at the source and a specified static pressure at the delivery location, p_2, which we wrote in dimensionless form, $F = p_2/\rho g z_1$. Given the geometry of the site, including mean slope s and tortuosity λ, the specification of F allowed us to solve Eqn (2.44) for D required to pass a specified volume flow rate of water, Q. The analysis was straightforward and the solutions were obtained either graphically (in Chapter 5) or by using a `Mathcad` worksheet, which allowed the inclusion of minor losses (Chapter 8). In the case of a multiple-pipe network, the static pressures at the locations where the multiple pipes are connected are not known. We must determine the values for the static pressures at these "junctions" (or internal "nodes") from other information or guidelines[1] and, using these values, evaluate D for each pipe by solving a *system* of (nonlinear) energy equations for the flow in multiple pipes in a simultaneous manner. The solution of simultaneous nonlinear algebraic equations was discussed in Section 4.4.1. It is important to note that the need to specify the junction pressures to be able to solve for D uniquely is entirely consistent with the developments in Chapter 6 where, to solve for the Natural diameter distribution in the network, we first prescribed a static pressure distribution. The resulting solution for D from the energy equation is, in fact, the definition of the Natural diameter.

[1]Other information could be the condition of minimum cost, the requirement of a suitably large static pressure at the junction to eliminate potential contamination of the clean water, or an acceptably low static pressure such that pressure limitations for the pipe and fittings are not exceeded.

11.2 BACKGROUND

11.2.1 Past Approaches to the Problem

The analysis and design of multiple-pipe networks forms the bulk of the few books and chapters of books written on the topic water distribution (Jeppson, 1976; Nayyar, 2002; Trifunovic, 2006; Swamee and Sharma, 2008). As opposed to the relatively simple representations of the solutions for single-pipe networks that we saw in Chapter 5, those for multiple-pipes will *always require a numerical solution* even for minor-lossless flow. The literature shows two different approaches to the problem. The first assumes values for all pipe diameters (D) and solves for volume flow rates (Q) and static pressure head values (h_j) at all junctions. The second assumes known values of Q and solves for D and h_j. Both approaches will be thoroughly considered in the sections that follow. Optimization is often employed such that network total cost is minimized. Linear programming, where optimization is performed with the energy equations in *linearized* form, is sometimes used [see Schrijver (1998)].

11.2.2 Pressure Head Recommendations

For pumped water flow networks, the hydraulic design requires a specification of a minimal static pressure in the distribution mains. These are ranges of values set by the communities or their legislators. In mountainous regions like parts of Austria, the standard for these pressures can be as large as 120 m, while in other locations like Rio de Janeiro are as small as 25 m (Trifunovic, 2006). A reasonable average range is ~40–60 m. In gravity-driven water networks, for all points beyond the source,[2] only static pressure can drive the flow once it has been converted from potential energy. Thus, static pressures may be considerably larger in these. For example, analysts and designers of these networks may encounter the need for static pressure heads nearing 100 m to satisfy the requirements of a design. Pipe materials and wall thicknesses, along with rated pressures for the different pipe candidates, need to be seriously considered, in addition to sound construction and operation practices. This includes the method of joining pipe including cementing for plastic pipe and threaded joints for galvanized iron (see Chapter 3). The need for break-pressure tanks, air vents, and vacuum-breakers in the network will also enter the design and, as discussed in Chapter 13, will be crucial for its successful operation.

11.3 OUR APPROACH

Consistent with the developments and terminology in Chapter 2, we will designate the unknown static pressure, p_1, at one end of the pipe (state 1) as $\hat{F}_1 = p_1/\rho g(z_1 - z_2) = h_1/(z_1 - z_2)$ and the one at the other end of the pipe (state 2) as $\hat{F}_2 = p_2/\rho g(z_1 - z_2) = h_2/(z_1 - z_2)$. Equation (2.44), the energy equation for minor-lossless flow in a pipe,

[2] A reservoir or reservoir tank at atmospheric pressure

becomes

$$\frac{1+\hat{F}_1-\hat{F}_2}{\lambda\sqrt{1+s^{-2}}}-\frac{8Q^2}{\pi^2 g}\frac{f(Q,D)}{D^5}=0 \tag{11.1}$$

where D and, in general, $\hat{F}_1$ and $\hat{F}_2$ are unknowns. It is understood that the heads h_1 and h_2 in the definitions for $\hat{F}$ are the static pressure heads at the pipe ends. The reader will note that Eqn (11.1) is consistent with Eqn (2.44) for a single-pipe (i.e., $\hat{F}_1 = 0$ if the static pressure at state 1 is atmospheric). Also, recall from Fig. 2.11 that $z_2 = 0$ for a single-pipe network. However, in the present situation where we have any number of pipes of any lengths, z_2 is not generally zero as it was for a single-pipe network. Because of this, the denominator of each $\hat{F}$ term is $z_1 - z_2$, instead of just z_1 as it appears in the definition of F.

In previous chapters, the energy equation for pipe flow was able to be simplified if $s \ll 1$. Obtain

$$\frac{s}{\lambda}(1+\hat{F}_1-\hat{F}_2)-\frac{8Q^2}{\pi^2 g}\frac{f(Q,D)}{D^5}=0, \quad \text{for} \quad s \lesssim 0.5 \tag{11.2}$$

If minor losses in the network are to be considered, we include them by writing Eqn (11.2) as,

$$\frac{s}{\lambda}(1+\hat{F}_1-\hat{F}_2)-\frac{8Q^2}{\pi^2 g}\frac{f(Q,D)}{D^5}\left[1+\frac{D}{L}\sum_{i=1}^{M}\left.\frac{L_e}{D}\right|_i+\frac{1}{f(Q,D)}\frac{D}{L}(\alpha+\sum_{i=1}^{N}K_i)\right]=0 \tag{11.3}$$

where, in the square braces, the major loss is represented by 1 followed by the minor terms using either the equivalent length (L_e/D) or loss-coefficient (K) methods.[3] From our inspection of Eqn (11.3), the origin of the recommendations in Section 7.4 concerning the threshold level for minor losses to be significant becomes clear. They are established by comparing the size of the major loss, the 1 in Eqn (11.3), with those of the minor loss terms.

As an aid to understanding, the reader may wish to consider the term in square brackets in Eqn (11.3) as a dimensionless factor > 1 (for nonzero minor losses) that multiplies the major loss term and, in this way, accounts for the effect of minor losses in the network.

The term α is included in Eqn (11.3) if it is needed. Recall that, to this point, α is known to account for the kinetic energy change between a quiescent reservoir at the source or open tank and the developed flow speed in a downstream pipe. At the junction of two pipes each having a different diameter, for example, the flow speed in each will not be very different. This means that the kinetic energy change experienced by the flow passing between the pipes will be negligibly small. In other words, in this case the effect of α may be neglected and α dropped from Eqn (11.3).

Where there is a junction of three or more pipes, either one of two approaches may be used. If there are many outlets, one can imagine the mixing of flows from/to

[3]Remember that only the loss-coefficient (K) approach *or* the equivalent length method (L_e/D) is used, never use both methods for the same minor loss elements or else the effect of the minor losses will be erroneously doubled.

multiple pipes as taking place in a small mixing "box". In this box, the static pressure is approximated as uniform throughout; p is the same for all pipes at that location. The mixing box will also need to be relatively large, compared with a pipe diameter to accommodate the flow from/to multiple pipes. Therefore, for the first approach, the designer may approximate the velocity in this mixing box as small compared with the velocity in a pipe (i.e., the approximation $\overline{u} = 0$ at a junction may be invoked). This approximation is conservative because it will add a small "minor loss" of α to the flow entering each pipe from a junction. Recall that the value of α is ~1 for turbulent flow and 2 for laminar flow (see Fig. 2.2). Both of these values are small compared with many of the minor-loss K values appearing in Table 2.1.

The second approach applies if there is a single inlet and two outlets, such as what occurs with branching flow in a tee fitting. In this case, the minor loss from Table 2.1 would be applied to either the "branch" flow (a turning of the flow of 90°) or the "run" flow, which is straight through the tee; α in Eqn (11.3) is ignored in favor of the minor-loss term. This model for energy losses in a branch is most frequently used.

It is worthwhile to emphasize in our discussion of losses associated with branching flows that the effect of the acceleration term in the energy equation is generally small compared with the pressure and potential energy terms for flows in gravity-driven water networks.[4] Low-flow networks, where the elevation heads are small, are a possible exception to this guideline.

The general procedure for analyzing a multiple-pipe network is as follows:

1. Apply the energy equation for pipe flow, Eqn (2.7) or (11.3), to each leg of the network for which there is a pipe of uniform diameter. This means that the energy equation is written between the inlet and outlet for the uniform-diameter pipe. The inlet of a pipe of one diameter joined by a reducer or an expander to the outlet of a pipe of a different diameter forms a "junction" or "node". Junctions also occur at all sources and wherever pipes join a tank[5] or any branch fitting such as a tee, even though the pipe diameter may not change across the tank or tee[6]. Besides these junctions, all appropriate local high and low points in the network, as defined in Section 2.7, should also be treated as junctions (we may refer to these as "design points" rather than junctions) even though the pipe diameter may not change at these locations. Local high and low points, where the values for the static pressures may be locally too low or high, are worthy of our inspection.

[4]As discussed in Section 13.13 the normally recommended peak flow speed in a plastic pipe is ~3 m/s. From this, a simple calculation of the kinetic energy per unit mass gives ~0.5 m of head. This is what is meant by the acceleration term in the energy equation is generally small compared with the pressure and potential energy terms. However, for a low-head gravity-driven water network, small minor losses and α should be considered. This was emphasized in Section 7.4.

[5]This is because the pressure at the surface of the source or tank is atmospheric and is thus known. The flow upstream and downstream of the tank and downstream from the source is affected by this fixed condition.

[6]The inlets and outlets of a tee may have the same or different diameters; if different, the tee is referred to as a "reducing" or "expanding" tee.

2. At each junction in the network, mass conservation requires that the sum of the volume flow rates into the junction must be zero. For example, if there are n pipes at a junction, mass conservation requires $\sum Q_{in} - \sum Q_{out} = 0$ as discussed in Section 2.5, where the summation is implied over n pipes. For the simplest case, where there is a connection of two pipes, each of a different diameter, the volume flow rates in each pipe are clearly equal.

3. In pipe networks where closed loops appear, use is made of the fact that the pressure change around *any* closed loop must be zero. This arises because the static pressure at any point in the network must be single valued. A loop network will be considered below. Further information on looped networks is presented in a Section 11.7 and in Gagliardi and Liberatore (2002) and Swamee and Sharma (2008). The Hardy Cross method, presented in some fluid mechanics books (Potter and Wiggert, 2002), is used to solve this type of network problem for arbitrarily specified pressure at pipe junctions.

The following simplifications apply to the energy equation for each leg of the network as appropriate:

1. For all reservoirs and tanks open to atmospheric pressure, $p = 0$ and $\overline{u} = 0$, as discussed in Chapter 2.

2. In all mixing boxes, as discussed in the preceding paragraph, the static pressure is uniform and $\overline{u} = 0$.

3. As noted and discussed in Section 7.5, for a faucet valve at a tapstand, the pipe network leading to the tapstand is designed based on flow conditions occurring for a fully open valve. The same applies to a globe valve at the entrance to a tank. When the faucet is open, the static pressure of the fluid at the valve outlet is zero (atmospheric pressure or zero gage pressure). When a globe valve at the entrance to a tank is open, the static pressure of the fluid at the valve outlet is equal to the hydrostatic head of the water in the tank. In both cases, the minor loss for the full-open valve could be included if carrying out a complete analysis using, say, a `Mathcad` worksheet. From Table 2.1 and the associated discussion, we see that the K value for a full-open valve is ~8–10, small enough so that it may be neglected in a preliminary analysis. For an example where the minor loss is included, see the simple-branch network in Section 11.4. Note in this discussion that the minor loss K value for the highly dissipative (that is, nearly closed) globe or faucet valve can be 100 or larger (Table 2.1). Of course, if the valve is shut, the pipe diameters have no effect on the static pressure in the system, which depends on just the local elevation.

In this chapter, we will consider the following cases for flow in multiple-pipe networks:

- A simple-branch network; this could be applied to water distribution from a single pipe to multiple delivery locations, or tapstands, and serves as a simple introductory case for more complicated multiple-pipe networks. This case is

the building block for branching flows that occur frequently in all multiple-pipe networks in large urban areas including those that are pressure driven.

- A number of pipes of different diameters in series, often used in large networks, where the dissipation of potential energy is tailored to match of contour of the pipeline,
- A multiple-branch network; an extension of the first case. This is probably the most common type of multiple-pipe network for rural applications.
- A loop network.

As a group, these encompass nearly all the situations encountered in the design of gravity-driven water distribution networks.[7] In the case where there is needed a more-complex model of any number of pipes connected in any manner, typical of a large urban water-distribution network, please see Jeppson (1976); Streeter et al. (1998); Gagliardi and Liberatore (2002); Trifunovic (2006), and Swamee and Sharma (2008). In these, general but more complex than those used in this text, computer codes are available to solve the nonlinear equations of the flow network. This topic is considered in Section 11.8.

For uniformity, pipe is assumed to be IPS sch. 40 PVC for all of the numerical examples presented in this chapter. Application of the methodologies in this chapter to other pipe of interest is clearly very easily done (see Chapter 3).

11.4 A SIMPLE-BRANCH NETWORK: FLOW FROM A JUNCTION TO MULTIPLE TAPSTANDS

Consider the three-pipe network as shown in Fig. 11.1. The pipes are labeled a, b, and c and they meet at the junction (subscript j) where the pressure is p_j. Each pipe has a mean flow speed $\overline{u}$, volume flow rate Q, diameter D, and length measured along the path of the pipe L. The change in elevation between the top and bottom of each pipe is Δz. For example, Δz_a is the elevation change between the top and bottom of pipe a, where the bottom of this pipe is located where the static pressure is p_j. The required head at each outlet for pipes b and c, h_{del}, is nonzero as indicated in Fig. 11.1.

The values appearing in Table 11.1 apply to this problem. Note that the volume flow rates are prescribed for each pipe, which are based on the measured, or perhaps measured and projected into the future, demands of the communities to be served. As specified in Table 11.1, the continuity equation is satisfied. The elevation changes for pipes a and b are positive, and that for pipe c is negative meaning that the flow is moving upward against gravity toward the delivery location at the end of this pipe.

[7]Note that the case of flow from multiple sources or tanks to a single pipe is identical to the first of these cases. The only difference is that the flow is into the branch from multiple pipes instead of from the branch through multiple pipes.

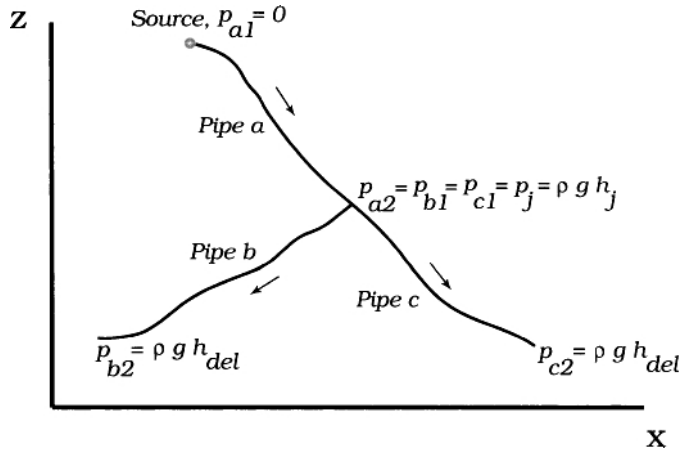

Figure 11.1 A three-pipe branch network. Possible application is flow from a branch to multiple tapstands located at the delivery locations (ends of pipes b and c). The source is at the top of pipe a.

Table 11.1 Values for the Design Parameters for the Branch Three-Pipe Network of Fig. 11.1

Pipe	L (m)	Q (L/s)	K	L_e/D	Δz (m)	h_{del} (m)
a	365	0.5	50	60	33	
b	120	0.2	10	120	5	7
c	210	0.3	10	90	−1	7

As an introduction to the topic of multiple-pipe networks, we will formulate this problem two ways. The first will be in terms of "primitive variables" (i.e., p, z, and L, along with D and Q). The word primitive refers to the solution of a problem where its fundamental dimensional quantities appear as opposed to the variables rewritten in dimensionless forms. With the primitive approach we begin by writing the fundamental energy equation for pipe flow for each pipe, simplify them to eliminate the energy terms that appear, but are not relevant to the problem at hand, and then solve them to obtain, for example, the sought-after values for D.

The second approach to the formulation is to use the framework developed earlier in this book for single-pipe networks where p, z, and L are replaced by the *dimensionless* parameters F, s, and λ [see Eqn (11.3)]. As we will see, this approach, while very convenient for a single-pipe network, is less so for one with multiple pipes because elevations and static pressures at the pipe ends are generally nonzero.

Whether the problem is solved in primitive or dimensionless form, there will *always* be the need for three steps to the solution of a multiple-pipe problem, where

D for each segment (or leg) of the network is unknown.[8] The first step is referred to as the "forward solution." In this step, we solve the energy equation for pipe flow to determine the theoretical values for D needed to satisfy the prescribed volume flow rates in the network, network overall geometry, and specified or calculated static pressures at all pipe junctions. Once the values for D are obtained, in step 2, the designer adjusts these to correspond to actual inside diameters for the nominal pipe sizes chosen. As discussed in Chapter 3, the nominal pipe size normally chosen is one where its inside diameter is slightly larger than D.

In step 3, the "reverse solution" is obtained where, given the actual values for D corresponding to the nominal pipe sizes, the actual volume flow rates of water along with the actual static pressures at each junction are determined.[9] The differences between the actual and specified values for p at each junction and Q may be small, such that the actual values will satisfy the needs of the design to an acceptable level. If not, the actual D may be adjusted by choosing different nominal pipe sizes and step 3 repeated. Other adjustments in the design that will bring the calculated flow rates more in agreement with those required by the design include simulating the presence of globe valves (and thus including them in the design) by adding the appropriate values for their minor loss coefficients at specific locations. This, in particular, is employed in the first type of multiple-pipe network explored in this section. Thus, we see that engineering design enters this process in all three steps, where the designer needs to choose static pressure at the junctions in step 1, choose corresponding nominal pipe sizes in step 2, and decide on adjustments to these after inspecting the results from step 3.

To summarize, the three-step process is illustrated schematically below.

$$\underbrace{\text{Known } z, L, K, L_e/D, \text{ Prescribed } p_j, Q_a, Q_b, Q_c, \ldots \rightarrow \text{Theoretical } D_a, D_b, D_c \ldots}_{\text{"Forward Solution"}}$$

$$\underbrace{\text{Theoretical } D_a, D_b, D_c \ldots \rightarrow \text{Actual } D_a, D_b, D_c \ldots}_{\text{From Pipe Data (see Chapter 3)}}$$

$$\underbrace{\text{Known } z, L, K, L_e/D, \text{ Actual } D_a, D_b, D_c \ldots \rightarrow \text{Actual } p_j, Q_a, Q_b, Q_c \ldots}_{\text{"Reverse Solution"}}$$

Embedded in this process will be the need for the designer to determine the acceptability of the static pressures at all pipe junctions. Solutions of the energy equations

[8]This was done for single-pipe networks above, but the process was never formalized because of the simplicity of this type of network. In the case of multiple-pipe networks, the first and last steps are more computationally intensive so that it is worthwhile providing structure to the three-step solution process. This process has been referred to as a "continuous diameter approach" to distinguish it from one where the diameters corresponding to only nominal pipe sizes are considered as candidates in the solution (Swamee and Sharma, 2008).

[9]For networks where there are branching pipes, such as those illustrated in Fig. 11.1, the actual volume flow rates of water along with the actual static pressures at each junction are determined in step 3. For a network of pipes in series, each having a different diameter, only the actual static pressures at each junction are determined in this step since the volume flow rate is the same for each pipe and is thus known.

for pipe flow may need to be adjusted to meet this need along with an assessment of the impact of these adjustments on performance of the network and, perhaps, cost. We will consider the pipe material cost of the network in this chapter. In contrast with a single-pipe network, the multiple-pipe network is characterized by the existence of an optimal design point because the static pressures at pipe junctions, which do not exist for a single pipe, affect the diameters of different pipes in competing ways. This will become clearer as we explore the next few sections.

11.4.1 Solution in Terms of Primitive Variables

11.4.1.1 Setting up the Problem and Solving The energy equation is from Eqn (2.7),

$$(\frac{p_1}{\rho} + \alpha_1 \frac{\overline{u}_1^2}{2} + gz_1) - (\frac{p_2}{\rho} + \alpha_2 \frac{\overline{u}_2^2}{2} + gz_2) = C_L \frac{L\overline{u}^2}{2D} \tag{11.4}$$

where C_L is the loss coefficient that includes the major and minor loss terms,

$$C_L = f(\overline{u}, D)(1 + \frac{D}{L}\sum_{i=1}^{M} \frac{L_e}{D}\Big|_i) + \frac{D}{L}\sum_{i=1}^{N} K_i \tag{11.5}$$

Note that C_L for each pipe depends on $\overline{u}$, or flow rate Q, and D through the Reynolds number (Re)) for each pipe, and the values of the minor loss coefficients, K and L_e/D. Our inspection of Eqn (11.5) shows that C_L is of the order of f which, as noted in Chapter 2, is of the order of 0.01 for order-of-magnitude purposes.

From Fig. 11.1 and the guidelines discussed in Section 11.1, we recognize that $p_{a1} = \rho g h_1$ and the flow speed in the (assumed for this example) mixing box at the pipe junction is zero. With these, Eqn (11.4) is written for pipes a, b, and c to get

$$\begin{aligned}
\Delta z_a - h_j &= (C_{L,a} + \alpha\frac{D_a}{L_a})\frac{L_a\overline{u}_a^2}{2gD_a}, && \text{Pipe } a \\
\Delta z_b + h_j - h_{del} &= (C_{L,b} + \alpha\frac{D_b}{L_b})\frac{L_b\overline{u}_b^2}{2gD_b}, && \text{Pipe } b \\
\Delta z_c + h_j - h_{del} &= (C_{L,c} + \alpha\frac{D_c}{L_c})\frac{L_c\overline{u}_c^2}{2gD_c}, && \text{Pipe } c
\end{aligned} \tag{11.6}$$

where $h_j = p_j/\rho g$ and $h_{del} = p_{del}/\rho g$.

The continuity equation for each pipe relates Q to $\overline{u}$ through $\overline{u} = 4Q/\pi D^2$ [see Eqn (2.21)]. Substituting this into Eqn (11.6), we obtain

$$\begin{aligned}
\Delta z_a - h_j &= (C_{L,a} + \alpha\frac{D_a}{L_a})\frac{8L_aQ_a^2}{\pi^2 g D_a^5}, && \text{Pipe } a \\
\Delta z_b + h_j - h_{del} &= (C_{L,b} + \alpha\frac{D_b}{L_b})\frac{8L_bQ_b^2}{\pi^2 g D_b^5}, && \text{Pipe } b \\
\Delta z_c + h_j - h_{del} &= (C_{L,c} + \alpha\frac{D_c}{L_c})\frac{8L_cQ_c^2}{\pi^2 g D_c^5}, && \text{Pipe } c
\end{aligned} \tag{11.7}$$

Equation (11.7) is the energy equation written for flow in pipes a, b, and c. By choosing a value for the head, h_j, the three nonlinear algebraic equations of Eqn (11.7) are solved with the continuity equation,

$$Q_a - Q_b - Q_c = 0 \tag{11.8}$$

to obtain diameters D_a, D_b, and D_c. Equation (11.8) is satisfied by the flow-rate data in Table 11.1. Note that the only unknown in each of the equations in Eqn (11.7) is the respective pipe diameter, D. Because only a different, single unknown appears in each equation, the system of equations represented by Eqn (11.7) is not simultaneous. This means that each equation may be independently solved for D_a, D_b, and D_c which, as noted above, is the forward solution. It is important to keep in mind that the pipe diameters are a function of static pressure, p_j, or equivalently head h_j, and vice versa.

Once acceptable nominal pipe sizes are selected based on D from the solution of Eqn (11.7), the problem is then re-solved with the known values for D_a, D_b, and D_c (corresponding to the selected nominal pipe sizes) to get the actual head, h_j, and the actual flow rates, Q_a, Q_b, and Q_c.[10] This is the reverse solution and we note that for this a simultaneous solution of Eqn (11.7) is needed because a change in the flow rate in one pipe affects those in the remaining two through the continuity equation.

The results of the solution, obtained in `Mathcad` using the `Given...Find` construct, are presented in Fig. 11.2 for a wide range of values for h_j. The `Mathcad` worksheet for this example appears in Figs. 11.3–11.5, for the preliminaries, and the forward and reverse solutions, respectively. Before the results for this problem are explored, the format of the `Mathcad` worksheets for multiple-pipe networks is presented and discussed.

11.4.1.2 Format of the Mathcad Worksheets Most worksheets are divided into three sections. These are preliminaries, and the forward and reverse solutions. The preliminary calculations needed for a solution using `Mathcad` are as follows:

- Definition of water properties of density, ρ, and viscosity, ν.
- A convergence tolerance, `TOL`, used in `Mathcad` to determine when a root-finding algorithm has found the root to sufficient accuracy.
- Definition of Re as a function of Q and D, and α as a function of Re.
- Definition of the absolute roughness of the pipe wall.
- The friction factor function as defined by Eqs (2.16) and (2.17).
- The correspondence between nominal pipe size and D for the pipe material and type (schedule or SDR as necessary) of pipe under consideration.

[10]Note that Eqn (11.7) consists of 3 equations and 4 unknowns (h_j, D_a, D_b, and D_c) when solving for diameters as a function of head, h_j, when all flow rates are known. However, there are 4 equations [Eqs (11.7) and (11.8)] and 4 unknowns (h_j, Q_a, Q_b, and Q_c) when solving for head, h_j, and flow rates when all pipe diameters are known. Thus, this is proof that the problem is uniquely specified in the latter case and subject to an arbitrary value for h_j in the former.

- Cost data for the pipe as a function of nominal pipe size.

The forward solution using `Mathcad` includes the following:

- Initial guesses for the values of D (diameters ranging from 0.5 in. to 4 in. are good guesses for nearly all problems considered in this book).
- Values for the input parameters for each pipe segment in the network, including L, Q, the appropriate minor loss coefficients, and elevation changes.
- Definition of the energy equation for each pipe segment of the network. Each is given a symbol r and the needed functional dependence.
- A formula for the total pipe material cost, T_{cost}.
- The solution of the energy equations using either the `Given...Find` construct or `Given...Minimize` construct. The latter was first discussed in Chapter 10 and further in Section 11.4.4.
- Plots of the results or secondary calculations, such as checking to ensure that all equations are satisfied to the desired tolerance.

The reverse solution using `Mathcad` includes the following:

- Initial guesses for the values of Q (from earlier in the worksheet) and static pressure heads at the junctions.
- Values for the input parameters for each leg in the network as in the forward solution; normally only K will be included here.
- The solution of the energy equations using either the `Given...Find` construct or `Given...Minimize` construct, as above.
- Secondary calculations as above.

While presented in the context of Figs. 11.3–11.5, the above format is generally consistent with all `Mathcad` worksheets for multiple-pipe networks.

11.4.1.3 Discussion of the Solution We now return to the solution of the problem at hand. From inspection of Fig. 11.2, we see that the diameter for pipe b is not very sensitive to the head, h_j; D_b corresponds to $\frac{3}{4}$ in. nominal. On the other hand, D_c is very sensitive to h_j at small values of h_j, where the driving force for the flow in pipe c approaches the elevation head of $\Delta z_c = -1$ m. Recall that the negative value for Δz_c means that there is an elevation increase from the junction to the delivery location for pipe c. Likewise, D_a is very sensitive to h_j at large values of h_j where h_j approaches the hydrostatic head at the junction of 33 m. These bounding cases will be used to provide a guideline for choosing the junction pressures for this simple-branch network (see Section 11.4.2).

The total pipe material cost for this three-pipe network is plotted in Fig. 11.6. The cost data for the assumed IPS sch. 40 PVC pipe appear in the worksheet of Fig. 11.3.

Based on this calculation, we see that minimal cost for the pipe for this network occurs at $h_j \approx 15$ m of head (21.3 psig). At this head, the results from Fig. 11.2 provide the final values for pipe diameters D_a, D_b, and D_c of 1, $\frac{3}{4}$, 1 in. nominal sizes, respectively[11]. With these pipe sizes and the specified design parameters, the reverse solution from Fig. 11.5 shows that all flow rates will not meet the design specifications. However, by partially closing globe valves installed in all pipes corresponding to values $K_a = 120$, $K_b = 20$, and $K_c = 80$, all design conditions are satisfied with the static pressure at the junction, h_j, of 12.2 m. This value is large enough such that no vacuum conditions will exist at the junction under any ordinary operating conditions. The globe valves at the end of pipe segments b and c would be faucet valves normally planned as part of the design. A globe valve before the junction in Fig. 11.1 in pipe a, on the other hand, would not normally be planned, but its need is made clear by recognizing these results. This example shows the important role played by throttling valves in providing acceptable flow balance in a branch network. This was first discussed in Chapter 1 and emphasized in Section 11.6.5.

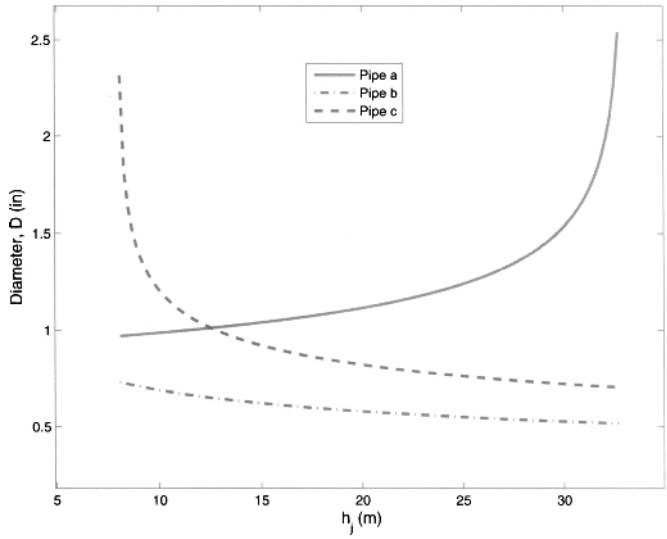

Figure 11.2 Pipe diameters for the case of a branch three-pipe network versus head at the pipe junction.

We may generalize the equations for the case of any number of pipes, $a, b, c, \ldots n$, connected in the manner shown in Fig. 11.1. The energy equation for flow in pipe a remains as it is written as the first of Eqn (11.7). For every other pipe in the network, the form is identical to the remaining two equations in Eqn (11.7). That is, for the ith

[11]Where it is necessary for clarity, we will designate the diameters and other variables and parameters from an optimized solution with the superscript *opt*. In most places, this is cumbersome and will not be used. The optimized nature of these results should be clear from the text that describes them.

Branching flow 3-pipe problem solved in Forward and Reverse ways

Water properties $\rho := 1000\frac{kg}{m^3}$ $\nu := 13.0710^{-7}\cdot\frac{m^2}{sec}$ $sec := 1\cdot s$ $TOL := 1\cdot10^{-6}$

ORIGIN := 1

IPS sch. 40 PVC pipe cost

$$diam := \begin{pmatrix} 0.622 \\ 0.824 \\ 1.049 \\ 1.610 \\ 2.067 \\ 2.469 \\ 3.068 \\ 4.026 \end{pmatrix}\cdot in \qquad cost := \begin{pmatrix} 0.60 \\ 0.82 \\ 1.02 \\ 1.74 \\ 2.40 \\ 3.94 \\ 5.58 \\ 7.75 \end{pmatrix}\frac{dollar}{m} \qquad dollar := 1$$

$$Re(Q,D) := \frac{4\cdot Q}{\pi\cdot D\cdot\nu} \qquad \varepsilon := 5\cdot10^{-6}\cdot ft$$

absolute roughness, ft (increase 100 times for galvanized steel)

friction factor that spans the laminar/turbulent range. ebyD is relative roughness.

$$funct(f,R,ebyD) := \frac{f}{2} - \left[\left(\frac{4}{R\cdot\sqrt{\frac{f}{8}}}\right)^{24} + \left[\left(\frac{18765}{R\cdot\sqrt{\frac{f}{8}}}\right)^{8} + \left[3.29 - \frac{227}{R\cdot\sqrt{\frac{f}{8}}} + \left(\frac{50}{R\cdot\sqrt{\frac{f}{8}}}\right)^{2} \ldots + \frac{1}{0.436}\cdot\ln\left(\frac{R\cdot\sqrt{\frac{f}{8}}}{1 + 0.301R\cdot\sqrt{\frac{f}{8}}\cdot ebyD\cdot 2}\right)\right]^{16}\right]^{-\frac{3}{2}}\right]^{\frac{1}{12}}$$

$$fric\_fac(Re,ebyD) := root(funct(f1,Re,ebyD),f1,0.0001,0.2)\cdot 4$$ friction factor

$$\alpha(R) := if(R < 2100, 2, 1.05)$$

For PVC or galvanized steel pipe:

nominal 1.5 in	$D_4 := 1.61\cdot in$	nominal 4 in	$D_8 := 4.026in$
nominal 1 in	$D_3 := 1.049in$	nominal 3 in	$D_7 := 3.068in$
nominal 0.75 in	$D_2 := 0.824in$	nominal 2.5 in	$D_6 := 2.469in$
nominal 0.5 in	$D_1 := 0.662in$	nominal 2 in	$D_5 := 2.067in$

Figure 11.3 Mathcad worksheet for a simple three-pipe branch network: preliminaries include Re definition, pipe material costs, friction factor, α definition, and pipe-size equivalences. Mathcad worksheet `BranchingPipeExample.xmcd`.

A 3-pipe network solved in forward way (specify volume flow rates and solve for pipe diameters vs. range of hj):

$D_a := 1\cdot in \quad D_b := 1\cdot in \quad D_c := 1\cdot in$ guesses $h_{del} := 7\cdot m$

Input Parameters:

$L_a := 365m \quad Q_a := 0.5\frac{liter}{sec} \quad K_a := 50 \quad L_{ebyD\_a} := 2.30 \quad \Delta z_a := 33\cdot m$

$L_b := 120m \quad Q_b := 0.2\frac{liter}{sec} \quad K_b := 10 \quad L_{ebyD\_b} := 4.30 \quad \Delta z_b := 5\cdot m$

$L_c := 210m \quad Q_c := Q_a - Q_b \quad K_c := 10 \quad L_{ebyD\_c} := 3.30 \quad \Delta z_c := -1\cdot m$

Define energy equation functions:

$$r_a(h_j, Q_a, D_a, K_a) := \Delta z_a - h_j - \left[K_a + \alpha\left(Re\left(|Q_a|, D_a\right)\right) + fric\_fac\left(Re\left(|Q_a|, D_a\right), \frac{\varepsilon}{D_a}\right)\left(\frac{L_a}{D_a} + L_{ebyD\_a}\right)\right]\cdot\frac{8\cdot Q_a^{\,2}}{\pi^2\cdot g\cdot D_a^{\,4}}$$

$$r_b(h_j, Q_b, D_b, K_b) := \Delta z_b + h_j - h_{del} - \left[K_b + \alpha\left(Re\left(|Q_b|, D_b\right)\right) + fric\_fac\left(Re\left(|Q_b|, D_b\right), \frac{\varepsilon}{D_b}\right)\left(\frac{L_b}{D_b} + L_{ebyD\_b}\right)\right]\cdot\frac{8\cdot Q_b^{\,2}}{\pi^2\cdot g\cdot D_b^{\,4}}$$

$$r_c(h_j, Q_c, D_c, K_c) := \Delta z_c + h_j - h_{del} - \left[K_c + \alpha\left(Re\left(|Q_c|, D_c\right)\right) + fric\_fac\left(Re\left(|Q_c|, D_c\right), \frac{\varepsilon}{D_c}\right)\left(\frac{L_c}{D_c} + L_{ebyD\_c}\right)\right]\cdot\frac{8\cdot Q_c^{\,2}}{\pi^2\cdot g\cdot D_c^{\,4}}$$

$$Tcost(D_a, D_b, D_c) := linterp(diam, cost, D_a)L_a + linterp(diam, cost, D_b)L_b + linterp(diam, cost, D_c)L_c$$

Solve in Given...Find block

Given $0 = r_a(h_j, Q_a, D_a, K_a) \quad 0 = r_b(h_j, Q_b, D_b, K_b) \quad 0 = r_c(h_j, Q_c, D_c, K_b)$

$D_p(h_j) := Find(D_a, D_b, D_c) \quad h_j := 8.1\cdot m, 8.3\cdot m .. 32.7\cdot m$

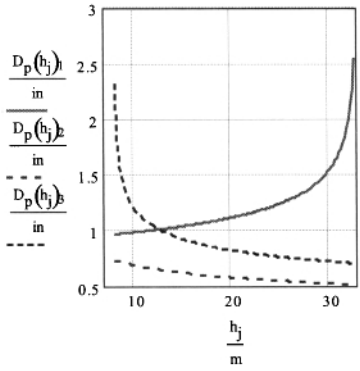

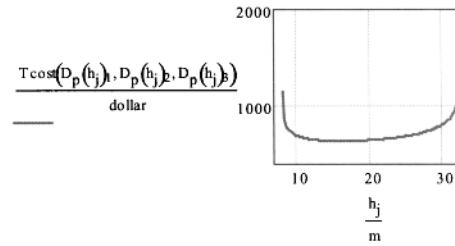

Figure 11.4 Mathcad worksheet for a simple three-pipe branch network for the forward solution. Note that the minimum pipe material cost for this network occurs at $h_j \approx 10$ m. See Fig. 11.3 for the preliminary material needed for this calculation. Mathcad worksheet `BranchingPipeExample.xmcd`.

A 3-pipe network solved in reverse way (specify pipe diameters and solve for the volume flow rates):

$h_j := 10\,m$ guess

Input Parameters:

$K_a := 120$ Increase to 120 to account for partially open globe valve

$K_b := 20$ Increase to 20 to account for partially open globe valve

$K_c := 180$ Increase to 180 to account for partially open globe valve

Given $0 = r_a(h_j, Q_a, D_a, K_a)$ $0 = r_b(h_j, Q_b, D_b, K_b)$ $0 = r_c(h_j, Q_c, D_c, K_b)$ $Q_a - Q_b - Q_c = 0$

$$Q_p(D_a, D_b, D_c) := \text{Find}\left(\frac{Q_a}{\frac{liter}{sec}}, \frac{Q_b}{\frac{liter}{sec}}, \frac{Q_c}{\frac{liter}{sec}}, \frac{h_j}{m}\right)$$

$$Q_p(D_3, D_1, D_3) = \begin{pmatrix} 0.509 \\ 0.201 \\ 0.308 \\ 12.170 \end{pmatrix}$$

Figure 11.5 Mathcad worksheet for a simple three-pipe branch network for the reverse solution. Note that K_a and K_b were increased in value to account for the partially open globe valves installed at the end of these pipes (see Fig. 11.3 for the preliminary material needed for this calculation). Mathcad worksheet BranchingPipeExample.xmcd.

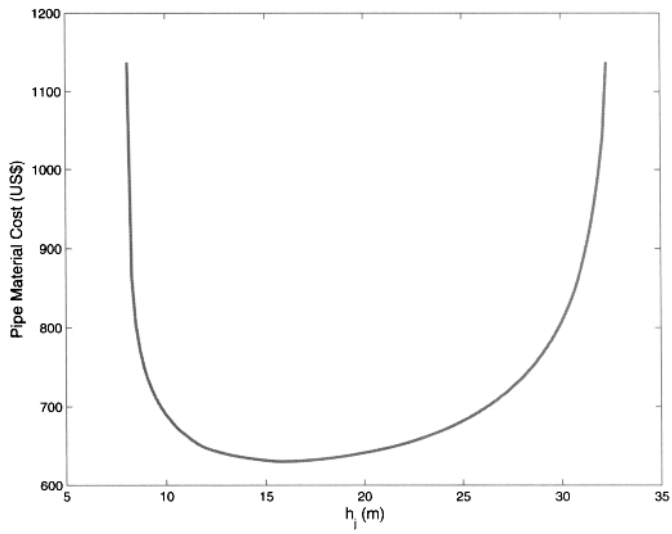

Figure 11.6 Pipe material cost of three-pipe branch network versus head at the pipe junction.

pipe, $i = b, c, d, \ldots, n$ in the network we can write the energy equation as

$$\Delta z_i + h_j - h_{del} = (C_{L,i} + \alpha \frac{D_i}{L_i}) \frac{8 L_i Q_i^2}{\pi^2 g D_i^5} \tag{11.9}$$

The continuity equation is written in the usual way [Eqn (2.23)] as

$$\sum Q_{in} - \sum Q_{out} = 0$$

The solution of the resulting n nonlinear algebraic equations in terms of $D_a, D_b, D_c \ldots D_n$ is obtained once a value for static pressures at the pipe junction is prescribed. For the reverse solution, $Q_a, Q_b, Q_c \ldots Q_n$ and the value for static pressure at the pipe junction are determined once the inside diameters corresponding to the chosen nominal pipe sizes are established.

11.4.2 Bounds on Junction Pressures

The head at any junction in a network has a *maximum* in the limit of zero flow. Thus, the *upper bound* on the static pressure head at any junction is from hydrostatics and is

$$\boxed{h_{j,max}(z) < z_1 - z} \tag{11.10}$$

where z_1 is the elevation of the source. Evidence of this limiting case for the above example is obtained by inspecting Fig. 11.2 as h_j approaches the hydrostatic head of 33 m at the junction. In this limiting case, the pipe diameter plays no role in the problem because there is no flow. That is, the energy equation reduces to Eqn (2.20), where D does not appear. However, the pipe must be able to withstand the hydrostatic pressures that are larger than the static pressures, once motion begins, at all points in the network.

In multiple-pipe networks, the *lower bound* on the static pressure head at any junction is imposed by considerations of water quality and integrity of the network. Values in the range of 7–10 m of head are often prescribed. The reasons for this have been noted in several places in this book and will not be visited again here. Alternately, *unique junction pressures*, provided they are $>$ 7–10 m, may be obtained by considering other constraints, such as minimized network cost. In the sections below that follow this particular strategy, a simple network cost model is considered.

Table 11.2 Values for Design Parameters for Four-Pipe Network

Pipe	L (m)	Q (L/s)	K	L_e/D	Δz (m)	h_{del} (m)
a	135	1.5	50	80	48	
b	54	0.7	10	100	21	7
c	38	0.3	10	40	4	7
d	79	0.5	10	90	12	7

B.11.1 Exploration: Extension to a Four-Pipe Branch Network

Consider the network of Fig. 11.1 and extend to four pipes, a, b, c, and d, where the end of pipe a joins the beginning of pipes b, c, and d. The data from Table 11.2 apply. Modify the Mathcad worksheet `BranchingPipeExample.xmcd` to accommodate the four pipe network and determine the static pressure head at the junction that minimizes the pipe material cost. Report this cost and the optimal values for the theoretical pipe diameters D_a, D_b, D_c, and D_d.

We begin by making the following additions and changes to the worksheet `BranchingPipeExample.xmcd`:

- Add the initial guess of $D_d = 1$ in.
- Add the data from Table 11.2. Need an additional row for pipe d data.
- Under the energy equation for pipe c, add (by copy-and paste to reduce typing) the energy equation for pipe d [from Eqn 11.9]. In Mathcad syntax is will appear as

$$\begin{aligned} r_d(h_j, Q_d, D_d) &= \Delta z_d + h_j - h_{del} - [K_d + \alpha(\mathrm{Re}(|Q_d|, D_d)) \\ &+ fric\_fac(\mathrm{Re}(|Q_d|, D_d), \frac{\epsilon}{D_d})(\frac{D_d}{L_d} + L_{ebyD_d})] \cdot \\ &\cdot \frac{8Q_d^2}{\pi^2 g D_d^4} \end{aligned}$$

- In the expression for $Tcost$, add "+`linterp(diam, cost, Dd)`" and D_d as an argument in the $Tcost$ function (after the addition it should read $Tcost(D_a, D_b, D_c, D_d) = \ldots$).
- In the `Given...Find` block, add $0 = r_d(h_j, Q_d, D_d)$ after $0 = r_c(h_j, Q_c, D_c)$.
- Change `Find` to include D_d. It will appear as $\mathtt{D_p(h_j)} = \mathtt{Find(D_a, D_b, D_c, D_d)}$.

Extension to a Four-Pipe Branch Network (Cont'd)

Using the guidance from Section 11.4.2 on the range of h_j, we plot results of the solution for 7 m $< h_j <$ 48 m (the lower bound is considered minimally acceptable and the upper bound is the hydrostatic limit), we find the minimum cost of ~$1363 occurs at $h_j \approx 30$ m. At this static pressure head, $D_a, D_b, D_c, D_d = 1.57, 0.959, 0.888, 0.530$ in., respectively.

11.4.3 Solution in Terms of Dimensionless Variables

In this section, we wish to write Eqn (11.3), which is the energy equation for pipe flow written in dimensionless form, for each of the three pipes in the network. Referring to Fig. 11.1, the data from Table 11.1 is used to produce expressions for values for s/λ [recall Eqn (2.38)], $\hat{F}_1$, and $\hat{F}_2$. The details are as follows:
Pipe a:

$$\begin{aligned} \frac{s_a}{\lambda_a} &= \frac{\Delta z_a}{L_a} = \frac{33}{435} = 0.0759 \\ \hat{F}_{a1} &= \frac{p_{a1}}{\rho g \Delta z_a} = 0 \\ \hat{F}_{a2} &= \frac{p_{a2}}{\rho g \Delta z_a} \end{aligned} \tag{11.11}$$

Pipe b:

$$\begin{aligned} \frac{s_b}{\lambda_b} &= \frac{\Delta z_b}{L_b} = \frac{5}{12} = 0.417 \\ \hat{F}_{b1} &= \frac{p_{a2}}{\rho g \Delta z_b} = \frac{\Delta z_a}{\Delta z_b} \hat{F}_{a2} = 6.60 \hat{F}_{a2} \\ \hat{F}_{b2} &= \frac{p_{b2}}{\rho g \Delta z_b} = \frac{h_{del}}{\Delta z_b} = 1.40 \end{aligned} \tag{11.12}$$

Pipe c:

$$\begin{aligned} \frac{s_c}{\lambda_c} &= \frac{\Delta z_c}{L_c} = -\frac{1}{21} = -0.0476 \\ \hat{F}_{c1} &= \frac{p_{a2}}{\rho g \Delta z_c} = \frac{\Delta z_a}{\Delta z_c} \hat{F}_{a2} = -33.0 \hat{F}_{a2} \\ \hat{F}_{c2} &= \frac{p_{c2}}{\rho g \Delta z_c} = \frac{h_{del}}{\Delta z_c} = -7.00 \end{aligned} \tag{11.13}$$

Equation (11.3) is written for pipes a, b and c to get,

$$\begin{aligned}
\frac{s_a}{\lambda_a}(1+\hat{F}_{a1}-\hat{F}_{a2}) &= (C_{L,a}+\alpha\frac{D_a}{L_a})\frac{8Q_a^2}{\pi^2 g D_a^5}, \quad \text{Pipe } a \\
\frac{s_b}{\lambda_b}(1+\hat{F}_{b1}-\hat{F}_{b2}) &= (C_{L,b}+\alpha\frac{D_b}{L_b})\frac{8Q_b^2}{\pi^2 g D_b^5}, \quad \text{Pipe } b \qquad (11.14) \\
\frac{s_c}{\lambda_c}(1+\hat{F}_{c1}-\hat{F}_{c2}) &= (C_{L,c}+\alpha\frac{D_c}{L_c})\frac{8Q_c^2}{\pi^2 g D_c^5}, \quad \text{Pipe } c
\end{aligned}$$

The next step is to substitute the results from Eqs (11.11)–(11.13) into Eqs (11.14) and solve for D_a, D_b, and D_c using `Mathcad`. Note that the single free parameter in the dimensionless form of the energy equations [Eqs (11.14)] is not h_j as it was for the primitive variables form of Eqs (11.7). Instead, it is the dimensionless parameter $\hat{F}_{a2}$.

Once the terms and values from Eqs (11.11)–(11.13) are included, we note that Eqn (11.14) becomes identical to Eqn (11.7).[12] Thus, the only difference between the primitive and dimensionless variables approach is the need to calculate the values of the dimensionless groups that appear in Eqs (11.11)–(11.13). Since the end result is identical either way, and it is normally not desirable to spend extra time calculating the values of the dimensionless groups, the use of the dimensionless form of the energy equation for multiple-pipe networks is discouraged compared with the primitive variables form. In fact, the reason why the dimensionless groups were used at all for single-pipe networks is that the simplifications of $p_1 = z_2 = 0$ reduced the energy equation so that it could be written in terms of just a few parameters, namely, s, λ, and F and the application is *only a single pipe*. The easy-to-use design charts of Chapter 5 were the result of this simple representation. Evidence from the example in this section shows that this outcome is clearly not the same for multiple-pipe networks.

11.4.4 Minimal-Cost Solution

In Section 11.4.1.3, we saw that the static pressure at the junction in a simple three-pipe branch network was, in fact, uniquely valued if we required the cost of pipe to be minimized. We wish to further explore this finding to understand why this has occurred and if it is to be generally expected. Specifically, we will try to answer the question *what is the optimal value for the static pressure at the junction that produces D values that minimize total pipe cost?* To facilitate insight, we assume turbulent flow in smooth pipe and that minor losses are negligible. The requirement that Re of $>$ 3000 can be verified after we perform the design calculations. The results of Section 9.3 correspond to these conditions so that we are able to write an

[12]Obviously, this must be the case because the energy equation is the same whether written in dimensional or dimensionless form. The reader is encouraged to verify this either by substituting the terms and numbers as indicated or by simply moving L for each pipe to the left side of Eqn (11.7) and extracting $\Delta z/L$, which is the mean slope. After a few steps of algebra, the equivalence of Eqs (11.7) and (11.14) will become clear.

Table 11.3 Values for Design Parameters for a Branching Three-Pipe Network of Fig. 11.1

Pipe	L (m)	Q (L/s)	K	L_e/D	Δz (m)	h_{del} (m)
a	464	1.5	0	0	77	
b	199	0.75	0	0	11	7
c	199	0.75	0	0	11	7

explicit formula for each of the pipe diameters that appear in Fig. 11.1. To illustrate a minimal-cost solution for a multiple-pipe network problem, values for each of the design parameters as appearing in Table 11.3 will be assumed. For simplicity, and to reduce the number of free parameters, the conditions for pipes b and c are assumed to be identical. The results of this analysis are in no way less general because of this assumption.

Equation (9.8) is written for each of the three pipes in the geometry of Fig. 11.1 to obtain

$$\begin{aligned} D_a &= 0.741\left(\frac{\Delta z_a + \Delta h_a}{L_a}\right)^{-4/19}\left(\frac{Q_a\,\nu^{1/7}}{g^{4/7}}\right)^{7/19} \\ D_b = D_c &= 0.741\left(\frac{\Delta z_b + \Delta h_b}{L_b}\right)^{-4/19}\left(\frac{Q_b\,\nu^{1/7}}{g^{4/7}}\right)^{7/19} \end{aligned} \tag{11.15}$$

where Δz and Δh are the change in z and static pressure head at the junction, respectively, along the pipeline coordinate measured from the top of the pipe.

Our inspection of Fig. 11.1 shows that $\Delta h_a = h_{1a} - h_{2a} = 0 - h_j = -h_j$, $\Delta h_b = h_{1b} - h_{2b} = h_j - h_{del}$, and $\Delta h_c = h_{1c} - h_{2c} = h_j - h_{del}$. With these, Eqn (11.15) becomes

$$\begin{aligned} D_a &= 0.741\left(\frac{\Delta z_a - h_j}{L_a}\right)^{-4/19}\left(\frac{Q_a\,\nu^{1/7}}{g^{4/7}}\right)^{7/19} \\ D_b = D_c &= 0.741\left(\frac{\Delta z_b - h_{del} + h_j}{L_b}\right)^{-4/19}\left(\frac{Q_b\,\nu^{1/7}}{g^{4/7}}\right)^{7/19} \end{aligned} \tag{11.16}$$

As we first saw in Chapter 10, the cost per unit length for pipe over a nominal range of pipe diameters normally follows a power-law relationship,

$$\boxed{C' = a\left(\frac{D}{D_u}\right)^b} \tag{11.17}$$

where D is the inside diameter (ID), a is a coefficient, b is an exponent, and D_u is a unit diameter taken to be 1 in.[13] For the calculations presented in this chapter, we

[13]Even though Eqn (11.17) is a continuous function that predicts a cost for *any* pipe diameter, we clearly understand that it is applied only to the diameters that correspond to nominal pipe sizes.

will assume 2007 cost data for IPS-series sch. 40 PVC pipe in central Nicaragua. A correlation of these data gives $a = 1.067$ \$/m and $b = 1.40$. A quick glance at Eqn (11.17) will convince the reader that pipe material cost per unit length is proportional to pipe diameter; large-diameter pipe costs more than small-diameter pipe per unit length.

With Eqn (11.17) the general expression for the total cost for the pipe material, C_T, is obtained by summing over all pipe segments ij,

$$\boxed{C_T = a \sum (\frac{D_{ij}}{D_u})^b L_{ij}} \tag{11.18}$$

For the present problem this becomes,

$$C_T = a\,[(\frac{D_a}{D_u})^b L_a + (\frac{D_b}{D_u})^b L_b + (\frac{D_c}{D_u})^b L_c] = a\,[(\frac{D_a}{D_u})^b L_a + 2(\frac{D_b}{D_u})^b L_b] \tag{11.19}$$

A close inspection of Eqn (11.16) in combination with Eqn. (11.19) will reveal the origin of the existence of an optimal h_j for the design of this network. From the discussion in Section 11.1, recall that we are free to vary h_j; the static pressure head where the three pipes meet. As h_j increases, say from a small value like 1 m, the static pressure difference between the junction and the bottom of pipe b (and c) increases. Since the volume flow rates in each pipe are fixed, as specified in Table 11.3, an increase in pressure drop across pipe b (and c) requires a reduction in D_b (and D_c). This is evident from our inspection of the second of Eqn (11.16), where we see that D_b and D_c are both proportional to $(\Delta z_a - h_{del} + h_j)^{-4/19}$; $(\Delta z_a - h_{del} + h_j)^{-4/19}$ decreases as h_j increases.

How is the diameter of pipe a affected by the increase in h_j? Because the top of pipe a is at atmospheric pressure (~10 m, absolute) an increase in h_j will decrease the pressure drop between the top of pipe a and the junction.[14] Thus, compared with pipes b and c, the opposite effect occurs in pipe a; D_a increases with increasing h_j. For insight on how the energy equation supports this explanation, note that the first of Eqs (11.16) requires that $D_a \approx (\Delta z_a - h_j)^{-4/19}$ *increases* as h_j increases.

It is clear from the above brief discussion that for increasing h_j there is a competition between the *decrease* of D_b (and D_c) and an *increase* in D_a. Once the effect of D on pipe cost is included through Eqn (11.19), as h_j increases we see that the cost for pipes b and c decrease, and the cost for pipe a increases. A consequence of this competition is the existence of an optimum, in this case an optimal value for h_j, that produces the smallest possible cost. A plot of the total pipe material cost over a range of h_j is presented in Fig. 11.7, where we see that the total pipe cost is indeed minimized for $h_j = h_j^{opt} \approx 25$ m. Values of h_j either smaller or larger than h_j^{opt} will increase cost; in fact, large deviations from h_j^{opt} will result in large cost increases. Once the optimal value for h_j is identified, either by a plot or by a more-formal and

[14]The varaiable h_j is not restricted to be less than atmospheric pressure. In fact, the pressure drop for pipe a could actually be negative valued. The only constraint on h_j is that it cannot be $> \Delta z_a$ [see the first of Eqn (11.16), where the calculation of D_a would be meaningless for $h_j > \Delta z_a$].

more-general method to be discussed below, the values for all pipe diameters can be calculated from Eqs (11.16). For this problem we will find $D_a = 1.28$ in. and $D_b = D_c = 0.937$ in. The appropriate corresponding nominal pipe sizes can be selected from these. A graph showing the *sensitivity* to the head at the junction appears in Fig. 11.8, where we note there to be a very large range of possible pipe diameters depending on the value of h_j. A plot such as this, when used with Eqn (11.19), will instruct the designer on the extent of the cost increase due to an non-optimal choice of h_j for his/her design.

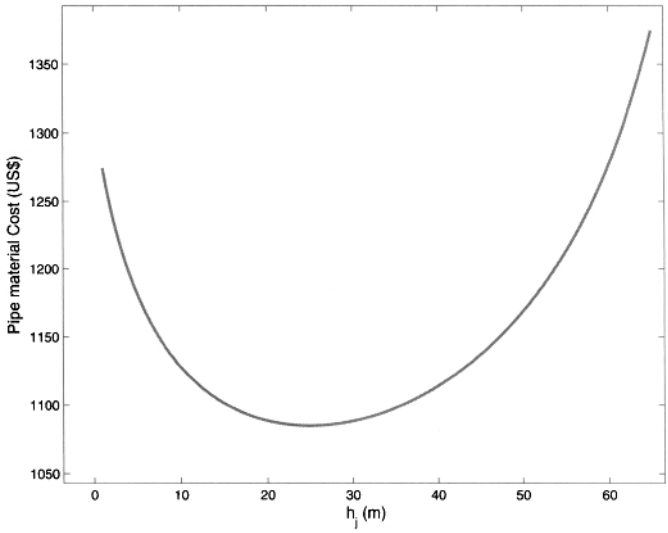

Figure 11.7 Sensitivity of pipe material cost for a three-pipe network versus head at the pipe junction.

The smallest value of Re for this three-pipe network is ~48,000, thus validating the assumption of turbulent flow.

A few comments are needed to complete our discussion on this topic. First, the equations that determine total pipe cost for even the simple-branch network considered in this section are highly nonlinear. Because it is very difficult, if not impossible, to generalize the solutions for optimal h_j for any pipe network, we will use a methodology implemented in `Mathcad` that attempts to find the minimum pipe material cost subject to the following two constraints:

- A designer-specified minimum value of static pressure at all junctions in a network.
- A maximum value of static pressure based on hydrostatics.

In cases where obtaining the minimum cost solution from `Mathcad` is too time consuming, a trial-and-error approach can be used to get approximate results for a minimum cost design. This is pursued in Section 11.7. In addition to this, an alternate

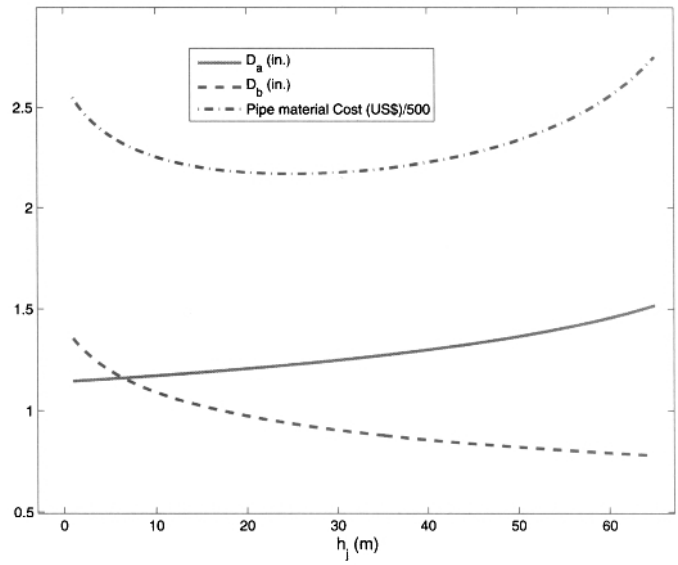

Figure 11.8 Sensitivity of pipe material cost and pipe diameters for a three-pipe network versus head at the pipe junction.

approach is to use the approximate formula developed in Section 11.6.6, where no minimization function is needed. Wherever it is practical, plots of pipe diameters as functions of a range of reasonable junction pressures should be part of the process in any good design methodology. These will normally provide insight and understanding about the network and the sensitivity of pipe sizes, and ultimately costs, to junction pressures. This exploration is highly recommended. However, it is neither practical nor efficient to produce plots of pipe sizes versus *all* of the junction pressures in a complex network having many branches or loops.

Second, the use of pipe material cost in this section as the function to be minimized was assumed for convenience, simplicity, and to an extent, relevance. The choice was made because in many of gravity-driven water networks designed and installed by service-learning students, the installation labor comes from the local community and, as such, has no well-defined associated cost. In addition, the material cost for the network is of prime importance since it normally comes from funds raised by Nongovernmental organizations or grants, where there is seldom a required repayment (no mortgage on these funds) but where the funds are always in short supply. For these reasons material cost as a stand-alone quantity was chosen as the objective function in this work. Note, however, that the economics of gravity-driven water networks in other cases is most likely more complex and includes costs associated with materials, labor, operation and maintenance, depreciation, taxes (if any), and salvage, among others. The time value of money also needs to be considered, which includes interest rates, amortization, and estimation of network lifetimes. Several of

these are fixed costs that are independent of pipe sizes and lengths and others, as we saw from the example above, are pipe-diameter- and length-dependent. For a more thorough treatment of network costs, and their minimization [see Burmeister (1998); Swamee and Sharma (2000) or any good textbook on thermal or hydraulic system design].

Finally, publications on optimizing branching networks based on a variety of simplifying assumptions exist (Bhave, 1983; Chiplunkar and Khanna, 1983; Varma et al., 1997). For example, frictional head loss is written simply as the product of Q and D raised to different powers. Others convert a looped network to the branching type before solving. While the methodologies in these works have varying degrees of soundness, the fundamentals approach in the present treatment imposes few, if any, assumptions that are unrealistic under a broad range of design conditions.

B.11.2 An Interim Recap

Thus far, we have applied the fundamental principles of conservation of energy and mass to flow in a simple-branch network. Along the way we have learned a few things about the approach, assumptions, method of solution, and a few interesting outcomes from the solutions that can be summarized by

- The analysis of multiple-pipe networks follows closely that for a single pipe; the fundamental difference is that static pressures (or static pressure heads) at both ends of each pipe segment are generally not zero [for a single pipe, flow from a reservoir or into a tank was always from/to zero (atmospheric) pressure]. The continuity equation also needs to be included in the solution for a network where there is branching. Because of both of these differences, numerical methods, like those used in `Mathcad` are normally needed to solve multiple-pipe network problems.

- Because of the additional complexity of possibly two nonzero static pressures for each pipe segment, the solution of pipe-flow problems using primitive variables (the fundamental dimensional quantities) is preferred over the use of the dimensionless form of the governing equations that enjoyed success for single-pipe networks. Only the primitive form of the energy equation will be used for the solutions of multiple-pipe networks.

- The usual, realistic assumptions of zero flow speed in a reservoir, the inclusion of the kinetic energy correction factor (α) only where there is flow from a reservoir or tank into a pipe, and the inclusion of (at least) minor loss factors for open globe valves in many segments of the network will be made in multiple-pipe networks. The strategic placement and use of the throttling globe valve, as we will see below, is important for flow balancing and network maintenance.

An Interim Recap (Cont'd)

- There are typically three steps in the analysis and design of a multiple-pipe network. In the *forward* solution, the theoretical values for D needed to satisfy the prescribed volume flow rates, overall geometry, and designer-specified static pressures at all pipe junctions are obtained. After this step, the designer adjusts D to correspond to actual inside diameters for the nominal pipe sizes chosen. The *reverse* solution is then obtained where, given the actual values for D corresponding to the nominal pipe sizes, the actual volume flow rates along with the actual static pressure heads at each junction are determined.
- For the forward solution, we use the energy and continuity equations to solve for D. In this solution, the following apply:
  - In the absence of any other constraints, like cost, the static pressure head at each junction is *arbitrary but always bounded by hydrostatic conditions from above and a designer-prescribed constraint from below.* The latter is a minimum value of -7 m.
  - Once pipe cost is considered, a *unique value for the static pressure heads at all junctions can be found* as a result of the competition of increasing and decreasing pipe sizes on either side of each junction. The constraint of minimum cost adds additional equations that provide uniqueness to the forward solution for multiple-pipe networks.

11.5 PIPES OF DIFFERENT DIAMETERS IN SERIES: CONTROLLED DISSIPATION OF POTENTIAL ENERGY

11.5.1 The Problem

In gravity-driven water distribution systems, the contour of the pipe follows that of the land, which generally has a non-uniform slope. If a pipe of a single diameter is used, the rate of dissipation of potential energy due to the major loss is uniform along the flow path. Recall the discussion of the HGL from Chapter 6. For example, when the contour changes from a small slope to a larger one, the static pressure in the pipe will build because the rate of potential energy loss (that is, the conversion from potential into pressure energy) is greater than that dissipated by the constant-volume flow rate in the constant-diameter pipe. To remedy this difficulty, designers often require a diameter change (for this example, a reduction in pipe diameter) to better match the dissipation due to friction with the rate of change of elevation head. In this way, the HGL will more closely follow the contour of the land in which the pipe is buried and there will be less static pressure build-up in the pipe. The excess energy in the flow at the delivery point, say a tank or tapstand, will not need to be dissipated by a single

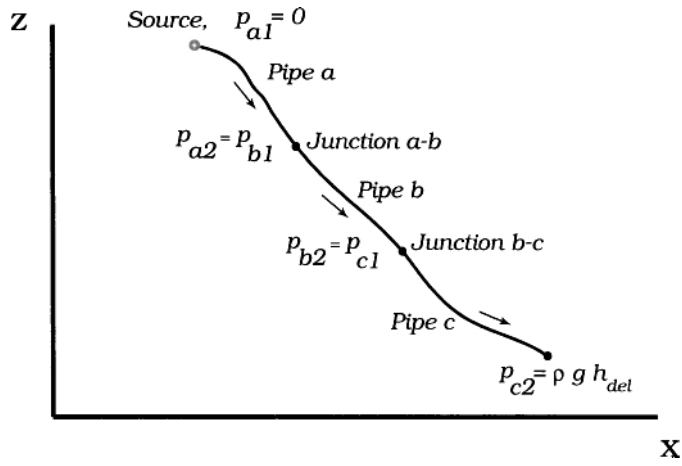

Figure 11.9 A three-pipe serial network.

nearly-closed globe valve. The latter could be noisy and produce unwanted vibrations in the system, experience premature wear, and is not considered good engineering practice.

Consider the series-connected three-pipe system as shown in Fig. 11.9.[15] The pipes are labeled a, b, and c, and each has a mean flow speed, $\overline{u}$, diameter, D, and length measured along the path of the pipe, L. As before in this chapter, the change in elevation between the top and bottom of each pipe is Δz. The volume flow rate, Q, is the same for each pipe, thus satisfying the continuity equation.

The energy equation is from Eqn (11.4). As above, we first use the continuity equation, Eqn (2.21), to rewrite Eqn (11.4) in terms of Q instead of $\overline{u}$. The energy equations for each of the three pipes becomes

$$\begin{aligned}
\frac{\Delta z_a + \Delta h_a}{L_a} &= (C_{L,a} + \alpha \frac{D_a}{L_a}) \frac{8Q^2}{\pi^2 g D_a^5}, && \text{Pipe } a \\
\frac{\Delta z_b + \Delta h_b}{L_b} &= C_{L,b} \frac{8Q^2}{\pi^2 g D_b^5}, && \text{Pipe } b \qquad (11.20) \\
\frac{\Delta z_c + \Delta h_c}{L_c} &= C_{L,c} \frac{8Q^2}{\pi^2 g D_c^5}, && \text{Pipe } c
\end{aligned}$$

[15]This type of network is sometimes referred to as a serial, or serial-pipe, network.

where $\Delta h = (p_1 - p_2)/\rho g$ for all pipes. Note that only in pipe a is there included an acceleration from zero flow speed (at the surface of the reservoir) to the flow speed in the pipe.[16] For pipe junctions a–b and b–c, the acceleration of the flow is negligible.

Referring to Fig. 11.9, the static pressure at all junctions is continuous, so that $p_{b1} = p_{a2}$ and $p_{c1} = p_{b2}$. With the static head at the delivery location of h_{del} and the static pressure of zero at the source ($h_{c2} = h_{del}$, $p_{a1} = 0$), we obtain

$$\begin{aligned}
\frac{\Delta z_a - h_{j,ab}}{L_a} &= (C_{L,a} + \alpha\frac{D_a}{L_a})\frac{8Q^2}{\pi^2 g D_a^5}, && \text{Pipe } a \\
\frac{\Delta z_b + h_{j,ab} - h_{j,bc}}{L_b} &= C_{L,b}\frac{8Q^2}{\pi^2 g D_b^5}, && \text{Pipe } b \qquad (11.21) \\
\frac{\Delta z_c + h_{j,bc} - h_{del}}{L_c} &= C_{L,c}\frac{8Q^2}{\pi^2 g D_c^5}, && \text{Pipe } c
\end{aligned}$$

where the term $h_{j,ab}$ is the static pressure head at junction of pipes a and b, and so on.

11.5.2 Solution and Mathcad Worksheet

Equation (11.21) contains three nonlinear algebraic equations in the unknowns D_a, D_b, and D_c. To solve, we need to supply the static pressure heads at the two junctions, $h_{j,ab}$ and $h_{j,bc}$. To illustrate the solution, consider the data of Table 11.4. The value for Q is 2.10 L/s. Guided by the discussion in Section 11.4.2 and from the previous example, we choose 7 m of head for $h_{j,ab}$ and $h_{j,bc}$. The solution is carried out in the `Mathcad` worksheet using the `Given...Find` construct (see Figs. 11.10 and 11.11). The forward solution for D_a, D_b, and D_c gives 2.287, 1.623, and 1.352 in., respectively. Thus, we choose nominal $2\frac{1}{2}$-in., 2-in, and $1\frac{1}{2}$ PVC pipe. The reverse solution shows a considerable increase in the values for the junction pressure heads compared with the values that we initially prescribed. Though large, they are within acceptable pressure limits for IPS series, sch. 40 PVC pipe (Table 3.3).[17] A throttling valve, normally installed at the bottom of pipe c, will reduce the static pressure head before the tapstand at the outlet.

11.5.3 An Extension: Sensitivity Study Revisited

Suppose we wish to extend our analysis of this problem and perform a sensitivity (or "parametric') study on the effect of junction pressure head on D. The results of this are presented in Figs. 11.12 and 11.13. In Fig. 11.12, the effect of junction pressure head $h_{j,ab}$ is shown for fixed values of $h_{j,bc} = 7$ m and $h_{del} = 10$ m. Diameters D_b and D_c show little sensitivity to $h_{j,ab}$ because the dominant source of energy for flow

[16]The numerical value for $\alpha D_a/L_a$ may, in fact, be negligible compared with $C_{L,a}$.

[17]Recall from the discussion in Section 3.5 that pressure energy in a gravity-driven water network is the only local energy source over which the designer normally has control. Thus, high pressures are desirable for a design provided they are not unacceptable from the standpoint of the pipe pressure rating.

Solved in forward way (specify volume flow rates and solve for pipe diameters vs. junction heads):

$D_a := 1 \cdot in \quad D_b := 1 \cdot in \quad D_c := 1 \cdot in$ guesses

Input Parameters:

$L_a := 427 \cdot m \quad Q := 2.1 \cdot \frac{liter}{sec} \quad K_a := 50 \quad L_{ebyD\_a} := 0 \quad \Delta z_a := 14 \cdot m$

$L_b := 710 \cdot m \quad h_{del} := 10 \cdot m \quad K_b := 0 \quad L_{ebyD\_b} := 0 \quad \Delta z_b := 46 \cdot m$

$L_c := 187 \cdot m \quad K_c := 0 \quad L_{ebyD\_c} := 0 \quad \Delta z_c := 32 \cdot m$

Define energy equation functions:

$$r_a(h_{jab}, D_a) := \Delta z_a - h_{jab} - \left[K_a + \alpha\left(Re(|Q|, D_a)\right) + fric\_fac\left(Re(|Q|, D_a), \frac{\varepsilon}{D_a}\right)\left(\frac{L_a}{D_a} + L_{ebyD\_a}\right)\right] \cdot \frac{8 \cdot Q^2}{\pi^2 \cdot g \cdot D_a^4}$$

$$r_b(h_{jab}, h_{jbc}, D_b) := \Delta z_b + h_{jab} - h_{jbc} - \left[K_b + fric\_fac\left(Re(|Q|, D_b), \frac{\varepsilon}{D_b}\right)\left(\frac{L_b}{D_b} + L_{ebyD\_b}\right)\right] \cdot \frac{8 \cdot Q^2}{\pi^2 \cdot g \cdot D_b^4}$$

$$r_c(h_{jbc}, D_c) := \Delta z_c + h_{jbc} - h_{del} - \left[K_c + fric\_fac\left(Re(|Q|, D_c), \frac{\varepsilon}{D_c}\right)\left(\frac{L_c}{D_c} + L_{ebyD\_c}\right)\right] \cdot \frac{8 \cdot Q^2}{\pi^2 \cdot g \cdot D_c^4}$$

Solve in Given...Find block

Given $\quad 0 = r_a(h_{jab}, D_a) \quad 0 = r_b(h_{jab}, h_{jbc}, D_b) \quad 0 = r_c(h_{jbc}, D_c) \quad D_s(h_{jab}, h_{jbc}) := Find(D_a, D_b, D_c)$

$D_a(h_{jab}, h_{jbc}) := D_s(h_{jab}, h_{jbc})_1 \quad D_b(h_{jab}, h_{jbc}) := D_s(h_{jab}, h_{jbc})_2 \quad D_c(h_{jab}, h_{jbc}) := D_s(h_{jab}, h_{jbc})_3$

$h_{jab} := 7 \cdot m \quad h_{jbc} := 7 \cdot m \quad D_a(h_{jab}, h_{jbc}) = 2.287in \quad D_b(h_{jab}, h_{jbc}) = 1.623in \quad D_c(h_{jab}, h_{jbc}) = 1.352in$

$h_{jabv} := 1 \cdot m, 1.1 \cdot m .. 13 \cdot m$

$h_{jbcv} := 1 \cdot m, 2 \cdot m .. 31 \cdot m$

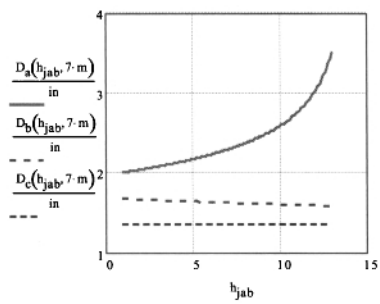

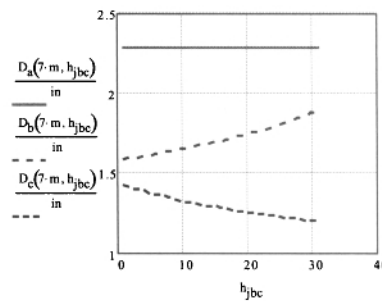

Figure 11.10 Mathcad worksheet for a three-pipe series network. Forward solution (see Fig. 11.3 for the preliminary material needed for this calculation). Mathcad worksheet NumberPipesSeries_Example.xmcd.

Table 11.4 The Design Parameter Values for a Serial Network of Three Pipes

Pipe	L (m)	K	L_e/D	Δz (m)	h_{del} (m)
a	427	50	0	14	
b	710	0	0	46	
c	187	0	0	6	10

Solved in reverse way (specify pipe diameters and solve for the junction pressure heads):

$h_{jab} := 7 \cdot m \qquad h_{jbc} := 7 \cdot m$ guesses

Input Parameters:

$K_a := 50 \qquad K_b := 0 \qquad K_c := 0$

$$r_a(h_{jab}, D_a) := \Delta z_a - h_{jab} - \left[K_a + \alpha\left(Re\left(|Q|, D_a\right)\right) + fric\_fac\left(Re\left(|Q|, D_a\right), \frac{\varepsilon}{D_a}\right)\left(\frac{L_a}{D_a} + L_{ebyD\_a}\right)\right] \cdot \frac{8 \cdot Q^2}{\pi^2 \cdot g \cdot D_a^4}$$

$$r_b(h_{jab}, h_{jbc}, D_b) := \Delta z_b + h_{jab} - h_{jbc} - \left[K_b + fric\_fac\left(Re\left(|Q|, D_b\right), \frac{\varepsilon}{D_b}\right)\left(\frac{L_b}{D_b} + L_{ebyD\_b}\right)\right] \cdot \frac{8 \cdot Q^2}{\pi^2 \cdot g \cdot D_b^4}$$

$$r_c(h_{jbc}, h_{del}, D_c) := \Delta z_c + h_{jbc} - h_{del} - \left[K_c + fric\_fac\left(Re\left(|Q|, D_c\right), \frac{\varepsilon}{D_c}\right)\left(\frac{L_c}{D_c} + L_{ebyD\_c}\right)\right] \cdot \frac{8 \cdot Q^2}{\pi^2 \cdot g \cdot D_c^4}$$

Given $0 = r_a(h_{jab}, D_a) \quad 0 = r_b(h_{jab}, h_{jbc}, D_b) \quad 0 = r_c(h_{jbc}, h_{del}, D_c) \quad h_s(D_a, D_b, D_c) := Find(h_{jab}, h_{jbc}, h_{del})$

$$h_s(D_6, D_5, D_4) = \begin{pmatrix} 9.068 \\ 40.598 \\ 60.018 \end{pmatrix} m$$

Figure 11.11 Mathcad worksheet for a three-pipe series network. Reverse solution (see Figs. 11.3 and 11.10 for the preliminary material needed for this calculation). Mathcad worksheet NumberPipesSeries_Example.xmcd.

in these two pipes is potential energy, not pressure, as we can see from inspection of Table 11.4. This is contrasted with D_a, which demonstrates considerable sensitivity to $h_{j,ab}$ especially as $h_{j,ab}$ approaches the elevation head of 14 m between the source and the pipe junction. The plot of D_a versus $h_{j,ab}$ in this figure is also consistent with the results seen in Fig. 11.11. That is, the actual diameter associated with nominal $2\frac{1}{2}$-in. pipe, which is greater than the calculated theoretical diameter for $h_{j,ab} = 7$ m, produced a pressure head at the a-b junction of > 9 m.

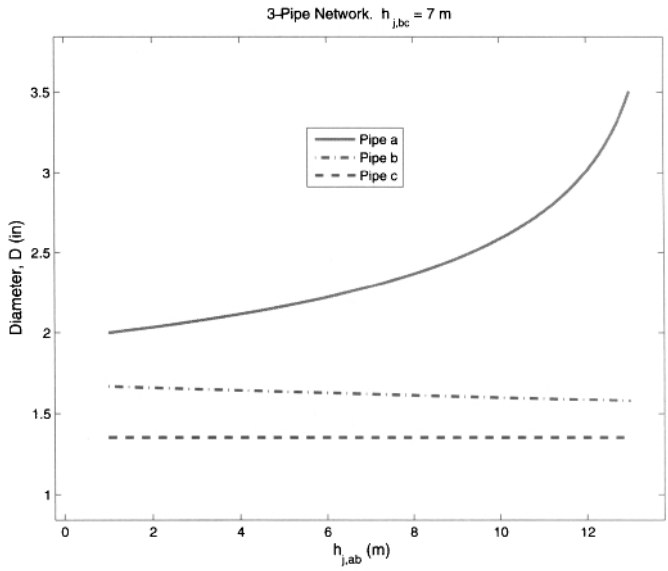

Figure 11.12 The diameters for a serial three-pipe network. $h_{j,bc} = 7$ m and $h_{del} = 10$ m.

Figure 11.13 shows no sensitivity of D_a to $h_{j,bc}$ simply because $h_{j,ab}$ and Q are both fixed values. However, D_c decreases and D_b increases with increased $h_{j,bc}$. To understand this, recall that Δz values, Q, and h_{del} are all fixed. Increasing $h_{j,bc}$ increases the pressure drop between junction bc and the delivery location. To balance this increase in pressure drop the friction must increase between these two points. For fixed Q and Δz_{bc}, this is accomplished with reducing D_c (the smaller cross–sectional area for pipe c increases the flow speed, $\overline{u}_c$, and thus friction). The same argument applies to D_b where the pressure drop between junctions ab and bc decreases with an increase in $h_{j,bc}$. Here, D_b must increase to balance this decreasing pressure difference.

For an n-number of series connected pipes of different diameters, $D_a, D_b, D_c, \ldots, D_n$, where the flow passes from pipe $i = a$, then pipe $i = b$, and so on, the energy equations can be generalized from Eqn (11.21) and written as

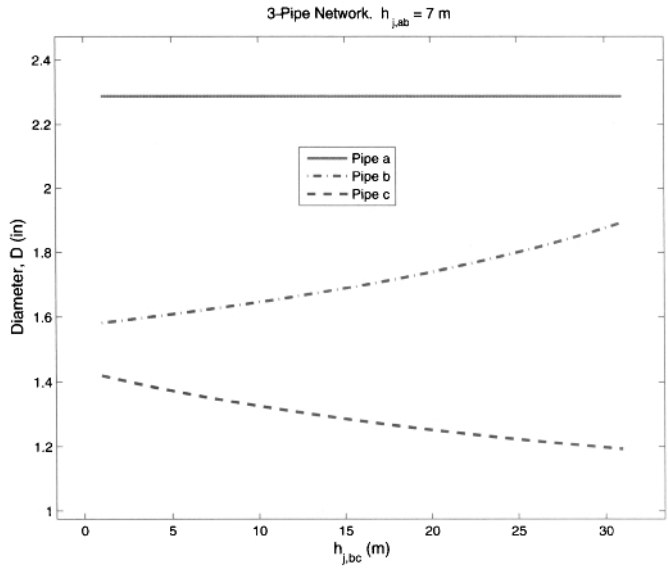

Figure 11.13 The diameters for a three-pipe serial network. $h_{j,ab} = 7$ m and $h_{del} = 10$ m.

$$\begin{aligned}
\frac{\Delta z_a - h_{j,ab}}{L_a} &= (C_{L,a} + \alpha\frac{D_a}{L_a})\frac{8Q^2}{\pi^2 g D_a^5}, \quad \text{Pipe } a \\
\frac{\Delta z_i + h_{j,(i-1)i} - h_{j,i(i+1)}}{L_i} &= C_{L,i}\frac{8Q^2}{\pi^2 g D_i^5}, \quad \text{Pipe } b \leq i \leq n-1 \quad (11.22) \\
\frac{\Delta z_n + h_{j,(n-1)n} - h_{del}}{L_n} &= C_{L,n}\frac{8Q^2}{\pi^2 g D_n^5}, \quad \text{Pipe } n
\end{aligned}$$

where the pipes are lettered $i = a, b, c, \ldots, n$, and it is understood that letter sequencing $b = a - 1$, $c = b - 1$, $d = c - 1$, ... and $a = b + 1$, $b = c + 1$, $c = d + 1$, ... apply. With known pressure heads at all junctions and the delivery location, $h_j = h_{j,ab}, h_{j,bc}, h_{j,cd}, \ldots, h_{j,(n-1)n}, h_{del}$, the solution of Eqn (11.22) is carried out to determine $D = D_a, D_b, D_c, \ldots, D_n$ in the forward solution and, upon setting the values of actual D based on chosen nominal pipe sizes, we solve for $h_j = h_{j,ab}, h_{j,bc}, h_{j,cd}, \ldots, h_{j,(n-1)n}, h_{del}$ in the reverse solution.

We recognize that the indexing scheme in Eqn (11.22) is cumbersome for large problems of the type considered here; using letters as numbers, and so on. See Exercise 41 for a representation of Eqn (11.22) in nodal format that will be used starting with Section11.6.1. The result is Eqn (16.22), which is recommended over the form appearing as Eqn (11.22).

In Section 11.4, we saw that optimal pipe diameters existed for a branch network if we add the constraint of minimum overall pipe cost. The same calculation is performed for the present case of flow in a series of pipes of different diameters. The

static pressure head at the junctions is required to be no less than 7 m and $h_{del} = 10$ m. As we see by inspection of Fig. 11.14, the minimum-cost solution is found where h_j *is equal* to 7 m for all junctions. Thus, pipe cost <$2872 can be obtained only by reducing the allowable values for h_j.

B.11.3 A High-Head, Single-Pipe Network with Local Peak

Communities that are candidates for gravity-driven water networks located in very mountainous regions often need to analyze and design networks of the type in this textbox. Consider the network of Fig. 11.15 and accompanying data in Table 11.5. The topography of the region requires a sharp fall-off in elevation from the source at atmospheric pressure to junction *b–c*, and a 43-meter climb to a local peak at junction *c–d*. You are asked to determine the theoretical pipe diameters for each of the five segments of this network that minimize the total pipe cost. The following constraints apply: static pressure heads at the junctions must be 10 m or more and less than hydrostatic. Before beginning the analysis, we will assure ourselves that the hydrostatic pressure is less than the rated pressure for the pipe material and wall thickness we are considering. A factor of safety should be included in this, as will be discussed in Chapter 13. Report all values for D and h_j. For this problem, $Q = 3.6$ L/s and $h_{del} = 10$ m.

Modify the `Mathcad` worksheet `SeriesPipeExample_equalQ_3pipe_withcost.xmcd` to include the data in Table 11.5. Accurate initial guesses can be supplied by considering hydrostatic conditions and the above constraints. We use $h_{j,ab} = 37$ m, $h_{j,bc} = 55$ m, $h_{j,cd} = 10$ m, and $h_{j,de} = 35$ m. The guess for $h_{j,ab}$ comes from the fact that the head at this location will be slightly less than hydrostatic (39 m), and head $h_{j,bc}$ must be large enough to drive the flow upward 43 m in pipe *c* with a reserve head of 10 m at junction *c–d* and overcome friction along the way.

The solution appears in Table 11.6. The high head at junction *b–c* of ~6 atm (87.5 psig) is not excessive and, with the resulting diameter for pipe *c*, guarantees a minimum of 10 m of head at junction *c–d* [from Section 8.9, the minimum static pressure occurs slightly downstream from junction *c–d* because of friction; we can investigate this by solving for the local pressure distribution from Eqn (6.12)]. The total pipe cost is $3523. A sensitivity study shows that a variation of ±8 m for the heads $h_{j,ab}$ and $h_{j,bc}$ about their respective optimal values of 33.9 m and 61.5 m increases the pipe cost to ~$4200. This gives the designer an feel for the sensitivity of the design to off-optimal conditions.

This completes the forward solution. The next step, if we were to continue this problem, would be to select nominal pipe sizes corresponding to the theoretical diameters, and then complete the reverse solution to determine flow rates and static pressure heads for the actual pipe sizes.

A 3-pipe network solved in forward way (specify volume flow rate and solve for pipe diameters vs. junction heads):

$D_a := 1 \cdot in \quad D_b := 1 \cdot in \quad D_c := 1 \cdot in$ guesses

Input Parameters:

$L_a := 427 m \quad Q_a := 2.10 \frac{liter}{sec} \quad K_a := 50 \quad L_{ebyD\_a} := 0 \quad \Delta z_a := 14 \cdot m$

$h_{del} := 10 \cdot m \quad L_b := 710 m \quad Q_b := 2.10 \frac{liter}{sec} \quad K_b := 0 \quad L_{ebyD\_b} := 0 \quad \Delta z_b := 46 m$

$h_j := 7 \cdot m \quad L_c := 187 m \quad Q_c := 2.10 \frac{liter}{sec} \quad K_c := 0 \quad L_{ebyD\_c} := 0 \quad \Delta z_c := 32 \cdot m$

$$Tcost(D_a, D_b, D_c) := linterp(diam, cost, D_a) L_a + linterp(diam, cost, D_b) L_b + (linterp(diam, cost, D_c) L_c)$$

Define energy equation functions: Cost (objective) function

$$r_a(h_{jab}, D_a, Q_a) := \Delta z_a - h_{jab} - \left[K_a + \alpha\left(Re\left(|Q_a|, D_a\right)\right) + fric\_fac\left(Re\left(|Q_a|, D_a\right), \frac{\varepsilon}{D_a}\right)\left(\frac{L_a}{D_a} + L_{ebyD\_a}\right)\right] \cdot \frac{8 \cdot Q_a^2}{\pi^2 \cdot g \cdot D_a^4}$$

$$r_b(h_{jab}, h_{jbc}, D_b, Q_b) := \Delta z_b + h_{jab} - h_{jbc} - \left[K_b + fric\_fac\left(Re\left(|Q_b|, D_b\right), \frac{\varepsilon}{D_b}\right)\left(\frac{L_b}{D_b} + L_{ebyD\_b}\right)\right] \cdot \frac{8 \cdot Q_b^2}{\pi^2 \cdot g \cdot D_b^4}$$

$$r_c(h_{jbc}, D_c, Q_c) := \Delta z_b + h_{jbc} - h_{del} - \left[K_c + fric\_fac\left(Re\left(|Q_c|, D_c\right), \frac{\varepsilon}{D_c}\right)\left(\frac{L_c}{D_c} + L_{ebyD\_c}\right)\right] \cdot \frac{8 \cdot Q_c^2}{\pi^2 \cdot g \cdot D_c^4}$$

Solve in Given...Find block

Given

$0 = r_a(h_{jab}, D_a, Q_a) \quad 0 = r_b(h_{jab}, h_{jbc}, D_b, Q_b) \quad 0 = r_c(h_{jbc}, D_c, Q_c)$

$Ds(h_{jab}, h_{jbc}) := Find(D_a, D_b, D_c)$

$Tc(h_{jab}, h_{jbc}) := Tcost(Ds(h_{jab}, h_{jbc})_1, Ds(h_{jab}, h_{jbc})_2, Ds(h_{jab}, h_{jbc})_3)$

$h_{jab} := \Delta z_a - 1 \cdot m \quad h_{jbc} := \Delta z_b + h_{jab} - 1 \cdot m$ guesses

Problem is in terms of unknowns h.jab, h.jbc. Minimize Tc subject to inequality constraints below.

Given

$h_{jab} \geq h_j \quad h_{jbc} \geq h_j$ h.jab, h.jbc > h.j

$h_{jab} < \Delta z_a \quad h_{jbc} < \Delta z_a + \Delta z_b$ h.jab and h.jbc < hydrostatic

$(h_{jab}\ h_{jbc}) := Minimize(Tc, h_{jab}, h_{jbc})^T \quad (D_a\ D_b\ D_c) := Ds(h_{jab}, h_{jbc})^T$

$Tcost(D_a, D_b, D_c) = 2871.76 dollars \quad D_a = 2.287 in \quad D_b = 1.623 in \quad D_c = 1.246 in \quad h_{jab} = 7 m \quad h_{jbc} = 7 m$

Figure 11.14 Mathcad worksheet for a three-pipe serial network with minimum cost. Forward solution (see Fig. 11.3 for the preliminary material needed for this calculation). Mathcad worksheet SeriesPipeExample_equalQ_3pipe_withcost.xmcd.

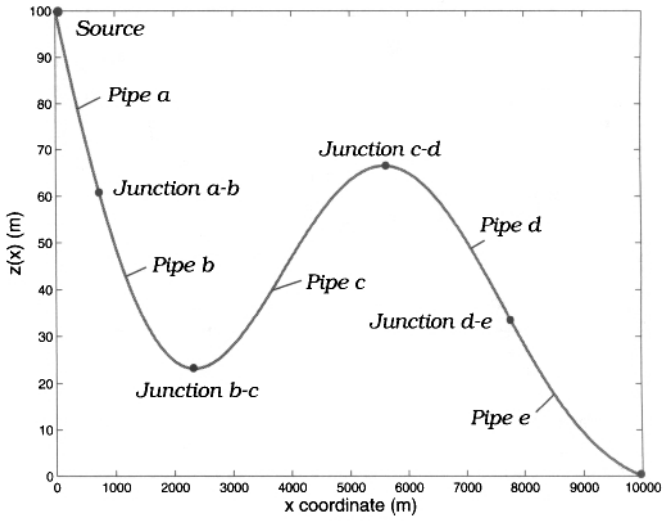

Figure 11.15 A high-head network with local peak.

Table 11.5 Design Parameters for High-Head Network with a Local Peak

Pipe	L (m)	Δz (m)	K	L_e/D
a	187	$100 - 61 = 39$	50	0
b	310	$61 - 24 = 37$	0	20
c	280	$24 - 67 = -43$	0	20
d	220	$67 - 35 = 32$	0	20
e	155	$35 - 0 = 35$	0	20

Table 11.6 Results for High-Head Network with a Local Peak

Pipe	D (in.)	h_j (m)
a	2.71	$h_{j,ab} = 33.9$
b	2.33	$h_{j,bc} = 61.5$
c	2.33	$h_{j,cd} = 10$
d	1.68	$h_{j,de} = 10$
e	1.53	$h_{del} = 10$

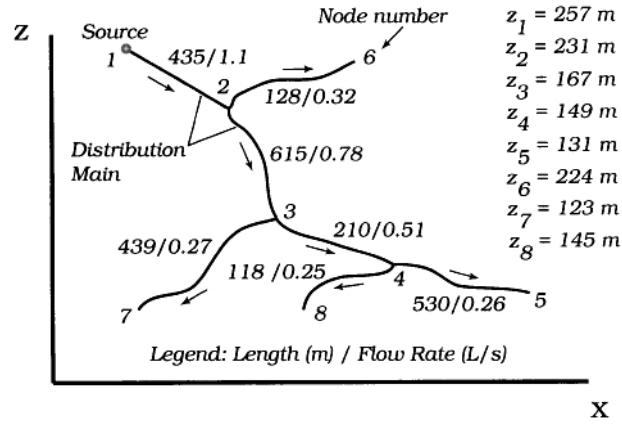

Figure 11.16 A multiple-branch network. Globe valves are installed in all pipe segments except 1–2. Not to scale.

11.6 MULTIPLE-BRANCH NETWORK

11.6.1 The Problem

The multiple-branch network, as an example Fig. 11.16, has elements of both the series and simple-branching networks from the above sections. Specifically, the diameter of the trunk or main[18] normally changes in the direction of flow to account for flow to (for multiple sources) or from the many branches. Because of its ability to cover very large areas having large elevation changes, and the possibility of branching-off of branches in a repeatable manner, it may be the most common of all types of multiple-pipe networks. We will consider this construct now.

First, as the complexity of the network increases it becomes necessary to use a different method than above (where letters were used to designate each pipe) for labeling pipe and other network parts. Each junction, including all starting (source) and ending (delivery) points are labeled with a *node* number, as shown in Fig. 11.16. It is common to start the order of numbering with the source as node 1 and label each node sequentially along the trunk line. Note that in the present case, the trunk line may be thought of as arbitrarily composed of four pipe segments; 12, 23, 34, and 45. The distribution pipes are normally labeled last. Any characteristic for a pipe connected by any two nodes has a symbol (like D, Q, etc.) with the two node numbers appearing as subscripts (a hyphen is used if double-digit nodes are encountered, and if desired for single digit nodes). For example, the pipe connecting nodes 2 and 3 in Fig. 11.16 has an as-yet unknown nominal diameter D_{23}, actual length $L_{23} = 615$ m, and volume flow rate $Q_{23} = 0.78$ L/s, as shown. The elevations for each node are presented in this figure. For diagrams of large networks where there may be inadequate space

[18]This part of network is sometimes referred to as a "distribution main" which we will adopt in this book.

Table 11.7 The Design Parameters for a Multiple-Branch Network

Pipe Subscript, ij	L_{ij} (m)	Q_{ij} (L/s)	$z_i - z_j = \Delta z_{ij}$ (m)	K_{ij}	$(L_e/D)_{ij}$
12	435	1.10	$257 - 231 = 26$	50	0
23	615	0.78	$231 - 167 = 64$	10	20
34	210	0.51	$167 - 149 = 18$	10	20
45	530	0.25	$149 - 131 = 18$	10	20
26	128	0.32	$231 - 224 = 7$	10	60
37	439	0.27	$167 - 123 = 44$	10	60
48	118	0.26	$149 - 145 = 4$	10	60

for all of the labels and numbers that characterize the network, or insufficient detail given concerning pipe fittings and valves, a table can be produced with the relevant information (Table 11.7).[19] Note that we have included several minor losses for each leg of the network that correspond to either entry losses (for pipe 12) or losses from elbows, reducers, and fully opened globe valves, which are shown in Fig. 11.16. Here, h_{del} $(= h_5 = h_6 = h_7 = h_8)$ is fixed at 10 m for this design.

As we have seen in the past, the static pressure heads at each internal node (nodes 2, 3, and 4) are arbitrary and can be determined either by specifying a safe positive value say, 7 m or greater, or by minimizing the cost of the network. We will perform both solutions for the present example.

Using the primitive variable approach, as discussed above, we begin by writing the energy equation for each of the seven pipes in this network. By now, we should be comfortable with doing this. We recognize that the energy equation is from Eqn (11.4) and write it in terms of Q using the continuity equation [see Eqn (2.21)]. With this, the energy equation in general form for a multiple-branch network is

$$\Delta z_{ij} + \Delta h_{ij} = (C_{L,ij} + \alpha_{ij}\frac{D_{ij}}{L_{ij}})\frac{8L_{ij}Q_{ij}^2}{\pi^2 g D_{ij}^5} \tag{11.23}$$

where the subscript ij is a placeholder to identify a pipe with node numbers at its beginning, i, and end, j, and $\Delta h_{ij} = h_i - h_j = (p_i - p_j)/\rho g$. For programming in `Mathcad`, we introduce the definition of C_L from Eqn (11.5) to get

$$\boxed{\Delta z_{ij} + \Delta h_{ij} = \{K_{ij} + \alpha_{ij} + f(Q_{ij}, D_{ij})[\frac{L_{ij}}{D_{ij}} + (\frac{L_e}{D})_{ij}]\}\frac{8Q_{ij}^2}{\pi^2 g D_{ij}^4}} \tag{11.24}$$

In Eqn (11.24), the summation symbols for minor loss terms have been suppressed for simplicity. Thus, it is understood that $K_{ij} = \sum K_{ij}$ and $(\frac{L_e}{D})_{ij} = \sum(\frac{L_e}{D})_{ij}$, where each summation is performed over all minor loss elements in pipe ij.

[19]The peak elevation head of > 100 m was chosen for this example for illustrative purposes only. Though even sch. 40 PVC pipe could withstand the hydrostatic pressure for this design, elevations this large would normally prompt the use of a break-pressure tank thus reducing the peak elevation head.

Following Eqn (11.24), the energy equations for the seven pipes in Fig. 11.16 are

$$
\begin{aligned}
0 &= \Delta z_{12} - h_2 - \{K_{12} + \alpha_{12} + f_{12}[\frac{L_{12}}{D_{12}} + (\frac{L_e}{D})_{12}]\}\frac{8Q_{12}^2}{\pi^2 g D_{12}^4}, && \text{Pipe 12}\\
0 &= \Delta z_{23} + \Delta h_{23} - \{K_{23} + f_{23}[\frac{L_{23}}{D_{23}} + (\frac{L_e}{D})_{23}]\}\frac{8Q_{23}^2}{\pi^2 g D_{23}^4}, && \text{Pipe 23}\\
0 &= \Delta z_{34} + \Delta h_{34} - \{K_{34} + f_{34}[\frac{L_{34}}{D_{34}} + (\frac{L_e}{D})_{34}]\}\frac{8Q_{34}^2}{\pi^2 g D_{34}^4}, && \text{Pipe 34}\\
0 &= \Delta z_{45} + h_4 - h_{del} - \{K_{45} + f_{45}[\frac{L_{45}}{D_{45}} + (\frac{L_e}{D})_{45}]\}\frac{8Q_{45}^2}{\pi^2 g D_{45}^4}, && \text{Pipe 45}\\
0 &= \Delta z_{26} + h_2 - h_{del} - \{K_{26} + f_{26}[\frac{L_{26}}{D_{26}} + (\frac{L_e}{D})_{26}]\}\frac{8Q_{26}^2}{\pi^2 g D_{26}^4}, && \text{Pipe 26}\\
0 &= \Delta z_{37} + h_3 - h_{del} - \{K_{37} + f_{37}[\frac{L_{37}}{D_{37}} + (\frac{L_e}{D})_{37}]\}\frac{8Q_{37}^2}{\pi^2 g D_{37}^4}, && \text{Pipe 37}\\
0 &= \Delta z_{48} + h_4 - h_{del} - \{K_{48} + f_{48}[\frac{L_{48}}{D_{48}} + (\frac{L_e}{D})_{48}]\}\frac{8Q_{48}^2}{\pi^2 g D_{48}^4}, && \text{Pipe 48}
\end{aligned}
\tag{11.25}
$$

where f_{ij} for $ij = 12, 23, \ldots$ means $f(Q_{ij}, D_{ij})$. As we saw in the previous sections, only in pipe 12 is there included an acceleration from zero-flow speed at the surface of the reservoir to the flow speed in the pipe (i.e., an α term). For the remainder of the pipe junctions, the acceleration of the flow through a tee is accounted for with a K-type loss coefficient. As noted in the above paragraph, in Eqs (11.25) the terms h_2, h_3, and h_4 are unknown. Finally, we note that the continuity equation is *identically* satisfied by the specification of the volume flow rates for this problem. That is, the sum of the volume flow rates at each node is zero.

The solution for this design is performed in the Mathcad worksheet `BranchPipe Example_4pipe_withcost_ver2.xmcd`. It appears in Figs. 11.17 and 11.18 for the forward solution and for the reverse solution, Fig. 11.19. As a reminder, the forward solution uses the specified volume flow rates and dimensional data (pipe lengths and elevations) to determine the theoretical inside diameter for each pipe in the network. After selecting pipes of nominal sizes corresponding to this solution (from Chapter 3), the actual inside diameters of the pipes are used together with the specification of the delivery pressures to determine the actual volume flow rates and junction pressures. Most of the design content in sizing pipe for the network comes in the latter step where adjustments to pipe sizes and minor loss coefficients (corresponding to the opening or closing of a globe valve) are made to meet the design specifications.

11.6.2 Mathcad Worksheet

The Mathcad worksheet of Figs. 11.17–11.19 is slightly more involved than those from above so a brief description of the entries in this worksheet will be given before the results are discussed.

- To begin the forward solution, initial guesses for pipe diameters are made (all equal to 1 in.) and the data from Table 11.7 are entered into the worksheet as seen at the top of Fig. 11.17.

- A function for the total cost of the pipe, $Tcost$, is defined and the energy equations from Eqn (11.25) are input, where each is defined as a function r_{ij}, where $ij = 12, 23, 34, \ldots, 48$.

- The energy equations are then solved in functional form in the `Given...Find` block at the top of Fig. 11.18 and the solution for the pipe diameters D_{12}, D_{23}, D_{34}, D_{45}, D_{26}, D_{37}, and D_{48} stored in the row vector $Ds(h_2, h_3, h_4)$. Ds stands for the Diameter solution. For example, diameters D_{12} and D_{23} occupy the first two positions in Ds, which means $D_{12} = Ds_1$, $D_{23} = Ds_2$, and so on. The arguments h_2, h_3, h_4 appear for Ds because the diameters are known to depend on the static pressure heads at nodes 2, 3, and 4.

- The total cost of the pipe material, $T_c(h_2, h_3, h_4)$, is defined next based on the function $Tcost$ identified in Fig. 11.17.

- Preparation for the numerical solution for the minimum pipe cost is done next. The initial guesses for h_2, h_3, h_4 are made (see Section 11.6.4).

- To provide a check on the accuracy of the worksheet thus far, and to get a sense for the pipe diameters, $Ds(h_2, h_3, h_4)$ is evaluated for $h_2 = h_3 = h_4 = 10$ m. The values range from 1.49 to 0.696 in. These results are in scale with the range of pipe sizes typical for moderate-size, gravity-driven water networks. An estimate of the total pipe cost at these values of h is ~$2415.

- In a `Given...Minimize` block in the middle of Fig. 11.18, we solve for the junction heads and pipe diameters that produce a minimum pipe cost. The first part of this block is the constraints. These are that the static pressure heads at each junction must be at least equal to a minimum value; in this case h_{del} of 10 m,

$$h_2 \geq h_{del}, \qquad h_3 \geq h_{del}, \qquad h_4 \geq h_{del} \tag{11.26}$$

  This establishes the lower bound for the junction pressure heads. The upper bound is that the junction pressure heads must be less than the hydrostatic pressure at the respective locations. Thus,

$$h_2 < \Delta z_{12}, \qquad h_3 < \Delta z_{12} + \Delta z_{23}, \qquad h_4 < \Delta z_{12} + \Delta z_{23} + \Delta z_{34} \tag{11.27}$$

  Of course, it is assumed that the designer has already checked to ensure that the hydrostatic pressure is always less than the rupture pressure of the pipe. The second part of the `Given...Minimize` block is the `Minimize` function. This, together with the constraints, produces the solution for the junction heads and pipe diameters. The run time on a dual-core laptop PC with a 2.66-MHz processor for `Mathcad` ver. 14 is ~1 min. Earlier versions of `Mathcad` will run slower.

- The results for total cost, diameters, and junction pressure heads, are shown in the last two lines in Fig. 11.18.
- In Fig. 11.19, actual nominal pipe sizes are first chosen from the results of the forward solution.
- The reverse solution begins next by copying and pasting in the worksheet the values for the minor loss (K) coefficients from Fig. 11.17. These will be adjusted as needed (see Section11.6.3) as part of the design process.
- The total cost based on the selected nominal pipe sizes is calculated.
- The energy equations and continuity equations for flow at each node are solved in a `Given...Find` block for the actual flow rates for each pipe and actual static pressure heads at each junction. The values are reported on the last two lines of this figure.

11.6.3 Solution

The results for this problem are presented in Table 11.8. Nominal $1\frac{1}{2}$-in. sch. 40 PVC pipe is chosen for pipe segment 12 (1.61-in. ID) where the required pipe size is 1.49 in. Globe valves downstream from this segment will compensate for the larger-than-required ID of the chosen pipe size. A 1-in. nominal pipe is chosen for segment 23, this despite the required diameter of 1.12 in. (the ID for 1-in. nominal pipe is 1.049 in.). The reason for this choice is the cost savings between a nominal 1-in. and nominal $1\frac{1}{2}$-in. PVC pipe because of the large length of this segment (615 m). While the cost savings is an obvious benefit, the penalty in using the smaller pipe is that the flow rate in pipe segment 37 is reduced from its design value by $< 10\%$ (worst case). While this is not large, the slightly reduced Q_{37} may be undesirable. In this case, the possibility of obtaining $1\frac{1}{4}$-in. sch. 40 PVC pipe should be investigated, though it is not always available. The pipe sizes for the rest of the segments follow the usual rule of selecting the nominal size that produces an inside diameter slightly larger than the theoretical value.

Our inspection of Table 11.8 shows that the results were obtained by balancing the flow using partially closed globe valves. The solution with full-open valves gives results in decent agreement with the design specifications of Table 11.7. Adjustments to the valves (meaning an adjustment to the K values)[20] allows the designer to gage the sensitivity of the design to the flow-rate demand variations in the various segments of the network. For example, $K_{34} = 100$ for the globe valve installed in this segment functions to slightly reduce D_{34}, increasing the friction in this segment, and forcing additional flow into segments 26 and 37. If, for instance, $K_{34} = 10$ (corresponding to an open globe valve), $Q_{37} = 0.24$ L/s; if $K_{34} = 400$ (corresponding to partially closed globe valve), $Q_{37} = 0.27$ L/s. The designer is encouraged to perform this sensitivity study to get a sense for the balance characteristic of the network.

[20]The equivalent-length minor loss coefficients are unchanged from those specified.

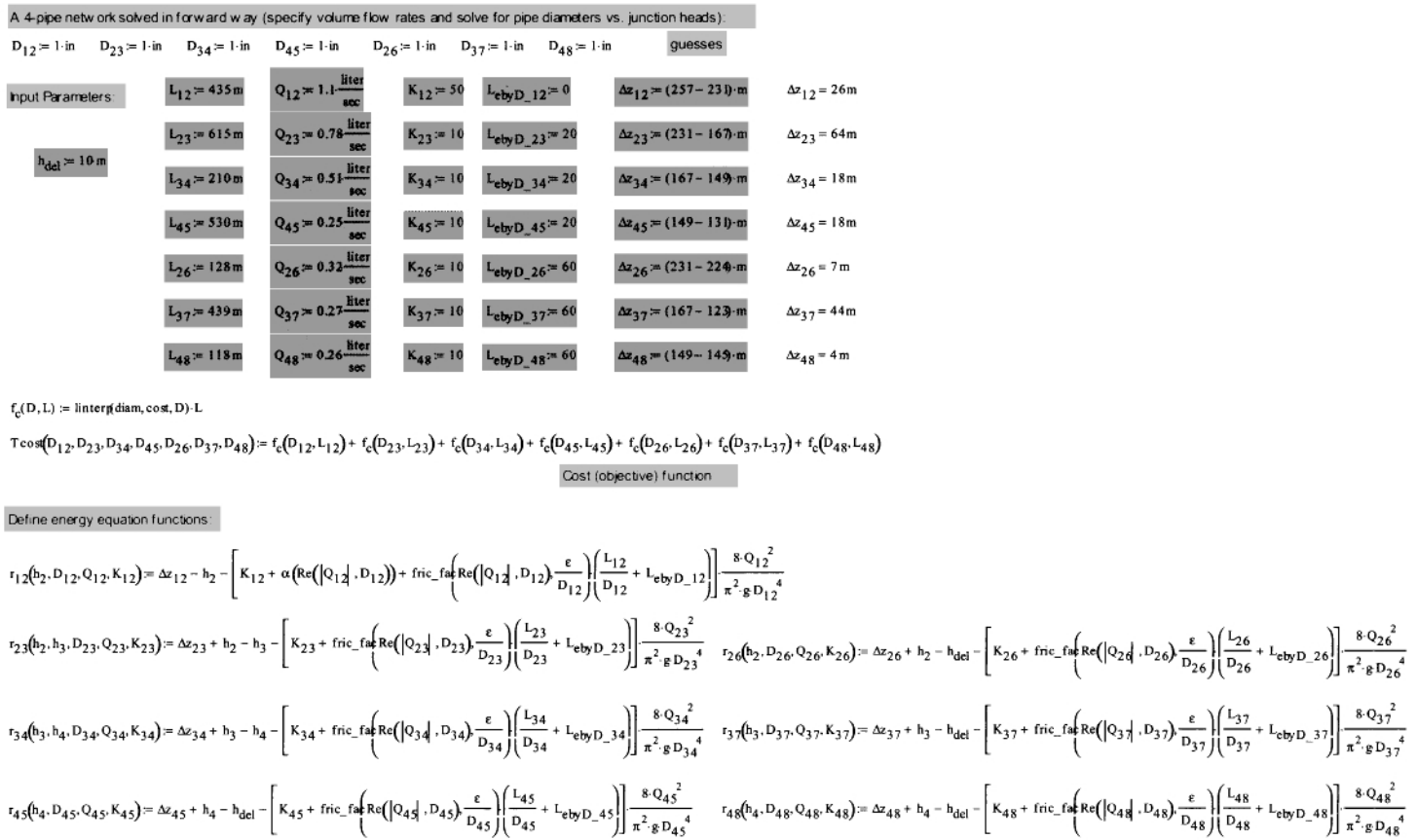

Figure 11.17 Part 1 of Mathcad worksheet for a four-pipe branch network with minimum cost. Forward solution (see Fig. 11.3 for the preliminary material needed for this calculation). Continued in Fig. 11.18. Mathcad worksheet BranchPipeExample_4pipe_withcost_ver2.xmcd.

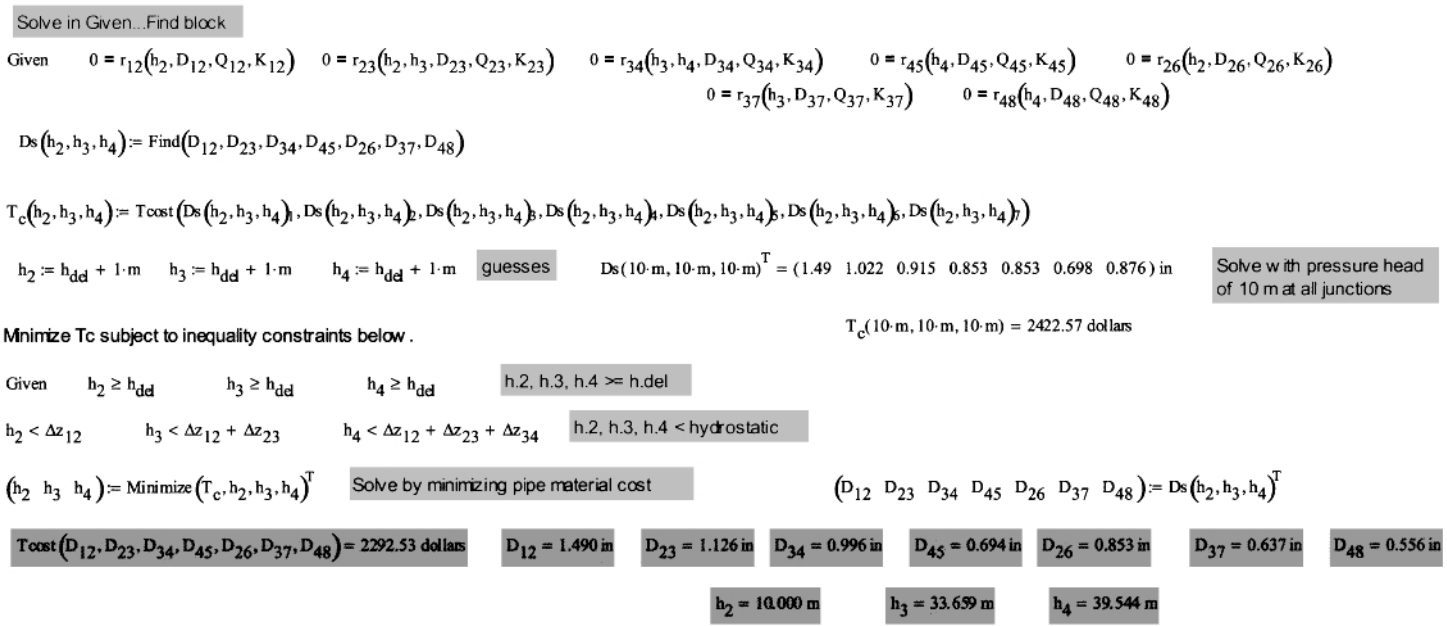

Figure 11.18 Part 2 of Mathcad worksheet for a four-pipe branch network with minimum cost. Forward solution. Continued from Fig. 11.17. Mathcad worksheet BranchPipeExample_4pipe_withcost_ver2.xmcd.

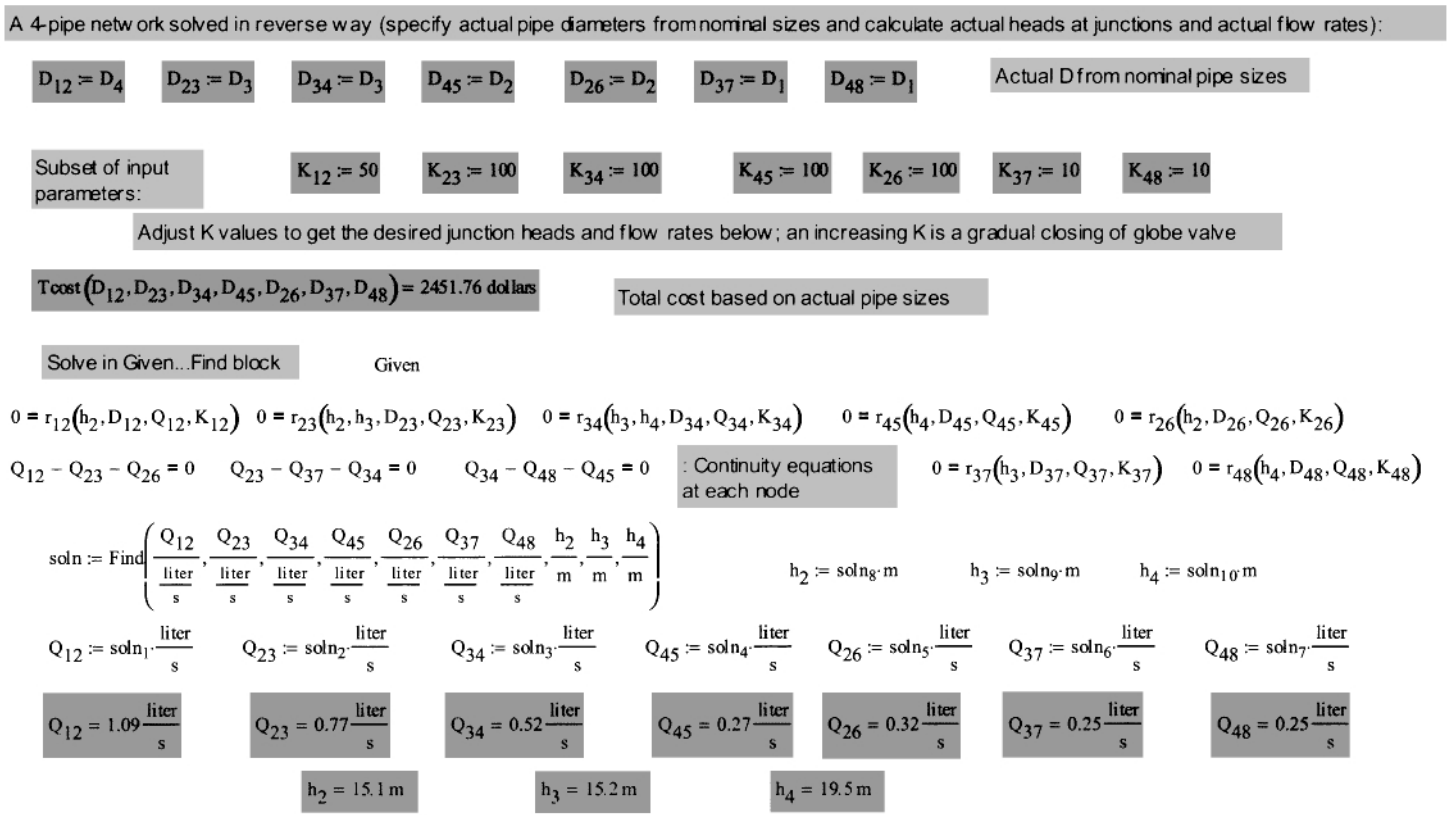

Figure 11.19 Part 3 of Mathcad worksheet for a four-pipe branch network with minimum cost. Reverse solution. Mathcad worksheet BranchPipeExample_4pipe_withcost_ver2.xmcd.

Table 11.8 Solution for a Multiple-Branch Network

Subscript, ij	L_{ij} (m)	Q_{ij}[a] (L/s)	Δz_{ij} (m)	K_{ij}[b]	D_{ij}[c] (in.)	Nom. D (in.)
12	435	1.09 [1.10]	26	50	1.49	$1\frac{1}{2}$
23	615	0.77 [0.78]	64	100	1.13	1
34	210	0.52 [0.51]	18	100	0.996	1
45	530	0.27 [0.25]	18	100	0.694	$\frac{3}{4}$
26	128	0.32 [0.32]	7	100	0.853	$\frac{3}{4}$
37	439	0.25 [0.27]	44	10	0.637	$\frac{1}{2}$
48	118	0.25 [0.26]	4	10	0.556	$\frac{1}{2}$

[a]Actual flow rates from the reverse solution. Values in square braces are design-specified flow rates (all valves open) from Table 11.7.
[b]Required to produce flow rates Q_{ij}.
[c]From the forward solution.

An extension of this sensitivity study would be to assess the performance of the design when parts of the network are turned off. In the reverse solution (only) in the Mathcad worksheet this is done by:

- In the Given...Find block, setting the flow rate for this segment to zero (using CTRL =).

- Removing[21] the energy equation for the turned-off segment from inside the Given...Find block,

Examples of this type of sensitivity study are given in Figs. 11.20 and 11.21. In the first of these, the flow in segment 48 is turned-off. In the second, flows in segments 45 and 48 are turned-off. Note in the latter case, the energy equation for segments 48, 45, and 34 are removed since there is no flow in segment 34 if the flow in segments 45 and 48 stops. The reader will note that, for this type of branching network, flow rates in the remaining active branches generally increase over their design values once flows in other parts of the network are turned-off. In all of the above results, the static pressure heads at nodes 2, 3, and 4 are > 10 m, as required by the solution.

Evidence that the minimum-cost solution has indeed been found for this problem is presented in Figs. 11.22–11.24, where total pipe cost is plotted as a function of the static pressure heads at nodes 2, 3, and 4, respectively. The trend in these plots follows those in Figs. 11.25–11.27, where the pipe-size sensitivity to the static pressure heads at nodes 2, 3, and 4 is shown.

[21]Note that the equation need not be physically removed. Mathcad allows for disabling an evaluation. Right click the mouse while the cursor sits on the equation to get this option. A disabled equation will have a square black dot at its upper-right-most corner.

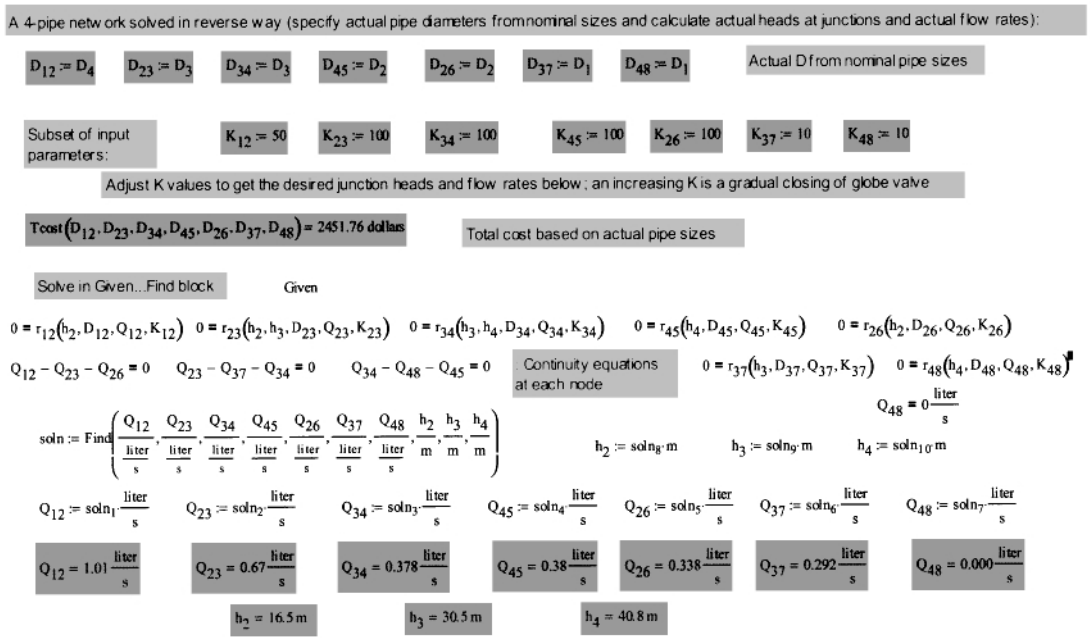

Figure 11.20 Results of a sensitivity study: One segment turned off.

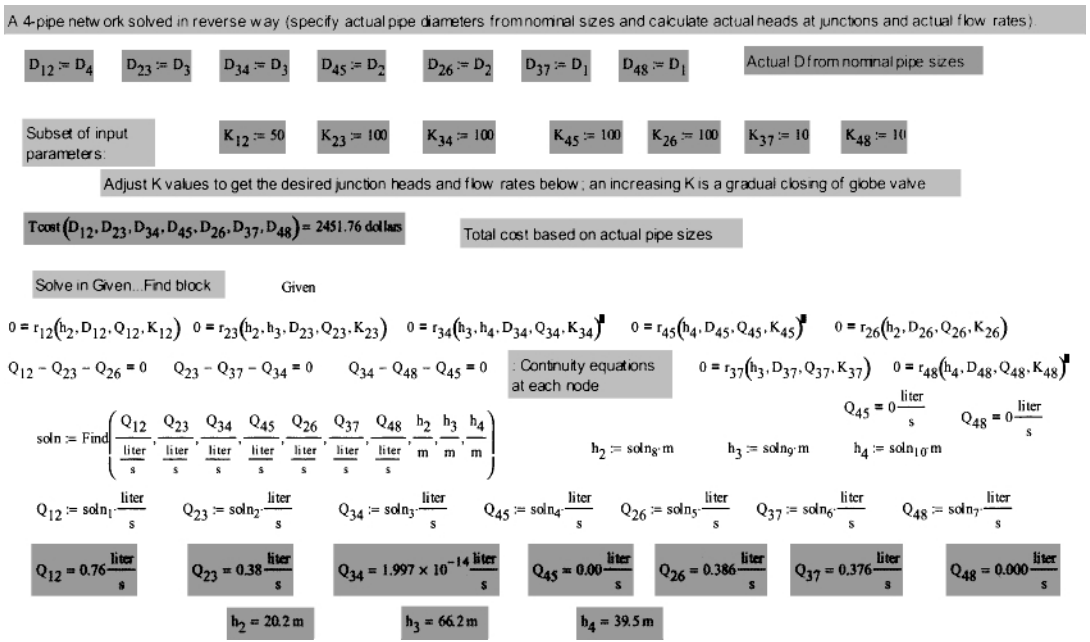

Figure 11.21 Results of a sensitivity study: Two segments turned off.

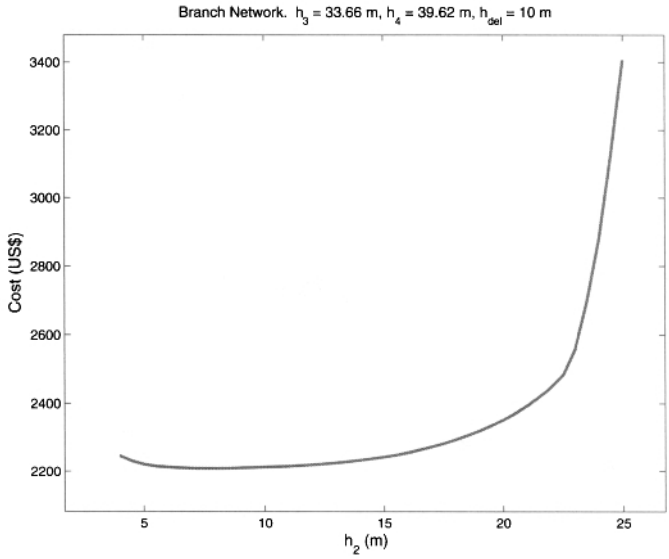

Figure 11.22 Sensitivity of pipe material cost to h_2 for a branch network.

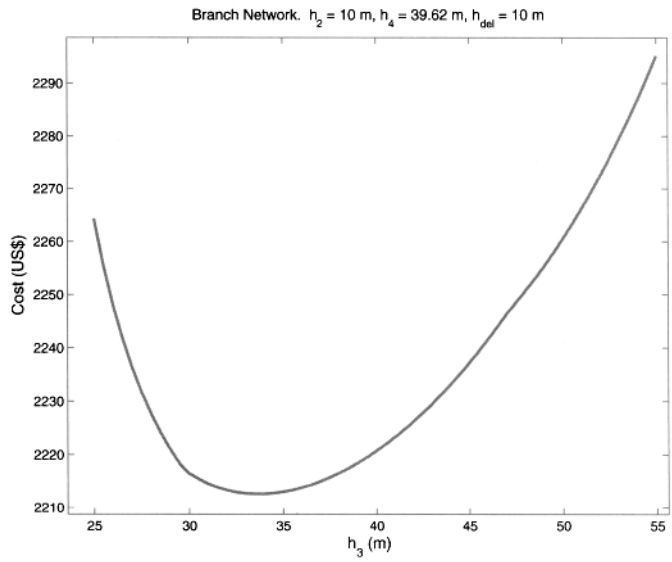

Figure 11.23 Sensitivity of pipe material cost to h_3 for a branch network.

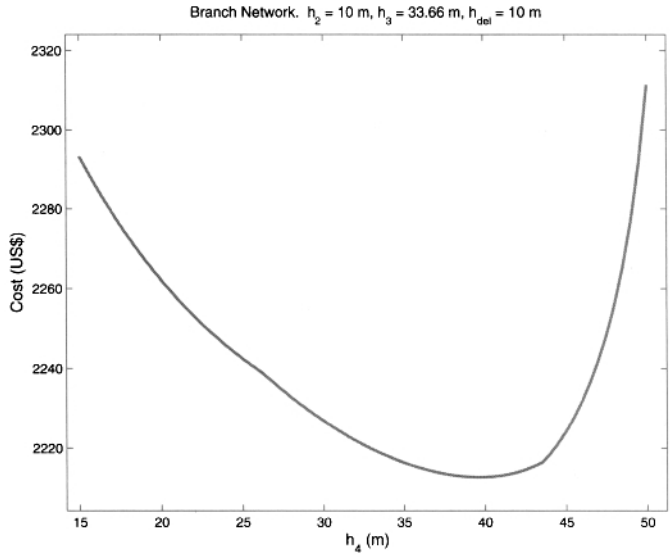

Figure 11.24 Sensitivity of pipe material cost to h_4 for a branch network.

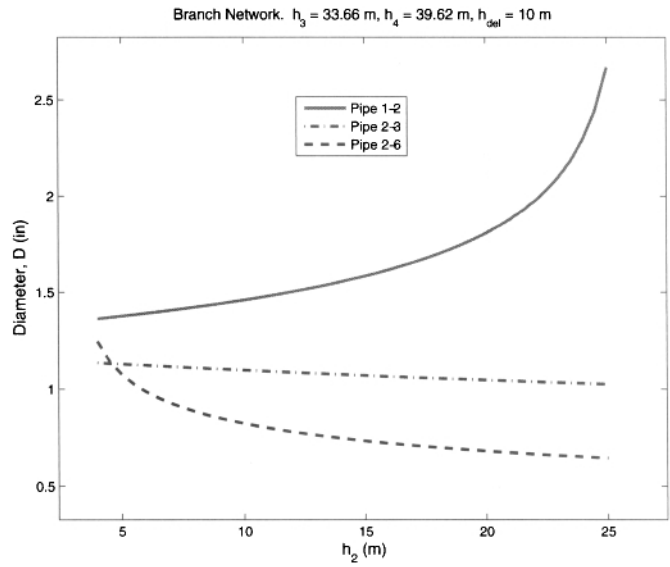

Figure 11.25 Sensitivity of D to h_2 for a branch network with minimum cost. Forward solution.

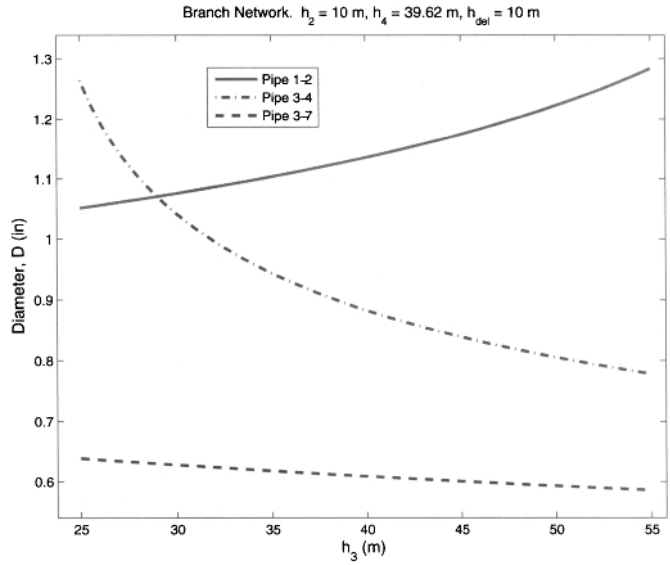

Figure 11.26 Sensitivity of D to h_3 for a branch network with minimum cost. Forward solution.

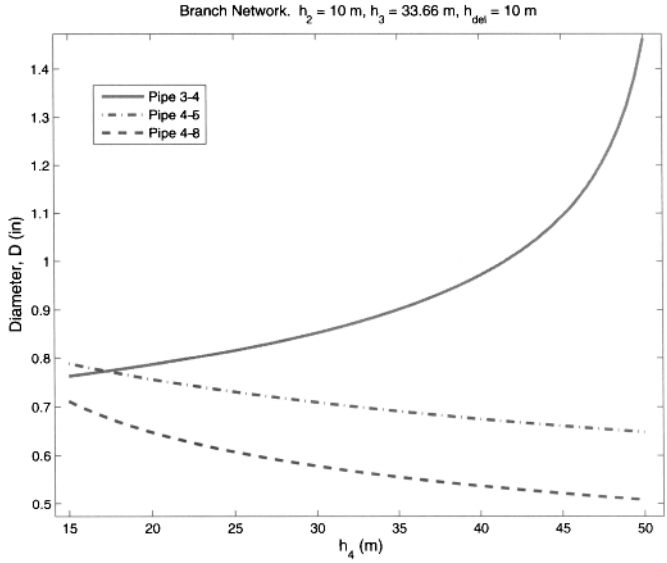

Figure 11.27 Sensitivity of D to h_4 for a branch network with minimum cost. Forward solution.

11.6.4 Choosing Initial Guesses for Static Pressure Heads at Junctions

The numerical solution of the system of equations for multiple-pipe networks requires initial guesses for D and h_j. For convergence of the numerical method, the guessed values of h_j must be realistic for the problem under consideration (so do the initial guesses for D but, as indicated in earlier sections, values ranging from 0.5 to 4 in. are reasonable selections for the scale of networks considered in this book). Inappropriate initial guesses for h_j will cause divergence of the numerical method and no solution will be obtained. In `Mathcad` the equation where the divergence is encountered will turn red, thus indicating a problem.

There are two methods for providing initial guesses for h_j. The first is simply to choose them by following a few basic rules from fluid mechanics. These are

1. $h_j < z_1 - z$, the hydrostatic head, where z is the local elevation of the junction and z_1 is the maximum elevation of the network. See 4 below for details.

2. $h_j > 0$. As noted in Section11.4.2, h_j >7–10 m for network integrity.

3. For a local low point in the network, h_j must be greater than that needed to provide a specified positive head at the highest point downstream when the elevation head difference between this point and the local low point and friction are considered. In equation form this is

$$h_j > \underbrace{\Delta z_{high-low}}_{\Delta z \text{ between highest point downstream and local low point}} + \underbrace{\Delta h_{frict}}_{\text{Frictional head loss between highest point downstream and local low point}} + \underbrace{h_{j,peak}}_{\text{Static pressure head at higest point downstream}}$$

   For example, if a local low point is followed by a peak 25 m higher than it, an initial guess for h_j of 25 m or less will cause divergence of the numerical solution.

4. For a local high point in the network, h_j must be less than the elevation head at the source less the friction between the source and the local high point. In equation form this is

$$h_j < \underbrace{z_1 - z}_{\Delta z \text{ between source and local high point}} - \underbrace{\Delta h_{frict}}_{\text{Frictional head loss between between source and local high point}}$$

   For example, an initial guess for the static pressure head at any junction greater than the elevation of the source is clearly incorrect.

5. For cases where the junction is neither a local high or low point, any initial guess for h_j between hydrostatic and 7–10 m is adequate.

In 3 and 4, Δh_{frict} must be estimated by the designer. Many of the Mathcad worksheets supplied with this book have initial guesses for h_j that use this method.n

The second method is a more systematic approach to supplying the initial guesses for h_j by using the energy equation. Rearranging Eqn (11.24), we obtain

$$-\Delta h_{ij} = \Delta z_{ij} - \{K_{ij} + \alpha_{ij} + f(Q_{ij}, D_{ij})[\frac{L_{ij}}{D_{ij}} + (\frac{L_e}{D})_{ij}]\}\frac{8Q_{ij}^2}{\pi^2 g D_{ij}^4} \quad (11.28)$$

Once initial guesses for D are made, the entire right side of Eqn (11.28) is known and Eqn (11.28) may be applied repeatedly for each node along the distribution main starting from the source, where $h_j = 0$.

To illustrate this procedure, apply Eqn (11.28) to the multiple-branch network of Fig. 11.16. Initial guesses for h_2, h_3, and h_4 are needed for the solution of this problem, along with initial guesses for all D_{ij}. h_2, h_3, and h_4 are calculated from

$$\begin{aligned} h_2 - h_1 = h_2 &= \Delta z_{12} - \{K_{12} + \alpha_{12} + f(Q_{12}, D_{12})[\frac{L_{12}}{D_{12}} + (\frac{L_e}{D})_{12}]\}\frac{8Q_{12}^2}{\pi^2 g D_{12}^4} \\ h_3 - h_2 &= \Delta z_{23} - \{K_{23} + f(Q_{23}, D_{23})[\frac{L_{23}}{D_{23}} + (\frac{L_e}{D})_{23}]\}\frac{8Q_{23}^2}{\pi^2 g D_{23}^4} \\ h_4 - h_3 &= \Delta z_{34} - \{K_{34} + f(Q_{34}, D_{34})[\frac{L_{34}}{D_{34}} + (\frac{L_e}{D})_{34}]\}\frac{8Q_{34}^2}{\pi^2 g D_{34}^4} \end{aligned}$$

where the value of h_2 is calculated from the first of these, h_3 from the second, and h_4 from the third.

Care must be taken to ensure that $h_j > 0$ for all junctions when using this method; see 2 above. Negative h_j values may appear if the initial guesses of D are too small for one or more of the pipe segments upstream from the junction under consideration. Thus, cases where negative values of h_j are calculated can be easily corrected by increasing the size of the initial guesses of D for one or more these pipe segments.

With correct application of either of the above methods, $\Delta z_{ij} + \Delta h_{ij} > 0$ for all segments of the distribution main[22], and the numerical method of solution for the equations of the network should proceed toward convergence.

11.6.5 Importance of Throttling Valves and Their Placement for Flow Balancing

One of the key "takeaway" points from Section11.6.3 is the importance of strategically placed globe valves in most of the segments of a multiple-branch network. This was first noted in Section 3.5 and included here for re-emphasis. For most networks, an

[22]This is a necessary condition since the frictional head loss must be positive. See Eqn (11.24).

open globe valve [having $K =\sim 10$; see Eqn (2.11)] does not measurably penalize performance. Thus, other than possibly valve cost, there is little or no disadvantage to their strategic installation. As discussed in Section 3.5, and illustrated with the example above, globe valves give the designer flexibility in balancing flows in multiple branch and (and as we will see below, loop) networks and, when closed, allow the removal of pipe and components for maintenance and repair.

B.11.4 Getting Started: Working with `Mathcad` Worksheet for a Multiple-Branch Network

The first step in gaining confidence to solve the more challenging multiple-branch network problems is to just "dive in" to an appropriate `Mathcad` worksheet. The easiest way to do this is to make a simple change to an existing worksheet, like with the serial-network problem above, and examine and scrutinize the results of the change. This can be repeated for several cases until we begin to feel comfortable with the worksheet and get a sense for cause and effect in the networks we are modeling. With this in mind, consider the network of Fig. 11.16 and accompanying data in Table 11.7. In the worksheet `BranchPipeExample_4pipe_withcost_ver2.xmcd`, increase all flow rates by 50% and reduce all elevations by a product of 80% and examine the solutions for the cases listed below. Report the theoretical pipe diameters and total pipe cost. Comment on the changes. Do they make sense from an engineering standpoint? How do the pipe sizes and total cost change with different values for the junction static pressure heads over their range as recommended in Section 11.4.2? To reduce the execution time, ignore by deleting or disabling the lines beyond the text line "Minimize Tc subject to inequality constraints below" and calculate the diameters for fixed values of h_2, h_3, and h_4. Choose h_2, h_3, and h_4 of 7 m (lower limit; Case 1), 10 m (Case 2), 15 m (Case 3), 20 m (Case 4) and, as an upper limit, 90, 80, and 70% of the hydrostatic pressures at nodes 2, 3, and 4, respectively (Case 5).

Make the requested changes in Q_{ij} and Δz_{ij} to obtain the values for actual pipe diameters. Examine the cases where the pressure heads at the junctions are:

- Uniform at 7, 10, 15, and 20 m (Cases 1–4).
- Vary according to 90, 80, and 70% of the hydrostatic pressures at nodes 2, 3, and 4 ($0.9 \cdot \Delta z_1, 0.8 \cdot (\Delta z_1 + \Delta z_2), 0.7 \cdot (\Delta z_1 + \Delta z_2 + \Delta z_3)$ (Case 5).

Our inspection of the results presented in Table 11.9 prompts several interesting observations. First, as h_1 increases, we expect D_{12} to increase as seen in Table 11.9 because a larger pipe size is needed to reduce the segment-12 friction loss to achieve the larger values of h_1. The difference between the static pressure

Working with `Mathcad` Worksheet for a Multiple-Branch Network (Cont'd)

heads at nodes 2, 3, and 4 is zero for cases 1–4. The pipe sizes for segments 23 and 34 are thus determined solely by the elevation changes Δz_{23} and Δz_{34}, respectively [see Eqs (11.25)], so D_{23} and D_{34} do not change for these cases as observed in Table 11.9. The competition between the increase in D_{12} and decrease in D_{45}, D_{26}, D_{37}, and D_{48} produces an optimal result for h of ~10 m at each internal node. The actual result determined by running the worksheet for the flow rates and elevations modified as above does indeed give h_2 of 10 m. Another observation is that D_{26}, D_{37}, and D_{48} all reduce in value for cases 1–4 as expected because of the increasingly larger pressures at nodes 2–4. Finally, we see that the largest total cost is associated with the largest static pressure heads at nodes 2–4, case 5. Thus, we see different engineering tradeoff here. The desirable larger pressures at internal nodes, which can allow flexibility in the network, say for unanticipated future expansion, come at a price of larger pipe sizes.

Keep in mind that it is seldom necessary to start a worksheet in `Mathcad` from scratch. Always modify an existing worksheet that already successfully performs calculations similar, or identical, to those you are attempting. For example, you would modify an existing worksheet for an 18-leg network if you have one that already runs for a 12-leg network.

B.11.5 The Effect of Turning Off Segments of a Multiple-Branch Network

The following exercise is worthwhile to become familiar with the sensitivity of flow in the remaining active parts of the network when flow is shut off in the other parts. Consider the network of Fig. 11.16 and accompanying data Table 11.7. In the worksheet `BranchPipeExample_4pipe_withcost_ver2.xmcd`, independently turn off the flow in the branches of segments 26, 37, 48, and 45 in the *reverse* solution. The nominal pipe sizes for the network as shown in Table 11.8 apply as well as the final values for K. Examine the response of the flow rates through the remaining segments. Follow the procedure described in Section 11.6.3.

There are two simple changes to the worksheet `BranchPipeExample_4pipe_withcost_ver2.xmcd` needed for the solution of any one of these four cases:

- Inside the `Given...Find` block, set the flow rate to zero for the segment you wish to shut-off.
- Disable the energy equation for this segment (inside the `Given...Find` block).

Table 11.9 Results from Textbox B.11.4 – Working with a `Mathcad` Worksheet for a Multiple-Branch Network

Case	h_1 (m)	h_2 (m)	h_3 (m)	D_{12} (in.)	D_{23} (in.)	D_{34} (in.)	D_{45} (in.)	D_{26} (in.)	D_{37} (in.)	D_{48} (in.)	Total Cost ($)
1	7	7	7	1.801	1.245	1.116	1.090	1.227	0.865	1.949	3259
2	10	10	10	1.899	1.245	1.116	1.037	1.040	0.849	1.068	3111
3	15	15	15	2.173	1.245	1.116	0.973	0.908	0.825	0.873	3314
4	20	20	20	3.354	1.245	1.116	0.927	0.836	0.805	0.789	4750
5	18.72	57.60	60.48	2.719	1.681	1.170	0.754	0.851	0.708	0.585	4207

The Effect of Turning Off Segments of a Multiple-Branch Network (Cont'd)

The result reported by Mathcad should show that the flow rate in the segment that is turned off is indeed zero. Refer to Figs. 11.20–11.21 for the appearance of the worksheet with these changes.

The results of this analysis are presented in Table 11.10. From our inspection of this table, we see that when the flow to one segment is shut off, the flow rates to the remaining active segments of the network increase over their respective values that existed when all segments were open. Thus, a general conclusion from this exercise is that *shutting off segments of a multiple-branch network of the type seen in Fig. 11.16 will provide more than the design-specified flow rates to those segments that remain open.* Of course, the designer can modify the Mathcad worksheet to investigate the effects of turning off various combinations of two or more segments, but it expected that the above conclusion will apply in all cases.

11.6.6 Contribution of Cost Minimization to the Solution

In this section, we look at how imposing cost minimization on the problem of gravity-driven water flow in networks makes the forward solution unique. Refer to the example of the four-pipe, three-branch network of Fig. 11.16 for a moment. Note that there are seven energy equations [Eqs (11.25)] and seven unknown pipe diameters. The volume flow rates are specified and thus mass conservation is identically satisfied. However, the three static pressure heads, h_2, h_3, and h_4, at the junctions are unknown and in the absence of any other constraint, have arbitrary values. With no additional constraint the forward solution, which gives the theoretical pipe diameters, is clearly non-unique. This issue was the subject of footnote 10. In this note, we also saw that the reverse solution is unique because the energy *and continuity* equations are used.

We have claimed above that introducing cost minimization adds the constraint needed to determine the static pressure heads to make the forward solution unique. But, exactly how does it perform this task? We will explore the answer to this question now.

In addition to pipe lengths (the values for which are fixed), the total cost depends on the diameters for all of the pipes in the network. For the case of Fig. 11.16, we get,

$$C_T = C_T(D_{12}, D_{23}, D_{34}, D_{45}, D_{26}, D_{37}, D_{48}) \tag{11.29}$$

Our inspection of Eqs (11.25) shows that D_{12}, D_{23}, and D_{26}, in turn, depend on h_2; D_{23}, D_{34}, and D_{37} depend on h_3, and so on. With this, Eqn (11.29) is written in "functional form" as,

$$C_T = C_T(D_{12}(h_2), D_{23}(h_2, h_3), D_{34}(h_3, h_4), D_{45}(h_4), D_{26}(h_2), D_{37}(h_3), D_{48}(h_4)) \tag{11.30}$$

Table 11.10 Results from Effect of Turning Off Segments of a Multiple-Branch Network[a]

Case	h_1 (m)	h_2 (m)	h_3 (m)	Q_{12} (L/s)	Q_{23} (L/s)	Q_{34} (L/s)	Q_{45} (L/s)	Q_{26} (L/s)	Q_{37} (L/s)	Q_{48} (L/s)
Segment 26 Off	19.83	16.95	20.45	0.789	0.789	0.535	0.278 [0.26]	0 [0.32]	0.255 [0.27]	0.256 [0.25]
Segment 37 Off	16.61	32.25	29.03	0.998	0.658	0.658	0.323 [0.26]	0.340 [0.32]	0 [0.27]	0.335 [0.25]
Segment 48 Off	16.45	30.54	40.78	1.008	0.670	0.378	0.378 [0.26]	0.338 [0.32]	0.292 [0.27]	0 [0.25]
Segment 45 Off	16.23	28.14	37.54	1.021	0.686	0.401	0 [0.26]	0.335 [0.32]	0.286 [0.27]	0.401 [0.25]

[a] Values in square braces are design-specified flow rates (all valves open) from Table 11.7.

Using the chain rule from calculus, the total differential of Eqn (11.30) is written as,[23]

$$\begin{aligned} dC_T &= \frac{\partial C_T}{\partial D_{12}}\frac{\partial D_{12}}{\partial h_2}\,dh_2 + \frac{\partial C_T}{\partial D_{23}}\frac{\partial D_{23}}{\partial h_2}\,dh_2 + \frac{\partial C_T}{\partial D_{26}}\frac{\partial D_{26}}{\partial h_2}\,dh_2 \\ &+ \frac{\partial C_T}{\partial D_{23}}\frac{\partial D_{23}}{\partial h_3}\,dh_3 + \frac{\partial C_T}{\partial D_{34}}\frac{\partial D_{34}}{\partial h_3}\,dh_3 + \frac{\partial C_T}{\partial D_{37}}\frac{\partial D_{37}}{\partial h_3}\,dh_3 \\ &+ \frac{\partial C_T}{\partial D_{34}}\frac{\partial D_{34}}{\partial h_4}\,dh_4 + \frac{\partial C_T}{\partial D_{45}}\frac{\partial D_{45}}{\partial h_4}\,dh_4 + \frac{\partial C_T}{\partial D_{48}}\frac{\partial D_{48}}{\partial h_4}\,dh_4 \end{aligned} \tag{11.31}$$

Recalling material from Chapter 10, the minimum value of C_T is found once $dC_T = 0$ (this condition is necessary, but not sufficient; we also need to verify that the second derivative of C_T is positive thus indicating that C_T is a minimum). Require this and group terms common to multipliers of dh_2, dh_3, and dh_4, respectively, from Eqn (11.31) to obtain three independent algebraic equations,

$$\begin{aligned} 0 &= \frac{\partial C_T}{\partial D_{12}}\frac{\partial D_{12}}{\partial h_2} + \frac{\partial C_T}{\partial D_{23}}\frac{\partial D_{23}}{\partial h_2} + \frac{\partial C_T}{\partial D_{26}}\frac{\partial D_{26}}{\partial h_2} \\ 0 &= \frac{\partial C_T}{\partial D_{23}}\frac{\partial D_{23}}{\partial h_3} + \frac{\partial C_T}{\partial D_{34}}\frac{\partial D_{34}}{\partial h_3} + \frac{\partial C_T}{\partial D_{37}}\frac{\partial D_{37}}{\partial h_3} \\ 0 &= \frac{\partial C_T}{\partial D_{34}}\frac{\partial D_{34}}{\partial h_4} + \frac{\partial C_T}{\partial D_{45}}\frac{\partial D_{45}}{\partial h_4} + \frac{\partial C_T}{\partial D_{48}}\frac{\partial D_{48}}{\partial h_4} \end{aligned} \tag{11.32}$$

The cost C_T is from Eqn (11.17), so the derivatives like $\partial C_T/\partial D_{12}$ in Eqn (11.32) are written in general as

$$\frac{\partial C_T}{\partial D_{ij}} = a\,b\frac{D_{ij}^{b-1}}{D_u^b}L_{ij} \tag{11.33}$$

for any segment ij, where a, b, and D_u are the constants defined in Section 11.4.4.

The derivatives like $\partial D_{12}/\partial h_2$ in Eqn (11.32) are obtained by taking the partial derivative of the pipe diameter with respect to the relevant static pressure head in the appropriate energy equation. For equations like Eqs (11.25), where D appears in a nonlinear way in more than one location, this is done using numerical methods. However, for illustrative purposes, if we restrict our interest to a range of *minor-lossless, turbulent flow in smooth pipe*, we can use the energy equations like Eqs (11.16), where the friction factor has been approximated based on the developments in Chapter 9. We obtain for segment 12, for example,

$$\frac{\partial D_{12}}{\partial h_2} = 0.156\left(\frac{\Delta z_{12} - h_2}{L_{12}}\right)^{-23/19}\left(\frac{\nu^{1/7}Q_{12}}{g^{4/7}L_{12}^{19/7}}\right)^{7/19} \tag{11.34}$$

[23]For uniformity and ease, all derivatives on the right side of this equation are written as partial derivatives though in some cases it is clear that a particular diameter depends on just a single static pressure head, not two or more. In these cases, it is mathematically correct to write these derivatives as ordinary.

For segment 23, we get

$$\frac{\partial D_{23}}{\partial h_2} = -0.156\left(\frac{\Delta z_{23} + h_2 - h_3}{L_{23}}\right)^{-23/19}\left(\frac{\nu^{1/7} Q_{23}}{g^{4/7} L_{23}^{19/7}}\right)^{7/19} \tag{11.35}$$

and for segment 26,

$$\frac{\partial D_{26}}{\partial h_2} = -0.156\left(\frac{\Delta z_{26} + h_2 - h_{del}}{L_{26}}\right)^{-23/19}\left(\frac{\nu^{1/7} Q_{26}}{g^{4/7} L_{26}^{19/7}}\right)^{7/19} \tag{11.36}$$

Equations 11.33)–(11.36 are combined with the first of Eqs (11.32) to produce a single algebraic equation that depends on h_2 and h_3, as well as D_{12}, D_{23}, and D_{26},

$$\begin{aligned} 0 &= D_{12}^{b-1} Q_{12}^{7/19}\left(\frac{\Delta z_{12} - h_2}{L_{12}}\right)^{-23/19} \\ &- D_{23}^{b-1} Q_{23}^{7/19}\left(\frac{\Delta z_{23} + h_2 - h_3}{L_{23}}\right)^{-23/19} \\ &- D_{26}^{b-1} Q_{26}^{7/19}\left(\frac{\Delta z_{26} + h_2 - h_{del}}{L_{26}}\right)^{-23/19} \end{aligned} \tag{11.37}$$

Introducing D_{12}, D_{23}, and D_{26} from Eqs (11.16), we get,

$$\begin{aligned} 0 &= Q_{12}^{7b/19}\left(\frac{\Delta z_{12} - h_2}{L_{12}}\right)^{-(1+4b/19)} \\ &- Q_{23}^{7b/19}\left(\frac{\Delta z_{23} + h_2 - h_3}{L_{23}}\right)^{-(1+4b/19)} \\ &- Q_{26}^{7b/19}\left(\frac{\Delta z_{26} + h_2 - h_{del}}{L_{26}}\right)^{-(1+4b/19)} \end{aligned} \tag{11.38}$$

The same procedure is repeated for the second and third equations in the group designated as Eqn (11.32) to obtain a total of three algebraic equations for h_2, h_3, h_4. In the forward solution, these three equations are included with the energy equations and solved to obtain unique solutions for the static pressure heads at the three junctions, as well as all of the values for D in the distribution main and branches.

The general form of Eqn (11.38), written at any junction, is

$$\boxed{\begin{aligned} 0 = &\sum_{ij,in} Q_{ij}^{7b/19}\left(\frac{\Delta z_{ij} + \Delta h_{ij}}{L_{ij}}\right)^{-(1+4b/19)} \\ &- \sum_{ij,out} Q_{ij}^{7b/19}\left(\frac{\Delta z_{ij} + \Delta h_{ij}}{L_{ij}}\right)^{-(1+4b/19)} \end{aligned}} \tag{11.39}$$

where, as usual, $h_1 = 0$ (at the source, $\Delta h_{12} = h_1 - h_2 = -h_2$), and $h = h_{del}$ at the end of each delivery pipe segment. The convention that we apply to the continuity equation also applies to Eqn (11.39). This is the meaning of the index ij, in and ij, out on the summations.

A reminder that Eqn (11.39) applies strictly to minor lossless, turbulent flow in smooth pipes. From our experience, however, we can use it as a first-approximation for optimal h_j for flow in the rougher-wall, GI pipe and, in fact, with all pipe under all minor lossless flow conditions.

Equation (11.39) is an alternative to the `Given...Minimize` block in `Mathcad` to minimize the network cost and determine optimal h_j. One difference between the two is that the block evaluates all of the above derivatives numerically[24] and thus includes Eqs (11.32) in the solution process, even though it is not evident. This increases the accuracy compared with Eqn (11.39). However, the `Given...Minimize` block, though a little simpler to implement in `Mathcad`, takes considerable longer to execute.

B.11.6 Use of Eqn (11.39): Optimal Static Pressure Heads at Branch Junctions

To demonstrate the use of Eqn (11.39), we apply it to the simple-branching network of Fig. 11.1. We make the following assumptions to enable an analytical solution: $L_a = L_b = L_c = L$, $Q_b = Q_c = Q_a/2$, $h_{del} = 0$, and $\Delta z_a = \Delta z_b = \Delta z_c = \Delta z$. Substitute these into Eqn (11.39) and, after some rearranging, we get $h_j^{opt} = (1 - C)/(1 + C)\Delta z$, where $C = 2^{(7b-19)/(4b+19)}$. The optimal head h_j^{opt} depends only on Δz for this case because of the simplifying assumptions. For $b = 1.4$ as above, obtain $C = 0.772$ and $h_j^{opt} = 0.129\Delta z$. For example, for $\Delta z = 60$ m, $h_j^{opt} = 7.74$ m. See Exercises 37 and 38 related to this textbox.

Table 11.11 Comparison Between `Given...Minimize` Block and Eqn (11.39): D

Subscript, ij	D_{ij} (in.) From `Given...Minimize` Block	D_{ij} (in.) From Eqn (11.39)
12	1.49	1.45
23	1.13	1.10
34	0.996	0.937
45	0.694	0.732
26	0.853	0.922
37	0.637	0.651
48	0.556	0.603

[24]Derivatives like $\partial D_{12}/\partial h_2$ are produced from the complete form of the energy equation, not the approximate one that was used in the above example.

Table 11.12 Comparison Between `Given...Minimize` block and Eqn (11.39): Cost and h_j

	From `Given...Minimize` Block	From Eqn (11.39)
cost ($)	2292.53	2298.54
h_2 (m)	10.0	7.88
h_3 (m)	33.7	27.1
h_4 (m)	39.5	28.9

B.11.7 Comparison of Results Using Eqn (11.39) and the `Given...Minimize` Block

To gain confidence in the ability of Eqn (11.39) to produce the same results achieved with the `Given...Minimize` block in `Mathcad`, we apply Eqn (11.39) to the multiple-pipe network of Fig. 11.16. The results using the `Given...Minimize` block appear in Table 11.8. The `Mathcad` worksheet `BranchPipeExample_4pipe_withcost_ver3.xmcd` was used that contains Eqn (11.39) written at the three branches of this network instead of the `Given...Minimize` block. The results compare very favorably as we see by inspecting Tables 11.11 and 11.12. In particular, the total cost is nearly identical for the two approaches. The differences in results come from linear interpolation among the pipe cost data used in the `Given...Minimize` approach instead of the curve-fit to the same cost data as reflected in Eqn (11.39). The execution time using Eqn (11.39) is considerably less than for the `Given...Minimize` block.

11.7 LOOP NETWORK

11.7.1 Characteristics

Because of the greater cost and complexity, single loop networks[25] like the example appearing in Fig. 11.28 are less common than the multiple-branch type just considered. However, loop networks have a couple of advantages which are

- Greater reliability; a loop network is designed so that flow can approach each delivery point from more than one direction. With appropriate placement of valves, repairs to the network may be made without complete service interruption.
- In some cases, because the flow can approach a delivery point from more than one direction, the cross-sectional area for flow is effectively greater than for a

[25]Multiple loop networks that have common pipe segments also exist, but are unusual for the scale of gravity-driven water networks considered here.

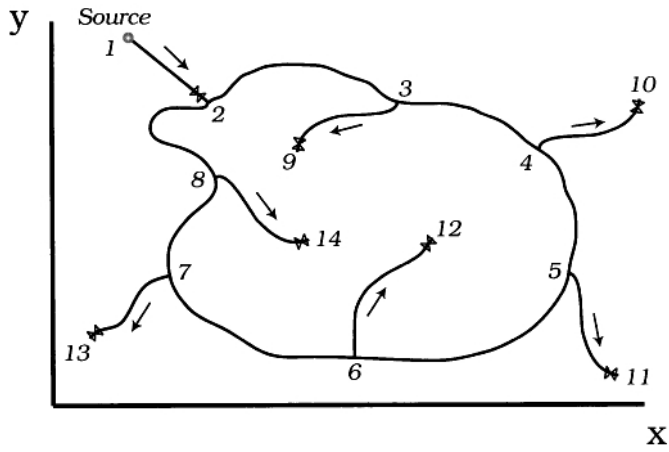

Figure 11.28 A loop network having six distribution segments (see Table 11.13 for data).

comparable branch-type network. This allows for possible increase in water demand and lessens sensitivity of flow rates at a given tap to the demands elsewhere in the network.

Generally, loop networks are candidates for water supply in communities in which there is not much elevation change among water taps. The character of the loop requires a zero change in elevation around the loop measured from any point. Therefore, the assistance of the flow due to a reduction in elevation is always balanced by a loss in assistance as the flow climbs back to its original elevation. Since static pressure is the only energy source driving flow upward against gravity, it is not desirable to have large elevation changes that require large changes in static pressure to accomplish this.

11.7.2 The Approach

The approach for analysis and design of a loop network follows closely to that for a multiple-branch type. There are four fundamental differences.

1. The volume flow rates in the various segments of the loop are not known *a priori*. This means that we need to solve for the volume flow rate distribution in the loop using the continuity equation written for each node.

2. A corollary to the above is that flows will occur in opposite directions at different locations in a loop network. This requires that we define a sign convention for positive flows. We will assume flow rates in the clockwise direction around the loop to be positive in value. Values for flow rates that move in the counterclockwise direction around the loop will be negative. The continuity equation for flow at a branch, Eqn (2.23), remains unchanged.

Table 11.13 The Design Parameters for a Loop Network

Pipe Subscript, ij[a]	L_{ij} (m)	Q_{ij} (L/s)	$z_i - z_j = \Delta z_{ij}$ (m)	K_{ij}	$(L_e/D)_{ij}$
12	235	2.89	$81 - 25 = 56$	50	16
23	415	TBD	$25 - 27 = -2$	0	32
34	210	TBD	$27 - 29 = -2$	0	32
45	330	TBD	$29 - 31 = -2$	0	32
56	539	TBD	$31 - 28 = 3$	0	32
67	108	TBD	$28 - 28 = 0$	0	32
78	147	TBD	$28 - 32 = -4$	0	32
82	183	TBD	$32 - 25 = 7$	0	32
39	111	0.35	$27 - 30 = -3$	10	60
4–10	98	0.46	$29 - 30 = -1$	10	60
5–11	118	0.81	$31 - 28 = 3$	10	60
6–12	143	0.26	$28 - 31 = -3$	10	60
7–13	85	0.63	$28 - 32 = -4$	10	60
8–14	101	0.38	$32 - 34 = -2$	10	60

[a]Refer to Fig. 11.28. $h_{del} = 10$ m for this design.

3. In the past, as we saw with single-pipe and branching multiple-pipe networks, the direction of the flow was always known. In the absence of any elevation change, head losses from friction always had the effect of reducing static pressure in a known direction. However, in the case of a loop network, the flow can move in either direction in a pipe segment. This means that the friction term in the energy equation needs to be directionally sensitive. To account for this, we will make a small addition to the friction term for the energy equation written for any segment on the loop.

4. Along any flow path, the pressure at any fixed location is clearly single valued. If we apply this to a loop network, the change in elevation and static pressure head around a closed loop must be identically zero. A quick inspection of the energy equation applied around a closed loop will reveal this. By further considering the energy equation, this also means that the change in pressure due to friction from node-to-node around a closed loop must sum to zero. This is referred to as the "loop equation", which is an auxiliary equation unique to a loop network. We will explore this more thoroughly in Section 11.7.3.

11.7.2.1 An Introductory Problem It is worthwhile to first consider a simpler variation of the loop network of Fig. 11.28 (see Fig. 11.29). The reason for this is that with several simplifying assumptions we are able to develop simple analytical solutions for the pipe diameters and total pipe cost. By our inspecting and understanding these solutions, issues concerned with determining static pressure heads at the junctions and the associated cost optimization the loop network will be highlighted. Later on, we may better be able to deal with these in more complex loops.

The loop of Fig. 11.29 consists of four, equal-elevation, loop segments of smooth pipe each having equal lengths ($L_{23} = L_{34} = L_{45} = L_{52} = L_{12}/2 = 50$ m). Valves on each of the equal-elevation branches are adjusted such that the flow rate in each

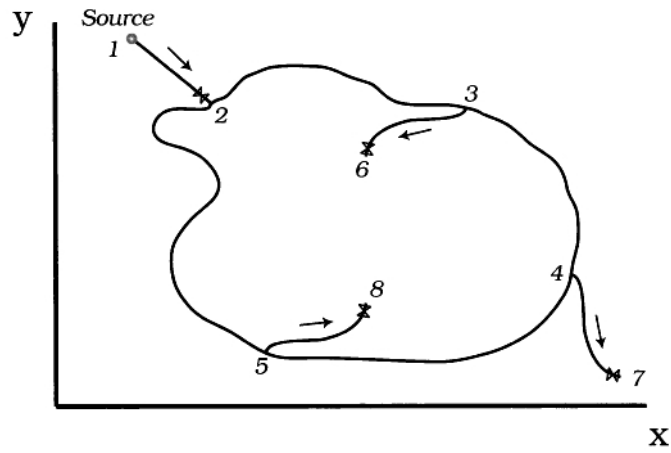

Figure 11.29 Geometry for a simple loop network.

branch is equal to $Q_{12}/3$, where we assume $Q_{12} = 3.10$ L/s for this design. The flow rate distribution in the network is from the continuity equation. Thus,

$$Q_{23} = \frac{Q_{12}}{2}, \quad Q_{34} = \frac{Q_{12}}{6}, \quad Q_{36} = \frac{Q_{12}}{3}, \quad Q_{47} = \frac{Q_{12}}{3} \tag{11.40}$$

Because of symmetry, we need only solve for the flow in branches 36 and 47 (the flow in branch 58 is identical with that in branch 36). To simplify the solution, we will neglect the major friction loss in favor of a minor loss having a large value of $K = 200$ in each branch and segment of the loop. We will assume $K = 50$ for segment 12.

The energy equations, Eqn (11.24), for each segment of the loop and branch are written as

$$\begin{aligned}
0 &= \Delta z_{12} - h_2 - K_{12}\frac{8Q_{12}^2}{\pi^2 g D_{12}^4} \\
0 &= h_2 - h_3 - K_{23}\frac{2Q_{23}^2}{\pi^2 g D_{23}^4} \\
0 &= h_3 - h_4 - K_{34}\frac{2Q_{34}^2}{9\pi^2 g D_{34}^4} \\
0 &= h_3 - h_{del} - K_{36}\frac{8Q_{36}^2}{9\pi^2 g D_{36}^4} \\
0 &= h_4 - h_{del} - K_{47}\frac{8Q_{47}^2}{\pi^2 g D_{47}^4}
\end{aligned} \tag{11.41}$$

where h_{del} is assumed to be 7 m. To allow us to represent the solution as a function of just a single parameter, we will let $h_2 - h_3 = h_3 - h_4 \equiv \Delta h$. With this, the

formulas for h_2 and the pipe diameters become,

$$\begin{aligned} h_2 &= \Delta z_{12} - K_{12}\frac{8Q_{12}^2}{\pi^2 g D_{12}^4} \\ D_{23} &= [K_{23}\frac{2Q_{12}^2}{\pi^2 g \Delta h}]^{1/4} \\ D_{34} &= [K_{34}\frac{2Q_{12}^2}{9\pi^2 g \Delta h}]^{1/4} \\ D_{36} &= [K_{36}\frac{8Q_{12}^2}{9\pi^2 g (h_2 - h_{del} - \Delta h)}]^{1/4} \\ D_{47} &= [K_{47}\frac{8Q_{12}^2}{9\pi^2 g (h_2 - h_{del} - 2\Delta h)}]^{1/4} \end{aligned} \tag{11.42}$$

By assuming a value of $D_{12} = 2$ in., we solve for the first of Eqn (11.42) to get a fixed value of $h_2 (= 32.04$ m), and then solve the remaining four equations for D_{23}, D_{34}, D_{36}, and D_{47}, respectively, as a function of Δh. The results of these calculations are shown in Figs. 11.30–11.32. The relationships between h_3, h_4, and Δh are

$$h_3 = h_2 - \Delta h, \qquad h_4 = h_2 - 2\Delta h \tag{11.43}$$

Finally, we note that the loop equation does not appear here, because it is identically satisfied because of the symmetry of this problem.

Our inspection of Eqs (11.42) shows the following:

- D_{23} and D_{34} are proportional to $\Delta h^{-1/4}$; both decrease as Δh increases.
- D_{36} and D_{47} are proportional to $(h_2 - h_{del} - \Delta h)^{-1/4}$ and $(h_2 - h_{del} - 2\Delta h)^{-1/4}$, respectively. This means that both D_{36} and D_{47} increase as Δh increases.

Both of these observations are evident from Fig. 11.30, although the increase of D_{36} over the range of Δh that is plotted is not very striking. As noted several times before in this text, the competing effects of the decrease of D_{23} and D_{34} and increase D_{36} and D_{47} with increase in Δh leads to the existence of an optimal value for the diameters as a function of Δh, once cost is considered. The pipe cost for the loop is from Eqn (11.18), rewritten here for convenience,

$$C_T = a \sum (\frac{D_{ij}}{D_u})^b L_{ij}$$

where a, b, and D_u are the constants defined in Section 11.4.4 and the summation in Eqn (11.18) is taken over four pipe segments, 23, 34, 36, and 47.

A plot of the total pipe cost as a function of Δh is shown in Fig. 11.31. The existence of a minimum cost at Δh of ~7.9 m ($h_3^{opt} = 24.2$ m and $h_4^{opt} = 16.3$ m; see Fig. 11.32) is clear. Note that there are very large cost increases due to increased pipe sizes at small Δh and $h_2 - h_{del} - 2\Delta h$ approaching zero ($\Delta h \rightarrow (h_2 - h_{del})/2 \approx 12.5$ m).

From the above value for optimal Δh , the optimal theoretical pipe diameters for D_{23}, D_{34}, D_{36} and D_{47} are 1.87, 1.08, 1.25, and 1.46 in., respectively.

The important observations from our inspection of this introductory problem are the following:

- Generally, there exist optimal static pressure heads at the junctions of a loop network, just as there was for simple- and multiple-branch networks. These are h_j values that, as an ensemble, minimize the cost of the network.
- A close inspection of a loop network of length L reveals that it acts like two parallel flow paths, connected at both ends, each over approximate length $L/2$. This is because of clockwise flows in one leg of the loop over a distance of ~$L/2$, and counterclockwise flow in the opposite leg. Thus, compared with a multiple-branch network of an equal overall length, the loop network is effectively shortened by about half. Accordingly, because of this and the lack of elevation changes along the flow path, the range of variation of the static pressure heads at the junctions may be expected to be smaller for a loop than for an equal-length multiple-branch network.
- A consequence of the previous bullet is that as the number of nodes in the loop increases, it becomes increasingly challenging to find solutions for optimal junction-h values. Because of this, care needs to be taken in the numerical solution of loop problems to achieve a solution with reasonable execution times. We will elaborate on this below. In cases where the number of nodes in the loop is fewer than ~20, a trial-and-error approach with just the reverse solution is probably the quickest and most reliable way to determine near-optimal static pressure heads at the branches of loop network and near-optimal cost. The forward solution is skipped. This is very tedious, however. Trial-and-error is employed below in the solution of the loop of Fig. 11.28 along with the `Mathcad` solution using the usual `Given...Minimize` structure. Recall that the reverse solution uses actual inside diameters from chosen nominal pipe sizes to calculate actual flow rates and actual static pressure heads at all junctions.

11.7.3 Formulation

We return to the problem of Fig. 11.28 and begin by writing the governing equations. The energy equation for each segment of the loop network is written as done for Eqn (11.25). The segment label is the subscript on the function r_{ij} for each. Obtain

$$r_{12} = \Delta z_{12} - h_2 - \{K_{12} + \alpha_{12} + f_{12}[\frac{L_{12}}{D_{12}} + (\frac{L_e}{D})_{12}]\}\frac{8Q_{12}^2}{\pi^2 g D_{12}^4} = 0$$

$$r_{23} = \Delta z_{23} + h_2 - h_3 - \{K_{23} + f_{23}[\frac{L_{23}}{D_{23}} + (\frac{L_e}{D})_{23}]\}\frac{8Q_{23}|Q_{23}|}{\pi^2 g D_{23}^4} = 0$$

$$r_{34} = \Delta z_{34} + h_3 - h_4 - \{K_{34} + f_{34}[\frac{L_{34}}{D_{34}} + (\frac{L_e}{D})_{34}]\}\frac{8Q_{34}|Q_{34}|}{\pi^2 g D_{34}^4} = 0$$

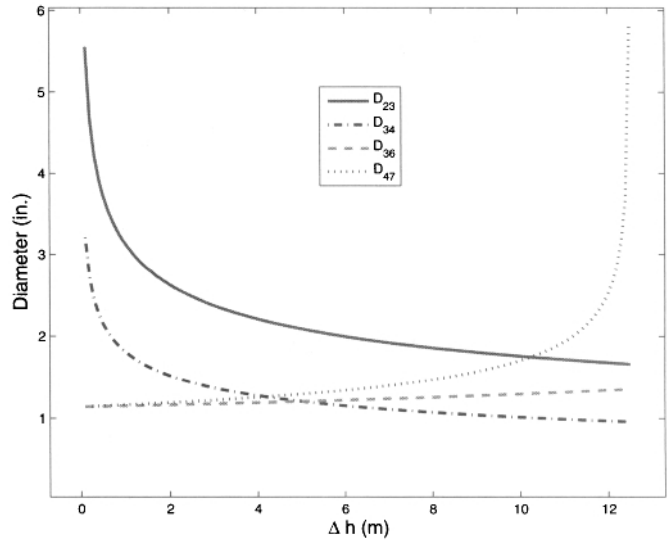

Figure 11.30 Pipe diameters versus Δh for loop network.

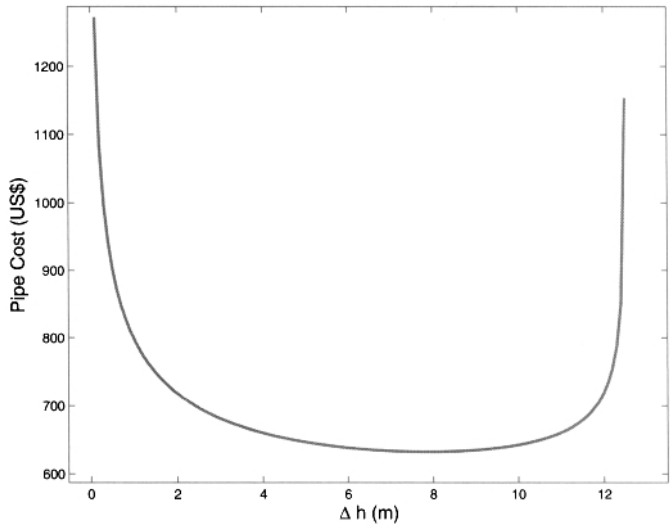

Figure 11.31 Total pipe cost versus Δh for loop network.

$$r_{45} = \Delta z_{45} + h_4 - h_5 - \{K_{45} + f_{45}[\frac{L_{45}}{D_{45}} + (\frac{L_e}{D})_{45}]\}\frac{8Q_{45}|Q_{45}|}{\pi^2 g D_{45}^4} = 0$$

$$r_{56} = \Delta z_{56} + h_5 - h_6 - \{K_{56} + f_{56}[\frac{L_{56}}{D_{56}} + (\frac{L_e}{D})_{56}]\}\frac{8Q_{56}|Q_{56}|}{\pi^2 g D_{56}^4} = 0$$

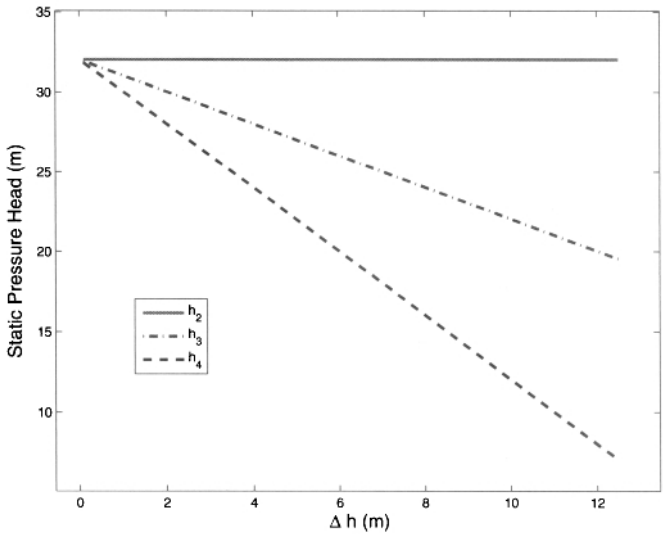

Figure 11.32 Static pressure heads, h_2, h_3, and h_4, versus Δh for loop network.

$$
\begin{aligned}
r_{67} &= \Delta z_{67} + h_6 - h_7 - \{K_{67} + f_{67}[\frac{L_{67}}{D_{67}} + (\frac{L_e}{D})_{67}]\}\frac{8Q_{67}|Q_{67}|}{\pi^2 g D_{67}^4} = 0 \\
r_{78} &= \Delta z_{78} + h_7 - h_8 - \{K_{78} + f_{78}[\frac{L_{78}}{D_{78}} + (\frac{L_e}{D})_{78}]\}\frac{8Q_{78}|Q_{78}|}{\pi^2 g D_{78}^4} = 0 \\
r_{82} &= \Delta z_{82} + h_8 - h_2 - \{K_{82} + f_{82}[\frac{L_{82}}{D_{82}} + (\frac{L_e}{D})_{82}]\}\frac{8Q_{82}|Q_{82}|}{\pi^2 g D_{82}^4} = 0 \\
r_{39} &= \Delta z_{39} + h_3 - h_{del} - \{K_{39} + f_{39}[\frac{L_{39}}{D_{39}} + (\frac{L_e}{D})_{39}]\}\frac{8Q_{39}^2}{\pi^2 g D_{39}^4} = 0 \\
r_{410} &= \Delta z_{410} + h_4 - h_{del} - \{K_{410} + f_{410}[\frac{L_{410}}{D_{410}} + (\frac{L_e}{D})_{410}]\}\frac{8Q_{410}^2}{\pi^2 g D_{410}^4} = 0 \\
r_{511} &= \Delta z_{511} + h_5 - h_{del} - \{K_{511} + f_{511}[\frac{L_{511}}{D_{511}} + (\frac{L_e}{D})_{511}]\}\frac{8Q_{511}^2}{\pi^2 g D_{511}^4} = 0 \\
r_{612} &= \Delta z_{612} + h_6 - h_{del} - \{K_{612} + f_{612}[\frac{L_{612}}{D_{612}} + (\frac{L_e}{D})_{612}]\}\frac{8Q_{612}^2}{\pi^2 g D_{612}^4} = 0 \\
r_{713} &= \Delta z_{713} + h_7 - h_{del} - \{K_{713} + f_{713}[\frac{L_{713}}{D_{713}} + (\frac{L_e}{D})_{713}]\}\frac{8Q_{713}^2}{\pi^2 g D_{713}^4} = 0 \\
r_{814} &= \Delta z_{814} + h_8 - h_{del} - \{K_{814} + f_{814}[\frac{L_{814}}{D_{814}} + (\frac{L_e}{D})_{814}]\}\frac{8Q_{814}^2}{\pi^2 g D_{814}^4} = 0
\end{aligned}
\tag{11.44}
$$

where f_{ij} for $ij = 12, 23, \ldots$ means $f(Q_{ij}, D_{ij})$. As we saw for the multiple-branch network, only in pipe 12 is there included an acceleration from zero flow speed at the surface of the reservoir to the flow speed in the pipe (i.e., an α term). For the remainder of the pipe junctions, the acceleration of the flow through a tee is accounted for with a K-type loss coefficient. h_{del} is taken to be 7 m for this design. Also as above, in Eqn (11.44) the static pressure heads at all branches, h_i are unknown. These are constrained through pipe material cost minimization as we have seen in the past.

The term $Q_{ij}|Q_{ij}|$ in Eqn (11.44) behaves like Q_{ij}^2 and accounts for the possible change in direction of the friction head loss for energy equations written for segments on the loop. $Q_{ij}|Q_{ij}| > 0$ for $Q_{ij} > 0$ and $Q_{ij}|Q_{ij}| < 0$ for $Q_{ij} < 0$.

As discussed above, the loop equation states that the sum of the head loss (this can be positive or negative valued depending on the direction of flow) between consecutive nodes around the loop must be zero. Note that the sum of difference in static pressure heads and elevation heads between consecutive nodes around the loop must also sum to zero. This is *identically* satisfied by summing, around the loop, the elevation head and static pressure-head terms, respectively, in Eqn (11.44). The loop equation is

$$\begin{aligned}
0 &= \{K_{23} + f_{23}[\frac{L_{23}}{D_{23}} + (\frac{L_e}{D})_{23}]\}\frac{Q_{23}|Q_{23}|}{D_{23}^4} \\
&+ \{K_{34} + f_{34}[\frac{L_{34}}{D_{34}} + (\frac{L_e}{D})_{34}]\}\frac{Q_{34}|Q_{34}|}{D_{34}^4} \\
&+ \{K_{45} + f_{45}[\frac{L_{45}}{D_{45}} + (\frac{L_e}{D})_{45}]\}\frac{Q_{45}|Q_{45}|}{D_{45}^4} \\
&+ \{K_{56} + f_{56}[\frac{L_{56}}{D_{56}} + (\frac{L_e}{D})_{56}]\}\frac{Q_{56}|Q_{56}|}{D_{56}^4} \\
&+ \{K_{67} + f_{67}[\frac{L_{67}}{D_{67}} + (\frac{L_e}{D})_{67}]\}\frac{Q_{67}|Q_{67}|}{D_{67}^4} \\
&+ \{K_{78} + f_{78}[\frac{L_{78}}{D_{78}} + (\frac{L_e}{D})_{78}]\}\frac{Q_{78}|Q_{78}|}{D_{78}^4} \\
&+ \{K_{82} + f_{82}[\frac{L_{82}}{D_{82}} + (\frac{L_e}{D})_{82}]\}\frac{Q_{82}|Q_{82}|}{D_{82}^4}
\end{aligned} \tag{11.45}$$

From Eqn (2.23), the continuity equations for each branch starting from node 2 and moving clockwise are written as

$$\begin{aligned}
Q_{82} - Q_{23} + Q_{12} &= 0 \\
Q_{23} - Q_{34} - Q_{39} &= 0 \\
Q_{34} - Q_{45} - Q_{410} &= 0 \\
Q_{45} - Q_{56} - Q_{511} &= 0 \\
Q_{56} - Q_{67} - Q_{612} &= 0 \\
Q_{67} - Q_{78} - Q_{713} &= 0 \\
Q_{78} - Q_{82} - Q_{814} &= 0
\end{aligned} \tag{11.46}$$

In the forward solution only, one continuity equation is replaced by the loop equation. In fact, by substituting the continuity equations, Eqs (11.46), successively into Eqn (11.45), we can show that the loop equation depends only on the known values of Q_{12} and the branch flow rates, and just a single unknown, for example, Q_{82}. In this case, the loop equation replaces the final continuity equation in Eqs (11.46).

11.7.4 Mathcad Worksheets

A `Mathcad` worksheet, `LoopExample_withcost_ver3.xmcd`, was written to solve this problem in the usual way. First, the forward solution is carried out where the theoretical pipe diameters and optimal static pressure heads at the junctions are found using the `Given...Minimize` structure. Then, the reverse solution is performed after choosing appropriate nominal pipe sizes. This worksheet is too large for presentation here,[26] but the following list highlights the principal features of the solution procedure.

- We chose to solve this problem by assuming a fixed value for $D_{12} = 2$ in. (nom.). Together with the prescribed value of Q_{12} this produces $h_2 = 42.89$ m, which remains fixed, along with D_{12}, for the forward calculation.
- The choice of initial guesses for the unknowns in `Mathcad` is crucial to obtain a solution with reasonable execution times. This is done by the following sequence:
  - Based on the prescribed branch flow rates and segment lengths, provide reasonable guesses for the unknown pipe diameters.
  - Initial guesses for the flow rate distribution in the loop are made by assuming that nearly half the flow goes clockwise starting at node 2. This is referred to as the "flow split" in `LoopExample_withcost_ver3.xmcd`.
  - After defining the energy equations for each segment in the usual way, initial guesses for h at each junction are obtained by solving each energy equation around the loop for h_j. For example, h_3 comes from the solution (in `Mathcad` syntax) $h_3 := \text{root}(r_{23}(h_2, h_3, D_{23}, Q_{23}, K_{23}), h_3)$, and so on.
  - Finally, the loop equation, Eqn (11.45), is used to improve the values for the flow rate distribution in the loop.
- The energy and continuity equations, and the loop equation are solved as a function of the unknown h_j values at the six junctions (nodes 3–8) in a `Given...Find` block in the usual way.
- Optimal values for h_j at the junctions are obtained from the `Given...Minimize` block wherein the inequality constraints of $h_j \geq h_{del}$ and $h_j < z_1 - z_j$ (h_j must be less than the hydrostatic head) at each junction node, j.

[26] It is included with this book, however.

- An optimal (minimum cost) solution is obtained in ~18 min on a dual-core laptop PC with a 2.66-MHz processor for Mathcad ver. 14.

For comparison purposes, a trial-and-error method was also used to solve just the problem (just the reverse solution) where actual inside diameters from a series of nominal pipe sizes were selected. The worksheet for this calculation, LoopExample_withcost_ver8.xmcd, appears in Figs. 11.33–11.36. The procedure in this worksheet follows the reverse solutions seen in previous sheets. The input for the calculations is nominal pipe sizes for all segments of the loop and branches. The execution time on a dual-core laptop PC with a 2.66 MHz processor for Mathcad ver. 14 was < 30 s/case.

11.7.5 Results

The results for this analysis and design are presented in Tables 11.14–11.16. The results of the Mathcad worksheet, LoopExample_withcost_ver3.xmcd are presented in Table 11.14. The forward solution converges where the minimal cost is ~$4077. The nominal pipe sizes are assigned as shown in column 7 of Table 11.14 based on the usual guideline for selecting these and the theoretical values for D_{ij} from column 5. We see that the design flow rates can be achieved with slight adjustments to globe valves located in segment 12 and in the branches. The total pipe cost based on actual pipe sizes selected is ~$4500.

For the trial-and-error solution, candidate values for D range from 2-in. (nom.) for segments 12, 23, and 82 to $\frac{1}{2}$ in. (nom.) for some of the distribution segments. To save time, values for the minor loss coefficients used in this analysis are as specified in Table 11.13 with the exception of K_{12}, which is adjusted to match the required flow rate of 2.89 L/s in segment 12. We see in Table 11.15 that the total pipe cost falls as the average pipe size of the network decreases. The minimum cost satisfying all of the branch flow requirements and static pressure head constraints ($h_j \geq 10$ m and h_j less than hydrostatic) is ~$4791 (case 5). The volume flow rates for all distribution pipes appear in Table 11.16. For all cases some of the branch flow rates are below specification and must be adjusted upward. This is done by partially closing the globe valves (meaning increasing their K values) in the branch segments that have flow rates higher than specified.

Although it is straightforward and will normally return a converged solution, the designer should be aware that the trial-and-error method is very tedious and subject to errors because of this. Though execution times are considerable, the Mathcad worksheet is generally preferred. Of course, as the number of nodes increases, the trial-and-error method becomes prohibitively cumbersome and should be used only for cursory investigation purposes or to verify a calculation performed using another method.

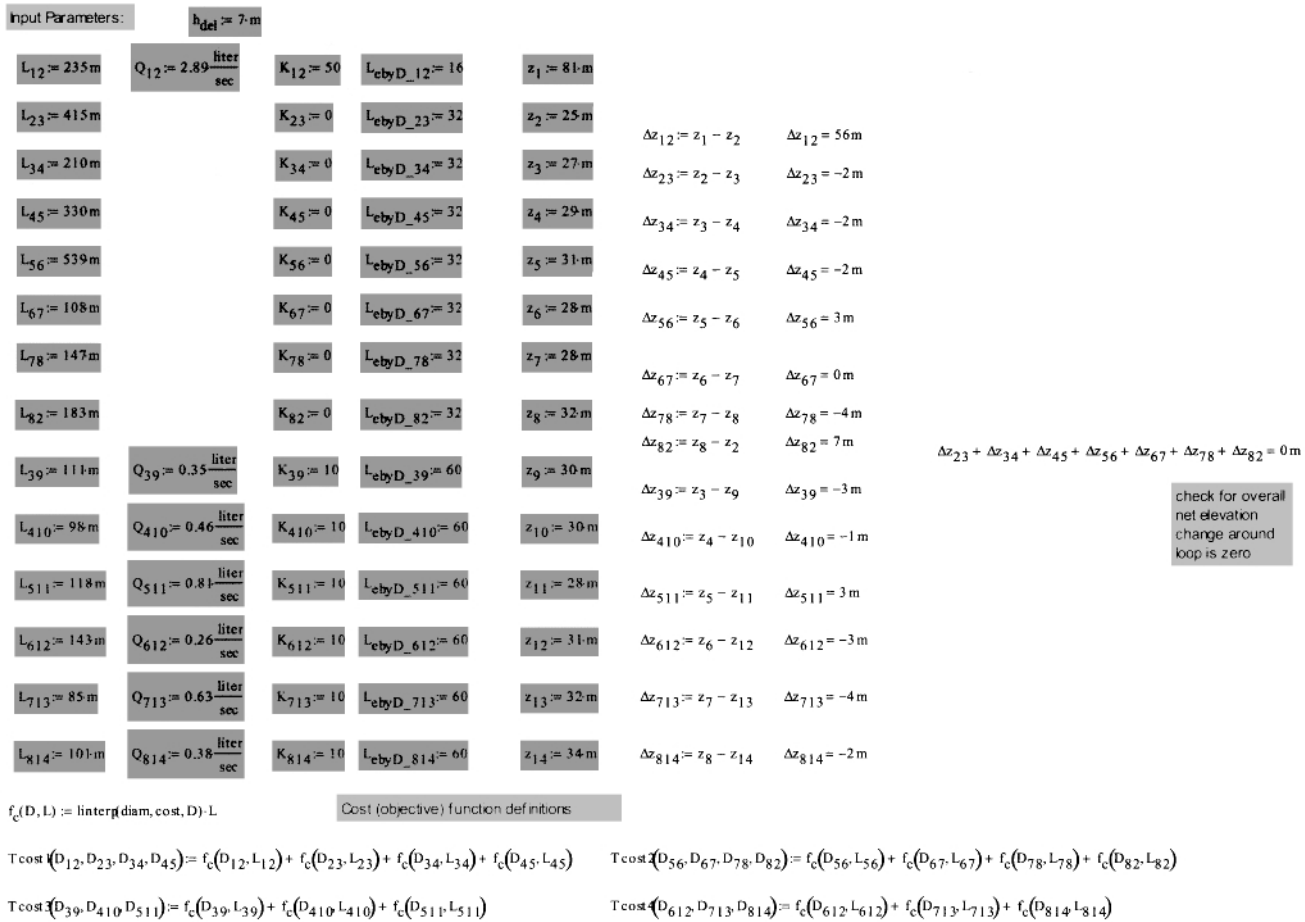

Figure 11.33 Part 1 of `Mathcad` worksheet for loop network (see Fig. 11.3 for the preliminary material needed for this calculation). `Mathcad` worksheet `LoopExample_withcost_ver8.xmcd`.

Figure 11.34 Part 2 of Mathcad worksheet for loop network. Mathcad worksheet LoopExample_withcost_ver8.xmcd.

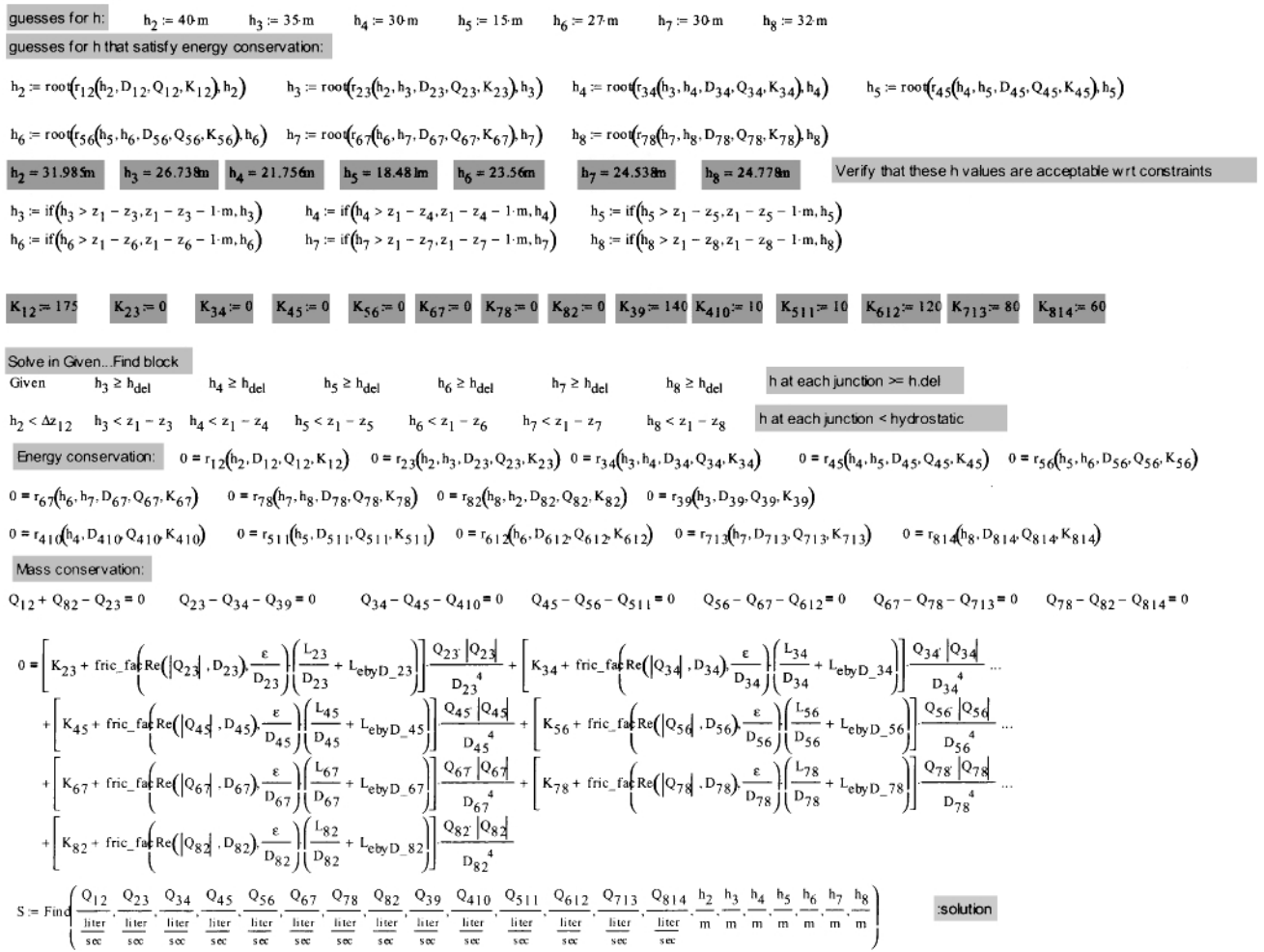

Figure 11.35 Part 3 of Mathcad worksheet for loop network. Mathcad worksheet LoopExample_withcost_ver8.xmcd.

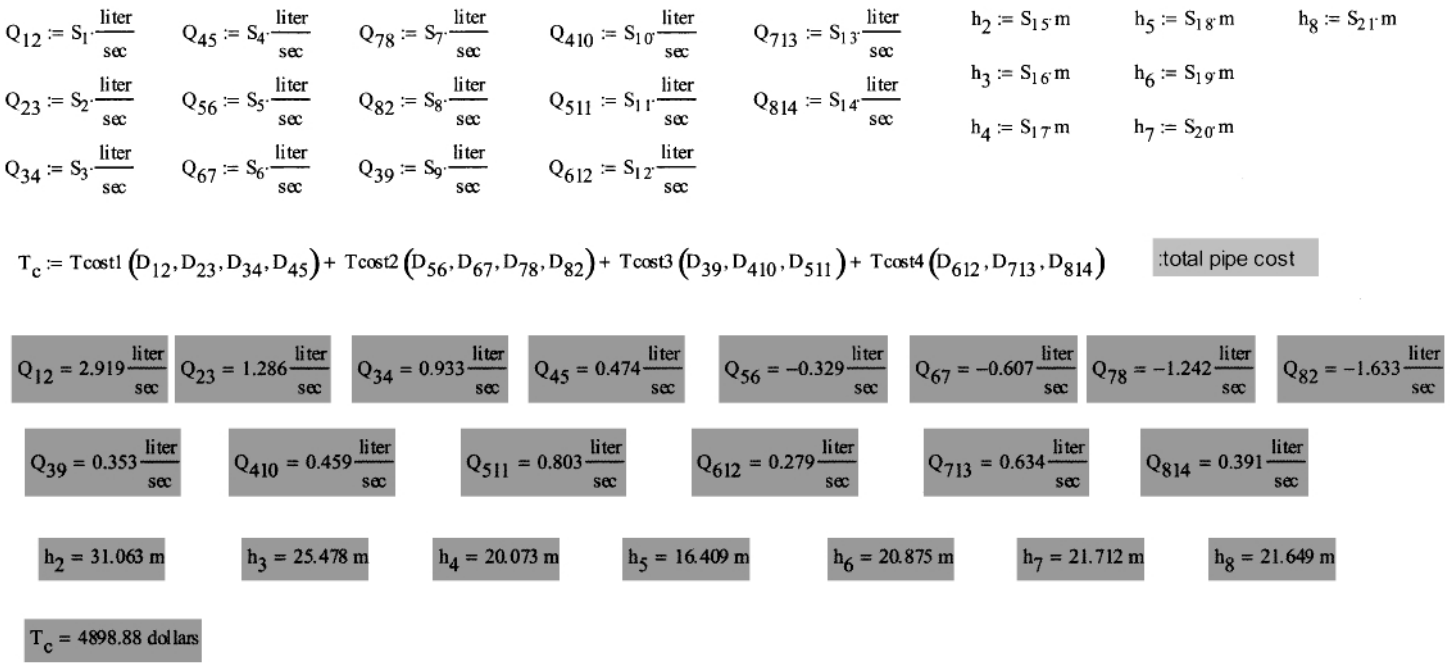

Figure 11.36 Part 4 of Mathcad worksheet for loop network. Mathcad worksheet LoopExample_withcost_ver8.xmcd.

Table 11.14 Results from Mathcad Solution for a Loop Network

Pipe Subscript, ij	L_{ij} (m)	Design Q_{ij} (L/s)	Initial Guess D_{ij} (in.)	Theoretical D_{ij} (in.)	Theoretical Q_{ij} (L/s)	Selected Nominal D_{ij} (in.)	Actual Q_{ij} (L/s)	Actual K_{ij}
12	235	2.89	2.067	2.067	2.89	2	2.90	185
23	415	TBD[a]	1.7	1.72	1.24	2	1.28	0
34	210	TBD	1.5	1.71	0.889	$1\frac{1}{2}$	0.916	0
45	330	TBD	1.3	1.27	0.429	$1\frac{1}{2}$	0.466	0
56	539	TBD	1.3	1.21	−0.381	$1\frac{1}{2}$	−0.328	0
67	108	TBD	1.5	1.46	−0.641	$1\frac{1}{2}$	−0.576	0
78	147	TBD	1.7	1.66	−1.27	$1\frac{1}{2}$	−1.20	0
82	183	TBD	1.8	1.74	−1.65	2	−1.62	0
39	111	0.35	1	0.668	0.35	$\frac{3}{4}$	0.351	140
4–10	98	0.46	1	0.737	0.46	$\frac{3}{4}$	0.456	10
5–11	118	0.81	2	0.982	0.81	1	0.801	10
6–12	143	0.26	1	0.643	0.26	$\frac{1}{2}$	0.254	180
7–13	85	0.63	1	0.809	0.63	$\frac{3}{4}$	0.634	80
8–14	101	0.38	1	0.683	0.38	$\frac{1}{2}$	0.381	65

[a]TBD means to be determined.

Table 11.15 Cost Results from Trial-and-Error Solution for Loop Network[a]

Case	D_{12}	D_{23}	D_{34}	D_{45}	D_{56}	D_{67}	D_{78}	D_{82}	D_{39}	D_{410}	D_{511}	D_{612}	D_{713}	D_{814}	Total Pipe Cost ($)
1	2	2	$1\frac{1}{2}$	$1\frac{1}{2}$	$1\frac{1}{2}$	$1\frac{1}{2}$	$1\frac{1}{2}$	2	1	1	1	1	1	1	4989
2	2	2	$1\frac{1}{2}$	$1\frac{1}{2}$	$1\frac{1}{2}$	$1\frac{1}{2}$	$1\frac{1}{2}$	2	1	1	1	$\frac{3}{4}$	1	$\frac{3}{4}$	4940
3	2	2	$1\frac{1}{2}$	$1\frac{1}{2}$	$1\frac{1}{2}$	$1\frac{1}{2}$	$1\frac{1}{2}$	2	$\frac{3}{4}$	$\frac{3}{4}$	1	$\frac{3}{4}$	1	$\frac{3}{4}$	4899
4	2	2	$1\frac{1}{2}$	$1\frac{1}{2}$	$1\frac{1}{2}$	$1\frac{1}{2}$	$1\frac{1}{2}$	2	$\frac{1}{2}$	$\frac{3}{4}$	1	$\frac{1}{2}$	1	$\frac{3}{4}$	4794
5	2	2	$1\frac{1}{2}$	$1\frac{1}{2}$	$1\frac{1}{2}$	$1\frac{1}{2}$	$1\frac{1}{2}$	2	$\frac{1}{2}$	$\frac{3}{4}$	1	$\frac{1}{2}$	$\frac{3}{4}$	$\frac{1}{2}$	4791
6	2	2	$1\frac{1}{2}$	$1\frac{1}{2}$	$1\frac{1}{2}$	$1\frac{1}{2}$	$1\frac{1}{2}$	2	$\frac{3}{4}$	$\frac{3}{4}$	1	$\frac{1}{2}$	$\frac{3}{4}$	$\frac{1}{2}$	4819

[a] D_{ij} is nominal in inches.

Table 11.16 Branch Flow (Q in L/s) Results from Solution for Loop Network

Case	Q_{39}	Q_{410}	Q_{511}	Q_{612}	Q_{713}	Q_{814}
1	0.588	0.489	*0.518*[a]	0.360	*0.459*	0.487
2	0.648	0.554	*0.576*	0.235	*0.573*	*0.317*
3	0.429	*0.392*	*0.696*	0.287	0.698	0.385
4	*0.268*	*0.443*	0.772	*0.183*	0.802	0.436
5	*0.317*	0.534	0.926	*0.239*	*0.567*	*0.310*
6	0.516	0.487	0.859	*0.220*	*0.522*	*0.284*

[a]Italicized entries are below specified values for this design.

B.11.8 Reinforcement of Concepts for Loop Network

We can gain confidence to solve the loop-network problem as we did for multiple-branch networks by diving in to the appropriate Mathcad worksheet. Modify the existing worksheet LoopExample_withcost_ver3.xmcd to solve the following problem. The neglect of the major friction loss in the Introductory Problem above (Section 11.7.2.1) is the most restrictive of all the assumptions made. Resolve this problem by adding pipe friction to produce an improved, more realistic solution. The energy equations will now be nonlinear and nonseparable so that we will be unable to write explicit formulas for the pipe diameters in the manner of Eqs (11.42). Mathcad will be used instead. Keep all of the other conditions in the problem statement the same, except for the K values. For this exercise, set K for each segment in the loop and branches to 10 (an open globe valve). To simplify, assume $h_2 = 32.04$ m (for $D_{12} = 2$ in.) so that the calculations in the Mathcad worksheet will not include segment 12.

Modify the worksheet LoopExample_withcost_ver3.xmcd to include the parameter values, energy equations, and solutions in the Given...Find and Given...Minimize blocks for only pipe segments 23, 34, 36, and 47. The total pipe cost also depends on these diameters only. The resulting Mathcad worksheet appears in Fig. 11.37. The optimal value of Δh is 7.94 m, and the theoretical pipe diameters D_{23}, D_{34}, D_{36} and D_{47} are 1.27, 0.827, 0.917, and 1.05 in., respectively. All of these values are smaller than when major pipe friction was neglected. It is reasonable to expect the pipe diameters to decrease when major friction loss is included; the additional friction loss (above that for the minor loss already included) is due to a reduction in pipe diameters.

As an alternate solution, if we let h_3 and h_4 vary independently rather than letting $h_2 - h_3 = h_3 - h_4$, the solution will depend on h_3 and h_4 and not simply Δh. In this case, we obtain the optimal values for h_3 and h_4 of 22.7 and 16.2 m, respectively, and the theoretical pipe diameters D_{23}, D_{34}, D_{36} and D_{47} are 1.23, 0.863, 0.934, and 1.05 in., respectively. The Given...Minimize block takes < 30 s to converge. The interested reader is encouraged to modify the worksheet of Fig. 11.37 to verify these results.

A loop network solved in forward way (specify volume flow rates and solve for pipe diameters vs. junction heads):

Input Parameters:

$h_{del} := 7 \cdot m$ $\quad Q_{12} := 3.1 \cdot \frac{liter}{sec}$ $\quad L_{ebyD\_12} := 0$ $\quad L_{ebyD\_36} := 0$ $\quad z_1 := 63 \cdot m$ $\quad z_4 := 25 \cdot m$

$L_{12} := 100 \cdot m$ $\quad K_{12} := 50$ $\quad L_{34} := 50 \cdot m$ $\quad K_{34} := 10$ $\quad L_{ebyD\_23} := 0$ $\quad L_{ebyD\_47} := 0$ $\quad z_2 := 25 \cdot m$ $\quad z_6 := 25 \cdot m$

$L_{23} := 50 \cdot m$ $\quad K_{23} := 10$ $\quad L_{36} := 50 \cdot m$ $\quad K_{36} := 10$ $\quad L_{ebyD\_34} := 0$ $\quad z_3 := 25 \cdot m$ $\quad z_7 := 25 \cdot m$

$L_{47} := 50 \cdot m$ $\quad K_{47} := 10$ $\quad \Delta z_{12} := z_1 - z_2$ $\quad \Delta z_{12} = 38\,m$ $\quad \Delta z_{23} := z_2 - z_3$ $\quad \Delta z_{23} = 0\,m$ $\quad \Delta z_{34} := z_3 - z_4$ $\quad \Delta z_{34} = 0\,m$

$\Delta z_{36} := z_3 - z_6$ $\quad \Delta z_{36} = 0\,m$ $\quad \Delta z_{47} := z_4 - z_7$ $\quad \Delta z_{47} = 0\,m$

$f_c(D, L) := linterp(diam, cost, D) \cdot L$

Cost (objective) function definitions

$Tcost(D_{12}, D_{23}, D_{34}, D_{36}, D_{47}) := f_c(D_{12}, L_{12}) + f_c(D_{23}, L_{23}) + f_c(D_{34}, L_{34}) + f_c(D_{36}, L_{36}) + f_c(D_{47}, L_{47})$

Flow rates:

$Q_{23} := \frac{Q_{12}}{2}$ $\quad Q_{34} := \frac{Q_{12}}{6}$ $\quad Q_{36} := \frac{Q_{12}}{3}$ $\quad Q_{47} := \frac{Q_{12}}{3}$

h.2:

$h_2 := 32.04\,m$

guesses for D:

$D_{12} := 2 \cdot in$ $\quad D_{23} := 2 \cdot in$ $\quad D_{34} := 1.5 \cdot in$ $\quad D_{36} := 1 \cdot in$ $\quad D_{47} := 1 \cdot in$

Define energy equation functions:

$$r_{23}(\Delta h, D_{23}, Q_{23}, K_{23}) := \Delta z_{23} + \Delta h - \left[K_{23} + fric\_fac\left(Re\left(|Q_{23}|, D_{23}\right), \frac{\varepsilon}{D_{23}}\right)\left(\frac{L_{23}}{D_{23}} + L_{ebyD\_23}\right)\right] \cdot \frac{8 \cdot Q_{23}^2}{\pi^2 \cdot g \cdot D_{23}^4}$$

$$r_{34}(\Delta h, D_{34}, Q_{34}, K_{34}) := \Delta z_{34} + \Delta h - \left[K_{34} + fric\_fac\left(Re\left(|Q_{34}|, D_{34}\right), \frac{\varepsilon}{D_{34}}\right)\left(\frac{L_{34}}{D_{34}} + L_{ebyD\_34}\right)\right] \cdot \frac{8 \cdot Q_{34}^2}{\pi^2 \cdot g \cdot D_{34}^4}$$

$$r_{36}(\Delta h, D_{36}, Q_{36}, K_{36}) := \Delta z_{36} + (h_2 - h_{del} - \Delta h) - \left[K_{36} + fric\_fac\left(Re\left(|Q_{36}|, D_{36}\right), \frac{\varepsilon}{D_{36}}\right)\left(\frac{L_{36}}{D_{36}} + L_{ebyD\_36}\right)\right] \cdot \frac{8 \cdot Q_{36}^2}{\pi^2 \cdot g \cdot D_{36}^4}$$

$$r_{47}(\Delta h, D_{47}, Q_{47}, K_{47}) := \Delta z_{47} + (h_2 - h_{del} - 2 \cdot \Delta h) - \left[K_{47} + fric\_fac\left(Re\left(|Q_{47}|, D_{47}\right), \frac{\varepsilon}{D_{47}}\right)\left(\frac{L_{47}}{D_{47}} + L_{ebyD\_47}\right)\right] \cdot \frac{8 \cdot Q_{47}^2}{\pi^2 \cdot g \cdot D_{47}^4}$$

Solve in Given...Find block

Energy conservation:

$Given \quad 0 = r_{23}(\Delta h, D_{23}, Q_{23}, K_{23}) \quad 0 = r_{34}(\Delta h, D_{34}, Q_{34}, K_{34}) \quad 0 = r_{36}(\Delta h, D_{36}, Q_{36}, K_{36}) \quad 0 = r_{47}(\Delta h, D_{47}, Q_{47}, K_{47})$

$S(\Delta h) := Find(D_{23}, D_{34}, D_{36}, D_{47})$:solution

Check solution for guessed values of h: $\Delta h := 2 \cdot m$ $\quad S(\Delta h)^T = (1.716 \;\; 1.114 \;\; 0.86 \;\; 0.877)\,in$

$T_c(\Delta h) := Tcost(D_{12}, S(\Delta h)_1, S(\Delta h)_2, S(\Delta h)_3, S(\Delta h)_4)$:total cost of pipe $\quad T_c(\Delta h) = 466.05 dollars$

Minimize Tc subject to inequality constraints below.

Given $\quad h_2 - \Delta h < z_1 - z_3$ $\quad h_2 - 2 \cdot \Delta h < z_1 - z_4$ h at each junction < hydrostatic

$h_2 - \Delta h \geq h_{del}$ $\quad h_2 - 2 \cdot \Delta h \geq h_{del}$ h at each junction >= h.del

$\Delta h := Minimize(T_c, \Delta h)$ $\quad \Delta h = 7.94\,lm$ $\quad T_c(\Delta h) = 432.74 dollars$ $\quad S(\Delta h)^T = (1.27 \;\; 0.827 \;\; 0.917 \;\; 1.049)\,in$

Figure 11.37 Mathcad worksheet for solution of example in textbox B.11.8.

B.11.9 A Reminder

It is worthwhile to periodically recall one of the important points discussed in Chapter 1. In gravity-driven water networks, for all points beyond the atmospheric-pressure source, energy that drives the flow comes from only static pressure when converted from potential energy. The challenge as analysts and designers is to manage this energy. Pipe sizes that are too small cost less than large ones but dissipate too much energy in friction. Pipes that are too large may unnecessarily increase the cost of the network and possibly present control problems. Thus, energy from static pressure in the network is our friend because it allows us flexibility in our designs and potential for future expansion of the network.

11.8 LARGE, COMPLEX NETWORKS

11.8.1 Comments

Water distribution networks having hundreds of nodes or more, joined in branch and loop patterns, with pipe lengths extending over many kilometers are typical of large towns and urban areas. The analysis and design of these large-scale networks is the subject of a number of books (Jeppson, 1976; Nayyar, 2002; Trifunovic, 2006; Swamee and Sharma, 2008) and many journal and conference publications covering the network subfeatures. Although this application is not the target of the present book of small-scale networks and emphasis on fundamentals, it is worthwhile spending some time discussing the approaches and methodologies for the analysis and design of these large systems, along with a few pertinent results.

Among the differences between the approaches explored so far in this book and those used for the solution to large, complex networks are the following:

- Large computer codes, written in classical programming languages like `Fortran` to solve large systems of nonlinear simultaneous equations, are nearly always used.

- Indexing of the elements of the problem is done so that the computer programs can take advantage of execution speed increases resulting from the use of vectorization.

- As the scale of the network increases, it is appropriate to make simplifying assumptions that are at least slightly more applicable in the large scale but less so with smaller-scale networks. Lumped-equivalent and distributed-equivalent models for branching flows from a distribution main (Swamee and Sharma, 2008) and equivalent diameters and lengths (Trifunovic, 2006) that, in some cases, come from treating the friction factor as constant are examples of this.

Two examples of large computer codes are those presented in Swamee and Sharma (2008), written in `Fortran`, and the `EPANET 2` code (Rossman, 2000) of the United States Environmental Protection Agency. In general, numerical methods like Newton–Raphson (Gerald and Wheatley, 1999), Hardy Cross (Potter and Wiggert, 2002), Levenberg–Marquardt (Levenberg, 1944; Marquardt, 1963), and Conjugate Gradient (Hestenes and Stiefel, 1952) are used to solve the systems of nonlinear algebraic equations that arise in water-flow networks. Iteration, starting with initial guesses of the solutions and repeating of the calculation until suitable convergence of the solution is found, is common among all of these methods.

From our experience thus far with the analysis of water distribution networks, we see there are many examples of the same calculations repeated for different parts of the network. For example, for a given problem we solve the same energy equation many times over for different segments of the network to obtain the diameter of each segment. With vectorization, if it can be used in our computer program or platform, this calculation is done as if it were for just a single segment. The result is a considerable savings in execution time.

Vectorization is implemented by first defining a vector of diameter values $\vec{D} = [D_1 D_2 D_3 \ldots D_n]$, flow rates $\vec{Q} = [Q_1 Q_2 Q_3 \ldots Q_n]$, lengths $\vec{L} = [L_1 L_2 L_3 \ldots L_n]$, and changes in elevation heads $\vec{\Delta z} = [\Delta z_1 \Delta z_2 \Delta z_3 \ldots \Delta z_n]$, and so on. Instead of writing the energy equation for a particular segment ij, in which there would appear D_{ij}, Q_{ij}, L_{ij}, and Δz_{ij}, etc., we write it for the entire *vector* of $\vec{D}$, $\vec{Q}$, $\vec{L}$, and $\vec{\Delta z}$ values. The energy equation, Eqn (11.24), in vectorized form becomes

$$\boxed{\vec{\Delta z} + \vec{\Delta h} = \{\vec{K} + \vec{\alpha} + f(\vec{Q}, \vec{D})[\frac{\vec{L}}{\vec{D}} + (\frac{\vec{L_e}}{D})]\}\frac{8\vec{Q}^2}{\pi^2 g \vec{D}^4}} \tag{11.47}$$

Normally, a vectorized calculation on a computer takes much less time, and can be programmed in a much more compact form, than one that is not vectorized (that is, performed on each of the scaler quantities that are components of the vector). For these reasons, vectorization of calculations is highly recommended where possible.

Major losses dominate as the size of a network increases. With the exception of those for throttling valves, minor losses at branches[27] and other parts of the network are ignored for large water-flow networks. In most cases, this is justified because of the weak effect that the minor loss has on the solution. In other cases, the neglect of things like minor loss and changes in acceleration are made out of the need to simplify an equation to obtain a tractable problem. In this case, validation of the solution, or solutions to a class of problem, is needed to give confidence in the accuracy of the result.

One simplification related to the latter case is the occasional treatment of the friction factor as a constant in the governing equations of some developments (Swamee and

[27] As has been discussed previously, when flow to a branch is directed either with or against another flow, there is a local change in static pressure that adds to or subtracts from the energy at that location (Jones and Galliera, 1998; Jones and Lior, 1994). For a combining flow where the branch and main run of pipe are perpendicular, this is a very weak effect. If a dividing flow, there is a stronger effect. Minor loss coefficients appearing in Table 2.1 account for these losses.

Sharma, 2008; Mihelcic et al., 2009). The friction factor is clearly not constant but can vary considerably, as discussed in Chapter 2. By making this simplification, the analyst is freed from the task of having to consider the dependence of pipe diameter, and perhaps flow rate, in the function for friction factor. The benefit of this assumption is simplification of the analytical result but a price is paid because of the need to include in the solution an iterative procedure to account for the above dependencies.

11.8.2 Optimization for Large Multiple-Branch Networks: Use of Vectorization

For large multiple-branch networks, where we expect only turbulent flow, Swamee and Sharma (2008) report closed-form expressions for minimal network cost for both gravity-driven and pumped flows. The analysis begins with the energy equation written for the entire distribution main (composed of segments 12, 23, 34, and 45), as seen in Fig. 11.16. We will neglect minor losses since they are normally small relative to friction in this long pipeline. With this assumption, the energy equation [Eqn (11.24)] becomes

$$\hat{l} = 0 = \Delta z_n - h_{del} - \sum_{ij=12}^{n} \frac{8f(Q_{ij}, D_{ij})L_{ij}Q_{ij}^2}{\pi^2 g D_{ij}^5}, \tag{11.48}$$

where $\Delta z_n = z_1 - z_n$ and n is the index for the final segment of the main. That is, Δz_n is the total elevation change between the source and the delivery location at the bottom of the distribution main. Following the developments for Lagrange multipliers in Chapter 10, $\hat{l}$ is an equality constraint that is equal to zero.

The total network cost (pipe cost in the present work) is from Eqn (11.17) and is written for this problem as

$$C_T = a \sum_{ij=12}^{n} (\frac{D_{ij}}{D_u})^b L_{ij} \tag{11.49}$$

where a, b, and D_u are the constants defined in Section 11.4.4.

We wish to minimize C_T subject to the constraint of Eqn (11.48). We will use Lagrange multipliers. Obtain for the overall cost function, $C_{T,o}$,

$$C_{T,o} = a \sum_{ij=12}^{n} (\frac{D_{ij}}{D_u})^b L_{ij} + \hat{\lambda}\hat{l} \tag{11.50}$$

or

$$C_{T,o} = a \sum_{ij=12}^{n} (\frac{D_{ij}}{D_u})^b L_{ij} + \hat{\lambda}(\Delta z_n - h_{del} - \sum_{ij=12}^{n} \frac{8f(Q_{ij}, D_{ij})L_{ij}Q_{ij}^2}{\pi^2 g D_{ij}^5}) \tag{11.51}$$

Immediately clear from our inspection of the cost function of Eqn (11.51) is the competition between the first term on the right side where cost increases with D_{ij}^b ($b >$

0) and that due to friction where cost is approximately proportional to $\sum_{ij=12}^{n} 1/D_{ij}^5$; the opposite effect on cost. Following the procedure for Lagrange multipliers, we take the partial derivative of $C_{T,o}$ with respect to D_{ij}, set it equal to zero, and solve for the optimal diameter, D_{ij}^{opt}. Obtain

$$D_{ij}^{opt} = [\frac{40\hat{\lambda} f(Q_{ij}, D_{ij}^{opt}) D_u^b Q_{ij}^2}{\pi^2 \, g \, a \, b} \cdot (1 + \frac{D_{ij}^{opt}}{5 f(Q_{ij}, D_{ij}^{opt})} \frac{\partial f_{ij}}{\partial D_{ij}}\Big|_{D_{ij}=D_{ij}^{opt}})]^{\frac{1}{b+5}} \tag{11.52}$$

The term $\partial f_{ij}/\partial D_{ij}$ is obtained from taking the derivative of the Colebrook equation, Eqn (2.12),

$$\frac{\partial f_{ij}}{\partial D_{ij}} = \frac{2.650[\epsilon_{ij}/3.7D_{ij}^2 - 4.156(\nu^9/Q_{ij}^9 D_{ij})^{0.1}]}{\delta_{ij} \, \ln(\delta_{ij})} \tag{11.53}$$

where $\delta_{ij} = \epsilon_{ij}/3.7D_{ij} + 4.618(\nu \, D_{ij}/Q_{ij})^{0.9}$.

The unknown Lagrange multiplier, $\hat{\lambda}$, in Eqn (11.52) is eliminated by the following procedure:

1. Write Eqn (11.52) for the first pipe segment ($ij = 12$) and divide this by Eqn (11.52), which is for D_{ij}^{opt}. This ratio is $D_{12}^{opt}/D_{ij}^{opt}$; independent of $\hat{\lambda}$.

2. Substitute this expression into Eqn (11.48) to eliminate D_{ij} in favor of D_{12}. Keep f written as $f(Q_{ij}, D_{ij}^{opt})$.

3. Equate this result, which is an expression for D_{12}, to the formula for D_{12} from step 1. The result of this step is a final equation for D_{ij}^{opt},

$$\boxed{D_{ij}^{opt} = (\beta_{ij} \, f_{ij} \, Q_{ij}^2)^{\frac{1}{b+5}} [\frac{8}{\pi^2 g(\Delta z_n - h_{del})} \sum_{ij=12}^{n} \frac{L_{ij} \, (f_{ij} \, Q_{ij}^2)^{\frac{b}{b+5}}}{(\beta_{ij})^{\frac{5}{b+5}}}]^{\frac{1}{5}}} \tag{11.54}$$

where β_{ij} is from

$$\boxed{\beta_{ij} = 1 + \frac{D_{ij}^{opt}}{5 f_{ij}} \frac{\partial f_{ij}}{\partial D_{ij}}\Big|_{D_{ij}=D_{ij}^{opt}}} \tag{11.55}$$

and it is understood that $f_{ij} = f(Q_{ij}, D_{ij}^{opt})$ (or $f_{ij} = f(Q_{ij}, D_{ij})$ in $\partial f_{ij}/\partial D_{ij}$).

Equation (11.54) is a single nonlinear algebraic equation for the optimal diameters for the distribution main of a multiple-branch network. This equation is nonlinear because of f_{ij} and β_{ij} on the right side, both of which depend on D_{ij}^{opt}. The term β_{ij} does not appear in the development of Swamee and Sharma (2008) since they assumed constant f_{ij}. The diameter-dependence of f_{ij} in their solution was included in the problem through iteration.

Once D_{ij}^{opt} are obtained, and with Δz_{ij} and Q_{ij} known for all indices ij, the energy equations for the distribution main segments are easily used to determine the static pressure heads at the junctions, h_j, at the branches. The diameters for the branching distribution pipes are also determined by their respective energy equations with Δz_{ij}, Q_{ij}, and h_j as known quantities. The selection of nominal pipe sizes follows this, together with the reverse solution as usual.

11.8.3 Example Problem: Use of Vectorization

Consider the example below based on Fig. 11.16, which is a variation of the example in Section 11.6.1. The relevant design data are presented in Table 11.17. The focus is optimization of the pipe sizes for the distribution main, D_{12}, D_{23}, D_{34}, and D_{45}. We will solve this problem in two different ways: using the analytical result of Eqn (11.54) and using the `Given...Minimize` block both of which will be in `Mathcad`. The `Mathcad` worksheet for the approach using `Given...Minimize` is as discussed in Section 11.6.1 and will not be shown because of its length. The worksheet that implements the solution of Eqn (11.54) (`BranchPipeExample_4pipe_withcost_vectorized_ver3.xmcd`) appears in Figs. 11.38-11.40.

Vectorization is used in the latter worksheet to demonstrate its benefits of speed and compactness. The first task is to convert all input parameters from the normal designation, D_{ij}, Q_{ij}, and so on, to vector notation (see Fig. 11.39). Thus, $D_1 = D_{12}, D_2 = D_{23}, D_3 = D_{34} \ldots$.[28] The next several lines in Fig. 11.39 are devoted to producing good initial guesses including those for $\vec{D}_m$ (the vector of diameters for the distribution main), $\vec{f}$, and $\vec{\beta}$. The solution for $\vec{D}_m$ is obtained in the `Given...Minimize` block at the bottom of Fig. 11.39. Only three simultaneous equations sit inside this block: $\vec{f}$, $\vec{\beta}$, $\vec{D}_m$. Note that all are vectorized in the manner as required by `Mathcad`. It turns out that Eqn (11.54) is somewhat challenging to solve with the default value of convergence tolerance (`CTOL`) of 0.001. Instead, `CTOL` is set to 0.1, and a procedure to improve the initial guesses was used. This is done using the `WRITEPRN` and `READPRN` statements in Fig. 11.39. `WRITEPRN` is first used to write the initial guess for $\vec{D}_m$ to a file, `D_file.prn`. The `WRITEPRN` statement just after the `Find` statement writes the most recent values of $\vec{D}_m$ to this file. By keeping the cursor on the `READPRN`, positioned just before the `Given...Find` block, and pressing the F9 key to execute the program, successively improved solutions for $\vec{D}_m$ will be calculated[29]. This happens because `READPRN` reads the most recent solutions for $\vec{D}_m$, the `Given...Find` block improves them, and `WRITEPRN` writes $\vec{D}_m$ so that it may be read again by `READPRN`. After ~3–4 cycles of this, the values for $\vec{D}_m$ no

[28] In `Mathcad` there are two types of subscripts. The first is a literal one like L that modifies the definition of h in h_L to produce the symbol for head loss. The second one designates the component of a vector. In the expression $D_1 = D_{12}$, the subscript 1 is the component of the D vector and the subscript 12 is a literal label, not really a number. The literal subscript in `Mathcad` is produced by a period after a symbol. A placeholder for the vector component is produced using CTRL-[. Care should be taken to not confuse these or else considerable head-scratching will be needed to debug your worksheets.

[29] `Automatic Calculation` must be turned off in the `Tools ... Calculate` menu before performing this step.

Table 11.17 Design Parameters for a Multiple-Branch Network with Vectorization (see Fig. 11.16)

Pipe Subscript, ij	L_{ij} (m)	Q_{ij} (L/s)	$z_i - z_j = \Delta z_{ij}$ (m)	K_{ij}	$(L_e/D)_{ij}$
12	435	2.20	$236 - 195 = 41$	0	0
23	615	1.56	$195 - 177 = 18$	0	0
34	410	1.02	$177 - 159 = 18$	0	0
45	530	0.50	$159 - 151 = 8$	0	0
26	128	0.64	$195 - 185 = 10$	10	60
37	439	0.54	$177 - 176 = 1$	10	60
48	118	0.52	$159 - 151 = 8$	10	60

Table 11.18 Results for Multiple-Branch Network with Vectorization (Solution by Eqn (11.54) and `Given...Minimize` block in `Mathcad`)

Pipe Subscript, ij	D_{ij}^{opt} (in.) From Eqn (11.54)	D_{ij}^{opt} (in.) From `Given...Minimize`
12	1.758	1.761
23	1.593	1.594
34	1.411	1.411
45	1.153	1.152

longer change and convergence is achieved. The solution for static pressure heads at junctions of all branches is obtained next (Fig. 11.40) by solving the energy equation for the distribution main in vectorized form. From this result, we define the vector of Δh values at the three junctions having components $h_2 - h_{del}$, $h_3 - h_{del}$, and $h_4 - h_{del}$, and solve the energy equations for the branches. The solution is the vector of branch diameters, $\vec{D}_b$. The execution time for the entire worksheet is few seconds.

Results are presented in Table 11.18. The diameters calculated by both methods are in near-perfect agreement. Because of the much greater execution speed using Eqn (11.54) compared with the `Given...Minimize` block, the former method is generally recommended. However, the designer needs to be aware that with Eqn (11.54), the optimization is performed only for the distribution main, not the *entire* network. With the `Given...Minimize` block-approach, the diameters determined are based on optimization of the entire network. For cases where the distribution main, because if its larger diameter and/or length, is much more costly than the distribution branches, there will be little difference between the results of the two approaches.

If the flow rates in each pipe segment in the distribution main are equal, the problem becomes that studied in Section 11.5.1, where we considered the characteristics of single, variable-diameter pipe. With constant Q_{ij}, our inspection of Eqn (11.54) shows that it produces the same D_{ij} for all ij. In fact, if $Q_{ij} = 2$ L/s for all pipe segments for the example considered in this section, Eqn (11.54) yields $D_{ij} = 1.79$ in. for all ij. Thus, we conclude from this brief inspection that the minimal cost design for the problem of series-connected pipes of possibly different diameters is, in fact, a network of uniform diameter pipe. Of course, the designer may wish to vary the

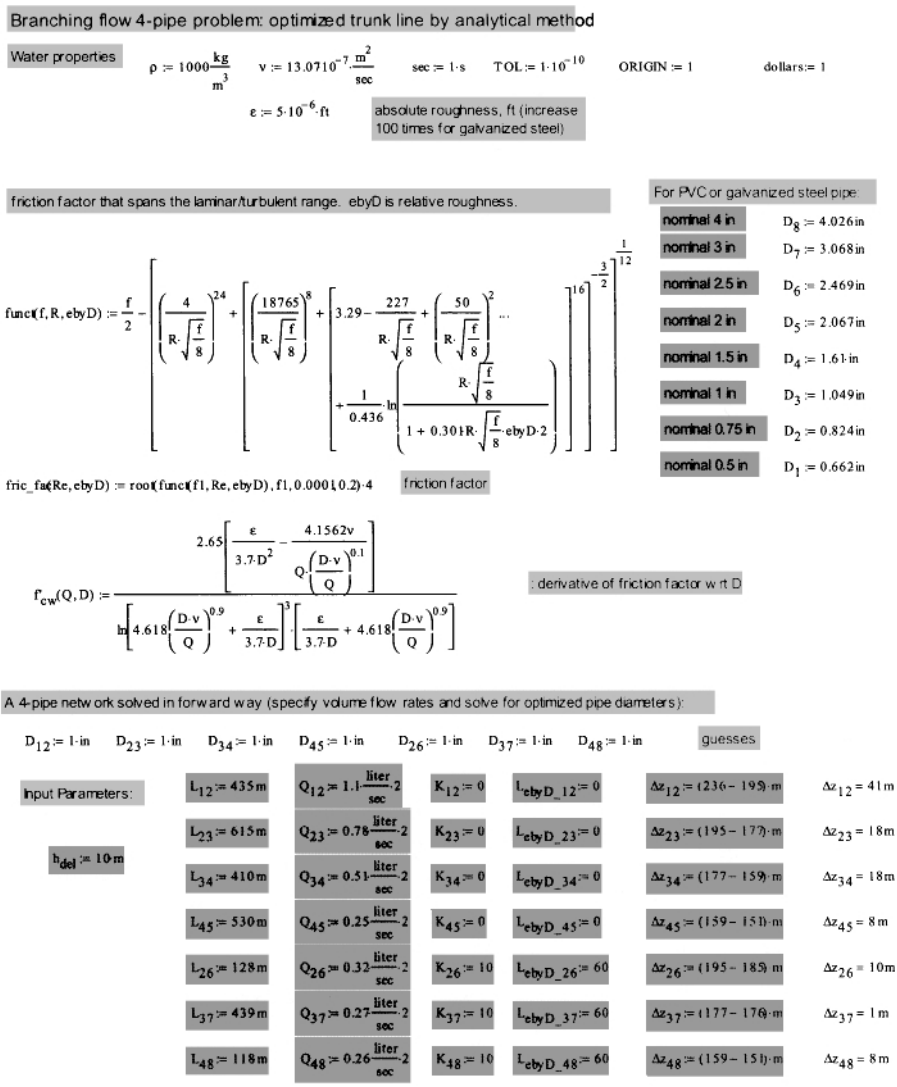

Figure 11.38 Page 1 of Mathcad worksheet for solution of vectorized optimization of a multiple-branch network. Worksheet `BranchPipeExample_4pipe_withcost_vectorized_ver3.xmcd`.

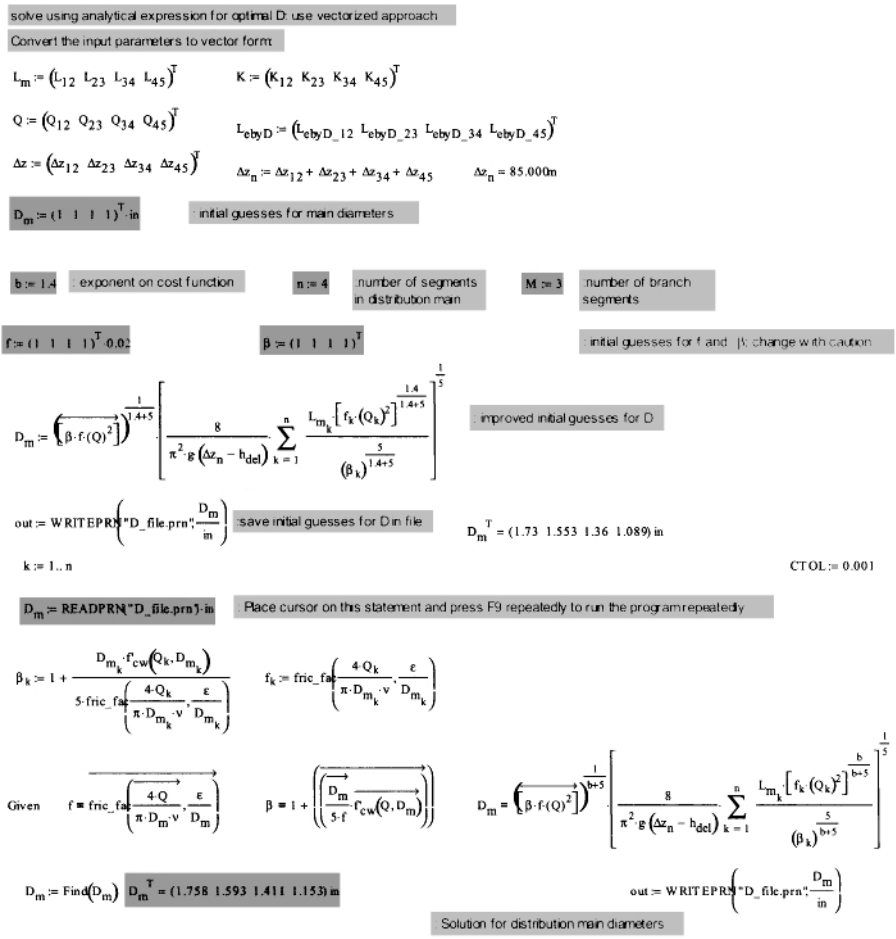

Figure 11.39 Page 2 of `Mathcad` worksheet for solution of vectorized optimization of a multiple-branch network. Worksheet `BranchPipeExample_4pipe_withcost_vectorized_ver3.xmcd`.

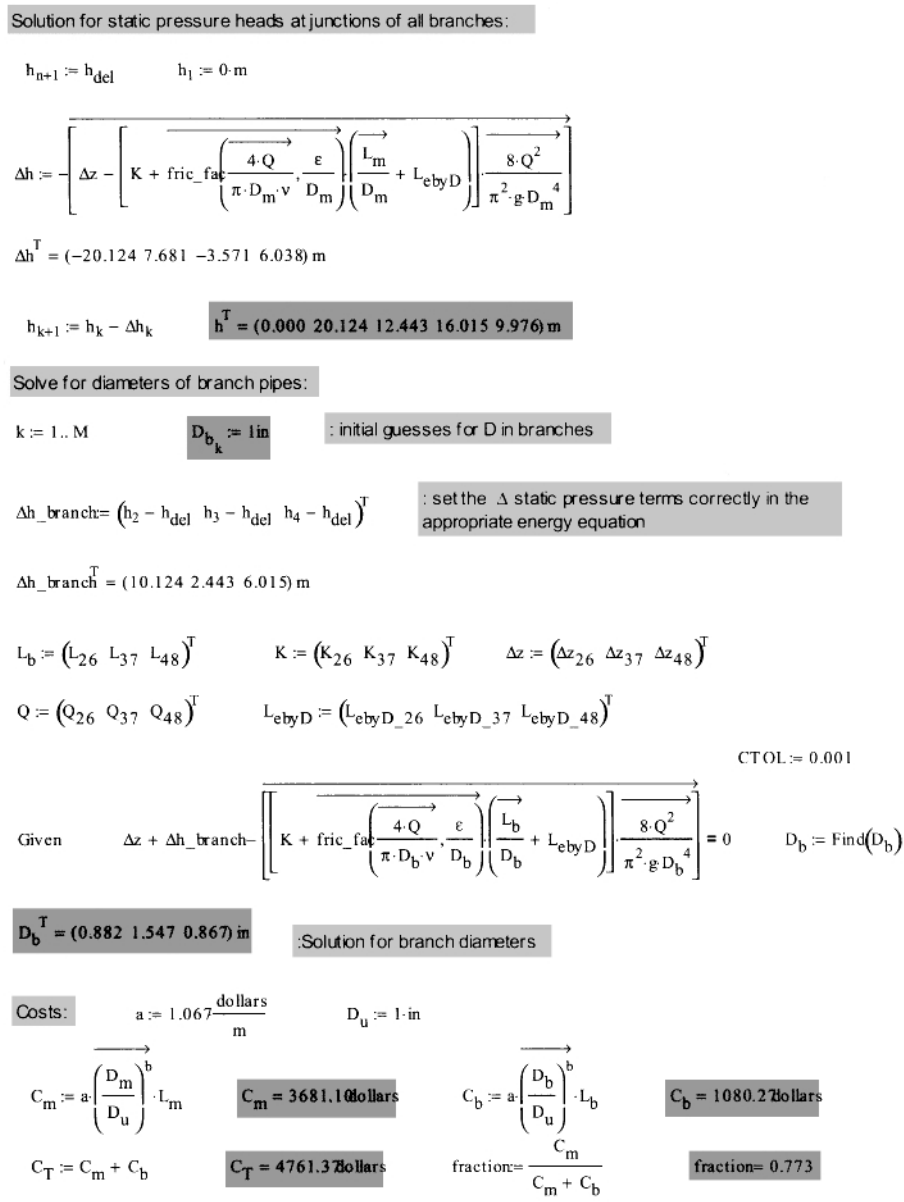

Figure 11.40 Page 3 of Mathcad worksheet for solution of vectorized optimization of a multiple-branch network. Worksheet `BranchPipeExample_4pipe_withcost_vectorized_ver3.xmcd`.

pipe diameters to satisfy considerations other than cost (like too large a peak static pressure) for a series-connected single-pipe network. A slightly different problem is where we require a minimum static pressure head at each junction. Under some conditions, and subject to this constraint, we note that a minimum cost solution does indeed exist as illustrated in Section 11.5.3. This solution produces different D_{ij} than those from Eqn (11.54). No constraint on static pressure heads at the junctions was made in the development of Eqn (11.54).

Unfortunately, there is no optimization formula, like Eqn (11.54), for a loop network. Either the `Given...Minimize` block in `Mathcad` can be used, as in the problem of Section 11.7, or a "loop-cutting" approach as discussed in Swamee and Sharma (2008) and Trifunovic (2006). The latter method is like that used in Section 11.7.2.1, where we cut the loop into two parts and treat each part as the distribution main (a "quasimain') of a branching network. Equation (11.54) can the be used. Iteration, as well as the choice of the larger of the two pipe diameters for the same pipe segments that are common to more than one quasimain, are used. Generally, this solution is carried out using large computer programs as discussed above.

In Section 11.6.6, we obtained an equation [Eqn (11.39)] that can be solved to find optimal values for static pressure heads at the junctions of a multiple-branch network. The principal difference between Eqn (11.39) and Eqn (11.54) is that solutions from Eqn (11.39 reflect optimization of the entire branch network, including branches, whereas Eqn (11.54) is based on only an optimal distribution main.

B.11.10 Optimization of 16-Node Multiple-Branch Network: Use of `Mathcad` with Vectorization

Consider the 16-node branching network in Fig. 11.41. Modify the `Mathcad` worksheet `BranchPipeExample_4pipe_withcost_vectorized_ver3.xmcd` by including the data from Table 11.19. Calculate the theoretical pipe diameters that minimize the cost of the distribution main part of this network. Report all pipe diameters and the vector of static pressure heads at the junctions. Calculate the cost of the distribution main and compare with the total pipe cost. How confident are you that your diameter results optimize the overall network? $h_{del} = 8$ m for this problem.

Follow the worksheet and the discussion in Section 11.8.3 to make the modifications to the worksheet. Make `CTOL` as large as 0.1 if needed and reduce in size to 0.001 as $\vec{D}_m$ converges. The results for optimal pipe diameters, ($\vec{D}^{opt} =$) $\vec{D}_m$ and $\vec{D}_b$, appear in Table 11.20. Nominal sizes are selected next based on the theoretical diameters in this table. The static pressure head vector for the junctions in the distribution main is $\vec{h}^{opt} = [0\ 19.2\ 20.2\ 23.8\ 23.3\ 19.0\ 11.9\ 9.98\ 8.00]$ m.

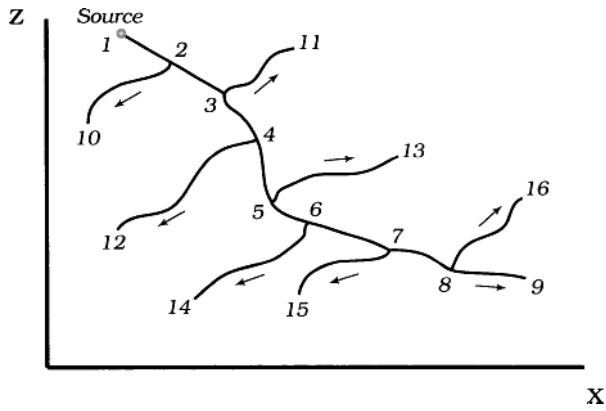

Figure 11.41 Geometry for optimization of a 16-node multiple-branch network. Refer to Table 11.19 for values of design parameters.

Table 11.19 Parameter Values for Optimization of a Multiple-Branch Network (See Fig. 11.41)

Pipe Subscript, ij	L_{ij} (m)	Q_{ij} (L/s)	$z_i - z_j = \Delta z_{ij}$ (m)	K_{ij}	$(L_e/D)_{ij}$
12	135	3.50	$223 - 195 = 28$	0	0
23	115	3.00	$195 - 187 = 8$	0	0
34	110	2.75	$187 - 177 = 10$	0	0
45	230	2.25	$177 - 165 = 12$	0	0
56	335	2.00	$165 - 152 = 13$	0	0
67	415	1.50	$152 - 140 = 12$	0	0
78	210	1.25	$140 - 133 = 7$	0	0
89	230	1.00	$133 - 126 = 7$	0	0
2–10	128	0.50	$195 - 180 = 15$	10	60
3–11	139	0.25	$187 - 173 = 14$	10	60
4–12	118	0.50	$177 - 165 = 12$	10	60
5–13	128	0.25	$165 - 158 = 7$	10	60
6–14	439	0.50	$152 - 141 = 11$	10	60
7–15	118	0.25	$140 - 133 = 7$	10	60
8–16	698	0.25	$143 - 120 = 23$	10	60

Optimization of 16-Node Multiple-Branch Network (Cont'd)

Note that all of the components of this vector at interior branch nodes (the ones calculated in this problem) are $> h_{del}$. The cost for the distribution main is \$3774, ~72% of the total pipe cost. With just 28% of the pipe cost not included in the optimization calculations, we are confident that the network is nearly optimized in an overall sense.

Table 11.20 Results for Optimization of a Multiple-Branch Network

Pipe Subscript ij	D_{ij}^{opt} (in.)	ij	D_{ij}^{opt} (in.)	ij	D_{ij}^{opt} (in.)	ij	D_{ij}^{opt} (in.)
12	1.96	56	1.67	2–10	0.760	6–14	1.013
23	1.88	67	1.54	3–11	0.597	7–15	0.696
34	1.83	78	1.46	4–12	0.739	8–16	0.842
45	1.73	89	1.37	5–13	0.608		

11.9 MULTIPLE-PIPE NETWORKS WITH FORCED FLOW

It has been noted before in several places that the equations and methods of solution, as well as the Mathcad worksheets, may be used for forced (i.e., pumped) flows in addition to those that are gravity driven. In all cases, the only change that is needed is in the energy equation for the first pipe segment. Instead of the atmospheric-pressure source, where $h_1 = 0$, the actual nonzero value of $h_1 = p_1/\rho g z_1$ is entered. This is a very simple change so no example is needed to illustrate it. However, the reader is urged to modify any one of the Mathcad worksheets from this chapter in the above manner to obtain results with forced flow at the source for comparison with that which is solely gravity driven (see Exercise 51).

11.10 PERSPECTIVE: CONVENTIONAL APPROACH TO SOLVING MULTIPLE-PIPE NETWORK PROBLEMS[31]

To place the work from this chapter in perspective, we consider the conventional formulation and solution of flow problems for multiple-path networks that might be found in a fluid mechanics textbook. Obviously, the energy equation [Eqn (11.4)] solved in the present work is also solved in the conventional approach. The major difference between the two is the *manner* of the solution. It has been noted above that if we are solving the energy equation for the flow rate, Q, or the flow speed, $\overline{u}$, the equation or system of equations is nonlinear because Q or $\overline{u}$ appears in the energy equation in a nonlinear way, (i.e., with an exponent of 2). The dependence of the friction factor on Q or $\overline{u}$ also contributes to the nonlinear nature of the energy equation.

As we discussed in Chapter 4, nonlinear problems can generally be solved using the method of iteration, referred to as Gauss–Seidel iteration (Gerald and Wheatley, 1999). In this method, the equations are written so that one dependent variable appears alone on the left side of the equal sign for each equation, a different dependent variable for each equation. All other variables and parameters in each equation are moved to the right side of the equal sign. In cases where the dependent variable appears more than once in a separable way in any equation, the most dominant of these is

[31]This section may be skipped if appropriate without loss of continuity.

the one moved to the left side of the equal sign. Next, the values for the dependent variables (that is, the solution) are guessed so that the expressions on the right side of the equal sign for all equations may be numerically evaluated. This provides updated estimates of the values for the dependent variables which, in turn, become improved (in the sense that the values might be getting closer to the solution of the problem) guesses. These are then substituted into the right sides of all equations again and the calculation repeated. This "iterative" procedure continues until the value for each dependent variable changes very little, usually to within a relative "tolerance" of 1%, or less, of the value from the previous cycle of the procedure. The Hardy Cross or Newton-Raphson methods are alternates to this, but still require iteration to solve.

Iteration is the conventional method of solution for multiple-path pipe flow problems and is often supplemented with a linearization technique called "Regula Falsi" (Chapra and Canale, 2002). Almost every fluid mechanics textbook gives an example of a two- or three-pipe parallel flow problem that illustrates this method (Fox and McDonald, 1992). A variation of this method is used by (Jordan Jr., 2004) to solve for flow in multiple-pipe problems. Normally, the flow rate or flow speed in each branch of the pipe is guessed, the friction factor calculated, and the energy and continuity equations applied to obtained improved estimates of the flow rate or speed in each branch. The procedure continues until flow rate or flow speed in each branch from two consecutive iterations agree to within the tolerance specified by the designer. Paper and pencil are the normal means of executing such iterative methods of solution, though a computer program written in `Excel` or `Mathcad` could easily be used.

In the present work, the iterative procedure described here is replaced by the `Given...Find` construct in `Mathcad`, which is a quick and efficient way for solving individual or systems of nonlinear algebraic equations, including the ones that arise in multiple-path fluid flow problems.

To illustrate this procedure, consider the example problem in Section 11.4 for parallel flow in a three-pipe network. Recall that we wish to solve for the pipe diameters D_a, D_b, and D_c in this problem for prescribed values of Q_a and Q_b (Q_c is determined from these two and the continuity equation) and for arbitrary values of p_2. Equation (11.7), solved in `Mathcad` above, is now rewritten for solution by iteration as described in the above paragraphs. Obtain[32]

$$
\begin{aligned}
D_a &= \left(\frac{4Q_a}{\pi}\right)^{1/2}\left[\frac{\rho(\alpha - C_{L,a}(D_a))}{2(p_2 - \rho g \Delta z_a)}\right]^{1/4}, \quad \text{Pipe } a \\
D_b &= \left(\frac{4Q_b}{\pi}\right)^{1/2}\left[\frac{\rho(C_{L,b}(D_b) - \alpha)}{2(p_2 + \rho g \Delta z_b)}\right]^{1/4}, \quad \text{Pipe } b \\
D_c &= \left(\frac{4Q_c}{\pi}\right)^{1/2}\left[\frac{\rho(C_{L,c}(D_c) - \alpha)}{2(p_2 + \rho g \Delta z_c)}\right]^{1/4}, \quad \text{Pipe } c
\end{aligned}
\tag{11.56}
$$

[32]Note that for diameters to be real and physical in Eqs (11.56), the base of each exponential term must be positive. Since it was noted above that C_L is greater than the order of one and α is of the order of one, the equations for pipes b and c present no problem in this regard. For pipe a, this condition requires that $p_2 - \rho g \Delta z_a < 0$ or that $\rho g \Delta z_a > p_2$ for a real solution for D_a to exist. This provides an upper bound for the value of p_2.

where the loss coefficients, $C_{L,a}(D_a)$, $C_{L,b}(D_b)$, and $C_{L,c}(D_c)$ are written with their appropriate arguments to remind us that the C_L depend on the respective pipe diameters, which are the dependent variables in the problem [see Eqn (11.5)]. With guessed values of D_a, D_b, and D_c, and a prescribed arbitrary value for p_2, all of the terms on the right side of Eqn (11.56) are calculable. This provides updated values for D_a, D_b, and D_c which are then used as improved guesses. The iterative procedure continues in this manner until D_a, D_b, and D_c no longer change with further iterations. The solution is then said to be "converged" and the problem is solved.

Of course, the static pressure at the junction, p_2 is unknown in the above procedure. In nearly all instances, designers choose values for these static pressures based on lower-bound values that were discussed in Section 11.4.2. Practitioners sometimes refer to these as "tapping pressures." For one reason or another, network optimization using cost minimization as described in this chapter is seldom done for the scale of gravity-driven water networks considered in this book. Cost minimization is clearly desirable in and of itself, and the static pressure heads at all junctions in a multiple-pipe network could be uniquely determined once cost minimization is performed.

11.11 CLOSURE

At this point, we can all imagine a big sigh of relief after diligently working though some 90 pages of hydraulic analysis and design of multiple-pipe, gravity-driven water networks. Depending on your understanding of the material and comfort with it, this is quite an accomplishment. With a little practice, you should shortly begin to feel confident about your abilities to carry out successful hydraulic designs for realistic networks. If needed, review this chapter frequently, especially the examples, to increase your understanding and comfort level. We are now finished with most of the technical core of the book, so our hydraulic analysis and design toolbox is nearly complete. Now is the time to work a few exercise problems in Chapter 16 to cement and compliment your knowledge base.

Here are the takeaway concepts for this chapter beginning from textbox B.11.2.

- Although the focus of nearly all hydraulic analysis and design is on satisfying the energy and continuity equations, the addition of the economic equation (i.e., total cost of the network) is critical to make the forward solution unique. This means that minimizing the total network cost provides an additional equation or set of equations that, when solved, gives the solutions for optimal static pressure heads at all junctions of a multiple-pipe network. The reverse solution is always unique since values for Q and h at the junctions are the unknowns (see footnote 10).

- With its `Given...Find` and `Given...Minimize` blocks and the ability to easily include the appropriate inequality constraints on static pressure heads at the junctions, `Mathcad` is a suitable platform for solving the nonlinear simultaneous equations that arise in small- and moderate-scale gravity-driven water

networks. For large, complex networks having hundreds of nodes or more, and without vectorization, the large execution times will make the use of Mathcad prohibitive, however. Two alternatives are available in these cases:

1. Equation (11.54), which was developed based on the minimal cost of the distribution main of a multiple-branch network. Recall that the solutions from this equation do not reflect a minimal cost for the entire network, just the distribution main.
2. Large, commercially available computer programs that are described in Swamee and Sharma (2008) and Trifunovic (2006), including that from Rossman (2000).

- Strategically placed throttling (or globe) valves in many of the segments, including the branch segments, of multiple-branch and loop networks are crucial to give the designer flexibility in balancing flows and, when closed, allow the removal of pipe and components for maintenance and repair. For most networks, an open globe valve [of $K = 10$ or slightly less; see Eqn (2.11)] does not measurably penalize performance so there is little or no disadvantage to their strategic installation.

- Though having greater reliability, loop networks are less common than multiple-branch type because of their greater cost and complexity. The analysis and design of loop networks is also more complex because of the need to solve the continuity equation for each junction and loop equation, in addition to the usual energy equation for each segment. The loop equation is an auxiliary equation unique to a loop network and comes from the requirement that the change in pressure due to friction from node-to-node around a closed loop must sum to zero. Because of large execution times in Mathcad using the usual Given...Find and Given...Minimize blocks, for small- and moderate-scale loop networks we recommend a simple trial-and-error approach to solve for the optimal static pressure heads at the junctions.

- It is worthwhile to keep in mind that it is almost never necessary to start a worksheet in Mathcad from scratch. Always modify an existing worksheet that already successfully performs calculations similar, or identical, to those you are attempting.

- The experienced Mathcad user will probably quickly tire of entering redundant equations in a worksheet for each leg of large networks. Vectorization, as explored in Section 11.8, can be used with the Given...Find and Given...Minimize blocks to greatly reduce the time to set up a worksheet for a given problem. For details on how to do this, see the vector structure in worksheet BranchPipeExample_4pipe_withcost_vectorized_ver3.xmcd.

As noted above, all of the material in this chapter, and most in the others, is unique to gravity-driven water flow *only because we have an atmospheric reservoir at the source in all of our problems.* That is, all of the formulas, equations, assumptions,

methods of solution, interpretations of results, and other characteristics the problems that we have covered may be applied to forced-flow (that is, pump-driven) simply by setting h_1 to the nonzero value appropriate to the forced-flow problem.

The next step is to move forward into the design and engineering phase. We will do this after covering a brief chapter on the interesting topic of microhydroelectric power production, which is a close companion to gravity-driven water supply.

References

P. R. Bhave. Optimization of gravity-fed water distribution systems: Theory. *J. Environ. Eng.*, 109(1):189–205, 1983.

L. Burmeister. *Elements of Thermal-Fluid System Design.* Prentice Hall, New York, NY, 1998.

S. C. Chapra and R. P. Canale. *Numerical Methods for Engineers.* McGraw-Hill, New York, NY, 4th edition, 2002.

A. V. Chiplunkar and P. Khanna. Optimal design of branched water supply networks. *J. Environ. Eng.*, 109(3):604–618, 1983.

R. W. Fox and A. T. McDonald. *Introduction to Fluid Mechanics.* John Wiley & Sons, Inc., New York, NY, 4th edition, 1992.

M. G. Gagliardi and L. J. Liberatore. *Piping Handbook*, chapter on Water Systems Piping. McGraw-Hill, New York, NY, 7th edition, 2002.

C. F. Gerald and P. O. Wheatley. *Applied Numerical Analysis.* Addison Wesley, New York, NY, 5th edition, 1999.

M. R. Hestenes and E. Stiefel. Methods of conjugate gradients for solving linear systems. *J. Res. Nat. Bur. Stand.*, 49(2), 1952.

R. W. Jeppson. *Analysis of Flow in Pipe Networks.* Ann Arbor Science Pubs., Ann Arbor, MI, 1976.

G. F. Jones and J. M. Galliera. Isothermal flow distribution in coupled manifolds: Comparison of results from CFD and an integral model. In *Proceedings ASME International Congress and Exhibition, ASME FED 247*, page 189. ASME, 1998.

G. F. Jones and N. Lior. Flow distribution within manifolded solar collectors with negligible buoyancy effects. *Solar Energy*, 52:289, 1994.

T. D. Jordan Jr. *Handbook of Gravity-Flow Water Systems.* ITDG Publication, London, UK, 2004.

K. Levenberg. A method for the solution of certain non-linear problems in least squares. *Quart. Appl. Math.*, 2:164–168, 1944.

D. Marquardt. An algorithm for least-squares estimation of nonlinear parameters. *SIAM J. Appl. Math.*, 11:431—-441, 1963.

J. R. Mihelcic, L. M. Fry, E. A. Myre, L. D. Phillips, and B. D. Barkdoll. *Field Guide to Environmental Engineering for Development Workers*. ASCE Press, Reston, VA, 2009.

M. L. Nayyar. *Piping Handbook*. McGraw-Hill, New York, NY, 7th edition, 2002.

M. C. Potter and D. C. Wiggert. *Mechanics of Fluids*. Brooks/Cole (Thomson), Tampa, FL, 2002.

L. A. Rossman. EPANET 2 Users Manual, EPA_600_R-00_57. Technical report, Water Supply and Water Resources Division, U.S. Environmental Protection Agency, Cincinnati, OH, September 2000.

A. Schrijver. *Theory of Linear and Integer Programming*. John Wiley & Sons, Inc., New York, NY, 1998.

V. L. Streeter, E. B. Wylie, and K. W. Bedford. *Fluid Mechanics*. McGraw-Hill, New York, NY, 1998.

P. K. Swamee and A. K. Sharma. Gravity flow water distribution network design. *J. Water Supply: Res. and Technol.-AQUA*, 49(4):169–179, 2000.

P. K. Swamee and A. K. Sharma. *Design of Water Supply Pipe Networks*. John Wiley & Sons, Inc., Hoboken, NJ, 2008.

N. Trifunovic. *Introduction to Urban Water Distribution*. Taylor & Francis, New York, NY, 2006.

K. V. K. Varma, S. Narasimhan, and S. M. Bhallamundi. Optimal design of water distribution systems using an NLP method. *J. Environ. Eng.*, 123(4):381–388, 1997.

Future Nicaraguan engineers in front of a
25 kW(e) Pelton water turbine.

This page intentionally left blank

CHAPTER 12

MICROHYDROELECTRIC POWER GENERATION

"It's Simple, but not Easy."
– John C. Bogle, Founder of The Vanguard Group, Inc., 2009

12.1 BACKGROUND

Microhydroelectric power generation has been used in developing regions for many years. Installed in remote areas, and not connected to a larger electrical power grid, these are classified as micro because they range from ~10–200 kW (Anon., 2007). This is contrasted with large power plants of the order of megawatts (thousands of kW) that are connected to a central electrical power grid for distribution over large areas. Many microhydroelectric power plants in the Philippines and the Pacific Rim, Central Asia, Africa, and Central America have been build in the recent past.

Hydroelectric power generation works by converting the potential energy of a mass of water to electrical energy. Actually, there are three steps to this process. First, the potential energy in the water is converted to kinetic and pressure energy (if the flow is

Gravity-Driven Water Flow in Networks. By Gerard F. Jones

in a closed pipe) by reducing its elevation.[1] The conduit that carries water in this step is called a *penstock*. Next, this energy is converted to mechanical energy in a *turbine*. Finally, the mechanical energy is used to rotate the shaft of an electrical *generator* to produce electricity. In some applications, hydropower is used to drive a mechanical process, such as grinding of grain, in which case the final step is obviously not used.

It can be argued that a gravity-driven water network and hydroelectric power are highly complementary. The former requires dissipation of energy in pipes and valves and the latter is a dissipator of this energy where the result is useful electric power; that is, energy from the source in a gravity-driven water network could be dissipated in a productive manner. It appears, however, that the two are seldom coupled. There are several likely reasons for this. Among them is that water flow rates required for electrical power are generally very much larger than what might be supplied by a spring delivering an acceptable flow of fresh water to a community. A subset of this is that a water storage tank is not used in a microhydroelectric plant (see Section 12.2), but is almost always needed for a clean-water network. Another reason that microhydroelectric and water-supply networks are seldom coupled could include water quality requirements that are significantly higher for a potable water system. There also may be the lack of simultaneous need for both water and power in a given community, or there is a strong community focus on either one or the other, not both.

From a community standpoint, electrification creates opportunities for growth of new businesses and population, increasing the quality of life for many. The author has witnessed this in travels to Nicaragua. In one case, a milk-processing plant was built in rural Waslala that collected milk from farms in the surrounding communities. The facility had installed several electric-powered chillers to cool the milk to several degrees above freezing for transport to a pasteurization plant in Matagalpa, ~4 h away by a tortuous road. The initially cool temperatures allowed the milk to arrive at its destination unspoiled. The benefit of electrification was not only to the many end-users of the product, but also the plant owners and their families and the many who supplied the milk to the plant at a greatly reduced cost compared to that if they were to transport raw milk to Matagalpa themselves.

12.2 THE SYSTEM

As shown in the schematic of Fig. 12.1, the microhydroelectric power generation system consists of a device for diverting flow from a river, a settling basin, pipe (the penstock) that conducts water from the source to a turbine, and turbine discharge. The turbine is normally connected through a transmission (consisting of a belt or gear drive) to an electrical generator. From this point, the electric power passes through an electrical or electronic circuit that attempts to match the power output from the

[1] Of course, the relatively high elevation of water at the source is achieved by solar evaporation of the earth's surface water and the deposit of it at high elevations through precipitation. We see that hydroelectric power is simply another form of solar power.

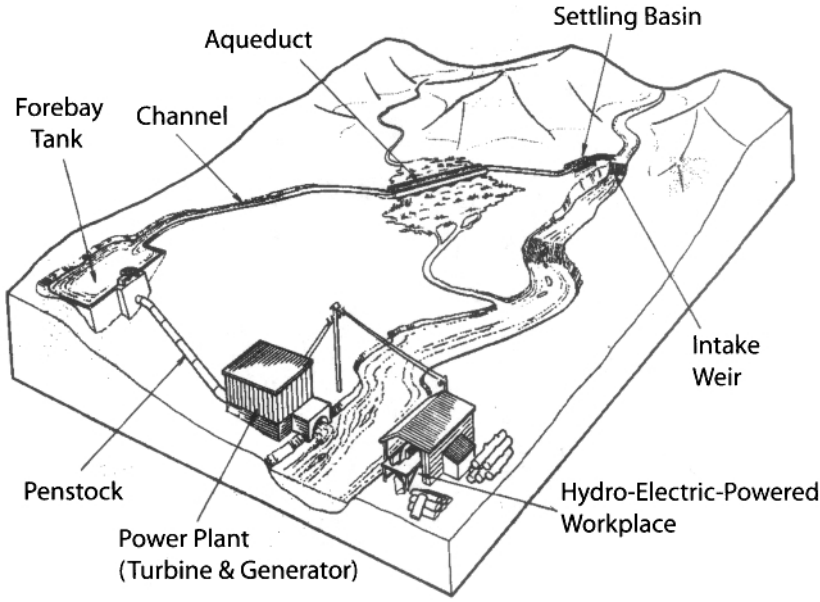

Figure 12.1 Run-of-river hydroelectric schematic. Available from http://practicalaction.org/energy/micro_hydro (with permission).

turbine (and proportionally, the power input to the turbine from the water flow) to the electrical demand (or load). If required for power transmission over large distances, a transformer is used to increase the voltage, otherwise the voltage output from the generator is distributed to the community through overhead transmission lines.

The flow diversion device is a characteristic of a so-called "run-of-river" system, where water flow through the turbine comes directly from the river. This means there is no dam or storage tank and, consequently, reduced costs. The run-of-river system is contrasted with a gravity-driven water network where there is almost always the need for a storage tank because of the mismatch in water supply and demand.

The turbine is classified as an "impulse" or "reaction" type. In an impulse turbine, a cylindrical or planar jet of water impacts a "bucket" or "blade" attached to the wheel that rotates a shaft that is connected to the generator. Atmospheric pressure surrounds this entire process so that the electrical power comes from the change of momentum, or impulse, of the water when striking the wheel. The most common forms of an impulse turbine are the Pelton (Lester A. Pelton, 1829–1908) and Cross-flow types. In a Pelton turbine, a single or multiple *cylindrical* jets of water are used to drive the device. The rotor assembly of a Pelton turbine is shown in Fig. 12.2 (Wikipedia, 2009a). The bucket assembly of a smaller Pelton wheel is shown in Fig. 12.3, where the nozzle that passes the single cylindrical water jet is visible at the bottom. The fact

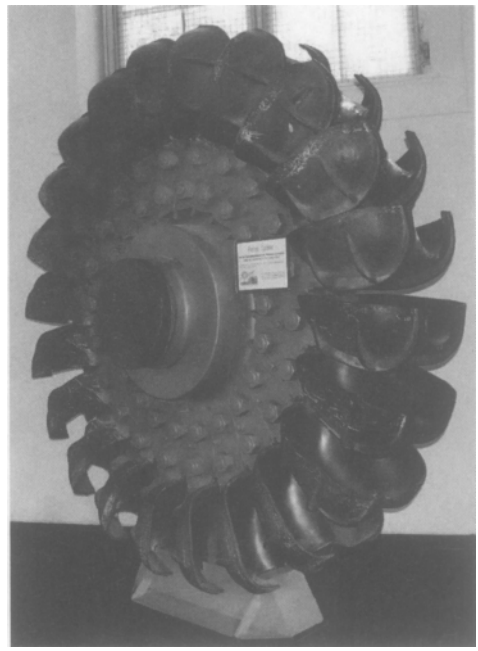

Figure 12.2 Old Pelton wheel from Walchensee Power Plant, Germany.

that all impulse turbines, including the Pelton one, operate at atmospheric pressure means there is no pressure casing required for this type. Pressure vessels or casings are normally expensive to purchase and operate since maintenance must be performed to assure their leak tightness. As indicated by Harvey et al. (2008) impulse turbines are better suited to large elevation heads than reaction types.

Reaction turbines, which are designed for higher flow rates and lower heads, operate in the manner of a centrifugal pump run in reverse. Reaction turbines are enclosed in a pressure vessel because of the large change in static pressure across the turbine blades. The high flow rate and large change in static pressure is the source of power in this type. Like the centrifugal pump, reaction turbines fall into two classes. This includes radial flow, where the motion of water is primarily in the radial direction when acting on the turbine blades. In an axial-flow turbine, the flow passes through the unit parallel to the turbine rotating axis. The axial-flow water turbine is similar to the gas-turbine jet engine on the wing of a commercial aircraft, except there is no combustion of an expanding gas to drive the turbine.

A cross-flow turbine is similar to a Pelton-type in that it operates immersed in atmospheric pressure, but it is not bucket-like. Instead, it resembles a squirrel cage [Fig. 12.4, Wikipedia (2009b)]. A *planar* jet of water is directed onto the blades of the rotor to produce the impulse needed to drive the generator. The roundness of the rotor requires that the water jet impinges on the rotor blades twice, once when entering it and once when leaving. The first impingement is clearly more powerful

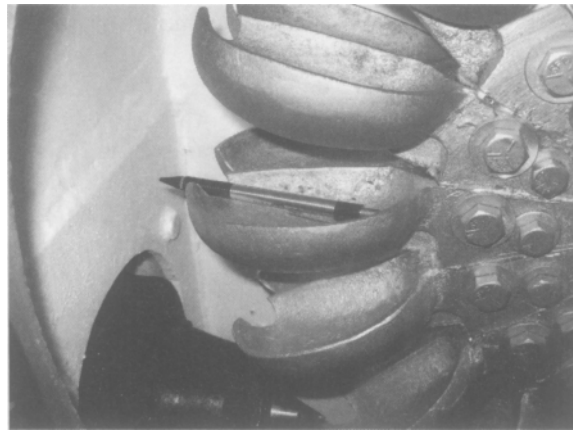

Figure 12.3 Buckets from Pelton wheel in Nicaragua. A 6-in.-long (15 cm) pencil appears for the purpose of scale. The nozzle and "spear" valve appear in the lower part of this figure.

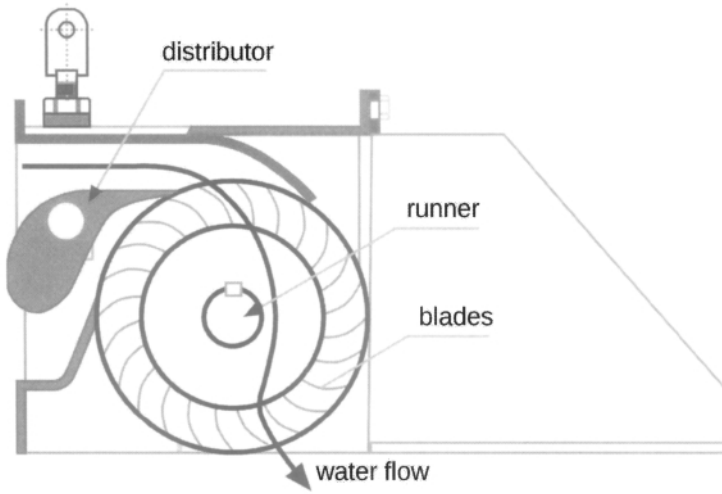

Figure 12.4 Schematic of a cross-flow turbine.

than the second, but the latter adds to the performance, increasing it perhaps by ~30%. As discussed in Harvey et al. (2008) cross-flow turbines are preferred in low-head, high-flow-rate designs over the Pelton type.

When designing a gravity-driven water network, it would seem intuitive to attempt capture whatever energy remains in the flow after it is delivered to the end use. However, as noted in Section 12.1, in many instances this does not happen. Costs are a major consideration including those for the turbine and generator, as well as that for the larger pipe sizes normally needed to transport the larger water flow rates needed

for hydroelectric power production. Where the turbine and generator are purchased from commercial vendors, the costs are relatively large. For example, as of this writing one of the smallest available turbines costs ~$1500 without the generator; perhaps about a quarter of the cost of the water network itself. For this reason, using commercial turbine-generators may not be practical in cases where the focus is on providing clean water, not electrical power. There are many references in the literature on user-constructed turbines (Harvey et al., 2008; Fraenkel et al., 1991; Anon., 2007; Opdenbosch, 2009) and relatively inexpensive options like automobile generators and alternators (Smith, 1994) that can lower these costs considerably. Depending on the financial resources available for a design, elevation head, water flow rates, and other factors, the designer may wish to consider a user-constructed turbine in the microhydroelectric power system in conjunction with the gravity-driven water network. See Section 12.5 for further discussion on this topic.

12.3 APPROACH

Two levels of analysis and design will be considered in this chapter. The first is at the system level (the energy equation applied to the turbine as a work engine), and the second at the detail level (fluid flow in the nozzle, torque and power to the rotor, etc.) The treatment of the latter will not be broad nor deep and will be discussed where relevant in the treatment of the much-broader system-level analysis and design, and briefly as applied to the power production in a Pelton turbine. The interested reader is referred to references, such as Harvey et al. (2008), a source book that has considerable breadth and, in specific areas, depth and textbooks on fluid mechanics and machinery for depth in the component areas (Smits, 2000; White, 1999; Streeter et al., 1998; Munson et al., 1994).

Two different approaches can be taken in the design of a microhydroelectric power plant. The first is by specifying the volume flow rate of water (referred to as a "flow-driven" design). Together with the elevation head, penstock diameter, and a few other characteristics, we can calculate the power production from the developments below. The second is a "demand-driven" design. In this case, the electrical demand is specified and, knowing that the demand and supply of electrical power must be equal, the design calculations determine the volume flow rate of water needed to supply this power. We will discuss both approaches in Section 12.4.1.

12.4 ANALYSIS

12.4.1 Hydraulic System Model

The focus in this section is to develop a mathematical model for the electrical power produced by a water-powered turbine-generator. First, we consider the energy equation, Eqn (2.2) written for the single-pipe network geometry of Fig. 12.5, where the

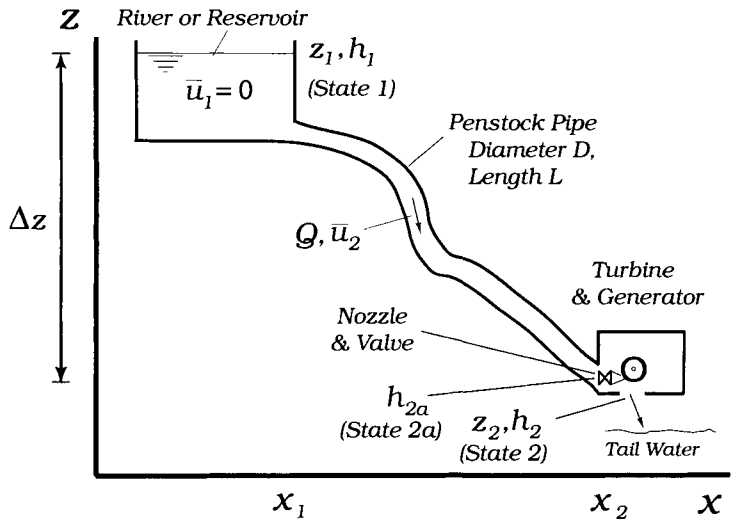

Figure 12.5 Microhydroelectric power plant geometry.

work term is retained[2] to account for the work extracted from the system to be used for electrical power production. Equation (2.2) is rewritten here for convenience,

$$\dot{m}[(\frac{p_1}{\rho} + \alpha_1 \frac{\bar{u}_1^2}{2} + gz_1) - (\frac{p_2}{\rho} + \alpha_2 \frac{\bar{u}_2^2}{2} + gz_2)] = \dot{w}_{th} + \dot{m}H_L$$

where the subscript th on the work term $\dot{w}$ indicates the *theoretical* rate of work done. The theoretical work is distinguished from the actual rate of work, $\dot{w}_a$, through efficiencies for the turbine and generator.[3] Efficiencies are parameters that have values of one or less (normally < 1) that characterize the overall performance of a component at a fine level of detail. The level of detail is so fine that we do not, or cannot, produce a mathematical model of it with certainty. The values for efficiency are normally determined by laboratory experiments or field tests. An equation for the actual work will be developed below.

If z is measured from the location of the turbine, $z_2 = 0$. We will neglect the normally small energy change associated with the velocity head, $\alpha_2 \bar{u}_2^2/2g$, and minor losses. These could be included by using an equivalent length, L_e, instead of the physical length, L (see Section 12.4.2). With Eqn (2.4), and $\dot{m} = \rho Q$ from Eqn (2.24), Eqn (2.2) can be rewritten as

$$\dot{w}_{th} = \rho g Q[z_1 - f(\bar{u}_2, D)\frac{L}{D}\frac{\bar{u}_2^2}{2g}] = \rho g Q L[\frac{z_1}{L} - f(\bar{u}_2, D)\frac{\bar{u}_2^2}{2gD}] \qquad (12.1)$$

[2]There was no work done or extracted when we applied the energy equation to a pipe flow for water-delivery networks.

[3]Other inefficiencies exist. See textbox B.12.1.

The second term in the square braces is the head loss from the Darcy–Weisbach equation, whereas the first term is the hydraulic gradient, S (upper-case S). Thus,

$$S = \frac{\Delta z}{L} = \frac{z_1}{L} \tag{12.2}$$

Previously, we have seen S written two different ways. Where multiple-pipe networks were considered (chapters 9 and 11), the hydraulic gradient was written with primitive parameters as

$$S = \frac{\Delta z + \Delta h}{L} \tag{12.3}$$

where $\Delta z = z_1 - z_2$, $\Delta h = h_1 - h_2$, and points 1 and 2 are at the inlet and outlet of a pipe segment, respectively. For the current problem, z_2 and Δh are zero (Fig. 12.5).

In chapters that dealt with single-pipe networks (2, 5, 7, 8, and 9), and with Eqn (2.39), the hydraulic gradient has appeared as

$$S = \frac{\Delta z + \Delta h}{L} = \frac{z_1(1 - h_2/z_1)}{L} = \frac{s(1 - F)}{\lambda} \tag{12.4}$$

where s is the mean slope (lower-case s), λ is the tortuosity of the penstock pipe, and F is the ratio of the static pressure head at the turbine outlet to the elevation of the reservoir or stream. Recall that $s \tilde{<} 0.5$ (mean slope of 27° or smaller) must be satisfied for validity of this representation of the hydraulic gradient; this is normally not an issue. If using representation Eqn (12.4), s and λ would be specified by the designer of the hydroelectric power system. $F = 0$ for this application.

With either of these representations, and the continuity equation [Eqn (2.21)], Eqn (12.1) becomes,

$$\dot{w}_{th} = \rho g Q L[S - f(Q, D)\frac{8Q^2}{\pi^2 g D^5}] \tag{12.5}$$

Note that for the energy equation for pipe flow [without a turbine; Eqn (2.45)], the term in square braces in Eqn (12.5) is identically zero indicating that all potential energy in the network is dissipated in losses (major and minor). In the present case, the term in square braces should be a positive nonzero value proportional to the theoretical work done by the turbine.

Our inspection of the energy equation for a turbine, Eqn (12.5), shows that $\dot{w}_{th}$ depends on Q, L, S, and D. We wish to simplify this to provide insight. Define a "volume flow rate scale," Q_{sc}, where Q_{sc} is the flow rate that is produced in a pipe (with no turbine installed) of prescribed diameter, D_{sc}, given the hydraulic gradient, S, for the microhydroelectric system. Thus, Q_{sc} is from the solution to Eqn (2.45),

$$\boxed{S = f(Q_{sc}, D_{sc})\frac{8Q_{sc}^2}{\pi^2 g D_{sc}^5}} \tag{12.6}$$

The diameter D_{sc} is arbitrarily assigned, but a reasonable choice that is in scale with the size of hydroelectric plants under consideration in this section is 6 in. The choice of D_{sc} has no effect on the equation for the power generation that we seek.

Using Eqn (12.6) to eliminate $8/\pi^2 g$ in Eqn (12.5), the energy equation for the theoretical power of a turbine becomes,

$$\boxed{\frac{\dot{w}_{th}}{\dot{w}_{th,sc}} = \frac{Q}{Q_{sc}}\left[1 - \frac{f(Q,D)/D^5}{f(Q_{sc},D_{sc})/D_{sc}^5}\left(\frac{Q}{Q_{sc}}\right)^2\right]} \tag{12.7}$$

where $\dot{w}_{th,sc}$ is[4]

$$\boxed{\dot{w}_{th,sc} = \rho g Q_{sc} L S} \tag{12.8}$$

The ratio of the theoretical turbine power, $\dot{w}_{th} = \dot{w}_{th}(Q, D, S, L)$, to $\dot{w}_{th,sc} = \dot{w}_{th,sc}(S, L)$ from Eqn (12.7) is presented in Fig. 12.6 for nominal IPS sch. 40 smooth pipe sizes of 3, 4, 5, and 6 in. The value for D_{sc} is arbitrarily set to 6 in. for this figure and $S = 1$.[5] Even a cursory inspection of Fig. 12.6 reveals a competition that was introduced and discussed in Chapter 10. In the present case, $\dot{w}_{th}$ competes with frictional losses in the pipe. At small values of Q/Q_{sc}, Fig. 12.6 shows that little power is produced. This is attributed to the first Q/Q_{sc} term on the right side of Eqn (12.7). At large values of Q/Q_{sc}, the turbine power decreases with increasing Q because of large frictional losses in the penstock pipe. This trend is caused by the effect of the second term in square braces in Eqn (12.7), which is attributable to friction. In fact, at the highest flow rates for each curve in Fig. 12.6, *all power* is dissipated in pipe friction (this is Natural flow, see Section 2.6.2). Between these extremes, there exists an optimal point in Q, for all D, which represents a perfect balance between power production and production of internal energy due to friction. *Optimal (i.e., maximal)* $\dot{w}_{th}$ *occurs at* Q^{opt} *for any* D.

In addition to the extremum behavior evident in Fig. 12.6, note that the peak power increases with increasing D. This effect exhibits no optimal character.

A plot of the locus of all optimum points from Fig. 12.6 appears in Fig. 12.7 for a range of S typical of microhydroelectric power plants. It is clear that Q^{opt} increases with increases in D and S as more cross-sectional area for water flow is made available with the larger pipe sizes and as more energy becomes available as manifested by an increase in S. The latter can be explained in one of two ways. More energy becomes available due to an increase in mean slope of a fixed pipe length and constant λ [see Eqn (12.4)], or an increase in elevation head per unit of pipe length [see Eqn (12.3)].

Two companion plots for Fig. 12.6 are presented in Figs. 12.8–12.9. We see from Fig. 12.8 that the theoretical power scale for $S = 0.1$ ranges from 10 to > 100 kW. Figure 12.9 shows that the volume flow rate required to produce this power is ~90 L/s. From Fig. 12.6, the optimal pipe size for this flow rate is just under 8 in. inside diameter (ID). All of the figures under discussion in this section were produced assuming smooth pipe.

[4]The term $\dot{w}_{th,sc}$ is the theoretical power scale; the power produced by a lossless system. For example, for Q_{sc} =100 L/s and $LS = \Delta z = 100$ m of elevation head, $\dot{w}_{th,sc} = 100$ kW to within 2%.

[5]Here, S is merely a scale factor since it affects only the volume flow rate scale of Q_{sc}. The shapes of the curves in Fig. 12.6 remain unchanged for all values of S.

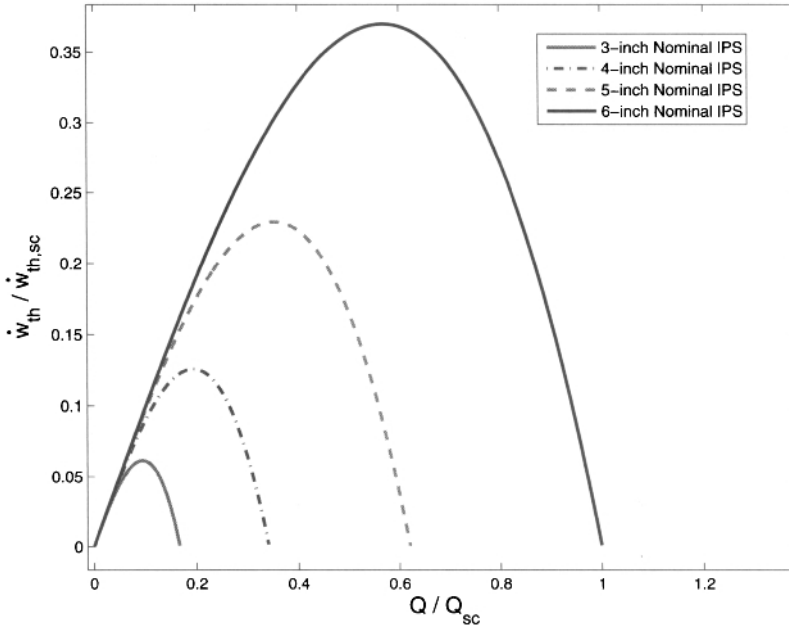

Figure 12.6 Theoretical power production versus Q for several values of D.

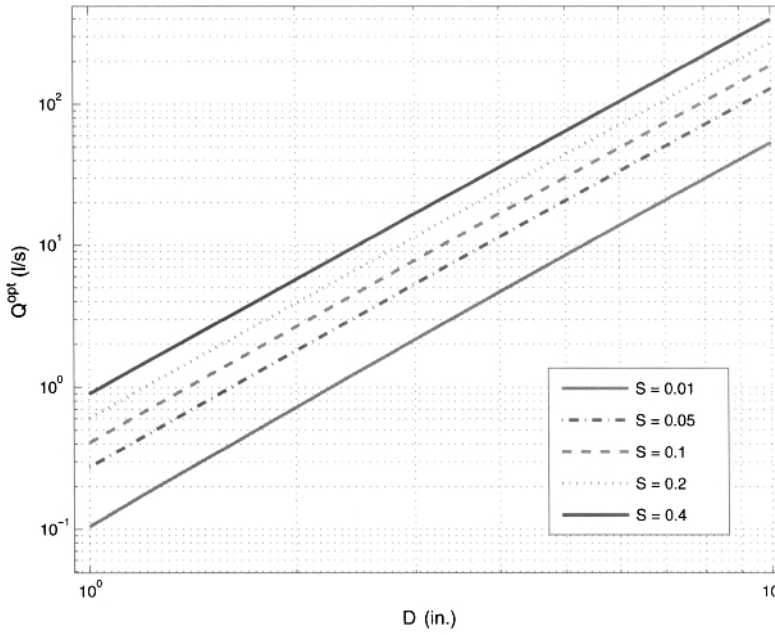

Figure 12.7 Optimal Q versus D for fixed values of hydraulic gradient, S.

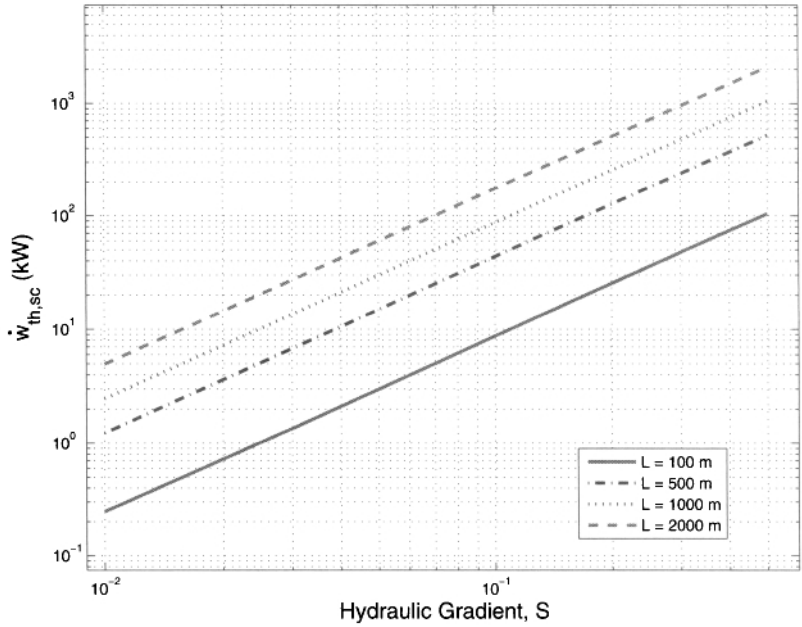

Figure 12.8 Theoretical power scale versus S for several values of L.

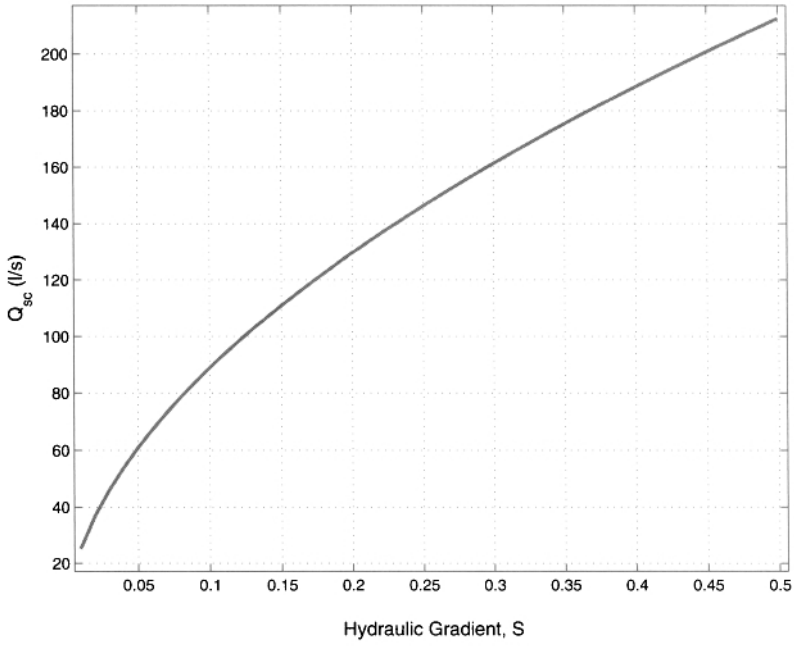

Figure 12.9 Volume flow rate scale versus S.

The results in Fig. 12.7 can be fit to the following function[6]:

$$Q^{opt} = 1.511 \text{ L/s} \cdot S^{4/7}(\frac{D}{D_u})^{19/7} \tag{12.9}$$

where D_u is a unit diameter of 1 in. Equation (12.9) is valid for smooth pipe where the flow is turbulent[7].

It is interesting to note that if we maximize $\dot{w}_{th}$ by taking the Q derivative of Eqn (12.5) *subject to constant* $f(Q, D) = f$, setting this result equal to zero, and solving for Q^{opt}, obtain

$$Q^{opt} = \frac{0.116 \text{ L/s}}{\sqrt{f}} S^{1/2}(\frac{D}{D_u})^{5/2} \tag{12.10}$$

For example, for $f = 0.01$, $0.116/\sqrt{f} = 1.16$. This coefficient is considerably different from 1.511 in Eqn (12.9), but the exponents for S (0.571 versus 0.500) and D (2.714 versus 2.500) are in general range of each other. However, the numerical results from Eqs (12.9) and (12.10) differ greatly, in many cases 40% or more. This underscores the magnitude of importance of the effect of flow dependence on f.

For a flow-driven design, it is always desirable to calculate D from designer-prescribed Q rather than the inverse as given by Eqn (12.9). By taking $Q = Q^{opt}$ and inverting Eqn (12.9), for smooth pipe, we get

$$\boxed{D^{opt} = 0.8589 \text{ in.} \cdot S^{-4/19}(\frac{Q}{Q_u})^{7/19}} \tag{12.11}$$

where Q_u is a unit flow rate of 1 L/s. For a given value of S, D^{opt} is such that Q^{opt} matches the prescribed flow rate Q for the problem, thus ensuring an optimal operating point for the turbine. The usual procedure of choosing a nominal pipe size having a slightly larger inside diameter than D^{opt} applies here.

Similar correlations for GI pipe, of roughness 100-times larger than that for smooth pipe, are

$$Q^{opt} = 1.248 \text{ L/s} \cdot S^{0.540}(\frac{D}{D_u})^{2.628} \tag{12.12}$$

and

$$\boxed{D^{opt} = 0.9192 \text{ in.} \cdot S^{-0.2054}(\frac{Q}{Q_u})^{0.3805}} \tag{12.13}$$

[6]While a curve fit will give correct results, it is not necessary. By substituting the Blasius formula for $f(Q, D)$ in Eqn (12.5), taking the first derivative of $\dot{w}_{th}$ with respect Q, and setting this result equal to zero, we can solve for $Q = Q^{opt}$ and write it as Eqn (12.9). The coefficient and exponents in Eqn (12.9) are thus determined *analytically* not through curve fitting. This is why the exponents appear in terms of rational numbers, not decimals, in the referenced equation.

[7]The exponents in Eqn (12.9) are identical with those of Eqn (9.4) (for flow in a pipe with no turbine) but the coefficients are different. D from Eqn (12.9) produces a pipe cross-sectional area about 53% larger than that for flow in a pipe with no turbine. The additional flow area reduces frictional loss so that work can be performed in the turbine.

The accuracy of Eqs (12.12) and (12.13) is ±5% or less for at least 3 in. $\leq D \leq$ 16 in. and $0.003 < S < 0.3$. If better estimates of Q^{opt} or D^{opt} are required, the reader is referred to the `Mathcad` worksheet below where Q^{opt} and D^{opt} are determined by accurate numerical differentiation of the theoretical turbine power.

It is of interest to investigate the fraction of available power at the source that is converted to work in the turbine, η_{sys}, at the optimal operating point for the system. Taking the ratio of Eqn (12.5) to the power at the source, $\rho g Q L S = \rho g Q \Delta z$, we get

$$\eta_{sys} = 1 - f(Q, D^{opt}) \frac{8Q^2}{\pi^2 g (D^{opt})^5 S} \tag{12.14}$$

where $D^{opt} = D^{opt}(Q, S)$ is from Eqn (12.11) or (12.13). The power converted in the turbine includes the useful power output from it, as well as windage, and losses in the nozzle and bearings (see Section 12.4.4). A plot of Eqn (12.14) appears in Fig. 12.10 for smooth pipe. The system efficiency curves are relatively flat at ~65% for a broad range of flow rates and S values. Thus, at the optimal points in Fig. 12.6, nearly 2/3 of the available potential energy is theoretically converted into useful work by the flow Q [consistent with Daugherty et al. (1985)]. The rest is dissipated in friction in the penstock pipe. Including turbine, generator, and other efficiencies will reduce the value to less than this. The usual practice of choosing a pipe size larger than D^{opt} will increase the above fraction. For smooth pipe, if D is selected 20% larger than D^{opt} ($D = 1.2D^{opt}$), the system efficiency increases to ~85% and to ~90% for $D = 1.3D^{opt}$ [consistent with Harvey et al. (2008)].

For GI pipe, there is a much larger range of system efficiencies for different values of S (Fig. 12.11) compared with smooth pipe. However, for the range of S considered in this figure, the average fraction of available power at the source that is converted to useful power in the turbine is still ~2/3.

Turbine efficiencies, η_t, range from 65% to >80%. Harvey et al. (2008) recommends the low end of this range for locally made cross-flow turbines, and 75% for Pelton types, although Opdenbosch (2009) cites much larger total (turbine and generator) efficiencies of 85% and higher. In the absence of test data for the particular turbine-generator set of interest, turbine efficiencies of 70–75% are conservative, will not over-extend the design, and are thus recommended.

Generator efficiencies, η_g, can be larger than η_t. In fact, commercial generators are almost always more efficient than turbines. Harvey et al. (2008) notes values near 85%. However, information available on the world wide web from manufacturers and vendors supports values higher than this, perhaps as large as 91% for generator powers as low as 25 kW and upward of 95% for larger units (Stamford Power Systems Ltd., 2006).

The final expression for the electrical power output, or actual rate of work, from the microhydroelectric turbine-generator is from Eqn (12.5) which, when the above efficiencies are included, becomes

$$\dot{w}_a = \eta_t \, \eta_g \, \dot{w}_{th} \tag{12.15}$$

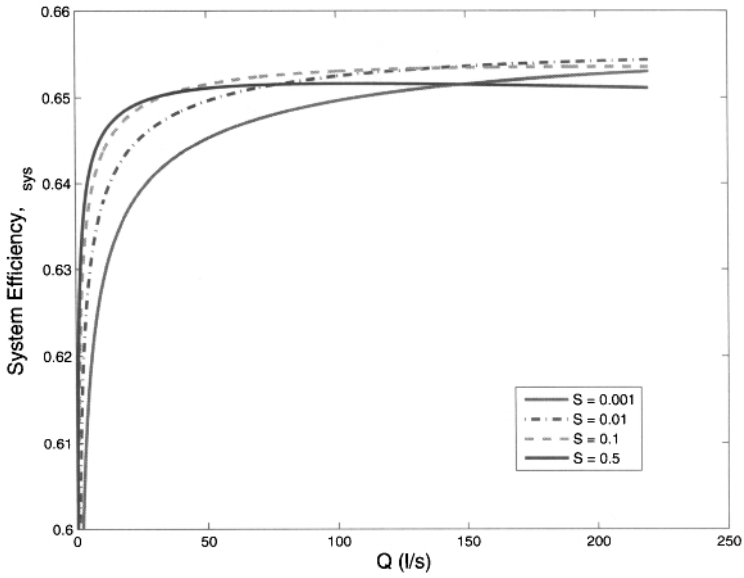

Figure 12.10 Maximum fraction of available power at the source converted in the turbine. Smooth pipe.

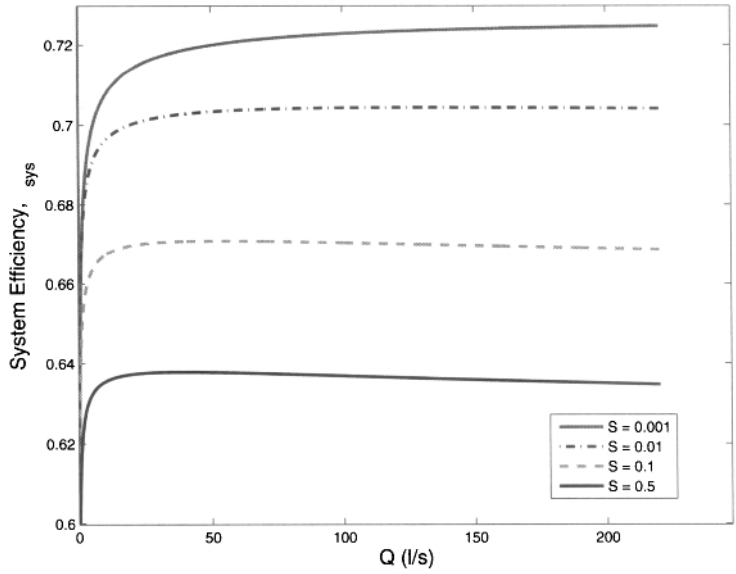

Figure 12.11 Maximum fraction of available power at the source converted in the turbine. GI pipe.

or,

$$\boxed{\dot{w}_a(Q, D, S, L) = \eta_t \, \eta_g \, \rho g \, Q \, L[S - f(Q, D)\frac{8Q^2}{\pi^2 g D^5}]} \tag{12.16}$$

where the functional dependence of $\dot{w}_a$ is included.

The above equations are solved in a `Mathcad` worksheet supplied with this book. See textbox B.12.1 for details.

B.12.1 Microhydroelectric Turbine: Flow-Driven Example

A community is considering the merits of installing a microhydroelectric power plant. The community engineer has determined the need for 65 kW(e) (electrical power) based on the current and future population and their needs. These include the growth of several small industries, one of which produces clay filters for household water purification. The elevation head from a stream located 1050 m (the run of the penstock) from the planned location of the turbine is 80 m and flow measurements taken there indicate that ~230 L/s can be diverted to produce power. Determine the plan's feasibility and recommend alternatives if the design conditions cannot meet the power demand.

The `Mathcad` worksheet `microhydro_theoretical_power.xmcd` is used to evaluate Eqn (12.16) to predict the actual electrical power that can be produced for the prescribed design conditions. The calculations are as follows.

The hydraulic gradient is from Eqn (12.3),

$$S = \frac{\Delta z}{L} = \frac{80 \text{ m}}{1050 \text{ m}} = 0.07619$$

We will first consider the use of PVC pipe since it is less expensive and easier to install than GI. From Table 3.3, the pressure rating of large-diameter sch. 40 PVC pipe is greater than the elevation head of 85 m so sch. 40 PVC pipe is acceptable pressure wise.

The optimal pipe size, subject to the design value of $Q = Q^{opt} = 230$ L/s in the penstock is from Eqn (12.11),

$$\begin{aligned} D^{opt} &= 0.8589 \text{ in.} \cdot S^{-4/19}(\frac{Q}{Q_u})^{7/19} \\ &= 0.8589 \text{ in.} \cdot 0.07619^{-4/19} \cdot 230^{7/19} = 10.96 \text{ in.} \approx 11 \text{ in.} \end{aligned}$$

Flow-Driven Example (Cont'd)

For sch. 40 IPS pipe, the ID is within 1% of the nominal size for nominal size of 4 in. and larger (Table 3.1). Thus, because 11-in. pipe is unavailable (see Chapter 3), we choose nominal 12-in. sch. 40 PVC pipe. The flow speed is 3.15 m/s, sightly above the maximum recommended of 3 m/s when considering abrasion. This value is close enough to 3 m/s, that abrasion should not be an issue.

The energy equation for the actual turbine power output is Eqn (12.16),

$$\dot{w}_a = \eta_t \, \eta_g \, \rho g \, Q \, L[S - f(Q, D)\frac{8Q^2}{\pi^2 g D^5}]$$

Let us assume $\eta_t = 0.75$ and $\eta_g = 0.85$. With $f(Q, D) = 0.0126$ from the Mathcad worksheet (or Fig. 2.4), obtain,

$$\begin{aligned} \dot{w}_a &= 0.75 \cdot 0.85 \cdot 999.7 \text{ kg/m}^3 \cdot 9.807 \text{ m/s}^2 \cdot 230 \times 10^{-3} \text{ m}^3\text{/s} \cdot 1050 \text{ m} \\ &\cdot \; [0.0762 - 0.0126\frac{8 \cdot (230 \times 10^{-3} \text{ m}^3\text{/s})^2}{\pi^2 \cdot 9.807 \text{ m/s}^2 \cdot (12/39.372 \text{ m})^5}] = 83.3 \text{ kW} \end{aligned}$$

Since $83.3 > 65$ kW as required by the community, we conclude the above design specifications will meet the electrical power demand. However, there are other inefficiencies in the system for which we need to account, mostly on the electrical side. Among these are transformer and power transmission losses that together will reduce the power output by ~15%.

If D were exactly equal to D^{opt} of 10.96 in., reducing or increasing Q from the prescribed value of 230 L/s will *reduce* power output from the turbine. Note that this is not the same effect as increasing D. As seen in Fig. 12.6, the peak power will always increase with increasing D. This effect exhibits no optimal character. Also note that η_t may be affected by changes in Q and S.

The pressure rating for 12-in. sch. 40 PVC pipe of 130 psig (91.4 m of water head) is from Table 3.3. This is greater than the elevation head of 85 m, 12-in. sch. 40 PVC pipe is acceptable.

If GI instead of PVC pipe were selected, $D^{opt} = 12.3$ in, subject to the design value of $Q = Q^{opt} = 230$ L/s from Eqn (12.13). With 12-in. nominal pipe, the electrical power generation falls to 71.4 kW, due to more friction in the GI pipe compared with PVC (see Exercise 55).

For a demand-driven design, the final expression for the electrical power output from the generator is the same as Eqn (12.16) with D replaced by D^{opt} from either

Eqn (12.11) (for smooth pipe) or Eqn (12.13) (for GI pipe). Thus,

$$\dot{w}_d(Q, S, L) = \eta_t \eta_g \rho g Q L[S - f(Q, D^{opt})\frac{8Q^2}{\pi^2 g (D^{opt})^5}] \tag{12.17}$$

where $\dot{w}_d = \dot{w}_a$ is power demand. Note that diameter dependence has disappeared in Eqn (12.17) since $D = D^{opt}$ depends only on Q and S. Once the designer specifies a value for $\dot{w}_d$, Eqn (12.17) can be solved for Q to produce this power subject to given S and L. A root-finder in `Mathcad` is needed to solve Eqn (12.17) because Q appears nonlinearly. Once Q is obtained, the designer is free to explore the sensitivity of Q to a range of actual D that is not optimal.

B.12.2 Microhydroelectric Turbine: Demand-Driven Example

Calculate the volume flow rate needed to produce 120 kW(e) for an elevation head of 105 m and penstock length of 1750 m. Neglect minor losses for now, and assume $\eta_t = 0.80$ and $\eta_g = 0.90$. Choose sch. 40 PVC pipe.

The hydraulic gradient is from Eqn (12.3).

$$S = \frac{\Delta z}{L} = \frac{105\text{ m}}{1750\text{ m}} = 0.060$$

The energy equation written for demand-driven design is Eqn (12.17).

$$\begin{aligned}\dot{w}_d &= \eta_t \eta_g \rho g Q L[S - f(Q, D^{opt})\frac{8Q^2}{\pi^2 g (D^{opt})^5}],\\ &= 0.80 \cdot 0.90 \cdot 999.7\text{ kg/m}^3 \cdot 9.807\text{ m/s}^2 \cdot Q \cdot 1750\text{ m} \cdot [0.060\\ &- f(Q, D^{opt})\frac{8Q^2}{\pi^2 \cdot 9.807\text{ m/s}^2 \cdot (D^{opt})^5}]\end{aligned}$$

where $\dot{w}_d = 120$ kW and D^{opt} is from Eqn (12.11). Using `root` in `Mathcad`, we solve this equation to get $Q = 247.5$ L/s and $D^{opt} = 12.4$ in. for this value of Q. Once these are calculated, the designer has a baseline to explore the choice of different Q and D on the performance of the system. If the stream can supply 247.5 L/s and this is acceptable to the community at large, the design is feasible.

12.4.2 Minor Loss Considerations

Minor losses were neglected for convenience in the above developments. This effect could be included in the appropriate equations by adding the equivalent lengths of all of the minor-loss elements to the actual pipe length, L, in the calculation of the hydraulic gradient (only). This reduces the hydraulic gradient, S, and performance of the system because less energy is supplied to the turbine.

The large scale of the run of the penstock pipe and good planning in the field will reduce the need for most serious minor-loss elements like 90° elbows. Table 2.1 shows the equivalent length for each 90° elbow is 30. Ten elbows in a 12-in. pipe of length 1000 m adds ~91 m to L, reducing S by ~9%. This effect is halved if 45° elbows are used. Turbine performance is impacted by roughly the same amount as Eqs (12.7) and (12.8) show that actual turbine power decreases nearly in direct proportion to S. For PVC pipe, long runs of pipe may be able to bend to conform to the contour of the land, provided the diameter is not too large. Clearly, this is less likely with GI pipe not only because of the stiffer pipe material, but also because large bending stresses on threaded joints will reduce the integrity of the pipeline.

From Table 2.1 note that couplings and gate valves (used for on–off only, not throttling) negligibly contribute to the minor loss.

B.12.3 The Effect of Minor Losses

In textbox B.12.1, the penstock is known to have 18–45° elbows, 175 couplings, and a globe valve for flow control. Calculate the reduction in electrical power output from the system if minor losses are included.

The equivalent length, L_e/D, for a 45° elbow is 16 (Table 2.1). Assuming the globe valve to be open and for 12-in. pipe, Eqn (2.11) gives $K = 4.48$. Since the friction factor, f, for the penstock is 0.0126, the equivalent L_e/D for a globe valve is from $K = fL_e/D$ or $L_e/D = 356$. The minor loss for each coupling is small, but there are many of them. Account for this uncertainty by increasing the number of 45° elbows to 20. The total L_e/D is

$$\frac{L_e}{D} = 20 \cdot 16 + 356 = 676$$

For 12-in. pipe, the minor losses add $(676 \cdot 12/39.372 \text{ m} =)206$ m to the physical length of the penstock in the calculation of the hydraulic gradient only. The hydraulic gradient becomes,

$$S = \frac{80 \text{ m}}{1050 \text{ m} + 206 \text{ m}} = 0.0637$$

This is 16% less than for the minor-lossless design. The optimal pipe diameter is calculated from Eqn (12.11) as $D^{opt} = 11.37$ in., so 12-in. sch. 40 PVC pipe is chosen as it was for the minor-lossless design. From the `Mathcad` worksheet `microhydro_theoretical_power.xmcd`, the electrical power output is 64.2 kW, ~19 kW less than the textbox B.12.1 example. Conclude that this design will not meet the electrical power demand with the above minor losses. Minor losses must be reduced or other parts of the design changed (such as increasing the head or penstock diameter) to increase power output.

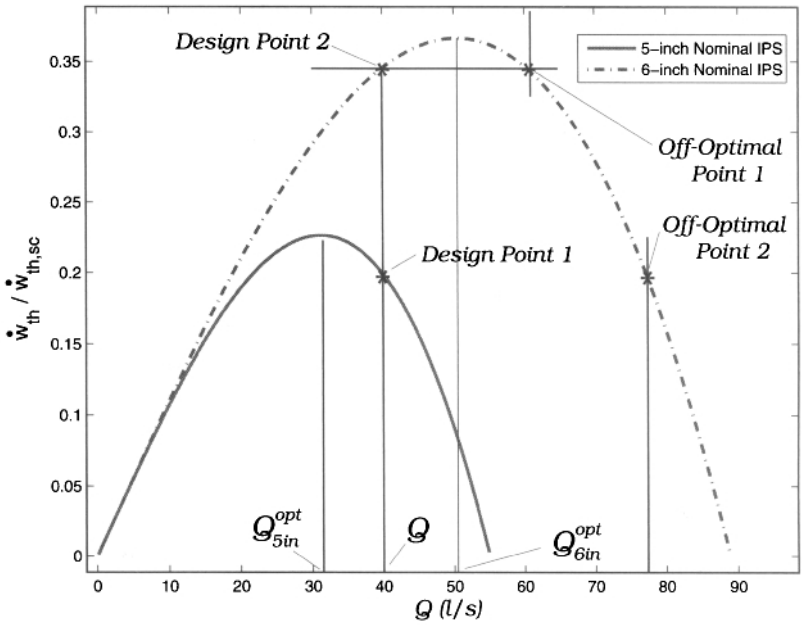

Figure 12.12 Power versus volume flow rate; off-optimal conditions.

12.4.3 Sensitivity to Off-Optimal Conditions

In Section 12.4.1, we saw the optimal character of the theoretical power done by the turbine as affected by the volume flow rate. We explore this more fully with a simple example. Suppose a small community wishes to install a microhydroelectric power plant of the order of 15–20 kW. They have available a water supply of $Q = 40$ L/s or more with a head that will produce a hydraulic gradient of $S = 0.10$. The elevation head is small enough that pressure considerations allow the use of PVC pipe. The optimal pipe size for this design is from Eqn (12.11),

$$D^{opt} = 0.8589 \text{ in.} \cdot 0.10^{-4/19} \cdot 40^{7/19} = 5.42 \text{ in.} \tag{12.18}$$

We will choose 6-in. nominal sch. 40 pipe for the penstock that has an ID of $D = 6.065$ in; slightly larger than D^{opt}. One of the members of the Community Engineer's Office suggests that a 5-in. (nom.) pipe should be selected, which the community has available for purchase, to save resources. In addition, this member also suggests the likelihood of increasing power from the plant by increasing water flow rate at some time in the future. What should the response to these questions be?

A plot of the relative power from the turbine [Eqn (12.7)] is shown in Fig. 12.12 for this example where two power curves appear, one each for the 5 and 6-in. pipes. The two design points identified in Fig. 12.12 fall along a line of constant $Q = 40$ L/s. Design Point 1 intersects with the power curve for the 5-in. pipe and gives a relative power value of ~0.20. The relative power value for Design Point 2, which intersects

the 6-in. power curve, is ~0.35. Thus, we see that we can achieve a 75% increase in power output by choosing a 6-in. penstock instead of 5-in. This should be very convincing even for the most skeptical members of the Engineer's Office!

In addition to this immediate increase in power with the choosing of 6-in. pipe, if the flow rate is increased in the future, power production will decrease with an increase in flow for the 5-in. candidate, whereas for the 6-in. penstock, it will increase.

The issue of increasing flow rate is addressed by the remaining vertical lines and the off-optimal points in Fig. 12.12. The optimal flow rates for the two pipe candidates are Q_{5in}^{opt} and Q_{6in}^{opt}, from Eqn (12.11), are ~31 L/s and 50 L/s, respectively. If the current design flow rate of 40 L/s is increased, the power will increase as Design Point 2 moves to the right toward the peak of the power curve for the 6-in. pipe; up to a relative power value of ~0.37 at which $Q = 50$ L/s. Increasing the flow rate greater than this will reduce the power. In fact, the power output is the same for the design flow rate of 40 L/s (Design Point 1) and 61 L/s (Off-Optimal Point 1), more than a 50% increase in flow. Further flow rate increases continue to reduce power output as an increasing fraction of the available potential energy of the system is dissipated in pipe friction. It is very interesting to see that if $Q \approx 77$ L/s, the power produced by the plant would be the same as operating the system at 40 L/s with the smaller 5-in. penstock pipe (Off-Optimal Point 2).

Of course, if there really is an interest in the larger flow rates of the scale at the Off-Optimal Points, the engineer will want to consider a larger pipe size at the outset. This would produce a third power curve in Fig. 12.12 that will fall above and to the right of that for the 6-in. candidate.

12.4.4 Component Models

The turbine efficiency discussed in Section 12.4.1 includes the complex fluid mechanics when a water jet at high speed contacts a bucket of a turbine, such as that for a Pelton wheel (see Fig. 12.3). The parameters needed to describe the power produced by this interaction are shown in Fig. 12.13. Water flow from the penstock enters the turbine and is immediately accelerated in a converging nozzle as shown. The jet from the nozzle impacts the bucket imparting some momentum to it, and the bucket "pushes back" in a sense that accelerates the flow backward in the direction from which it came. If it were possible for the water to deflect an angle $\beta = 180°$, the flow would lose an amount of momentum equal to ρV_1^2 to decelerate it to zero speed at the surface of the bucket, and another ρV_1^2 to accelerate it to V_1 in the opposite direction.[8] This is the "impulse" that drives a Pelton turbine. The relative velocity between the incoming jet at V_1 and the tangential speed of the wheel, ωr, gives rise to a torque acting at the wheel's center.[9] We have (Smits, 2000; White, 1999; Streeter

[8]This description is based on an observer fixed at the surface of the bucket.

[9]The symbols in this section are used only in their contexts in this section; as such, they do not appear in the Nomenclature and, where possibly used in other parts of this book, will have different meanings.

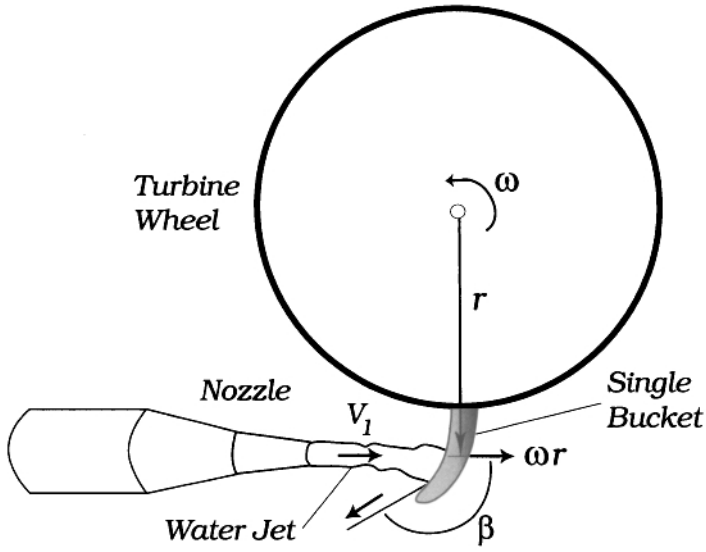

Figure 12.13 Parameters to describe torque and power for a Pelton water turbine.

et al., 1998; Munson et al., 1994),

$$T_{shaft} = \rho Q r(V_1 - \omega r)(1 - \cos\beta) \tag{12.19}$$

where T_{shaft} is the torque (a rotational force) on the shaft of the Pelton wheel resulting from the momentum change of the water jet at a radius of r. The product of the torque and rotational speed, ω, is the rate of work done by the water. Obtain

$$\dot{w}_{shaft} = \rho Q \omega r(V_1 - \omega r)(1 - \cos\beta) \tag{12.20}$$

where ωr is the tangential velocity of the wheel at radius r.

Several comments concerning Eqs (12.19) and (12.20) are in order. First, the power to the wheel includes the product $1 - \cos\beta$. For $\beta = 180°$, this term becomes 2, which is its maximum value. Because of physical constraints where the incoming and outgoing water jets cannot occupy the same space at the same time, the bucket is typically designed for $\beta \approx 165°$. This is of little consequence from a performance standpoint since $1 - \cos(165°) = 1.966$ is very close to the maximum of 2.

Second, Eqn (12.20) shows that power depends on the difference between the incoming jet speed and the tangential speed of the wheel. Although torque is a maximum when the wheel is not moving [$\omega r = 0$ in Eqn (12.19) produces maximum torque], the wheel must move for power to be produced as seen by our inspecting Eqn (12.20). To determine maximum power as affected by the water jet and rotational wheel speeds, we take the derivative of $\dot{w}_{shaft}$ with respect to ωr, set this equal to zero, and solve for ωr. The result is $\omega r = V_1/2$. Thus, for fixed values of Q and β,

the maximum power from the wheel is

$$\dot{w}_{shaft,max} = \frac{1}{4}\rho Q V_1^2(1 - \cos\beta) \tag{12.21}$$

Finally, if the load were removed from the shaft, intuitively the wheel would speed up to a point where $\omega r = V_1$. Our inspection of Eqn (12.20) verifies that no work is done under this condition and Eqn (12.19) shows that the torque is zero, as well. In this case, the jet of water is passing through the wheel without any loss of its momentum.

If the nozzle were frictionless, the static pressure energy and kinetic energy just upstream from the nozzle would convert to the kinetic energy of the jet according to Bernoulli's equation [Eqn (2.3)]. In fact, the nozzle is imperfect and energy losses from between 2 and 8% are expected because of friction (White, 1999). Bernoulli's equation is written for the nozzle flow as

$$V_1 = C_v\sqrt{2gh_{2a}} \tag{12.22}$$

where C_v is an experimentally determined "velocity coefficient" of value $0.92 \leq C_v \leq 0.98$, and h_{2a} is the sum of the static pressure and kinetic energy heads at the inlet to the nozzle (Fig. 12.5).[10]

When solving problems in turbomachinery, which is how the present topic is known, the equations that describe the performance of the machine are often written in terms of dimensionless groups. The groups themselves are nearly always ratios of two independent effects in the problem. For example, the Reynolds number (Re), which appears often in this book, can be shown to be the ratio of the inertial effects to viscous effects in a flow. A flow that has $\mathrm{Re} \gg 1$ is highly energetic (like turbulent flow), and one that has $\mathrm{Re} \ll 1$ is sluggish because friction dominates. Two dimensionless groups relevant to the present problem are the power coefficient, defined as

$$C_p = \frac{\dot{w}_{shaft}}{\rho Q g h_{2a}} = \frac{\dot{w}_{shaft}}{Q\Delta p} \tag{12.23}$$

and the "peripheral-velocity factor"

$$\xi = \frac{\omega r}{\sqrt{2gh_{2a}}} \tag{12.24}$$

Equation (12.20) becomes with these,

$$\boxed{C_p = 2\xi(C_v - \xi)(1 - \cos\beta)} \tag{12.25}$$

where C_p has the meaning of efficiency, in this case a hydrodynamic efficiency for the Pelton turbine. The denominator in Eqn (12.23) is the power in the flow at the inlet to the turbine. It is written in two identical forms in Eqn (12.23), one in terms of the head

[10]The kinetic energy is negligible relative to the pressure energy at the turbine inlet.

h_{2a}, and the other in terms of the static pressure drop across the turbine, Δp. Recall, the pressure at the turbine outlet is atmospheric. From Eqn (12.25), the optimal value for ξ is $C_v/2 \approx 0.47$. The reader can verify this by taking the derivative of C_p with respect to ξ, setting it equal to zero, and solving for ξ. With $\beta = 165°$ and $\xi = 0.47$, Eqn (12.25) gives $C_p = 0.887$. Thus, 88.7% of the rate of work done by the water becomes shaft work at the turbine outlet. One should not be misled by this apparent high value. Other physics needs to be considered when "calculating" the turbine efficiency. The hydrodynamics is just one part of this. The other important effects include windage (or shearing of air) between the rotating wheel and the casing, and friction in the bearings and transmission between the turbine and generator. Windage resistance, bearing, and transmission losses are normally determined by lab tests.

A plot of Eqn (12.25) appears in many references cited in this and the above sections. The performance curve of C_p as a function of ξ (where $0 \leq \xi \leq 1$) is nearly parabolic and peaks at $C_p = 0.887$ located at $\xi = 0.47$; the parabola is shifted a small amount to the left of center of this plot.

The cross-sectional area for the nozzle can be calculated by combining the continuity equation and Eqn (12.22). Obtain

$$A_n = \frac{Q}{C_v\sqrt{2g\,h_{2a}}} = \frac{Q}{C_v\sqrt{2g\,\eta_{sys}\,z_1}} \tag{12.26}$$

where η_{sys} is from Fig. 12.6 for smooth pipe or Fig. 12.11 for GI pipe. For smooth pipe, for example, $0.65\tilde{\leq}\eta_{sys}\tilde{\leq}0.9$, where the larger number corresponds to a pipe diameter of $1.3D^{opt}$.

B.12.4 Example: Nozzle Diameter

Calculate the nozzle diameter, D_n, and jet speed, V_1, for the textbox B.12.1 example. Assume smooth pipe of diameter $D = D^{opt}$ for the penstock.

From Fig. 12.6, $\eta_{sys} \approx 0.65$. Assuming $C_v = 0.95$ at its mid-range, Eqn (12.26) becomes,

$$A_n = \frac{230 \times 10^{-3}\ \text{m}^3/\text{s}}{0.95\sqrt{2 \cdot 9.807\ \text{m/s}^2 \cdot 0.65 \cdot 80\ \text{m}}} = 7.58 \times 10^{-3}\ \text{m}^2 = 11.75\ \text{in.}^2$$

If the nozzle is round, its diameter is

$$D_n = (4A_n/\pi)^{1/2} = 3.86\ \text{in.}$$

With C_v near its optimal point, the efficiency of the turbine, $C_p \approx 88.7\%$.

Nozzle Diameter (Cont'd)

The speed of the water jet is

$$V_1 = \frac{Q}{A_n} = \frac{230 \times 10^{-3}\ \text{m}^3/\text{s}}{7.58 \times 10^{-3}\ \text{m}^2} = 30.3\ \text{m/s}$$

The tangential velocity of the Pelton wheel, ωr, is optimally half of this value.

For $D = 12$ in. $> D^{opt}$ for textbox B.12.1 example above, Eqn (12.26) gives,

$$A_n = \frac{230 \times 10^{-3}\ \text{m}^3/\text{s}}{0.95\sqrt{2 \cdot 9.807\ \text{m/s}^2 \cdot 57.96\ \text{m}}} = 7.18 \times 10^{-3}\ \text{m}^2 = 11.13\ \text{in.}^2,$$

where $h_{2a} = 57.96$ m is from Mathcad worksheet `microhydro_theoretical_power.xmcd` (Fig. 12.5). Thus $\eta_{sys} = 57.96\ \text{m}/80\ \text{m} \approx 75\%$. The nozzle diameter is reduced by only 2.5% compared with $D = D^{opt}$.

12.5 HYBRID HYDROELECTRIC POWER AND WATER NETWORK

One of the discussions in Section 12.1 centered on how microhydroelectric power and the delivery of gravity-driven clean water are potentially a good marriage from the standpoint of the need for power to be dissipated in both systems. Difficulties with water quality and mismatches in volume flow rates that were discussed in Section 12.1 can be solved with simple existing technologies and designs. Once these problems are solved, at least two alternative designs can be considered. The first could be to move the power station to a higher elevation thereby sacrificing some elevation head but creating an elevation head for the gravity-water network. Water from the tail (see Fig. 12.5) would run into a storage tank located below the plant. The tank could be partially sunken into the earth with concrete block, brick, or ferrocement walls and rigid top to support the weight of the turbine and generator. Gravity-driven water flow from the tank to the community would be distributed in the normal way. No additional hardware would be necessary.

The second alternative is to maintain the power plant location to obtain the largest possible elevation head and use an electrically powered pump to move water to an elevated storage tank for gravity distribution. This system is most desirable because of the ready availability of electricity for the pump, there is no loss of elevation head or need to bury the tank which could be costly and, most importantly, pumping would take place during night-time hours where there is little or no electrical demand. In this case, most of the water is bypassing the turbine. The only addition to this proposed system compared with a stand-alone power station or stand-alone gravity-driven water network is the pump. This will likely be small, perhaps 0.6 L/s, the flow rate required

to fill a 20-m^3 tank in a 10-h period. The discharge head is required to reach the tank, perhaps 20 m or less. This pump would require $< 1/4$ horsepower to operate.

12.6 SUMMARY

We briefly touched on the companion topic of microhydroelectric power production in this chapter. Below are listed some of the key ideas and results from this discourse.

- Impulse turbines are well matched with high-head and low flow rates typical to many microhydroelectric power candidates where relatively small streams in mountainous regions are the energy sources. Impulse turbines include the Pelton wheel and Cross-flow types.
- The energy equation for a hydroelectric power plant exhibits optimal volume flow rate, Q^{opt}, for fixed penstock pipe diameter and hydraulic gradient, S. For $Q < Q^{opt}$, power reduces dues to lack of flow rate, and for $Q > Q^{opt}$, power reduces due to increasing pipe friction.
- By setting the actual flow rate for a flow-driven design to Q^{opt}, correlations for the pipe diameter that corresponds to the optimal power have been obtained for smooth and GI pipe. These allow the designer to quickly determine the pipe size that maximizes power output for a given Q and S.
- The same energy equation applies to designs that are driven by demand power. In this case, we use numerical methods (a root-finder) to solve for Q, which appears nonlinearly in the energy equation.
- Minor losses in the penstock pipe can play a major role in reducing power output. Serious attention should be given to this. Minor losses are included in the analysis and design by using the equivalent-length model (see Chapter 2), artificially increasing the penstock length, and thereby reducing the hydraulic gradient that drives the system.
- From our investigation of the sensitivity of the performance to off-optimal design conditions, it is important that the design point lies on a performance curve (power as a function of Q with D as a parameter; see Fig. 12.12) for a fixed D that has positive slope. In this way, an increase in Q will increase power output. If the design point lies on a performance curve having negative slope, an increase in Q will reduce power output. The exception to this is for cases where there will be a reduction in Q during the operation of the power plant. Reducing Q will increase power output where the design point lies on a performance curve of negative slope.
- The theoretical hydrodynamic efficiency of the nozzle/water jet/bucket system for a Pelton wheel is ~89%. Additional effects like friction in the bearings and transmission and windage losses in the air between the rotating wheel and turbine housing, all of which are experimentally determined, will reduce this value.

References

Anon. Micro-hydro Power. Technical report, Practical Action, The Schumacher Centre for Technology & Development, Bourton Hall, Bourton-on-Dunsmore, Rugby, Warwickshire, UK, 2007.

R. L. Daugherty, J. B. Franzini, and E. J. Fennemore. *Fluid Mechanics with Engineering Applications*. McGraw-Hill, New York, NY, 8th edition, 1985.

P. Fraenkel, O. Paish, V. Bokalders, A. Harvey, and A. Brown. Micro-hydro power: A guide for development workers. Technical report, ITDG Publishing, London, UK, 1991.

A. Harvey, A. Brown, P. Hettiarachi, and A. Inversin. Micro-hydro Design Manual. Technical report, ITDG Publications, London, UK, 2008.

B. R. Munson, D. F. Young, and T. H. Okiishi. *Fundamentals of Fluid Mechanics*. John Wiley & Sons, Inc., New York, NY, 2nd edition, 1994.

G. Opdenbosch. OGI, LLC. Personal Communication, 2009.

M. Smith. Motors as Generators for Micro-Hydro Power. Technical report, ITDG Publications, London, UK, 1994.

A. J. Smits. *A Physical Introduction to Fluid Mechanics*. John Wiley & Sons, Inc., New York, NY, 2000.

Stamford Power Systems Ltd. Technical data sheet BCM184J. `http://www.stamfordgeneratorsuk.com`, 2006.

V. L. Streeter, E. B. Wylie, and K. W. Bedford. *Fluid Mechanics*. McGraw-Hill, New York, NY, 1998.

F. M. White. *Fluid Mechanics*. McGraw-Hill, New York, NY, 4th edition, 1999.

Wikipedia. Pelton wheel — wikipedia, the free encyclopedia, 2009a. URL `\url{http://en.wikipedia.org/w/index.php?title=Pelton\_wheel\&oldid=297560369}`. [Online; accessed 24-August-2009].

Wikipedia. Cross-flow turbine — wikipedia, the free encyclopedia, 2009b. URL `\url{http://en.wikipedia.org/w/index.php?title=Cross-flow\_turbine\&oldid=330157532}`. [Online; accessed 14-December-2009].

CHAPTER 13

NETWORK DESIGN

By G. F. Jones and J. Ermilio

"If Practice and Theory Don't Agree, Investigate the Theory."
– C. M. Allen, 19th & 20th Century Hydraulic Engineer

13.1 THE DESIGN PROCESS

The process of gravity-driven water network design includes both hydraulic and non-hydraulic parts as discussed in Chapter 1. The process follows that in Jordan Jr. (2004); Jeppson (1976); Nayyar (2002); Trifunovic (2006); Swamee and Sharma (2008), among others.

1. From land survey data, elevation and plan-view drawings that identify locations and elevations of all elements of the network (see Fig. 1.1), which include pipe lengths, mean slopes of each pipe segment where relevant, etc., are produced. In this step, uncertainties in locations and elevations based on the instrument used in the survey are addressed and will be systematically included in the design calculations at a later step.

Gravity-Driven Water Flow in Networks. By Gerard F. Jones

2. From a water-demand survey of the community, and an estimate of the rate of population growth, the current and future water demands for on-average and peak conditions are calculated.

3. The water storage requirement is assessed and volume of the water storage tank is calculated.

4. The need for break-pressure tank(s) is assessed.

5. From steps 1 and 2, the intake (normally a single-pipe network) and distribution (normally a multiple-pipe network) pipelines are designed. The intake is from the source(s) to a storage tank, and the distribution mains distribute flow from the tank to the community. This includes selecting the pipe material, calculating actual inside diameters (ID), choosing nominal pipe sizes, and investigating flow control; that is, the sensitivity of the performance of the network to the partial closing of globe valves installed in the pipe segments and sizing of these valves. The latter step is referred to as the "reverse solution" in Chapter 11. Alternative designs are normally considered in this step, such as variations in the run of pipe and the use of different pipe materials. Determining the ability of the pipe and fittings to withstand the hydrostatic pressures in the network is also part of this step.

6. The details of the hydraulic design (including valve types and locations; by-passes; flow speed limits; the need for and location of cleanouts, air vents, and vacuum breakers; and consideration of air pockets and water hammer effects) and nonhydraulic design (reservoir construction at the source; structural considerations for the storage and possible break-pressure tanks and pipe supports, etc.) are executed.

7. Operating and maintenance issues are considered.

8. Costs are estimated, a final design selected, and drawings are prepared for the engineering and construction teams.

Most of these steps are applied to a design considered in the case study of Chapter 15. In this chapter, we will address some of the key elements of this process.

13.2 OVERVIEW

There are very many aspects of a sound gravity-driven water network. Correct sizing of the pipelines and placement of globe valves to meet the design specifications for flow rate are just two of them. The intent of this chapter is to discuss some features of the design of a few of the elements of the water network. For others, we will refer to appropriate references for further information. One of the better available references for the details of the *design* of most components of gravity-driven water networks at the time of this writing is Jordan Jr. (2004).

We will consider the following topics:

- Surveying the site to obtain accurate dimensional data.
- Calculating design information from site-survey data.
- Measuring and calculating water supply and uniform and peak demand.
- The need for and sizing of storage tanks.
- Features associated with the reservoir and development of the source.
- The tapstand.
- Air vents, vacuum breakers, and cleanouts.
- Issues associated with hydrostatic pressure.
- Flow speed limits.
- Dissipating potential energy in valves and fittings.
- Break-pressure and sedimentation tanks.
- Issues with oversized pipe.
- The composite pipeline.
- Water hammer.

13.3 ACCURATE DIMENSIONAL DATA FOR THE SITE

A design is only as good as the data on which it is based. With Global Positioning System (GPS) technology, there is a tendency to ascribe high accuracy (and precision) to the readings. In reality, GPS data are much more uncertain than those from a high-quality optical surveying instrument. This especially applies to elevation data. Normally, five or more satellites are required to obtain an even partially reliable altitude measurement from a GPS (see Appendix B). This is difficult to achieve if there is a tree canopy that covers the source. With a multitude of satellites, the altitude reading from a GPS is still subject to ± 15 m uncertainty. This means that, for low-head systems, GPS-based elevation data are practically meaningless. A calibrated altimeter may be reliable for small systems that can be surveyed in a short period of time. For large systems that take most of a day or more to survey, data from the altimeter must be assumed subject to uncertainties, of the same order as from a GPS, that arise from changing barometric pressure over this time scale. The solution to obtaining reliable length and position data is for a careful and systematic survey of the site using an Abney level or a transit. Readers not familiar with the operation and accuracy of an Abney level are referred to footnote 1 in Chapter 8 or (Jordan Jr., 2004) for further details. For inexperienced surveyors, a survey with an Abney level and a good measuring tape is best carried by two independent teams and the results of one team checked by the other.

A transit is a more sophisticated form of an Abney level that, in addition to slope or angle, allows for the direct measurement of distance between the instrument and a fixed end point. Thus, no measuring tape is required when a transit is used. Details of surveying with these instruments is presented in numerous sources (Brinker and Wolf, 1977).

13.4 CALCULATING DESIGN INFORMATION FROM SITE-SURVEY DATA

If the site were surveyed by a GPS, the first step to produce data for a design is to convert GPS latitude and longitude to Universal Transverse Mercator (UTM) coordinates. See Appendix B for the definition of UTM, this procedure, and notes on uncertainty of the measurements. With survey data in length dimensions, either from GPS or Abney level (or transit), we proceed to calculate local path lengths between any two arbitrary points along the water-flow path. For example, suppose we have recorded 18 survey points, or nodes, using a GPS or an Abney level (or transit). Each node has coordinates (x_i, y_i, z_i), where i is the node number. A plot of these points in three-dimensional (3D) space appears in Fig. 13.1. If the distance between the nodes is much less than the pipeline total length, we can imagine the pipeline as being constructed of 18 straight segments of pipe, each having a length calculated by the Pythagorean theorem. Thus, each segment length is from,

$$L_{(i-1)-i} = [(x_i - x_{i-1})^2 + (y_i - y_{i-1})^2 + (z_i - z_{i-1})^2]^{1/2} \tag{13.1}$$

where $i = 2, 3, \ldots, 18$. The local length, $L_{\ell,n}$, measured from the origin to an arbitrary node n is the running sum of the segment lengths to node n. Obtain,

$$L_{\ell,n} = L_{1-2} + L_{2-3} + \cdots + L_{(n-1)-n} = \sum_{i=2}^{n} L_{(i-1)-i} \tag{13.2}$$

The total length of the pipeline is $L_{\ell,18}$ for this example. With the above notation, it is understood that the pipeline length from its origin to node 2 is L_{1-2}, from node 2 to node 3 is L_{2-3}, and so on, as seen in Fig. 13.1.

Further discussion on this topic is presented in Section 8.7.

Elevation changes, needed in the energy equation for the solution of pipe diameters, are easily obtained in the same manner using just the z component of the position point (or vector). See Exercise 58.

13.5 ESTIMATING WATER SUPPLY AND DEMAND

One of the first considerations when designing a water supply network is the availability of water (the supply) in comparison with the water needs (demand) in the community. This consideration falls into four parts: the supply flow rate, the quality of this flow, and the uniform and peak water demand flow rates. The uniform demand needs to be considered to determine the adequacy of water flow rate from the

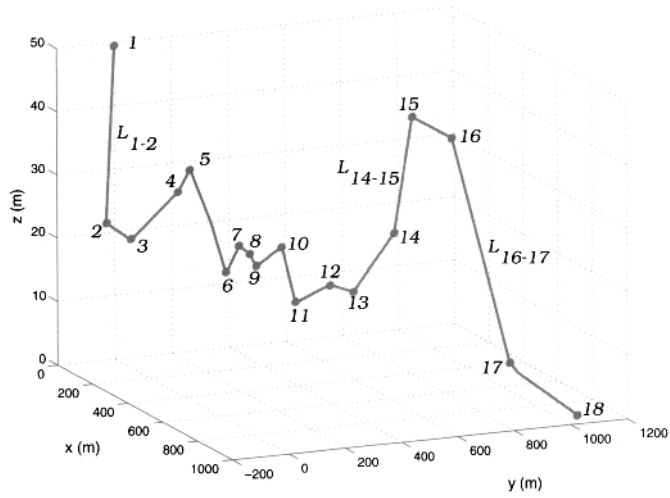

Figure 13.1 A 3D plot for pipeline from survey data. Here, L_{1-2}, L_{14-15}, and L_{16-17} are shown as sample segment lengths.

source(s), and the peak demand is part of the sizing of the water storage tank. The latter will be considered in Section 13.6.

The rate of water flow from a spring is easily determined by taking several measurements of timed collection of a known volume of water; say, a 2-L soft drink bottle for small springs or a barrel of known volume for large ones. Averaging the results over several, say 5–10, trials will ensure an accurate reading.

Water flow rate in a flowing stream may be estimated by measuring the surface speed, $\overline{u}$, of the flow using any object like a floating leaf timed over a known distance. From the continuity equation, Q is equal to $\overline{u}A$ [Eqn (2.21)]. The cross-sectional area, A, of the stream is estimated by measuring the depth of the stream at various locations and taking a suitable average. The product of the average depth and the measured width of the stream produces the cross-sectional area, A. Assuming that the flow speed is uniform over the entire cross-sectional area, the continuity equation is used to estimate Q for the stream.

Water quality of the source is an important consideration before proceeding with plans for network development. In most cases, if a spring is properly protected from contaminated runoff and solid matter, it will provide a reliable supply of good quality water. There are many types of water sampling and testing kits that are available for water-quality testing. These are available from commercial vendors or perhaps borrowed from the local District Health Office.

Once the present population is known for the community for which the water network is being built, the present and future water demand may be estimated. The future population is based on the formula for simple compounding,

$$P_F = P_P(1 + i)^t \tag{13.3}$$

Table 13.1 A Starting Point for Estimating Water Demand

Type of Water Supply	Average Consumption (L/person/day)	Range (L/person/day)
Public Water Collection Point		
Distance (500–1000 m)	7	5–10
Distance (250–500 m)	12	10–15
Distance (<250 m)	25	15–50
Private Connection		
Single Connection	50	30–80
Multiple Connections[a]	120	70–250

[a]As reference, eight months of data collected in 2008 from the rural community of Los Morales, Nicaragua show a range of 78-115 L/person/day with an average consumption of 90 L/person/day. This system was designed for private connections and has multiple connections per household.

where P_F is the future population, P_P is the present population, i is the growth rate per year (%/100), and t is the design lifetime in periods (years, in our case). For example, the rate of growth in a community may be 3.5%/year. Assuming a lifetime of 20 years, typical for the networks being designed, Eqn (13.3) shows that the future population will be approximately twice that at present.

The daily, uniform water demand for the community is considered next. There are a number of techniques that can be used based on the current water consumption. However, in most cases, the water consumption will change when a new system is constructed. This is usually because the rate of water consumption per person is, to a large extent, a function of water availability; increasing accessibility to water will correlate with an increase in consumption. This is important because an increase in water consumption often results in improvements in health and hygiene. If we explore the relationship between water availability and consumption further, we find that water demand can be accurately estimated based on the distance that people have to travel to collect it. For example, if someone has a direct household connection, then they will naturally consume more water than someone who has to travel a long distance. The water demand will also depend on the end-use of the water. If people have household gardens, then they might have an additional demand for irrigation. If someone has livestock, this will also increase the demand. At the same time, we should always keep in mind that there might be another source of water that can be used to supplement the demand for these secondary needs.

The following tables (Tables 13.1–13.3) can be used as a starting point to estimate water demand (Hofkes, 1983). Slightly more liberal estimates are presented by Jordan Jr. (2004).

An initial estimate of domestic per-capita water consumption with very little secondary demand (for livestock and farming) is between 15–50 L/person/day.[1] This

[1]In a World Health Organization (WHO) report concerning minimum drinking-water intake levels, Grandjean (2009) notes "Given the extreme variability in water needs which are not solely based on differences in metabolism, but also in environmental conditions and activity, there is not a single level of water intake

Table 13.2 Water Demand Estimates for Various Facilities

Type of Facility	Range (L/person/day)
School	15–30
Hospital	220–300
Restaurant	65–90
Church	25–40
Office	25–40

Table 13.3 Water Demand Estimates for Various Livestock

Type of Livestock	Range (L/unit/day)
Cattle	25–35
Horse	20–25
Sheep	15–95
Pigs	10–15
Chickens	0.015–0.025

includes allowances for drinking, cooking, personal washing, and a small amount for secondary needs (Jordan Jr., 2004). A recommended conservative estimate is 100 L/person/day that includes an allowance for some gardening and other small secondary uses. By using a larger water demand, we will also be able to account for the possibility that people will eventually connect a private water pipe to their houses so, this estimate will allow for expansion in the future.

The present demand can then be written as,

$$Q_{d,P} = \frac{P_P \cdot 100\ \text{L/person/day}}{60\ \text{s/min} \cdot 60\ \text{min/h} \cdot 24\ \text{h/day}} = 1.16 \times 10^{-3} \cdot P_P\ \text{L/s} \qquad (13.4)$$

A community of 300 persons, for example, will require a uniform water flow rate of ~0.35 L/s from the source(s). The future demand (in 20 years), $Q_{d,F}$, will be twice this value based on the above assumptions.

At this point in the design process, there is the need to verify that the available supply from the yield of the sources is greater than the present *and future* demand. This is determined by calculating the instantaneous rate of water supply available from the sources, Q_R, and comparing it with the instantaneous water demand, Q_d. If $Q_R > Q_d$ for the present, as well as the future, water demand, plans can be made to proceed with development of the source(s). If this condition is not met, the current and future demands should be considered to see if it makes sense to develop additional sources as a measure to meet both.

that would ensure adequate hydration and optimal health for half of all apparently healthy persons in all environmental conditions." However, WHO recommends the availability of a *minimum* of 20 L/person/day from a source within 1 km of the community (Mihelcic et al., 2009).

B.13.1 Water Supply and Demand Example

Three springs have been found to potentially supply clean water to a community seeking to develop a water network. The yields from the springs are $Q_{R,1}$ of 0.85 L/s, $Q_{R,2}$ of 0.30 L/s, and $Q_{R,13}$ of 0.55 L/s. A community of 520 persons is proposing to develop some or all of these sources for their use. The population growth rate is estimated at 2.5%/year. Assuming a 20-year lifetime and 100 L/person/day at present, report to the community leaders which sources you would recommend developing.

The present water demand is estimated from Eqn (13.4),

$$Q_{d,P} = \frac{520 \text{ persons} \cdot 100 \text{ L/person/day}}{60 \text{ s/min} \cdot 60 \text{ min/h} \cdot 24 \text{ h/day}} = 0.602 \text{ L/s}$$

The future population is estimated from Eqn (13.3),

$$P_F = 520 \text{ persons} \cdot (1 + 0.025)^{20} = 852 \text{ persons}$$

from which the future demand becomes,

$$Q_{d,F} = \frac{852 \text{ persons} \cdot 100 \text{ L/person/day}}{60 \text{ s/min} \cdot 60 \text{ min/h} \cdot 24 \text{ h/day}} = 0.986 \text{ L/s}$$

Our comparison of the future demand with the yields from the three sources shows that source 1 with either source 2 or source 3 will be adequate, whereas just sources 2 and 3 together will not be able to meet the future demand. Sources 2 and 3 together can meet the present demand, however. Depending on the relative locations of the sources, available funding, and local issues with obtaining the rights to use each, the community may want to consider source 1 with either source 2 or source 3 or reconsider the future demand model to determine its appropriateness. If water demand for the future is 0.85 L/s (the sum of $Q_{R,2}$ and $Q_{R,3}$) or smaller, the recommendation would be to consider developing source 2 and source 3 if more desirable than source 1 and either of the remaining two. Cost will need to be considered in this recommendation.

Note that it is not uncommon for there to be a seasonal variation in the available water supply at the source between the rainy and the dry seasons. For this reason, developing source 1 and one other may account for this difference in the event of a reduced water supply during the dry season.

This example above typifies a semianalytical solution for assessing the development of a number of potential sources for a network. Clearly, a full-analytical solution could be carried out where the pipes for the gravity mains are sized for the various

candidate sources to the tank and the cost of pipe and associated fittings is included in the calculation. From among these candidates, the minimum-cost solutions would likely be those recommended for development (see Exercise 59).

13.6 THE RESERVOIR TANK

When the water demand of the community cannot be met by direct flow from the source a reservoir (or storage) tank is generally required. A storage tank can be constructed of reinforced concrete, ferrocement (Watt, 1978), or prefabricated ultraviolet (UV)-resistant plastic, like polyethylene. The latter are becoming more common and can be cost-competitive with concrete tanks, but are typically no larger than ~12 m^3 and, for large volumes, may be difficult to transport to the site.

The tank is sized by first considering typical water demand schedules appropriate to the community under consideration. One schedule is presented in Chapter 15, and two in Jordan Jr. (2004). The schedule appearing in Fig. 15.3 is thought to apply to many communities worldwide. It consists of high hourly demand over a period of a few hours in the morning (40% of daily demand), a smaller peak over a 2-h period at midday (20%), and high hourly demand over a several-hour period in late afternoon/early evening (30%). Other schedules have been proposed (Ermilio, 2005). All schedules report in terms of fraction of total demand so that they can be applied to any community where the total daily water demand is known. As we will see in the example below, the high hourly demand in the morning or evening are normally the bases for sizing the storage tank.

The remaining 10% of the daily demand falls in between the morning and evening peaks. Water demand between late-evening and early-morning (e.g., 7 pm–5 am) is generally negligible.

The relationship between storage volume and the rates of water supply and demand is determined by the following integral formula, written by considering the definition of volume flow rate,

$$V_S(t) = V_S(0) + \int_0^t Q_s(\hat{t}) - Q_d(\hat{t})\, d\hat{t} \tag{13.5}$$

where $V_S(0)$ is the initial volume of water in the tank (at the start of the day; the end of hour 1 or 1 am) and $\hat{t}$ is a dummy variable of integration. The integrand in Eqn (13.5) is the net flow rate that enters the tank. A positive value of $V_S(t)$ at the end of any hour indicates that the tank contains some water for use at that time, whereas a zero or negative value of $V_S(t)$ shows that the tank is empty. During the latter periods, there is obviously no water available to meet demand. The volume of the tank is determined by a trial-and-error procedure by choosing a series of increasing tank volumes (starting from a small value) and calculating from Eqn (13.5) the water volume in the tank for each at the end of every hour of the day. In these calculations, we assume that the tank is full at $t = 0$ because of the normal fill-up during the evening hours when there is no water demand, but supply continues unabated. *An acceptable volume, in principle, is that which eliminates all zero or negative values*

of water volume at the end of each hour. The tank volume calculated by this approach will normally be conservative compared with other methods. For practical reasons, a volume is normally chosen that keeps the number of hours where there are zero or negative volumes to perhaps just one or two. The understanding here is that communities will tend to adjust their schedules to accommodate water availability once the network is installed and functioning (Jordan Jr., 2004). Uncertainty of the design data would also argue for the acceptability of an hour of empty tank.

As suggested by Mihelcic et al. (2009), to get a sense for the appropriateness of the final value for the tank volume, the flow rate per capita able to be delivered to the community (in 1 day) in the event of a source shutdown can be calculated. If this result provides for less than the WHO recommended minimum availability of 20 L/person/day, the tank volume should be increased if practical.

In many areas, the general operation of a community-based water system is not completely understood by the local residents. In some cases, household beneficiaries will be accustomed to having running water at or near their homes throughout the day and night. This habit is a result of previous water collection and delivery techniques that simply insert a hose to a running stream and extend it to a private home. This type of water collection can be beneficial for private homes in areas where water resources are sufficient. However, the habit of leaving the water system open at all times can do serious harm to a community-based gravity water system that uses water storage to manage peak demands. As a result, it is important to incorporate education about system operation and maintenance into any water supply project.

B.13.2 Example: Sizing of Storage Tank

Consider the textbox B.13.1 example. The community has reconsidered its future water needs and has decided to restrict the per-capita demand rate to 74 L/person/day (for the maximum of 852 persons) and to develop sources 2 and 3. Thus, the yield is 0.85 L/s. Based on the demand model of Fig. 15.3, size the storage tank for this community.

The calculations are carried out in the spreadsheet (supplied with this book) that solves Eqn (13.5). By trial-and-error, we select a range of tank sizes from 14,000 to 16,000 L. A plot of tank volume versus hour of the day is shown in Fig. 13.2 for 14,000, 15,000, and 16,000 L. At 6–7 pm the 15,000 L tank is empty whereas for 16,000 L it remains filled the entire day. We would recommend a tank volume between these two, say, 15,500 L (15.5 m^3). The numerical values for the volumes versus the hour of day are shown in Table 13.4 for the recommended tank size.

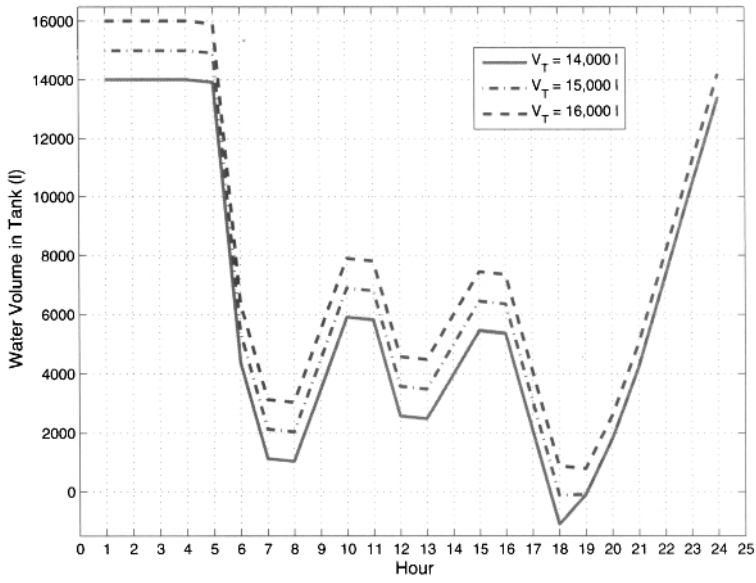

Figure 13.2 Water volume in tank versus hour of day. Hour 1 is at 1 am.

Example: Sizing of Storage Tank (Cont'd)

Note that the tank would overflow for several hours in the early morning hours. Overflow from storage tanks is normal. If there were an integrated approach to managing this water supply, the overflow volume could be used for other purposes, such as irrigating fields or livestock demand.

The flow rate per capita able to be delivered to the community (in 1 day) in the event of a source shutdown is 15,500 L / 852 persons / day = 18.2 L/person/day. This is slightly less than the minimum value recommended by WHO. Consideration should be given to increasing the tank size to ~17,000 L to meet the WHO-recommended target.

Planning for the construction of a reinforced-concrete tank is a time-consuming task. This is because of the need for the many different constituents of the reinforced concrete (cement, gravel, sand, steel reinforcing rod, wire mesh, and tie wires) along with forming timber to hold the concrete in place while it hardens. Once the volume of the tank walls is calculated using elementary volume formulas from geometry,[2]

[2]A quick estimate of the volume of concrete needed for a tank can be had by adding up the product of the wall (and floor) areas from lengths measured midway through the wall thicknesses and the appropriate

Table 13.4 Water Volume in Tank versus Hour of Day for a Tank Volume of 15,500 L.

Hour	Q_s (L/h)	Demand Percentage	Q_d (L/h)	Water Volume (L)	State of Tank
1	3060	0	0	15,500	Overflow
2	3060	0	0	15,500	Overflow
3	3060	0	0	15,500	Overflow
4	3060	0	0	15,500	Overflow
5	3060	5	3,150	15,410	Filling
6	3060	20	12,600	5,870	Filling
7	3060	10	6,300	2,630	Filling
8	3060	5	3,150	2,540	Filling
9	3060	1	630	4,970	Filling
10	3060	1	630	7,400	Filling
11	3060	5	3,150	7,310	Filling
12	3060	10	6,300	4,070	Filling
13	3060	5	3,150	3,980	Filling
14	3060	2.5	1,575	5,465	Filling
15	3060	2.5	1,575	6,950	Filling
16	3060	5	3,150	6,860	Filling
17	3060	10	6,300	3,620	Filling
18	3060	10	6,300	3,80	Filling
19	3060	5	3,150	2,90	Filling
20	3060	2	1,260	2,090	Filling
21	3060	1	630	4,520	Filling
22	3060	0	0	7,580	Filling
23	3060	0	0	10,640	Filling
24	3060	0	0	13,700	Filling

the amounts of constituents can be calculated for a prescribed strength of concrete. See, for example, the spreadsheet of Ermilio (2005).

13.7 THE TAPSTAND

Communal water collection points are referred to as tapstands and are designed to deliver water to a central location in an area to provide equal access to the collection facility. A picture of a completed tapstand is presented in Fig. 1.12. This topic is discussed in some detail in Section 15.3.3.4. The reader is referred to this section for tapstand features and design recommendations.

13.8 ESTIMATING PEAK WATER FLOW RATES

One could imagine the demand of the household daily consumption (of, say Q_d = 100 L/person/day) for a community as being spread out uniformly over the day. However, the demand model of Fig. 15.3 shows that it is not. In fact, in this model, 40% of water flow from the storage tank to the community is delivered in an approximate

wall thicknesses. A wall thickness of about 6 in. is necessary for most reservoir tanks in the 8–12 m^3-size range.

3-h period in the morning peak. If there were uniform (nonpeak) demand during this period, one would expect 3 h/24 h = 1/8 = 12.5% of the demand to occur during these hours. Thus, we need to increase the volume flow rate delivered to the distribution main from 12.5 to 40% by multiplying the uniform, or on-average, volume flow rate by a factor of 40/12.5 = 3.2 to obtain the peak flow rate.[3] The value 3.2 is called a "peak factor" and given the symbol PF. The peak volume flow rate determined in this manner is referred to as the "peak (or design) volume flow rate". The expression relating the peak flow rate to the uniform flow rate for any segment i–j in the network is then,

$$Q_{i-j,P,p} = PF \cdot Q_{i-j,P} \tag{13.6}$$

where the p subscript on $Q_{i-j,p}$ means the peak or design flow rate, and P refers to the present time.

The peak flow rates in the future are determined in the same way except that Q_{i-j} in Eqn (13.6) are the future flow rates, based on the future population from Eqn (13.3).

It is worth noting that the peak factor of 3.2 calculated above applies to the demand model of Fig. 15.3. For other demand models, the largest of the peak factors is used to calculate the design flow rates for the network.

B.13.3 Example: Peak Water Flow Rates

Consider the multiple-branch network of Fig. 11.16. Using a peak factor of $PF = 3.2$, and assuming the flow rates shown in this figure are on-average during the day, calculate the design flow rates for each segment of the network. If the flow rates shown in Fig. 11.16 are based on the present population, calculate the design flow rates that would accommodate the future population. Assume an annual growth rate, i, of 3% and a 20-year network lifetime.

For pipe segment 1–2, for example, from Eqn (13.6) the design flow rate becomes,

$$Q_{1-2,P,p} = PF \cdot Q_{1-2} = 3.2 \cdot 1.1 \text{ L/s} = 3.52 \text{ L/s}$$

For an annual growth rate, i, of 3% and a 20-year network lifetime, the result from Eqn (13.3) shows the design flow rates need to increase a factor of 1.806 to accommodate the future population. Thus, for pipe segment 1–2,

$$Q_{1-2,F,p} = (1+i)^t \cdot Q_{1-2,P,p} = 1.806 \cdot 3.52 \text{ L/s} = 6.36 \text{ L/s}$$

[3]Note that the morning peak produces a peak factor larger than the mid-day and late-afternoon–evening peaks. We will select pipe diameters based on the largest of the three peak factors.

Table 13.5 Uniform and Peak Water Flow Rates for the Multiple-Branch Network of Fig. 11.16

Pipe Segment, $i-j$	$Q_{i-j,P}$ (L/s)	$Q_{i-j,P,p}$ (L/s)	$Q_{i-j,F,p}$ (L/s)
1–2	1.10	3.52	6.36
2–3	0.78	2.50	4.52
3–4	0.51	1.63	2.94
4–5	0.25	0.80	1.44
2–6	0.32	1.02	1.84
3–7	0.27	0.86	1.55
4–8	0.26	0.83	1.50

Peak Water Flow Rates (Cont'd)

The flow-rate results for this network are presented in Table 13.5. Recall that the subscripts on the flow rate are i–j, the pipe segment indices; P, present; F, future; and p, peak.

13.9 SOURCE DEVELOPMENT

The primary considerations for a water supply system are source selection and source protection. Source selection considers the quantity of water available and the quality of the supply. Groundwater is water that can be accessed through the proper design and development of a borehole or well that taps into an underground water bearing stratum called an aquifer. Groundwater is generally of good-to-excellent quality. Surface water is a combination of groundwater that interacts with the surface of the terrain and runoff that collects within the watershed and becomes channelized during precipitation. Spring water is groundwater that comes into contact with the ground's surface due to subsurface geological conditions. Springs typically occur in mountainous areas because of steep elevation changes that cause infiltrated rainfall to emerge from fractured rock.

Source protection includes measures for preventing contamination from entering the supply. The primary consideration with groundwater is protecting against contamination that results from leaking septic tanks and pit latrines that are within 20 m from any extraction points. Surface water generally has poor-to-moderate quality. It should be assumed that any water supply that uses surface water, such as a small stream or river, requires water treatment using physical, biological, and chemical processes (Ermilio, 2005).

The primary concern with protecting surface water intakes is preventing agricultural runoff from entering the system. This is because agriculture-based pollutants, such as pesticides, are difficult to measure and expensive to remediate. Despite having

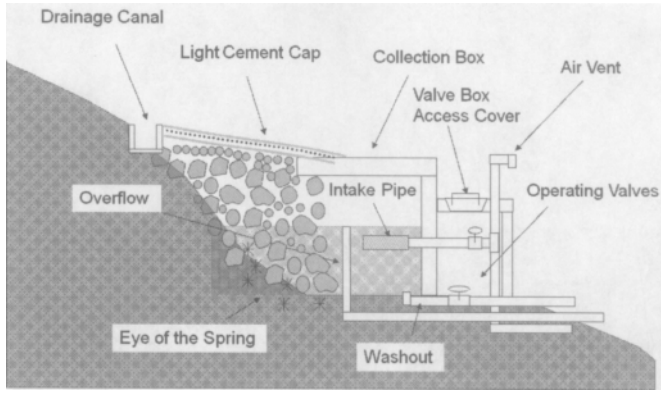

Figure 13.3 Source design.

generally lower yields than ground or surface water, springs are often the preferred water resource for community-based water supply projects. This is because a properly protected spring can typically provide a sustainable supply of high-quality water for a community. Springs are easier to contain than ground or surface water and are also easier to protect against contamination.

The components of a properly protected spring intake-reservoir are (see Fig. 13.3):

- A concrete retaining wall, or a spring box (Fig. 13.4) to capture the supply,
- A stone filter for screening of large debris,
- A concrete cap,
- A drainage canal to prevent surface runoff from entering the supply.

A removable cover should be included in the cap to allow for inspection of the water in the reservoir and to facilitate periodic cleanout of the reservoir if needed. See Fig. 13.4 and those from Fig. 1.2.

Source development is discussed in detail in other works on international development [cf. Jordan Jr. (2004)].

The outlet pipe penetrates the retention wall — the downstream part of the reservoir (if there is water storage at the source) or spring box, and forms the beginning of the "intake" part of water network. There are several things associated with the outlet that are important. First, a gate valve should be installed just downstream of the retention wall in the outlet pipe.[4] The gate valve is necessary to isolate the reservoir or spring-box when maintenance on the network is performed. Second, the intake end of the outlet pipe, submerged in water held by the reservoir or spring box, should

[4]Since no throttling will be done at the source there is no need for a globe valve. The latter are more expensive than gate valves and a full-open gate valve has less pressure drop (that is, a smaller K value) than a full-open globe valve.

Figure 13.4 A spring box under construction in central Nicaragua. A cast-in-place concrete cap was installed after this photo was taken (see Fig. 1.2).

have a filter, perhaps constructed of a fine-mesh screen, installed. This is important to eliminate sand and other particles, normally present in the flow, from entering the flow. When designing the screen, care should be taken to maintain a flow area as large as possible for water to enter the pipe. This will ensure a small loss coefficient that, if large, could result in substantial negative gage pressure immediately downstream of the source. This was discussed in Chapter 7.

Third, a 2 or 3-in. cleanout pipe is installed near the bottom of the reservoir or spring box to allow for periodic clean-out of debris that settles during operation. The clean-out also allows draining if a large-scale cleaning of the source is needed. Gate valves should also be installed at local low points along the entire pipe flow path to facilitate the clean out of sand and other debris that tends to accumulate over time at these parts. The size of these valves is small, generally of the order of $\frac{3}{4}$-in.

To ensure against undesirable vacuum conditions in the pipe coming from the source, an air vent or "vacuum breaker" should be installed at the source. This pipe, say of 1/2-in. GI, branches off of the outlet pipe just downstream from the gate valve (noted above), rises above the level of the reservoir surface, and is open to the atmosphere. Its purpose is to allow air into the system should negative pressures tend to occur in the outlet pipe. This would normally occur when the network is shut down for maintenance. This construction thus serves to "break the vacuum" in the network should it begin to form. More details on this construct are in Jordan Jr. (2004).

The presence of air in the network presents its own set of concerns. If the contour of the piping system has high and low points, the air trapped between a high and low point in the pipeline forms a cylinder-like compression chamber where there is no water. Because the air is trapped in a downward-directed leg, the density of water contributes nothing to the elevation pressure head at the low point (air density is effectively zero compared with that of water). The net effect is a reduction in the elevation head available to drive the water-flow network. In addition to this dominant effect, as water on either side of a high point attempts to move the cylinders of trapped air through the system, it compresses the air, doing work in the process, and dissipating energy from the flow. Some of this energy is recovered with expansion of the air upon reduction in static pressure. For both of these reasons, trapped air in the network acts as an additional minor loss. Should this loss become large, these "air blocks" could severely restrict the performance of the system.

The addition of manually operated or automatic air vent valves located at the local high points in the system, relative to nearby local low points, can always be used to remediate this problem, but they represent a maintenance issue. A brief discussion of air blocks is in Jordan Jr. (2004) and a more thorough treatment is given by Corcos (2004). The problem is approached from a fundamentals standpoint and presented briefly in Chapter 14.

Finally, gate valves should be installed at the lowest end of all runs of pipe that form valleys. These will allow for periodic cleaning of solid debris from the pipe that accumulates over time.

13.10 HYDROSTATIC PRESSURE ISSUES

Because of the energy dissipation associated with a fluid in motion in a pipe, the static pressure in a moving fluid is always less than when fluid motion ceases and the pressure becomes hydrostatic. Thus, the ultimate stress associated with pressure is exerted on the piping when the water in the network is static. Care must be taken to consider the hydrostatic pressure when designing pipe for the network. The pressure rating for Class III high-density polyethylene (HDPE; refer to Chapter 3 and Jordan Jr. (2004)) is equivalent to ~60 m of water head, whereas for the thicker wall, and more expensive, Class IV HDPE pipe, it is 100 m of water head. For polyvinyl chloride (PVC) pipe, the pressure rating for a wide range of appropriate pipe sizes, including SDR 26, is 160 psig, or ~112 m of head (Table 3.4). Break-pressure tanks (Jordan Jr., 2004), discussed briefly below, allow the static pressure to return to atmospheric and should be installed in any network where the change in elevation even approaches these levels. The pressure rating for heavy-wall galvanized steel (GI) pipe is high enough (1500 m of head) such that rupture from pressure is not normally a concern. However, a corroded or poorly assembled fitting will normally be the point of potential failure for GI pipe.

13.11 THE BREAK-PRESSURE TANK

A break-pressure tank (see Fig. 1.7) is used in a gravity-driven water network to reduce the static pressure in the pipe flow to atmospheric pressure. Break pressure tanks are used in high-head gravity-driven water networks, where the build-up of static pressure at lower elevations would require thick-wall plastic or GI pipe; both expensive alternatives. In all cases, the reliability of pipe and fittings in the water network suffers as the static pressure encroaches on the values discussed in Section 13.10.

A break-pressure tank is needed in the following two instances:

- For the segments in the network that are feeding water to a tapstand, a break-pressure tank is needed if the static pressure at the tapstand will be greater than ~20–30 m of water head. Larger values may cause the water tap valve (one like a globe valve, except it has a rubber washer as the seat material; see Fig. 1.11) to leak or wear prematurely. Also, static pressures that are too large at the water tap valve will create difficulty in drawing water without severe splashing. See more discussion in this topic in Section 15.3.3.4.

- For the segments in the network that are *not* feeding water to a tapstand, a break-pressure tank is needed if the static pressure in the pipeline will exceed those values presented in Section 13.10 or the pressure limits as specified by the pipe or fitting manufacturers. The rule-of-thumb for this case is that one break-pressure tank is needed for every 100 m of elevation change in the network.

Be aware that a water storage tank acts in the same manner as a break-pressure tank to reduce the static pressure to atmospheric level. This should be considered in the decision to install and where to locate a break-pressure tank.

Unlike water storage tanks, the capacity of a break-pressure tank is not a major design consideration since there should be no accumulation within the tank; inflow and outflow rates should match. In practice, this is done by using a float valve (one that turns off if the water level in the tank reaches a preset level; like a ball-float valve used in western toilets) Several good conceptual drawings of a break-pressure tank exist and will not be reproduced here [see Mihelcic et al. (2009) and Jordan Jr. (2004)].

13.12 THE SEDIMENTATION TANK

Sedimentation is a physical process used to pretreat water that has high levels of suspended particles, such as stone, sand, silt, and other insoluble materials. Sedimentation will occur in these suspensions when the flow speed of water is reduced sufficiently in a "retention chamber" or water tank and turbulence in the flow is reduced. This process allows for the particles of density greater than that of water to settle out of suspension. A conceptual drawing with dimensions approximately to scale for a horizontal-flow sedimentation tank is shown in Fig. 13.5.

The "settling velocity" of a particle, which is independent of the flow speed in the sedimentation tank, can be determined experimentally and should be verified prior to the tank design and construction. Analysis may be used to obtain a first approximation of the settling velocity. The theory is based on Stokes flow of a small spherical particle.[5] Settling velocities for a number of different materials appear in Jordan Jr. (2004). For typical materials found in water supplies in rural communities, these range from 0.023 m/h for silty-clay to 9.36 m/h for silt. The efficiency of the settling process is reduced significantly if turbulence is present in the flow and is not considered in the design.[6]

Figure 13.6 shows results of an analysis with tank specifications for typical sedimentation facilities used in community water supply projects. The assumed tank length-to-width ratio of three generally produces a one-dimensional (1D) flow. We see from this figure that the tank width is largely dependent on the type of material being settled. In systems where silty-clay material is present, the sedimentation tank can be fitted with additional measures to reduce the tank dimensions by including level spreaders within the tank. These are flat plates installed horizontally in the tank each of which acts as a pseudo-tank bottom to catch particles as they settle. This topic is covered in more detail in Anon. (1981). Simple techniques to ensure a uniform velocity across the tank should be included in the design so that water flow is evenly divided over the width and depth of the tank (Anon., 1981).

[5]Stokes flow of a solid particle in a fluid occurs where the flow speed and particle size are both small. This gives rise to a Reynolds number (Re, based on equivalent particle diameter) $\ll 1$.

[6]One of the characteristics of turbulence is localized intense mixing. Mixing will prevent the dense solid matter from settling in the sedimentation tank.

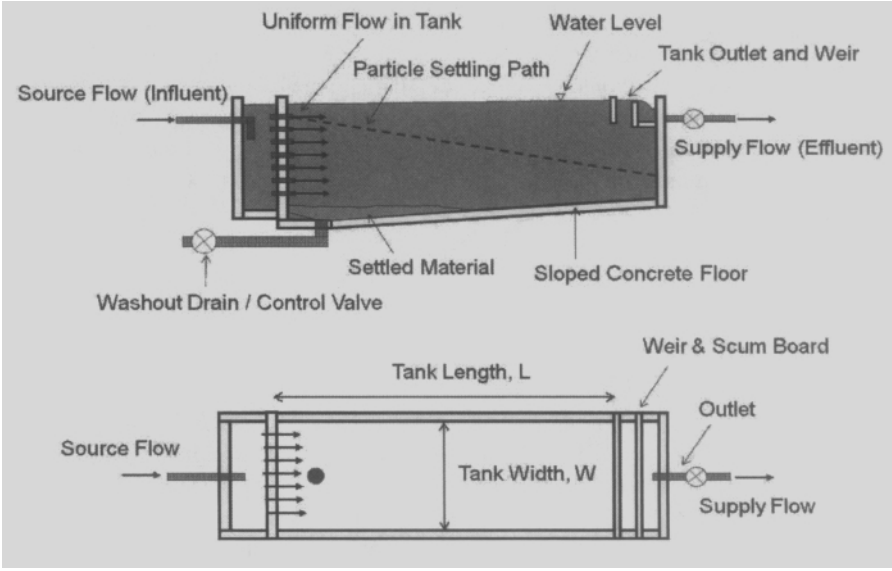

Figure 13.5 Elevation view (top) and plan view (bottom) for a horizontal-flow sedimentation tank.

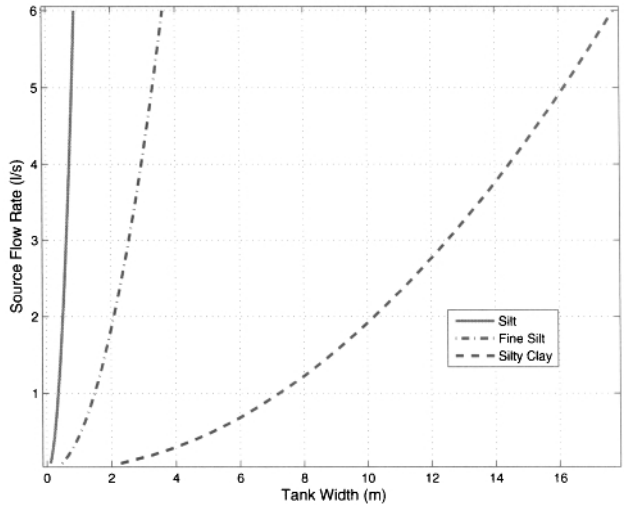

Figure 13.6 Sedimentation tank performance.

13.13 FLOW SPEED LIMITS

Erosion of plastic pipe caused by suspended particles in the flow is known to occur for high flow speeds. The problem worsens as flow speeds increase, based on rec-

ommendations in the literature (Jordan Jr., 2004), a designer should limit the extent of pipe exposed to speeds exceeding ~3 m/s. The erosion is especially problematic just downstream from sharp bends, like 90° elbows and the branches of tees. The speed of 3 m/s is also the recommended peak speed for a pipe flow to keep flow noise to acceptable levels for cases where pipe is to be run in or around living spaces. At the other end of the spectrum, should the flow speed fall to much less than ~0.7 m/s, there is likelihood of sedimentation from small particles, such as sand and small bits of organic matter, normally entrained in the flow. Pipe diameters that result in flow speeds $\gg$ 3 m/s and $\ll$ 0.7 m/s should be avoided. For more discussion related to this topic, see Section 13.15.

13.14 DISSIPATION OF POTENTIAL ENERGY

There are a limited number of discrete pipe diameters from which to choose when designing a pipe-flow network. Thus, it is seldom that we are able to design a system such that the elevation head (the potential energy) is exactly offset by energy dissipation from pipe friction between the pipe inlet and outlet. The imbalance between the potential energy and pipe friction requires the use of either a fixed or variable energy-loss device (Section 7.5) in the pipeline. Jordan Jr. (2004) refers to the above imbalance as "excess energy" and the act of dissipating it as "burn-off". In the fields of thermodynamics or fluid mechanics, the process of dissipating energy (with no heat transfer from the pipe) is referred to as "throttling".

A variable-loss device is normally a globe valve, which has been noted often in this text, and discussions about it appear in Sections 1.3.4 and 7.5. The globe valve works by forcing the flow to pass through a small cross section where friction between the flow and the valve body can be very large. The cross-sectional area for flow is adjustable based on how it is set by turning the valve handle. A cross-sectional view of a globe valve is presented in Section 1.3.4. A globe valve is designed to perform in a partially open state. Another type of valve, such as a gate valve, should not be used in place of a globe valve for throttling because it is not constructed to throttle the flow and will likely be noisy when operating and fail prematurely. It is often difficult and time consuming to replace a failed valve in a pipe-flow network.[7] Throttling with a ball valve is not recommended because of the difficulty of controlling the flow near the closure point for this type of valve. As discussed in several places above, including Chapter 11, globe valves are used at various locations in every pipe gravity-driven water flow network to allow the designer and operators flexibility in the flow and pressure conditions throughout. The presence of a globe valve in the pipe has the effect of reducing the pipe diameter from its actual ID. In this sense, the globe valve

[7]Special considerations are needed in networks where galvanized iron (or galvanized steel; GI) pipe is used. Because of the possible need to replace a throttling valve upstream of a tank or tapstand, for example, unions (Section 1.3.2) are recommended to be installed upstream and downstream of the valve to facilitate the replacement. Otherwise, the pipe must be cut, rethreaded, and rejoined which is inconvenient and costly.

allows the designer to more-closely match the diameter corresponding to the chosen nominal pipe size with the required theoretical inside diameter.

What is not widely understood about throttling valves is that they have pressure-drop limitations. Throttling in a globe valve reduces the pressure across its flow restriction, causing a pressure drop, Δp, between the upstream and far-downstream (say, just after the body of the valve) locations, as discussed in the above paragraph. This occurs in two parts. The first part occurs between the inlet and that immediately downstream from the seat area of the valve (see Fig. 1.11) where the pressure falls to *more* than Δp between the inlet and this location.[8] In the second part, there is a "static pressure recovery" effect just downstream from the first, where there is a slight static pressure increase. For liquid flows, a pressure-drop limitation arises if the absolute static pressure resulting from the first part of the pressure drop attempts to fall below the local vapor pressure of the liquid.[9] If the local static pressure becomes equal to the vapor pressure of the liquid, the flow will locally vaporize and bubbles will form. Under this condition, the flow is said to be "choked," a consequence of which is that no further pressure drop can be produced by further closing of the valve (the pressure drop across the valve is controlled by the vapor pressure just downstream from the valve seat). A further consequence occurs when the bubbles collapse as they move slightly downstream and are exposed to the higher pressures in the second part of the above process. If the collapse occurs near t,he valve seat or pipe wall, the seat or wall will erode as if being hit with small projectiles of dense fluid. Since failure over time will likely occur under this condition, cavitation should be avoided.

If cavitation is detected (cavitation sounds like small rocks moving in the flow), the suspect valve should be replaced with one or more globe valves in series or by a fixed energy-loss device (see below). The former may be adjusted so that just a fraction of the overall required pressure drop occurs across each of the valves thus eliminating cavitation. More on this topic is found in the control valve literature. See, for example, the design handbook from Fisher Controls (Anon., 2005).

A fixed energy-loss device is a restriction placed in the flow. One type of restriction, given by Jordan Jr. (2004) (frictional diffuser), consists of a PVC cap inserted into a 32-mm PVC pipe where a small hole is drilled into the cap. The flow restriction caused by the hole produces a large amount of energy dissipation that reduces the static pressure from the inlet to the outlet of the diffuser.

Care should be taken when planning to use this diffuser, since the small hole may very easily become completely blocked with small particles and organic matter that are normally present in the flow. This characteristic of the diffuser necessitates that it be designed for easy removal (say, by the use of two unions, one immediately upstream and the other immediately downstream) for periodic cleaning.[10] In addition,

[8]In fluid mechanics, this region is referred to as the "vena contracta," the point of minimum cross-sectional area for flow in the valve. In the vena contracta the highest local flow speed and approximately the lowest local static pressure as predicted by Eqn (2.3) result.

[9]This depends on temperature. At 10°C the vapor pressure of water is ~0.178 psia or ~1.2% of an atm.

[10]Note that a bypass pipe, with the appropriate valves and unions, need to be included in this arrangement [see Jordan Jr. (2004)].

the pressure drop across the diffuser is very sensitive to the diameter of the hole in the cap, an effect that changes over time as the hole will become partially clogged. This uncertainty requires that the diffuser be calibrated before placed into service in the field. Only a simple liquid manometer and a pump are required to carry out an accurate calibration. Partial clogging over time argues for a globe valve to always be installed in series with the frictional diffuser to enable a throttling adjustment.

As a final comment on energy dissipation, we note that dissipation can be *useful* in contrast with the understanding of it from the above paragraphs in this section where energy dissipation is viewed as a bothersome task. For example, a water turbine coupled to a generator may be installed in place of a globe valve. In the turbine-generator, mechanical power that would have been dissipated as waste heat can now be put to use to benefit the community. This topic was discussed in Chapter 12.

13.15 DESIGNING FOR PEAK DEMAND: PIPE OVERSIZING

In designs where the peak factor, $PF > 1$, the pipe diameters in the distribution and gravity mains downstream from the storage tank will be oversized for the nonpeak periods. For example, for PF of 3.2 in the example of Section 13.8, the increase in flow rate to the peak values increases the pipe diameters by 53% [$D \sim Q^{7/19}$, see Eqn (9.4)]. This translates to a 235% increase in the cross-sectional area of each of the pipes. If we make the conservative assumption of constant friction factor for the sake of simplicity, the energy equation [Eqn (2.44)] shows that, in each of these pipes, the major loss (pipe friction) falls to ~12% of its value when sized for the nonpeak periods (the major loss is proportional to D^5 if f is assumed constant). In this way, in a gravity-driven water network, *much of the pipe in the network is oversized for operation during most of the day to accommodate the needs of the peak periods.*

Another consideration is that small sources, such as springs, may not remain constant over time. Variations in rain amounts and soil percolation rates, and changes in the topology and extent of ground cover in the region, both natural and man-made, around the source can cause variations in water production rates at the source. This may also contribute to the reduction in water flow rates and oversized pipe.

This topic is included to highlight it, and to shed light on the importance of trying to ascertain peak and future water demands as accurately as possible. As discussed in Section 13.14, oversized pipe will normally require that a greater fraction of the potential energy of the network be dissipated in minor-loss elements like globe vales. This is unavoidable. For the case of $PF = 3.2$, the increase in minor-loss-element dissipation is equal to about 88% of the major-loss pressure drop that would have occurred if the pipe were sized for non-peak periods. Overestimating peak and future water demands will unnecessarily increase the cost of the network (because of the higher cost of larger pipe) and place a greater load on the throttling devices, or require more of them, throughout. Controllability of the flows in the network will become more challenging and premature wear of the throttling devices is possible under these conditions.

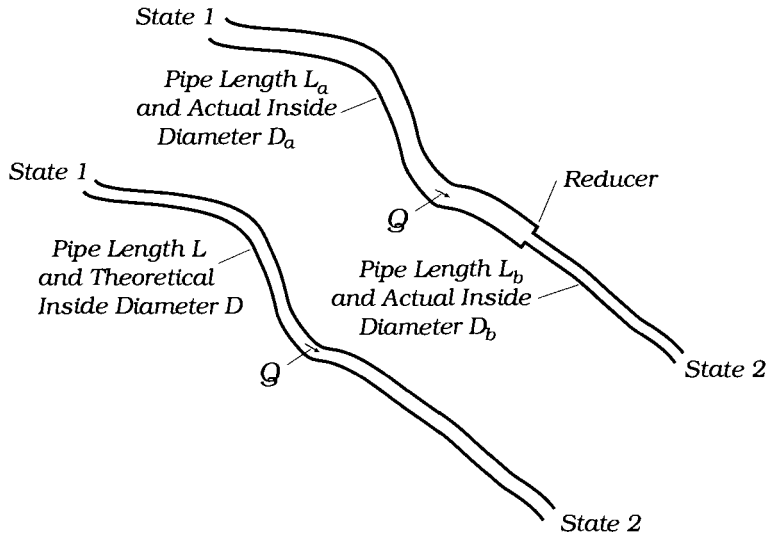

Figure 13.7 A pipe (bottom) and its composite form (top) that produces approximately the same head loss.

13.16 THE COMPOSITE PIPELINE

When selecting a nominal pipe size corresponding to a calculated theoretical pipe diameter, we saw in Section 3.5 that the choice is made for the nominal size that produces an inside diameter slightly larger than the theoretical value. If we are restricted to just a single pipe of a single nominal size, this method may result in excessive energy dissipation in a globe valve and other minor loss elements if the theoretical diameter is much less than the inside diameter for the chosen pipe size. As discussed in Section 13.14 this may not be desirable. A remedy to this problem is the composite pipeline. When used in place of a single pipe, a composite pipeline will dissipate energy as required by the design in major loss, thus relieving the minor-loss elements of this task.

A composite pipeline (Fig. 13.7) consists of two series-connected pipes of different diameters, D_a and D_b, and lengths, L_a and L_b, that produce the same head loss as that for a uniform pipe of theoretical diameter D and length $L = L_a + L_b$. The fluid flow rate in each pipe is identical. Relative to the uniform-diameter pipe, this is possible if $D_a > D$ (resulting in reduced head loss over length L_a) and $D_b < D$ (resulting in an increase in head loss over length L_b). Thus, it is clear that $D_b < D < D_a$. The order of pipes of D_a and D_b as shown in Fig. 13.7 may be interchanged with no overall

effect on the performance of this pipeline.[11] Normally the choice is made to install the larger pipe size upstream of the smaller one to maintain a high a static pressure over the run of pipe a in case a branch may be needed from this pipe in the future.

For sufficiently long pipelines, the minor losses for the reducer and other possible fittings are small relative to the major loss and may be neglected. If an exceptional case is encountered, the following simple development may be modified to include minor losses as needed. The requirement that the head loss in the single and composite pipes be identical gives

$$h_L = h_{L,a} + h_{L,b} \tag{13.7}$$

The Darcy–Weisbach equation (Eqn (2.10)) is introduced to obtain

$$f(\overline{u}, D)\frac{L\,\overline{u}^2}{D} = f(\overline{u}_a, D_a)\frac{L_a\,\overline{u}_a^2}{D_a} + f(\overline{u}_b, D_b)\frac{L_b\,\overline{u}_b^2}{D_b} \tag{13.8}$$

Combining the continuity equation [Eqn (2.21)] with this, and with $L = L_a + L_b$, we get

$$f(Q, D)\frac{L}{D^5} = f(Q, D_a)\frac{L_a}{D_a^5} + f(Q, D_b)\frac{L - L_a}{D_b^5} \tag{13.9}$$

Rearrange this to obtain

$$\frac{L_a}{L} = \frac{D^{-5} f(Q, D) - D_b^{-5} f(Q, D_b)}{D_a^{-5} f(Q, D_a) - D_b^{-5} f(Q, D_b)}, \qquad D_b < D < D_a \tag{13.10}$$

Once the theoretical pipe diameter, D, is determined from the solution of the energy equation, and the actual inside diameters for the two nominal pipe sizes, D_a and D_b, that bound D are identified, Eqn (13.10) can then be solved for the length L_a. The friction factor is from Eqs (2.16) and (2.17). For smooth pipe over the range of Re where the Blasius formula for friction factor applies [see Eqn (2.19) and Section 9.3], a closed-form equation may be easily developed from Eqn (13.10).

$$\frac{L_a}{L} = \frac{D^{-19/4} - D_b^{-19/4}}{D_a^{-19/4} - D_b^{-19/4}}, \qquad D_b < D < D_a \tag{13.11}$$

[11] A composite pipeline generally falls under the category of the serial network of Section 11.5.1. The difference between this and the treatment in the current section is that the static pressure at the junction of the two pipes in the upper part of Fig. 13.7 is assumed to be acceptable for the composite pipeline. That is, there is no attempt to calculate this pressure in the analysis associated with the composite pipeline.

B.13.4 Example: Composite Pipeline

Determine the lengths L_a and L_b (see Fig. 13.7) for a composite pipeline of 1078-m-long, sch. 40 PVC pipe, where the theoretical value for D is calculated as 6.830 in. Assume, and then verify, that the flow is turbulent such that Eqn (13.11) applies. The flow rate is 3.4 L/s.

From Table 3.1, two actual inside diameters that bound D are 6.065 in. (6-in. nom.) and 7.981 in. (8-in. nom.). Equation (13.11) becomes

$$\frac{L_a}{L} = \frac{6.830^{-19/4} - 6.065^{-19/4}}{7.981^{-19/4} - 6.065^{-19/4}} = 0.591$$

Thus, $L_a = 0.591 \cdot 1078$ m = 638 m, and $L_b = 440$ m. A composite pipeline of these lengths of 6 and 8-in. (nom.) pipe will produce approximately the same head loss as one of $D = 6.830$ in. for the total length, L.

Re based on pipe b (the smaller size) is

$$\mathrm{Re}_b = \frac{4Q}{\pi \nu D_b} = \frac{4 \cdot 3.4 \times 10^{-3}\ \mathrm{m}^3/\mathrm{s}}{\pi \cdot 1.307 \times 10^{-6}\ \mathrm{m}^2/\mathrm{s} \cdot (6.065/39.372)\ \mathrm{m}} = 21,500$$

a turbulent flow. For the larger pipe size, Re_a = 16,340. Thus, Eqn (13.11) is valid for this problem.

A couple of notes of caution concerning the composite pipeline are in order. First, recall from the discussion in Section 3.5 that one of the reasons for choosing a pipe diameter larger than theoretical is that this approach adds flexibility to the design. In keeping with this idea, if a composite pipeline is to be used, it is recommended to reduce the length of the smaller-diameter pipe as calculated by Eqn (13.10) (or 13.11) by perhaps a factor of 0.8–0.9. By doing this, there will be excess static pressure not dissipated by major loss that can be used if needed for unanticipated needs.

Second, a composite pipeline and globe valve both serve to reduce static pressure by energy dissipation. The fundamental difference between them is that a globe valve is adjustable during network operation whereas the composite pipeline is not. As discussed in Section 11.6.5, globe valves give the designer flexibility in balancing flows in multiple branch and loop networks and, when closed, allow the removal of pipe and components for maintenance and repair. The recommendation is do not replace a globe valve by a composite pipeline if this leg of the network requires static pressure control or anticipated frequent maintenance.

13.17 WATER HAMMER

When a liquid flows in a network of pipes, there is a considerable kinetic energy due to its density and flow speed. If a valve in the pipe is closed rapidly, the liquid attempts to come to a complete stop over a short period of time. If the valve is closed rapidly enough, this time is so small that there is little opportunity for the closing valve to dissipate all of the kinetic energy in friction. The excess energy that is not dissipated produces an internal wave in the liquid that moves back-and-forth in the pipeline, dissipating energy in the process. This effect is referred to as water hammer. Thus, water hammer produces a pressure wave, with an amplitude perhaps much higher that the hydrostatic pressure, that travels at a high speed through the liquid. Water hammer causes noise, can result in sudden movement of the pipe, or burst a pipe if the pressure rise exceeds the safe operating pressure of the pipe or fittings. The perturbations could also be severe enough to break joints between pipe and fittings, or loosen pipe anchors, and so it is worth our consideration.

The following simple analysis can be used to approximate the pressure rise resulting from the instantaneous closing of a valve in a pipeline. Because of the assumptions on which it is based, this analysis will predict the worst-case effect from water hammer. Nonetheless, the results are valuable in that they highlight the need for the designer to take steps to mitigate potential water-hammer problems in the completed network.

The increase in pressure, Δp, associated with a sudden reduction in flow speed, $-\Delta \bar{u}$, in a pipe flow is from the Joukowski equation[12] developed by considering mass conservation at the location of a shock wave in the liquid,

$$\Delta p = -\rho a_w \Delta \bar{u} \tag{13.12}$$

where ρ is the density of, and a_w is wave speed in, the liquid. The wave speed in water at standard conditions (10°C) is ~1483 m/s if the pipe wall behaves as rigid. If the pipe wall is elastic, which is a good assumption for plastic pipe, the expression for the wave speed is much less than this value and is from,

$$a_w = \sqrt{\frac{B/\rho}{1 + 2 \cdot (B/E)/(D_{out}/D_{in} - 1)}} \tag{13.13}$$

In Eqn (13.13), B and E are the bulk modulus of water (a thermodynamic property that is ~2.110 GPa at 10°C, where 1 GPa = 10^9 Pa), and elastic modulus of the pipe wall, respectively. For PVC, $E \sim 2.90$ GPa, and for steel (or GI), $E \sim 200$ GPa. The terms D_{out} and D_{in} are the outer and inner diameters of the pipe, respectively.

Equations (13.12) and (13.13) can be used to conservatively estimate the magnitude of the pressure wave that arises in a pipe after the sudden closing of a valve.

[12]The details of this development ar beyond the scope of the present work, but are found in several textbooks on fluid mechanics (Streeter et al., 1998; Potter and Wiggert, 2002).

B.13.5 Example: Pressure Rise in Water Hammer

Consider $Q = 2.25$ L/s of water flow at 10°C in a 2-in. nominal sch. 40 PVC pipe. A gate valve in the pipeline is suddenly closed. Calculate the amplitude of the pressure wave resulting from this closure. How would your results change if the pipe material were steel or GI?

For this size pipe, Table 3.1 gives $D_{out} = 2.375$ in. and $D_{in} = 2.067$ in. For water at 10°C at which the density is $\rho = 999.7$ kg/m^3, Eqn (13.13) becomes

$$\begin{aligned} a_w &= \sqrt{\frac{(2.110 \cdot 10^9 \text{ N/m}^2)/999.7 \text{ kg/m}^3 \cdot (1 \cdot \text{kg m/s}^2)/\text{N}}{1 + 2 \cdot (2.11 \cdot 10^9/2.90 \cdot 10^9)/(2.375/2.067 - 1)}} \\ &= 442.8 \text{ m/s} \end{aligned}$$

The flow speed in the pipe before the valve is closed, $\bar{u}$, is from the continuity equation, Eqn (2.21),

$$\bar{u} = \frac{Q}{A} = \frac{2.25 \text{ L/s} \cdot 0.001 \text{ m}^3/\text{l}}{\pi/4 \cdot (2.067 \text{ in.})^2} = 1.04 \text{ m/s}$$

The change in flow speed is thus,

$$\Delta\bar{u} = 0 - \bar{u} = -1.04 \text{ m/s}$$

The magnitude of the pressure wave resulting from the sudden valve closure is from Eqn (13.12),

$$\Delta p = -999.7 \text{ kg/m}^3 \cdot 452.1 \text{ m/s} \cdot -1.04 \text{ m/s} = 460 \text{ kPa}$$

or ~47 m of water head at the location of the valve. A quick calculation will show that the pressure rise would more than double to ~1413 kPa if the pipe material were GI, or ~144 m of head. We see that PVC pipe has a damping effect on water hammer compared with GI. As the pressure wave travels over distances away from the valve, the magnitude of this wave will be damped by viscous forces between water and pipe wall. This damping may take perhaps several seconds to tens of seconds. The calculations here provide a worst-case estimate of the pressure rise.

Our inspection of the above example shows that very large pressure rises are possible, especially if steel (galvanized iron) pipe is used. This points to the need to consider water hammer in the design stage to take appropriate steps to reduce it. Among these are

- Design the distribution network to reduce excessive flow speeds (see Section 13.13),
- Ensure that operators of the water network are made aware of the water hammer problem and are instructed to close all valves slowly, especially those where the flow speeds are high,
- For pipelines where water hammer is known or suspected to be a serious problem, accumulators or expansion tanks may be installed at locations where large pressure rises may occur to absorb and dissipate the energy of the pressure wave. These units, which have an air pocket separated from the water by a flexible rubber bladder, may be purchased from many commercial vendors.

References

Anon. Small community water supplies: Technology of small water supply systems in developing countries - technical paper series 18. Technical report, IRC: The International Rescue Committee, Rijswijk, The Netherlands, 1981.

Anon. Control Valve Handbook. Technical report, Fisher Controls International LLC,, Marshalltown, IA, 2005. URL \url{http://www.documentation.emersonprocess.com/groups/public/documents/book/cvh99.pdf}. [Online; accessed 08-December-2009].

R. C. Brinker and P. R. Wolf. *Elementary Surveying*. IEP Press, 1977. New York, NY.

G. Corcos. Air in water pipes, a manual for designers of spring-supplied gravity-driven drinking water rural delivery systems. Technical report, Agua Para La Vida, Berkeley, CA, 2004.

J. Ermilio. A case study for a water distribution network for the community of Kiangan, the Philippines. Course material for ME 4801, Department of Mechanical Engineering, Villanova University, Villanova, PA, 2005. URL Jordan.Ermilio@Villanova.edu.

A. C. Grandjean. Water requirements, impinging factors, and recommended intakes. http://www.who.int/water_sanitation_health/dwq/nutrientschap3.pdf, 2009. [Online; accessed 02-December-2009].

E. H. Hofkes. *Small community water supplies; technology of small water supply systems in developing countries*. John Wiley & Sons, Inc., Chichester, UK, 1983.

R. W. Jeppson. *Analysis of Flow in Pipe Networks*. Ann Arbor Science Pubs., Ann Arbor, MI, 1976.

T. D. Jordan Jr. *Handbook of Gravity-Flow Water Systems*. ITDG Publication, London, UK, 2004.

J. R. Mihelcic, L. M. Fry, E. A. Myre, L. D. Phillips, and B. D. Barkdoll. *Field Guide to Environmental Engineering for Development Workers.* ASCE Press, Reston, VA, 2009.

M. L. Nayyar. *Piping Handbook.* McGraw-Hill, New York, NY, 7th edition, 2002.

M. C. Potter and D. C. Wiggert. *Mechanics of Fluids.* Brooks/Cole (Thomson), Tampa, FL, 2002.

V. L. Streeter, E. B. Wylie, and K. W. Bedford. *Fluid Mechanics.* McGraw-Hill, New York, NY, 1998.

P. K. Swamee and A. K. Sharma. *Design of Water Supply Pipe Networks.* John Wiley & Sons, Inc., Hoboken, NJ, 2008.

N. Trifunovic. *Introduction to Urban Water Distribution.* Taylor & Francis, New York, NY, 2006.

S. B. Watt. Ferrocement Water Tanks and their Construction. Technical report, ITDG Publications, London, UK, 1978.

A water technician in East Timor.

CHAPTER 14

AIR POCKETS IN THE NETWORK

"Let all you who Thirst, Come to the Water!"
– Isaiah 55:1

14.1 THE PROBLEM

If the contour of the piping network has high and low points, the air trapped in the high points forms cylinder-like compression chambers. This is an idealization, but is useful for visualization of the relatively complicated process of liquid flow in a partially filled pipe with air. As the denser water on either side of the air attempts to move the cylinders of trapped air through the system, it compresses the air, doing work in the process, and dissipating energy from the flow. Nearly all of this energy is recovered with expansion of the air upon reduction in static pressure so that the work to compress the air can normally be neglected.

More importantly, the fact that air of essentially negligible density occupies a fraction of the pipe length reduces the elevation head available to drive flow through

Gravity-Driven Water Flow in Networks. By Gerard F. Jones

the system. For this reason, trapped air in the system, referred to as an "air block,"[1] acts as a reduction in the driving head or, as an alternate interpretation, an additional minor loss. Should this minor loss be large, the presence of air could severely restrict the performance of the system. The addition of manually operated or automatic air vent valves located at the highest points in the network, relative to nearby local low points, can always be used to remediate this problem, but they are a maintenance issue. A brief discussion of air pockets is in Jordan Jr. (2004) and a more thorough treatment is given by Corcos (2004).

Here, we explore this problem from a fundamentals viewpoint and suggest a methodology different from that in the previous references to access the impact of air pockets on the performance of a gravity-driven water system.

14.2 THE PHYSICS OF AIR/LIQUID PIPE FLOWS: FLOW IN A STRAIGHT PIPE

Consider the flow of water in a straight inclined pipe initially filled with air, as shown in Fig. 14.1. As the denser water flows to the bottom of the pipe, some of the air is pushed out by the direct movement of water or entrained in the water and carried out, and some of the lighter air is displaced to the top. In steady state (Fig. 14.1), we see that the effect of the initial air-filled pipe is to reduce the elevation head of the system, from z_1 to z_1'. In an extreme case, the elevation head driving the flow in the system can be reduced to a small fraction of z_1. Flow rates will consequently suffer and conditions of the design may not be met.

The volume of air in the pipe at any time depends on the volume pushed out and entrained by the water flow, and the pressure of the water on the air. To explore this further, imagine a pipe of volume V_{pipe} initially filled with air at atmospheric pressure, p_{atm}. For the moment, assume that no air is removed when water is introduced into the pipe. In steady state, the static pressure at the top of the pipe is known to be p_1. Recall that air is compressible and, if we assume that the temperature of the air remains constant as the water flows in the pipe,[2] the ideal gas law may be written between the initial state and that of Fig. 14.1 as

$$p_{atm}V_{pipe} = p_1 V' \tag{14.1}$$

or

$$\frac{V'}{V_{pipe}} = \frac{p_{atm}}{p_1} \tag{14.2}$$

where p is absolute static pressure in all of the equations in this chapter. The symbol V' refers to the volume of compressed air depicted in Fig. 14.1. If the pipe is constant diameter, volume terms in Eqn (14.2) may be written as proportional to length and

[1]This term is unfortunate in that for most cases air does not actually block the flow, but reduces it from the Natural-flow value. The term "air pocket" may be more representative of the phenomenon.

[2]This is reasonable since the ground in which the pipe is buried is approximately at constant temperature.

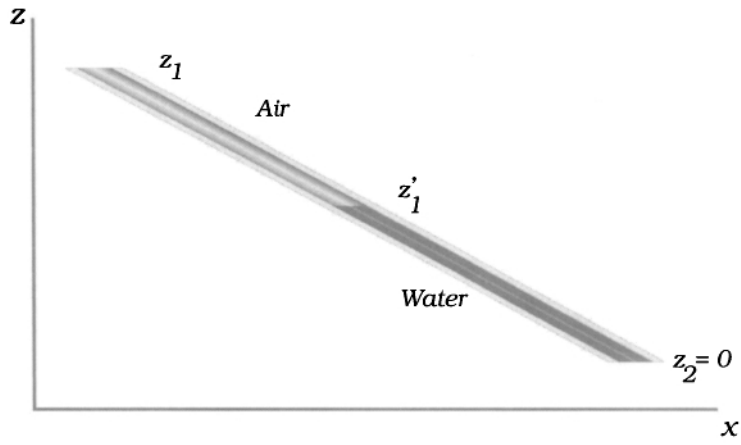

Figure 14.1 Water flow in a straight inclined pipe partially filled with air. Gravity acts downward. Drawings in this chapter are courtesy of Erin Vogel, Villanova University.

Eqn (14.2) becomes

$$\frac{z_1'}{z_1} = \frac{p_{atm}}{p_1} \tag{14.3}$$

where z_1'/z_1 is the fraction of the length of the pipe containing only air. Since it is reasonable to assume that some air will always be pushed out of the system by flowing water, either directly or through entrainment, the results of Eqn (14.3) represent a worst-case or "upper-bound" estimate of the effect of trapped air in gravity-driven flow of water in a straight, inclined pipe. For this case, for example, if we know that p_1 is twice atmospheric pressure, the air will occupy half of the length of the pipe. The actual elevation head driving the flow, z_1', will be $z_1/2$. Clearly, this is not a desirable situation since the design flow rate may not be satisfied with the reduced value for the elevation head.

Of course, no system is designed as just a straight pipe without incorporating in the design some way to remove air from the system. In the case of Fig. 14.1, the designer needs to include an air vent at the top of the system and the air will, over a reasonably short period of time from start-up, be pushed from the high part of the pipe by pressure. Note that the static pressure just downstream from z_1 is slightly larger than atmospheric due to the positive elevation head at this location.

The problem of a straight pipe is considered here to illustrate how air in a pipe reduces the elevation head. It is very idealistic. The more realistic problem, which we consider in Section 14.3, is one where there are local high points where air can become trapped.

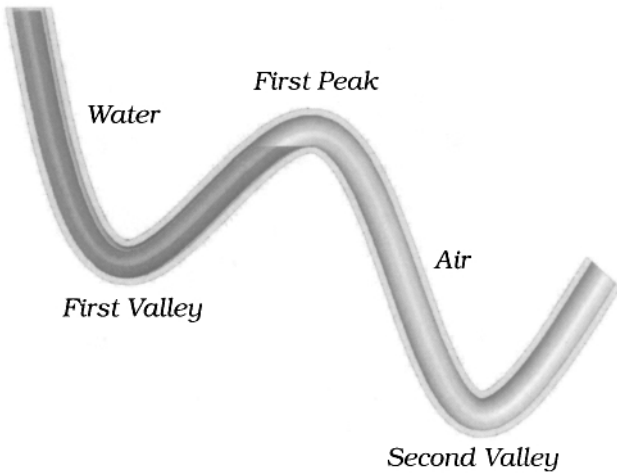

Figure 14.2 Water flow in a wavy inclined pipe partially filled with air. Before formation of air pocket.

14.3 FLOW IN A PIPE WITH LOCAL HIGH POINTS

Consider an initially air-filled pipe of uniform diameter with local high points. The situation of filling the pipe with water is depicted in Fig. 14.2. As water flows into the pipe, the first valley becomes filled. Water trickling over the first peak fills the second valley and, by doing so, traps a mass of air between the first peak and the second valley. This trapped air becomes the first "air pocket" and appears as shown in Fig. 14.3.[3] The static pressure in the pipe at the location of the first peak is greater than atmospheric because of the elevation head difference between the inlet and the first peak. Thus, the air in the first air pocket is compressed, reducing its volume to less than the volume of the leg of pipe connecting the first peak with the second valley (refer to Fig. 14.3).

As the pipe continues to fill, each leg of pipe that has a positive slope fills up to its peak along with the valley that immediately follows it. Air is trapped and compressed between this peak and valley to form another air pocket. Thus, each peak/valley combination forms one air pocket that contains compressed air at the pressure of the water at the peak. Recall that the density of air is small compared with water by a factor of ~1000. As we saw in Section 14.2, negligible-density air in the pipe displaces large-density water and reduces the elevation head that drives the flow. The water flow rate, obtained from the solution of the energy equation, that includes

[3]Note that there is no air formation above the first valley since air can normally escape upward and be released through the surface of the reservoir.

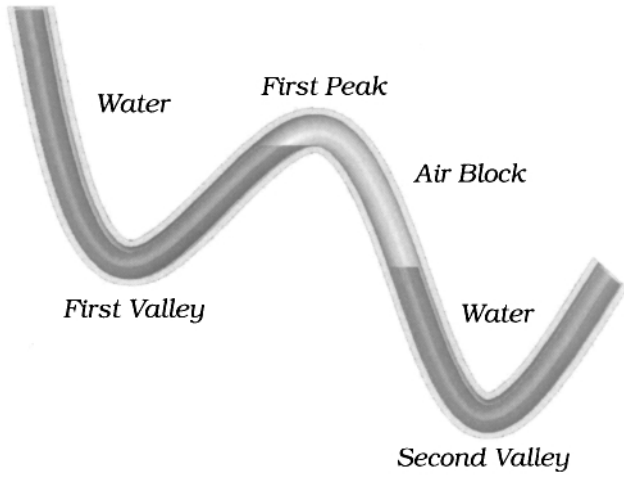

Figure 14.3 Water flow in a wavy inclined pipe partially filled with air. After formation of air pocket.

this "reduced elevation head," may not be able to satisfy the design requirements for the system. *This is the fundamental problem associated with air pockets.*

We see that to assess the impact of air pockets on the performance of a gravity-driven water network, there is a need to solve the energy equation for flow rate by using the reduced elevation head. Also needing our attention is the major loss term since the wetted surface area of the pipe, where the major loss occurs, is less than that for a totally water-filled pipe. Thus, the major loss in a partially air-filled pipe is less than its totally water-filled counterpart.

There are several things to keep in mind while assessing the effect of air pockets on network performance. First, as noted above, the results of our analysis are worst-case because to keep the problem tractable, we must assume that all air that was initially in the pipe remains during the filling process. Air that is directly removed by the flowing water or entrained in the water and carried away, reduces the negative impact of air pockets on the water flow rate.

Second, the situation depicted in Fig. 14.3 is idealized. For there to be flow in the system, water must trickle from each peak to the following valley. Therefore, the pipe is not full and the energy equation needs to be modified to account for this. For reasons of simplicity and because this effect is not large, we will neglect this in the analysis that follows.

Third, vent valves installed at the high point in the system, especially those closest to the source of water, may be used to reduce or eliminate any penalty in flow rate arising from air pockets. However, it must be kept in mind that these valves, if manual, must be operated in a reliable way by personnel in the local community. Whether they are manual or automatic, regular check-ups and maintenance must be performed on them to ensure they remain in good working condition. If not regularly attended, the

air valves will not function as designed and the system may accumulate air over time. Thus, the models developed in this chapter are worthwhile since they can predict the worst-case performance of the network if it is left unattended.

Finally, the presence of air in the system is not just the result of filling an initially air-filled pipe with water. Air can get into the system in many ways including air released from the water itself (even cold water contains dissolved air), and through vacuum breakers installed at the source (see Section 13.9). Thus, removal of air from gravity-driven water networks is an on-going responsibility of a community to ensure proper performance of the network.

14.4 THE EFFECT OF AIR POCKETS ON FLOW RATE

The fundamental problem associated with air pockets is the presence of air in the system that reduces the driving force for flow. There are two ways of analyzing this problem. The first, referred to as the "simple approach", neglects the compressibility of air. In doing so, a single, relatively simple, single linear algebraic equation for Q is obtained, which we can use to calculate the effect of air pockets on Q. The second includes the effect of air compressibility but at the expense of the need to solve a system of nonlinear algebraic equations for the pressure distribution in the network and Q. The computational effort for the latter is considerably greater than for the former. In both cases, the value for Q is conservative, meaning that it is an underestimate of the true value for Q.

Because of the simplicity of the simple approach, it is tempting to first assess the problem of air pockets using this one. Based on the outcome of this calculation, the designer can then judge the need to carry out a more-complete and more-realistic assessment by including the compressibility of air.

Perhaps a more compelling reason for using the simple approach is that it forms the *fundamental basis for understanding the more-complete problem where air compressibility is included.* In other words, the more-complicated, more-exact problem is more easily understood by first learning the simpler one.

14.4.1 A Simple Approach

The simplest approach to determine the effect of air pockets on the flow is to neglect compressibility of the air. This approach overestimates the length of pipe occupied by the air and produces a lower-than-actual estimate of the elevation head that drives flow in the system. In this sense, the present approach is "worst-case" (or conservative) but, since the compressibility effect of the air is neglected, relatively simple formulas may be obtained for the reduced elevation head and wetted (with water) pipe length.

Consider the geometry shown in Fig. 14.4, which consists of an inclined pipe of constant diameter, D, having numerous local peaks and valleys. The air pockets have already formed in the manner as discussed above and appear in Fig. 14.4 as pipe segments b, d, and f. Water resides in each of the valleys and fills up to the peaks that immediately follow. These are shown as pipe segments a, c, e, and g. The pressures

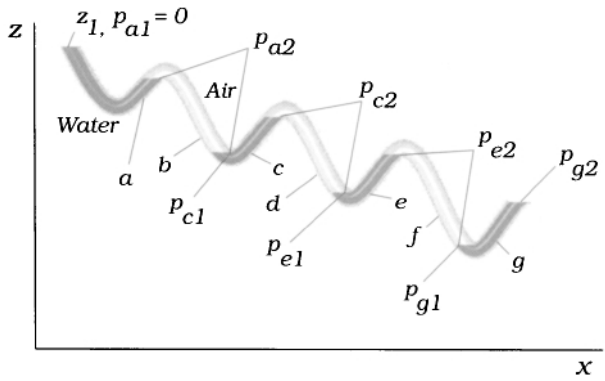

Figure 14.4 Water flow in a wavy inclined pipe partially filled with air after formation of many air pockets. Water appears dark and air appears lighter.

are designated as 1 at the start of each pipe segment (in the x direction) and 2 at the end of the segment. For example, for segment a, the static pressure at the inlet of this segment is p_{a1} and its outlet, p_{a2}. Because of the negligible density of the air and the fact that no air is flowing, the static pressures at the top and bottom of each leg of air are equal. Thus, for example, $p_{a2} = p_{b1} = p_{b2} = p_{c1}$, and so on, as shown in Fig. 14.4.

Because we have neglected the compressibility of air, the length of each pipe segment is completely determined by the geometry of the pipe. Using the usual symbol for length, L, we can write, for example, the length of pipe segment a as L_a. Also, for pipe segment c, L_c is the length of pipe between the valley at the start of segment c to the peak at the end of this segment.

We begin the analysis by writing the energy equation, Eqn (11.4), for each pipe segment containing water. We have

$$\begin{aligned}
g\Delta z_a - \left(\frac{p_{a2}}{\rho} + \alpha_a \frac{\bar{u_a}^2}{2}\right) &= C_{L,a}\frac{\bar{u_a}^2}{2}, \quad \text{Segment } a \\
g\Delta z_c + \frac{p_{c1}}{\rho} - \frac{p_{c2}}{\rho} &= C_{L,c}\frac{\bar{u_c}^2}{2}, \quad \text{Segment } c \\
g\Delta z_e + \frac{p_{e1}}{\rho} - \frac{p_{e2}}{\rho} &= C_{L,e}\frac{\bar{u_e}^2}{2}, \quad \text{Segment } e \\
g\Delta z_g + \frac{p_{g1}}{\rho} - \frac{p_{g2}}{\rho} &= C_{L,g}\frac{\bar{u_g}^2}{2}, \quad \text{Segment } g
\end{aligned} \tag{14.4}$$

where, as above, the terms Δz refer to the elevation change from the top to the bottom of a pipe segment measured in the coordinate system of Fig. 14.4. For example, as shown in Fig. 14.4, Δz_a appears as a positive value, whereas Δz_c, Δz_e, and Δz_g are negative valued. If we assume uniform pipe diameter, D, for the moment, we can

write $\bar{u}$ as $4Q/\pi D^2$ [using Eqn (2.21)] in Eqn (14.4). Obtain

$$\begin{aligned}
\rho g \Delta z_a - p_{a2} &= \frac{\rho}{2}(C_{L,a} + \alpha)(\frac{4Q}{\pi D^2})^2, \quad \text{Segment } a \\
\rho g \Delta z_c + p_{c1} - p_{c2} &= \frac{\rho}{2} C_{L,c}(\frac{4Q}{\pi D^2})^2, \quad \text{Segment } c \\
\rho g \Delta z_e + p_{e1} - p_{e2} &= \frac{\rho}{2} C_{L,e}(\frac{4Q}{\pi D^2})^2, \quad \text{Segment } e \\
\rho g \Delta z_g + p_{g1} - p_{g2} &= \frac{\rho}{2} C_{L,g}(\frac{4Q}{\pi D^2})^2, \quad \text{Segment } g
\end{aligned} \tag{14.5}$$

We also note that certain static pressures in Eqn (14.5) are equal; $p_{c1} = p_{a2}, p_{e1} = p_{c2}$, and $p_{g1} = p_{e2}$. By adding the equations in Eqn (14.5) and canceling the appropriate pressures, $p_{c1} - p_{a2}$, and so on, we obtain

$$\Delta z_a + \Delta z_c + \Delta z_e + \Delta z_g - h_{del} = (C_{L,a} + C_{L,c} + C_{L,e} + C_{L,g} + \alpha)\frac{8Q^2}{\pi^2 g D^4} \tag{14.6}$$

where $h_{g2} = h_{del}$ is the prescribed delivery static pressure head, say, at a tapstand, and $\Delta z_a, \Delta z_c$, etc. are from the geometry of the network as shown in Fig. 14.4.

Equation (14.6) is to be solved for the flow rate Q, where D has been already determined from the methods developed in Chapter 11. Note that the elevation head, referred to as the reduced elevation head above, $\Delta z_a + \Delta z_c + \Delta z_e + \Delta z_g$, is not as large as that for a water-filled pipe. In contrast to a wavy pipe that is entirely filled with water, if there are air pockets, as shown in Fig. 14.4, the constant air pressure on the left side of each valley does not add to the overall elevation head.

When solving Eqn (14.6), recall from Chapter 11 that C_L is the loss coefficient that includes the major and minor loss terms [see Eqn (11.5)]. C_L for each segment depends on Q and D for the pipe (through Re), the segment lengths L, and the values of the minor loss coefficients, K and L_e/D, if they are to be considered.

Equation (14.6) may be generalized for any number of local valleys, N, written in a compact form,

$$\sum_{j=1}^{N} \Delta z_j - h_{del} = (\alpha + \sum_{j=1}^{N} C_{L,j})\frac{8Q^2}{\pi^2 g D^4} \tag{14.7}$$

and solved for Q to assess the effect of air pockets on flow, subject to the assumption of incompressible air. Note that in Eqn (14.7) the summations are assumed to be taken only over the segments of the pipe that contain water.

If the pipe diameter changes along the flowpath such that $D_a \neq D_c \neq D_e \neq D_g$, Eqn (14.7) becomes

$$\sum_{j=1}^{N} \Delta z_j - h_{del} = \frac{\alpha}{D_1^4} + \frac{8Q^2}{\pi^2 g}\sum_{j=1}^{N} \frac{C_{L,j}}{D_j^4} \tag{14.8}$$

It is obvious from our inspection of Eqs (14.7) or (14.8) that $\sum_{j=1}^{N} \Delta z_j - h_{del} \geq 0$ for any flow to occur. From this result, it is easy to see that flow in the system will be choked if air pockets are such that $\sum_{j=1}^{N} \Delta z_j < h_{del}$.

14.4.2 Consideration of Compressibility of Air

The fundamental picture of the formation of air pockets is unchanged once the air is considered to be compressible. Complexity is added to the problem because the lengths of the water-filled segments of pipe and the elevation heads for each of these segments are no longer determined solely by pipe geometry. This is because when the air compresses under the effect of pressure, the length of each air segment shrinks, and correspondingly, the lengths of the water-filled segments increase. This can be easily visualized using Fig. 14.4. One outcome is that any negative-valued elevation heads that appear in Eqn (14.7) become less negative valued. This will serve to increase the volume flow rate, Q, relative to that determined from the solution of Eqs (14.7) or (14.8). An additional outcome is that there is slightly more major loss since more of the total length of pipe is wetted by the water. However, this effect is not large enough to offset the reduction of the negative-valued elevation heads.

It is not possible to write a single equation for Q once the compressibility of air is considered. The reason for this is that the terms Δz and L (embedded in C_L) in Eqn (14.5) are influenced by the static pressures at each peak through the ideal gas law. Thus, a system of equations needs to be solved simultaneously that includes Eqn (14.5), which was written for the water-bearing pipe segments, and the ideal gas law written for each pipe segment that contains air.

We now outline the solution procedure. The energy equation for flow in segment a is unchanged as it appears in Eqn (14.5) since the start and end of segment a is defined only by pipe geometry. Next, we calculate the length of the column of air in pipe segment b. For this segment, Eqn (14.3) may be written as

$$\frac{L'_b}{L_b} = \frac{p_{atm}}{p_{a2}} \tag{14.9}$$

where L'_b/L_b is the fraction of the length of pipe segment b that contains air as measured from the first peak in Fig. 14.4. In Section 14.4.1, we ignored compressibility, so $L'_b/L_b = 1$. Once compressibility is considered, we see that $L'_b/L_b < 1$. Pressure p_{a2} is the source of compression of the air, which is initially at atmospheric pressure, p_{atm}, just before filling begins. From an elevation drawing of the pipe and known L'_b/L_b from Eqn (14.9), the designer can then determine the values for Δz_c and L_c (to be used in the major loss calculation for $C_{L,c}$). That is,

$$\begin{aligned} \Delta z_c &= \Delta z_c\left(\frac{L'_b}{L_b}\right) = \Delta z_c\left(\frac{p_{atm}}{p_{a2}}\right) \\ L_c &= L_c\left(\frac{L'_b}{L_b}\right) = L_c\left(\frac{p_{atm}}{p_{a2}}\right) \end{aligned} \tag{14.10}$$

where Δz_c and L_c are functions of L'_b/L_b or, alternately, p_{atm}/p_{a2} as seen in Eqn (14.10).

The procedure continues by considering the effect of pressures p_{c2} on Δz_e and L_e, and p_{e2} on Δz_g and L_g, respectively. The following two equations, similar to

Eqn (14.10), result

$$\begin{aligned} \Delta z_e &= \Delta z_e(\frac{L'_d}{L_d}) = \Delta z_e(\frac{p_{atm}}{p_{c2}}) \\ L_e &= L_e(\frac{L'_d}{L_d}) = L_e(\frac{p_{atm}}{p_{c2}}) \end{aligned} \tag{14.11}$$

and

$$\begin{aligned} \Delta z_g &= \Delta z_g(\frac{L'_f}{L_f}) = \Delta z_g(\frac{p_{atm}}{p_{e2}}) \\ L_g &= L_g(\frac{L'_f}{L_f}) = L_g(\frac{p_{atm}}{p_{e2}}) \end{aligned} \tag{14.12}$$

Introducing Eqs (14.10)–(14.12) into Eqn (14.5), we obtain

$$\begin{aligned} \rho g \Delta z_a - p_{a2} &= \frac{\rho}{2}(C_{L,a} + \alpha)(\frac{4Q}{\pi D^2})^2, \quad \text{Segment } a \\ \rho g \Delta z_c(\frac{p_{atm}}{p_{a2}}) &+ p_{a2} - p_{c2} \\ &= \frac{\rho}{2} C_{L,c}(L_c(\frac{p_{atm}}{p_{a2}}))(\frac{4Q}{\pi D^2})^2, \quad \text{Segment } c \\ \rho g \Delta z_e(\frac{p_{atm}}{p_{c2}}) &+ p_{c2} - p_{e2} \\ &= \frac{\rho}{2} C_{L,e}(L_e(\frac{p_{atm}}{p_{c2}}))(\frac{4Q}{\pi D^2})^2, \quad \text{Segment } e \\ \rho g \Delta z_g(\frac{p_{atm}}{p_{e2}}) &+ p_{e2} - p_{del} \\ &= \frac{\rho}{2} C_{L,g}(L_g(\frac{p_{atm}}{p_{e2}}))(\frac{4Q}{\pi D^2})^2, \quad \text{Segment } g \end{aligned} \tag{14.13}$$

where static pressure p_{a1} (=14.7 psi) has been added to the first of these equations since all pressures are in absolute.

The equations of Eqn (14.13) are a system of four nonlinear algebraic equations in four unknowns, Q, p_{a2}, p_{c2}, and p_{e2}. The static pressure $p_{del} = p_{g2} = \rho g h_{del}$ is the static pressure at the delivery location as prescribed by the designer. The functions Δz_c, Δz_e, and Δz_g, and L_c, L_e, and L_g come from the geometry of the pipe also specified by the designer. Equation (14.13) can are solved in `Mathcad` using the `Given...Find` construct for solving system of nonlinear algebraic equations that we employed frequently in the study of multiple-pipe networks.

Clearly, the time and effort needed to solve the system of equations that arises when one considers air compressibility [Eqn (14.13)] is considerably larger than when compressibility is neglected [Eqn (14.7)]. The designer can weigh the benefits against this investment in time and effort when deciding the course of action. However, we have found for the cases studied in this text that the flow-rate result based on the neglect of air compressibility is overly conservative in many of these.

14.5 AN EXAMPLE

Consider the elevation view of a simple gravity water distribution pipe, of nominal $1\frac{1}{2}$ in. PVC, as shown in Fig. 14.5. The coordinates, (x, z), at the source, intersections

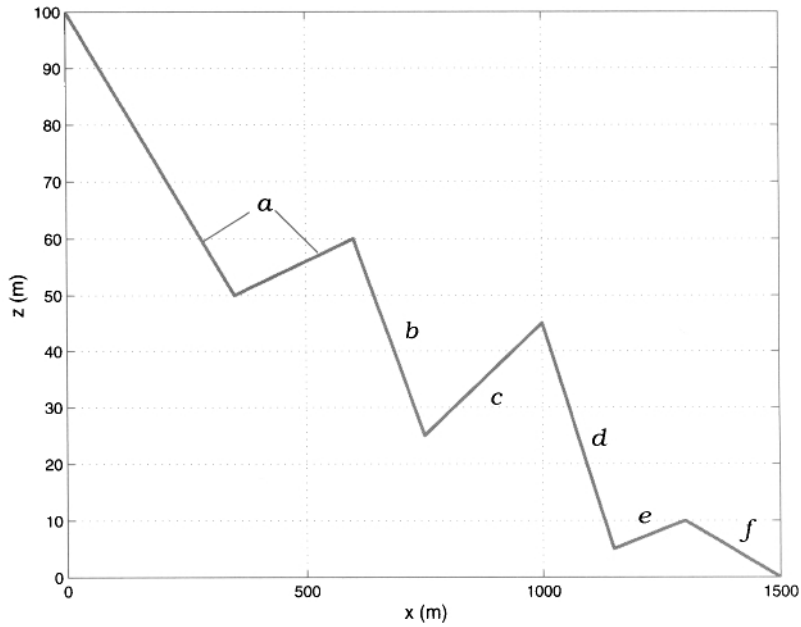

Figure 14.5 Elevation view of a simple gravity water distribution pipe with peaks and valleys. The source is at the entrance to segment a, and the delivery location is at the outlet of segment f. Note the large difference between the horizontal and vertical scales.

of the pipe segments, and delivery location are: (0,100), (350,50), (600,60), (750,25), (1000,45), (1150,5), (1300,10), and (1500,0) m. We wish to assess the effect of the air pockets on the volume flow rate of water in the system. Based on the material presented in Section 14.3, our inspection of Fig. 14.5 indicates that two air pockets will form, one in segment b and one in d. Our approach will be to use Eqn (14.7), the simple approach where air compressibility is neglected, and Eqn (14.13) where compressibility is included. We will compare the results of the two, and with the case of no air pockets.

To simplify the calculation, all minor losses will be neglected. This is justified if the sharp turns in the pipes as seen in Fig. 14.5 are instead well rounded, reducing the minor loss in the network. The static (gage) pressure head at delivery is assumed to be 10 m of water (about one atmosphere of pressure). As always, the static pressure at the source is atmospheric. Recall that for the equations from Section 14.4.2, where the problem depends on pressure through the ideal gas law, all pressures must be in

absolute units. Thus, we add 14.7 psi (10.34 m of water) to each gage pressure to get absolute pressure. Obtain, p_{a1} = 14.7 psi and h_{del} = 19.34 m.

First, we find the flow rate if there are no air pockets. The mean slope between the source and delivery points is calculated from Fig. 14.5 as $s = 0.0467$. We will use the design figures from Section 5.4, where the source pressure is zero gage pressure. We calculate the dimensionless delivery static pressure, F, to be $F = h_{del}/z_1$ = 10 m / 100 m = 0.1. From Fig. 14.5, the total length of pipe in the system is determined to be $L = 1514$ m, and the length of pipe if it were straight between the source and delivery is 1503 m. Thus, λ = 1511 m / 1502 m = 1.0072. Following the procedure of Section 5.4, we first use Fig. 5.5, for $F = 0.1$ and $\lambda = 1$, to get $Q = 1.9$ L/s (result reported to only two significant digits; refer to textbox B.14.1). Since the value for λ of 1.0072 is very close to 1, it is not necessary to use Fig. 5.9, for $F = 0.1$ and $\lambda = 1.5$, and then interpolate between these two. Therefore, flow rate is $Q = 1.9$ L/s. It is interesting to note that both Eqs (9.2) and (9.3), which assume turbulent flow in smooth pipe, predict $Q = 1.93$ L/s; this is perhaps an easier alternative to the use of the design graphs and almost as accurate.

B.14.1 The Significance of Significant Digits

It is noteworthy for the above calculation that we did not write Q as 1.90 L/s because the visual nature of the solution for Q from the graphs produces uncertainty beyond two significant digits. By writing $Q = 1.90$ L/s, we say that we are certain of the answer to three significant digits, 1, 9, and 0. If the sheet were used to calculate Q, we may be able to write the solution to at least three digits of accuracy because of the certainty we have in the formulas used in the calculations and in the input data. This is because the friction factor correlation used in `Mathcad` worksheet is accurate to at least three significant figures. Please be aware that the certainty of the input data, such as elevations, slopes, and so on, will normally determine the overall certainty of the design. By allowing the value of each parameter to vary according to its certainty, it is straightforward to determine the effect of the uncertainty of each parameter on the design.

Next, we neglect air compressibility and use Eqn (14.7) to calculate Q. For this, we employ the `Mathcad` worksheet `pipe sizing for air block example.xmcd` since the friction factor as a function of Q is needed to solve Eqn (14.7). Alternately, Eqs (9.2) and (9.3) may be used since minor losses are neglected. Pipe segments b and d contain air over the entire segment lengths. The remainder of the pipe segments flow water. The reduced elevation head, $\Delta z_a + \Delta z_c + \Delta z_e + \Delta z_f$, is $(40 - 20 - 5 + 10)$ m = 25 m, and the length of pipe flowing water, $L_a + L_c + L_e + L_f$, is (603.75 + 250.80 + 150.08 + 200.25) m = 1204.9 m. The corresponding values for s and λ are 25 m/1500 m = 0.0167 and 1204.9 m/1503 m = 0.802, respectively. Through the `Mathcad` worksheet, we calculate Q = 0.066 L/s, a reduction of ~96% compared with no air pockets. Thus, it is very clear that the effect of air pockets in the

worst case of neglecting air compressibility, is to significantly reduce the flow rate in the system. $Q = 0.066$ L/s is the lowest flow rate one would expect for this system, which may occur on start-up where there is much trapped air in the network. It could occur during steady state operation of the system, as well, if there is a continual inflow of air, say though a vacuum breaker, at the source.

If air compressibility is included, we use Eqn (14.13) together with the same `Mathcad` worksheet as above to calculate the flow rate. Consider Fig. 14.6 which is Fig. 14.5 with notation added for elevations and pressures. The ideal gas law [e.g.,

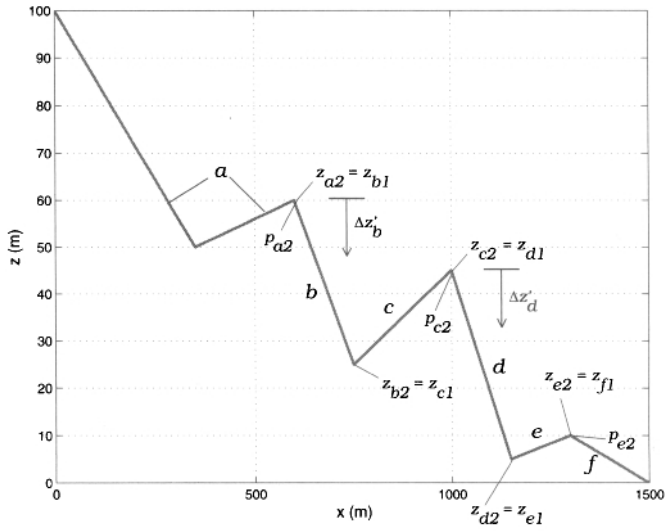

Figure 14.6 Same as Fig. 14.5 with notation added for elevations and pressures.

see Eqn 14.11] for pipe segment b is written as

$$\frac{L'_b}{L_b} = \frac{p_{atm}}{p_{a2}} = \frac{\Delta z'_b}{\Delta z_b} \tag{14.14}$$

where $\Delta z_b = z_{b1} - z_{b2}$ and $\Delta z'_b = z_{b1} - z'_b$. The elevation z'_b is the location of the water surface in pipe segment b measured in the vertical direction from the top of the segment at z_{b1}. In Eqn (14.14), L'_b is the location of the water surface in pipe segment b measured along the length of the pipe from the top of the segment at z_{b1} (see Fig. 14.6). L_b is the length of pipe segment b.

Likewise for pipe segment d, we obtain

$$\frac{L'_d}{L_d} = \frac{p_{atm}}{p_{c2}} = \frac{\Delta z'_d}{\Delta z_d} \tag{14.15}$$

The elevation change between the free surfaces of the leg of water in pipe segment c may then be written as

$$\Delta z_c = z_{b2} - z_{c2} + \Delta z_b - \Delta z'_b \tag{14.16}$$

Substituting for $\Delta z_b'$ from Eqn (14.14), Eqn (14.16) becomes

$$\Delta z_c = z_{b2} - z_{c2} + (z_{b1} - z_{b2})(1 - \frac{p_{atm}}{p_{a2}}) \tag{14.17}$$

The first two terms on the right side of Eqn (14.17) represent the elevation change between the bottom and top of pipe segment c. This is the elevation change that would arise if the air were incompressible and it is negative valued as seen by our inspection of Fig. 14.6. The third term on the right side of Eqn (14.17) is the head of water that resides at the bottom of pipe segments b and c and partially fills pipe segment b. This is a positive-valued elevation head that offsets some of the negative-valued head of the first two terms. The third term on the right side of Eqn (14.17) appears only if air is treated as compressible, and in fact, we see that the head of water, $(z_{b1} - z_{b2})(1 - p_{atm}/p_{a2})$, depends on the air static pressure that sits above it, p_{a2}.

An equation similar to Eqn (14.17) may be written for the elevation change between the free surfaces of the leg of water in pipe segment e,

$$\Delta z_e = z_{d2} - z_{e2} + (z_{d1} - z_{d2})(1 - \frac{p_{atm}}{p_{c2}}) \tag{14.18}$$

Finally, because of similar triangles, the above equations for elevations may also be written for the water-filled pipe lengths, L. To write these, we let L^* be the sum of the length of the water-filled pipe segment plus the length of a partially water-filled pipe segment that adjoins it. Obtain

$$\begin{aligned} L_c^* &= L_c + L_b - L_b', \\ &= L_c + L_b(1 - \frac{p_{atm}}{p_{a2}}) \end{aligned} \tag{14.19}$$

for water-filled pipe segment c and,

$$L_e^* = L_e + L_d(1 - \frac{p_{atm}}{p_{c2}}) \tag{14.20}$$

for water-filled pipe segment e. In each of these equations the second term on the right sides accounts for the length of water-filled pipe for segments b and d that join segments c and e at their respective valleys (see Fig. 14.6).

It is interesting to note that as the static pressures p_{a2} or p_{c2} become infinite, air is compressed to a infinitesimally small volume. Both Eqs (14.19) and (14.20) show that, in this limiting case, the lengths of pipe are completely filled with water, $L_c^* = L_c + L_b$ and $L_e^* = L_e + L_d$ for segments c and e, respectively.

Equations (14.17)–(14.20) represent the functions $\Delta z_c(\frac{p_{atm}}{p_{a2}})$, $\Delta z_e(\frac{p_{atm}}{p_{c2}})$, $L_c(\frac{p_{atm}}{p_{a2}})$, and $L_e(\frac{p_{atm}}{p_{c2}})$, respectively, in Eqn (14.13).

The next step is to substitute numbers for all of the terms in Eqs (14.17)-(14.20) and carry out the solution. This is done in `Mathcad`. Equations (14.17)-(14.20) become for this example

$$\Delta z_c(p_{a2}) = [25 - 45 + (60 - 25)(1 - \frac{14.7 \text{ psia}}{p_{a2}})], \text{ m} \tag{14.21}$$

$$\Delta z_e(p_{c2}) = [5 - 10 + (45 - 5)(1 - \frac{14.7 \text{ psia}}{p_{c2}})], \text{ m} \tag{14.22}$$

$$L_c^*(p_{a2}) = [250.80 + 154.03(1 - \frac{14.7 \text{ psia}}{p_{a2}})], \text{ m} \tag{14.23}$$

and

$$L_e^*(p_{c2}) = [150.08 + 155.24(1 - \frac{14.7 \text{ psia}}{p_{c2}})], \text{ m} \tag{14.24}$$

Equations (14.13) for this example are written as

$$\rho g \Delta z_a - p_{a2} + p_{a1} = \frac{\rho}{2}(C_{L,a} + \alpha)(\frac{4Q}{\pi D^2})^2, \quad \text{Segment } a$$

$$\begin{aligned} \rho g \Delta z_c(p_{a2}) &+ p_{a2} - p_{c2} \\ &= \frac{\rho}{2} C_{L,c}(L_c^*(p_{a2}))(\frac{4Q}{\pi D^2})^2, \quad \text{Segment } c \end{aligned}$$

$$\begin{aligned} \rho g \Delta z_e(p_{c2}) &+ p_{c2} - p_{e2} \\ &= \frac{\rho}{2} C_{L,e}(L_e^*(p_{c2}))(\frac{4Q}{\pi D^2})^2, \quad \text{Segment } e \end{aligned} \tag{14.25}$$

$$\begin{aligned} \rho g \Delta z_f &+ p_{e2} - p_{del} \\ &= \frac{\rho}{2} C_{L,g}(\frac{4Q}{\pi D^2})^2, \quad \text{Segment } g \end{aligned}$$

where p_{a1} (=14.7 psi) has been added to the first of these equations since all static pressures are in absolute.

Equation (14.25) is solved in the Mathcad worksheet `pipe sizing for air block example.xmcd` for p_{a2}, p_{c2}, p_{e2}, and Q. After converting all static pressures to gage values, we obtain $p_{a2} = 24.5$ psig, $p_{c2} = 8.4$ psig, $p_{e2} = 10.9$ psig, and $Q = 1.49$ L/s (~21% less than with no air pockets). The heads $\Delta z_c(p_{a2})$ and $\Delta z_e(p_{c2})$ are 1.86 and 20.0 m, respectively, both positive values (compare these with -20 and -5 m for the case where we assume incompressible air from above). Thus, although a conservative estimate of the effect of air pockets on flow in the network is obtained by assuming compressible air, this result is much more realistic when compared with the case where we neglected air compressibility. In this case, the reduction of flow rate by 96% compared with no air, is not realistic. However, there is considerably more time and effort invested in obtaining the solution for the case of compressible air.

This example illustrates the methodology for estimating the effect of air-pockets on the flow rate in the network. Obviously, to reduce the negative impacts of air pockets, the designer is encouraged at the outset to reduce the number of localized peaks and their magnitudes in the design to whatever extent possible. The major slopes in the network for this example (Fig. 14.5) appear in pipe segments at the very beginning and near the end that gives rise to large static pressures p_{a2} and p_{e2}. However, in

general, in a well-designed gravity-driven water system, static pressure is smallest at the top and largest near the delivery location. Recall Eqn (14.14), where we see that the amount of air in the pocket is inversely proportional to the air pressure. With static pressure generally the lowest at the top localized peak of the system, the amount of trapped air should be the largest at that location. Thus, air vents, when used, should first be located at the highest local peak to assist in the removal of air.

14.6 SUMMARY

Based on the discussion and developments in this chapter, we can summarize the above as follows:

- Air pockets in a gravity-driven water network are realistic, and their formation must be anticipated in any system where there are local peaks and valleys,
- The impact of an air pocket is always to reduce the water flow rate relative to the Natural flow rate, that which would occur in the absence of any air pockets,
- A vacuum breaker installed at any location in the network may continuously introduce air into the system. While desirable from the perspective of reducing the local static pressure at key points in the network to prevent possible pipe-wall collapse, a vacuum breaker is undesirable in the sense that it introduces air that assists in the formation of air pockets.
- By neglecting the compressibility of air, it is relatively easy to estimate the flow rate that occurs in the presence of air pockets. However, this produces a conservative result, and for the limited number of cases tested for this writing, may not be of much practical value. The more-realistic approach is to model air as compressible. However, the calculations are significantly more complicated and time consuming.
- The problem of air pockets, and their negative impact on the flow, can be greatly reduced by installing air vent valves at local peaks. Manually operated vent valves must be opened on a regular schedule if they are to be effective. Even if automatic valves are used, air vent valves are maintenance items and need routine inspection to ensure proper operation.

References

G. Corcos. Air in water pipes, a manual for designers of spring-supplied gravity-driven drinking water rural delivery systems. Technical report, Agua Para La Vida, Berkeley, CA, 2004.

T. D. Jordan Jr. *Handbook of Gravity-Flow Water Systems*. ITDG Publication, London, UK, 2004.

CHAPTER 15

CASE STUDY

By J. Ermilio and G. F. Jones

"One is trusted because one trusts, and one can trust because one knows one is trusted."

– Brother John of Taizé on trust between a teacher and student

15.1 ENGINEERING DESIGN: SCIENCE AND ART

Engineering design, as discussed in Chapter 1, is composed of differing weights of engineering science and art. The science part consists of most of the hydraulic design that is the core topic of this book, along with other quantitative-based design perhaps associated with pipe supports, structural integrity of tanks, and so on. The art of water distribution network design consists of "rules-of-thumb" or guidelines, passed along by engineers and other experienced workers, that normally lack a fundamental theoretical basis.[1] An example of this would be the recommended range of flow

[1] In other applications, the art of design may also address the conceptual or graphical aspects of a process or product that have no little or no quantitative bases.

Gravity-Driven Water Flow in Networks. By Gerard F. Jones

speeds in a pipe from the standpoint of pipe-wall erosion at high flow speeds and sedimentation of particulates in the flow at low speeds. It is unlikely that extensive systematic studies have been performed for erosion rates of different types of pipe materials with flows of different fluids at different speeds and different particle loadings to determine a theoretical value of speed below which erosion may be neglected. Likewise, the theoretical minimum flow speeds for various particulate-loaded fluids where precipitation begins are not commonly modeled. As noted in Chapter 13, flow speeds between ~0.7 and ~3 m/s are known from experience to be such that neither sedimentation nor erosion should be a problem in most cases.

Both the science and art of design will be considered in the case below.

The case presented in this chapter pertains to an actual system with actual dimensional and flow rate data, and application and discussion of real-world constraints. Thus, the case amplifies and, in certain instances, goes beyond the analysis and design content already treated in this text. In addition, it gives the reader an opportunity to work with the appropriate `Mathcad` worksheets to carry out the design calculations. Engineering tradeoffs and sensitivity (or parametric) studies, like those discussed in Chapter 11, will be demonstrated and discussed where appropriate.

15.2 DESIGN PROCESS REVISITED

The design procedure for this case study follows that in Chapter 13 and in Jordan Jr. (2004); Jeppson (1976); Nayyar (2002); Trifunovic (2006); Swamee and Sharma (2008) among others. It includes the following:

- From survey data, elevation and plan-view drawings are produced that identify locations and elevations of all elements, pipe lengths, mean slopes, and so on.
- From a water-demand survey of the community, and an estimate of the rate of population growth, the current and future water demands, peak and on-average, are calculated.
- The water storage requirement is assessed and the volume of the water storage tank is calculated.
- Knowing water flow rates, the intake (normally a single-pipe network) and distribution (normally a multiple-pipe network) pipelines are designed. This includes selecting the pipe material, calculating actual inside diameters (ID), choosing nominal pipe sizes, and investigating flow control; (i.e., the sensitivity of the performance of the network to the partial closing of globe valves installed in the pipe segments).
- The details of the hydraulic design (including valve types and locations; bypasses; flow speed limits; the need for and location of clean-outs, air vents, and vacuum breakers; and consideration of air pockets and water hammer effects) and nonhydraulic design (reservoir construction at the source; structural considerations for the storage and possible break-pressure tanks and pipe supports, etc.) are executed.

- Costs are estimated, and final drawings are prepared for the engineering and construction teams.

15.3 THE CASE

15.3.1 Background

You are an engineer working for an engineering company that specializes in the design and construction of large-scale water supply and distribution systems. Having had many years of engineering experience, you decide to volunteer with a service organization to provide technical assistance on water supply projects in remote communities in the Philippines. As a part of this service, you have committed to giving assistance to field volunteers who are working on water supply projects. You were at an orientation seminar last month and you met a number of young engineers who are working on projects throughout the country. One particular volunteer mentioned a project she was working on and asked if she could fax you some details to get your input.

A couple of weeks later, you are in your office and you receive a fax from the field volunteer who you met at the seminar. She is currently in the Philippines living and working in Mountain Village, and she is asking for your engineering assistance.

15.3.2 The Request

The fax you received reads as follows:

To: You
From: Ms. Volunteer, Mountain Village, Philippines

Dear Sir,
It was very nice meeting you at the technical seminar the other week. I have been in Mountain Village working for the past 6 months and, would like to ask your advice on a few things. After arriving here, I put together a map of the community using my hand-held Global Positioning System (GPS) (Figs. 15.1 and 15.2) and, as a result, I have basically been appointed to serve as the town engineer. Recently, there has been an outbreak of diarrhea in this area, and the District Health Official is planning to visit (with some representatives from the President's cabinet) in the next couple of weeks to investigate. The President's wife has family in this area and because this is an election year, she wants to help solve this problem so that her husband looks good at the national level. As a result, if I can put together a comprehensive plan for this visit, I could get funding to build a water system in this area and help alleviate the current health crisis.

To give you a background of this area; Mountain Village is composed of six small neighborhoods with a total of 159 households and an estimated population of 795 people. I looked up statistics from the national census and it looks as if there is an estimated 2% growth rate in rural areas of the Philippines. The area is relatively poor and people here earn an estimated $4,000 annually per capita, primarily from raising livestock, such as cattle and growing rice. The area is very mountainous and there is an estimated 47 in. of rainfall annually, with a dry season that lasts about ~3 months. Included in the fax is a map I created using a GPS. This map shows some key features in the community including the village centers, estimated number of households, and approximate elevations. In regards to water resources, there are a number of natural springs that are being considered for development and a couple of small streams that flow through the area. These streams currently serve as the primary source for most houses who typically divert a portion of the water upstream into a hose and deliver water to their homes by gravity. Whereas, this technique has been successful in the past, the current health problems and issues with population growth have caused the community to consider creating a public utility. Several of the key data I have collected appear in Tables 15.1–15.3. Thank you for your suggestion regarding collecting and tabulating these data.

In regards to materials, there is a supplier within a few hours who can deliver to this area. I am not sure about different piping materials but, there are local contractors here who can construct concrete water tanks. I looked into the cost for various materials and, it appears the storage tank that they plan to build (roughly 8 m^3) is going to cost ~$2,000 dollars for the materials. This would require an estimated 60 bags of cement. Also there is PVC drain pipe that costs roughly $1.00/m for 1-in. diameter pipe. So, if we were to construct a system with 1000 meters of piping, then we would probably need a total of $3000 for the project. Does this sound like a reasonable approach?

As per your suggestion at the seminar, I collected some general information about the sources of water and I sketched a site map of the area with some rough distances and elevations. Finally, included in this fax is a preliminary layout of a piping system that basically follows the path of a local road and some footpaths. Thank you so much for your help. If you can reply with some general recommendations about these options, this would be very useful for me.

Sincerely,

Ms. Volunteer

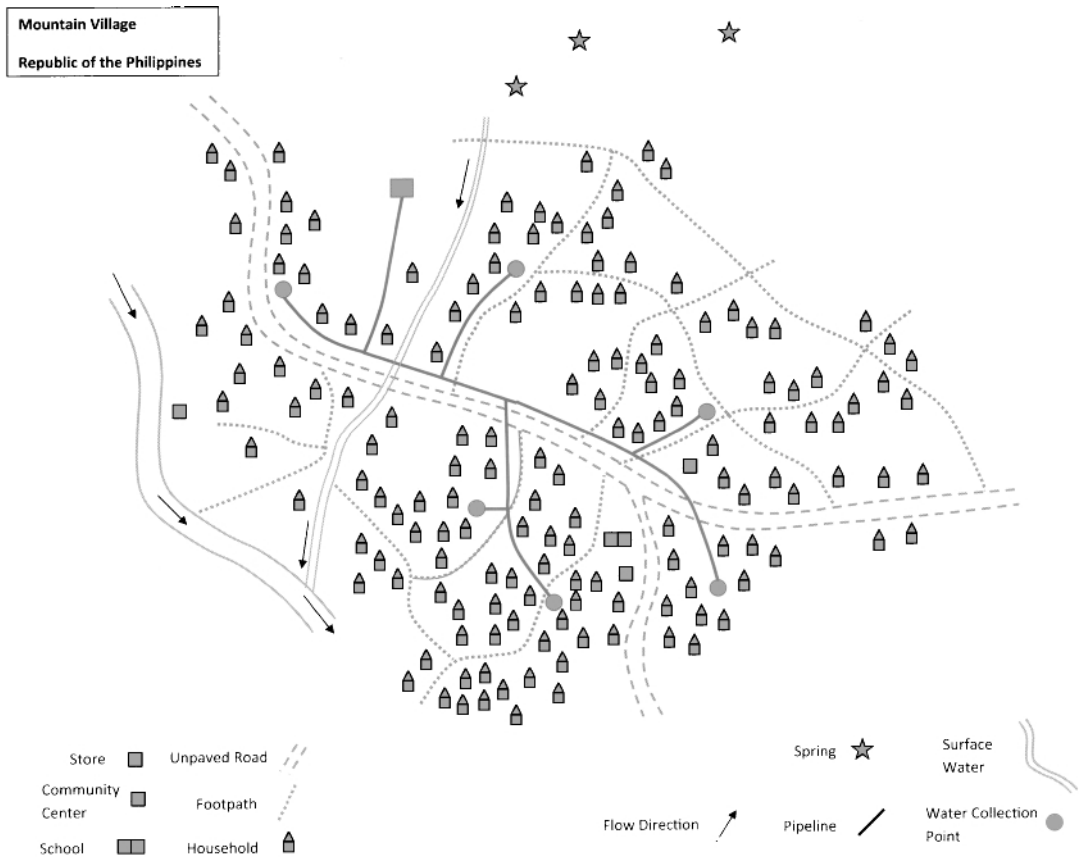

Figure 15.1 Site map.

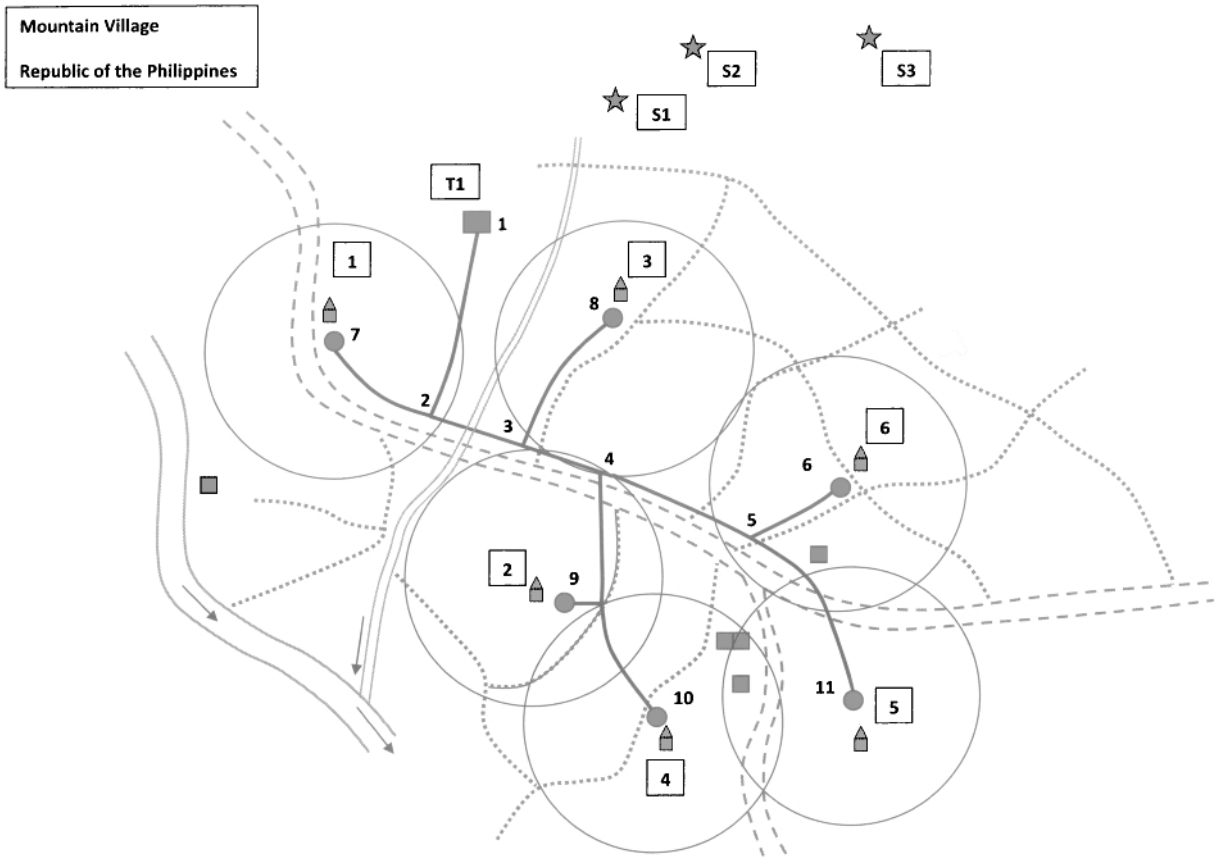

Figure 15.2 Spot map. Community identification numbers are boxed.

Table 15.1 Water Resources

Identification Symbol (id)	Description	Safe Yield (Q, L/s)	Elevation (m)	Straight-Line Distance to Proposed Tank Location (m)
S1	Spring	0.8	310	200
S2	Spring	1.2	350	944
S3	Spring	1.3	320	1300
T1(A)	Storage Tank $V = 8,000$ L (Proposed)	NA[a]	290.4	NA[a]

[a]Not available = NA.

Table 15.2 Water Collection Points

ID	Village Name	Households (HH)	Average Elevation (m)
1	Pasa Buena	25	275.8
2	El Barrio	23	273.7
3	Buena Vista	27	276.5
4	Rio Blanco	31	271.7
5	Piedra	25	275.5
6	Barrial	28	272.9

Table 15.3 Proposed Water Network Details

Node	Distance (m)	Elevation (m)	Comment[a]
1	0	290.4	Storage Tank location, T1
2	76	276.4	Dist. from 1 to 2
3	113	275.4	Dist. from 2 to 3
4	19	274.8	Dist. from 3 to 4
5	54	275.1	Dist. from 4 to 5
6	135	272.9	Dist. from 5 to 6, Barrial community, id-6, 28 HH[b]
7	80	275.8	Dist. from 2 to 7, Pasa Buena community, id-1, 25 HH
8	99	276.5	Dist. from 3 to 8, Buena Vista community, id-3, 27 HH
9	75	273.7	Dist. from 4 to 9, El Barrio community, id-2, 23 HH
10	95	271.7	Dist. from 9 to 10, Rio Blanco community, id-4, 31 HH
11	75	275.5	Dist. from 5 to 11, Piedra community, id-5, 25 HH

[a]See Fig. 15.2.
[b]Households = HH.

15.3.3 Your Response

Dear Ms. Volunteer,

It was nice to meet you at the orientation seminar the other week. It sounds like you have a very good opportunity to make a difference in the lives of the people who live in Mountain Village. I admire the commitment you have made to this project and, I am willing to help in any way that I can.

In regard to your inquiry, please keep in mind that in the analysis and design of all water-supply problems you need to satisfy the following conservation laws from engineering science:

- Conservation of mass (continuity).
- Conservation of energy (first law of thermodynamics).

In addition to these, you will also be interested in minimizing the cost of your network.

I will emphasize and elaborate on these in the appropriate parts of my response below. In particular, cost mnimization will allow the unique determination of the static pressures throughout the entire pipe network that you design. First, however, you need to complete the planning part of the project. You have begun this with your GPS-survey of the area, and recording of elevations and longitude-latitude coordinates which, I assume, you converted to x–y (or Easting–Northing) coordinates for your maps (see Appendix B in Jones (2010) for this material). The tables on water flow rates from the available sources, the number of households, and the tapstand node locations, distance, and elevations are a good first step in the hydraulic design of the network.

In order to size the storage tank, and to determine the adequacy of the sources, you will need to consider water supply and demand. Let us cover this first.

15.3.3.1 Water Supply and Demand One of the first considerations when designing a water supply network is the availability of water (supply) in comparison with the water needs (demand) in the community. Based on the information you have provided, it appears that your community is very fortunate to have three springs that collectively have a good yield and (it appears) enough elevation potential to serve the project area. Another variable to consider is the water quality of these sources. In most cases, if a spring is properly protected, it will provide a reliable supply of good quality water. There are many types of water sampling and testing kits that might help you determine which source is the best. Consult with the District Health Office before they arrive and inquire about borrowing water testing equipment. Keep this in mind when determining which source to develop.

It appears that all three springs are capable of supplying the water demands. If you consider the 2% growth rate, you can estimate the future population in this area. In order to do this, you have to first choose a design life for the infrastructure, often 20–30 years for this type of system. Choosing a 20-year design life, we can calculate

the future population in this area using[2]

$$F = P(1 + i)^t$$

where F is the future population, P is the present population, i is the growth rate (%/100) per period (a year), and t is the number of periods (years) in the design lifetime. From this equation, we estimate that the future population in 20 years will be $F = 1181$ persons.

Next, you have to determine the daily water demand for this community. There are a number of techniques that can be used based on the current water consumption. However, in most cases, the water consumption will change when a new system is constructed. This is usually because the rate of water consumption per person is, to a large extent, a function of water availability; increasing accessibility to water will correlate with an increase in consumption. This is important because an increase in water consumption often results in improvements in health and hygiene. If we explore the relationship between water availability and consumption further, we would discover that water demand can be accurately estimated based on the distance that people have to travel to collect it. For example, if someone has a direct household connection, then they will naturally consume more water than someone who has to travel a long distance. The water demand will also depend on the end-use of the water. If people have household gardens, then they might have an additional demand for irrigation. If someone has livestock, this will also increase the demand. At the same time, we should always keep in mind that there might be another source of water that can be used to supplement the demand for these secondary needs.

The following tables (Tables 15.4–15.6) can be used as a starting point to estimate water demand (Hofkes, 1983).

Based on the drawing you provided, it appears that you are planning to construct a system that uses communal water collection points, commonly called tapstands, to which the walking distance from each house is < 250 m. This usually means that there would be very little secondary demand for water, so the average domestic consumption could be estimated between 15 and 50 L/person/day. For the sake of this design problem, let us assume that the current water demand is conservatively estimated as 100 L/person/day, which includes an allowance for some light gardening. By using a larger water demand, we will also be able to account for the possibility that people will eventually connect a private water line to their houses so, this estimate will allow for expansion in the future. This becomes more important later when we start sizing the water distribution system, which is the piping network from the storage tank to the various neighborhoods in the community.

The next step is to verify that the available supply from the yield of the springs is greater than the present and future demand. This is determined by calculating the

[2]Some of the equations in this chapter appear elsewhere in this book. The symbols in this case study are as would be used by you, the professional, responding to the aid-worker's request for help with the design. The symbols may or may not coincide with those appearing elsewhere for the same quantities. This is intended for the purpose of exposing the readers to a variety of symbols and terminology for the same or similar things that may be used in the hydraulics community.

Table 15.4 A Starting Point for Estimating Water Demand

Type of Water Supply	Average Consumption (L/person/day)	Range (L/person/day)
Public Water Collection Point		
Distance (500–1000 m)	7	5–10
Distance (250–500 m)	12	10–15
Distance (<250 m)	25	15–50
Private Connection		
Single Connection	50	30–80
Multiple Connections[a]	120	70–250

[a]As reference, eight months of data collected in 2008 from the rural community of Los Morales, Nicaragua show a range of 78-115 L/person/day with an average consumption of 90 L/person/day. This system was designed for private connections and has multiple connections per household.

Table 15.5 Water Demand Estimates for Various Facilities

Type of Facility	Range (L/person/day)
School	15–30
Hospital	220–300
Restaurant	65–90
Church	25–40
Office	25–40

Table 15.6 Water Demand Estimates for Various Livestock

Type of Livestock	Range (L/unit/day)
Cattle	25–35
Horse	20–25
Sheep	15–95
Pigs	10–15
Chickens	0.015–0.025

instantaneous rate of water supply available, Q_s, and comparing it with the instantaneous rate of water demand, Q_d. Thus, if

$$Q_s > Q_d$$

is satisfied, you can proceed with the proposal to develop the source. Otherwise, you should consider the current demand to see if it makes sense to develop the source as measured to meet it.

In your project proposal, there are two sources available. Let us call these $Q_{s,1}$ and $Q_{s,2}$, where

$$Q_{s,1} = 0.8 \text{ L/s} \cdot 60 \text{ s/min} \cdot 60 \text{ min/h} \cdot 24 \text{ h/day} = 69,120 \text{ L/day}$$

Furthermore, the future demand in 20 years is

$$Q_{d,20} = 1,181 \text{ persons} \cdot 100 \text{ L/person/day} = 118,100 \text{ L/day}$$

The present demand is

$$Q_{d,0} = 79,500 \text{ L/day}$$

Therefore, the available supply at Spring 1 is not sufficient to meet the future or present demand for the community. This means that you should consider Spring 2 and determine the available supply of this source. Obtain

$$Q_{s,2} = 1.2 \text{ L/s} \cdot 60 \text{ s/min} \cdot 60 \text{ min/h} \cdot 24 \text{ h/day} = 103,680 \text{ L/day}$$

Whereas the available supply at Spring 2 is sufficient to meet the present demand in the community, it is not sufficient to meet the future demand. A combination of Springs 1 and 2, however, would be sufficient to meet the water demand of Mountain Village well beyond the 20-year population growth and should therefore be considered in the initial proposal. Ultimately, the final decision will depend on the available funding. Spring 2 will suffice for the present demand but, if funding is available, both sources should be developed. Additionally, it is not uncommon for there to be a seasonal variation in the available water supply at the source between the rainy and the dry seasons. For this reason, developing both sources may account for this difference in the event of a reduced water supply during the dry season.

The conclusions from the discussion in this section are,

$$Q_{s,1} < Q_{d,0} \text{ and } Q_{s,1} < Q_{d,20}, \quad \text{Unacceptable}$$

$$Q_{s,2} > Q_{d,0}, \quad \text{Acceptable}$$

and

$$Q_{s,1} + Q_{s,2} > Q_{d,20}, \quad \text{Acceptable; recommended if funding available.}$$

15.3.3.2 Water Storage Requirement The next element in the design that we will consider is the required volume of water storage. The reason for water storage is to ensure enough water supply for the times of peak water demand in the community. Whereas, the water supply (on average) for this system is

$$Q_{s,1} + Q_{s,2} = 2 \text{ L/s}$$

the instantaneous demand will vary throughout the day. At times, the demand will likely be > 2 L/s, and other times it will be less. In fact, during the late evening hours, the demand will most likely tend toward zero when most of the community is asleep. Intuitively, during morning hours when people first wake up, water consumption will increase. This is called the "morning-peak demand". Furthermore, it follows that there is an expected afternoon peak during the lunch-time hours and an evening-peak

during the dinner hours, mostly related to food preparation and bathing.[3] The peak demand will also be an important variable when designing the water distribution system which will use a peak factor to determine the design flow rate. The design flow rate along with mean slopes and tortuosities of all pipe, and static pressure distributions at all pipe junctions are the primary variables affecting the pipe diameters in the network.

A rough estimate for the water storage could be determined by allowing for 30–50% of the total daily demand to be available in storage. This estimate would not account for the continuous supply and could grossly overestimate water storage where the supply is large enough to meet the peak demand. For example, *if the peak demand at any time of the day is less than the available supply, it would be feasible to build the network without water storage*. Thus,

$$\text{If } Q_s > Q_{d,p} \rightarrow \text{ Storage Not Required}$$

where the subscripts s and d, p mean supply and peak demand, respectively.

For your project proposal, use Figs. 15.3–15.4 to determine the water storage requirement. Figure 15.3 shows a typical demand schedule for understanding the peak water demand. From this figure we see that there are usually a morning peak of 40%, an afternoon peak of 20%, and an evening peak of 30%, where each is a percentage of the total daily demand. The additional 10% of the daily demand occurs during the time periods separating these periods. In many cases, the morning peak-demand determines the water-storage volume because it is the largest of the three.

The relationship between storage volume and the rates of water supply and demand is determined by the following integral formula,

$$V_S(t) = V_S(0) + \int_0^t Q_s(\hat{t}) - Q_d(\hat{t})\, d\hat{t} \tag{15.1}$$

where $V_S(0)$ is the initial volume of water in the tank (at the start of the day; the end of hour 1 or 1 am) and $\hat{t}$ is a dummy variable of integration. The integrand in Eqn (15.1) is the net flow rate that enters the tank. A positive value of $V_S(t)$ at the end of any hour indicates that the tank contains some water for use at that time, whereas a zero or negative value of $V_S(t)$ shows that the tank is empty. During the latter periods, there is obviously no water available to meet demand. The volume of the tank is determined by a trial-and-error procedure of choosing a series of increasing tank volumes and calculating the water volume in the tank for each at the end of every hour of the day.[4] In these calculations, we will assume that the tank is full at $t = 0$ because of the normal

[3]This schedule is based on three meals a day and bathing during random hours and may need to be adjusted depending on local customs. For example, Jordan Jr. (2004) notes a two-meal schedule in Nepal with ritual bathing before each, which will produce a different demand schedule. In any case, water demand between 6 or 7 pm and 5 or 6 am is generally negligible.

[4]A spreadsheet, like Excel, is the best way to carry out the calculations described here.

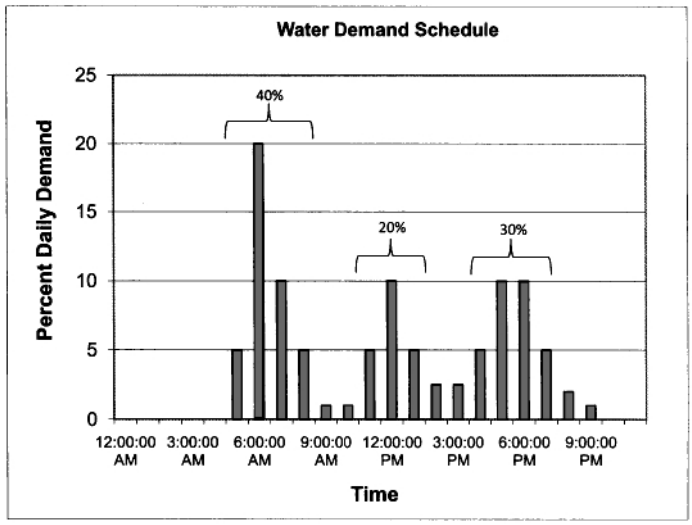

Figure 15.3 Typical water demand schedule for the case of three meals per day.

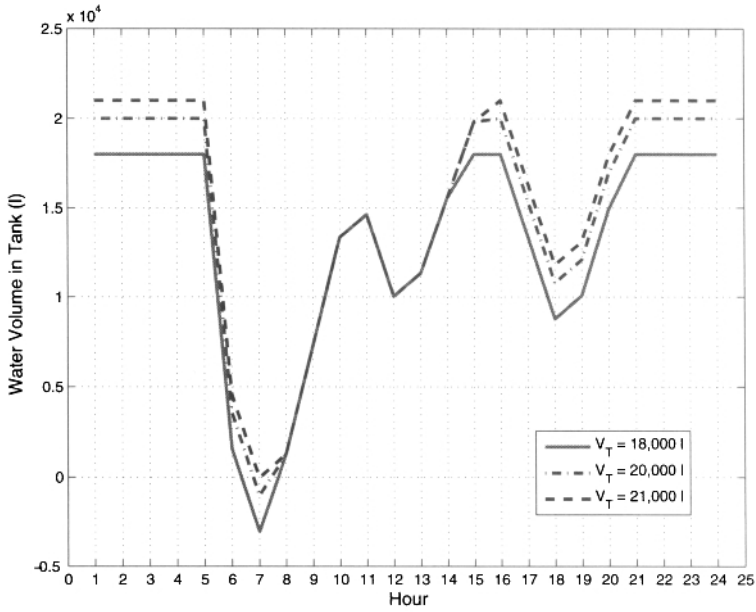

Figure 15.4 Water volume in tank versus hour of the day. Hour 1 is at 1 am.

fill-up during the evening hours.[5] *An acceptable volume, in principal, is that which eliminates all zero or negative values of water volume at the end of each hour.* For practical reasons, a volume is normally chosen that keeps the number of hours where there are zero or negative volumes to just one or two. The understanding here is that communities will tend to adjust their schedules to accommodate water availability once the network is installed and functioning (Jordan Jr., 2004). Uncertainty of the design data would also argue for the acceptability of an hour of empty tank.

From this analysis and Fig. 15.4 (the data appear in Table 15.7) we see that a 20,000-L tank (20 m^3) experiences a water deficit of ~1000 L for only one hour (at 7 am). Further calculation will show that the deficit at this hour reduces to ~30 L for a tank volume of 21,000 L. Based on the understanding of Jordan Jr. (2004) as above, I would recommend a 21-m^3 tank (if the budget is available) or one of 20 m^3 for your design, though I suspect the cost difference will be small.

Another useful piece of information is the time required to fill the water storage tank. This result will indicate if the tank is over- or under-sized. In this example, if you were to construct a 20,000-L tank and the supply to the tank is $Q_s = 2$ L/s on average, the time to fill the tank is

$$t_S = \frac{V_{S,T}}{Q_s} \tag{15.2}$$

Equation (15.2) shows that the tank will fill in $t_S = 10,000$ s, or ~2.8 h. This means that during the evening hours when the community is not using water, typically about a 10-h period (see the evening hours in Fig. 15.3 or 15.4), the tank would overflow for > 7 hours in the evening (see Table 15.7 for this evidence). Overflow of water is normal for nearly all networks. If there was an integrated approach to managing this water supply, which I recommend, this water could be used for other purposes such as irrigating fields or livestock demand.

Because the peak elevation head of your proposed design is just 14 m, there is clearly no need for a break-pressure tank in this design.

15.3.3.3 Piping Design The largest part of engineering design in a water supply project is the proper sizing of the water distribution network. This problem requires maintaining a minimum static pressure in the network during peak hours of water demand in order to ensure its integrity (low pressures, in the presence of even a small leak in a pipe connection will allow contaminated ground water to seep into the pipe flows). At the same time, financial constraints play a key role in the design of these systems because local governments usually have a limited budget for infrastructure projects. As a result, finding a balance between the system cost and the system design is very important for the engineer on a project like this.

In the past, pipe-flow hydraulics problems were solved using a series of complicated charts, tables, nomographs, or computer programs. Data from these sources

[5]The designer should verify that this assumption is correct for her/his design. For example, if the source-flow is diverted for night-time use elsewhere, the tank may be less than full at $t = 0$. In this case, $V_S(0)$ is calculated for the particular design.

Table 15.7 Water Volume in Tank Versus Hour of Day for 20,000-L Tank

Hour	Q_s (L/h)	Demand Percentage	Q_d (L/h)	Water Volume (L)	State of Tank
1	7200	0	0	20,000	Overflow
2	7200	0	0	20,000	Overflow
3	7200	0	0	20,000	Overflow
4	7200	0	0	20,000	Overflow
5	7200	5	5,905	20,000	Overflow
6	7200	20	23,620	3,580	Filling
7	7200	10	11,810	−1,030	Empty
8	7200	5	5,905	1,295	Filling
9	7200	1	1,181	7,314	Filling
10	7200	1	1,181	13,333	Filling
11	7200	5	5,905	14,628	Filling
12	7200	10	11,810	10,018	Filling
13	7200	5	5,905	11,313	Filling
14	7200	2.5	2,952.5	15,561	Filling
15	7200	2.5	2,952.5	19,808	Filling
16	7200	5	5,905	20,000	Overflow
17	7200	10	11,810	15,390	Filling
18	7200	10	11,810	10,780	Filling
19	7200	5	5,905	12,075	Filling
20	7200	2	2,362	16,913	Filling
21	7200	1	1,181	20,000	Overflow
22	7200	0	0	20,000	Overflow
23	7200	0	0	20,000	Overflow
24	7200	0	0	20,000	Overflow

always required verification before using and were sometimes in question because of the lack of appropriateness of the equations on which they were based.

The computer programs are typically "opaque" in that the user is not made aware, or chooses not to be aware, of the program's basis. This means that an executable file is run on a computer, which is the result of a compilation of a source program written in perhaps `Fortran` or `C++`.

Optimizing the network for minimum cost is, even today, not regularly done no matter what design tool is used.

Fortunately, there are "transparent" computer programs used today that employ the correct friction factor for pipe flow, address pipe cost appropriately, and simplify the procedure for solving complex pipe-flow hydraulics problems. Though these programs are very convenient, fundamental knowledge of fluid flow in pipe networks is very important to correctly program, and understand and interpret the design results. One of the better books that bracket all of the above is *Gravity-Driven Water Flow in Networks: Theory and Design* (Jones, 2010). This book is the only reference that I know of that places all developments, equations, and design formulas on a sound fundamentals footing, includes simple charts for the design of single-pipe networks (for the intake part of the network covered below), and supplies computational (`Mathcad`) Worksheets for the solution of the more-complex distribution part of the network, all of which include the constraint of minimum network cost. The Worksheets contain the solution procedure in an easy-to-read, step-by-step manner, and appears as if it

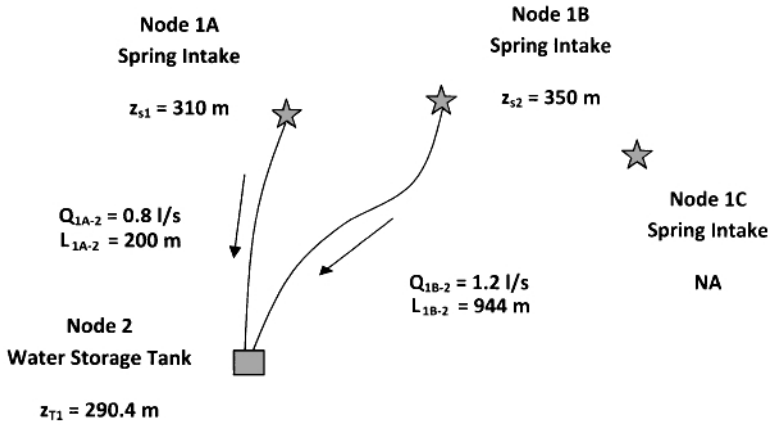

Figure 15.5 Intake line diagram.

were written on paper. I have included the Worksheet for your information with this mailing.

Based on the charts developed by Jones (2010), we solve this problem by first starting at the source and designing the intake system to provide water to the storage tank. Using the appropriate `Mathcad` worksheet provided by Jones (2010), we will then solve the problem of delivering water to key locations in the community taking into consideration peak demands in the distribution system.

Intake System The connection between a source and the tank is by a pipe having a single diameter. If there are no local high points in this pipeline (from your drawings, none appear), this is known as a single-pipe network (or subnetwork, since it is a part of a larger one, but we seldom refer to it this way; a pipe that distributes water to an end point by gravity and has no branches along its length is known as a gravity main) and there is a particularly simple tool available to design these as I will discuss below[6]. First, we need to know the flow rate from each source ($Q_{1A,2}$ and $Q_{1B,2}$), the mean (or average) slope of each pipe ($s_{1A,2}$ and $s_{1B,2}$), and the actual pipe length between each source and the tank. I have revised the map that you provided to identify the values for these parameters (Fig. 15.5).

From the data you have already provided, I know that $Q_{1A,2} = 0.8$ L/s and $Q_{1B,2} = 1.2$ L/s. The slopes are calculated from data in Table 15.1 and Fig. 15.5.

$$s_{1A,2} = \frac{310 \text{ m} - 290 \text{ m}}{200 \text{ m}} = 0.10$$

[6]I will neglect minor losses that come from fittings, such as elbows, because these are nearly always small.

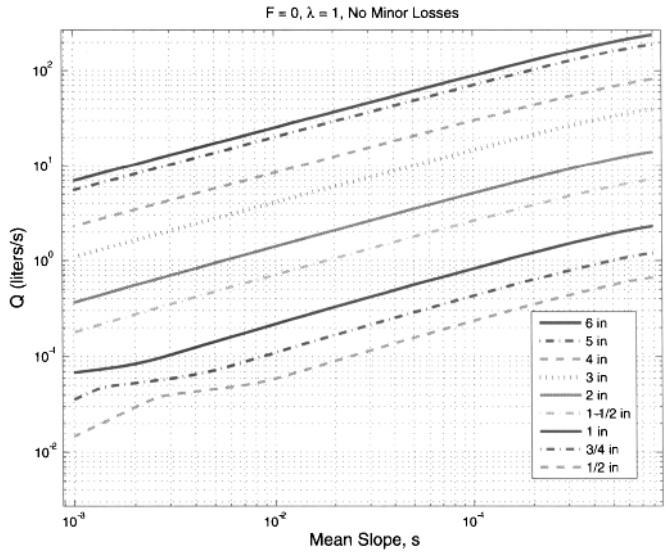

Figure 15.6 Design graph for intake system for sch. 40 PVC pipe and $\lambda = 1.0$. $F = h_d/z_1 = 0$.

where I rounded down 290.4 m to 290 m because 0.4 m is unrealistically precise given that it is from a GPS device. For the second pipe, I calculate a slope of $s_{1B,2} = 0.064$ using the same method.

Now, let us begin to calculate the pipe sizes needed for the intake system. The three parameters that are needed are volume flow rate, mean slope, and a term called the tortuosity, λ, of the pipe. The tortuosity is the ratio of the actual length of pipe to that if it were run directly (along a straight line) between the source and tank. There are insufficient data for me to calculate this from what you have supplied. However, typical values for many networks where there is a normal amount of circuitousness in the pipelines between the source and storage tank is $\lambda \sim 1.25$. I will assume $\lambda = 1.25$ for each pipe.

The appropriate design charts for the case of $\lambda = 1.0$ and 1.5 are presented in Figs. 15.6 and 15.7, respectively, for PCV sch. 40 pipe. I will interpolate between these to get results for $\lambda = 1.25$ since there is no single chart for this value of λ. Also, note that these figures assume that the tank is at atmospheric pressure (since, of course, it is open to the atmosphere). If we were trying to design a pipeline from the tank to a tapstand where we desire a nonzero static pressure head, we would specify a value for the ratio $F = h_d/z_1$. Here, h_d is the static pressure head at the delivery location and z_1 is the elevation head of the source, and we would use the design chart appropriate to a value nearest this value of F. Of course, in our case $F = 0$ since the static pressure head at the top surface of the water in the tank is zero.

For $Q_{1A,2} = 0.8$ L/s and $s_{1A,2} = 0.1$, obtain 1-in. sch. 40 PVC pipe for $D_{1A,2}$ from *both* Figs. 15.6 and 15.7. In the same manner, for $Q_{1A,2} = 1.2$ L/s and $s_{1A,2} =$

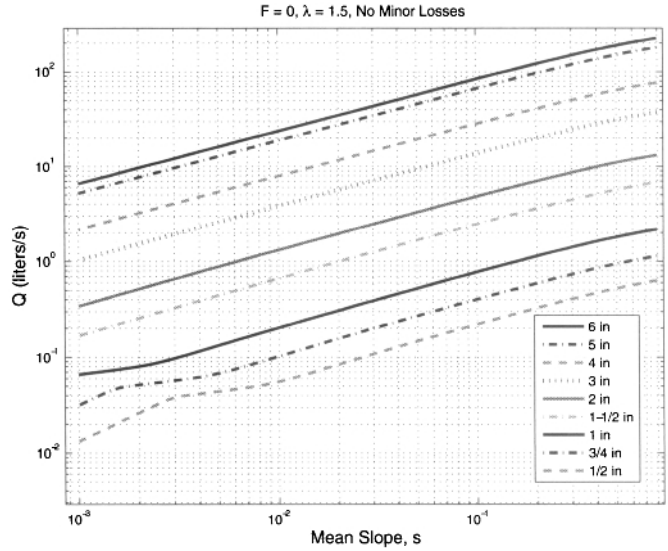

Figure 15.7 Design graph for intake system for sch. 40 PVC pipe and $\lambda = 1.5$. $F = h_d/z_1 = 0$.

0.064, obtain a $1\frac{1}{2}$-in. sch. 40 PVC pipe for $D_{1B,2}$ from *both* figures. Because the same pipe diameter is obtained from charts for $\lambda = 1.0$ and 1.5, we see the lack of sensitivity of pipe size to tortuosity in the range of $1.0 \leq \lambda \leq 1.5$ for this design.

If PVC pipe is not available, or you are required to use galvanized (GI) pipe because of local restrictions, you should refer to Fig. 5.13 of Jones (2010) for the chart appropriate to GI pipe. In this case, the Jones Charts yield a pipe diameter of $1\frac{1}{2}$-in. sch. 40 GI pipe for $D_{1A,2}$ and 2-in. sch. 40 GI pipe for $D_{1B,2}$. The differences between the results for PVC and GI pipe are attributed to the difference in the pipe relative roughness for these materials. The PVC pipe is smoother and thus exhibits less frictional loss.

Note the following: In your initial letter, you mentioned a supplier who can provide PVC drain pipe. This is *not* recommended for water distribution networks that are pressurized. Take time to visit the supplier to determine if there is pipe available appropriate for pressurized water. Different suppliers will provide pipe material specifications as either sch. 20 (thin-wall), sch. 40 (standard-wall), or sch. 80 (heavy-wall). A sch. 20 pipe is drain pipe and is not suitable for pressurized networks. You should use sch. 40 pipe wall thickness. A sch. 80 pipe wall is too heavy duty and is normally for industrial applications. Some suppliers may also reference pipe using SDR (Standard Diameter Ratio). This is the ratio of the pipe outside diameter to the wall thickness. Normally, SDR 26 or SDR 13.6 pipe would be appropriate for your network. Keep in mind that pressure pipe can be significantly more expensive than drain pipe. It is not uncommon for unscrupulous contractors to try to save money

on a contract by using a lesser-quality pipe than specified. For this reason, close supervision during installation is needed to ensure the use of proper materials.

Before moving on to design of the distribution part of the network, I offer a few comments on how what we have just done relates to the fundamentals of fluid flow. You may be curious about this. First, mass is conserved for the flow in both of the pipes since the volume flow rate that enters a pipe is the same that leaves it. Second, the design charts used above are developed from the solution of the energy equation (really, mechanical energy equation) for pipe flow. From your education, you may recall this as the first law of thermodynamics,

$$\dot{m}[(\frac{p_1}{\rho} + e_1 + \alpha_1 \frac{\overline{u}_1^2}{2} + gz_1) - (\frac{p_2}{\rho} + e_2 + \alpha_2 \frac{\overline{u}_2^2}{2} + gz_2)] = \dot{w} - \dot{q}$$

where $\dot{m}$ is the mass flow rate, e is the internal energy per unit mass, g is the acceleration of gravity, and $\dot{q}$ and $\dot{w}$ are the rates of heat transfer to and work done by the system, respectively. States 1 and 2 are at any two arbitrary locations along the pipe flow path, where the normal convention is that state 1 is upstream and state 2 is downstream. The terms in each parentheses on the left side of this equation account for pressure energy, kinetic energy, and potential energy, all per unit mass of fluid. The term α is the ratio of the kinetic energy in the flow to the kinetic energy based on the mean flow speed, $\overline{u}$. It accounts for the non-uniform velocity distribution through the cross section of the flow and is connected with the acceleration of the flow between two different flow speeds in the pipe. For example, if the velocity distribution were uniform through the cross section of the pipe, α would equal 1. Of course there is no rate of work done on or by the water flow in a pipe , so $\dot{w} = 0$.

Upon simplifying this equation with zero static pressure at the source and tank, and negligible change in kinetic energy due to flow acceleration from the source to the pipe, we get

$$\frac{s(1-F)}{\lambda} - \frac{8Q^2}{\pi^2 g} \frac{f(Q,D)}{D^5} = 0$$

Here, $f(Q, D)$ is the Darcy friction factor (the one you would normally read from the Moody diagram), Q is the volume flow rate, and s, F, and λ are as defined a few paragraphs above. Thus, when using the design charts Figs. 15.6 and 15.7, you are really using the energy equation to solve for the pipe diameter, D, for your problem.

Distribution System Using the table you provided in your fax, I have revised the spot map that you also provided (Fig. 15.2) to identify all of the key locations in the network (see Fig. 15.8; the trunk pipeline in the network in this figure is sometimes referred to as a "distribution main"). The label attached to each of the key locations is commonly called a node. I also included some important information about the expected number of households at each connection, as well as information about the expected peak flow rates through each section of pipe. We will then look at each section in the system and size the piping so that it will deliver a minimum pressure of 10 psig (~7 m of water head) at the required peak flow rate.

Before explaining the water system design specifications, we should first discuss how the peak volume flow rate was determined. Using the same method as above,

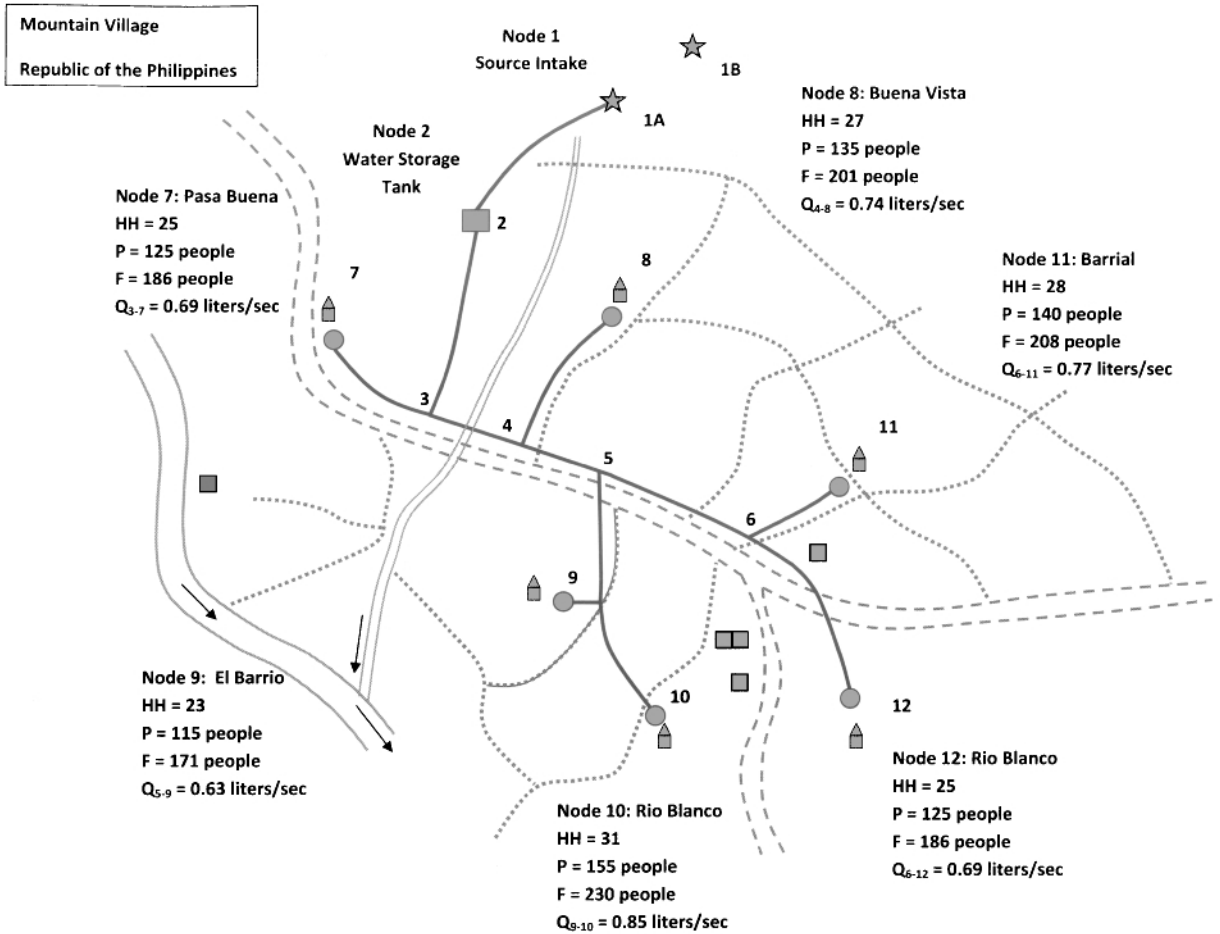

Figure 15.8 Detailed schematic diagram.

Table 15.8 Summary of Results for Peak Design Flow Rates

Household Size	5 persons/house
Growth Rate	2%
Design Life	20 years
Daily Demand	100 L/person/day
Peak Factor	3.2

we first determine the expected future population at each service location by using a 2% growth rate for a 20-year lifetime. Note that we use an average household (HH) size of 5 persons/household based on the information you provided. Thus,

$$F = P(1 + i)^t$$

where, for node 7 for example, $P = 25$ houses $\cdot$ 5 persons/house $= 125$ persons, and $F = 186$ persons is the population at node 7, where t is 20 years in the future.

The next step is to determine the total daily demand at the node based on an average household daily consumption of $Q_d = 100$ L/person/day. For the pipe connected by nodes 3 and 7 (designated by subscript 3-7) for example, this is the amount of water that would have to pass through this pipe over a 24 hour period. Thus,

$$Q_{3-7} = F_{3-7} \cdot Q_d = 18,600 \text{ l/day} = 0.215 \text{ L/s}$$

Finally, we need to account for the peak demand on the system which, based on the demand model from Fig. 15.3, is 40% of the total daily demand in a 3-h period during the morning peak. This is the highest of the three peaks seen in Fig. 15.3 so this 3-h period is the basis for the calculation of the peak demand. If there were uniform (nonpeak) demand during this period, one would expect 3 h/24 h = 1/8 = 12.5% of the demand. Thus, we need to increase the volume flow rate from 12.5 to 40% by multiplying the nonpeak volume flow rate by a factor of 40/12.5 = 3.2 to obtain the peak flow rate. The value 3.2 is called a "peak factor". The peak volume flow rate determined in this manner is referred to as the "peak (or design) volume flow rate". For example, for pipe segement 3–7 in Fig. 15.8, we obtain $Q_{3-7,p} = 3.2 \cdot 0.215$ L/s $= 0.688$ L/s ≈ 0.69 L/s. The subscript p on the flow rate refers to peak.

The results of this discussion on peak volume flow rate are summarized in Table 15.8.

Using the same procedure from the above paragraphs, we calculate the design volume flow rate for each external node (or community tapstand) and for each segment of the distribution main (at internal nodes) shown in Fig. 15.8. Using the law of mass conservation (also known as the continuity equation) we can determine the design volume flow rate for each segment of pipe in the network.

The continuity equation is written as

$$\sum Q_{in} - \sum Q_{out} = 0$$

Table 15.9 Volume Flow Rates for Distribution Network

Pipe Segment	HH Connected	Present Pop. (Persons)	Future Pop. (Persons)	Demand (L/day)	Peak Volume Flow Rate (L/s)
2–3	159	795	1,182	118,200	4.37
3–4	134	670	996	99,600	3.69
4–5	107	535	795	79,500	2.94
5–6	53	265	394	39,400	1.46
3–7	25	125	186	18,600	0.69
4–8	27	135	201	20,100	0.74
5–9	54	270	402	40,200	1.49
9–10	31	155	231	23,100	0.85
6–11	28	140	209	20,900	0.77
6–12	25	125	186	18,600	0.69

where the summations are taken over all of the inflows to a node (Q_{in}) and over all outflows from a node (Q_{out}). For example, apply the continuity equation for node 6 in Fig. 15.8 to get

$$Q_{5-6,p} = Q_{6-11,p} + Q_{6-12,p}$$

Knowing the design volume flow rates for the tapstands at nodes 11 and 12, we obtain

$$Q_{5-6,p} = 0.77 \text{ L/s} + 0.69 \text{ L/s} = 1.46 \text{ L/s}$$

The same procedure is followed for node 5 from which the value for $Q_{4-5,p}$ is determined, and so on.

The volume flow rate results for the distribution network are summarized in Table 15.9 and shown schematically in Fig. 15.9.

The `Mathcad` *Worksheet:* We are now ready to use a `Mathcad` worksheet to calculate the pipe diameters in the distribution system. The network of connected pipes in this system forms what is referred to as a "multiple-pipe network." To determine the diameters for each pipe segment, we need to solve an energy equation for each, where the volume flow rates are given in Table 15.9, and the pipe lengths and elevations of each node are from Table 15.3 which refers to your Fig. 15.2.

The Worksheet appears in Figs. 15.10–15.13 and I have attached a copy of the file to this mailing. The Worksheet is divided into three sections. These are preliminaries, and the forward and reverse solutions. The forward solution calculates the theoretical diameters that satisfy the energy equation for prescribed flow rates (Q), pipe lengths (L), and elevation changes (Δz) for each pipe segment in the network. Once obtained, a nominal pipe size having the next largest ID is normally chosen for each pipe [see Chapter 3 in Jones (2010) for pipe dimensions]. The reverse solution uses the actual ID of the selected pipe sizes to calculate the actual volume flow rates and static pressure heads at each junction in the network. The static pressure heads at each pipe junction in the forward solution are arbitrary if we consider just the continuity and energy equations. Cash conservation (i.e., minimization of pipe cost) is used as a constraint to determine unique values of junction static pressure heads, (i.e., those that minimize cost). This is done in the `MathcadWorksheet` using the construct `Given...Minimize`.

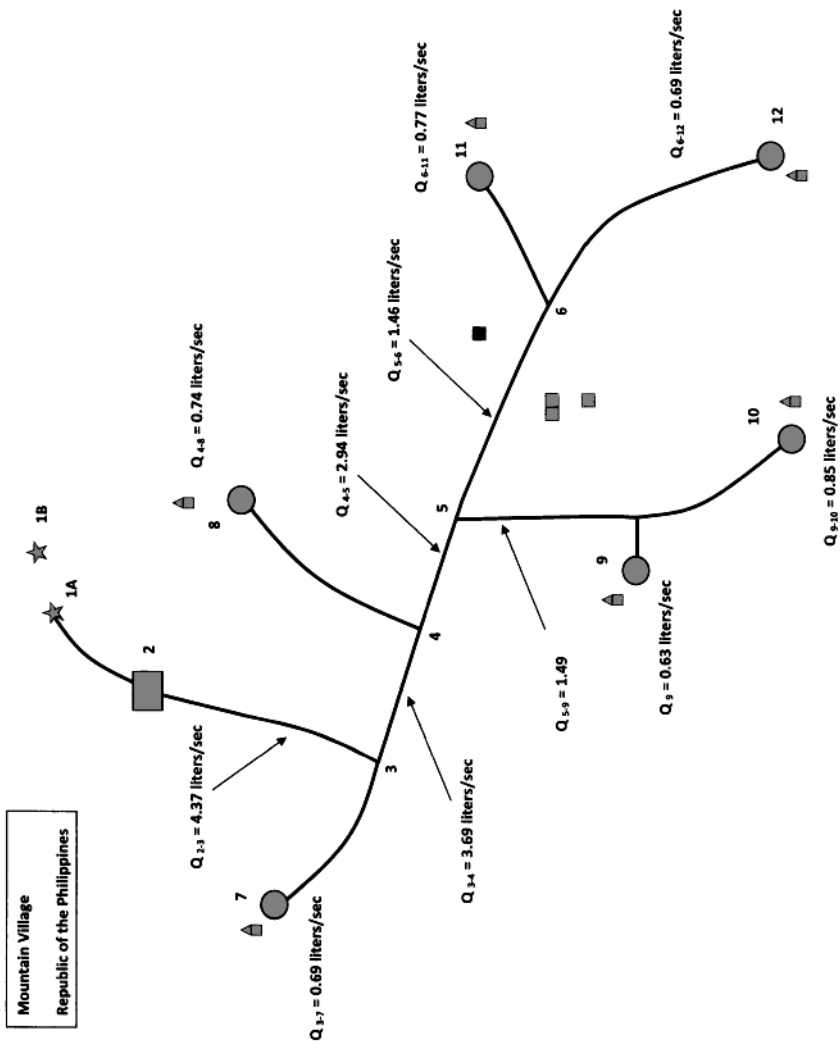

Figure 15.9 Schematic diagram showing the design volume flow rates.

The preliminary calculations in the Worksheet includes the following steps:

- Definition of water properties of density, ρ, and viscosity, ν.
- A convergence tolerance, `TOL`, used in `Mathcad` to determine when a root-finding algorithm. has found the root to sufficient accuracy.
- Definition of Reynolds number (Re) as a function of Q and D, and α as a function of Reynolds number.
- Setting the absolute roughness of the pipe wall.
- The friction factor function as defined by Eqs (2.16) and (2.17) in Jones (2010).
- The correspondence between nominal pipe size and D for the pipe material and type (schedule or SDR as necessary) of pipe under consideration (I will consider sch. 40, PVC pipe in this case).
- Cost data for the pipe as a function of nominal pipe size. You will need to adjust these values to pipe costs in your community. I assume values from central Nicaragua from several years ago.

The forward solution includes the following:

- Initial guesses for the values of D.
- Values for the input parameters for each pipe segment in the network, including pipe lengths L, volume flow rates Q, appropriate minor loss coefficients, K and $(\frac{L}{D})_e$, and elevations, z. I assumed a globe valve in each pipe segment and included $K = 10$ for each. This value corresponds to an open globe valve; see Chapter 2 in Jones (2010). I ignored all other possible minor losses for this analysis. Once nominal pipe sizes are selected after the forward solution is obtained, this valve can be adjusted to achieve the correct design flow rates in the distribution system.
- Definition of the energy equation for each pipe segment of the network. Each is given a symbol r and the needed functional dependence.
- Formula for the total pipe material cost, $T_{cost,1}$ and $T_{cost,2}$. They are added to get the total pipe cost, T_c.
- The solution of the energy equations using either the `Given...Find` construct or `Given...Minimize` construct. The latter is discussed in Chapter 10 and further in Section 11.4.4 in Jones (2010).
- Plots of the results or secondary calculations, such as checking to ensure that all equations are satisfied to the desired tolerance.

The reverse solution includes the following:

Table 15.10 Pipe Sizes for Distribution Network

Pipe Segment	Length (m)	Elevation Change (m)	Theor. D (in.)	Actual D (Nom.[a]) (in.)	Actual Q (L/s)	Actual K
2–3	76	14	2.88	3.068 (3)	TBD[b]	TBD
3–4	113	1	2.65	3.068 (3)	TBD	TBD
4–5	19	0	2.58	3.068 (3)	TBD	TBD
5–6	54	0	2.00	2.067 (2)	TBD	TBD
3–7	80	0	1.10	1.610 ($1\frac{1}{2}$)	TBD	TBD
4–8	99	−2	1.49	1.610 ($1\frac{1}{2}$)	TBD	TBD
5–9	75	1	1.64	1.610 ($1\frac{1}{2}$)	TBD	TBD
9–10	95	2	1.38	1.610 ($1\frac{1}{2}$)	TBD	TBD
6–11	135	2	1.33	1.610 ($1\frac{1}{2}$)	TBD	TBD
6–12	75	−1	1.49	1.610 ($1\frac{1}{2}$)	TBD	TBD

[a]Pipe is sch. 40 PVC.
[b]Entries labeled TBD need to be completed.

- Initial guesses for the values of Q (from earlier in the worksheet) and static pressure heads at the junctions of the distribution network.
- Values for the input parameters for each leg in the network as in the forward solution; normally only K will be included here.
- The solution of the energy equations using either the `Given...Find` construct or `Given...Minimize` construct, as above.
- Secondary calculations as above.

I refer you to Chapter 11 in Jones (2010), Section 11.6.1 for further details.

The theoretical and actual diameters for sch. 40 PVC pipe from the forward solution are presented in Table 15.10. The values range from 3-in. nominal for the segments having the largest flow rates to $1\frac{1}{2}$-in. nominal for the branches. For nearly all segments, I have chosen a nominal pipe size having ID slightly larger than the theoretical value for D. This allows me to adjust the minor loss value (K) for the globe valve in each pipe segment (in terms of the simulation in `Mathcad` this means increasing or reducing the value for K) to obtain volume flow rates that match design requirements.

Note that I have not completed this design. The reverse solution has been programmed correctly in the Worksheet, but the correct values for K for the pipe segments have not yet been selected and thus remain for you to complete. You will want to adjust the values of K to obtain the design flow rates. In this way, you will be assured that the network will perform as you specified. Since increasing K for a given globe valve corresponds to its closing, this result will also give you a feel for the sensitivity of the flow balance in the network to the throttling required in each segment. In any case, we understand that we are able to obtain the design flow rate in each pipe in the

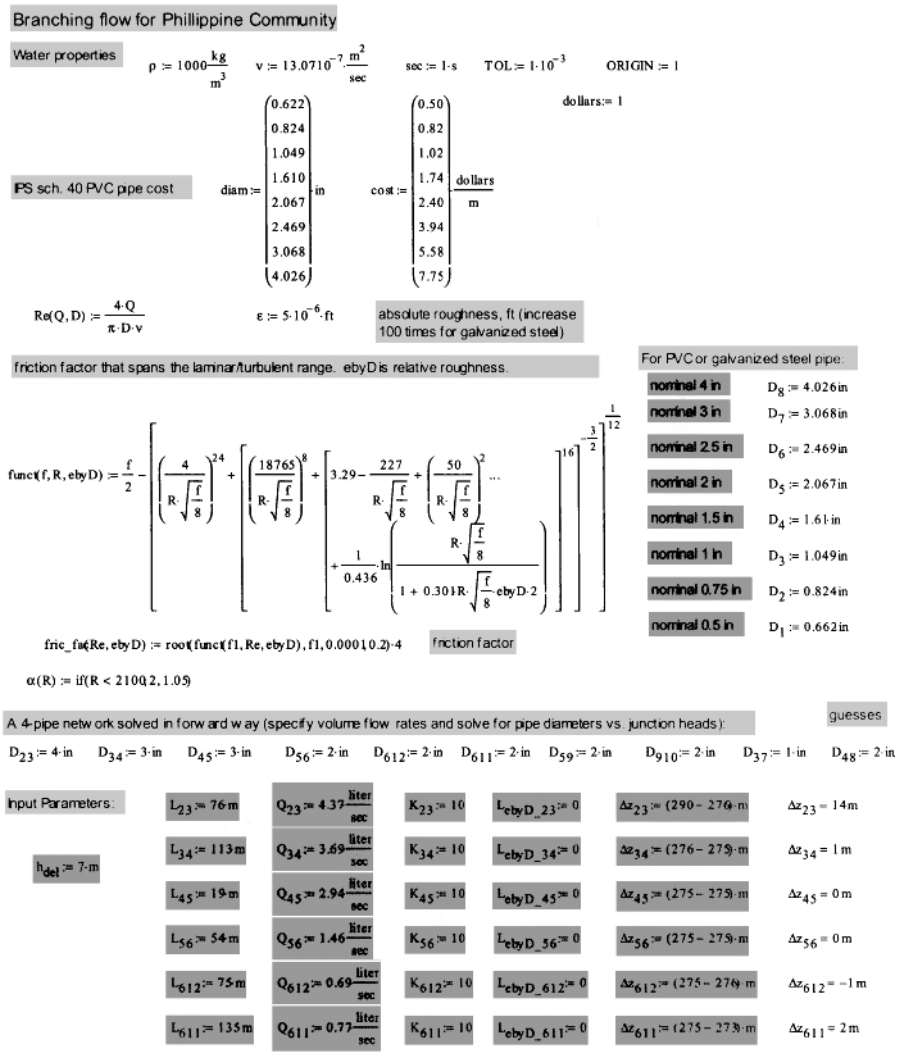

Figure 15.10 Page 1 of Mathcad worksheet for solution of distribution network. Worksheet `BranchNetwork_Philippines_withcost_ver1.xmcd`.

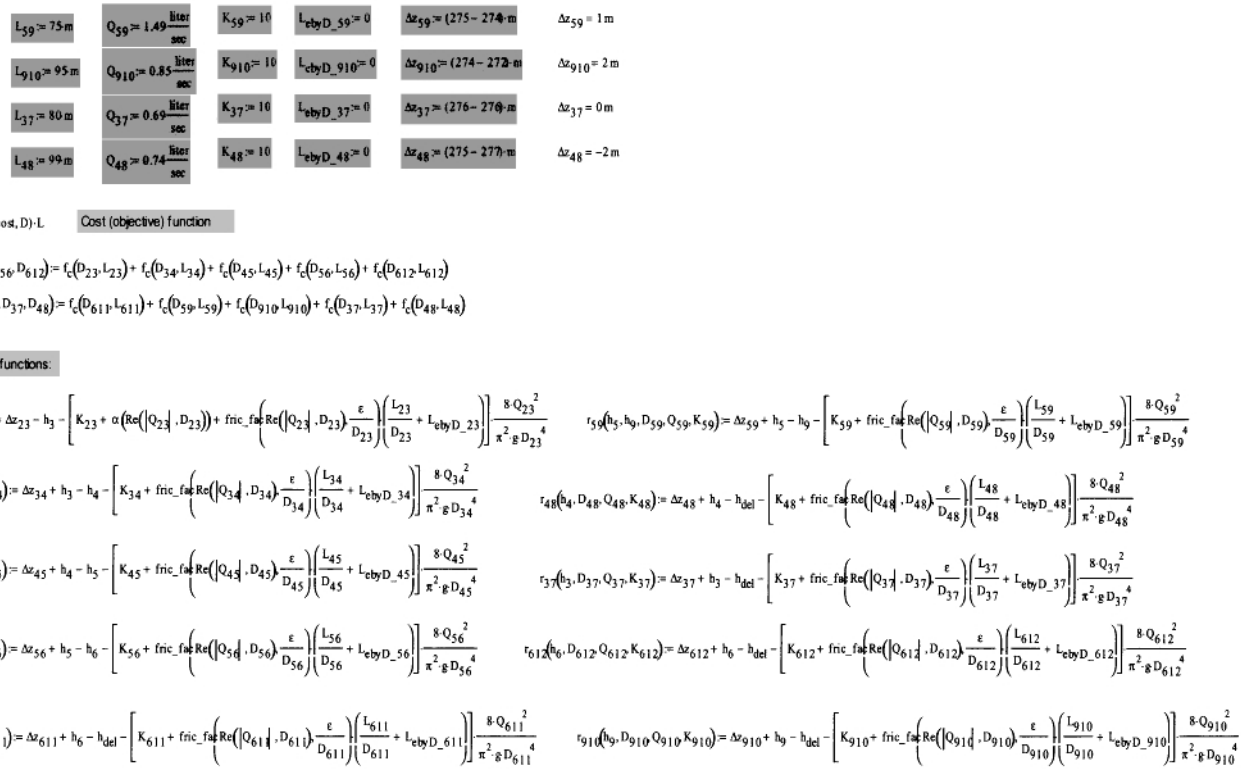

Figure 15.11 Page 2 of Mathcad worksheet for solution of distribution network. Worksheet `BranchNetwork_Philippines_withcost_ver1.xmcd`.

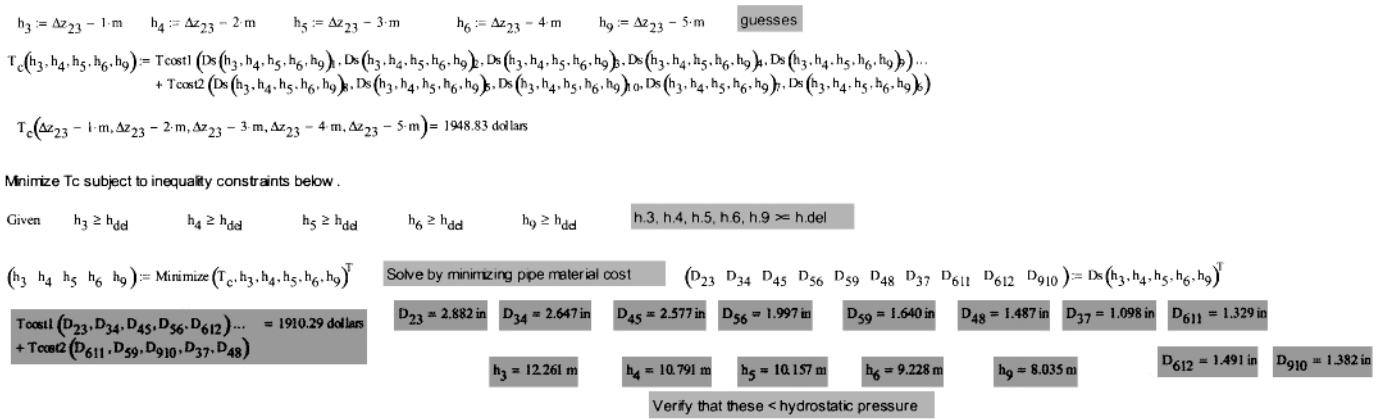

Figure 15.12 Page 3 of Mathcad worksheet for solution of distribution network. Worksheet BranchNetwork_Philippines_withcost_ver1.xmcd.

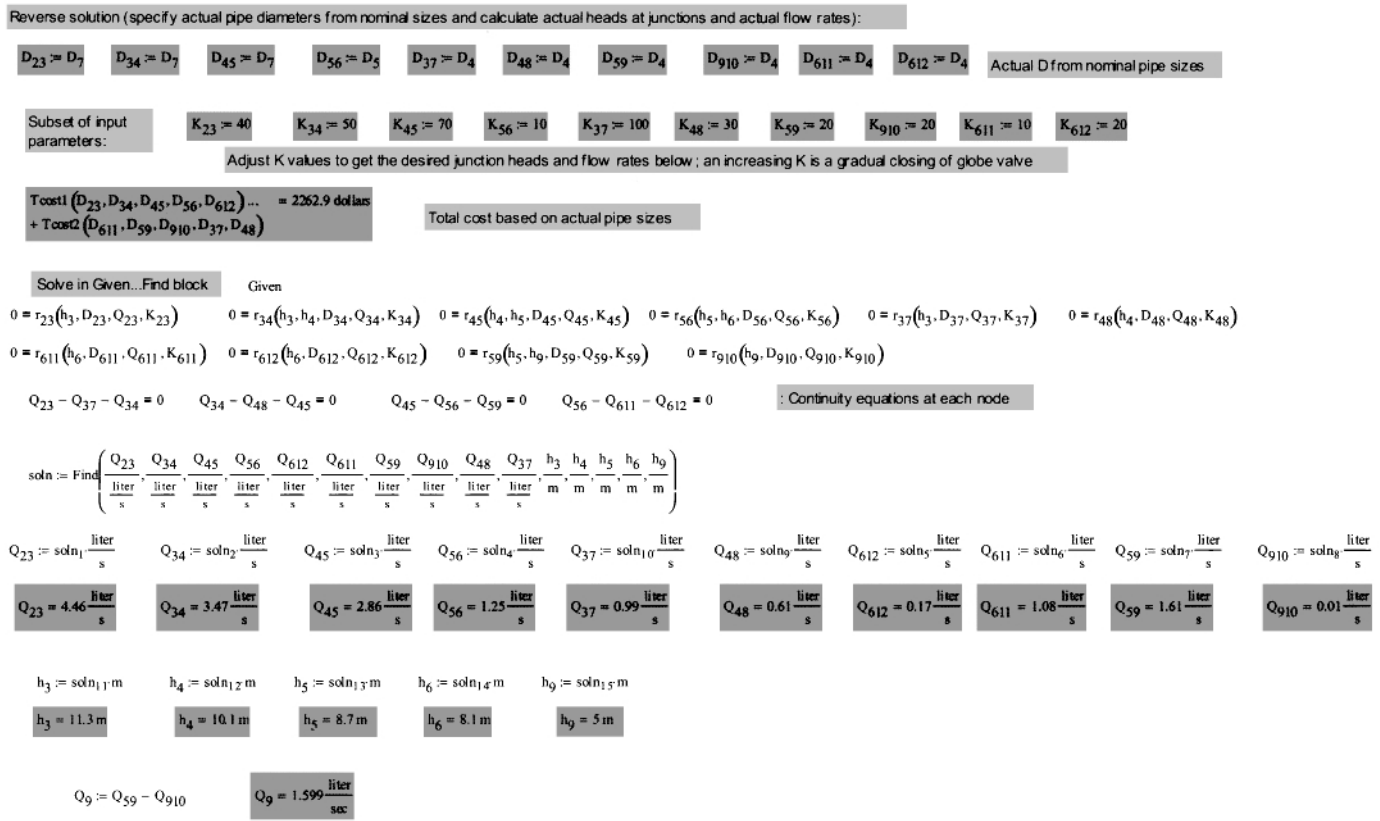

Figure 15.13 Page 4 of `Mathcad` worksheet for solution of distribution network. Worksheet `BranchNetwork_Philippines_withcost_ver1.xmcd`.

Table 15.11 Static Pressure Heads at the Junctions for Distribution Network

Node	Static Pressure Head (m) Based on Theor. D (Optimal)	Static Pressure Head (m) Based on Actual D
3	12.26	TBD[a]
4	10.79	TBD
5	10.16	TBD
6	9.23	TBD
9	8.04	TBD

[a]Entries labeled TBD need to be completed.

system because we chose a pipe size *larger* than theoretical for all segments (with one exception, but the theoretical and actual ID were nearly identical in this case). Be aware that a globe valve, whose job is to throttle the flow (in other words, reduce the static pressure), effectively reduces the pipe diameter in which it is installed.

As I mentioned above, if you plan to use GI pipe instead of PVC, you will need to rerun the Mathcad Worksheet with a roughness value (ϵ) 100 times larger than that for PVC pipe. Generally, you should expect slightly larger pipe sizes with GI pipe because of the rougher wall.

The static pressure heads at the junction of multiple pipes in this system are shown in Fig. 15.11. All values are acceptable because each is > 7 m as required by this design. Once you solve the reverse problem, you will want to inspect these values again to ensure their acceptability.

After adjusting the pipe diameters to correspond to nominal sizes, the total cost of \$2263 (central Nicaragua pipe-cost data,) is greater than the pipe cost of \$1910 based on the theoretical pipe diameters, as expected. The latter was obtained by determining the static pressure heads at the junctions that minimize pipe sizes and, thus, cost. A few plots of cost versus the static pressure heads can be made in the Mathcad Worksheet to determine the sensitivity of pipe size and cost to the pressure heads. We refer to this exercise as a "sensitivity" or "parametric" study.

Unfortunately, it appears that your original assumption of \$1000 for pipe will need to be adjusted by more than a factor of two. Perhaps the municipality or state government will consider making up the difference at your request.

One way to reduce the cost of the material for your network is to use a composite pipeline in place of a uniform-diameter pipe in one or more network segments. For example, in your design, the diameter of segment 3-4 is 2.65 in. We chose a 3-in. (nom.) PVC pipe having an ID of 3.068 in. for it (see Table 15.10). The choice of a pipe size larger than required has two effects: it costs more, and it does not dissipate as much potential energy as it should. A composite pipeline is one of two diameters in series that exhibits the same pressure drop as its uniform-diameter counterpart. One pipe has a diameter (D_a) larger than the theoretical one (of diameter D), and the other has a diameter (D_b) smaller than D. The formula, valid for PVC pipe, for the

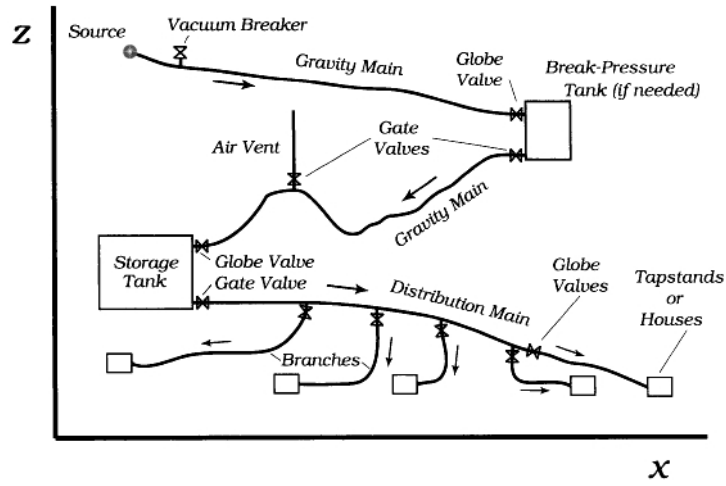

Figure 15.14 The elements of a gravity-driven water network.

ratio of the length of pipe a to the overall pipeline length, L, is

$$\frac{L_a}{L} = \frac{D^{-19/4} - D_b^{-19/4}}{D_a^{-19/4} - D_b^{-19/4}}, \qquad D_b < D < D_a.$$

Once this equation is used to calculate L_a/L, the lengths of pipes a and b are easily determined (note that $L = L_a + L_b$). These results assure us that the frictional head loss for the pipeline of theoretical diameter D will match that of the composite pipeline of D_a and D_b. For your design, the theoretical D of 2.65 in. is bounded by nominal 2-in. ($D_b = 2.067$ in.) and nominal 3-in. ($D_a = 3.068$ in.) pipe. With these, I calculate $L_a/L = 0.818$ and for $L = 113$ m, $L_a = 92$ m. This gives $L_b = 21$ m, slightly reducing the cost of the network since less nominal 3-in. pipe is used. To add flexibility to the design, I recommend reducing the length of the smaller-diameter pipe as calculated by the above formula by perhaps a factor of 0.8-0.9. By doing this, there will be "excess" static pressure not dissipated by major loss that can be used for unanticipated needs.

15.3.3.4 Miscellaneous Hydraulic Elements There are other hydraulic elements in the network you are designing that need to be considered. Among these are tapstands and miscellaneous things like valves, air vents, and vacuum breakers (see Fig.15.14).

Water Collection: There are typically three types of collection points in a gravity-driven water network. The water collection point can entail a communal water facility, a single household connection, or multiple household connections. It is important to understand that the amount of water consumed and the design flow rate increases significantly as the number of connections to system increases. A system that is designed to supply communal water collection will be under-designed if private households

begin connecting into the system after is has been installed. For this reason, it is often advisable to design the distribution mains to be able to provide for private connections regardless of the type of water collection. This often entails anticipating a future demand on the system and oversizing the water distribution mains to be able to account for a larger design flow rate. Since we estimated a demand of 100 L/person/day, we have essentially oversized the mains to accommodate private household connections.

A Tapstand – Communal Collection Point: Communal water collection points are often referred to as tapstands and are designed to deliver water to a central location in an area to provide equal access to the collection facility. The number of taps can be increased at a single collection point to provide more households with water and reduce the waiting time for collection. An important consideration in the design of a communal water collection system is the tapstand location. This can often be a sensitive issue in a community as every household will want a tapstand located close to home for convenience. For this reason, *the final design and location of a communal tapstand should include input from the local community.* One of the roles of the engineer or project manager in a communal water distribution system is to facilitate the decision-making process for determining the site location of community tapstands. Incorporating community participation in this phase of the project will also ensure that any cultural considerations are taken into account and that the final design is appropriate to the needs of the community. In most situations, a water collection point is more than a physical structure because it also serves as a meeting point where people make decisions about the community and spend a significant amount of time.[7] For this reason, another design consideration in addition to maintaining good drainage is having a clean, hygienic, and attractive place for people to socialize.

The project engineer is often involved in establishing minimum standards when facilitating the final design of a water collection facility. From a technical perspective, the number of tapstands in an area will depend on two variables, the number of users and the distance to the collection point. Additionally, the final design of a tapstand should take into consideration the site drainage as well as the structural integrity of the design and the pressure limits of the valves, meters and fittings. Tapstand designs are presented in Jordan Jr. (2004), Mihelcic et al. (2009), Anon. (1979), Anon. (1990), and Jones (2010). The final water collection points should be determined so as to provide for a convenient location for as many households as possible. The minimum standard for most water supply projects is (Anon., 2004),

- A maximum distance of 500 m to the nearest water collection point,
- A minimum of one tapstand for 250 people.

Whereas, this standard is commonly used for water projects aimed at maintaining a minimum standard, it is often more appropriate to determine the site locations based on geography, site topography, and the community's needs. Another approach would simply estimate the time required to collect water and define the area using a minimum recommended round-trip collection time.

[7]In sociological terms, this is like "the" local street corner or "watering hole" in an urban community.

A poorly designed tapstand can often limit access to water by not taking into account the site drainage and conveyance of waste water at the facility. This is primarily a concern because standing water can create breading areas for mosquitoes that is a vector transmission route for many environmental diseases in tropical climates. Additionally, poor drainage can often cause already vulnerable populations within a community to become more isolated. An example of this is handicapped or elderly people who already have difficulties accessing water. A properly designed tapstand will take site drainage into consideration by locating the facility in an area where standing water will not collect around the tap and where runoff will not impede access. A typical installation will include some type of conveyance for waste water such as a concrete channel or a drainage pipe that discharges the water to a natural swale or a stone-filled soak pit. In some cases, the community may decide to use the waste water for irrigation purposes.

The primary concern when designing the structural supports for a tapstand is protecting the valves and fittings. In most cases, some type of stone or brick masonry is used to support the stand-pipe; the water pipe that rises vertically to provide an easier means of collecting water. Some designs use a steel reinforced concrete column for this purpose, especially in areas where children have access to the tapstand. This additional protection is necessary to prevent damage that may result if children were to play around the water collection point.

An additional structural consideration is the protection of water meters or valves the tapstand connects into the branch pipe. Where water meters and valves are installed, a concrete or stone metering box with an access cover is often used to protect against corrosion and tampering. If a gate-valve is installed, it is feasible to protect the valve by simply using a 4-in. PVC pipe that is slotted at the bottom to fit around the valve and has an access cap at the surface.

Pressure limits for public tapstands are important and need to be considered. If the pressure is too high, the faucet valve may leak or prematurely wear when it is opened slightly. If the pressure is too low, the water flow rate will be too small. Most manufacturers of faucet valves rate the pressure limit in the range of 50–70 psig which translates to 35–50 m of water head [these generally agree with Jordan Jr. (2004)]. Under these conditions, the outlet velocity for a typical faucet with a design flow rate of 0.2 L/s is highly turbulent, and would create an intense jet and splashing during water collection that is not desirable. For this reason, the recommended pressure limits at a water collection point often range from between 10–30 psig or, 7–20 m of water head. In some circumstances, controlling the tapping pressure at the water connection is not feasible due to terrain and material limitations. In these instances, a pressure diffuser device [a fixed minor-loss element; see Chapter 7 in Jones (2010)] can be installed at the location where the delivery pipe connects to the water main. These devices should be designed specifically for the site conditions and can include a series-connected globe valve, or an orifice-type of flow restrictor (Jordan Jr., 2004).

Private Connections – Single and Multiple: It is very challenging for an external organization to control the number of connections to a community-based water system. The management of private connections to a gravity-flow water distribution system requires an intimate understanding of the day-to-day operations of the water

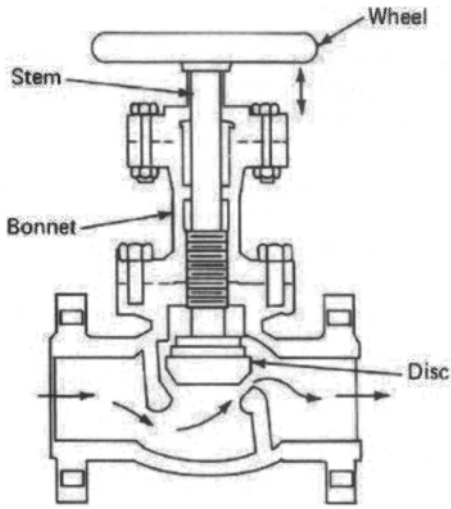

Figure 15.15 cross-sectional view of large globe valve.

supply network, as well as the specific needs of the community. For this reason, the role the project engineer is primarily to build the capacity of the local water association and provide them with the skills and knowledge to make good decisions about the water system. To meet these needs, it is recommended that the project engineer incorporates training and capacity-building workshops into the project implementation so that local technicians and managers can make informed decisions about the system's operations.

Valves, Air Vents, and Vacuum Breakers: Both gate and globe valves appear in Fig.15.14. A gate valve belongs to a class that may be thought of as "block" valves. The purpose of these is to either allow the full flow to pass or be totally turned off. No pressure reducing (throttling) should be performed with a gate valve because they are not designed for this purpose and will prematurely fail if operated in this way. The gate in this valve is moved up or down by rotating the handle. When the gate is down, the flow is blocked, and when up, is fully open and out of the way of the flow.

Although a globe valve can be used as an "on–off" valve, its primary function is to throttle or reduce the static pressure in the flow. The flow passageway between the metallic disk and valve seat as seen in Fig. 15.15 is adjustable. When the passageway is adjusted to be small, a large pressure drop occurs in the flow between the valve inlet and outlet. Because of the importance of energy management in gravity-driven water networks [see Section 1.5.1 in Jones (2010)], the globe valve is used in many locations especially where appropriate for control and flow balancing, in addition to intentional energy dissipation.

There is a need for air vents at local high points to vent trapped air in any water distribution network. This is discussed more fully in Chapter 14 in Jones (2010), where models for the potentially penalizing effect of trapped air in the network are also developed. A bucket-type air vent opens to vent air when there is an air–water

level in the body of the air vent. This level indicates the presence of air in the network. Alternately, a gate valve on the branch of a tee fitting installed at the local high point can be used to manually vent trapped air. Finally, a long vertical pipe attached to the local high point may be used to vent air automatically. In this case, the top end of the pipe is open to the atmosphere and its elevation must be approximately above the surface level of the reservoir or nearest tank upstream from it.

A vacuum breaker prevents the formation of negative gage pressure in a flowing pipe. Negative pressures in the flow are undesirable for many reasons which, I am sure you can imagine. A vacuum breaker can be a purchased unit that is installed in-line in the pipe. In this case, a spring in the body of the vacuum breaker allows air from the outside to enter the flow should the pressure fall below a pre-set value. In its simplest form, a vacuum breaker can be a vertical piece of pipe with an open end at the top. This would automatically bring air into the network when the pressure of the flow falls below atmospheric.

Finally, you will need to include gate valves at the lowest end of all runs of pipe that form valleys. These will allow for periodic cleaning of solid debris from the pipe that accumulates over time.

Non-hydraulic Design: Regarding the important topic of tank and reservoir construction, much is available in the literature, which I assume you have access to, so I will say just a few words. Water storage tanks are used for storing water during the nonpeak periods for use during the peak periods of consumption as discussed above. The design and construction of a water tank is a specialized field of engineering and needs to consider geotechnical issues with the tank's foundation and material selection for construction. In most cases, local expertise and resources can be utilized for addressing these concerns. It is recommended to consult with a local engineer once the final location of the storage tank facility has been selected. The local engineer should make the final decision if the site selected is feasible from a geotechnical point-of-view. A cross-sectional view of a typical water tank is shown in Fig. 15.16.

Local materials should be used for the construction of a water storage tank. In some countries, elevated steel water tanks are designed for municipal water systems. Elevated tanks can be complicated to construct and require very specialized skills in welding and project management. Given the mountainous nature of your project area, it is probably not necessary to plan for an elevated water tank.

Some areas of the world have successfully constructed water storage tanks using ferrocement technology rather than concrete. Ferrocement water tanks consist of a cement-rich mortar with a water-proofing agent that is plastered onto a steel-mesh frame. This saves significantly in material cost as the amount of cement required is much less than that for poured concrete tanks. It may even be feasible to construct a buried or semisubmerged water tank, if the tank location is sited properly. Buried tanks can be constructed with concrete block, brick, or ferrocement also have significant costsavings because of a reduction in wall thickness and steel reinforcement requirements.

Steel reinforced concrete water tanks are the most common type in developing countries because the masonry and carpentry skills for construction are often locally available. These water tanks are constructed using wood forms with steel-bar rein-

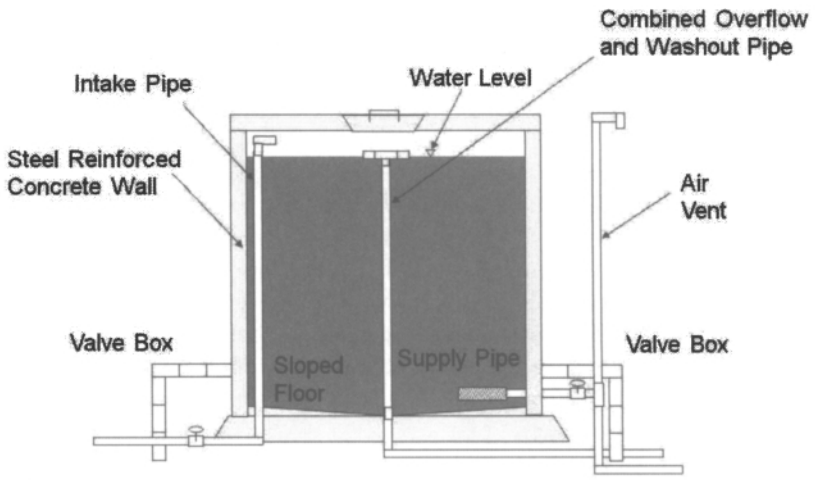

Figure 15.16 cross-sectional view of water storage tank.

forcement. After the forms and the steel have been assembled, a concrete mixture of Portland cement, sand, gravel and water is poured into the frame. The forms are then removed after a 3–7-day curing period. In any water tank design and construction, care should be taken to ensure that the water does not become contaminated as it sits in the tank. For this reason, a concrete cover or a wooden roof is constructed to prevent air-born contaminants from entering the tank. If a concrete cover is used, steel reinforcement is needed along with an access hole for maintenance. If a wooden roof is constructed, then some type of mess screen is needed to prevent animals from getting inside. Finally, care should also be taken to install the piping accessories prior to any concrete work. This entails determining the exact location, diameter and material for the inlet, outlet, overflow and the clean-out pipes for the water tank. See Fig. 15.17 for a picture of a protected valve box and Fig. 15.18 for a typical view of water inlet flow to a tank and overflow arrangement.

For further details, please see Jordan Jr. (2004), Mihelcic et al. (2009), or other references from reputable development guides.

I hope my response has been helpful to you. Please contact me if you have any questions.

Sincerely,

You

Figure 15.17 Protected valve box.

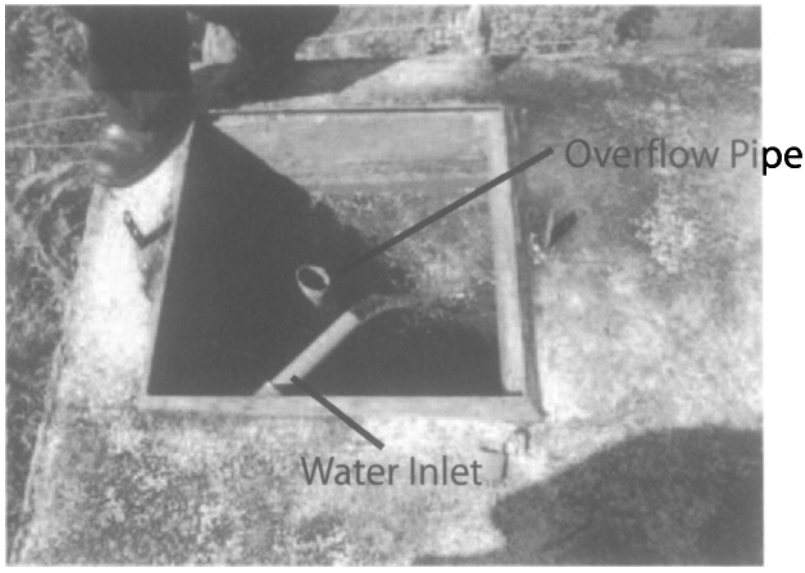

Figure 15.18 Tank inlet and overflow.

References

Anon. Public Standpost Water Supplies, A Design Manual - Technical Paper No. 14. Technical report, WHO International Reference Center for Community Water Supply, The Hague, The Netherlands, 1979.

Anon. Technical Brief No. 26/Public Standposts. *Waterlines*, 9(2):17–20, 1990.

Anon. The Sphere Project, Humanitarian Charter and Minimum Standards in Disaster Response. Technical report, 2004. URL `\url{http://www.sphereproject.org/content/view/27/84}`. [Online; accessed 12-December-2009].

E. H. Hofkes. *Small community water supplies; technology of small water supply systems in developing countries*. John Wiley & Sons, Inc., Chichester, UK, 1983.

R. W. Jeppson. *Analysis of Flow in Pipe Networks*. Ann Arbor Science Pubs., Ann Arbor, MI, 1976.

G. F. Jones. *Gravity-Driven Water Flow in Networks: Theory and Design*. John Wiley & Sons, Inc., Hoboken, NJ, 2010.

T. D. Jordan Jr. *Handbook of Gravity-Flow Water Systems*. ITDG Publication, London, UK, 2004.

J. R. Mihelcic, L. M. Fry, E. A. Myre, L. D. Phillips, and B. D. Barkdoll. *Field Guide to Environmental Engineering for Development Workers*. ASCE Press, Reston, VA, 2009.

M. L. Nayyar. *Piping Handbook*. McGraw-Hill, New York, NY, 7th edition, 2002.

P. K. Swamee and A. K. Sharma. *Design of Water Supply Pipe Networks*. John Wiley & Sons, Inc., Hoboken, NJ, 2008.

N. Trifunovic. *Introduction to Urban Water Distribution*. Taylor & Francis, New York, NY, 2006.

CHAPTER 16

EXERCISES

"Practice makes perfect."
– Proverbs

16.1 COMMENTS

The exercises below are specific to the chapter as noted. Their order of appearance generally matches that in the chapters. Unless directed otherwise, assume all pipe to be sch. 40, IPS series, PVC pipe. Assume the water temperature is 10°C. The solutions appear beginning midway through the chapter.

The index does not include entries in this chapter.

Gravity-Driven Water Flow in Networks. By Gerard F. Jones

16.2 THE PROBLEMS

Chapter 2

1. The turbulent velocity distribution, which appears as the middle curve in Fig. 2.2, may be approximated based on the "1/7-power law"

$$\frac{u(r)}{u_{max}} = (\frac{r}{R})^{1/7} \tag{16.1}$$

where u_{max} is the maximum velocity of the flow at the pipe centerline, r is the local radial location, and R is the outer radius of the pipe. Calculate u/u_{max} for r/R of 0.05, 0.1, 0.2, 0.4, 0.6, 0.8, 0.9, and 1.0 based on the 1/7-power law and qualitatively compare with the velocity distribution in this figure.

2. From the general energy equation, Eqn (2.7), develop Eqn (2.25). Simplify it to obtain Eqn (2.40) for minor-lossless flow.

3. Using Eqs (2.2), (2.6), and (2.9), calculate the temperature increase from inlet to outlet for water flow in a 100-m long, straight, 2-in. nom. PVC pipe at a flow rate of 1.2 L/s. Neglect minor losses and assume there is no heat transfer from the pipe to the surroundings. Comment on the significance of the results.

4. Make a list of the restrictions applied to the Bernoulli and energy equation and compare them. Interpret these restrictions in your own words.

5. The following flow speed and head loss data were collected in a lab test for steady flow of water in a straight, horizontal brass tube of inside diameter 1/4 in.

h_L	13.7	9.39	7.73	7.44	6.34	5.77	4.92	3.72	2.28	1.17
$\overline{u}$	2.5	2.1	1.83	1.72	1.61	1.5	1.4	1.14	0.9	0.6

h_L is in inches of Hg, and $\overline{u}$ is in m/s. Use this data to validate the Darcy–Weisbach equation [Eqn (2.10)]. Calculate and plot the friction factor against Re from the data and Eqn (2.10). How do the results from Eqn (2.10) qualitatively agree with these data?

6. Beginning with the energy equation for a single-pipe network where the pipe is straight, Eqn (2.33), develop the same for a minor-lossless flow in a pipe of arbitrary length and reasonably small slope, Eqn (2.45).

7. Consider a smooth, single-pipe network of mean slope $s = 5.5\%$, tortuosity $\lambda = 1.18$, and peak elevation $z_1 = 20$ m, with single globe valve installed at its lowest point. On the other side of the valve is atmospheric pressure. For a pipe with ID of 2.067 in., plot the volume flow rate as a function of the minor loss coefficient, K (K is proportional to the closure fraction of the valve). Vary K

from 10 (full open) to 500,000 (nearly closed). Ignore other minor losses and α in the network.

8. Calculate the volume flow rate in a galvanized iron pipe of ID 3.36 in. and $L = 3.4$ km long. The pipeline is under 3-atm of pressure at the inlet and the outlet discharges to atmospheric pressure. The elevation change, $z_1 - z_2$, is -10 m. There is a partially closed globe valve at the discharge for which $K = 350$. Neglect other possible minor losses.

9. Verify that 1° of longitude at the equator is ~111,300 m. Refer to Appendix B and use the Excel spreadsheet from Dutch (2009). What is the distance equivalence of 1° of longitude at 40° latitude?

10. Consider the GPS data (obtained by averaging over 10 readings each for latitude and longitude) in DMS format as shown in Table 16.1. Referring to the material in Appendix B, calculate the latitude and longitude of the source in decimal format and the mean slope between the source and delivery locations. The elevation change between the source and delivery locations, Δz, is 46.5 m obtained by averaging 10 GPS elevation readings.

Table 16.1 Data for Exercise 10

Name	Latitude	Longitude
Source	19° 13' 47"	-75° 18' 50"
Delivery	19° 15' 22"	-75° 19' 20"

Chapter 3

11. Look up and report the inside diameter and pressure rating for the pipe in the following table. Report pressure rating in values as supplied in Chapter 3 and in head of water (m). See Chapter 3 for the definition of the pipe materials PVC, PE, and ABS.

Nominal Size	Wall Thickness Reference	Material
1 in.	sch. 80	PVC
$3\frac{1}{2}$ in.	sch. 40	ABS
2 in.	sch. 40	PVC
$1\frac{1}{2}$ in.	sch. 80	PE
$\frac{1}{2}$ in.	SDR 11	PE
75 mm	SDR 13.6	PVC
25 mm	SDR 21	PE
4 in.	SDR 26	PVC

Chapter 4

12. An oil refinery requires a flow rate of water (10°C) at 0.3500 m^3/min. The length of supply pipe is 1345 ft between the main and delivery location and 34 m below the plant. It is known that the run will require 10–90° elbows and flow through the branch of a tee. Determine the minimum nominal galvanized steel pipe size required if the supply and delivery static pressures are known to be 1850 and 475 kPa, respectively. How is this calculation performed if Method 2 (see Section 4.2) is to be used to solve for D? What impact will the neglect of minor loss have on the calculation of D?

13. Use the Darcy–Weisbach equation, Eqn (2.9), and the friction factor from either the Colebrook equation [Eqn (2.12)] or the Churchill correlation [Eqn (2.16)] to calculate the head loss (in meters) per 100 m of straight pipe for volume flow rates between 0.1 and 5.0 L/s and for the standard PVC pipe dimensions contained in the appendices in Jordan (2004, reference Table V). For the absolute wall roughness, assume smooth pipe. The value for the absolute roughness for smooth pipe is presented in Chapter 2. Compare your results with those of Jordan Jr. (2004) presented in Reference Table XI. Comment on the extent of agreement between the two. Base Re on the kinematic viscosity of water at 10°C.

    Plot head loss (in m) per 100 m of straight pipe versus the volume flow rate and in the plot, ignore results for flow speeds less than 0.7 m/s and greater than 3 m/s.

14. In Exercise 13, the kinematic viscosity was based on 10°C. Rework this problem with the kinematic viscosity based on water at 27°C and compare it with the results of Exercise 13. What is the range of variation between these two sets of results, expressed as a percentage difference? Comment on the importance of this effect in your designs.

Chapter 5

15. By making the appropriate assumptions for gravity-driven flow in a vertical pipe, show that the energy equation, Eqn (2.40), reduces to Eqn (5.2). Using `Mathcad`, solve Eqn (5.2) and reproduce the results that appear in Fig. 5.2.

16. In the community of Arena Blanca in central Nicaragua, there is nearly a uniform slope between the source and the tank and between the tank and the tapstand in the village. Because of this we can assume the pipe to be straight [i.e., it will have no bends from elbows ($\lambda = 1$)]. A flow rate measurement at the source has determined $Q = 0.23$ L/s and an Abney level is used to find the slope of the system of $s = 0.015$. An altimeter and a GPS give the elevation difference between the source and the tank (z_1) of 452 m. Neglect minor losses.

(a) Calculate the PVC nominal pipe size between the source and the tank needed to satisfy the given geometry and flow conditions. What is the actual maximum volume flow rate of water with this pipe size? What is Re and is the flow laminar or turbulent? Check your result for D using the approximate formula, Eqn (9.2).

(b) If there is a water demand of $Q = 0.38$ L/s during the peak consumption periods of the day, calculate the smallest possible PVC pipe size (in inches) between the tank and the tapstand if the elevation difference between the two is 57 m and the distance measured along the ground between the two is 2840 m.

(c) If there is uncertainty of $\pm 10\%$ in the slopes between the source and the tank, and between the tank and the tapstand, how are the pipe sizes affected?

(d) If there is uncertainty of $\pm 20\%$ in the elevation measurement, how is the pipe size affected? Assume the slopes remain as specified above.

17. A low-head, high-flow gravity water system is proposed for the town of El Guayabo in central Nicaragua. The contour of the ground is not uniform and the flow path between the source and the tank is very circuitous. The pathlength between the source and the tank is 95 m and a survey of the land between the two with an Abney level gives a mean slope of $s = 0.08$. There are 23 bends in the system and we will approximate each as a 45° elbow. In addition, because of the locations of several buildings there are many 90° elbows causing an L_e/D value of 502. A filter at the source is known to have a K value of ~22. A flow rate measurement at the source has determined $Q = 0.55$ L/s. From the Abney level, the elevation difference between the source and the tank (z_1) is found to be 6 m.

    Analyze this system and recommend a nominal PVC pipe size from the source to the tank. Reassess the design if there is uncertainty of $\pm 20\%$ in the elevation measurement. How does the design change to accommodate an annual increase in the water demand of 2% over a 10-year time period? What is the effect of the minor losses? The elbows? The source filter? What is Re? Use the appropriate `Mathcad` worksheet or, for a first-cut estimate without minor losses, the design figures from above. Check your result for D using the approximate formula that appears in footnote 8 of Chapter 9.

Chapter 6

18. Using a few steps of algebra, show that Eqn (6.6), when written at $x = \ell$, reduces to Eqn (2.34) for a straight pipe of constant cross section and slope, s_ℓ.

19. Inspect Fig. 6.4 and explain the reasons for the variation in D^n in your own words. Focus on the inflection point in the 6000–7000-m range. Carry out this exercise by examining the terms in the energy equation, Eqn (6.7), without rereading Section 6.3.

20. Consider the following example of a three dimensional network. A single-pipe, gravity-driven water network in a hilly region is being planned and it is determined that the final run of the pipe is in the form of an inclined helix as shown in Fig 16.1. The parametric equations that describe this geometry are

$$\begin{aligned} x(t) &= \{400 - 40\pi t\} \text{ m} \\ y(t) &= \{200 + 20\cos(2\pi t) - 10t\} \text{ m} \\ z(t) &= \{0.3[200 + 20\sin(2\pi t) - 10t]\} \text{ m} \end{aligned}$$

where t is a parameter whose range is $0 \leq t \leq 3$. If the pipe is nominal $1\frac{1}{2}$, sch. 40 PVC and the flow rate is 2.0 L/s, calculate the static pressure distribution from Eqn (6.12) and plot it as a function of coordinate x. As the designer, are you satisfied with this distribution? Ignore minor loss, but include α at the source.

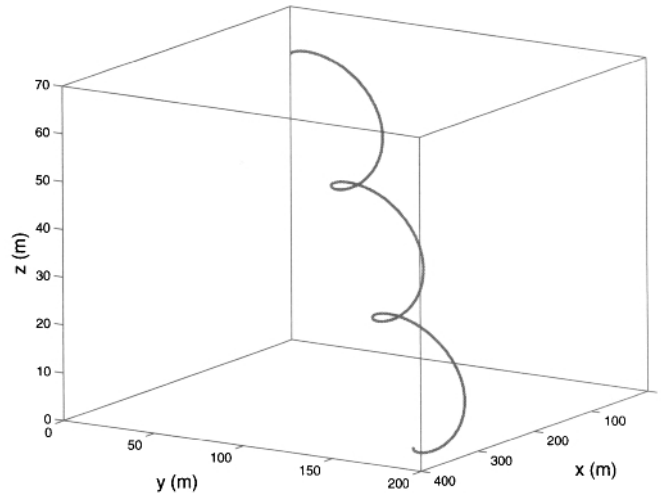

Figure 16.1 Network of Exercise 20. The vertical axis appears in a magnified scale.

Chapter 7

21. Follow the example of Section 7.2 and write a small worksheet to solve for the pressure distribution in a single straight pipe of uniform slope and pipe diameter with a series of three minor-loss elements uniformly spaced along the pipe (at $L/4$, $L/2$, and $3L/4$). To investigate the effect of the minor loss K-values, imagine each loss element is a globe valve. Plot the dimensionless pressure distribution, $p(z)/\rho g z_1$, for $s = 5\%$, $L = 1000$ m, and $Q = 4.3$ L/s for $K = 10, 400$, and 700 for each of the three valves. The pipe is 4-in. nominal, sch. 80 GI. The source is at atmospheric pressure.

Chapter 8

22. Consider a variation of the data set obtained from a site survey for a network in San Benito, Nicaragua, where the measured flow rate of water is 0.61 L/s. The survey data are presented in Table 16.2. (a) Use Mathcad to design the pipe to produce an acceptable positive static pressure at the station where the pipe is at its highest local peak. Multiple pipe diameters are permitted. (b) If the pipe sizes remain fixed at the values determined in part (a), determine the increase in the value for the flow rate if a static pressure at highest local peak is allowed to be atmospheric pressure.

Table 16.2 A Variation of the Survey Data for the San Benito Site

Station	x (m)	$y(x)$ (m)	$z(x)$ (m)	$L_\ell(x)$ (m)
0	0.0	0.0	24.7	0.0
5	−32.2	−47.1	13.2	58.2
8	−70.9	16.1	10.3	132.3
C3	−232.6	84.2	13.3	307.8
C4	−266.8	106.8	17.1	349.0
C5	−298.2	162.7	11.9	413.3
C6	−317.6	203.2	8.2	458.4
C7	−350.6	232.6	12.0	502.7
C8	−389.4	247.3	11.3	544.3
C9	−398.3	269.5	10.1	568.2
C11	−359.6	388.1	11.4	693.0
C12	−360.0	442.0	7.3	747.1
C13	−392.2	553.3	8.5	862.9
C15	−355.4	668.6	7.3	983.9
C17	−382.4	810.5	12.7	1128
C19	−347.7	917.4	19.5	1241
C21	−280.2	1121	22.3	1455
C23	−355.7	1307	4.0	1657
C24	−279.8	1421	2.7	1795
C28	−357.8	1636	0.0	2023

23. Demonstrate that the acceleration term, $L\frac{d^2\overline{u}_2}{dt^2}$, in Eqn (8.11) is negligible relative to the remaining two terms in this equation by making t in Eqn (8.11) dimensionless with respect to $\Delta t_{sc} = \frac{4A_t\Delta z_t(0)}{\pi D^2 \overline{u}_{2,\infty 1}}$. Show that Eqn (8.11) reduces to Eqn (8.14) once $L\frac{d^2\overline{u}_2}{dt^2}$ is neglected.

24. A large tank of 55,000-L capacity and $\Delta z_t = 4.5$ m high is to be drained. The tank is connected to a 2-in. nominal sch. 40 GI pipe, 187 m long, open to the atmosphere at its end. There are four 90° elbows and an open globe and gate valve in this pipeline. The elevation change from the bottom of the tank to the end of the pipe is $\Delta z_p = 12.5$ m. Calculate the steady state flow speeds for this process where the flow is driven by

- $\Delta z_t + \Delta z_p$
- Δz_p

to get $\overline{u}_{2,\infty 1}$ and $\overline{u}_{2,\infty 2}$, respectively (see Fig. 8.15). Calculate the time that it takes the flow to accelerate from zero speed to 99% of $\overline{u}_{2,\infty 1}$ and the time that it will take to drain the tank. Check your result by using the average flow rate over the drain time.

25. One favorite problem on the topic of inviscid flow in fluid mechanics is the frictionless syphon. To obtain a model for this, ignore the friction term in Eqn (8.17). The resulting equation can be solved for Q as a function of D. Compare the volume flow rates for D values of 1, 1.5, 2, 2.5, and 3 in. with those from Fig. 8.18 that includes the effect of friction. Comment on the reasonableness of the outcome.

26. Using the geometry of Fig. 8.17, determine the maximum height (i.e., the value for r) for a syphon of nominal 1-in. PVC pipe. HINT: The minimum static pressure corresponds to the saturation pressure for water at 10°C. Refer to footnote 13 in Chapter 8 for the value of this pressure.

Chapter 9

27. One of the formulas in the literature pertaining to gravity driven water flow in pipes is given in an earlier edition of the Piping Handbook (Nayyar, 1992) and in the Plastic Piping Handbook (Willoughby et al., 2002) as

$$Q = 27.5 D^{2.667} s^{0.5} \tag{16.2}$$

where it is understood that D is in inches and Q is the Natural flow rate in gallons per minute[1]. Another one is from a technical publication of the American Water Works Association (American Water Works Association, 2006).

$$Q = 42.2 D^{2.63} s^{0.54} \tag{16.3}$$

Assuming that $F = 0$ (for Natural flow, see Section 2.6.1) and $\lambda = 1$, and starting from Eqn (9.7), develop an equation in the form of Eqs (16.2) and (16.3). Comment on the differences between the expression that you develop and Eqs (16.2) and (16.3) and highlight the assumptions made to develop such formulas.

28. The Copper Tube Handbook (Copper Development Association, 2006) reports pressure drop results for smooth copper tube of various sizes. The Hazen–Williams formula on which their results are based is given as

$$\frac{\Delta p}{L} = \frac{4.52\, Q^{1.85}}{C^{1.85}\, D^{4.87}} \tag{16.4}$$

[1]The coefficient in Eqn (16.2) is 30.5 in Willoughby et al. (2002).

where $\Delta p/L$ is the pressure drop in psi per foot of tube length, Q is the flow rate in gallons per minute, D is the ID of the tube (inches), and C is a constant whose numerical value is 150.

By comparing Eqn (16.4) with the Darcy–Weisbach equation, Eqn (2.9), determine the assumptions upon which Eqn (16.4) is based. What are the units of the constant C? Plot the ratio of $\Delta p/L$ from Eqn (16.4) to that from the Darcy–Weisbach equation for tube diameters of $\frac{1}{2}$-in. nominal (D of 0.662 in.), 1-in. nominal (D of 1.049 in.), and 2-in. nominal (D of 2.067 in.), for Q ranging from 0.1 L/s to 7 L/s. Comment on your observations.

29. Develop Eqn (9.2). Simplify it to obtain Eqn (9.3). Note that this is similar to Exercise 27 except λ and F are retained as parameters in the energy equation.

30. Compare the results of Eqs (9.4) and (9.5) for smooth pipe. Take the ratio of the two and plot as a function of Q with h_L/L as a parameter to validate the statement that there is agreement to within $\pm 2\%$ over 0.1 L/s $\leq Q \leq$ 3 L/s and $0.001 \leq h_L/L \leq 1$. Also, show that this range of conditions generally produces $4,000 <$ Re $< 325,000$. To do this, plot Re as a function of Q with h_L/L as a parameter.

31. Compare the results of the correlation of Eqn (9.6) for GI pipe with the numerical solution from the `Mathcad` worksheet `SinglePipeNetworkDesign_Appendix.xmcd` for minor-lossless flow. Carry out this comparison for $Q = 0.012, 0.1, 1.0, 3.0$, and 5 L/s, and $h_L/L = 0.001, 0.01, 0.1$, and 1.0. Present your results in tabular form.

32. It was demonstrated in Chapter 9 that the solution for the energy equation for flow in a single pipe can be written such that only two dimensionless groups appear, one for the dimensionless volume flow rate and the other for the modified slope [see Eqn (9.7)]. Beginning with the form of the energy equation for flow in a pipe of arbitrary length, Eqn (2.40), recast this in the form of Eqn (9.7) by rearranging it after writing it in terms of Q instead of $\overline{u}$. In particular, identify the hydraulic gradient (or modified slope) term and the one that you would label as the dimensionless volume flow rate. Comment on the differences between the dimensionless groups from this exercise and those from Eqn (9.7).

Chapter 10

33. Give thought to, and list, several instances where optimization of a gravity-driven water network is possible other than those noted in Chapter 10.

34. A more realistic cost model for the heat exchanger considered in textbox B.10.3 is to include the cost for a variable tube surface area explicitly. In Eqn (10.13), this was accounted for as a lumped cost. Inside the heat exchanger are many tubes of small diameter, perhaps a centimeter, that flow the hot fluid. The cooler fluid passes over these tubes and this is where the heat transfer takes place.

With tube cost explicitly included, the improved cost model would be

$$\hat{F}(L,d,n) = \$400/\mathrm{m}^2 \frac{DLn^{1.5}}{n-1} + \$370.70/\mathrm{m}^{3.5} Ld^{2.5} + \$280.60/\mathrm{m}^2 Ld$$

where $\hat{F}$ is in dollars, d and L are the overall diameter and length of the exchanger (in meters), and n is the number of tubes. Here, D is the tube diameter, which is 1 cm. The overall volume of the exchanger is fixed at V = 15 m^3 and the required surface area is 350 m^2. The surface area of the tubes is from $A_s = n\pi DL$.

Use

- The method of Lagrange multipliers
- The `Given...Minimize` block in `Mathcad`

to solve this problem to obtain the optimal values for L, d, n, and total cost.

35. Three pipes are connected in series, as shown in Fig. 16.2. Each pipe is 100 m long and have diameters D_a, D_b, and D_c, respectively. The flow rate in each is Q = 6.1 L/s and the static pressure head at the outlet of pipe c is h_{del} = 10 m. The elevation changes for each pipe are $\Delta z_a = \Delta z$, $\Delta z_b = \Delta z/2$, and $\Delta z_c = \Delta z/3$, where Δz = 50 m. Determine the optimal pipe diameters for the network and the minimum total pipe cost. Are the static pressure heads at the junctions a–b and b–c acceptable from your engineering judgement? Recall that at all junctions the pressure has a single value; this means that the pressure at the end of one pipe is equal to that at the beginning of the one to which it is connected. Use pipe cost data for IPS series sch. 40 PVC pipe in central Nicaragua from the `Mathcad` worksheet and neglect minor loss throughout.

Chapter 11

36. Refer to Fig. 11.1 and the data from Table 11.1. Slightly modify the `Mathcad` worksheet `BranchingPipeExample.xmcd` to investigate the effect of $L_b = L_c$ over the range of 40–400 m, and Q_a over the range of 1–3 L/s. Assume all data from Table 11.1 apply, except the flow from pipe a is evenly split between pipes b and c for both investigations. Comment on the range of pipe sizes that you observe.

37. Obtain the analytical result for the optimal static pressure head, h_j^{opt}, using Eqs (11.16) for the three-pipe branch network in Fig. 11.1. Assume $L_a = L_b = L_c$, $D_b = D_c$, $Q_b = Q_c = Q_a/2$, and that cost is linear with pipe diameter.

38. Obtain the analytical result for the optimal static pressure head, h_j^{opt}, using Eqn (11.39) for the three-pipe branch network in Fig. 11.1 and data from Table 11.1. Use Eqn (11.17) with cost data for IPS-series sch. 40 PVC pipe in

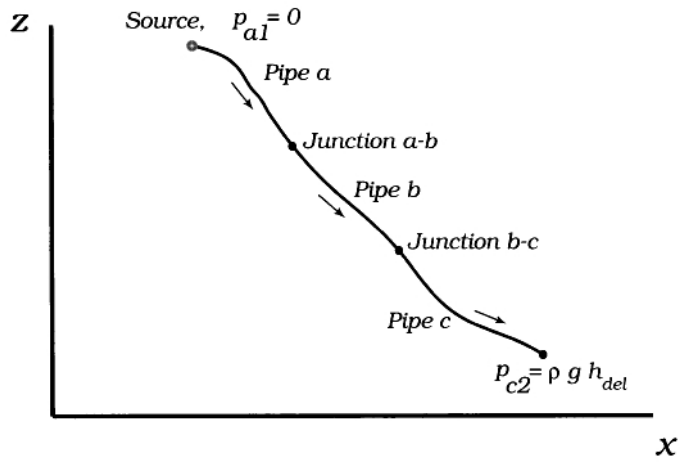

Figure 16.2 Optimization of series-connected pipe.

central Nicaragua. Compare your result with Fig. 11.6 for validation of your result. Note that the results of Fig. 11.6 include minor loss that is not included in the development of Eqn (11.39).

39. Develop Eqn (11.20) from the general energy equation, Eqn (2.25), and using the assumptions appropriate to the series-connected pipe, simplify Eqn (11.20) to get Eqn (11.21).

40. An interesting follow-on problem related to textbox B.11.3 is the response to increases in local peak elevation of the optimal pipe sizes (that minimize total pipe cost) located before the local peak. To do this, gradually increase the elevation of Junction *c–d* from 67 to 84 m. Modify the `Mathcad` worksheet `SeriesPipeExample_equalQ_3pipe_ withcost.xmcd` to include the data in Table 11.5 and the variable elevation of this junction. Report your results in a table. Use the cost data on the `Mathcad` worksheets.

41. The generalized form of the energy equation for a serial pipeline is from Eqs (11.22). In the section following the serial pipeline, we adopted a different method for labeling that included node numbers, not letters (recall that letters were carried over from the early developments of the energy equation for pipe flow from Chapter 2). With this in mind, recast Eqs (11.22) in nodal form, where the nodes at the junctions for a serial pipeline would be 2, 3, ... $n - 1$, where n is the total number of nodes (including the first one at the source and final one at the delivery location).

[ht]

Table 16.3 The Design Parameters for Four-pipe Distribution Network for El Guayabo

Pipe	L (m)	Q (L/s)	K	L_e/D	Δz (m)
a	287	0.81	100	60	12
b	51	0.33	12	360	4
c	37	0.15	12	124	−1
d	12	0.23	12	56	−3
e	48	0.10	12	320	6

42. For the El Guayabo network of Exercise 17, the data in Table 16.3 apply to the distribution pipes from the tank, through pipe a, to four tapstands, pipes b through e (see Fig. 11.1 for a two-tapstand design). A survey of the site provided the slope, pipe length, minor-loss coefficients, and Δz data for each pipe, and the number of people provides the water demand for each tapstand. Note that the flow rates in pipes b through e sum to the flow rate in pipe a, thus satisfying continuity.

    Calculate the nominal PVC pipe size for pipes a through e for this design. Use the appropriate `Mathcad` worksheet.

43. For the Kiangan community in the Philippines, one distribution main for a gravity-driven water network consists of the four pipe segments (Fig. 16.3). Each of the segments has a different flow rate because of attached branches. The relevant data is shown in Table 16.4. Segment 45 ends in a tapstand where a static pressure of 7 m of head is required.

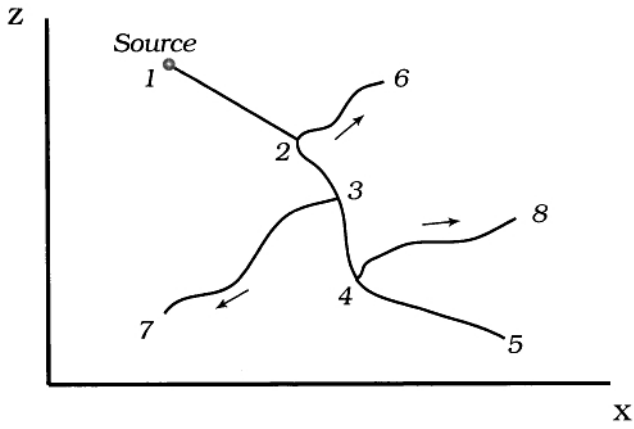

Figure 16.3 Part of a network for the Kiangan community in the Philippines.

Table 16.4 Design Parameters for One Leg of the Kiangan-community Network

Pipe Segment	Q (L/s)	L (m)	K	L_e/D	Δz (m)
12	1.23	76	30	60	18
23	1.04	113	0	90	10
34	0.83	19	0	90	8
45	0.42	75	0	90	6

Calculate the theoretical and nominal PVC pipe sizes for pipe segments for this design. Verify that the design flow rates can be achieved with junction static pressures of 7 m. Use the appropriate `Mathcad` worksheet. What is the total pipe cost?

44. Use the appropriate `Mathcad` worksheet to calculate the nominal PVC pipe size for pipe segments in the Kiangan community design (Fig. 16.3) by minimizing total pipe cost. Use Eqn (11.17) with cost data for IPS-series sch. 40 PVC pipe in central Nicaragua. Verify your numerical solutions using the analytical result from Eqn (11.54). How do your results, both theoretical and nominal diameters, compare with those of Exercise 43?

45. The lengths of all branches in Fig. 16.3 is 50 m and, for each branch, there is no elevation change between the branch and delivery at the end of the branch. Using the appropriate `Mathcad` worksheet, calculate the theoretical and nominal pipe diameters for the network by minimizing total pipe cost. Use cost data for IPS series sch. 40 PVC pipe in central Nicaragua from the `Mathcad` worksheet. Require the minimum static pressure head at all junctions to be 10 m. There is a minor loss in each branch of $K = 10$ (an open globe valve).

46. In Fig. 16.3, the flow to the branch at node 2 is turned off. Assuming nominal pipe sizes for the network of $D_{12} = D_{23} = 1\frac{1}{2}$ in., $D_{34} = 1$ in., $D_{45} = \frac{3}{4}$ in., and $D_{26} = D_{37} = D_{48} = \frac{1}{2}$ in. (from the results of solution 45), predict the flow rates in the branches that remain open. Assume that the K values in the branches from Exercise 45 also apply; globe valve positions remain. Use the appropriate `Mathcad` worksheet.

47. It has been suggested that an optimal set of pipe diameters exist for the following problem. There is a large change in surface contour for the gravity-driven water network shown in Figs. 16.4 and 16.5. The frontal (Fig. 16.4) and side views (Fig. 16.5) of the proposed pipe layout are presented. Following the thinking in Section11.5.1, the common-sense approach might be to reduce the size of the pipe in the segment where there is the steepest descent relative to that just downstream of the source. The length of pipe segment 12 is defined by angle γ and the radius of curvature of $R = 50$ m as shown. Segment 12 and 23 lengths sum to $\pi R/2$. The lengths and elevation changes for other segments are: $L_{34} = 230$, $L_{35} = 320$, $\Delta z_{34} = 43$, and $\Delta z_{35} = 39$ m. The flow rate

from the single source is 3.2 L/s and in segment 34, 1.2 L/s based on source measurements and a demand model. If minor losses are ignored, is there an optimal solution for this design? Comment on your findings. Use cost data for IPS series sch. 40 PVC pipe in central Nicaragua from the `Mathcad` worksheet.

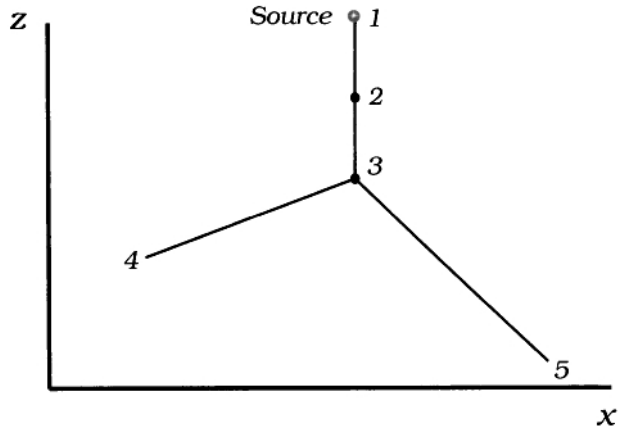

Figure 16.4 Front view of geometry for Exercise 47.

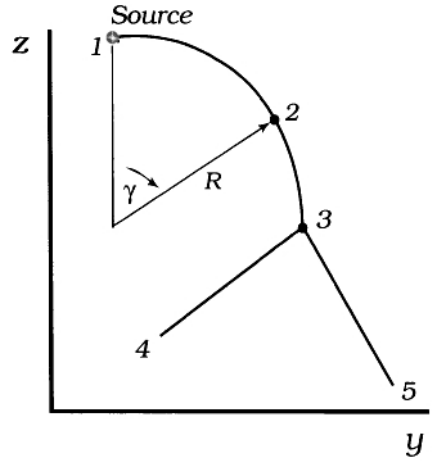

Figure 16.5 Side view of geometry for exercise 47.

48. Consider the loop of Fig. 11.29. The flow rate in segment 12 is $Q_{12} = 4.6$ L/s, and we know this flow is to be distributed in the following manner: $Q_{36} = 0.5Q_{12}, Q_{47} = 0.3Q_{12}$, and $Q_{58} = 0.2Q_{12}$. In addition, $L_{23} = L_{34} = L_{45} = L_{52} = L_{36} = L_{47} = L_{58} = 70$ m and all branch and delivery points are at

Table 16.5 Parameter Values for Optimization of a Multiple-Branch Network

Pipe Subscript, ij	L_{ij} (m)	Q_{ij} (L/s)	Δz_{ij} (m)
12	135	4.10	22
23	55	3.90	8
34	48	3.75	7
45	30	3.35	12
56	85	3.00	4
67	151	2.60	6
78	110	2.35	7
89	35	2.10	3
9–10	48	1.85	4
10–11	39	1.45	6
11–12	118	1.20	8
12–13	128	1.05	7
13–14	139	0.75	5
14–15	118	0.55	7
15–16	298	0.25	3

the same elevation. If the static pressure head at node 2 is 21 m, calculate the theoretical pipe sizes for the network that minimize total pipe cost. Assume an open globe valve ($K = 10$) is installed in each branch. Are the static pressure heads at each junction acceptable? Use Eqn (11.17) with cost data for IPS-series sch. 40 PVC pipe in central Nicaragua.

49. Data for the distribution main of a gravity-driven, multiple-branch network is given in Table 16.5. Modify the `Mathcad` worksheet `BranchPipeExample_4pipe_withcost_vectorized_ver3.xmcd` by including the data from this table and calculate the theoretical pipe diameters that minimize the cost of the distribution main part of this network. Report the pipe diameters and the vector of static pressure heads at the junctions. Assume $h_{del} = 10$ m at node 16 and that the pressure at node 1 is atmospheric.

50. Gravity-driven water networks that are supplied by more than one source are generally more reliable than with just a single source because of possible flow-rate depletion from either. Consider the dual-source network in Fig. 16.6 where the distance between the two sources is $2L_1$. The measured flow rate from one source is $Q_{13} = 2.1$ L/s and from the other is $Q_{23} = 1.3$ L/s. The object of the design is to supply water at $Q_{34} = 3.4$ L/s to the reservoir tank. There are two limiting cases for the piping of this network. The first is two pipes can be run, one from each source, over a distance L_3 directly to the tank. The second is that the two sources can be piped directly together along a straight line connecting the two. A tee fitting installed midway along this line will allow water to flow to the tank from both sources. For convenience, let the angle between the actual run of pipe segments 13 and 23 and the line connecting the two sources be γ (see Fig. 16.6). Using optimization methods from this chapter and Chapter 10, determine the optimal lengths and diameters for all pipes and the minimum pipe cost. Is the static pressure at the junction of the three pipes acceptable from

an engineering design standpoint? Use pipe cost data for IPS series sch. 40 PVC pipe in central Nicaragua from the Mathcad worksheet. The sources and the tank are at atmospheric pressure. Take $L_1 = 50$ m, $L_3 = 1600$ m, and $z_1 = z_2 = 64$ m above the tank. Ignore minor loss from all possible fittings in the network. The slope is uniform at 4% between the sources and tank and, as a first approximation, assume all pipes are straight.

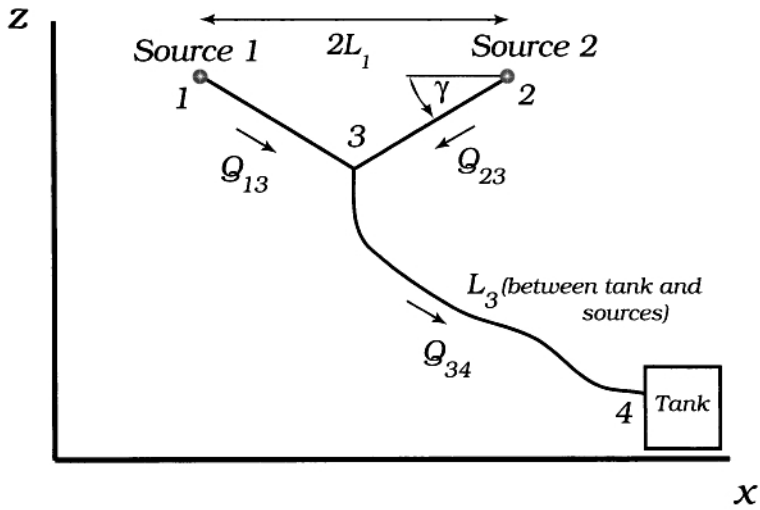

Figure 16.6 A network with dual sources.

51. Reconsider the branching network of Fig. 16.3. Instead of solving this problem as a gravity-driven flow, assume the flow to be pumped from node 5 *upward* toward node 1. The discharge pressure of the pump is 35 psig. Segment 12 ends in a tapstand where a static pressure of 7 m of head is required. Calculate the theoretical pipe diameters for this forced-flow network two ways. First, for fixed value of h_j of 7 m at each junction. Second, by minimizing the cost of the distribution main using Eqn (11.17) with cost data for IPS-series sch. 40 PVC pipe in central Nicaragua. Comment on the integrity of the network based on the values of the optimal static pressure heads at the three junctions. Neglect minor losses.

Chapter 12

52. Develop Eqs (12.6) and (12.7) from Eqs (2.45) and (12.5) to obtain the final form of the energy equation for a microhydroelectric turbine. Show that the hydraulic gradient can be extracted from the right side of Eqn (12.7) and thus becomes a scale factor.

Table 16.6 Survey Data for Exercise 58

Node, i	x_i (m)	y_i (m)	z_i (m)
1	0.0	0.0	49.3
2	−37.2	−52.1	22.2
3	−77.4	9.6	19.9
4	−241.0	75.7	29.6
5	−277.8	95.8	33.6
6	−312.5	148.4	25.2
7	−336.2	184.7	17.5
8	−374.7	208.4	22.5
9	−420.8	216.0	21.7
10	−439.1	228.7	20.0
11	−412.6	335.1	22.3
12	−428.9	373.1	13.5
13	−481.8	463.7	16.7
14	−471.9	552.1	15.0
15	−533.9	659.1	24.7
16	−544.5	720.5	43.0
17	−536.1	864.9	38.9
18	−688.4	974.3	5.2

53. Maximize $\dot{w}_{th}$ by taking the Q derivative of Eqn (12.5) subject to constant $f(Q, D) = f$. By setting this result equal to zero and solving for Q^{opt}, obtain Eqn (12.10).

54. By substituting the Blasius formula for $f(Q, D)$ in Eqn (12.7), taking the first derivative of $\dot{w}_{th}$ with respect Q, and setting this result equal to zero, solve for $Q = Q^{opt}$ to obtain Eqn (12.9).

55. Consider textbox B.12.1 example. Calculate the optimal penstock pipe size and electrical power generated if GI pipe were used.

56. Using Eqn (12.17), calculate the water flow rates required to produce electrical power ranging from 10to 100 kW for three cases of $S = 0.01, 0.05, 0.1$. Assume $L = 1000$ m, $\eta_g = 0.85$, $\eta_t = 0.80$. Plot your results on a log–log plot of Q versus power demand.

57. A Pelton turbine is under consideration for the conditions of Exercise 55. Calculate the nozzle diameter, D_n, jet speed, V_1, and system efficiency, η_{sys}, for this problem based on the actual penstock-pipe diameter.

Chapter 13

58. Consider the data of Table 16.6 that applies to Fig. 13.1. Using in formation in Chapter 13, calculate the running sum of the lengths of each of the 17 pipe segments starting with segment 1–2 and ending with segment 17–18. What is the total length of the pipeline? What is the elevation change between the source at node 1 and the next-highest location in the network?

59. Several springs have been identified that may contribute to a gravity-driven water network for a community. The yields from the springs are $Q_{R,1}$ of 0.95 L/s, $Q_{R,2}$ of 0.40 L/s, $Q_{R,3}$ of 1.46 L/s, and $Q_{R,4}$ of 0.55 L/s. A large community of 1050 persons is proposing to develop some or all of these sources for their use. The population growth rate is estimated at 1.5%/year. The distance to the identified storage tank location for each is $L_{R,1} = 32$ m, $L_{R,2} = 8$ m, $L_{R,3} = 53$ m, and $L_{R,4} = 21$ m. The elevations between the sources and the identified tank location for each is $\Delta z_{R,1} = 2$ m, $\Delta z_{R,2} = 3$ m, $\Delta z_{R,3} = 6$ m, and $\Delta z_{R,4} = 1$ m. Assuming a 20-year lifetime and 80 L/person/day at present, recommend to the community leaders which sources you would recommend developing and explain your reasoning. Perform a complete analytical solution by calculating the pipe sizes and costs for water delivery to the tank for each source. Assume the pipe to be IPS sch. 40 PVC.

60. From Exercise 59, developing sources 2 and 3 (producing a yield of 1.86 L/s) was determined as the most cost effective option. Based on per-capita demand rate of 80 L/person/day, 1819 persons, and the demand model of Fig. 15.3, size the storage tank for this community and justify your recommendation.

61. Consider the 16-node branching network in Fig. 11.41 that refers to data from Table 11.19. Using a peak factor of $PF = 3.2$, appropriate to 40% of the daily demand in a 3-h period, and assuming the flow rates shown in Table 11.19 are on-average during the day, calculate the design flow rates for each segment of the network. If the flow rates shown in Fig. 11.16 are based on the present population, calculate the design flow rates that would accommodate the future population. Assume an annual growth rate, i, of 1% and a 25-year network lifetime.

62. Given that the head loss in a uniform-diameter pipe is equal to that in a composite pipe composed of two pipes in series as in Fig. 13.7, use the continuity, Darcy–Weisbach, and Blasius equations to develop Eqn (13.10).

63. Determine the lengths L_a and L_b (see Fig. 13.7) for a pipeline of 378-meter-long, sch. 40 GI pipe, carrying 2.56 L/s where the theoretical value for D is calculated as 1.870 in. Re-calculate L_a and L_b if the pipe is changed to sch. 40 PVC.

64. Consider $Q = 48$ L/s of water flow at 10°C in a 6-in. nominal IPS sch. 40 PVC pipe that is supplying water to a 85-kW microhydroelectric turbine. An improperly designed control valve just upstream of the turbine closes suddenly when a loss of electrical load is detected by the turbine control circuitry. Calculate the amplitude of the pressure wave resulting from this closure. How would your results change if the pipe material were steel or GI?

Chapter 14

65. Consider a gravity-driven water system of 1-in. sch. 40 IPS PVC pipe as shown in Fig. 16.7. The coordinates, (x, z), at the source, intersections of the pipe segments, and delivery location are (0,200), (350,100), (600,120), (750,50), (1000,70), and (1300,30), all in meters (note that the lowest elevation is not zero). Assess the effect of the air pockets on the volume flow rate of water in the system by calculating the flow rate first assuming no compressibility for air, and then including the effect of air compressibility. Compare each with the flow rate if there were no air pockets. Neglect minor losses and assume h_{del} = 10 m.

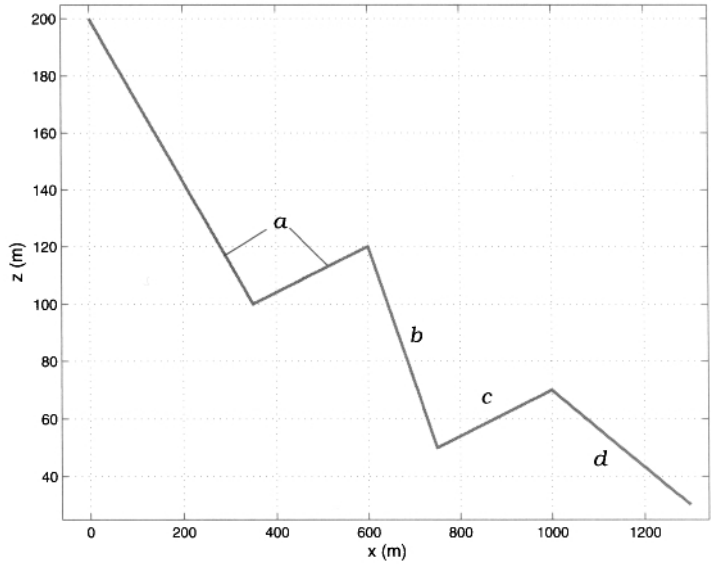

Figure 16.7 Geometry for Exercise 65.

References

The American Water Works Association. PE Pipe-Design and Installation, Manual of Water Supply Practices, M-55. `http://www.awwa.org`, 2006.

The Copper Development Association. The Copper Handbook. `http://www.copper.org`, 2006.

S. Dutch. Converting UTM to Latitude and Longitude (or vice versa). Technical report, University of Wisconsin – Green Bay, Green Bay, WI, 2009. URL `\url{http://www.uwgb.edu/DutchS/UsefulData/UTMFormulas.HTM}`. [Online; accessed 18-November-2009].

T. D. Jordan Jr. *Handbook of Gravity-Flow Water Systems.* ITDG Publication, London, UK, 2004.

M. L. Nayyar. *Piping Handbook.* McGraw-Hill, New York, NY, 6th edition, 1992.

D. A. Willoughby, R. D. Woodson, and R. Sutherland. *Plastic Piping Handbook.* McGraw-Hill, New York, NY, 2002.

16.3 THE SOLUTIONS

Chapter 2 Solutions

1. To be done by the student.

2. To be done by the student.

3. For a 2-in. PVC pipe and $Q = 1.2$ L/s, obtain $\overline{u} = 0.445$ m/s. Re=2.24×10^4, clearly a turbulent flow. The friction factor, $f(\overline{u}, D)$, for this flow is from Eqs (2.16)–(2.17) and is 0.0256. Combine Eqs (2.2), (2.6), and (2.9) and assume an adiabatic pipe to get

$$e_2 - e_1 = H_L = f(\overline{u}, D)\frac{L}{D}\frac{\overline{u}^2}{2} = c_v(T_2 - T_1) \tag{16.5}$$

Look up the value for c_v of water in any book on thermodynamics, heat transfer, or fluid mechanics to get $c_v = 4190$ J/kg·K. Upon substituting the numbers and units into Eqn (16.5), get $T_2 - T_1 = 0.00178°$C. This is almost an immeasurably small temperature rise. We see that the dissipation of potential energy that produces a Natural flow rate of 1.2 L/s causes a temperature increase that is negligible. This general outcome is caused by the relatively large value of c_v for water.

4. See the table below.

Bernoulli Equation	**Energy Equation**
Incompressible flow	Incompressible flow
Steady flow	Steady flow
Applies along streamline	Applies at any cross section of the flow
Inviscid flow	Inviscid or viscous flow
Applies strictly to laminar flow (Approximate for turbulent flow since) it is difficult to follow a streamline)	Valid for laminar and turbulent flow

5. The friction factor from the Darcy–Weisbach equation is written as

$$f = \frac{h_L/L}{\overline{u}^2/2gD} \tag{16.6}$$

where $L = 3$ m, $D = 0.25$ in., and h_L/L and $\overline{u}$ are from the test data. Since h_L are supplied in units of inches of mercury, we need to first convert this to meters of water using,

$$h_L \text{ (m of water)} = h_L \text{ (inches of Hg)} \frac{\rho_{Hg}}{\rho} \frac{1 \text{ m}}{39.372 \text{ in.}} \tag{16.7}$$

where the density of mercury is $\rho_{Hg} = 13579 \text{ kg/m}^3$. A plot of Eqs (16.6) and (2.9) versus Reynolds number appears in Fig. 16.8. The agreement is good, to within ~±7%, for this particular data set. The range of Re corresponds to the turbulent regime.

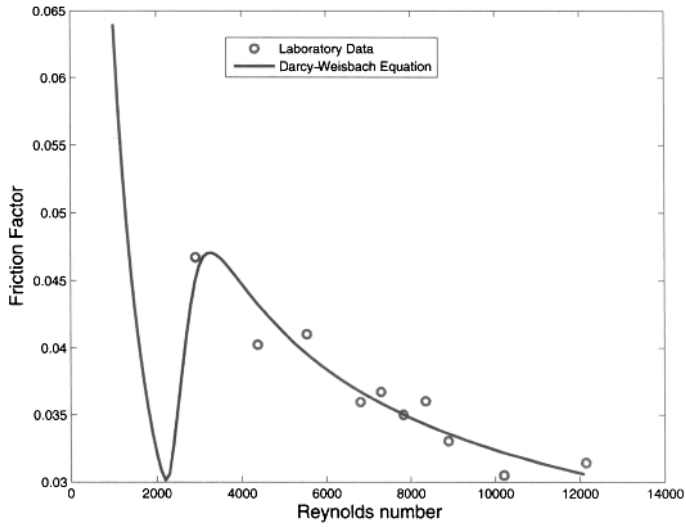

Figure 16.8 Friction factor laboratory test data compared with that from Darcy–Weisbach equation.

6. To be done by the student.

7. Solve the energy equation, Eqn (2.40), by first substituting the continuity equation (Eqn 2.21) to eliminate $\overline{u}$ in favor of Q. With only a single K-type minor loss, no α, and $F = 0$, we obtain

$$1 - [\lambda\sqrt{1 + s^{-2}} f(Q, D) + \frac{D}{z_1} K] \frac{8Q^2}{\pi^2 g D^5} = 0, \tag{16.8}$$

which we solve for Q as a function of K using the `root` function in `Mathcad`. D and z_1 are fixed as specified. The friction factor, $f(Q, D)$, depends on Q and D through Re and relative roughness of the smooth pipe. Re is

$$\mathrm{Re} = \frac{4Q}{\pi \nu D} \tag{16.9}$$

The solution appears in Fig. 16.9. Even with $K = 100,000$ the valve is still able to pass a few tenths of a L/s.

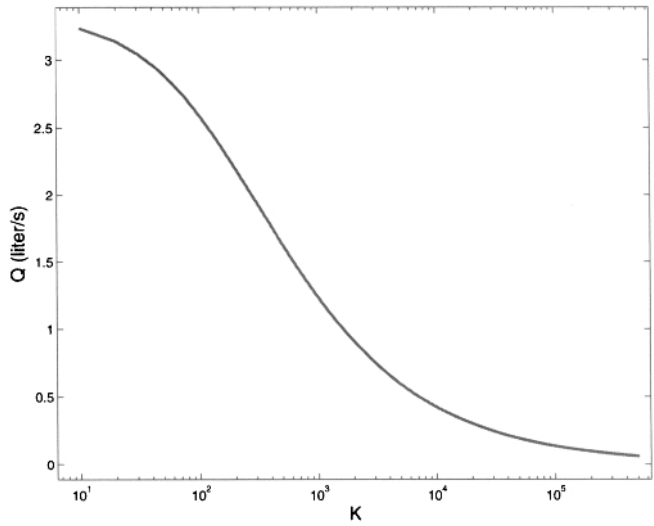

Figure 16.9 Volume flow rate versus closure fraction of globe valve for single-pipe network. K is minor loss coefficient.

8. The relevant energy equation is Eqn (2.46), where for this problem, it becomes

$$z_1 - \frac{p_2 - p_1}{\rho g} - [f(Q, D)L + D(\alpha + K)]\frac{8Q^2}{\pi^2 g D^5} = 0 \tag{16.10}$$

once it is written in terms of Q instead of $\overline{u}$ with the help of the continuity equation. The second term is

$$\frac{p_2 - p_1}{\rho g} = \frac{0 - 3 \text{ atm.} \cdot 1.01 \times 10^5 \text{ Pa/atm.}}{1000 \text{ kg/m}^3 \cdot 9.807 \text{ m/s}^2} = -31.0 \text{ m}$$

Equation (16.10) becomes

$$21.0 \text{ m} - \frac{8Q^2[f(Q, D) \cdot 3500 \text{ m} + 0.0853 \text{ m} \cdot (1.05 + 350)]}{9.807 \text{ m/s}^2 \cdot \pi^2 \cdot (0.0853 \text{ m})^5} = 0$$

Table 16.7 Solution to Exercise 11

Nominal Size	Wall Reference	Material	Inside Diameter	Press. Rating (As Spec'd)	Press. Rating [Head (m)]
1 in.	sch. 80	PVC	0.957 in.	630 psig	442.9
$3\frac{1}{2}$ in.	sch. 40	ABS	Not Given	190 psig	133.6
2 in.	sch. 40	PVC	2.067 in.	280 psig	196.9
$1\frac{1}{2}$ in.	sch. 80	PE	1.5 in.	160 psig	133.6
$\frac{1}{2}$ in.	SDR 11	PE	0.680 in.	160 psig	112.5
75 mm	SDR 13.6	PVC	63.8 mm	PN 16	160
25 mm	SDR 21	PE80	22 mm	PN 6.3	63
4 in.	SDR 26	PVC	4.134 in.	160 psig	112.5

This equation is solved in `Mathcad` using the `root` function or `Given...Find` block to get $Q = 3.04$ L/s. The absolute roughness for galvanized iron pipe is 0.152 mm. Clearly, the term α is negligible compared with K for this problem.

9. Use the Excel spreadsheet (supplied with this book) as discussed in Appendix B to get 111,383.0 m between arbitrarily chosen longitudes of -89 and $-90°$, 111,314.8 m for longitudes of -1 and $-2°$, and 111,280.7 m for longitudes of -44 and $-45°$. This is contrasted with the distance between longitudes of -89 and $-90°$ at 40° north latitude of ~85,408 m.

10. From Eqn (B.1), get 19.22972 and $-75.31389°$ for latitude and longitude, respectively, at the source. Both are recorded and reported to five decimal places.

    Use the Excel spreadsheet as discussed in Appendix B to solve the second part of this exercise. Obtain $\ell = 2920$ m and $s = \Delta z/\ell = 1.59\%$.

Chapter 3 Solutions

11. The results are reported in Table 16.7. The relevant conversions for pressure are 1 atm. = 1.013×10^5 Pa = 14.696 psi = 10.33 m. The dimensions for ABS pipe are not supplied in this chapter. No steel (or GI) pipe cases were examined here. The pressure ratings for this pipe are very large and may be found from numerous sources in web and paper format.

Chapter 4 Solutions

12. Following the developments in Section 4.2, Eqn (4.1) becomes

$$\frac{p_1 - p_2}{\rho g L} + \frac{z_1}{L} = \frac{h_L}{L} = \frac{8Q^2}{\pi^2 g D^5} f(Q, D)(1 + \frac{D}{L}\sum \frac{L_e}{D}) \qquad (16.11)$$

    where $z_1 = -34$ m (see Fig. 2.11) and the term for minor loss has been included. With $L = 1345$ ft, $Q = 0.3500$ m^3/min, $p_1 = 1850$ kPa, $p_2 = 475$ kPa,

$L_e/D = 30$ for a 90° elbow, and $L_e/D = 60$ for a flow-though-branch tee (Table 2.1), Eqn (16.11) is written as

$$0.2591 = \frac{h_L}{L} = 266.0(1 + 360\frac{D}{L})\frac{f(Q,D)}{D^5} \tag{16.12}$$

where the unit of D is inches and the summation of all L_e/D is 360. The formula for Re becomes

$$\mathrm{Re} = \frac{2.237 \times 10^5}{D} \tag{16.13}$$

where D is in inches.

Using Method 3 as in Section 4.2, we obtain $D = 1.956$ in. from the `Mathcad` worksheet. From Table 3.1, we choose a nominal 2-in. GI pipe. A calculation of the minor loss ($360\frac{L}{D}$ in Eqn (16.12)) shows that it is about 4.4% of the major loss [the 1 in Eqn (16.12)]. This is not a significant impact on the solution for D.

Method 2, which uses the head loss curve from Fig. 4.1 gives the same result for Q of 0.3500 m^3/min (or 5.8 L/s) and h_L/L of 0.26. Please be aware that *all head loss curves* from, for example, Figs. 4.1 and 4.2 *are only for straight pipe* (i.e., the effect of minor loss needs to be included by iteration). Specifically, this is done by calculating D by first neglecting the minor loss (the term $360\frac{D}{L}$ in Eqn (16.12)). The value for h_L/L is then modified by the most recent value for D as in Eqn (16.12), and the head loss curve used to recalculate D. This procedure is followed until D no longer changes with further iterations.

13. The head losses from Jordan Jr. (2004) are ~20–30% lower than those from the Darcy–Weisbach equation [see Figs. 16.10 and 16.11]. Since there is little systematic variation, it is difficult to determine the sources of this disagreement. However, these findings are consistent with the results of Exercise 28 where the pressure drop from a Hazen–Williams-type equation from the Copper Tube Handbook Copper Development Association (2006) predicts low by, at most, 35%. Thus, it appears that Jordan Jr. (2004) uses a similar formula to develop his results appearing in Reference Table XI.

14. The ratio of the head loss at 27 to 10°C for Class IV HDP pipe is shown in Fig. 16.12. There is ~10% difference between the two, the head loss for 27°C is smaller. This is not a dominant effect for most designs. The kinematic viscosity at 27°C is 8.576×10^{-7} m^2/s, and at 10°C, 13.07×10^{-7} m^2/s, a 52% difference.

Chapter 5 Solutions

15. To be done by the student.

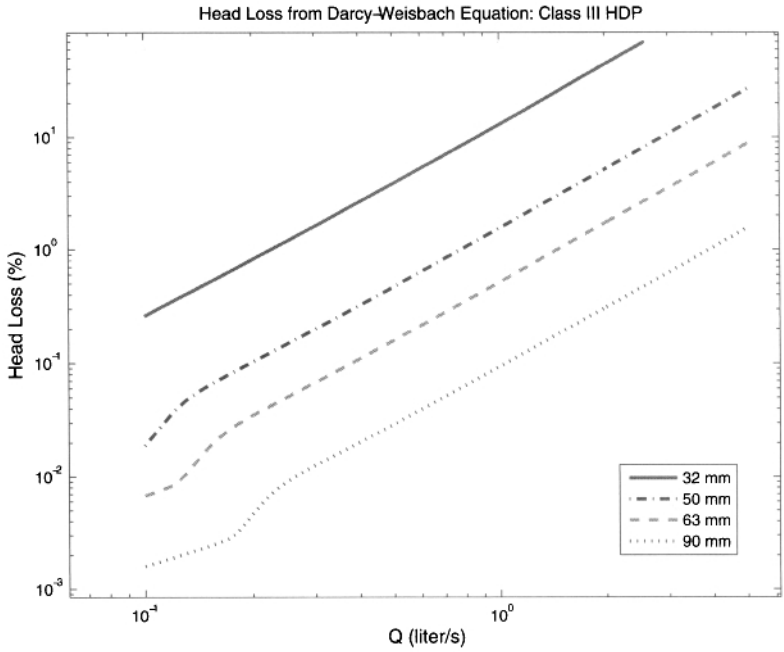

Figure 16.10 Head loss factors for Class III HDP pipe.

16. (a) *Solution from* `Mathcad` *worksheet or Fig. 5.4*: 1 in., 0.30 L/s which is 30% more than the design value. Re for this flow is ~14,000, which is turbulent. Equation (9.2) gives

$$\begin{aligned} D &= 0.741[\frac{\lambda(1+s^{-2})^{1/2}}{1-F}]^{4/19}(\frac{\nu Q^7}{g^4})^{1/19} \\ &= 0.741[(1+0.015^{-2})^{1/2}]^{4/19} \cdot \\ &\cdot\ [\frac{13.07\times10^{-7}\ \mathrm{m^2/s}\cdot(0.23\times10^{-3}\ \mathrm{m^3/s})^7}{(9.807\ \mathrm{m/s^2})^4}]^{1/19} \\ &= 0.0248\ \mathrm{m} = 0.978\ \mathrm{in.} \end{aligned}$$

which corresponds to a nominal 1-in. PVC pipe. Note that the simpler equation, Eqn (9.3), gives the same result as Eqn (9.2) because the mean slope $s \ll 1$.

(b) *Solution from* `Mathcad` *worksheet or Fig. 5.4*: The smallest possible pipe size that satisfies the above conditions occurs at a dimensionless delivery static pressure $F = 0$. With this value for F, and the calculated slope $s = 0.0201$, the nominal pipe size is $1\frac{1}{2}$ in.. The maximum volume flow rate that this pipe size can pass is 1.13 L/s, which is much larger than the current demand of 0.38 L/s. The recommended pipe size of $1\frac{1}{2}$ in. will

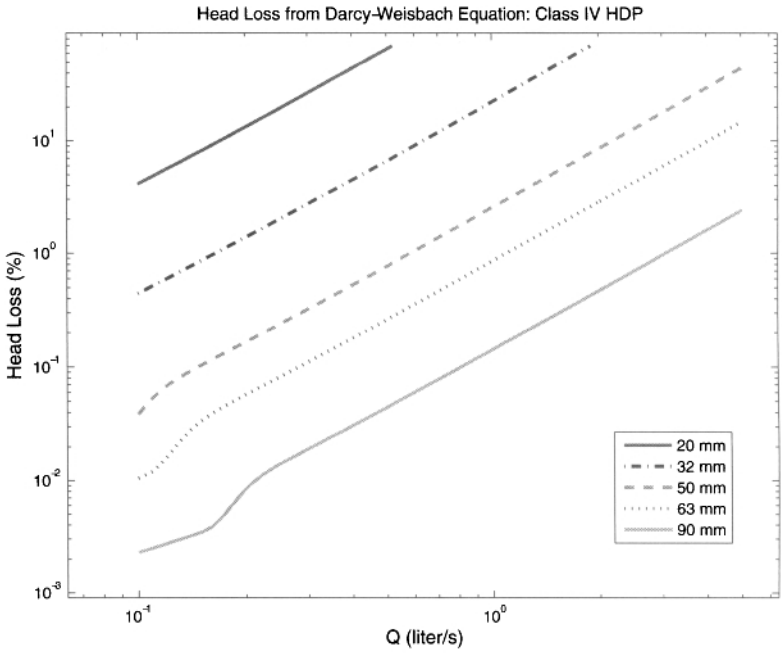

Figure 16.11 Head loss factors for Class IV HDP pipe.

allow plenty of increase in future demand. Re for this flow is ~20,000, which is turbulent.

(c) *Solution from* `Mathcad` *worksheet or Fig. 5.4*: The recommended pipe sizes remain unchanged.

(d) *Solution from* `Mathcad` *worksheet or Fig. 5.4*: Since minor losses are neglected and elevation changes enter into the problem only through the minor losses, the elevation difference between the source and the tank do not affect the recommended pipe size connecting the two. However, between the tank and the tapstand, the elevation is used to determine the slope. If the uncertainty is -20%, the calculated slope is 0.0161 and the nominal pipe size remains $1\frac{1}{2}$ in.. If the uncertainty is +20%, the calculated slope is 0.0241 and the nominal pipe size reduces to 1 in. However, the maximum flow that this pipe can pass is only ~0.39 L/s, which allows for very little increase in flow rate in future years. Therefore, it is best to recommend a nominal $1\frac{1}{2}$-in. pipe for this case.

17. *Solution from* `Mathcad` *worksheet*: From Table 2.1 for a 45° elbow, $L_e/D = 16$. The sum of L_e/D for all minor losses is $502+23\cdot16=870$. At an open tank, $F = 0$. From the mean slope and elevation, $\ell = 75$ m and $\lambda = 95\text{ m}/75\text{ m} = 1.267$. With both minor losses, the `Mathcad` worksheet gives nominal $1\frac{1}{2}$ in. PVC pipe to satisfy these conditions. If we suppress the minor losses due to

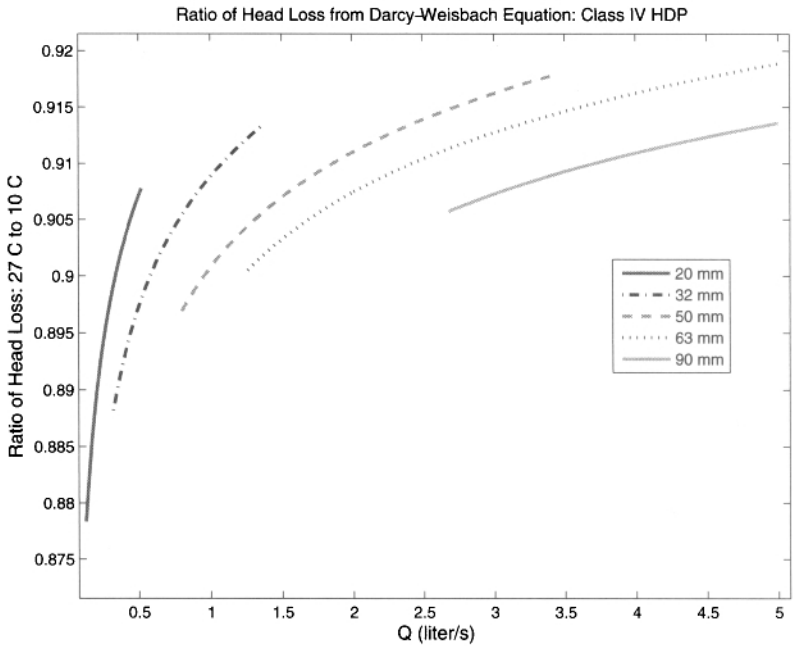

Figure 16.12 Ratio of head loss factors for Class IV HDP pipe for water at 27 and 10°C. Results for flow speeds < 0.7 m/s and > 3 m/s are not plotted.

the elbows, the pipe size is reduced to nominal 1-in. There is no effect on the nominal pipe size from the minor loss due to the filter at the source if the elbow loss is neglected. If the elbow loss is included, neglecting the K value for the source filter also reduces the pipe size to 1 in. Therefore, minor losses are important for this design.[2] With the $1\frac{1}{2}$ in. pipe, the maximum flow rate of water is 1.52 L/s, 2.76 times the present flow rate. The factor that we apply to the present flow rate to obtain that in 10 years is $1.02^{10} = 1.219$ or 1.219·0.55 L/s = 0.67 L/s. This is much less than a $1\frac{1}{2}$-in. pipe will flow based on current conditions. Therefore, for this low-head, high-flow system, a $1\frac{1}{2}$ in. nominal PVC pipe is recommended for the present conditions and those projected for the future. Re is ~30,000 corresponding to a turbulent flow.

[2]Note that the value for the right side of Eqn (7.3) is ~706. Since the sum of the minor losses from all the elbows is greater than this value, we see that Eqn (7.3) is a valid indicator of the importance of minor losses.

For this problem, the approximate formula for D from the footnote in Section 9.3 gives,

$$\begin{aligned} D &= 0.455(\lambda Q^2/g)^{1/5}(1+s^{-2})^{1/10} \\ &= 0.455[\frac{1.267(0.55\times 10^{-3}\ \mathrm{m^3/s})^2}{9.807\ \mathrm{m/s^2}}]^{1/5}(1+0.08^{-2})^{1/10} \\ &= 0.0249\ \mathrm{m} = 0.980\ \mathrm{in.} \end{aligned}$$

which corresponds to a nominal 1-in. PVC pipe, smaller than the $1\frac{1}{2}$ in. pipe predicted from the `Mathcad` worksheet because Eqn (9.2) neglects minor losses.

As for the uncertainty in elevation data, $\pm 20\%$ translates to ± 1.2 m of elevation uncertainty and slope uncertainty of ± 0.016. For the larger slope and elevation, a nominal 1-in. pipe will accommodate the current flow rate of 0.55 L/s but with little room for future flow-rate expansion (the maximum flow rate with 1-in. pipe is 0.59 L/s). Recommend the next largest pipe size. For the smaller slope and elevation, a nominal $1\frac{1}{2}$ in. pipe is required for the current flow rate and that of the future (the maximum flow rate with $1\frac{1}{2}$ in. pipe is 1.35 L/s). Thus, considering the uncertainty in slope, we should choose a nominal $1\frac{1}{2}$ in. PVC pipe.

Chapter 6 Solutions

18. To be done by the student.

19. As explained in Section 6.3.

20. The solution is carried out by breaking up the pipeline into a large number of increments (100 is used here) and solving Eqn (6.12) for the pressure distribution in each. This is referred to as *finite differences*. This approach follows that of Eqn (6.9) where, instead of dL, dx, and so on, we would write ΔL and Δx (see further description of this in Chapter 8). Accordingly, 100 increments in t are used between 0 and 3. The pathlength distribution is calculated from,

$$L_i = [(x_i - x_{i-1})^2 + (y_i - y_{i-1})^2 + (z_i - z_{i-1})^2]^{1/2} + L_{i-1}$$

where $2 \le i \le 100$ and $L_1 = 0$. A plot of the pathlength distribution is shown in Fig. 16.13. The dimensionless static pressure distribution is obtained in the same manner by writing Eqn (6.12) as

$$\frac{p_i}{\rho g z_1} = 1 - \frac{z_i}{z_1} - \frac{8Q^2}{\pi^2 g z_1 D^4}[\alpha_i + f(Q,D)\frac{L_i}{D}]$$

where $p_1 = 0$, and solving for p_i for $2 \le i \le 100$. $\alpha_2 = 1.05$ and all other α_i are zero. The solution appears in Fig. 16.14. The value of the $f(Q,D)$ for the prescribed flow rate and D is 0.0214 and is constant. The negative pressures downstream of the source for the first 50 m due to the elevation increase in this region and α are a concern. A change in the contour of the pipe in this region is recommended.

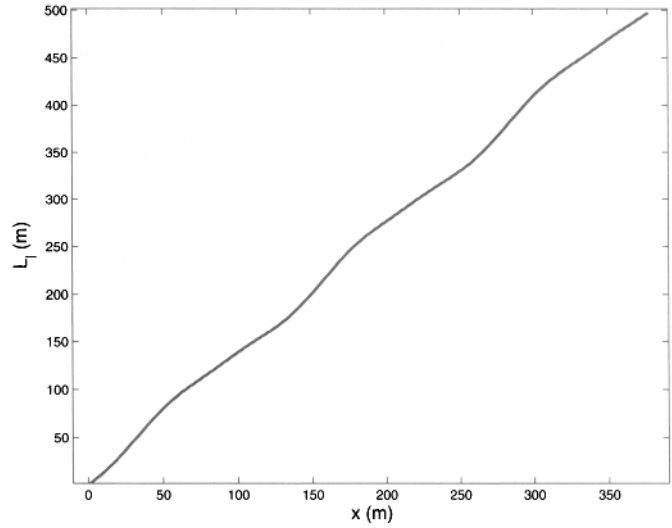

Figure 16.13 Pathlength distribution for Exercise 20.

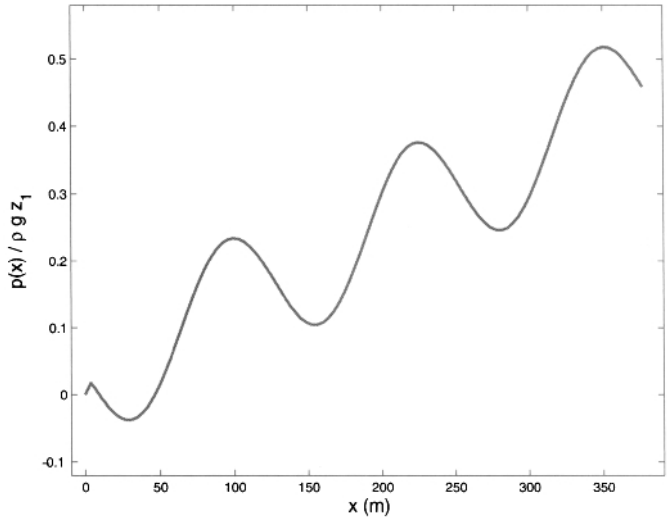

Figure 16.14 Dimensionless static pressure distribution for Exercise 20.

Chapter 7 Solutions

21. The solution comes from Eqn (7.2) that we write as

$$\frac{p_i}{\rho g z_1} = \frac{z_i^*}{z_1} - \frac{8Q^2}{\pi^2 g z_1 D^4}[\alpha + \sum_{j=1}^{i} K_i + f(Q,D)\frac{z_i^*}{sD}]$$

The elevation $z_i^* = 1 - z_i$ is measured from the *source*. To solve Eqn (7.2), we will use *finite differences* and break the pipe into 100 units. With this method, the integral in Eqn (7.2) becomes a summation. z_i^* is the independent variable,

$$\frac{z_i^*}{z_1} = \frac{i-1}{100-1}, \quad i = 1 \cdots 100$$

and K_i is the vector of 100 minor loss values that are all zero except for $i = 25, 50$, and 75, where they take on the values of 10, 400, or 700, respectively for the three different cases. The plot of the solution appears in Fig. 16.15. Note the weak effect for K of 10 and some negative static pressures (below atmospheric) for K of 700 immediately following the location of the minor loss element.

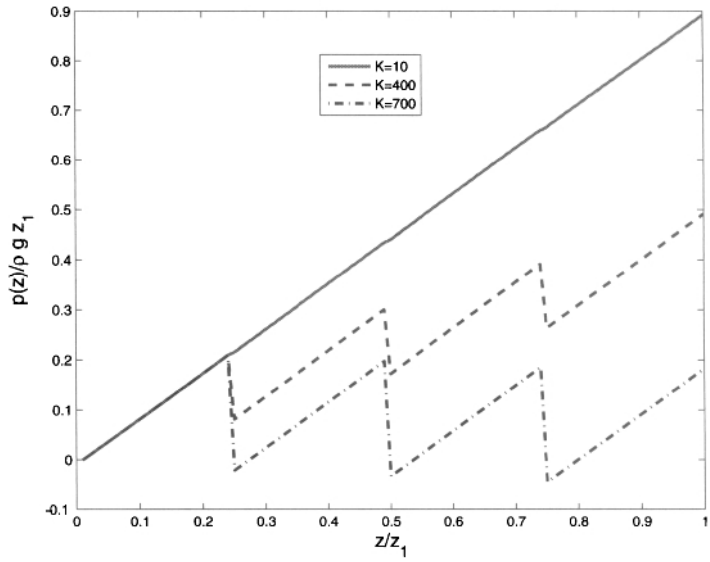

Figure 16.15 Dimensionless pressure versus elevation for Exercise 21.

Chapter 8 Solutions

22. The `Mathcad` worksheet used to solve this problem is a slight variation of that shown in Fig. 8.13. The changes from this worksheet are $Q = 0.61$ L/s, $z = 22.31$ m, and $L_\ell = 1455$ m. A plot of the pressure head at station C21, which is the highest local peak for the data set given, shows the need for a 3-in. nominal PVC pipe (see Fig. 16.16). That is, the pressure head for a $2\frac{1}{2}$-in. pipe (if it is even available) between the source and this station is only marginally positive. Any pipe size > 3 in. increases the static pressure at station C21

very little above the value corresponding to 3-in. pipe. Assuming a static pressure at station C21 of zero, the pipe size required between this station and the delivery location is 0.898 in. for which we choose a 1-in. nominal PVC pipe. This solution is from the procedure at the bottom of the Mathcad worksheet appearing in Fig. 8.13, except that $z_1 = 22.31$ m, $z = 0$ m and $L_\ell = 2023$ m $- 1455$ m $= 568$ m.

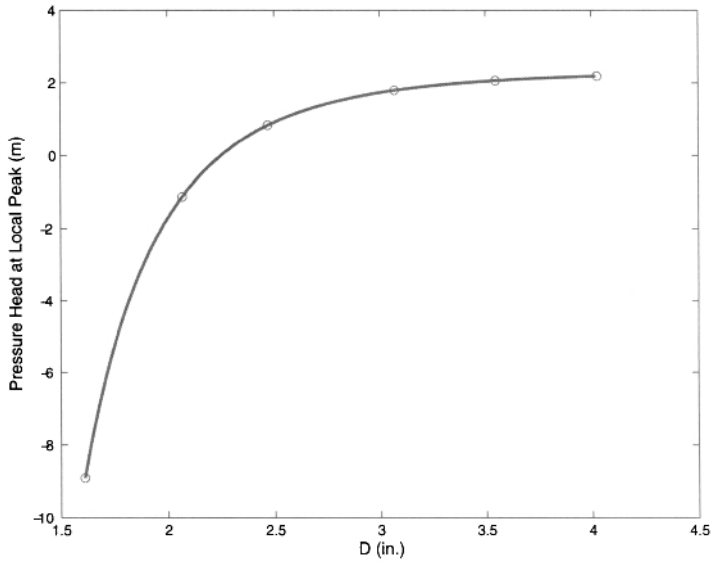

Figure 16.16 Pressure head versus pipe size for highest local peak for Exercise 22. Circles correspond to $1\frac{1}{2}$, 2, $2\frac{1}{2}$, 3, $3\frac{1}{2}$, and 4-in. nominal sch. 40 PVC pipe.

For a nominal 3-in. PVC pipe and $p(x)/\rho g z_1 = 0$, solve Eqn (6.12) in Mathcad for Q to obtain $Q = 1.44$ L/s, more than a factor of 2 greater than the design flow rate. There appears to be adequate room for an increase in volume flow rate before the static pressure at the local high peak becomes negative in value.

23. Let $\tau = t/\Delta t_{sc}$. With $t = \tau\, \Delta t_{sc}$, the time derivatives in Eqn (8.11) become

$$\frac{d^2\overline{u}_2}{dt^2} = \frac{1}{\Delta t_{sc}^2}\frac{d^2\overline{u}_2}{d\tau^2}$$

and

$$\frac{d}{dt} = \frac{1}{\Delta t_{sc}}\frac{d}{d\tau}$$

Substitute these into Eqn (8.11) and cancel Δt_{sc} which appears in all three terms. The result is

$$\frac{L}{\Delta t_{sc}}\frac{d^2\overline{u}_2}{d\tau^2} + \frac{g\Delta z_t(0)}{\overline{u}_{2,\infty 1}}\overline{u}_2 + \frac{d}{d\tau}\{[f(\overline{u}_2, D)\,\frac{L}{D} + 1 + K]\frac{\overline{u}_2^2}{2}\} = 0$$

Since $\overline{u}_2$ is of the order of 1 m/s, the derivatives in this equation are of the order of 1. Now, substitute values for the terms that comprise Δt_{sc} to show that $\frac{L}{\Delta t_{sc}}$ is of the order of 0.001 m/s. Substitute values for the terms in $\frac{g\Delta z_t(0)}{\overline{u}_{2,\infty 1}}$ to see that this group is of the order of 10 m/s. Thus, the acceleration term is negligible relative to the remaining terms in the equation. The friction term in Eqn (8.11) will always be important because it is fundamental to the problem.

Taking the derivatives and simplifying to get Eqn (8.14) are left as an exercise for the student.

24. The hydraulic gradient is $(\Delta z_t + \Delta z_p)/L = 0.0909$. Neglecting minor losses for the moment, use the `Mathcad` worksheet `HydraulicGradient.xmcd` to calculate $\overline{u}_{2,\infty 1} = 1.342$ m/s for the pipe ID of $D = 2.067$ in. (see Table 3.1). The friction factor is $f(\overline{u}_{2,\infty 1}, D) = 0.0520$. From Eqn (8.7), we obtain

$$t_{99\%} = 2.646 \frac{1.342 \text{ m/s}}{9.807 \text{ m/s}^2 \cdot 0.0909} = 3.98 \text{ s}$$

The length equivalent of an open globe valve ($K = 10$; see Eqn (2.11)) and 4–90° elbows is ~$504 \cdot D \approx 16.4$ m. The minor loss for the gate valve is negligible (Table 2.1). This reduces the hydraulic gradient by only ~8%. If minor losses were included, the value for $t_{99\%}$ will be nearly that as above.

Using the `Mathcad` worksheet `Tank_Draining.xmcd`, calculate $\overline{u}_{2,\infty 2} = 1.148$ m/s for the conditions given. The friction factor is $f(\overline{u}_{2,\infty 2}, D) = 0.0522$. Equations (8.11) and (8.12) are solved numerically to obtain a drain time of ~6.0 h. The minor losses were included in this solution.

The ratio of the tank volume to the mean volume flow rate obtained by averaging the flow speeds $\overline{u}_{2,\infty 1}$ and $\overline{u}_{2,\infty 2}$ gives a drain time of 5.7 h, within 18 minutes of the exact solution.

25. The volume flow rates for D values of 1, 1.5, 2, 2.5, and 3 in. are 10.0, 22.6, 40.1, 62.7, and 90.3 L/s, respectively. These are a factor of 2–5 times larger than from Fig. 8.18. This is to be expected since friction is clearly not negligible for the large size of the syphon considered here. Note from Eqn (8.17) that friction is independent of z_1 and the nonfriction term is proportional to $1/z_1$. For all else constant, the nonfriction effect is smaller than the friction effect by a factor of 20.

26. To solve this problem, we write the energy equation in three different forms and solve them simultaneously. The first is the energy equation written at $z = z_2$ or $x = x_2$, where the static pressure is atmospheric. This equation is Eqn (8.17) and it is solved for the volume flow rate, Q. The second equation identifies the location of the point of minimum pressure on the p versus x curve, x_{min} (see Fig. 8.20). Recognizing that this point is an extremum, by taking the derivative, d/dx, of Eqn (6.12) and setting it equal to zero, we solve this equation to obtain

x_{min}. Thus,

$$\frac{d}{dx}[\frac{z(x)}{z_1} + \frac{8Q^2}{\pi^2 g z_1}\frac{f(Q,D)L_\ell(x)}{D^5}] = 0 \tag{16.14}$$

The final equation is the energy equation written for the local static pressure, Eqn (6.12), where the pressure is set equal to the saturation pressure (at the specified temperature) at the location of minimum static pressure, x_{min}. Obtain,

$$\frac{-14.7 \text{ psia} + p_{min}}{\rho g z_1} = 1 - \frac{z(x)}{z_1} - \frac{8Q^2}{\pi^2 g z_1}(\frac{\alpha}{D^4} + \frac{f(Q,D)L_\ell(x)}{D^5}) \tag{16.15}$$

where $x = x_{min}$. For this problem, $p_{min} = 0.178$ psia which, for the left-side term gives $(-14.696 + 0.178)$ psia/(ρg·20 m) = -0.511. Equation (16.15) is solved for the height of the syphon. To do this, we first need to write $z(x)$ and $L_\ell(x)$ in terms of the geometry of the problem. Referring to Fig. 8.17, we can write

$$\frac{z(x)}{z_1} = 1 + \frac{1}{\gamma}\sqrt{1 - (\frac{\gamma x}{z_1} - 1)^2} \tag{16.16}$$

and

$$L_\ell(x) = \frac{z_1}{\gamma}\arccos(1 - \frac{\gamma x}{z_1}) \tag{16.17}$$

where $\gamma = z_1/r$, and r is the height of the syphon.

Equations (8.17) and (16.14)–(16.17) are solved simultaneously in `Mathcad` to obtain $r = 4.63$ m (Figs. 16.17 and 16.18). Note that the volume flow rate $Q = 2.16$ L/s from the `Mathcad` worksheet is nearly identical to that from Fig. 5.3 for terminal flow in vertical pipe. The slope for the current problem is 2.16, a very large value indeed.

Chapter 9 Solutions

27. After substituting the friction factor from the Blasius formula and simplifying, obtain

$$Q = 42.7 D^{2.714} s^{0.571} \tag{16.18}$$

It is clear that a different form for the friction factor as a function of Re was used to obtain the expressions in the two cited references since the exponents and the coefficient differ among the formulas. The value of the coefficient, 42.7 in Eqn (16.18), is affected by the kinematic viscosity of water that must be assumed in formulas of these types. This exercise illustrates the attempts at developing simple formulas for flow rate using Hazen–Williams-type approximations to the friction factor. With the ease at which we can solve for accurate flow rate and pipe diameter using fundamental equations of fluid mechanics and common software like `Mathcad`, there is little need for these approximations. When using a computational package the uncertainties in values for the design

Syphon exercise

$z_1 := 20 \cdot m$ $\quad TOL := 1 \cdot 10^{-4}$

Water properties at 10 C = 50 F $\quad \nu := 13.07 \cdot 10^{-7} \cdot \frac{m^2}{sec}$ $\quad \rho := 1000 \cdot \frac{kg}{m^3}$

$Re_D(V,D) := \frac{V \cdot D}{\nu}$ $\quad \varepsilon := 5 \cdot 10^{-6} \cdot ft$ absolute roughness, ft (increase 100 times for galvanized steel)

Moody friction factor that spans the laminar/turbulent range.
ebyD is relative roughness.

$alpha(R) := if(R < 2100, 2, 1.05)$

$$funct(f,R,ebyD) := \frac{f}{2} - \left[\left(\frac{4}{R \cdot \sqrt{\frac{f}{8}}} \right)^{24} + \left[\left(\frac{18765}{R \cdot \sqrt{\frac{f}{8}}} \right)^{8} + \left[3.29 - \frac{227}{R \cdot \sqrt{\frac{f}{8}}} + \left(\frac{50}{R \cdot \sqrt{\frac{f}{8}}} \right)^{2} \dots \right. \right. \right.$$
$$\left. \left. \left. + \frac{1}{0.436} \cdot \ln \left(\frac{R \cdot \sqrt{\frac{f}{8}}}{1 + 0.301 \cdot R \cdot \sqrt{\frac{f}{8}} \cdot ebyD \cdot 2} \right) \right]^{16} \right]^{-\frac{3}{2}} \right]^{\frac{1}{12}}$$

nominal 3 in $\quad D_1 := 3.068 \cdot in$ $\quad$ nominal 1 in $\quad D_4 := 1.049 \cdot in$

nominal 2 in $\quad D_2 := 2.067 \cdot in$ $\quad$ nominal 0.75 in $\quad D_5 := 0.824 \cdot in$

nominal 1.5 in $\quad D_3 := 1.61 \cdot in$ $\quad$ nominal 0.5 in $\quad D_6 := 0.662 \cdot in$

$f1 := 0.03$

$fric\_fac(Re, ebyD) := root(funct(f1, Re, ebyD), f1) \cdot 4$ Moody friction factor

$$p_{z2}(D,Q,\gamma) := 1 - \frac{8 \cdot Q^2}{\pi^2 \cdot g \cdot z_1} \cdot \left[\frac{alpha\left(Re_D\left(\frac{4 \cdot Q}{\pi \cdot D^2}, D \right) \right)}{D^4} + \frac{fric\_fac\left(Re_D\left(\frac{4 \cdot Q}{\pi \cdot D^2}, D \right), \frac{\varepsilon}{D} \right)}{D^5} \cdot \left(\pi \cdot \frac{z_1}{\gamma} + z_1 \right) \right]$$

Energy equation written at z = z.2 = 0

Figure 16.17 Mathcad worksheet for syphon exercise. See continuation of this worksheet in Fig. 16.18.

$$p(x,\gamma,D,Q) := 1 - \left[1 + \frac{1}{\gamma}\cdot\sqrt{1 - \left(\frac{x\cdot\gamma}{z_1} - 1\right)^2}\right] - \frac{8\cdot Q^2}{\pi^2\cdot g\cdot z_1}\cdot\left[\frac{\text{alpha}\left(\text{Re}_D\left(\frac{4\cdot Q}{\pi\cdot D^2}, D\right)\right)}{D^4} + \frac{\text{fric\_fac}\left(\text{Re}_D\left(\frac{4\cdot Q}{\pi\cdot D^2}, D\right), \frac{\varepsilon}{D}\right)}{D^5}\cdot\left(\frac{z_1}{\gamma}\cdot\text{acos}\left(1 - \frac{x\cdot\gamma}{z_1}\right)\right)\right]$$

Energy equation written at local x

$\gamma := 3.8$ guess

$$P_{min\_value} := \frac{-14.7\cdot psi + 0.178\cdot psi}{\rho\cdot g\cdot z_1} \qquad P_{min\_value} = -0.5105$$

$Q := 1\cdot\frac{liter}{sec}$ guess for Q $\qquad Q_{root}(D,\gamma) := root\left(p_{z2}(D,Q,\gamma),Q\right)$ Solution for Q from energy equation written at z = z 2

$x1 := \frac{z_1}{\gamma}$ $\quad x := root\left(\frac{d}{dx1}p(x1,\gamma,D_3,Q_{root}(D_3,\gamma)),x1\right)$ guess for x $\qquad x = 7.958\,m$

$D := D_4$ $\quad x_{root}(\gamma,D) := root\left(\frac{d}{dx}p(x,\gamma,D,Q_{root}(D,\gamma)),x\right)$ Condition of dp/dx = 0 at location of minimum static pressure

$\gamma_{root}(D) := root\left(p\left(x_{root}(\gamma,D),\gamma,D,Q_{root}(D,\gamma)\right) - P_{min\_value},\gamma\right)$ Solution for γ from energy equation written at location of minimum static pressure

$\gamma_{root}(D) = 4.318$ γ solution $\qquad Q_{root}\left(D,\gamma_{root}(D)\right) = 2.156\,\frac{liter}{sec}$ Volume flow rate

$\frac{z_1}{\gamma_{root}(D)} = 4.631\,m$ r; the height of the syphon above z.1 $\qquad \frac{4\cdot Q_{root}\left(D,\gamma_{root}(D)\right)}{\pi\cdot D\cdot v} = 7.883\times10^4$ Reynolds number

Figure 16.18 Mathcad worksheet for syphon exercise. Continued from worksheet in Fig. 16.17.

parameters can be assessed and included in the design in a much more informed manner.

28. When we write $\Delta p/L$ from the Darcy–Weisbach equation, Eqn (2.9), and for Eqn (16.4) and compare them, we can see that in this Hazen–Williams formula, f is assumed to be approximately proportional to $\text{Re}^{-0.15}$ (i.e., $f \approx \text{Re}^{-0.15}$). This approximation is a variation of the Blasius formula, Eqn (2.19) that is valid for only turbulent flow in smooth pipes where $\text{Re} < 10^5$. As discussed in Chapter 9, the Hazen–Williams formula applies to only turbulent flow and include other restrictions to which the designer's attention is needed.

The units of C are determined by substituting only the units for each dimensional term into Eqn (16.4). Obtain

$$[1] = \frac{D^{0.13}}{\rho C^{1.85} Q^{0.15}} \tag{16.19}$$

where [1] is a dimensionless number. The units for C are indeed very messy.

A plot of the ratio of $\Delta p/L$ from Eqn (16.4) to that from the Darcy–Weisbach equation is given in Fig. 16.19. The nonmonotonic behavior for the 2-in. pipe size reflects laminar flow for the smallest flow rates followed by transition and turbulent flow with increasing flow rate. The extent of disagreement between Eqn (16.4) and the Darcy–Weisbach-based pressure drop per length for the laminar flow and transition regimes is clear. The remaining two pipe sizes give evidence of only turbulent flow. Equation (16.4) under-predicts the actual pressure drop by 30–35% at the low flow-rate end and is relatively accurate for flow rates approaching 7 L/s for all pipe sizes. The general disagreement with the results of the Darcy–Weisbach equation, which we recall is based on fundamental fluid dynamics, should convince one to ignore the approximate Hazen–Williams formula for pipe flow calculations.

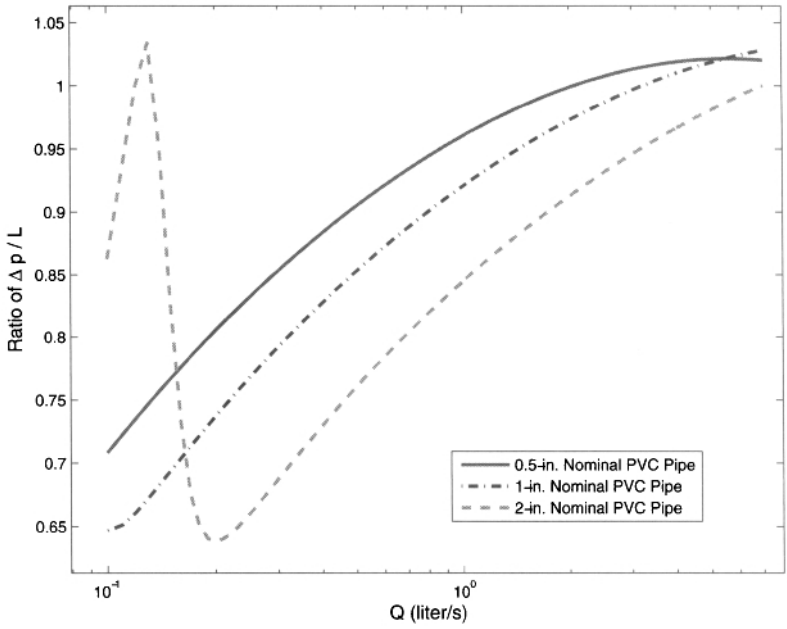

Figure 16.19 Ratio of $\Delta p/L$ from Eqn (16.4) to that from the Darcy–Weisbach equation for three pipe diameters.

29. To be done by the student.

30. The solutions are plotted in Fig. 16.20. The statements in Chapter 9 regarding this comparison are validated.

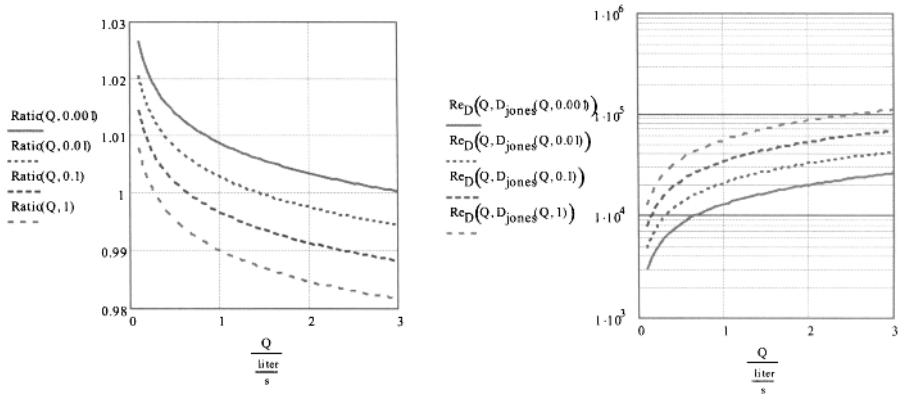

Figure 16.20 Solution for Exercise 30. The left-most plot is the ratio of D from Eqs (9.4) and (9.5). The other plot is Re over the requested range of Q and h_L/L.

31. The results of the correlation, Eqn (9.6), and the `Mathcad` worksheet `Single PipeNetworkDesign_Appendix.xmcd` are shown in Table 16.8. For minor-lossless flow in GI pipe, differences between D with the two approaches is $< 12\%$. For smooth pipe like PVC and PE, the agreement is 6% or better.

Table 16.8 Ratio of D from `SinglePipe NetworkDesign_Appendix.xmcd` to Eqn (9.6)

$h_L/L \rightarrow$	0.001	0.01	0.1	1.0
$\downarrow$ Q (L/s)				
0.012	0.997	0.965	0.884	0.987
0.1	1.026	1.033	1.012	1.001
1	1.006	0.992	0.983	0.978
3	0.994	0.984	0.977	0.973
5	0.990	0.982	0.976	0.972

32. Substituting the continuity equation, Eqn (2.21), into Eqn (2.40), obtain

$$1 - F - f(\overline{u}, D)\,\lambda\sqrt{1+s^{-2}}\frac{8Q^2}{\pi^2 g D^5} = 0 \tag{16.20}$$

Rearrange this equation to get

$$\frac{[f(Q,D)]^{1/2}\,Q}{g^{1/2}\,D^{5/2}} = 1.111\left[\frac{1-F}{\lambda(1+s^{-2})^{1/2}}\right]^{1/2} \tag{16.21}$$

The dimensionless volume flow rate is the term on the left side of this equation, and the modified slope is the group on the right. Note that for small s the modified slope becomes $s(1 - F)/\lambda$ the same as in Eqn (9.7). The exponent $1/2$ and the coefficient, 1.111, in Eqn (16.21) are both different from those in Eqn (9.7). Also, there is no explicit effect from the kinematic viscosity of the fluid, ν, since Re (where this appears) is embedded in the friction factor, $f(Q, D)$.

Chapter 10 Solutions

33. To be done by the student.

34. The solution appears in the Mathcad worksheet shown in Figs. 16.21–16.23. The solution using the Given...Minimize block follows exactly as in the example in Chapter 10 except that there are three unknowns for the present problem (L, D, and n) instead of two.

    For the Lagrange multiplier method, the cost function is

$$\begin{aligned}\hat{F}(L,d,n) &= \$400/\mathrm{m}^2 \frac{DLn^{1.5}}{n-1} + \$370.70/\mathrm{m}^{3.5} Ld^{2.5} \\ &+ \$280.60/\mathrm{m}^2 Ld + \hat{\lambda}_1 (V - \frac{\pi}{4} d^2 L) + \hat{\lambda}_2 (A_s - n\pi DL)\end{aligned}$$

    The last two terms are the constraints of fixed exchanger volume and tube surface area. $\hat{\lambda}_1$ and $\hat{\lambda}_2$ are two Lagrange multipliers. The derivatives $\partial\hat{F}/\partial L$, $\partial\hat{F}/\partial d$, $\partial\hat{F}/\partial n$, $\partial\hat{F}/\partial\hat{\lambda}_1$, and $\partial\hat{F}/\partial\hat{\lambda}_2$ are taken and set equal to zero, and appear in their own lines in Figs. 16.21 and 16.22. Mathcad has symbolic mathematics capability and will take a derivative and report the result symbolically. The five equations are nonlinear and cannot be solved by simple matrix inversion. Instead, they are solved simultaneously in a Given...Find block for $L^{opt}, D^{opt}, n^{opt}$ and $\hat{\lambda}_1$ and $\hat{\lambda}_2$. The latter two variables are of no interest to us. The units for each dependent variable are used to make each one dimensionless in the Find statement since the results are reported in a single column vector. They are converted to dimensional form after the solution is obtained. The solution reported in Mathcad for both methods is $d = 1.61$ m, $L = 7.41$ m, $n = 1504$, and the total cost is \$13,459.

35. The solution appears in Figs. 16.24 and 16.25. The optimal pipe diameters are $D_a^{opt} = 1.80$ in., $D_b^{opt} = 1.79$ in., and $D_c^{opt} = 1.79$ in., respectively; essentially equal diameters. The optimal static pressure heads at the junctions a–b and b–c of 22.6 m and 20.5 m, respectively, are acceptable. The minimum total pipe cost is \$602. Evidence that the minimal cost exists at the reported values of h_{ab}^{opt} and h_{bc}^{opt} comes from our inspection of the two plots at the bottom of Fig. 16.25 that show total cost versus h_j for the two junctions. These figures reveal that the total cost is not very sensitive to off-optimal values of h_{ab} and h_{bc}.

Optimization of Heat Exchanger

By Minimize function:

$V := 15\ m^3$ $A_s := 350\ m^2$ $dollars := 1$ $L := 1\ m$ $d := 1\ m$ $n := 300$ $D := 1\ cm$

$$F_{hat}(L,d,n) := 400\ \frac{dollars}{m^2}\ D\ \frac{n^{1.5}}{(n-1)}\ L + 370.7\ \frac{dollars}{m^{3.5}}\ d^{2.5}\ L + 280.6\ \frac{dollars}{m^2}\ d\ L$$

Given $\quad V - \frac{\pi}{4}\ d^2\ L = 0 \quad A_s - n\ \pi\ D\ L = 0 \quad \begin{bmatrix} L \\ d \\ n \end{bmatrix} := \text{Minimize}(F_{hat}, L, d, n)$

$$\begin{bmatrix} \frac{L}{m} \\ \frac{d}{m} \\ n \end{bmatrix} = \begin{matrix} 7.406 \\ 1.606 \\ 1.504\ \ 10^3 \end{matrix}$$

$F_{hat}(L,d,n) = 13458.69\ dollars$

By Lagrange multipliers:

$$400\ \frac{dollars}{m^2}\ D\ \frac{n^{1.5}}{(n-1)}\ L + 370.7\ \frac{dollars}{m^{3.5}}\ d^{2.5}\ L + 280.6\ \frac{dollars}{m^2}\ d\ L + \lambda_1\ \left(V - \frac{\pi}{4}\ d^2\ L\right) + \lambda_2\ (A_s - n\ \pi\ D\ L)$$

$$\frac{280.6\ d\ dollars}{m^2} - \pi\ D\ n\ \lambda_2 - \frac{\pi\ d^2\ \lambda_1}{4} + \frac{370.7\ d^{2.5}\ dollars}{m^{3.5}} + \frac{400\ D\ dollars\ n^{1.5}}{m^2\ (n-1)}$$

: derivative wrt L

Figure 16.21 Page 1 of Mathcad worksheet for heat exchanger optimization.

$$400\,\frac{\text{dollars}}{\text{m}^2}\,D\,\frac{n^{1.5}}{(n-1)}\,L + 370.7\,\frac{\text{dollars}}{\text{m}^{3.5}}\,d^{2.5}\,L + 280.6\,\frac{\text{dollars}}{\text{m}^2}\,d\,L + \lambda_1\,\left(V - \frac{\pi}{4}\,d^2\,L\right) + \lambda_2\left(A_s - n\,\pi\,D\,L\right)$$

$$\frac{280.6\ L\ \text{dollars}}{\text{m}^2} - \frac{\pi\ L\ d\ \lambda_1}{2} + \frac{926.75\ L\ d^{1.5}\ \text{dollars}}{\text{m}^{3.5}}$$: derivative wrt d

$$400\,\frac{\text{dollars}}{\text{m}^2}\,D\,\frac{n^{1.5}}{(n-1)}\,L + 370.7\,\frac{\text{dollars}}{\text{m}^{3.5}}\,d^{2.5}\,L + 280.6\,\frac{\text{dollars}}{\text{m}^2}\,d\,L + \lambda_1\,\left(V - \frac{\pi}{4}\,d^2\,L\right) + \lambda_2\left(A_s - n\,\pi\,D\,L\right)$$

$$\frac{600.0\ D\ L\ \text{dollars}\ n^{0.5}}{\text{m}^2\,(n-1)} - \frac{400\ D\ L\ \text{dollars}\ n^{1.5}}{\text{m}^2\,(n-1)^2} - \pi\ D\ L\ \lambda_2$$: derivative wrt n

$\lambda_1 := \frac{1000\text{dollars}}{\text{m}^3}$ $\lambda_2 := \frac{1000\text{dollars}}{\text{m}^2}$ $L = 7.406\ \text{m}$ $d = 1.606\ \text{m}$ $n = 1.504\ \ 10^3$

guesses

Given

$$0 = \frac{280.6\ d\ \text{dollars}}{\text{m}^2} - \pi\ D\ n\ \lambda_2 - \frac{\pi\ d^2\ \lambda_1}{4} + \frac{370.7\ d^{2.5}\ \text{dollars}}{\text{m}^{3.5}} + \frac{400\ D\ \text{dollars}\ n^{1.5}}{\text{m}^2\,(n-1)}$$: derivative wrt L

$$0 = \frac{280.6\ L\ \text{dollars}}{\text{m}^2} - \frac{\pi\ L\ d\ \lambda_1}{2} + \frac{926.75\ L\ d^{1.5}\ \text{dollars}}{\text{m}^{3.5}}$$: derivative wrt d

Figure 16.22 Page 2 of `Mathcad` worksheet for heat exchanger optimization.

$$0 = \frac{600.0\ \text{D L dollars}\ n^{0.5}}{m^2\,(n-1)} - \frac{400\ \text{D L dollars}\ n^{1.5}}{m^2\,(n-1)^2} - \pi\ \text{D L}\ \lambda_2$$: derivative wrt n

$$0 = V - \frac{\pi}{4} d^2 L \qquad 0 = A_s - n\,\pi\,D\,L$$: derivatives wrt λ.1 and λ.2

$$\begin{bmatrix} d \\ L \\ n \\ \lambda_1 \\ \lambda_2 \end{bmatrix} := \text{Find}\left[\frac{d}{m}, \frac{L}{m}, n, \lambda_1\ m^3, \lambda_2\ m^2\right]$$

$d := d\ m$ $\quad d = 1.606\ m$

$L := L\ m$ $\quad L = 7.411\ m$

$n = 1.504 \quad 10^3$

$F_{hat}(L, d, n) = 13478.37\ \text{dollars}$

Figure 16.23 Page 3 of `Mathcad` worksheet for heat exchanger optimization.

Series flow 3-pipe problem optimized for minimum cost

Water properties

$\rho := 1000\frac{kg}{m^3}$ $\nu := 13.0710^{-7}\cdot\frac{m^2}{sec}$ $sec := 1\cdot s$ $TOL := 1\cdot10^{-10}$ $ORIGIN := 1$

$dollars := 1$

IPS sch.-40 PVC pipe cost

$$diam := \begin{pmatrix} 0.622 \\ 0.824 \\ 1.049 \\ 1.610 \\ 2.067 \\ 2.469 \\ 3.068 \\ 4.026 \end{pmatrix}\cdot in \qquad cost := \begin{pmatrix} 0.50 \\ 0.82 \\ 1.02 \\ 1.74 \\ 2.40 \\ 3.94 \\ 5.58 \\ 7.75 \end{pmatrix}\cdot\frac{dollars}{m}$$

$$Re(Q,D) := \frac{4\cdot Q}{\pi\cdot D\cdot\nu}$$

$\varepsilon := 5\cdot10^{-6}\cdot ft$ absolute roughness, ft (increase 100 times for galvanized steel)

friction factor that spans the laminar/turbulent range. ebyD is relative roughness.

$$funct(f,R,ebyD) := \frac{f}{2} - \left[\left(\frac{4}{R\cdot\sqrt{\frac{f}{8}}}\right)^{24} + \left[\left(\frac{18765}{R\cdot\sqrt{\frac{f}{8}}}\right)^{8} + \left[3.29 - \frac{227}{R\cdot\sqrt{\frac{f}{8}}} + \left(\frac{50}{R\cdot\sqrt{\frac{f}{8}}}\right)^{2} \ldots + \frac{1}{0.436}\cdot\ln\left(\frac{R\cdot\sqrt{\frac{f}{8}}}{1 + 0.301R\cdot\sqrt{\frac{f}{8}}\cdot ebyD\cdot 2}\right)\right]^{16}\right]^{-\frac{3}{2}}\right]^{\frac{1}{12}}$$

$f1 := 0.2$ $fric\_fac(Re,ebyD) := root(funct(f1,Re,ebyD),f1)\cdot 4$ friction factor

$\alpha(R) := if(R < 2100, 2, 1.05)$

A 3-pipe network solved in forward way (specify volume flow rate and solve for pipe diameters vs. junction heads):

$D_a := 2\cdot in$ $D_b := 2\cdot in$ $D_c := 2\cdot in$ guesses

Input Parameters:

$L_a := 100m$ $Q := 6.10\frac{liter}{sec}$ $K_a := 0$ $L_{ebyD\_a} := 0$ $\Delta z_a := 50\cdot m$

$h_{del} := 10\cdot m$ $L_b := 100m$ $K_b := 0$ $L_{ebyD\_b} := 0$

$h_j := 7\cdot m$ $L_c := 100m$ $K_c := 0$ $L_{ebyD\_c} := 0$

Figure 16.24 Page 1 of solution for Exercise 35.

$$Tcost(D_a, D_b, D_c) := linterp(diam, cost, D_a)\,L_a + linterp(diam, cost, D_b)\,L_b + (linterp(diam, cost, D_c)\,L_c)$$

Define energy equation functions:

Cost (objective) function

$$r_a(h_{jab}, D_a) := \Delta z_a - h_{jab} - \left[K_a + \alpha\left(Re(|Q|, D_a)\right) + fric\_fac\left(Re(|Q|, D_a), \frac{\varepsilon}{D_a}\right)\left(\frac{L_a}{D_a} + L_{ebyD\_a}\right)\right]\cdot\frac{8\cdot Q^2}{\pi^2\cdot g\cdot D_a^4}$$

$$r_b(h_{jab}, h_{jbc}, D_b) := \frac{\Delta z_a}{2} + h_{jab} - h_{jbc} - \left[K_b + fric\_fac\left(Re(|Q|, D_b), \frac{\varepsilon}{D_b}\right)\left(\frac{L_b}{D_b} + L_{ebyD\_b}\right)\right]\cdot\frac{8\cdot Q^2}{\pi^2\cdot g\cdot D_b^4}$$

$$r_c(h_{jbc}, D_c) := \frac{\Delta z_a}{3} + h_{jbc} - h_{del} - \left[K_c + fric\_fac\left(Re(|Q|, D_c), \frac{\varepsilon}{D_c}\right)\left(\frac{L_c}{D_c} + L_{ebyD\_c}\right)\right]\cdot\frac{8\cdot Q^2}{\pi^2\cdot g\cdot D_c^4}$$

Solve in Given...Find block

Given

$0 = r_a(h_{jab}, D_a)$ $0 = r_b(h_{jab}, h_{jbc}, D_b)$ $0 = r_c(h_{jbc}, D_c)$

$Ds(h_{jab}, h_{jbc}) := Find(D_a, D_b, D_c)$

$T_c(h_{jab}, h_{jbc}) := Tcost(Ds(h_{jab}, h_{jbc})_1, Ds(h_{jab}, h_{jbc})_2, Ds(h_{jab}, h_{jbc})_3)$

$h_{jab} := h_{del} + 22\cdot m$ $h_{jbc} := h_{del} + 23\cdot m$ guesses

Problem is in terms of unknowns h.jab, h.jbc. Minimize Tc subject to inequality constraints below.

Given

$h_{jab} \geq h_j$ $h_{jbc} \geq h_j$ h.jab, h.jbc > h.j

$h_{jab} < \Delta z_a$ $h_{jbc} < \Delta z_a + \frac{\Delta z_a}{2}$ h.jab and h.jbc < hydrostatic

$(h_{jab}\ h_{jbc}) := Minimize(T_c, h_{jab}, h_{jbc})^T$ $(D_a\ D_b\ D_c) := Ds(h_{jab}, h_{jbc})^T$

$Tcost(D_a, D_b, D_c) = 602.86\,dollars$ $D_a = 1.801\,in$ $D_b = 1.794\,in$ $D_c = 1.794\,in$ $h_{jab} = 22.623\,m$ $h_{jbc} = 20.486\,m$

$h_{jplot} := 8\cdot m, 8.5\cdot m .. 35\cdot m$

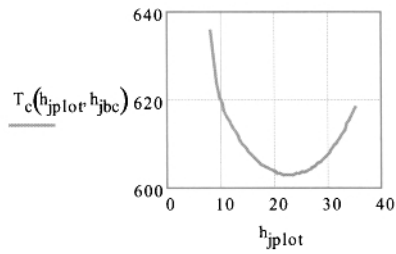

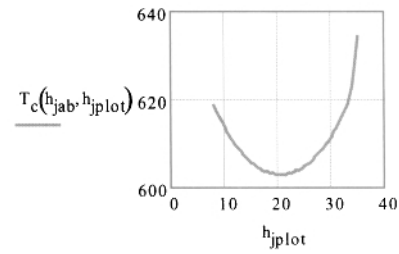

Figure 16.25 Page 2 of solution for Exercise 35.

Chapter 11 Solutions

36. The solutions are shown in Fig. 16.26. As we saw from the developments in Chapter 9 for turbulent, minor-lossless flow in a smooth pipe, $D \approx L^{4/19} \approx Q^{7/19}$. The results in Fig. 16.26 are in close agreement with these relationships.

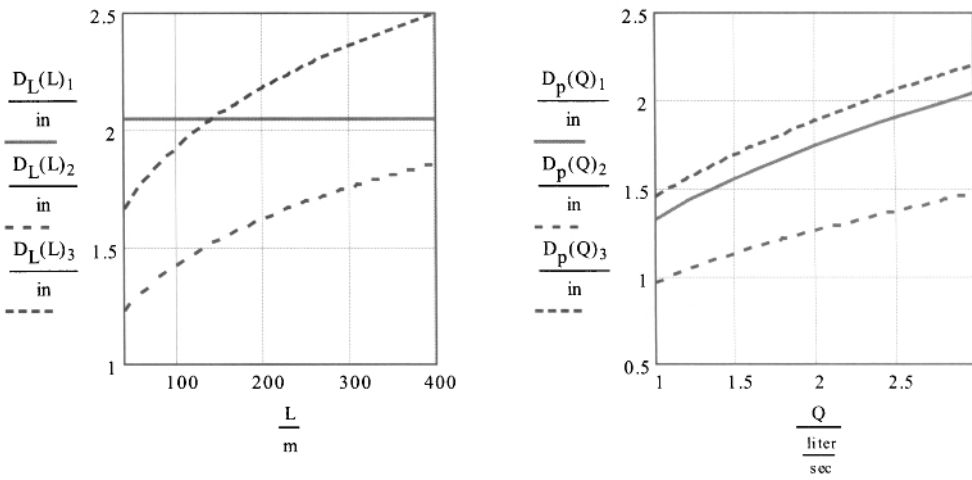

Figure 16.26 Solution for Exercise 36. D_a, D_b, and D_c appear in order on the vertical axis on both plots.

37. Into Eqs (11.16) substitute the assumptions: $L_a = L_b = L_c$, $D_b = D_c$, $Q_b = Q_c = Q_a/2$. Write the expression for total pipe cost assuming that cost for each pipe is linear with pipe diameter. After simplifying, take the derivative of total pipe cost with respect to h_j, set it equal to zero, and solve for $h_j = h_j^{opt}$. Obtain the analytical result: $h_j^{opt} = (2^{12/23}\Delta z_a - \Delta z_b + h_{del})/(1 + 2^{12/23})$. Under these assumptions, we see that h_j^{opt} is a linear combination of Δz_a, Δz_b, and h_{del}.

38. Add Eqn (11.39) to the `Mathcad` worksheet `BranchingPipeExample.xmcd` and solve for the single static pressure at the junction.

$$
\begin{aligned}
0 \;=\; & Q_a^{7b/19}\left(\frac{\Delta z_a - h_2}{L_a}\right)^{-(1+4b/19)} \\
- \; & Q_b^{7b/19}\left(\frac{\Delta z_b + h_2 - h_{del}}{L_b}\right)^{-(1+4b/19)} \\
- \; & Q_c^{7b/19}\left(\frac{\Delta z_c + h_2 - h_{del}}{L_c}\right)^{-(1+4b/19)}
\end{aligned}
$$

Table 16.9 D (in.) from Mathcad worksheet `SeriesPipe Example_equalQ_3pipe _withcost.xmcd`

z_d (m) →	67	72	78	84
↓ Pipe				
a	2.71	2.80	3.00	3.36
b	2.33	2.54	2.71	4.30
c	2.33	2.40	2.71	2.80
d	1.68	1.68	1.58	1.54
e	1.53	1.53	1.53	1.53

where $b = 1.4$. Solve this equation for h_j using the `Root` function or in a `Given...Find` block to obtain $h_j^{opt} = 16.8$ m. This agrees with Fig. 11.6.

39. To be done by the student.

40. The results are presented in Table 16.9. The static pressure head at Junction b–c for $z_d = 84$ m is 73.5 m or 7.1 atm (105 psig). The growth in pipe sizes with increasing z_d is expected as friction must play a more-diminishing role as the elevation of the local peak approaches z_1. Note that segments d and e are affected little by the elevation change in this problem.

41. The energy equation for a serial pipeline in nodal format is,

$$\Delta z_{ij} + \Delta h_{ij} = \{K_{ij} + \alpha_{ij} + f(Q_{ij}, D_{ij})[\frac{L_{ij}}{D_{ij}} + (\frac{L_e}{D})_{ij}]\}\frac{8Q^2}{\pi^2 g D_{ij}^4} \quad (16.22)$$

for $ij = 12, 23, 34, \ldots, (n-1)n$, where n is the total number of nodes in the pipe. It is understood that $\Delta h_{ij} = h_i - h_j$ for two consecutive nodes i and j, and h are the static pressure heads at the junctions. Also, $h_1 = 0$ and $h_n = h_{del}$ as always. The term α_{ij} is nonzero only for the first segment, $ij = 12$. Equation (16.22) is less cumbersome to use than Eqn (11.22) and is the form recommended for solutions to serial pipeline problems.

42. *Solution from* Mathcad *worksheet*: Following the above developments, the energy equation for each of the pipes is written as

$$
\begin{aligned}
p_2 &= \rho g \Delta z_a + \frac{\rho}{2}(-C_{L,a} + \alpha)\left(\frac{4Q_a}{\pi D_a^2}\right)^2, \quad \text{Pipe } a \\
p_2 &= -\rho g \Delta z_b + \frac{\rho}{2}(C_{L,b} + \alpha)\left(\frac{4Q_b}{\pi D_b^2}\right)^2, \quad \text{Pipe } b \\
p_2 &= -\rho g \Delta z_c + \frac{\rho}{2}(C_{L,c} + \alpha)\left(\frac{4Q_c}{\pi D_c^2}\right)^2, \quad \text{Pipe } c \\
p_2 &= -\rho g \Delta z_d + \frac{\rho}{2}(C_{L,d} + \alpha)\left(\frac{4Q_d}{\pi D_d^2}\right)^2, \quad \text{Pipe } d \\
p_2 &= -\rho g \Delta z_e + \frac{\rho}{2}(C_{L,e} + \alpha)\left(\frac{4Q_e}{\pi D_e^2}\right)^2, \quad \text{Pipe } e
\end{aligned}
$$

where C_L is defined in Eqn (11.4). These equations are solved simultaneously to obtain the solution for each D as a function of the arbitrary static pressure, p_2, at the end of pipe a. The results are shown in Fig. 16.27. From our inspection of this figure pipe a requires a $1\frac{1}{2}$-in. nominal PVC pipe size (actual diameter of 1.61 in.), and pipes b through e require a nominal $\frac{3}{4}$-in. size (actual diameter of 0.824 in.) or nominal $\frac{1}{2}$-in. size (actual diameter of 0.662 in.). As static pressure p_2 increases, the driving force for flow in pipe a is lessened so that the pipe diameter, D_a, must increase, which is clearly seen in Fig. 16.27. For the remaining four pipes, as static pressure p_2 increases, the driving force for flow increases and thus the pipe diameters decrease to satisfy the constrained water flow rates. This is also clear from our inspection of Fig. 16.27. Among the latter four pipes, pipe d demonstrates the greatest sensitivity to changes in p_2 because of the relatively large flow rate and the negative 3-m head that static pressure p_2 must overcome.

43. From the Mathcad worksheet, the elevation heads are large enough to satisfy the constraint of a 7-m head at the tapstand while satisfying the remainder of conditions for this design, which are shown in Table 16.10. The theoretical pipe diameters were obtained by assuming junction static pressures of 7 m. The final junction static pressures are $p_{12} = 19.3$ psig (13.6 m), $p_{23} = 28.0$ psig (19.7 m), and $p_{34} = 12.4$ psig (8.7 m). Pipe cost, which is \$341, was not optimized for this problem. The values for K represent partially closed globe valves in these pipe segments.

44. The results are shown in Table 16.11. The cost for the optimized network, based on theoretical D, is \$334, not very different from the solution of exercise 43. The choice for the nominal size of 1-in. for segment 34, instead of $\frac{3}{4}$ for problem 43, adds cost to the final design of the network but additional flexibility for future expansion. The solution from Eqn (11.54) gives $D_{ij}^{opt} = [1.13 \quad 1.08 \quad 1.01 \quad 0.832]$ in. The disagreement between the results from Eqn (11.54) and the Mathcad solution is because the optimal result shows

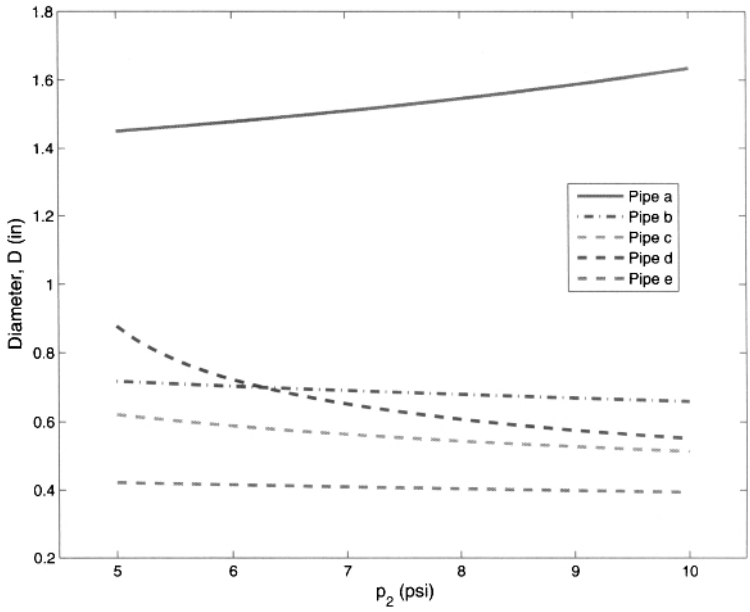

Figure 16.27 Solution for Exercise 42. Pipe a requires a $1\frac{1}{2}$-in. nominal PVC pipe size (actual diameter of 1.61 in.), and pipes b through e require a nominal $\frac{3}{4}$-in. size (actual diameter of 0.824 in.) or nominal $\frac{1}{2}$-in. size (actual diameter of 0.662 in.).

Table 16.10 Solution for the Theoretical and Nominal Pipe Diameters, and Actual Volume Flow Rates and K for Leg of the Kiangan-Community Network

Pipe Subscript	Theor. D (in.)	Nom. D (in.)	Q (L/s)	K
12	1.24	$1\frac{1}{2}$	1.24	50
23	1.18	$1\frac{1}{2}$	1.05	50
34	0.792	$\frac{3}{4}$	0.84	40
45	0.762	$\frac{3}{4}$	0.43	0

that $h_3^{opt} = 7$ m. That is, the optimal solution from `Mathcad` used the lower-bound static pressure head. There is no such constraint in the analytical solution of Eqn (11.54). The solution we should use is the one from `Mathcad`.

45. The results are presented in Table 16.12. The flow rates in segments 12, 45, and all branches are maintained as specified in Table 16.4 by adjusting globe valves in the branches as shown.

46. In `BranchPipeExample_4pipe_withcost_ver2.xmcd`, we solve only the reverse problem with the flow rate for the turned-off segment set equal to zero and the energy equation for this segment disabled in the `Given...Find` block as dis-

Table 16.11 Values for Design Parameters for a Leg of the Kiangan-Community Network

Pipe Segment	Q (L/s)	L (m)	K	L_e/D	Δz (m)
12	1.23	76	30	60	18
23	1.04	113	0	90	10
34	0.83	19	0	90	8
45	0.42	75	0	90	6

Table 16.12 Solution for the Theoretical and Nominal Pipe Diameters, and Actual Volume Flow Rates and K for Leg of the Kiangan-Community Network

Pipe Subscript	Theor. D (in.)	Nom. D (in.)	Q (L/s)	K
12	1.45	$1\frac{1}{2}$	1.25	30
23	1.19	$1\frac{1}{2}$	1.05	0
34	1.05	1	0.834	0
45	0.685	$\frac{3}{4}$	0.418	260
26	0.616	$\frac{1}{2}$	0.200	85
37	0.629	$\frac{1}{2}$	0.218	215
48	0.700	$\frac{1}{2}$	0.416	40

cussed in Section 11.6.3. The flow rates in the branches are $Q_{37} = 0.224$ L/s, $Q_{48} = 0.424$ L/s, and $Q_{45} = 0.424$ L/s; all slightly larger than required from Table 16.4 for this design.

47. The pathlengths and elevations for segments 12 and 23 are from geometry,

$$\begin{aligned} L_{12}(\gamma) &= R\gamma \\ L_{23}(\gamma) &= R(\frac{\pi}{2} - \gamma) \\ \Delta z_{12}(\gamma) &= R[1 - \cos(\gamma)] \\ \Delta z_{23}(\gamma) &= R\cos(\gamma). \end{aligned}$$

The energy equations for each of the four pipe segments are written. In each, D in its respective segment is unknown. In segments 12 and 23, h_2 is unknown, and in segments 23, 34, and 35, h_3 is unknown. Here, γ is the independent parameter and appears in the energy equations for segments 12 and 23. The solution is carried out consistent with past worksheets where optimal solutions were sought. The energy equations are first solved simultaneously in a `Given...Find` block for their respective pipe diameters as a function of h_2, h_3, and γ. The cost is then minimized using a `Given...Minimize` block and, by doing so, the value of h_2 and h_3 are determined as a function of angle γ. A plot of total cost versus γ will then reveal the optimal value for γ (i.e., the γ value that produces the lowest cost).

The solution appears in Figs. 16.28–16.31. The Mathcad worksheet displayed in Fig. 11.3 should be consulted for the preliminary calculations for the current worksheet. Our inspection of the results for this problem show that no optimal solution exists. The cost is essentially constant over all γ. This result is consistent with Section 11.5.1, where we saw that the minimum cost solution for a serial network is one where the pipe diameters are equal.

48. The solution is presented in Table 16.13. The final static pressure heads at the three junctions is $h_j^{opt} = [21.0 \quad 16.1 \quad 11.3 \quad 15.6]$ m for nodes 2, 3, 4, and 5. All are acceptable. Based on the correlation of pipe data from central Nicaragua, the optimal total pipe cost is \$776. Nominal pipe sizes are selected next, followed by the reverse solution where actual flow rates and static pressure heads at the junctions are determined.

Table 16.13 Solution for the Theoretical Pipe Diameters and Flow Rates for Loop Network

Pipe Subscript	Theor. D (in.)	Theor. Q (L/s)
12	1.07	4.60
23	1.93	3.55
34	1.32	1.25
45	0.592	−0.13
52	1.2	−1.05
36	1.52	2.30
47	1.47	1.38
58	1.08	0.920

49. Vectors of optimal pipe diameters for the distribution main and optimal static pressure heads at the junctions are: $\vec{D}_m^{opt} = [1.91 \quad 1.88 \quad 1.86 \quad 1.80 \quad 1.74 \quad 1.67 \quad 1.62 \quad 1.57 \quad 1.52 \quad 1.41 \quad 1.34 \quad 1.29 \quad 1.17 \quad 1.07 \quad 0.861]$ in. and $\vec{h}^{opt} = [0 \quad 8.66 \quad 11.3 \quad 13.8 \quad 23.0 \quad 19.6 \quad 13.2 \quad 11.6 \quad 11.9 \quad 12.5 \quad 16.0 \quad 16.9 \quad 16.6 \quad 14.7 \quad 16.5 \quad 9.99]$ m at the 16 nodes. All components of $\vec{h}$ are acceptable from an integrity standpoint.

50. The solution appears in the Mathcad worksheet in Figs. 16.32 and 16.33. In the energy equations, all pipe lengths (L_{13}, L_{23}, L_{34}) and elevations ($\Delta z_{13}, \Delta z_{23}, \Delta z_{34}$) depend on the angle γ through simple geometry (see Fig. 16.6). They are written as

$$\begin{aligned}
L_{13}(\gamma) &= \frac{L_1}{\cos(\gamma)} \\
L_{23}(\gamma) &= \frac{L_1}{\cos(\gamma)} \\
L_{34}(\gamma) &= L_3 - L_1 \tan(\gamma) \\
\Delta z_{13}(\gamma) &= sL_1 \tan(\gamma) \\
\Delta z_{23}(\gamma) &= sL_1 \tan(\gamma) \\
\Delta z_{34}(\gamma) &= z_1 - sL_1 \tan(\gamma)
\end{aligned}$$

The energy equations for the three pipes in the network are written where, in each, D and the static pressure head at the junction (h_j) are unknown, and γ is the independent parameter. The solution is carried out consistent with past worksheets where optimal solutions were sought. The energy equations are first solved simultaneously in a `Given...Find` block for their respective pipe diameters as a function of h_j and γ. The cost is then minimized using a `Given...Minimize` block and, by doing so, the value of h_j is determined as a function of angle γ. A plot of total cost versus γ will then reveal the optimal (i.e., the γ value that produces the lowest cost).

From the `Mathcad` worksheet, the optimal angle is $\gamma^{opt} = 77°$ and the minimal cost is \$4386. The theoretical pipe diameters are: $D_{13} = 1.91$ in., $D_{23} = 1.62$ in., and $D_{34} = 2.10$ in. The pipe lengths are: $L_{13} = 222$ m, $L_{23} = 222$ m, and $L_{34} = 1383$ m. These figures can be determined by using the graphical `trace` option in `Mathcad` or by requesting D and L values at $\gamma = \gamma^{opt}$.

At the optimal value of γ, the static pressure head is ~5.82 m. This is a marginally acceptable value based on our previous work. Note that there is a generally broad minimum as seen in the leftmost figure at the bottom of the solution in Fig. 16.33. For example, for $\gamma = 44°$ the total cost is ~\$4450, very close to the optimal cost. For values of $\gamma > \gamma^{opt}$, however, the total cost increases dramatically.

Finally, we note for optimal conditions, there is no possibility of water flow from one source to another. This may have occurred for small optimal values of γ but not for the optimal solution for this problem.

51. The energy equations for the distribution main from node 5 to node 1 are written as

$$
\begin{aligned}
0 &= \Delta z_{54} + h_5 - h_4 - (f_{54}\frac{L_{54}}{D_{54}})\frac{8Q_{54}^2}{\pi^2 g D_{54}^4} \\
0 &= \Delta z_{43} + h_4 - h_3 - (f_{43}\frac{L_{43}}{D_{43}})\frac{8Q_{43}^2}{\pi^2 g D_{43}^4} \\
0 &= \Delta z_{32} + h_3 - h_2 - (f_{32}\frac{L_{32}}{D_{32}})\frac{8Q_{32}^2}{\pi^2 g D_{32}^4} \\
0 &= \Delta z_{21} + h_2 - h_1 - (f_{21}\frac{L_{21}}{D_{21}})\frac{8Q_{21}^2}{\pi^2 g D_{21}^4}
\end{aligned}
$$

where $h_5 = 35$ psig = 24.61 m and $h_1 = 7$ m and it is understood that $\Delta z_{21} = -\Delta z_{12}$ and $L_{21} = L_{12}$, and so on. That is, the pump is raising water above the location of node 5. An appropriate `Mathcad` worksheet is modified to solve this problem.

For $h_j = 7$ m throughout, the pipe cost is \$290.50 and the diameters are $\vec{D} = [D_{54}\ D_{43}\ D_{32}\ D_{21}] = [1.02\ 1.17\ 0.777\ 0.642]$ in. When the pipe cost is minimized it becomes \$266.96 for which the optimized diameter results are

$\vec{D}^{opt} = [1.01 \;\; 0.963 \;\; 0.902 \;\; 0.742]$ in. The optimized static pressure heads at the three internal nodes are $\vec{h}_j^{opt} = [h_2^{opt} \;\; h_3^{opt} \;\; h_4^{opt}] = [7.34 \;\; 22.8 \;\; 18.8]$ m. All are acceptable from an integrity standpoint.

Chapter 12 Solutions

52. To be done by the student.

53. To be done by the student.

54. To be done by the student.

55. The `Mathcad` worksheet `microhydro_theoretical_power.xmcd` is used to solve this exercise. The calculations in this worksheet follow.

    The hydraulic gradient $S \approx 0.076$ from this example. The optimal pipe size, subject to the design value of $Q = Q^{opt} = 230$ L/s in the penstock is from Eqn (12.13),

$$\begin{aligned} D^{opt} &= 0.9192 \text{ in.} \cdot S^{-0.2054} \left(\frac{Q}{Q_u}\right)^{0.3805} \\ &= 0.9192 \text{ in.} \cdot 0.076^{-0.2054} 230^{0.3805} = 12.3 \text{ in.} \end{aligned}$$

    For sch. 40 IPS pipe, the inside diameter is within 1% of the nominal size for nominal size of 4 in. and larger (Table 3.1). Thus, we choose nominal 14-in. sch. 40 GI pipe. The flow speed is 2.3 m/s, below the maximum recommended of 3 m/s when considering abrasion.

    The energy equation for the actual turbine power output is Eqn (12.16),

$$\dot{w}_a = \eta_t \, \eta_g \, \rho g \, Q \, L[S - f(Q, D) \frac{8Q^2}{\pi^2 g D^5}]$$

    Assume $\eta_t = 0.75$ and $\eta_g = 0.85$. With $f(Q, D) = 0.01702$ from the `Mathcad` worksheet (or Fig. 2.4), obtain,

$$\begin{aligned} \dot{w}_a &= 0.75 \cdot 0.85 \cdot 999.7 \text{ kg/m}^3 \cdot 9.807 \text{ m/s}^2 \cdot 1050 \text{ m} \cdot [0.076 \\ &- 0.01702 \frac{8 \cdot (230 \times 10^{-3} \text{ m}^3/\text{s})^2}{\pi^2 \cdot 9.807 \text{ m/s}^2 \cdot (14/39.372 \text{ m})^5}] = 95.5 \text{ kW} \end{aligned}$$

    Since 95.5 kW > 65 kW as required by the community, we conclude the above design specifications will meet the electrical power demand. The designer needs to consider other inefficiencies in the system (transformer and power transmission losses), which will reduce this value by ~15%.

    The value for Q^{opt} is 324.7 L/s because of the need to select 14-in. GI pipe (13 in. pipe is normally not commercially available). This is much larger than

the design flow rate of $Q = 230$ L/s, and is the reason why the electrical power production is much higher than for textbox B.12.1 example. More power will be produced with GI pipe, but at a much greater pipe cost because the large pipe size is more than needed for optimal turbine performance.

56. Equation (12.17) is solved in `Mathcad` using the root-finder `root`. The solution appears in Fig. 16.34. The flow rates range from 23 L/s to > 2200 L/s.

57. In Exercise 55, the sch. 40 GI pipe size is $D = 14$ in. From the `Mathcad` worksheet `microhydro_theoretical_ power.xmcd`, the static pressure head just before the turbine is $h_{2a} = 66.26$ m (Fig. 12.5). Assuming $C_v = 0.95$ at its mid-range, Eqn (12.26) becomes

$$A_n = \frac{230 \times 10^{-3}\ \text{m}^3/\text{s}}{0.95\sqrt{2 \cdot 9.807\ \text{m/s}^2 \cdot 66.26\ \text{m}}} = 6.71 \times 10^{-3}\ \text{m}^2 = 10.4\ \text{in.}^2$$

The nozzle diameter is from

$$D_n = (4A_n/\pi)^{1/2} = 3.64\ \text{in.}$$

With C_v near its optimal point, the efficiency of the turbine, $C_p \approx 88.7\%$

The speed of the water jet is

$$V_1 = \frac{Q}{A_n} = \frac{230 \times 10^{-3}\ \text{m}^3/\text{s}}{6.71 \times 10^{-3}\ \text{m}^2} = 34.3\ \text{m/s}$$

The tangential velocity of the Pelton wheel, ωr, is optimally half of this value.

The system efficiency is $\eta_{sys} = 66.26\ \text{m}/80\ \text{m} = 82.8\%$, considerably larger than that based on $D = D^{opt}$.

Chapter 13

58. The solution is carried out using Eqs (13.1) and (13.2). The results for the running sum of the local lengths are presented in Table 16.14. The total length of pipeline is $L_{\ell,18} = 1454.3$ m. From our inspection of the given data set, the point in the network that is closest to the elevation of the source (at node 1) is node 17, where $\Delta z = 49.3 - 38.9$ m = 10.4 m.

59. The present water demand is estimated from Eqn (13.4)

$$Q_{d,P} = \frac{1350\ \text{persons} \cdot 80\ \text{L/person/day}}{60\ \text{s/min} \cdot 60\ \text{min/h} \cdot 24\ \text{h/day}} = 1.25\,\text{L/s}$$

The future population is estimated from Eqn (13.3)

$$P_F = 1350\ \text{persons} \cdot (1 + 0.015)^{20} = 1819\,\text{persons}$$

Table 16.14 Running Sum of Local Lengths for Exercise 58

Node, i	x_i (m)	y_i (m)	z_i (m)	$L_{\ell,i}$ (m)
1	0	0	49.3	0
2	−37.2	−52.1	22.2	69.5
3	−77.4	9.6	19.9	143.2
4	−241	75.7	29.6	319.9
5	−277.8	95.8	33.6	362.0
6	−312.5	148.4	25.2	425.6
7	−336.2	184.7	17.5	469.6
8	−374.7	208.4	22.5	515.1
9	−420.8	216	21.7	561.8
10	−439.1	228.7	20	584.2
11	−412.6	335.1	22.3	693.9
12	−428.9	373.1	13.5	736.1
13	−481.8	463.7	16.7	841.1
14	−471.9	552.1	15	930.1
15	−533.9	659.1	24.7	1054.1
16	−544.5	720.5	43	1119.1
17	−536.1	864.9	38.9	1263.8
18	−688.4	974.3	5.2	1454.3

Table 16.15 Flow Rate Data for Exercise 59

Present Demand (L/s)	Future Demand (L/s)	Source 1 Yield (L/s)	Source 2 Yield (L/s)	Source 3 Yield (L/s)	Source 4 Yield (L/s)
1.25	1.68	0.95	0.40	1.46	0.55

from which the future demand becomes

$$Q_{d,F} = \frac{1819 \text{ persons} \cdot 80 \text{ L/person/day}}{60 \text{ s/min} \cdot 60 \text{ min/h} \cdot 24 \text{ h/day}} = 1.68 \text{ L/s}$$

A comparison of the future demand with the yields from the sources is shown in Table 16.15 for convenience. Our inspection of the data in Table 16.15 shows the following combination of sources will meet the present and future demand:

(a) Source 3 and any one of the remaining sources.

(b) Sources 1, 2, and 4 together.

To produce a recommendation based on a full-analytical approach, proceed to calculate the pipe sizes needs to deliver water from each source to the storage tank. Design Fig. 5.4 is used ($F = 0$; Natural flow, and $\lambda = 1$) to calculate the nominal pipe sizes for each of the candidates. The results are shown in Table 16.16. Also shown in this table are the total pipe costs for developing each source, where the pipe cost per length is from any one of the appropriate `Mathcad` worksheets. Our inspection of the results of Table 16.16 shows that option a from the above list of options costs between $97.02 (Sources 3 and 2)

Table 16.16 Cost Data for the Four Sources in Exercise 59

Source	Mean Slope ($\delta z/L$)	Yield (L/s)	D (nom.) (in.)	Cost Per Length ($/m)	Length (m)	Total Pipe Cost (US$)
1	0.0625	0.95	2	2.40	32	76.80
2	0.375	0.40	$\frac{1}{2}$	0.60	8	4.80
3	0.113	1.46	$1\frac{1}{2}$	1.74	53	92.22
4	0.0476	0.95	2	2.40	21	50.40

and $169.02 (Sources 3 and 1). The total pipe cost for option b is $132. Therefore, the most economical choice is to develop sources 2 and 3 that produces a yield of 1.86 L/s. This recommendation assumes that binding commitments from the land owner(s) of the source(s) have been obtained for all of them, and that the owners have agreed to not disturb the native growth around each of the sources. Disturbing this growth, such as cutting of trees surrounding the sources could affect the yields from the springs in the future.

60. We use the spreadsheet `Storage Volume Calculation-Textbox_Example.xlsx`, supplied with this book, to calculate the volume of water in the tank at the end of each hour of the day. Trial-and-error dictate that we consider tank volumes in the range of 38,000–42,000 L; volumes below this range are empty > 2 h each day. Volumes greater than this are filled the entire day and have too many hours of overflow. Table 16.17 shows the results for a tank volume of 40,000 L (40 m^3). The recommended tank volume is between 40 and 41 m^3. For the latter value, the tank never empties.

61. For pipe segment 12, for example, from Eqn (13.6) the design flow rate becomes

$$Q_{12,P,p} = PF \cdot Q_{12} = 3.2 \cdot 3.5 \text{ L/s} = 11.2 \text{ L/s}.$$

For an annual growth rate, i, of 1% and a 25-year network lifetime, the result from Eqn (13.3) shows the design flow rates need to increase a factor of 1.282 to accommodate the future population. Thus, for pipe segment 12,

$$Q_{12,F,p} = (1+i)^t \cdot Q_{12,P,p} = 1.282 \cdot 11.2 \text{ L/s} = 14.4 \text{ L/s}$$

The flow-rate results for all segments of this network were calculated in the same manner and presented in Table 16.18.

62. To be done by the student.

63. For GI pipe, solve Eqn (13.10) in `Mathcad` using the friction factor from Eqs (2.16) and (2.17) to get L_a and L_b equal to 280.8 m, and 97.2 m, respectively. For PVC pipe either the `Mathcad` worksheet or Eqn (13.10) will give L_a and L_b equal to 277.3 m, and 100.7 m, respectively. The differences

Table 16.17 Water Volume in Tank versus Hour of Day for Tank volume of 40,000 L

Hour	Q_s (l/h)	Demand Percentage	Q_d (l/h)	Water Volume (l)	State of Tank
1	6696	0	0	40,000	Overflow
2	6696	0	0	40,000	Overflow
3	6696	0	0	40,000	Overflow
4	6696	0	0	40,000	Overflow
5	6696	5	7,276	39,420	Filling
6	6696	20	29,104	17,012	Filling
7	6696	10	14,552	9,156	Filling
8	6696	5	7,276	8,576	Filling
9	6696	1	1,455.2	13,817	Filling
10	6696	1	1,455.2	19,058	Filling
11	6696	5	7,276	18,478	Filling
12	6696	10	14,552	10,622	Filling
13	6696	5	7,276	10,042	Filling
14	6696	2.5	3,638	13,100	Filling
15	6696	2.5	3,638	16,158	Filling
16	6696	5	7,276	15,578	Filling
17	6696	10	14,552	7,722	Filling
18	6696	10	14,552	−134	Empty
19	6696	5	7,276	−580	Empty
20	6696	2	2,910.4	3,786	Filling
21	6696	1	1,455.2	9,026	Filling
22	6696	0	0	15,722	Filling
23	6696	0	0	22,418	Filling
24	6696	0	0	29,114	Filling

Table 16.18 Present and Future Design Volume Flow Rates for Exercise 61

Pipe Subscript, ij	$Q_{ij,P,p}$ (L/s)	$Q_{ij,F,p}$ (L/s)
12	11.2	14.4
23	9.6	12.3
34	8.8	11.3
45	7.2	9.2
56	6.4	8.2
67	4.8	6.2
78	4.0	5.1
89	3.2	4.1
2–10	1.6	2.1
3–11	0.8	1.0
4–12	1.6	2.1
5–13	0.8	1.0
6–14	1.6	2.1
7–15	0.8	1.0
8–16	0.8	1.0

between the results for PVC and GI hint that Eqn (13.11) is probably adequate as a first-order estimate for both GI and PVC pipe, especially when one applies the factor of 0.8-0.9 to allow for possible increase in water flow rate in the future. The Reynolds numbers for pipes of diameters D_a and D_b are 47,500 and 60,980, respectively; both are turbulent.

64. For the given pipe size, Table 3.1 reports $D_{out} = 6.625$ in. and $D_{in} = 6.065$ in. For water at 10°C at which the density is $\rho = 999.7$ kg/m^3, Eqn (13.13) becomes

$$\begin{aligned} a_w &= \sqrt{\frac{(2.110 \times 10^9 \text{ N/m}^2)/999.7 \text{ kg/m}^3 \cdot (1 \cdot \text{kg m/s}^2)/\text{N}}{1 + 2 \cdot (2.11 \cdot 10^9/2.90 \times 10^9)/(6.625/6.065 - 1)}} \\ &= 354.9 \text{ m/s} \end{aligned}$$

where the bulk modulus for water, $B = 2.110 \times 10^9$ N/m^2, and elastic modulus for PVC, $E = 2.90 \times 10^9$ N/m^2, are as given in Section 13.17.

The flow speed in the pipe before the valve is closed, $\bar{u}$, is from the continuity equation, Eqn (2.21),

$$\bar{u} = \frac{Q}{A} = \frac{48 \text{ L/s} \cdot 0.001 \text{ m}^3/\text{L}}{\pi/4 \cdot (6.065 \text{ in.})^2} = 2.58 \text{ m/s}$$

The *change* in flow speed is thus,

$$\Delta\bar{u} = 0 - \bar{u} = -2.58 \text{ m/s}.$$

The magnitude of the pressure wave resulting from the sudden valve closure is from Eqn (13.12)

$$\Delta p = -999.7 \text{ kg/m}^3 \cdot 354.9 \text{ m/s} \cdot -2.58 \text{ m/s} = 470 \text{ kPa}$$

or ~93 m of water head at the location of the valve.

If the pipe material were GI, the above becomes $a_w = 1311$ m/s and $\Delta p = 3374$ kPa. This is equivalent to ~344 m of water head. Although these results are worst case, water hammer in the presence of steel (or galvanized iron) pipe could fail the water delivery pipe. This is especially worrisome if both PVC and GI are used in the same network. In this case, a pressure wave of large magnitude is produced in the steel pipe which, when encountering the PVC pipe, would very likely rupture.

Chapter 14 Solutions

65. *Solution from* `Mathcad` *worksheet*: Based on the material presented in Section 14.3, our inspection of Fig. 16.7 indicates that one air block will form in segment *b*. Our approach will be to use Eqn (14.7), the simple approach where

air compressibility is neglected, and Eqn (14.13) where compressibility is included. When we include air compressibility, recall that p_{a1} = 14.7 psi since all static pressures must be in absolute and h_{del} = 20.3 m (abs). Otherwise, we can use gage pressures of p_{a1} = 0 psi and h_{del} = 10 m.

First, we find the flow rate if there are no air blocks. From the geometry of Fig. 16.7 calculate $s = 0.131$. With F = 10 m/170 m = 0.0588, and λ = 1333.8 m/1311.1 m = 1.11, the `Mathcad` worksheet gives $Q = 0.904$ L/s. By comparison, both Eqs (9.2) and (9.3), which assume a constant friction factor of 0.03, predict only 0.3% higher, in nearly perfect agreement with the exact solution.

Now, neglect air compressibility and use Eqn (14.7) to calculate Q. With compressibility neglected, pipe segment b contains air over the entire segment length. The remainder of the pipe segments flow water. The reduced elevation head, $\Delta z_a + \Delta z_c + \Delta z_d$, is (100−20−20+40) m = 100 m, and the length of pipe flowing water, $L_a + L_c + L_d$, is (614.81 + 250.80 + 302.65) m = 1168.3 m. The corresponding values for s, F, and λ are 100 m/1300 m = 0.0769, 10 m/100 m = 0.100, and 1168.3 m/1311.3 m = 0.891, respectively. Through the `Mathcad` worksheet, we calculate Q = 0.0925 L/s, a reduction of ~90% compared with the case where there are no air pockets.

With air compressibility included, we use Eqn (14.13) together with the `Mathcad` worksheet to calculate the flow rate. Please refer to the notation appearing in Fig. 14.6 above to write the equations for $\Delta z_c(p_{a2})$ and $L_c^*(p_{a2})$. Obtain

$$\Delta z_c(p_{a2}) = [50 - 70 + (120 - 50)(1 - \frac{14.7 \text{ psia}}{p_{a2}})], \text{ m} \tag{16.23}$$

$$L_c^*(p_{a2}) = [250.80 + 165.50(1 - \frac{14.7 \text{ psia}}{p_{a2}})], \text{ m} \tag{16.24}$$

Finally, Eqs (14.13) for this exercise are written as

$$\rho g \Delta z_a - p_{a2} + p_{a1} = \frac{\rho}{2}(C_{L,a} + \alpha)(\frac{4Q}{\pi D^2})^2, \quad \text{Segment } a$$

$$\begin{aligned} \rho g \Delta z_c(p_{a2}) &+ p_{a2} - p_{c2} \\ &= \frac{\rho}{2} C_{L,c}(L_c^*(p_{a2}))(\frac{4Q}{\pi D^2})^2, \quad \text{Segment } c \end{aligned} \tag{16.25}$$

$$\begin{aligned} \rho g \Delta h_{del} &+ p_{c2} - p_{del} \\ &= \frac{\rho}{2} C_{L,d}(\frac{4Q}{\pi D^2})^2, \quad \text{Segment } d \end{aligned}$$

where p_{a1} (=14.7 psi) has been added to the first of these equations since all static pressures are in absolute.

The equations of Eqn (16.25) are solved in the Mathcad worksheet for p_{a2}, p_{c2}, and Q. After converting all static pressures to gage values, we obtain $p_{a2} = 22.5$ psig, $p_{c2} = 2.198$ psig, and $Q = 0.837$ L/s (~7.4% less than with no air pockets). The head $\Delta z_c(p_{a2})$ is 22.3 m, a positive value. This is contrasted with -20 m for the case where we assume incompressible air from above. The neglect of air compressibility produces an overly conservative result as discussed in Chapter 14.

$h_{del} := 7\ m$ $h_j := 10\ m$ $D_{12} := 1\ in$ $D_{23} := 1\ in$ $D_{34} := 1\ in$ $D_{35} := 1\ in$ guesses

Input Parameters:

$L_{13} := 350\ m$ $L_{34} := 230\ m$ $L_{35} := 320\ m$

$Q_{12} := 3.7 \frac{liter}{sec}$ $Q_{23} := Q_{12}$ $Q_{34} := 1.2 \frac{liter}{sec}$ $Q_{35} := Q_{12} - Q_{34}$

$K_{12} := 0$ $K_{23} := 0$ $K_{34} := 0$ $K_{35} := 0$

$L_{ebyD\_12} := 0$ $L_{ebyD\_23} := 0$ $L_{ebyD\_34} := 0$ $L_{ebyD\_35} := 0$

$\Delta z_{34} := 43\ m$ $\Delta z_{35} := 39\ m$

$R := 50\ m$ $z(x) := \sqrt{R^2 - x^2}$ $x := 1\ m, 2\ m .. 50\ m$

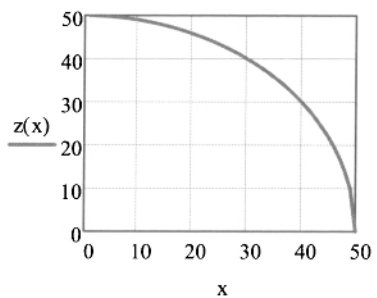

Δz.12, Δz.23, L.12, and L.23: $\Delta z_{12}(\gamma) := R\ (1 - \cos(\gamma))$ $\Delta z_{23}(\gamma) := R \cos(\gamma)$ $L_{12}(\gamma) := R\ \gamma$ $L_{23}(\gamma) := \frac{\pi}{2} R - R\ \gamma$

Figure 16.28 Page 1 of solution for Exercise 47.

$$\gamma := 0, 0.01 .. \frac{\pi}{2}$$

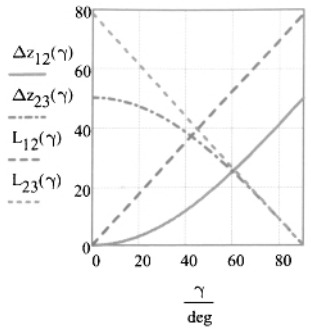

Define energy equation functions:

$$r_{12}(h_2, D_{12}, \gamma) := \Delta z_{12}(\gamma) - h_2 - K_{12} + \alpha\left(Re\left(|Q_{12}|, D_{12}\right)\right) + fric\_fac\ Re\left(|Q_{12}|, D_{12}\right), \frac{\varepsilon}{D_{12}} \quad \frac{L_{12}(\gamma)}{D_{12}} + L_{ebyD\_12} \quad \frac{8\ Q_{12}^{\ 2}}{\pi^2\ g\ D_{12}^{\ 4}}$$

$$r_{23}(h_2, h_3, D_{23}, \gamma) := \Delta z_{23}(\gamma) + h_2 - h_3 - K_{23} + \alpha\left(Re\left(|Q_{23}|, D_{23}\right)\right) + fric\_fac\ Re\left(|Q_{23}|, D_{23}\right), \frac{\varepsilon}{D_{23}} \quad \frac{L_{23}(\gamma)}{D_{23}} + L_{ebyD\_23} \quad \frac{8\ Q_{23}^{\ 2}}{\pi^2\ g\ D_{23}^{\ 4}}$$

$$r_{34}(h_3, D_{34}) := \Delta z_{34} + h_3 - h_{del} - K_{34} + fric\_fac\ Re\left(|Q_{34}|, D_{34}\right), \frac{\varepsilon}{D_{34}} \quad \frac{L_{34}}{D_{34}} + L_{ebyD\_34} \quad \frac{8\ Q_{34}^{\ 2}}{\pi^2\ g\ D_{34}^{\ 4}}$$

$$r_{35}(h_3, D_{35}) := \Delta z_{35} + h_3 - h_{del} - K_{35} + fric\_fac\ Re\left(|Q_{35}|, D_{35}\right), \frac{\varepsilon}{D_{35}} \quad \frac{L_{35}}{D_{35}} + L_{ebyD\_35} \quad \frac{8\ Q_{35}^{\ 2}}{\pi^2\ g\ D_{35}^{\ 4}}$$

Figure 16.29 Page 2 of solution for Exercise 47.

$$Tcost(D_{12}, D_{23}, D_{34}, D_{35}, \gamma) := linterp(diam, cost, D_{12})\, L_{12}(\gamma) + linterp(diam, cost, D_{23})\, L_{23}(\gamma) \ldots + linterp(diam, cost, D_{34})\, L_{34} + linterp(diam, cost, D_{35})\, L_{35}$$

Solve in Given...Find block

$$\text{Given} \quad 0 = r_{12}(h_2, D_{12}, \gamma) \quad 0 = r_{23}(h_2, h_3, D_{23}, \gamma) \quad 0 = r_{34}(h_3, D_{34}) \quad 0 = r_{35}(h_3, D_{35})$$

$$D_p(\gamma, h_2, h_3) := \text{Find}(D_{12}, D_{23}, D_{34}, D_{35})$$

$\gamma := 3\,\text{deg}, 5\,\text{deg} .. 89\,\text{deg}$ $\quad h_2 := 1\,\text{m}$ $\quad h_3 := 7\,\text{m}$: plot to see what solution will look like

$$T_c(h_2, h_3, \gamma) := Tcost(D_p(\gamma, h_2, h_3)_1, D_p(\gamma, h_2, h_3)_2, D_p(\gamma, h_2, h_3)_3, D_p(\gamma, h_2, h_3)_4, \gamma)$$

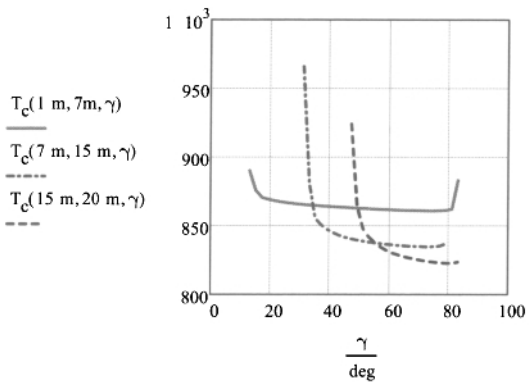

$\gamma := 60\,\text{deg}, 63\,\text{deg} .. 87\,\text{deg}$: seek to find h.2 and h.3 that minimize cost

$$\text{Given} \quad h_2 > 0\,\text{m} \quad h_3 > 0\,\text{m} \quad (h_{2soln}(\gamma) \;\; h_{3soln}(\gamma)) := \text{Minimize}(T_c, h_2, h_3)^T$$

Figure 16.30 Page 3 of solution for Exercise 47.

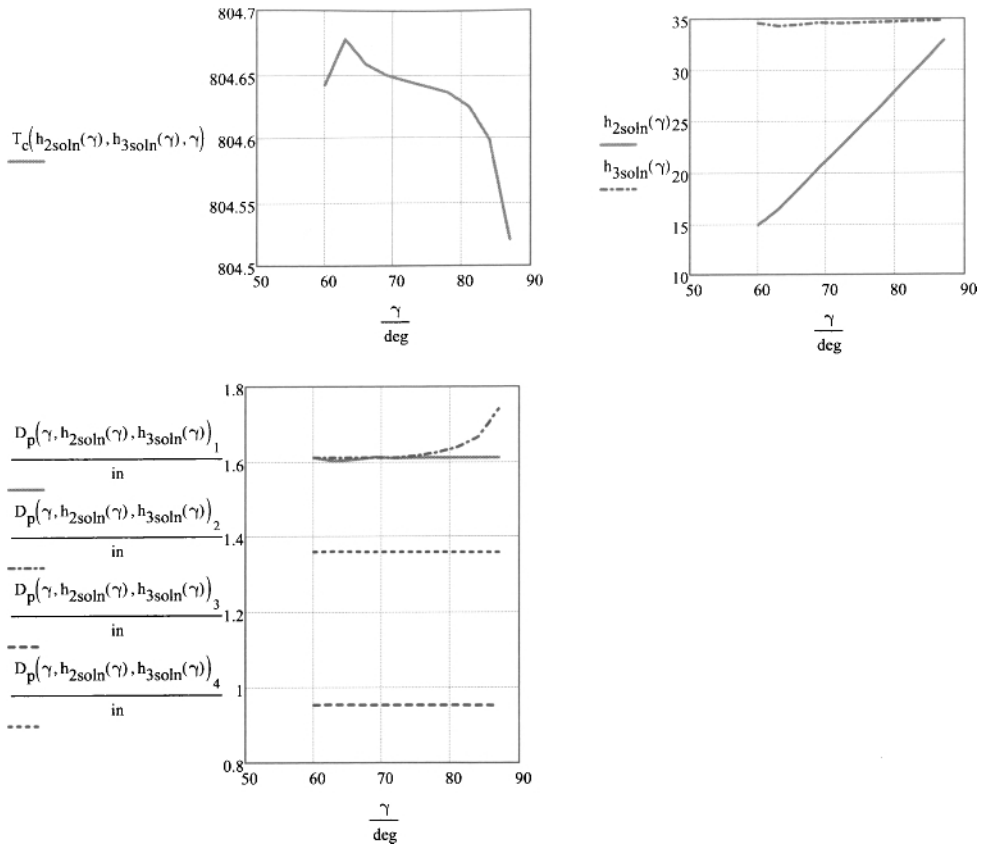

Figure 16.31 Page 4 of solution for Exercise 47.

Branching flow 3-pipe problem optimized

Water properties $\rho := 1000\frac{kg}{m^3}$ $\nu := 13.0710^{-7}\cdot\frac{m^2}{sec}$ $sec := 1\cdot s$ $TOL := 1\cdot10^{-10}$

ORIGIN := 1

dollar := 1

IPS sch. 40 PVC pipe cost

$$diam := \begin{pmatrix} 0.622 \\ 0.824 \\ 1.049 \\ 1.610 \\ 2.067 \\ 2.469 \\ 3.068 \\ 4.026 \end{pmatrix}\cdot in \qquad cost := \begin{pmatrix} 0.60 \\ 0.82 \\ 1.02 \\ 1.74 \\ 2.40 \\ 3.94 \\ 5.58 \\ 7.75 \end{pmatrix}\cdot\frac{dollar}{m}$$

$$Re(Q,D) := \frac{4\cdot Q}{\pi\cdot D\cdot\nu} \qquad \varepsilon := 5\cdot10^{-6}\cdot ft$$

absolute roughness, ft (increase 100 times for galvanized steel)

friction factor that spans the laminar/turbulent range. ebyD is relative roughness.

$$funct(f,R,ebyD) := \frac{f}{2} - \left[\left(\frac{4}{R\cdot\sqrt{\frac{f}{8}}}\right)^{24} + \left[\left(\frac{18765}{R\cdot\sqrt{\frac{f}{8}}}\right)^{8} + \left[3.29 - \frac{227}{R\cdot\sqrt{\frac{f}{8}}} + \left(\frac{50}{R\cdot\sqrt{\frac{f}{8}}}\right)^{2} \ldots + \frac{1}{0.436}\cdot\ln\left(\frac{R\cdot\sqrt{\frac{f}{8}}}{1 + 0.301\cdot R\cdot\sqrt{\frac{f}{8}}\cdot ebyD\cdot 2}\right)\right]^{16}\right]^{-\frac{3}{2}}\right]^{\frac{1}{12}}$$

$$fric\_fac(Re,ebyD) := root(funct(f1,Re,ebyD),f1,0.0001,0.2)\cdot4$$

friction factor

$\alpha(R) := if(R < 2100, 2, 1.05)$

guesses: $h_j := 10\cdot m$ $D_{13} := 1\cdot in$ $D_{23} := 1\cdot in$ $D_{34} := 2\cdot in$

Input Parameters:

$L_1 := 50\cdot m$ $Q_{23} := 2.1\cdot\frac{liter}{sec}$ $K_{13} := 0$ $L_{ebyD\_13} := 0$ $s := 4\cdot\%$

$L_3 := 1600m$ $Q_{13} := 1.3\cdot\frac{liter}{sec}$ $K_{23} := 0$ $L_{ebyD\_23} := 0$ $z_1 := L_3\cdot s$

$Q_{34} := Q_{13} + Q_{23}$ $K_{34} := 0$ $L_{ebyD\_34} := 0$ $z_1 = 64m$

$$\gamma_{max} := atan\left(\frac{L_3}{L_1}\right) \qquad \gamma_{max} = 88.21deg$$

: maximum angle for γ given the problem geometry

Figure 16.32 Page 1 of solution for Exercise 50.

Define energy equation functions:

$$r_{13}(h_j, D_{13}, \gamma) := s \cdot L_1 \cdot \tan(\gamma) - h_j - \left[K_{13} + \alpha\left(\mathrm{Re}\left(|Q_{13}|, D_{13}\right)\right) + \mathrm{fric\_fac}\left(\mathrm{Re}\left(|Q_{13}|, D_{13}\right), \frac{\varepsilon}{D_{13}}\right)\left(\frac{L_1}{D_{13}\cdot\cos(\gamma)} + L_{ebyD\_13}\right)\right] \cdot \frac{8 \cdot Q_{13}^2}{\pi^2 \cdot g \cdot D_{13}^4}$$

$$r_{23}(h_j, D_{23}, \gamma) := s \cdot L_1 \cdot \tan(\gamma) + h_j - \left[K_{23} + \alpha\left(\mathrm{Re}\left(|Q_{23}|, D_{23}\right)\right) + \mathrm{fric\_fac}\left(\mathrm{Re}\left(|Q_{23}|, D_{23}\right), \frac{\varepsilon}{D_{23}}\right)\left(\frac{L_1}{D_{23}\cdot\cos(\gamma)} + L_{ebyD\_23}\right)\right] \cdot \frac{8 \cdot Q_{23}^2}{\pi^2 \cdot g \cdot D_{23}^4}$$

$$r_{34}(h_j, D_{34}, \gamma) := z_1 - s \cdot L_1 \cdot \tan(\gamma) + h_j - \left[K_{34} + \mathrm{fric\_fac}\left(\mathrm{Re}\left(|Q_{34}|, D_{34}\right), \frac{\varepsilon}{D_{34}}\right)\left(\frac{L_3 - L_1 \cdot \tan(\gamma)}{D_{34}} + L_{ebyD\_34}\right)\right] \cdot \frac{8 \cdot Q_{34}^2}{\pi^2 \cdot g \cdot D_{34}^4}$$

$$\mathrm{Tcost}(D_{13}, D_{23}, D_{34}, \gamma) := \mathrm{linterp}(\mathrm{diam}, \mathrm{cost}, D_{13})\frac{L_1}{\cos(\gamma)} + \mathrm{linterp}(\mathrm{diam}, \mathrm{cost}, D_{23})\frac{L_1}{\cos(\gamma)} + \mathrm{linterp}(\mathrm{diam}, \mathrm{cost}, D_{34})\left(L_3 - L_1 \cdot \tan(\gamma)\right)$$

Solve in Given...Find block

Given $\quad 0 = r_{13}(h_j, D_{13}, \gamma) \quad 0 = r_{23}(h_j, D_{23}, \gamma) \quad 0 = r_{34}(h_j, D_{34}, \gamma) \quad D_p(\gamma, h_j) := \mathrm{Find}(D_{13}, D_{23}, D_{34})$

$\gamma := 3 \cdot \mathrm{deg}, 5 \cdot \mathrm{deg} .. \gamma_{max} \quad h_j := 0.1 \cdot m$

$T_c(h_j, \gamma) := \mathrm{Tcost}\left(D_p(\gamma, h_j)_1, D_p(\gamma, h_j)_2, D_p(\gamma, h_j)_3, \gamma\right)$

Given $\quad h_j > 0 \cdot m \quad h_j < s \cdot L_1 \cdot \tan(\gamma) \quad h_{soln}(\gamma) := \mathrm{Minimize}(T_c, h_j)$

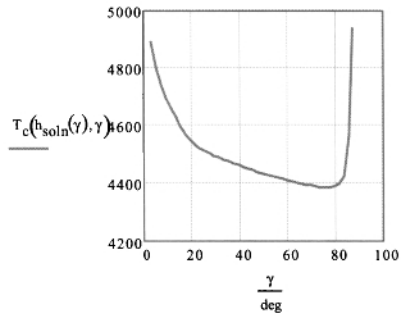

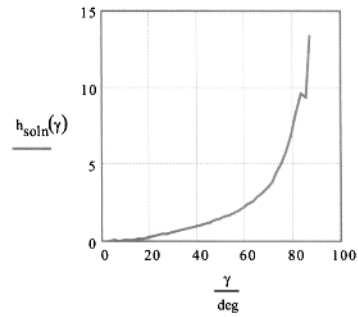

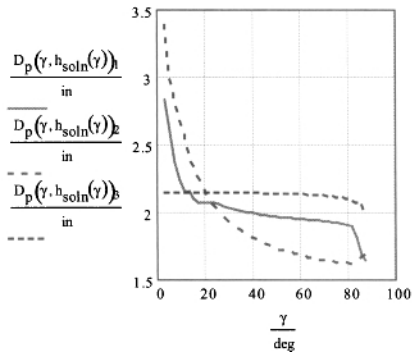

$$\frac{L_1}{\cos(77 \cdot \mathrm{deg})} = 222.3\mathrm{m}$$

$$L_3 - L_1 \cdot \tan(77 \cdot \mathrm{deg}) = 1383.4\mathrm{m}$$

Figure 16.33 Page 2 of solution for Exercise 50.

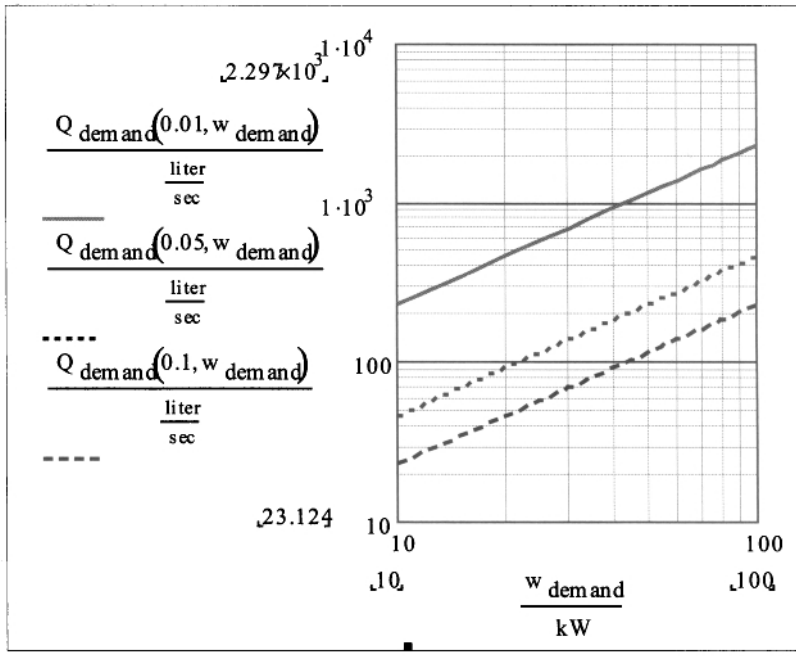

Figure 16.34 Solution for Exercise 56.

This page intentionally left blank

Appendix A

List of Mathcad Worksheets

The Mathcad worksheets (and other programs) supplied with this book and the sections in which they appear are as follows:

- Chapter 2:
  - friction factor.xmcd (Section 2.2.2)
  - HydraulicGradient.xmcd (textbox B.2.6)
- Chapter 4:
  - single pipe example-method 3.xmcd (Section 4.5.3)
- Chapter 8:
  - SinglePipeNetworkDesign_Appendix.xmcd (Sections 8.2- 8.5)
  - SinglePipeNetworkDesign_Metric_Appendix.xmcd (Sections 8.2-8.5)

*

  - example problem on peaks.xmcd (Section 8.6)
  - site_survey_data.xmcd (Section 8.7)
  - Tank_Draining.xmcd (Section 8.8)

- Chapter 10:
  - Optimization_TankHeightvsPipeSize.xmcd (Section 10.6)

- Chapter 11:
  - BranchingPipeExample.xmcd (Section 11.4)
  - NumberPipesSeries_Example.xmcd (Section 11.5.1)
  - SeriesPipeExample_equalQ_3pipe_withcost.xmcd (Section 11.5.1)
  - BranchPipeExample_4pipe_withcost_ver2.xmcd (Section 11.6.1)
  - BranchPipeExample_4pipe_withcost_ver3.xmcd (Section 11.6.6)
  - LoopExample_withcost_ver3.xmcd (Section 11.7)
  - LoopExample_withcost_ver8.xmcd (Section 11.7)
  - BranchPipeExample_4pipe_withcost_vectorized_ver3.xmcd (Section 11.8.3)

- Chapter 12:
  - microhydro_theoretical_power.xmcd (Section 12.2)

- Chapter 13:
  - Storage Volume Calculation-Textbox_Example.xlsx (A Microsoft Excel spreadsheet; Section 13.6)

- Chapter 14
  - pipe sizing for air block example.xmcd (Section 14.5)

- Chapter 15:
  - BranchNetwork_Philippines_withcost_ver1.xmcd (Section 15.3.3.3)

The worksheets have been successfully run on Mathcad versions 11, 13, and 14 (the current version at the time of this writing). There have been a few syntax changes and additions during the time of the release of these versions. One is for the root function. The earliest versions require an initial guess outside of the root function whereas, in the later versions, a range of values over which the root function looks for a solution is required within the root function itself. It appears that versions 11–14 allow the latter syntax. In the later versions, there also appear to be improvements to the Minimize function. The earliest versions take considerably longer to run worksheets that use Minimize compared with version 14; in some cases one or two orders-of-magnitude more time on the same computer. In addition, version 14 contains a time

function that can be used to calculate the execution time for a calculation. Earlier versions will not recognize this function.

Note that some worksheets have different extensions with the same name. These are written to run in two different versions of Mathcad. The extension mcd is for Mathcad version 11. The the extension xmcd is for Mathcad version 14 or later. Mathcad versions 11 and later can successfully read files with the extension mcd, but only Mathcad version 14 (or later) will read files with the extension xmcd.

Also, note that several worksheets appear in metric form where the worksheet name includes the word Metric. An example is SinglePipeNetworkDesign_Appendix and SinglePipeNetworkDesign_Metric_Appendix in the above list.

This page intentionally left blank

Appendix B

Calculating Pipe Length and Mean Slope from GPS Data

B.1 THE BASICS: NORTHING AND EASTING

Dimensions of the potential site for a water network can be measured with land-based surveying equipment, such as a transit or an Abney level and measuring tape. Alternately, more sophisticated electronic equipment may be used, such as a global positioning system or GPS. A GPS uses signals transmitted between itself and satellites to accurately determine the position of the device. The position is given in terms of three coordinates, latitude, longitude, and elevation from sea level. In principle, these are sufficient to allow us to determine everything we need for the survey. However, latitude and longitude are not immediately useful because they are angles measured from the equatorial plane for latitude (between 0 and 90°; positive for the northern hemisphere, negative for the southern) and the prime meridian for longitude

*

Gravity-Driven Water Flow in Networks. By Gerard F. Jones

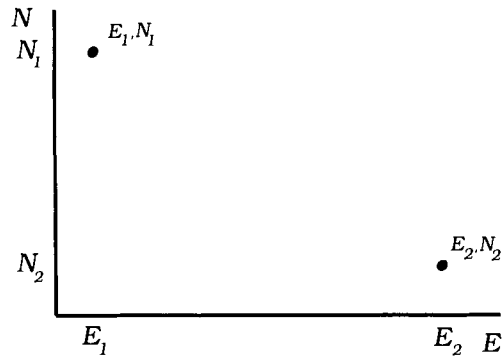

Figure B.1 Easting–Northing coordinates for two points on the earth's surface.

(between 1 and 180°, positive for the eastern hemisphere, negative for the western) and we require distances. A conversion is needed.

Universal Transverse Mercator (UTM[1]) coordinates are Cartesian coordinates that have been converted from latitude and longitude angles. The two coordinates are referred to as *Easting* and *Northing*, where Easting is the distance coordinate in the east–west direction (larger numbers are east of smaller numbers) and Northing is that in the north–south direction (larger numbers are north of smaller numbers). In engineering, we normally refer to Easting and Northing as the x and y coordinates, respectively; see Figs. B.1 and B.2 for a comparison between the two.

The conversion is accomplished by applying formulas from geometry relating angular measurements and distances at the earth's surface. For example, 1° of longitude at the equator (0° latitude) is 111.3 km to better than 0.1% depending on longitude. This distance gets smaller with increases in either north or south latitude. Fortunately, we do not have to program these formulas ourselves since others were kind enough to do this for us.

A Microsoft Excel spreadsheet written by Dutch (2009) is available for the conversions. The inputs include the model for the shape of the earth, latitude and longitude values entered in either decimal or degree-minutes-seconds (DMS) format, and specifications of north or south for latitude and east or west for longitude. For the DMS format there are 60 minutes in a degree and 60 seconds in a minute. The conversion between the DMS and decimal format is thus,

$$\Theta = D + \frac{M}{60} + \frac{S}{3600} \tag{B.1}$$

[1]The Transverse Mercator Projection that is used on many world maps is a cylindrical projection. In this projection, the earth is contained within an imaginary cylinder that contacts the globe along its equator. The earth is then projected on the cylinder to produce the Mercator Projection. To visualize this, imagine a flashlight positioned on the north-south axis (and normal to it) running through the globe, pointing outward toward the cylinder. Note that landmasses at the larger north and south latitudes will be compressed in the north–south direction relative to those at the equator once project onto the cylinder. This is a characteristic of the Mercator Projection.

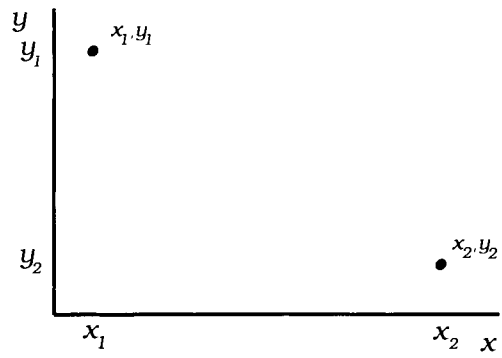

Figure B.2 Easting–Northing coordinates of Fig. B.1 written in conventional x-y form.

where Θ is the latitude or longitude angle in decimal format. For example, a latitude of 19°, 45', 33" converts to 19.759167°. Note the designations of a single prime for minutes and a double prime for seconds in the DMS format.

The model for the earth's shape essentially means the assumed diameters of the earth at the equator and poles; it is generally understood that the earth is larger at the equator than at the poles. Different models, referred to as "datums", use very slightly different diameters. The most recent datums are NAD83/WGS84 (World Geodetic System 1984) and GRS80 (the foundation for the North American Datum of 1983 or NAD83) which agree with each other to within 1 part in 10,000. Use the NAD83/WGS84 datum unless information is available to dictate otherwise.

A word about accuracy of the results from these calculations is in order. Since there are at most 111,300 m in 1° of longitude, 1 m of resolution in the Easting coordinate will require certainty in longitude to *five* decimal places. The same accuracy in latitude is required for the Northing coordinate. Longitude or latitude data to only four decimal places will produce, at best, certainty to ±10 m. The accuracy of readings from a standard GPS receiver is also unlikely to be greater than ±10 m.[2]. Thus, the understanding is that calculations involving dimensions from GPS data will be accurate only to this order of magnitude. To obtain the most meaningful results at any accuracy level, multiple latitude and longitude readings, say 10 or more, are recommended before converting the average of these readings to UTM coordinates.

More accurate horizontal and elevation measurements, at the cost of additional time and perhaps expense, are obtained by surveying the site with a transit as described in Chapter 13.

[2]One popular brand of GPS in the United States, Garmin, states that its GPS receivers are accurate to within 15 m on average (Anon., 2009) This is probably a worst-case estimate.

B.2 AN EXAMPLE

Consider the calculation of Northing and Easting coordinates for two locations listed in Table B.1.[3] Download the Excel spreadsheet (Dutch, 2009) and launch Excel to run the sheet. Input the data in DMS format and obtain the results as shown in Table B.2.

Table B.1 Data for a Northing-Easting Example

Name	Latitude	Longitude
Treasure Island	43° 33' 0"	−71° 17' 0"
Diamond Island	43° 34' 25"	−71° 19' 20"

Table B.2 Northing–Easting Results

Location	Northing Coordinate (m)	Easting Coordinate (m)
Treasure Island	$N_1 = 4,824,427.26$	$E_1 = 315,555.29$
Diamond Island	$N_2 = 4,827,136.64$	$E_2 = 312,487.09$

The Pythagorean theorem is used to calculate the distance between the two locations. Obtain

$$\ell = [(N_1 - N_2)^2 + (E_1 - E_2)^2]^{1/2} \tag{B.2}$$

The distance between the two locations is calculated as $\ell = 4093.24$ m. If this is the final result to be reported, it would be rounded to the nearest 10 m. We get $\ell = 4090$ m = 4.09 km.

To calculate the mean slope between these two locations, assuming a source at Treasure Island $\Delta z = 10$ m higher than the delivery location on Diamond Island, from the definition of slope, we use

$$s = \frac{\Delta z}{\ell} \tag{B.3}$$

from which we get $s = 0.244\%$.

From the Pythagorean theorem we can also calculate the pipe length if run directly from source to delivery or tank location. Thus,

$$L = (\ell^2 + \Delta z^2)^{1/2} = [(N_1 - N_2)^2 + (E_1 - E_2)^2 + \Delta z^2]^{1/2} \tag{B.4}$$

We get $L = 4093.25$ m. Because of the relatively small value of Δz, L and ℓ are essentially identical.

[3]The locations are on Lake Winnipesaukee, New Hampshire. This is the location of the author while completing this appendix.

References

Anon. How Accurate is GPS? http://www8.garmin.com/aboutGPS/, 2009. [Online; accessed 3-November-2009].

S. Dutch. Converting UTM to Latitude and Longitude (or vice versa). Technical report, University of Wisconsin – Green Bay, Green Bay, WI, 2009. URL \url{http://www.uwgb.edu/DutchS/UsefulData/UTMFormulas.HTM}. [Online; accessed 18-November-2009].

This page intentionally left blank

Appendix C

Mathcad Tutorial

The following tutorial was extracted from `Mathcad` ver. 11. (with permission). The areas covered include fundamental math operations (Figs. C.1–C.16), plotting (Figs. C.17–C.18), the `root` function (Figs. C.19–C.20), and `Given ... Find` construction (Fig. C.21). There is also a brief write-up on the `Minimize` function. If using a later version, or for information on other topics, please refer to the version's tutorial. Small changes in syntax (sometimes) and new features (usually) appear in later versions.

*

Basic Math

Entering Math Calculations

Math in a Mathcad worksheet appears in familiar math notation — multiplication as a raised dot, division with a fraction bar, exponents in a raised position, and built-up fractions just as you would see in a book. Entering math expressions is very straightforward. Here are some quick exercises to learn a few keystrokes and toolbar buttons. You will also learn how to get a numeric result and to modify its format.

Definitions

numeric expressions— expressions involving numbers and operators

symbolic expressions— expressions involving numbers, unknowns (variables), and operators

Calculator toolbar— toolbar containing buttons commonly found on a calculator and other math operator buttons

result— evaluation of numeric expression

result format— type of result, including: decimal, fractional, scientific, etc.

Practice

Entering a Numeric Expression

Type this:	Get this:	**Tip:** Don't press the Spacebar between parts of the expression. Mathcad enters the correct spacing as you type.
2+1/2	$2 + \frac{1}{2}$	

Type this:	Get this:
(9+3)/(2*4-5)	$\frac{(9 + 3)}{(2 \times 4 - 5)}$

Figure C.1 Mathcad tutorial - basic math; page 1.

Type this:	Get this:
3+\2	$3 + \sqrt{2}$

Entering a Symbolic Expression

Type this:	Get this:
3x+2y	$3x + 2y$
\16–d^2	$\sqrt{16 - d^2}$
log(x^2)–log(1000)	$\log(x^2) - \log(1000)$

Using the Calculator Toolbar

The **Calculator** toolbar is used primarily for work within the Worksheet window. It may already be on your desktop, but hidden under the Resources window. Click in the Worksheet window and move the **Calculator** toolbar over to the far left. Then bring your Resources window back up, which will make it the "active" window.

If the **Calculator** toolbar is not open, in the Worksheet window, follow these steps:

Select **Toolbars** ⇒ **Calculator** from the **View** menu:

Get this:

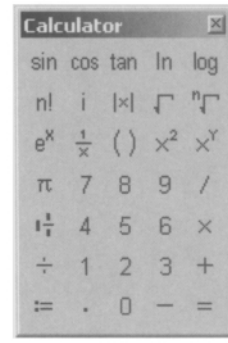

Tip: All toolbars are floating, which means you can move them wherever you want in the window by clicking the top, usually blue, bar and dragging it.

Figure C.2 Mathcad tutorial - basic math; page 2.

With your **Calculator** toolbar in view next to the Resources window and your Resources window active:

Click the following buttons in order:

2 π

Get this:

2π

Click the following buttons in order:

|x| − 8 · 9

Get this:

$|-8.9|$

Getting a Result

Type this:

2+1/2=

Get this:

$2 + \frac{1}{2} = 2.5$

Tip: Notice that the result is in **decimal** format, the Mathcad default.

Type or dick this:

[Shift]\−8.9=

or

|x| − 8 · 9 =

Get this:

$|-8.9| = 8.9$

Figure C.3 Mathcad tutorial - basic math; page 3.

Changing a Result to Fractional Format

Click on the right side of this result and select **Result** from the **Format** menu:

$$2 + \frac{1}{2} = 2.5$$

Get this:

$$2 + \frac{1}{2} = 2.5$$

Then this:

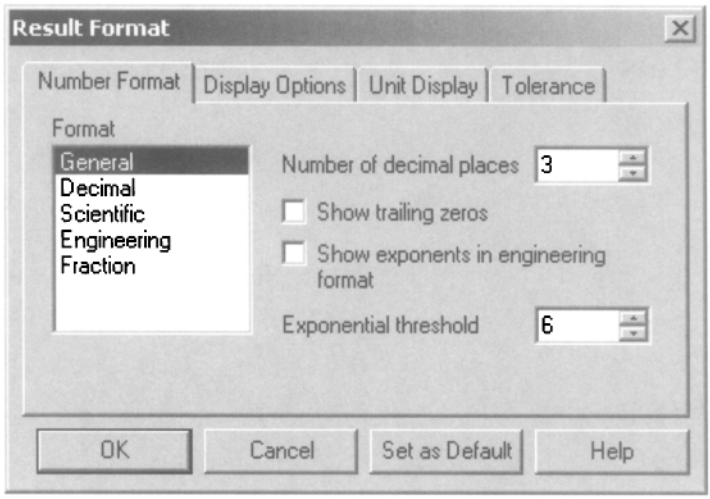

Click **Fraction** on the **Number Format** page to select it and click "OK":

Then this:

$$2 + \frac{1}{2} = \frac{5}{2}$$

Figure C.4 Mathcad tutorial - basic math; page 4.

Building Math Expressions

Click to position the red crosshair to the right and type the following examples. Pay particular attention to what happens when you press the spacebar. The spacebar moves you out of the denominator of a fraction.

EXAMPLE 1

Type this: Get this:

1/2 [Spacebar] +2 $\frac{1}{2} + 2$

When you are in an exponent and you want to continue entering more of the expression, you use the Spacebar to move down from the exponent.

EXAMPLE 2

Type this: Get this:

x^2 [Spacebar] +2x+1 $x^2 + 2x + 1$

Practice

Entering an Expression

3/4 [Spacebar] +8/9 $\frac{3}{4} + \frac{8}{9}$

Type this: Get this:

2x^3 [Spacebar] −3x^2 [Spacebar] +x−1 $2x^3 - 3x^2 + x - 1$

\a−1 [Spacebar] [Spacebar] + a $\sqrt{a - 1} + a$

Tip: You might need to press [Spacebar] two or more times to get to the right position in the expression before you can continue typing.

Type this: Get this:

\3/4 [Spacebar] +1/2 [Spacebar][Spacebar][Spacebar] /6

$$\frac{\sqrt{\frac{3}{4} + \frac{1}{2}}}{6}$$

Type this: Get this:

x+6[Spacebar]*(x^3[Spacebar]-1) $(x + 6)\left(x^3 - 1\right)$

The exponent operator in Mathcad is called a *sticky* operator because your keystrokes will stick to the exponent position until you specifically move back to the baseline by pressing [Spacebar]. Other sticky operators include square roots, subscripts, and division.

Figure C.5 Mathcad tutorial - basic math; page 5.

Using the Calculator Toolbar

Remember that to use the **Calculator** toolbar in conjunction with the Resources window, you must move it over to the far left in your Worksheet window. Then bring your Resources window back up, which will make it the "active" window.

With your **Calculator** toolbar in view next to the Resources window and your Resources window active:

Click and type this:

2 π r^2 [Spacebar] − 4 π r

Get this:

$2\pi r^2 - 4\pi r$

Click and type this:

1 [Tab] 2 [Tab] 3 [Spacebar] +5/8

Get this:

$1\frac{2}{3} + \frac{5}{8}$

Tip: If you select an operator, such as the mixed number operator, by clicking a button on the **Calculator** toolbar, you can use the Tab key to move from one placeholder to another.

Click and type this:

( ) x−1 [Spacebar] [Spacebar] ( )
x+2 [Spacebar] [Spacebar] [Spacebar]
/x+4

Get this:

$$\frac{(x-1)(x+2)}{x+4}$$

Getting a Result

Click and type this:

8 [Tab] 3 =

Get this:

$\sqrt[3]{8} = 2$

Tip: To get a result, you can press equal [=] no matter where the blue editing lines are in a numeric expression.

Click and type this:

log 1000 [Spacebar] − log 10000 =

Get this:

$\log(1000) - \log(10000) = -1$

Figure C.6 Mathcad tutorial - basic math; page 6.

Editing Math Expressions

Note: The exercises in this tutorial require you to work within the Worksheet window. To copy the contents of this lesson into the Worksheet window, choose **Select All** from the **Edit** menu. Then, either drag and or copy and paste all the regions into your Worksheet window.

Practice

Using the Spacebar, Backspace, Delete, Insert, and arrow keys to change math expressions:

1. Click between the 3 and 4 in the expression below; use the left arrow key to move the **blue editing bar** between the 1 and 2:

1234

Get this:

Then this:

Then press [Backspace] to delete the 1 and press 5 to change the whole number to 5234:

2. Click anywhere in the expression below; use the [Spacebar] to capture the entire expression with the blue editing lines:

$$\frac{1234}{12}$$

Get this:

or

Then this:

Then, if the vertical blue editing line is to the left, press **[Del]** to **highlight** the expression; if the vertical blue editing line is to the right, press [Backspace]:

Press [Del] or [Backspace] again to delete the region.

3. Click the 4 in the denominator of the fraction, 3/4. Use the right arrow key to move over to the 4 in the denominator of the fraction, 1/4:

$$\frac{3}{4} + \sqrt{\frac{1}{4} - 4}$$

Get this:

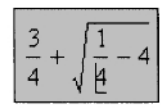

Then this:

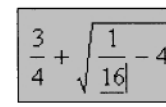

Figure C.7 Mathcad tutorial - basic math; page 7.

Press [Del] to delete the 4 and press 16 to change the fraction:

Press **[Insert]** to **move** the vertical blue editing line from right to left:

Then this:

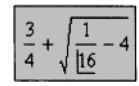

Then this:

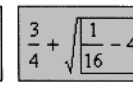

Press **[Spacebar]** enough times to select the entire expression under the root:

Press [Del] twice to delete the expression under the root and press 9= to get a result:

Then this:

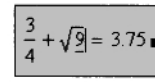

4. Click the 2 and then press [Del] to delete the +:

Get this:

Then this:

Press – to insert a subtraction sign:

Click the 1 and press [Spacebar] to select the fraction. Then press [Insert] to change the direction of selection:

Press [Backspace] to delete the subtraction sign. Then press + to put back the addition sign:

Then this:

Then this:

5. In white space near this expression, click, hold, and drag to select it:

Get this:

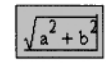

Press [Insert] to change the direction of selection. Then press + to insert an addition sign and an empty placeholder:

Then this:

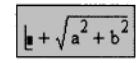

In the placeholder, type:

\a^2 [Spacebar] –b^2

Then this:

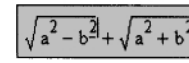

Then this:

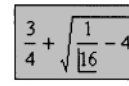

Then this:

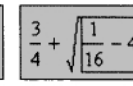

Press [Del] to delete the 4 and press 16 to change the fraction:

Press **[Insert]** to **move** the vertical blue editing line from right to left:

Press **[Spacebar]** enough times to select the entire expression under the root:

Press [Del] twice to delete the expression under the root and press 9= to get a result:

Then this:

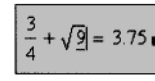

Figure C.8 Mathcad tutorial - basic math; page 8.

Defining Variables

Often you will want to define a value as a variable you can use in subsequent calculations. In this worksheet, you will practice defining and viewing single-value and range variables.

Practice

Defining a Single-Value Variable

Type this:	Get this:
x:2	$x := 2$
Type this:	Get this:
dist:25m	$dist := 25m$

Tip: If you don't know the abbreviation for a unit you are trying to use, select **Unit** from the **Insert** menu and browse for the units you want.

Type this:	Get this:
v.1:20mi/hr	$v_1 := 20\frac{mi}{hr}$

Tip: This definition uses a literal subscript, a common notation in science. You get a literal subscript by pressing the period (.) key after the variable name.

Notice that when you type the colon [:] key or press the assignment operator key

on the **Calculator** toolbar, Mathcad displays :=. The assignment operator (colon equals) in Mathcad is used for definitions.

Figure C.9 Mathcad tutorial - basic math; page 9.

Defining a Range Variable

Before starting these exercises, display the Matrix toolbar on your desktop by selecting **Toolbars ⇒ Matrix** from the **View** menu.

Remember that to use a toolbar in conjunction with the Resources window, you must move it over to the far left in your Worksheet window. Then bring your Resources window back up, which will make it the "active" window.

With your Matrix toolbar in view next to the Resources window and your Resources window active:

Click or type this:

g: **1 [Tab] 10**

Get this:

$g := 1..10$

Tip: This definition will give you a range of numbers between 1 and 10 at whole number increments.

Type this:

n:3.5;12.5

Get this:

$n := 3.5..12.5$

Tip: This definition will give you a range of numbers between 3.5 and 12.5 at whole number increments.

Notice that when you type the semicolon character, it displays on the screen as two dots (..) surrounded by placeholders. This is Mathcad's *range variable* operator.

n:3.5,4.0;12.5

Get this:

$n := 3.5, 4.0..12.5$

Tip: This definition will give you a range of numbers between 3.5 and 12.5 in increments of 0.5.

Type this:

h:1/4 [Spacebar] ,1/2 [Spacebar] ;7/4

Get this:

$h := \frac{1}{4}, \frac{1}{2}..\frac{7}{4}$

Tip: This definition will give you a range of numbers between $\frac{1}{4}$ and $\frac{7}{4}$ in increments of $\frac{1}{4}$.

Figure C.10 Mathcad tutorial - basic math; page 10.

Calculating with Variables

In this worksheet, you will practice calculating results based on variables you have defined. Then, you can practice modifying your variable values and watching your calculations update automatically.

Practice

Calculating a result based on one or more variables:

Type this:	Get this:
x:2	$x := 2$
Then, type this:	Get this:
y:x^2 [Spacebar] −1	$y := x^2 - 1$
Then, this:	Get this:
y=	$y = 3$

Type this:	Get this:
distance:1356ft	$distance := 1356ft$
Then, type this:	Get this:
rate:distance/42.4s	$rate := \frac{distance}{42.4s}$
Then, this:	Get this:
rate=	$rate = 9.748\frac{m}{s}$

Notice that Mathcad uses scientific units as the default unit. You can change the default unit system under **Tools ⇒ Worksheet Options**

Type this:	Get this:
a:39 and **b:52**	$a := 39$ $b := 52$
Then, type this:	Get this:
c:\a^2 [Spacebar]+b^2	$c := \sqrt{a^2 + b^2}$
Then, this:	Get this:
c=	$c = 65$

Modifying a Variable to Update a Result

Click the right side of this definition.
Backspace over 1, type 3, and press [Enter].

$time := 1hr$

Figure C.11 Mathcad tutorial - basic math; page 11.

Watch this calculation update:

$$\frac{50\text{m}}{\text{time}} = 0.031\text{mph}$$

Click the right side of the definition for "losses". Backspace over 3, type 4, and press [Enter].

wins:= 11

losses:= 3

Watch this calculation update:

$$\frac{\text{wins}}{\text{losses} + \text{wins}} = \frac{11}{14}$$

Click the right side of the definition for length. Backspace over 10m, type 12m, and press [Enter].

length:= 10m

Follow the same instructions to change the width from 30m to 31.6m

width:= 30yd

Watch this calculation update:

$$\text{Area} := \text{length} \times \text{width}$$

$$\text{Area} = 274.32\text{m}^2$$

Click the right side of the definition for height. Backspace over 2.9m, type 3m, and press [Enter].

height:= 2.9m

Watch this calculation update:

$$\text{Volume} := \text{Area} \times \text{height}$$

$$\text{Volume} = 795.528\text{m}^3$$

Tip: Notice that this definition uses definitions already given above. When you calculate a result, you can use any variable or definition above or to the left of the calculation.

Figure C.12 Mathcad tutorial - basic math; page 12.

Defining Functions

Here you will practice defining **functions**, calculations that can be used over and over again in your worksheet without being entered repeatedly.

EXAMPLE

Below is a function to define as the input and $2x + 1$ as the output. Notice that you use the *assignment operator* to define functions, just as you use the assignment operator to define variables in Mathcad.

$f(x) := 2x + 1$

The function is written in **function notation**, which is a compact way of saying that f is a rule that takes inputs represented by x and produces an output given by 2x + 1. Read "f(x)" as "f of x." It says, "What follows is the algebraic definition of what happens when the rule f is applied to the input x."

If you want to "call" or evaluate that function for a particular value, you enter this:

$f(2) = 5$

This call performed the calculation, 2(2) + 1, automatically by substituting 2 for x in the function f.

Practice

Defining and evaluating a function

Type this:	Get this:
g(x):15-x^2	$g(x) := 15 - x^2$
Then type this:	Get this:
g(2)=	$g(2) = 11$
g(3)=	$g(3) = 6$
Type this:	Get this:
d(s):s-1 [Spacebar] /s+1	$d(s) := \frac{s - 1}{s + 1}$

Tip: The algebraic expression on the right-hand side of your function definition must use the variable noted in parentheses on the left-hand side.

Figure C.13 Mathcad tutorial - basic math; page 13.

Then type this: Get this:

d(101)= $d(101) = 0.98$

Type this: Get this:

L(g):log(g) $L(g) := \log(g)$

and

n:10^30 $n := 10^{30}$

Then type this: Get this:

L(n)= $L(n) = 30$

Evaluating a Function with a Range Variable

Get this:

x:0;10 $x := 0..10$

Tip: Recall that a range variable is a variable that takes on a range of values from one endpoint to another at a specified increment.

Then type this: Get this:

f(x)=

$f(x) =$

1
3
5
7
9
11
13
15
17
19
21

Tip: The best method for performing the same calculation on a range of values is to use a range variable in conjunction with a function.

Tip: In this example, the function, f, was defined at the top of the worksheet. As long as a definition is above or to the left of where it is being used, it does not need to be close to calculations using it.

Type this: Get this:

function(y):y^2 $function(y) := y^2$

Y:3,3.5;5 $Y := 3, 3.5..5$

Then type this: Get this:

function(Y)=

$function(Y) =$

9
12.25
16
20.25
25

Tip: You can call a function with any variable defined in the worksheet.

Modifying a Function to Update Your Calculations

Figure C.14 Mathcad tutorial - basic math; page 14.

function(Y) =

9
12.25
16
20.25
25

Modifying a Function to Update Your Calculations

Inspect the results of evaluating the function, H, over the range variable, Y:

$H(x) := ceil(x)$

Y =
3
3.5
4
4.5
5

H(Y) =
3
4
4
5
5

Tip: The ceil function takes the input and rounds up to the nearest whole number.

Tip: You can display a range variable next to a function evaluated with that variable to show inputs and outputs.

Highlight the **ceil** on the right side of this function definition and delete it:

Get this:

$H(x) := \blacksquare(x)$

Then enter the **floor** function by typing:

floor

Get this:

$H(x) := floor(x)$

Tip: The floor function takes the input and rounds down to the nearest whole number.

Inspect the new results, above.

Entering a Built-in Function

To see a scrolling list of built-in functions along with brief descriptions, select **Function** from the **Insert** menu. The **Insert Function** dialog box, pictured below, lets you insert a function name directly into a math placeholder.

Get this:

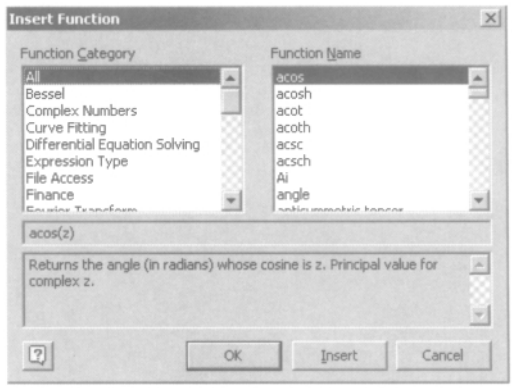

Figure C.15 Mathcad tutorial - basic math; page 15.

From the **Function Name** list, select the function **gcd** and click Insert.

Get this:

gcd(■,■,■,■)

Tip: Greatest Common Factor (**gcd**) is the largest number that evenly factors all the numbers in the list.

In the four function placeholders, type:

88 48 64 112

Get this:

gcd(88,48,64,112) = 8

You can use the [Tab] key to jump to the next placeholder. Press = to see a result.

From the Function Name list, select the function **mean** and click Insert.

Get this:

mean(■,■,■,■)

Tip: The built-in mean function automatically provides four placeholders for numbers you want to find the mean of, but you can always add more.

Click the first placeholder and type:

12 [Tab] 15 [Tab] 18 [Tab] 13,12.5,13.5=

Get this:

mean(12,15,18,13,12.5,13.5) = 14

Tip: If you know the name of the function you want to use, you can simply type it with its appropriate arguments. If not, use the **Insert Function** dialog box to find out the function's name and what arguments it takes.

Figure C.16 `Mathcad` tutorial - basic math; page 16.

Plotting Graphs

Plotting a Single Data Variable from One Data Table or Vector

1. Anywhere below or to the right of your data variable definition, define a range variable to index the data variable. For example, if your data variable is **data**, type "`i:0;length(data)` ".
2. Click below these definitions and choose **Graph ⇒ X-Y Plot** from the **Insert** menu or type "`[Shift]2` " to insert a 2D Graph.
3. In the x-axis placeholder, enter the name of the range variable (**i**).
4. In the y-axis placeholder type "`data[i` " to enter the name of the variable that contains your data subscripted with the range variable. Then, press [Enter].

Note: Arrays and tables have a starting index of 0 (zero) by default.

EXAMPLE

Here is a small set of data entered in a single column Data Table. The data represent the completion times for various speed trials of a car:

times :=

	0
0	13.4
1	14.5
2	13.9
3	14.1
4	15.2
5	15.1
6	15
7	14.8

i := 0..length(times)

The graph has been formatted to show the data as points and the axis limits have been adjusted.

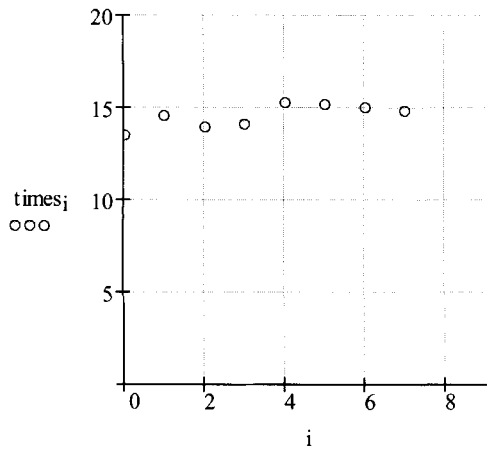

Figure C.17 Mathcad tutorial - plotting; page 1.

Plotting a Single Data Variable from One Data Table or Vector

1. Click anywhere below or to the right of your data table and choose **Graph ⇒ X-Y Plot** from the **Insert** menu or type "[Shift]2" to insert a 2D Graph.
2. In the x-axis placeholder, enter the name of the variable containing your independent data (usually time)
3. In the y-axis placeholder, enter the name of the variable containing your dependent data (usually what you measured) and press [Enter].

EXAMPLE

Here are two vectors containing time and population data and a plot of time versus population, below.

$$\text{time} := \begin{pmatrix} 0 \\ 5 \\ 10 \\ 15 \\ 20 \\ 25 \\ 30 \\ 35 \end{pmatrix} \qquad \text{population} := \begin{pmatrix} 0 \\ 6 \\ 11 \\ 25 \\ 50 \\ 90 \\ 153 \\ 230 \end{pmatrix}$$

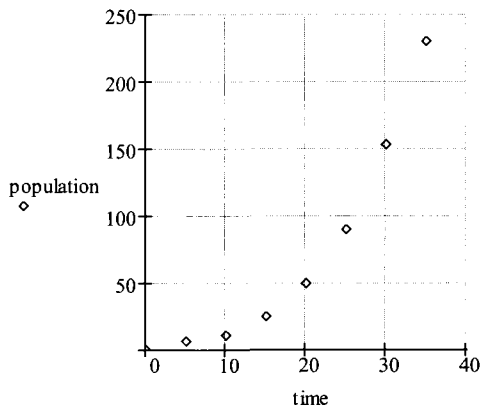

Figure C.18 Mathcad tutorial - plotting; page 2.

Using the `Root` Function; Solving a Single Nonlinear Algebraic Equation

To solve for a variable in an equation using the root function:

Often the equation you want to solve has a numerical solution but not an exact algebraic solution. This when you need the **root** function. To solve an equation using the root function:

1. In your worksheet window, define a guess value for the unknown variable.
2. Type the **root** function where the first argument is an expression equal to zero and the second argument is the unknown variable.

EXAMPLE

Solve the equation $\sin(x) = \frac{x + 1}{10}$.

It is a good idea to first plot the two functions to see approximately the number of times they intersect:

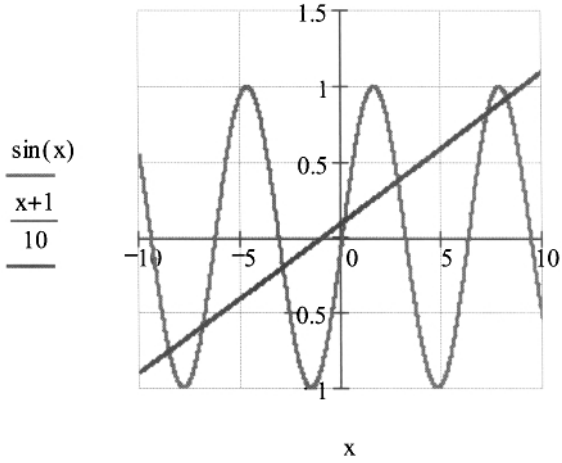

From the plot it looks like there are **seven** places where the two expressions are equal — the seven places where the blue line crosses the red sine curve. Use **root** to find these intersections.

The root function looks for places where an expression is equal to zero. So, first rearrange the equation into the form "something = 0."

$$\sin(x) - \frac{x + 1}{10} = 0$$

Figure C.19 Mathcad tutorial - root function; page 1.

The **root** function will find only a single solution; since there are actually seven solutions, you have to tell Mathcad which one you're after. Do this by defining a guess value for the solution. In fact even if there's only one solution, root requires a guess value to get it started. First try to find the largest solution. From the graph it looks like it's around $x = 9$, so use this guess:

$$x := 9$$

$$\text{root}\left(\sin(x) - \frac{x+1}{10}, x\right) = 8.245$$

Use a different guess value for x to try to find the smallest solution.

$$x := -9$$

$$\text{root}\left(\sin(x) - \frac{x+1}{10}, x\right) = -8.567$$

Figure C.20 Mathcad tutorial - root function; page 2.

Using the `Given ... Find` Construction; Solving Multiple Nonlinear Algebraic Equations

Solving a System of Equations Using a Solve Block

A **Solve Block** can be used to solve any solvable system of equations with any number of equations and unknowns. Here are the steps for setting up a Solve Block:

1. In your worksheet window, define guess values for the unknown variables using a definition equal sign. To do so, type : (colon) or click the Definition button on the **Calculator** toolbar.
2. Below that, type the word **given** (as in "given these equations") as a math region.
3. Below that, enter the equations using **[Ctrl]=**
4. Below that, type " **Find(x,y,z, etc.)** =". In the Find statement, enter all the variables that are unknown in the system.

EXAMPLE

Solve the following system of three equations and three unknowns:

$$3\cdot x + 4\cdot y - 4z = 2$$
$$-7\cdot x + y + z = 5$$
$$6x + 3y - z = 0$$

$x := 1 \quad y := -1 \quad z := 1$ Guess values

Given The word **given** as a math region

$3\cdot x + 4\cdot y - 4z = 2$

$-7\cdot x + y + z = 5$ The equations

$6x + 3y - z = 0$

$$\text{Find}(x,y,z) = \begin{pmatrix} -0.522 \\ 1.12 \\ 0.228 \end{pmatrix}$$ Find statement

Figure C.21 Mathcad tutorial - given ... find construction for solving simultaneous algebraic equations.

The Minimize Function

Minimize(f, var1, var2, ...)
Maximize(f, var1, var2, ...)

Returns the values of var1, var2... that satisfy the constraints in a Solve Block, and make the function f (var1, var2, ...) take on its smallest or largest value, respectively. Minimize and Maximize differ from Find and Minerr in that they refer to functions defined outside of the Solve Block, rather than defined in the body of the Block. Functions are used as objective functions, rather than as constraints, as they are with Find and Minerr. If you are solving for n variables, the solve block must have n equations. The functions choose an appropriate method from a group of available methods, depending on whether the problem is linear or nonlinear, and other attributes.

Arguments:
var1, var2,... are scalar or array variables found in the system of equations. Guess values for each variable must be defined above the Given keyword, or within the body of the Solve Block. If solutions are expected to be complex, complex guess values must be used. f is a function defined above the solve block. The function is supplied without its arguments to Maximize and Minimize.

Notes:
The universal notes on constructing Solve Blocks apply. Within the body of the block:
Equations: Equations to be solved must be defined using Boolean equals. Values in the equations and guess values may be defined within the body of the block using :=.

Constraints: Inequality constraints, using Boolean operators, are allowed.

Output may be assigned to a single variable, a vector of explicit variable names, or a function of argument names in the objective function. The resulting parameterized solve block can be used either to supply guess values for the solved variables in the objective function, or to supply parameters in the objective function or the constraints after the block. Even if the parameters don't appear in the objective function, they must be named as an argument to the function. If the solved variables have different units, they may only be assigned to an explicit vector of names, to avoid mixed units in matrices.

When there is one unknown scalar variable, the solution is a scalar. Otherwise the solution is a vector whose first element is var1, second element is var2, and so on. You cannot solve for a single element of a vector used in the block. All vector values are adjusted simultaneously to minimize the error.

The Levenberg-Marquardt method is not available for Maximize and Minimize.

TOL and CTOL can affect the solution to nonlinear systems. Setting these values too small may cause the solver to not converge. If adjusting these parameters does not help, try different guess values, or add an inequality constraint. If there are no constraints, the keyword Given is not necessary, and Maximize and Minimize may be used without a Solve Block, like a multivariable version of root. They still require guess variables.

Figure C.22 Mathcad tutorial - `minimize`.

INDEX

Gravity-Driven Water Flow in Networks. By Gerard F. Jones

AUTHOR INDEX

This page intentionally left blank

CUSTOMER NOTE: IF THIS BOOK IS ACCOMPANIED BY SOFTWARE, PLEASE READ THE FOLLOWING BEFORE OPENING THE PACKAGE.

This software contains files to help you utilize the models described in the accompanying book. By opening the package, you are agreeing to be bound by the following agreement: